THE ROLE OF DIFFERENT SUBCELLULAR ORGANELLES IN DNA DAMAGE RESPONSE

EDITED BY: Guoping Zhao, Lijun Wu, Shengmin Xu, Daoxiang Zhang and Randy Y. C. Poon

PUBLISHED IN: Frontiers in Cell and Developmental Biology

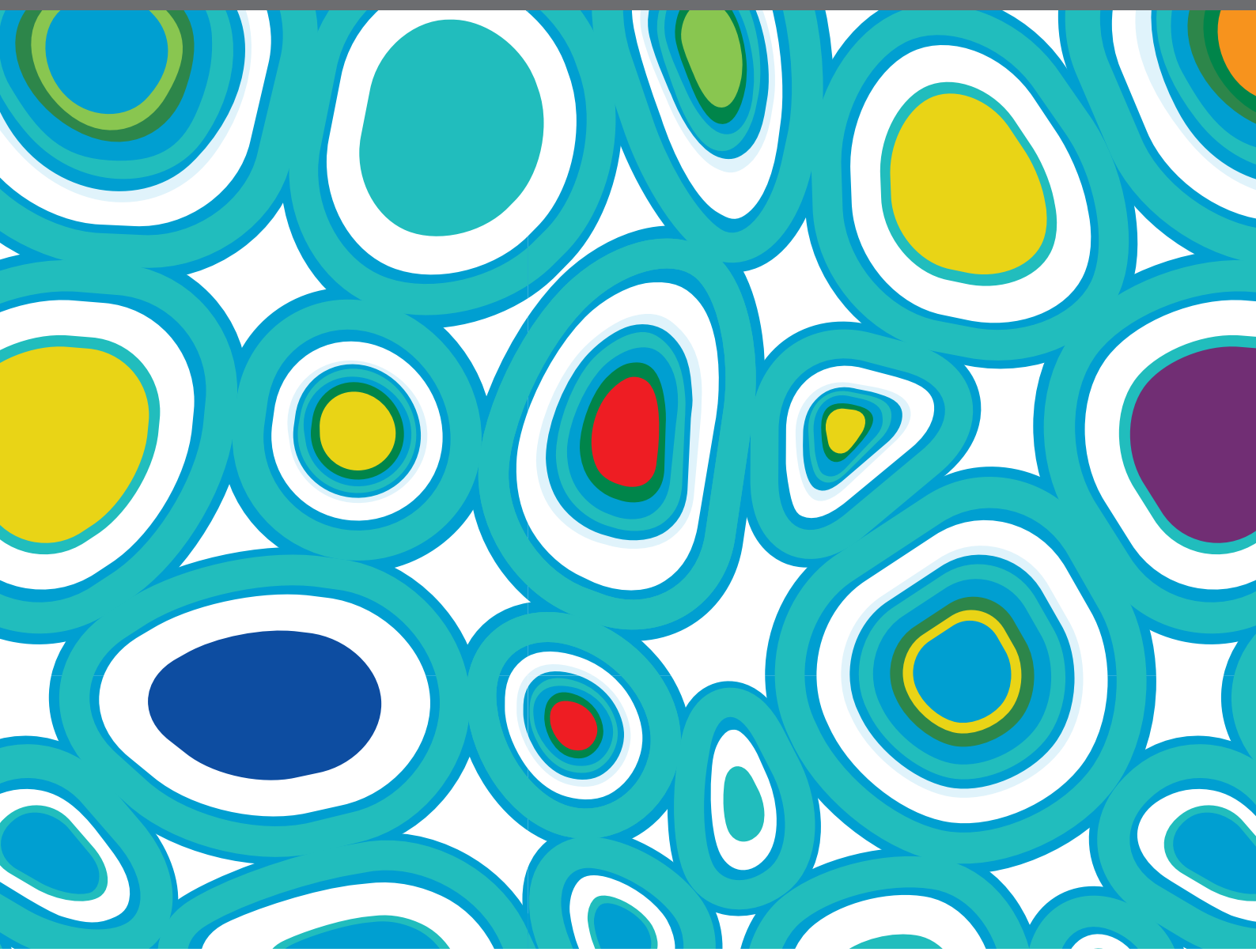

frontiers Research Topics

frontiers

ISSN 1664-8714
ISBN 978-2-88971-897-9
DOI 10.3389/978-2-88971-897-9

About Frontiers

Frontiers is more than just an open-access publisher of scholarly articles: it is a pioneering approach to the world of academia, radically improving the way scholarly research is managed. The grand vision of Frontiers is a world where all people have an equal opportunity to seek, share and generate knowledge. Frontiers provides immediate and permanent online open access to all its publications, but this alone is not enough to realize our grand goals.

Frontiers Journal Series

The Frontiers Journal Series is a multi-tier and interdisciplinary set of open-access, online journals, promising a paradigm shift from the current review, selection and dissemination processes in academic publishing. All Frontiers journals are driven by researchers for researchers; therefore, they constitute a service to the scholarly community. At the same time, the Frontiers Journal Series operates on a revolutionary invention, the tiered publishing system, initially addressing specific communities of scholars, and gradually climbing up to broader public understanding, thus serving the interests of the lay society, too.

Dedication to Quality

Each Frontiers article is a landmark of the highest quality, thanks to genuinely collaborative interactions between authors and review editors, who include some of the world's best academicians. Research must be certified by peers before entering a stream of knowledge that may eventually reach the public - and shape society; therefore, Frontiers only applies the most rigorous and unbiased reviews.
Frontiers revolutionizes research publishing by freely delivering the most outstanding research, evaluated with no bias from both the academic and social point of view. By applying the most advanced information technologies, Frontiers is catapulting scholarly publishing into a new generation.

What are Frontiers Research Topics?

Frontiers Research Topics are very popular trademarks of the Frontiers Journals Series: they are collections of at least ten articles, all centered on a particular subject. With their unique mix of varied contributions from Original Research to Review Articles, Frontiers Research Topics unify the most influential researchers, the latest key findings and historical advances in a hot research area! Find out more on how to host your own Frontiers Research Topic or contribute to one as an author by contacting the Frontiers Editorial Office: frontiersin.org/about/contact

THE ROLE OF DIFFERENT SUBCELLULAR ORGANELLES IN DNA DAMAGE RESPONSE

Topic Editors:
Guoping Zhao, Hefei Institutes of Physical Science (CAS), China
Lijun Wu, Anhui University, China
Shengmin Xu, Anhui University, China
Daoxiang Zhang, Washington University in St. Louis, United States
Randy Y. C. Poon, Hong Kong University of Science and Technology Kowloon, SAR China

Citation: Zhao, G., Wu, L., Xu, S., Zhang, D., Poon, R. Y. C., eds. (2021). The Role of Different Subcellular Organelles in DNA Damage Response.
Lausanne: Frontiers Media SA. doi: 10.3389/978-2-88971-897-9

Table of Contents

frontiers in Cell and Developmental Biology

EDITORIAL
published: 28 October 2021
doi: 10.3389/fcell.2021.760023

Editorial: The Role of Different Subcellular Organelles in DNA Damage Response

*Guoping Zhao**

Key Laboratory of High Magnetic Field and Ion Beam Physical Biology, Anhui Province Key Laboratory of Environmental Toxicology and Pollution Control Technology, Hefei Institutes of Physical Science, Chinese Academy of Sciences, Hefei, China

Keywords: DNA damage repair, subcellular organelles, mitochondria, lysosomes, crosstalk

Editorial on the Research Topic

The Role of Different Subcellular Organelles in DNA Damage Response

Cellular responses to DNA damage are important determinants of both cancer development and the outcome following radiation therapy and chemotherapy. The relationship between endonuclear repair proteins and DNA damage repair pathways during cancer genesis and treatment has been studied widely. However, the interaction between extra-nuclear subcellular organelles and DNA damage response has rarely been investigated. In this section, a comprehensive understanding of the role of different subcellular organelles in response to DNA damage and the possible mechanisms are described. This research provides new insights into cancer treatment with extra-nuclear subcellular organelles.

Mitochondria are considered to be one of the most important subcellular organelles that respond to various stressors, including DNA damage. Previous reports have indicated that exogenous threat-induced double strand breaks (DSBs) may be mediated by the production of mitochondrial reactive oxygen species (Ziech et al., 2011). Moreover, DNA damage repair is an energy-dependent process, and cellular energy depletion always leads to incomplete repair and cell death (Lans et al., 2012). Mitochondria regulate DNA damage repair pathways not only through the production of mitochondrial metabolites in the tricarboxylic acid cycle but also through mitochondria–nuclear signaling related to apoptosis and mitophagy. Han et al. proposed a key role for cytochrome C, a proapoptotic factor residing in mitochondria, in regulating DNA damage response (DDR) and radiosensitivity upon ultra-high dose rate (FLASH) radiation. Kim et al. described a comprehensive overview of mitophagy in the DNA damage response, which highlights a key mechanism for the induction of DDR through mitophagy. Similar to nuclear DNA, mitochondrial DNA (mtDNA) is also constantly assaulted by both exogenous and endogenous stresses. Rong et al. presented state-of-the-art knowledge on the role of base excision repair (BER), direct reversal (DR), mismatch repair (MMR), and double-strand break repair (DSBR) in the processing of the mtDNA repair system, which provides insights into the development of novel treatment strategies. In plants, chloroplasts are semiautonomous organelles with self-contained genetic materials (cp-DNA). Owing to its proximity with the reactive oxygen species (ROS)-generating electron transport system, the chloroplast genome is threatened by diverse forms of oxidative damages. Mahapatra et al. reviewed the existence of highly efficient repair machinery for DNA damage in chloroplasts, which has become an emerging field of research for better understanding of plant cell functions under stressed conditions.

Lysosomes are not only known as organelles that degrade waste materials but also serve as signaling hubs that regulate various metabolic pathways. Several results indicate that lysosomes are

OPEN ACCESS

Edited and reviewed by:
You-Wen He,
Duke University, United States

***Correspondence:**
Guoping Zhao
gpz@ipp.ac.cn

Specialty section:
This article was submitted to Cell Death and Survival, a section of the journal Frontiers in Cell and Developmental Biology

Received: *17 August 2021*
Accepted: *07 October 2021*
Published: *28 October 2021*

Citation:
Zhao G (2021) Editorial: The Role of Different Subcellular Organelles in DNA Damage Response. Front. Cell Dev. Biol. 9:760023. doi: 10.3389/fcell.2021.760023

related to the DNA damage response, and lysosome-targeting therapy can increase radiosensitivity (Zhang et al., 2021). Lysosomes were reported to play a critical role in mediating mTOR activation and, inhibiting mTOR impairs the recruitment of DNA repair proteins, BRCA1 and RAD51, to DNA repair foci, leading to the suppression of DNA damage repair (Zhang et al., 2018). Moreover, TFEB, which has recently been identified as a major regulator of lysosomal biogenesis, is also involved in the removal of oxidative stress and γH2AX formation (Brady et al., 2018). Yang et al. reported that through limited activation of lysosome-mediated autophagy, cancer stem cells achieve increased survival. Lysosomes also regulate the radio-resistance of tumor cells through hypoxia. Zhang et al. demonstrated that hypoxia is the most important factor contributing to radio-resistance. Hypoxia also affects the distribution of lysosomes and decreases mTOR activity. Thus, we assume that hypoxia-induced radio-resistance is lysosome-dependent. However, additional studies are required to verify this hypothesis.

Several studies have reported that DNA damage triggers Golgi fragmentation. This response requires the Golgi protein GOLPH3 to link the Golgi and DNA damage. Upon DNA damage, DNA-PK phosphorylation of GOLPH3 increases its binding to MYO18A, which consequently reduces trafficking and enhances the survival of cancer cells (Farber-Katz et al., 2014). Xie et al. demonstrated the significance of another Golgi protein, SPCA1, in the regulation of DNA repair. The increased SPCA1 level lowered the intracellular Ca^{2+} level, probably by pumping Ca^{2+} into the Golgi, leading to a reduction in ROS level, eventually decreasing MAPK activity and diminishing senescence after radiation. Crosstalk between DDR and ribosomes and DDR and endoplasmic reticulum (ER) has recently been reported. In general, autophagic recycling of ribosomes and the ER is one of the most representative events known to occur in response to DNA damage. Specific regulation of autophagy of ribosomes is mediated by the ubiquitin carboxyl terminal hydrolase Ubp3/Bre5 complex (Yin et al., 2020). DNA-damaging reagents induce the activity of the Ubp3/Bre5 complex, supporting the significance of ribophagy in DDR. Additionally, when ER stress is induced by DNA damage, IRE1a, PERK, and ATF6 play a role in the response to ER stress by interacting with DNA damage repair proteins, resulting in the formation of autophagosomes (Dufey et al., 2020). Kim et al. summarized the latest research that connects ribophagy and ER-phagy with defects in the DNA repair system and highlighted the importance of autophagy activated by DDR and appropriate regulation of autophagic organelles, suggesting insights for future studies.

Overall, this editorial described emerging relationships between the extra-nuclear subcellular organelles and DDR, which greatly contributes to further understanding of the regulatory networks and the potential applications of extra-nuclear subcellular organelles in DDR.

AUTHOR CONTRIBUTIONS

GZ wrote the manuscript, contributed to the article, and approved the submitted version.

FUNDING

This work was supported by the National Natural Science Foundation of China (31870845 and 11835014), the Dean's Fund of Hefei Institute of Physical Science (YZJJZX202014), and the CAS Pioneer Hundred Talents Program (GZ).

REFERENCES

Brady, O. A., Jeong, E., Martina, J. A., Pirooznia, M., Tunc, I., and Puertollano, R. (2018). The transcription factors TFE3 and TFEB amplify p53 dependent transcriptional programs in response to DNA damage. *Elife* 7:40856. doi: 10.7554/eLife.40856

Dufey, E., Bravo-San Pedro, J. M., Eggers, C., Gonzalez-Quiroz, M., Urra, H., Sagredo, A. I., et al. (2020). Genotoxic stress triggers the activation of IRE1alpha-dependent RNA decay to modulate the DNA damage response. *Nat. Commun.* 11:2401. doi: 10.1038/s41467-020-15694-y

Farber-Katz, S. E., Dippold, H. C., Buschman, M. D., Peterman, M. C., Xing, M., Noakes, C. J., et al. (2014). DNA damage triggers Golgi dispersal via DNA-PK and GOLPH3. *Cell* 156, 413–427. doi: 10.1016/j.cell.2013.12.023

Lans, H., Marteijn, J. A., and Vermeulen, W. (2012). ATP-dependent chromatin remodeling in the DNA-damage response. *Epigenet. Chromatin.* 5:4. doi: 10.1186/1756-8935-5-4

Yin, Z., Popelka, H., Lei, Y., Yang, Y., and Klionsky, D. J. (2020). The roles of ubiquitin in mediating autophagy. *Cells* 9:2025. doi: 10.3390/cells9092025

Zhang, X., Wang, J., Li, X., and Wang, D. (2018). Lysosomes contribute to radioresistance in cancer. *Cancer Lett.* 439, 39–46. doi: 10.1016/j.canlet.2018.08.029

Zhang, Z., Yue, P., Lu, T., Wang, Y., Wei, Y., and Wei, X. (2021). Role of lysosomes in physiological activities, diseases, and therapy. *J. Hematol. Oncol.* 14:79. doi: 10.1186/s13045-021-01087-1

Ziech, D., Franco, R., Pappa, A., and Panayiotidis, M. I. (2011). Reactive oxygen species (ROS)–induced genetic and epigenetic alterations in human carcinogenesis. *Mutat. Res.* 711, 167–173. doi: 10.1016/j.mrfmmm.2011.02.015

Conflict of Interest: The author declares that the research was conducted in the absence of any commercial or financial relationships that could be construed as a potential conflict of interest.

Publisher's Note: All claims expressed in this article are solely those of the authors and do not necessarily represent those of their affiliated organizations, or those of the publisher, the editors and the reviewers. Any product that may be evaluated in this article, or claim that may be made by its manufacturer, is not guaranteed or endorsed by the publisher.

frontiers in Cell and Developmental Biology

ORIGINAL RESEARCH
published: 25 March 2021
doi: 10.3389/fcell.2021.637454

The Roles of HIF-1α in Radiosensitivity and Radiation-Induced Bystander Effects Under Hypoxia

Jianghong Zhang[1], Yuhong Zhang[1], Fang Mo[1], Gaurang Patel[2], Karl Butterworth[2], Chunlin Shao[1] and Kevin M. Prise[2]**

[1] Institute of Radiation Medicine, Fudan University, Shanghai, China, [2] Patrick G Johnston Centre for Cancer Research, Queen's University Belfast, Belfast, United Kingdom

OPEN ACCESS

Edited by:
Shengmin Xu,
Anhui University, China

Reviewed by:
Hou Yuzhu,
University of Chicago, United States
Enyu Rao,
Xuzhou Medical University, China

***Correspondence:**
Kevin M. Prise
k.prise@qub.ac.uk
Chunlin Shao
clshao@shmu.edu.cn

Specialty section:
This article was submitted to Cell Death and Survival, a section of the journal Frontiers in Cell and Developmental Biology

Received: 03 December 2020
Accepted: 19 February 2021
Published: 25 March 2021

Citation:
Zhang J, Zhang Y, Mo F, Patel G, Butterworth K, Shao C and Prise KM (2021) The Roles of HIF-1α in Radiosensitivity and Radiation-Induced Bystander Effects Under Hypoxia. Front. Cell Dev. Biol. 9:637454. doi: 10.3389/fcell.2021.637454

Radiation-induced bystander effects (RIBE) may have potential implications for radiotherapy, yet the radiobiological impact and underlying mechanisms in hypoxic tumor cells remain to be determined. Using two human tumor cell lines, hepatoma HepG2 cells and glioblastoma T98G cells, the present study found that under both normoxic and hypoxic conditions, increased micronucleus formation and decreased cell survival were observed in non-irradiated bystander cells which had been co-cultured with X-irradiated cells or treated with conditioned-medium harvested from X-irradiated cells. Although the radiosensitivity of hypoxic tumor cells was lower than that of aerobic cells, the yield of micronucleus induced in bystander cells under hypoxia was similar to that measured under normoxia indicating that RIBE is a more significant factor in overall radiation damage of hypoxic cells. When hypoxic cells were treated with dimethyl sulfoxide (DMSO), a scavenger of reactive oxygen species (ROS), or aminoguanidine (AG), an inhibitor of nitric oxide synthase (NOS), before and during irradiation, the bystander response was partly diminished. Furthermore, when only hypoxic bystander cells were pretreated with siRNA hypoxia-inducible factor-1α (HIF-1α), RIBE were decreased slightly but if irradiated cells were treated with siRNA HIF-1α, hypoxic RIBE decreased significantly. In addition, the expression of HIF-1α could be increased in association with other downstream effector molecules such as glucose transporter 1 (GLUT-1), vascular endothelial growth factor (VEGF), and carbonic anhydrase (CA9) in irradiated hypoxic cells. However, the expression of HIF-1α expression in bystander cells was decreased by a conditioned medium from isogenic irradiated cells. The current results showed that under hypoxic conditions, irradiated HepG2 and T98G cells showed reduced radiosensitivity by increasing the expression of HIF-1α and induced a syngeneic bystander effect by decreasing the expression of HIF-1α and regulating its downstream target genes in both the irradiated or bystander cells.

Keywords: radiation, hypoxia, bystander, HIF1 alpha, micronuclei, hepatoma cells

INTRODUCTION

Hypoxic regions are a common feature of most solid tumors, have radioresistant biological effects, and represent the most aggressive fraction of a tumor (Horsman et al., 2012; Peitzsch et al., 2017; Busk et al., 2020). Recent experimental evidence has shown that cells may respond directly to radiation exposure or through communicated transmissible factors capable of inducing cellular responses in non-irradiated cells, which is referred to as the radiation-induced bystander effect (RIBE) (Shao et al., 2003; Kamochi et al., 2008; Lorimore et al., 2008; Shao et al., 2008a; Zhu et al., 2008; Heeran et al., 2019). The RIBE has been demonstrated in a range of experimental systems and been shown to induce DNA point mutations (Gaziev et al., 2008; Nikitaki et al., 2016), DNA double-strand breaks (Shikazono et al., 2009), genomic instability (Behar, 2008; Lorimore et al., 2008), micronucleus formation (Shao et al., 2005, 2006; Xie et al., 2015), change in gene expression (Xie et al., 2016), apoptosis, and cell killing (Yasui et al., 2017). There may be a close interrelationship between cellular bystander responses and systemic tissue responses to radiation exposure including abscopal effects and the involvement of immune signaling (Formenti and Demaria, 2009; Prise and O'Sullivan, 2009; Griffin et al., 2020a,b). Despite this, the role of RIBE in radiotherapy and cancer risks associated with environmental, occupational, and medical exposures remains to be fully elucidated. Furthermore, the impact of factors within the tumor microenvironment including hypoxia has not yet been determined.

The precise mechanisms underlying RIBE, especially under hypoxic conditions, are still unclear. There is evidence that a range of bystander signaling molecules, including free radicals (Dong et al., 2015), protein factors (Shao et al., 2008a; Xie et al., 2016), calcium ions (Shao et al., 2006), hormones, microRNA (Palayoor et al., 2014), and extracellular vesicles (EVs) (Bewicke-Copley et al., 2017), can be produced from irradiated cells and play a role in the induction of bystander responses. In addition, gap-junctional intercellular communication (GJIC) has been shown to play an important role in the bystander response of normal cells which have fully functional GJIC (Shao et al., 2003; Frank et al., 2006). RIBE can be triggered by irradiated tumor cells so that heritable damages are induced in surrounding tumor and normal cells. For example, we found that when a small fraction of glioblastoma cells T98G were targeted with localized ions from a microbeam, additional micronucleus could be induced in the neighboring cells of either T98G or normal human fibroblasts (Mayer et al., 2012), which suggests that bystander response may have two potential impacts on radiotherapy by increasing the efficacy of tumor cell killing but simultaneously increasing the secondary cancer risk via the production of genetic damage occurs in normal bystander cells.

It has been noted that hypoxia can increase radioresistance of malignant solid tumors through conspecific biological mechanisms (Moeller et al., 2007; Li et al., 2010; Sun et al., 2015). A key mechanism is via the transcription factor, hypoxia-inducible factor 1 (HIF-1). Extensive research has shown that increasing intratumoral hypoxia and HIF-1 activity correlate with incidences of both tumor recurrence and distant tumor metastasis as well as a poor prognosis and after radiation therapy. HIF-1 is able to promote the growth of endothelial cells after radiotherapy by inducing the expression of key downstream genes, including vascular endothelial cell growth factor (VEGF) (Ahn et al., 2014), carbonic anhydrase (CA9) (Chiche et al., 2009; Logsdon et al., 2016), and glucose transporter (GLUT1) (Dungwa et al., 2011), thus promoting the overall tumor radioresistance. HIF-1 is a heterodimeric transcription factor consisting of both an α-subunit (HIF-1α) and a β-subunit (HIF-1β). Its activity is mainly dependent on the stability of HIF-1α, which becomes relatively stable under hypoxia, then interacts with HIF-1β to form the HIF-1 active heterodimer. This binds to its enhancer sequence, the hypoxia-responsive element (HRE), and induces the expression of key genes related to adapting cellular metabolism to hypoxia, escaping or improvement in hypoxia, and the resistance of malignant tumor to chemo and radiation therapy (Prise and O'Sullivan, 2009; Semenza, 2009; Noman et al., 2019).

Here, we demonstrate a significant bystander response under hypoxic conditions in two cell models, which is comparable to that observed under oxic conditions, despite the reduction in direct effect. This highlights an overall increased role for bystander signaling under hypoxic conditions. A significant role for ROS and NO in mediating the response is reported. We also report that the increased expression of HIF-1α and its downstream proteins in hypoxic-irradiated cells leads to an increase of radioresistance but induces a bystander effect via downregulating HIF-1α expression in hypoxic non-irradiated bystander cells. These could have future benefits for the development of therapeutic strategies for treatment of hypoxic tumors.

MATERIALS AND METHODS

Cell Culture and Drugs

Human hepatoma cells HepG2 and human glioblastoma cells T98G were obtained from Cancer Research UK, London, and maintained in Dulbecco's minimum essential medium (DMEM, Gibco) supplied with 10% fetal calf serum (FCS, Gibco), 0.01% sodium pyruvate (Sigma), 2 mM L-glutamine, 100 units/ml penicillin, and 100 μg/ml streptomycin in humidified 95% air and 5% CO_2 at 37 °C. For hypoxic incubation, cells were maintained in an InvivO2-400 hypoxia workstation (Ruskinn Technology Ltd., United Kingdom) with 94.9% N_2, 5% CO_2, and 0.1% O_2 for at least 12 h. Target cells were placed into a sealed aluminum box at 37 °C with 95 % N_2 and 5% CO_2 for 4 h; after irradiation, target cells were transferred into the hypoxic workstation for further treatment. Bystander cells were cultured or treated while still in the hypoxia workstation.

Dimethyl sulfoxide (DMSO), aminoguanidine (AG), cobalt chloride ($CoCl_2$), cytochalasin B (CB), and 7-aminoflavone (AF) were purchased from Sigma (United Kingdom). HIF-1α siRNA (h2, sc-44225) and control siRNA were purchased from Santa Cruz Biotechnology, Inc (United Kingdom). Lipofectamine 2000 (Cat. No. 11668-019) was from Invitrogen (United Kingdom). Opti-MEM-I was from Gibco (United Kingdom).

Cell Irradiation

Log-phase cells were seeded and incubated overnight before being incubated in the hypoxic workstation for 12 h. One hour before irradiation, the culture medium was replaced by a serum-free and hypoxic medium containing 10 mM HEPES and the culture dishes were put into a custom-built aluminum box flushed with 95% N_2 and 5% CO_2 (BOC, United Kingdom) for cell irradiation. At room temperature, cells were irradiated with 225 kVp X-rays (2-mm copper-filtered, X-Rad 225, Precision X-ray Inc., United States) at a dose rate of 0.59 Gy/min.

In the experiments where cells were treated before irradiation with 1% DMSO or 20 μM AG for 1 h, after irradiation, the medium was immediately replaced by a complete medium for further experiments.

Generation of Conditioned Medium for Cell Treatment

After irradiation, the medium was changed immediately. Two hours later, the conditioned medium was collected from irradiated cells and filtered through a 0.2-μm filter. Then, non-irradiated cells were treated with the conditioned medium for 24 h with the following two methods. Group one ($N_2 \rightarrow N_2$), bystander hypoxic cells were treated with the conditioned medium generated from cells irradiated under hypoxia. Group two ($O_2 \rightarrow O_2$), normoxic bystander cells were treated with the conditioned medium harvested from irradiated normoxic cells.

Cell Co-culture

Under either normoxic or hypoxic condition, cells growing on one coverslip were irradiated with X-rays and were then co-cultured for 24 h with the same number of non-irradiated cells growing on another coverslip within the same culture dish. After this co-culture, micronucleus and cell survival were assayed in the non-irradiated cells.

Treatment of Reagents

For chemical hypoxic treatment, normoxic HepG2 or T98G cells were treated with 100 μM $CoCl_2$ for 4 h before irradiation. In specific experiments, hypoxic-irradiated cells were treated with 1% DMSO or 20 μM AG, an inhibitor for NO, 1 h before irradiation. AF was used to inhibit HIF-1α mRNA expression and HIF-1α protein accumulation, and hypoxic-irradiated or bystander cells were treated with 5 μM AF for 4 h before irradiation or conditioned-medium treatment, respectively. Transient inhibition of HIF-1α was carried out by transfection with HIF-1α siRNA or control siRNA-A using Lipofectamine^{TM} 2000 according to the manufacturer's instruction. After irradiation, the medium was immediately replaced by a complete medium on irradiated cells for further experiments.

Micronucleus Assay

Micronucleus induction was used as an endpoint for bystander damage. The frequency of micronucleus formation was measured using the cytokinesis-block technique (Fenech and Morley, 1986). After conditioned-medium treatment or co-culture procedure, the cells were treated with 1 μg/ml CB for 28 h, washed with PBS, fixed with methanol and acetic acid (9:1, v/v) for 20 min, stained with 10 μg/ml Hoechst 33342 plus 10 μg/ml acridine orange for 5 min, and washed in water. After air drying, the cells were mounted with Mount Medium (Sigma, United Kingdom) then at least 1000 binucleated cells were observed for micronuclei with a fluorescence microscope. The micronucleus yield (Y_{MN}) was calculated as the ratio of the number of micronuclei to the number of binucleated cells.

Cell Survival Assay

The irradiated HepG2 cells and T98G cells were trypsinized and replated on 60-mm dishes at appropriate dilutions immediately after irradiation with 0, 2, 4, or 8 Gy X-rays and incubated for 10–14 days at 37°C in a humidified atmosphere containing 5% CO_2 and 95% air. To measure viability in bystander cells, cells were treated with a conditioned medium for 24 h, then treated as above. The colonies from irradiated or bystander populations were fixed with 10% formalin, stained with 1% methylene blue, and the colonies containing ≥50 cells were counted to quantify clonogenic cell survival. Survival fraction was calculated as the ratio of the plating efficiency of the irradiated cells to the plating efficiency of cells which had not been irradiated (controls). Data from three separate experiments are presented as the mean ± SEM, and the error bars for all survival data represent the 95% confidence intervals for normalized data points as calculated by Fieller's theorem (Gupta et al., 1996). The cell survival curves were fitted with the multitarget single-hit mode of survival fraction = $1 - (1 - \exp(-D/D_0))^N$ by optimizing variable parameters D_0 and N. A modified OER (oxygen enhancement ration) was calculated as the ratio of D_0 at hypoxia as at ambient oxygen tension, i.e., OER = D_0 (hypoxia)/D_0 (normoxia).

Western Blotting

Cultured cells were harvested after the reported treatments (as described as above), washed with cold PBS on ice, and lysed with RIPA lysis buffer for protein extraction. After being denatured at 100°C for 10 min, aliquots of protein samples (20 μg) were separated by electrophoresis on an SDS-polyacrylamide gel (4% pycnotic gel and 10% separation gel, Bio-Rad Laboratories, Inc), then transferred onto a polyvinylidene difluoride membrane (Millipore Corporation), blocked for 1 h with 5% skimmed milk in 0.05% Tris-buffered saline/Tween (TBST), and incubated with a specific primary antibody (diluted 1:1000 in blocking buffer for the rabbit anti-HIF-1α; Cell Signaling Technology, London, United Kingdom), 1:500 for the rabbit anti-CA9 (Abcam, Cambridge, United Kingdom), 1:1000 for the mouse anti-VEGF, 1:1000 for mouse anti-Glut 1, and 1:1000 for mouse anti-β-actin (Abcam) overnight at 4°C. Then, the membrane was washed 3× with TBST at room temperature for 10 min and incubated with a secondary antibody (HRP-conjugated anti-mouse IgG or anti-rabbit IgG; 1:5000, Abcam) for 1 h. The membrane was detected by the enhanced chemiluminescence system (ECL Advance, Amersham Biosciences) after several washes, and the protein image was recorded using a BIO-RAD ChemiDoc XRS and analyzed using Quantity One software (Bio-Rad, Hercules, CA, United States).

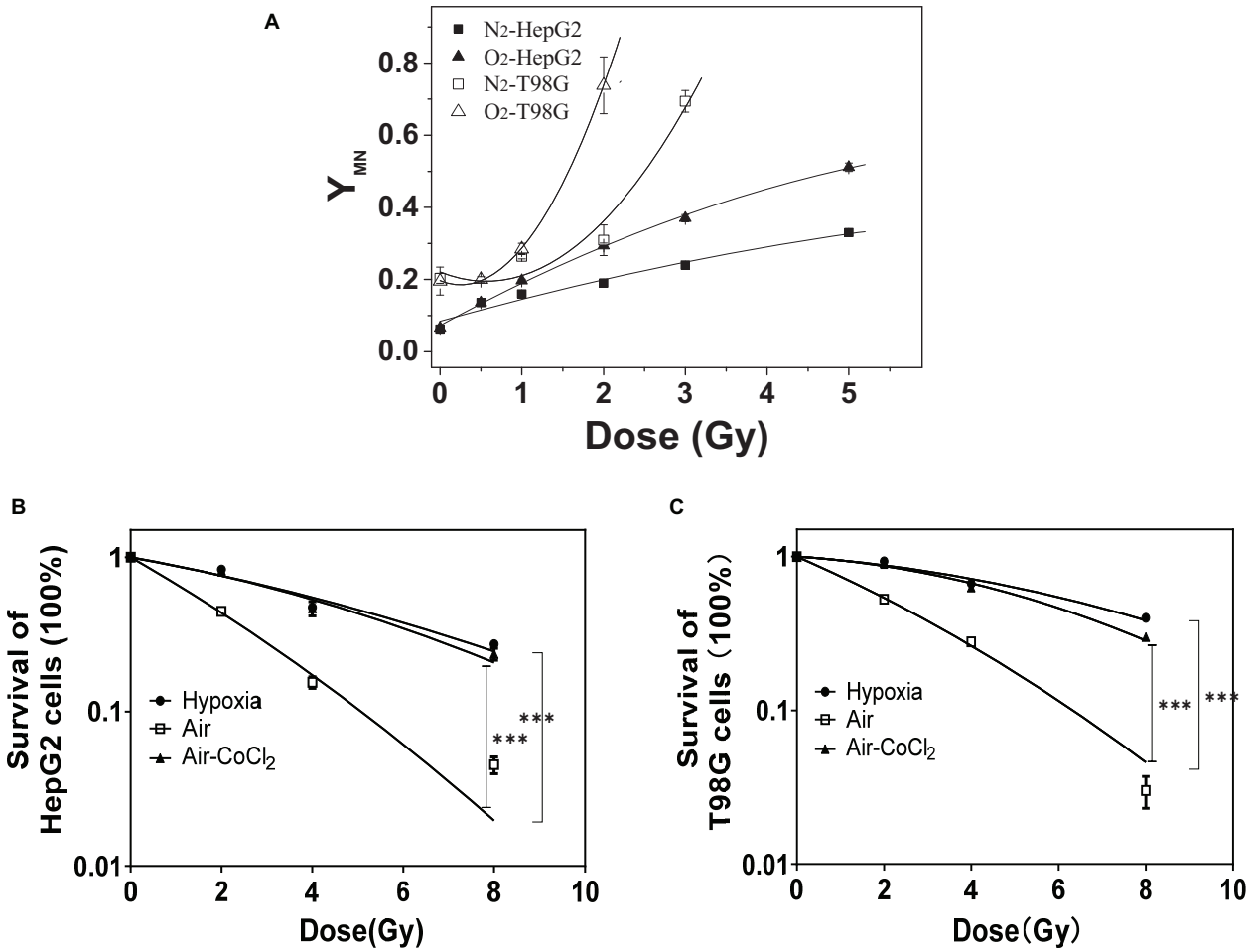

FIGURE 1 | The role of hypoxia on radioresistance in HepG2 and T98G cells. The micronucleus yields of irradiated HepG2 cells and T98G cells (with 0, 0.5, 1, 2, 3, or 5 Gy X-ray) were detected under normoxic or hypoxic conditions **(A)**. Cell survival was analyzed for HepG2 cells **(B)** and T98G cells **(C)** under normoxic, hypoxic, or 100 μM cobalt chloride ($CoCl_2$) pretreatment. ***$p < 0.01$ between indicated groups.

Statistical Analysis

Statistical analysis was performed on the means of data obtained from at least three independent experiments. Three replicates were counted for each data point to quantify the micronucleus induction. All results are presented as mean ± SEM, analyzed with an ANOVA test. Statistical significance was defined as $P < 0.05$.

RESULTS

Hypoxia-Induced Radioresistance

Chromosomal damage following direct irradiation was determined by measuring micronucleus induction after cell nuclear division. **Figure 1A** illustrates the yields of micronucleus in both HepG2 and T98G cell lines as a function of dose under normoxic and hypoxic conditions. T98G cells had higher yields of micronucleus under both conditions compared to HepG2 cells. For both cell lines, normoxic cell radiosensitivity was significantly higher than hypoxic cells. When the dose was 2 Gy, the yield of micronucleus in normoxic cells to the yield of micronucleus in hypoxic cells ratio was 1.6 and 2.4 for HepG2 cells and T98G cells, respectively. The radiosensitivity of hypoxic cells was increased under hypoxic conditions (**Figures 1B,C**). The OER of HepG2 and T98G cell was 2.56 and 2.66, respectively. Treatment of cells with $CoCl_2$ gave the OERs of 2.41 and 2.26 in HepG2 and T98G cells, respectively. These results clearly demonstrate that hypoxia induces significant radioresistance.

RIBE Played an Important Role in Radiation Damage Under Hypoxia Conditions

Figures 2A,B show that the micronucleus yields for both non-irradiated bystander HepG2 cells and T98G cells significantly increased when they were co-cultured with irradiated cells or treated with the conditioned medium harvested from irradiated cells under either normoxic or hypoxic conditions. It was found that, for both cell lines, the treatment of conditioned medium

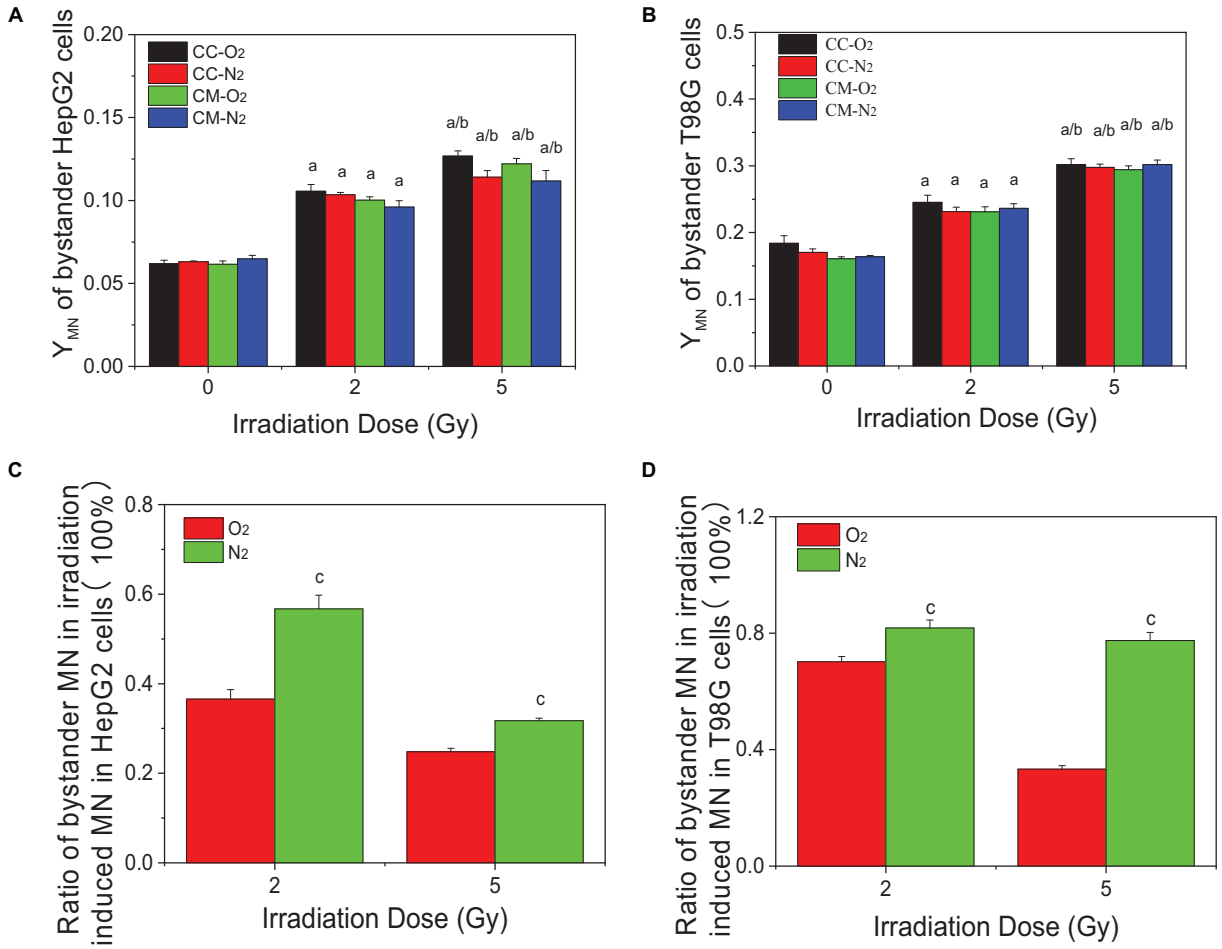

FIGURE 2 | Micronucleus induction in non-irradiated bystander cells of HepG2 and T98G under hypoxic and normoxic conditions. The bystander cells were either co-cultured with irradiated conspecific cells (CC-O_2 and CC-N_2) or treated with the conditioned medium (CM-O_2 and CM-N_2) harvested from irradiated conspecific cells under the same oxygen conditions. The ratio of bystander micronucleus **(A,B)** to radiation-induced micronucleus of HepG2 cells **(C)** and T98G cells **(D)** under hypoxic and normoxic conditions was plotted. a, $p < 0.05$ compared with the 0-Gy group; b, $p < 0.05$ compared with the 2-Gy group; c, $p < 0.05$ compared with the normoxic group.

and co-culture generated a similar bystander response leading to micronucleus induction. Moreover, the yields of bystander micronucleus were also similar under normoxic and hypoxic conditions. Although the hypoxic cells are radioresistant, the irradiated tumor cells can induce a similar bystander effect of micronucleus induction under different oxygen conditions. Further calculation showed that, for both cell lines, the ratio of the yield of micronucleus in bystander cells to the yield of irradiation-induced micronucleus in hypoxia was higher than that detected under normoxia (see **Figures 2C,D**). This result indicates that RIBE may play a more significant role in the overall radiation damage response of hypoxic cells.

RIBE Was Induced by Free Radical Under Hypoxic Conditions

Our previous studies have showed that ROS and NO contribute to the RIBE of normoxic tumor cells including HepG2 and T98G cells. To investigate whether these free radicals are involved in the RIBE in hypoxic cells, we incubated the hypoxic cells with either DMSO or AG 1 h before and during irradiation. Two hours post-irradiation, the conditioned medium without the drug was harvested and transferred to non-irradiated bystander cells that were further cultured for 24 h under hypoxic conditions until micronucleus or clonogenic assay. The representative results of bystander effects were illustrated in **Figure 3** where the donor tumor cells, with or without free radical scavenger treatment, were irradiated with 5 Gy X-rays. It can be seen that, for both HepG2 and T98G cells, treatment of cells with DMSO or AG significantly reduced the yield of bystander micronucleus (**Figures 3A,B**) and increased the relative cell survival (**Figures 3C,D**) of hypoxic cells, but the yields of remaining micronucleus, or the relative cell survival, did not completely return to control levels. This may be because free radicals and other related bystander signals were scavenged or inhibited by DMSO and AG only

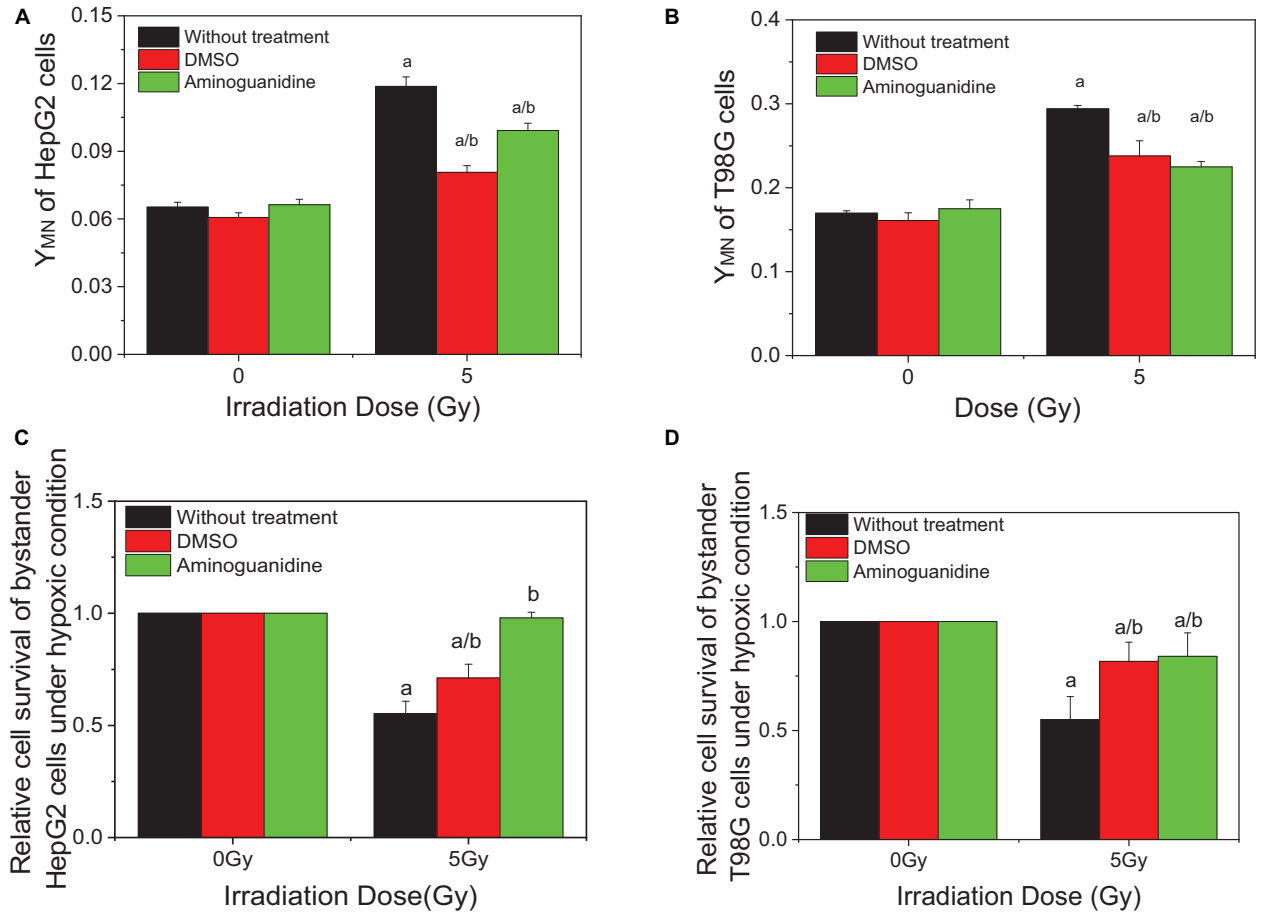

FIGURE 3 | Influence of DMSO and aminoguanidine (AG) on the bystander effect in HepG2 cells and T98G cells under hypoxic conditions. Bystander tumor cells were treated with the conditioned medium harvested from irradiated conspecific cells. **(A,C)** Micronucleus induction in the bystander cells. **(B,D)** Survival fractions of bystander cells. a, $p < 0.05$ compared with the 0-Gy group; b, $p < 0.05$ compared with the 5-Gy group without chemical treatment.

during irradiation, as the cell culture medium was replaced, after irradiation, with a fresh medium without scavenger. Subsequent bystander signaling factors could be released from irradiated cells in the conditioned medium further inducing bystander responses.

HIF-1α Status of Irradiated Cells Determined RIBE Under Hypoxia Conditions

To investigate the effect of HIF-1α on the RIBE under hypoxic conditions, cells were pretreated to inhibit HIF-1α (HIF-1α siRNA or chemical inhibitor AF) before irradiation, then harvested and the removed conditioned medium added to hypoxic bystander cells. Results showed that, for both HepG2 and T98G cells, pretreatment of irradiated cells with AF or siRNA inhibited the expression of HIF-1α and significantly reduced the yield of bystander micronucleus of hypoxic bystander cells although the yields of the remaining micronucleus were still higher than the control values (**Figures 4A,B**). The yields of micronucleus were decreased from 0.103 to 0.069 and 0.068 on HepG2 cells or from 0.31 to 0.215 and 0.234 on T98G cells by HIF-1α siRNA or AF treatment, respectively. Simultaneously, the relative cell survival of both hypoxic bystander cells were increased (**Figures 4C,D**) compared with 5 Gy without treatment; the survival fraction was increased from 0.66 to 0.804 and 0.859 in HepG2 cells or from 0.692 to 0.956 and 0.875 in T98G cells by the treatment of HIF-1α siRNA or AF, respectively. These data showed that, in hypoxic-irradiated cells, in the absence of HIF-1α expression the bystander damage in the hypoxic bystander cells was significantly reduced. It can be seen that HIF-1α also plays a key role in the RIBE under hypoxic conditions.

In order to explore the action of HIF-1α in the RIBE, both irradiated and bystander cells were pretreated with HIF1-α siRNA. Compared with irradiated controls, the yields of micronucleus of bystander cells were decreased from 0.105 to 0.085, 0.069, or 0.054 in HepG2 cells and from 0.307 to 0.265, 0.215, or 0.209 in T98G cells in three groups (bystander-inhibition group, target-inhibition group, and both bystander and target-inhibition group), respectively (**Figures 5A,B**). Significantly, the decrease in levels in the

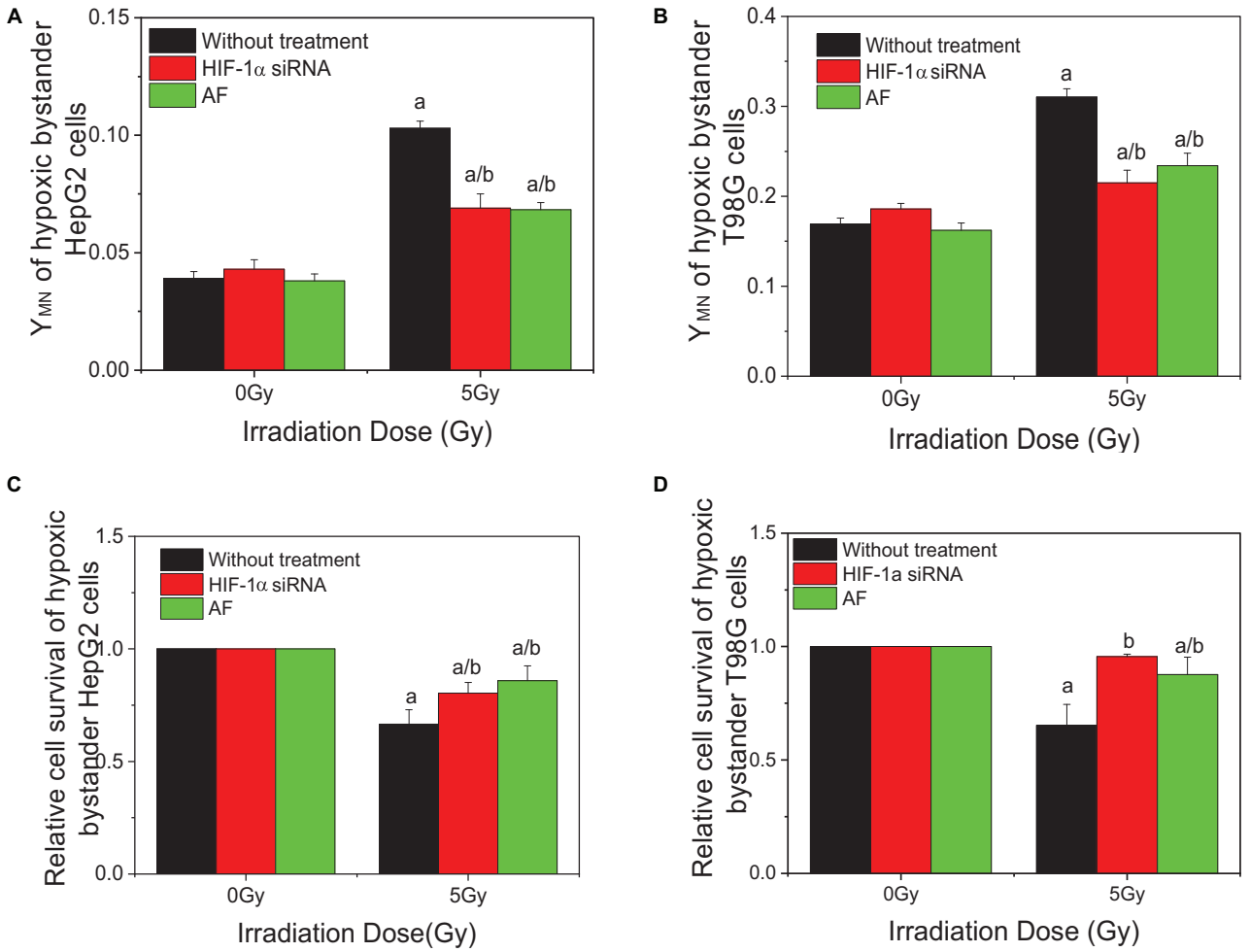

FIGURE 4 | Influence of HIF-1α on the bystander effect of HepG2 cells and T98G cells under hypoxic conditions. Bystander tumor cells were treated with the conditioned medium harvested from irradiated conspecific cells, which were pretreated with HIF-1α siRNA and 5 μM 7-aminoflavone under hypoxic conditions. **(A,C)** Micronucleus induction in the bystander cells. **(B,D)** Survival fractions of bystander cells. a, $p < 0.05$ compared with the 0-Gy group; b, $p < 0.05$ compared between the 5-Gy group under different oxygen conditions.

target-inhibition group or both target and bystander-inhibition group was higher than that of the bystander only-inhibition group. Similar results were observed for cell survival in both cell lines (shown in **Figures 5C,D**). The relative survival fraction was increased significantly from 0.666 to 0.804 or 0.811 for HepG2 cells and from 0.779 to 0.956 or 0.929 for T98G cells in the target-inhibition group or both target and bystander-inhibition group, respectively. Regardless of whether bystander cells were pretreated with HIF-1α siRNA, as long as target cells were pretreated with siRNA, the impact was higher than the other two groups (bystander-inhibition group and control group). Interestingly, if only bystander cells were pretreated with HIF-1α siRNA, the relative survival fraction was not markedly changed. These results confirm that HIF-1α is a key player in the RIBE detected under hypoxic conditions. It is significant that the hypoxic RIBE is regulated mainly by HIF-1α expression derived from irradiated cells, with no tight relationship with autochthonous HIF-1α expression level in hypoxic bystander cells.

HIF-1α Was Involved in Radiation Damage in Hypoxia-Exposed Cells by Controlling Downstream Genes

For both HepG2 cells and T98G cells, HIF-1α expression was increased markedly in hypoxic-irradiated cells and it was also increased along with the hypoxic incubation time and post-irradiation time (**Figure 6**). For HepG2 cells, the expression of GLUT-1 and CA9 showed a similar trend to HIF-1α expression. However, VEGF expression was only induced by hypoxia and not by irradiation. For T98G cells, the expressions of GLUT-1, CA9, and VEGF were all increased by hypoxia treatment and were increased slightly at 8 h and 4 h after irradiation. Overall, the changes in levels of GLUT-1, CA9, and VEGF all followed their upstream gene HIF-1α. In addition, for both HepG2 cells and

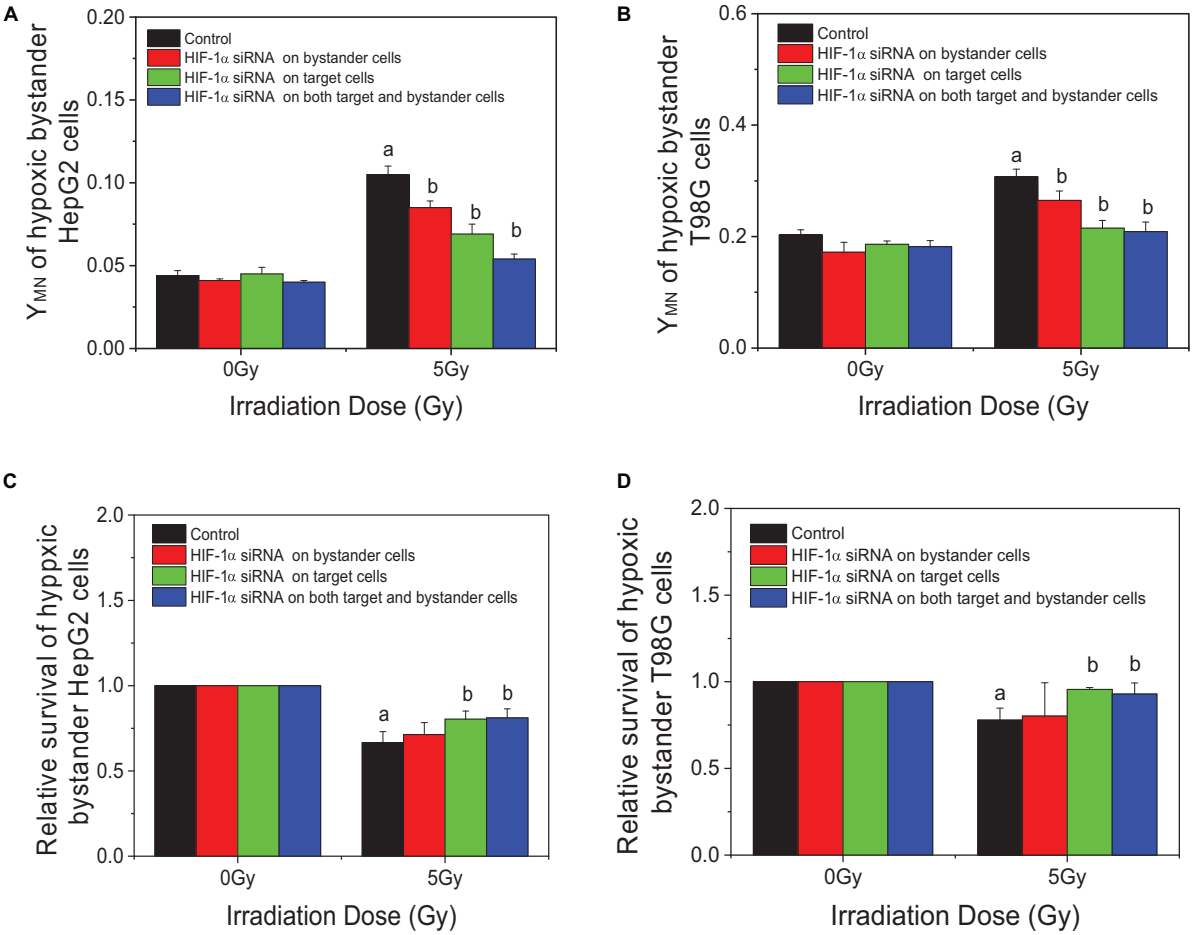

FIGURE 5 | Inhibition responses of HIF-1α expression on the target (irradiated) and/or bystander HepG2 cells and T98G cells under hypoxic conditions. Four groups in this experiment: Control group, bystander cells only were treated with the conditioned-medium from irradiated conspecific cells; Inhibition of bystander cells, only bystander cells were pretreated with HIF-1α siRNA, then incubated with the conditioned medium from irradiated conspecific cells. Inhibition of target cells, only target cells pretreated with HIF-1α siRNA, then harvested and the conditioned medium transferred to bystander cells. Inhibition on both target and bystander cells, target and bystander cells were pretreated with HIF-1α siRNA, then the conditioned medium added to bystander cells. **(A,C)** Micronucleus induction in the bystander cells. **(B,D)** Survival fractions of bystander cells. a, $p < 0.05$ compared with the 0-Gy group; b, $p < 0.05$ compared with the 5-Gy group without treatment.

T98G cells, $CoCl_2$ can induce an increased expression of HIF-1α to a similar extent to that produced by hypoxia (**Figure 7**). HIF-1α expression was markedly inhibited by both AF and HIF-1α siRNA pretreatment. Sequential irradiation did not promote HIF-1α expression under HIF-1α inhibitory conditions. The downstream expression of proteins such as CA9, GLUT-1, and VEGF was increased following the high expression of HIF-1α, either by hypoxia or with $CoCl_2$, and decreased with the low expression of HIF-1α by either siRNA or AF treatment. This confirmed that HIF-1α plays an important role in the irradiation-mediated damage response under hypoxic conditions and in controlling its downstream proteins.

Complex Mechanisms of HIF-1α Protein in Hypoxia Bystander Cells

Two hours after irradiation, the conditioned medium was harvested and transferred to bystander cells; 24 h later, the bystander expression of HIF-1α and downstream proteins was determined (**Figures 8A,B**). Interestingly, the expression of HIF-1α in hypoxic bystander HepG2 and T98G cells was significantly decreased by conditioned-medium treatment in contrast to the increase observed in directly irradiated cells. In bystander HepG2 cells, the conditioned medium also inhibited the expression of downstream signal factors VEGF and CA9, but there was no marked inhibition of GLUT-1. In contrast, to bystander T98G cells, following depressed expression of HIF-1α, VEGF was decreased slightly ($p > 0.05$), whereas CA9 and GLUT-1 were increased significantly ($p < 0.05$). In addition, the expression of bystander HIF-1α in hypoxic HepG2 cells and T98G cells was increased significantly by the conditioned medium from specific target cells which were pretreated with HIF-1α siRNA, but this had no notable impact on CA9, GLUT-1, and VEGF (**Figures 8C,D**). This illustrated that different cell lines have different signaling pathway responses to the conditioned medium under hypoxic conditions. In addition, the expressions of HIF-1α

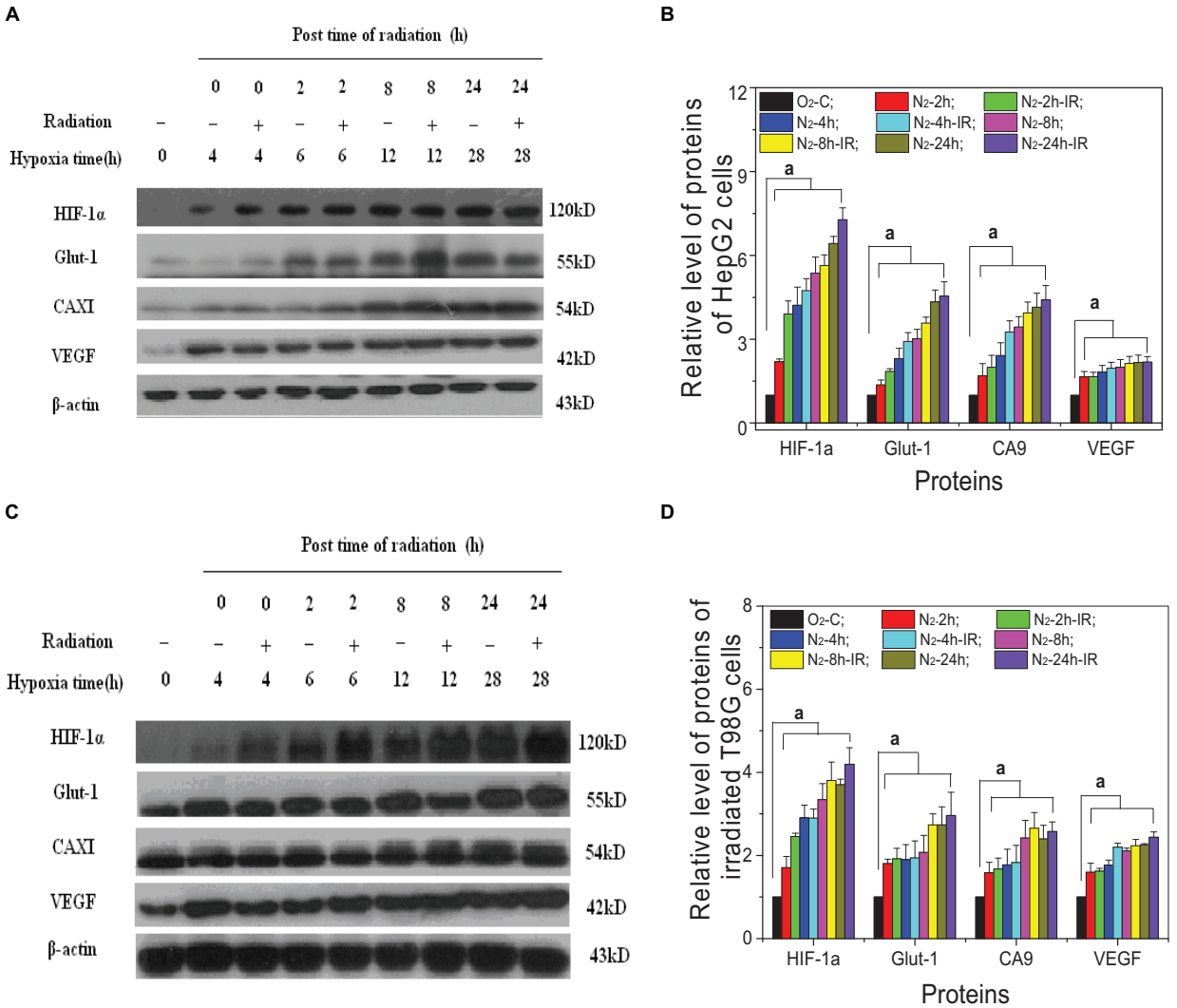

FIGURE 6 | Expression of HIF-1α and its downstream proteins in irradiated hepatoma cells. Proteins were obtained from the two cell lines of HepG2 cells **(A,B)** and T98G cells **(C,D)** at 0, 2, 8, and 24 h post 5 Gy X-ray irradiation. The expression level of HIF-1α and its downstream proteins was compared with the corresponding β-actin and then normalized to that protein from cells under normoxia conditions. a, $p < 0.05$, compared with the normoxic control in the absence of irradiation.

and downstream genes in bystander cells were mainly regulated by those signaling factors from target cells but not by the autologous hypoxic environment. It also highlights that HIF-1α plays a different role for the direct radiation damage effect and the radiation inducible bystander effect and leads to complex signal transmission in the RIBE under hypoxic conditions.

DISCUSSION

Hypoxia is a major barrier for effective tumor therapy as it increases a tumor's resistance to chemotherapy and radiotherapy (Span and Bussink, 2015; Busk et al., 2020). In addition, radiation-induced bystander effects may enhance the curative efficacy of external beam radiotherapy but may also cause fatal genetic damage to non-irradiated normal cells or induce adaptive responses to non-irradiated tumor cells, adversely affecting the overall outcome of radiotherapy (Prise and O'Sullivan, 2009; Xie et al., 2016; Griffin et al., 2020a,b). This study showed that the radiosensitivity of hepatoma cells and glioblastoma cells under normoxic conditions was higher than that under hypoxic conditions (shown in **Figure 1**), i.e., there is a hypoxia-mediated radioresistance effect on tumor cells. Our data also demonstrate that under hypoxic conditions irradiated tumor cells can release active signaling factors into the cell culture medium leading to damage in non-irradiated bystander cells (shown in **Figures 2A,B**). Interestingly, the yields of micronucleus in bystander cells under different oxygen conditions are not significant different so that the ratio of bystander micronucleus to radiation directly induced micronucleus in hypoxic cells is higher than that of normoxic cells (shown in **Figures 2C,D**). This result may have important implications for targeted tumor

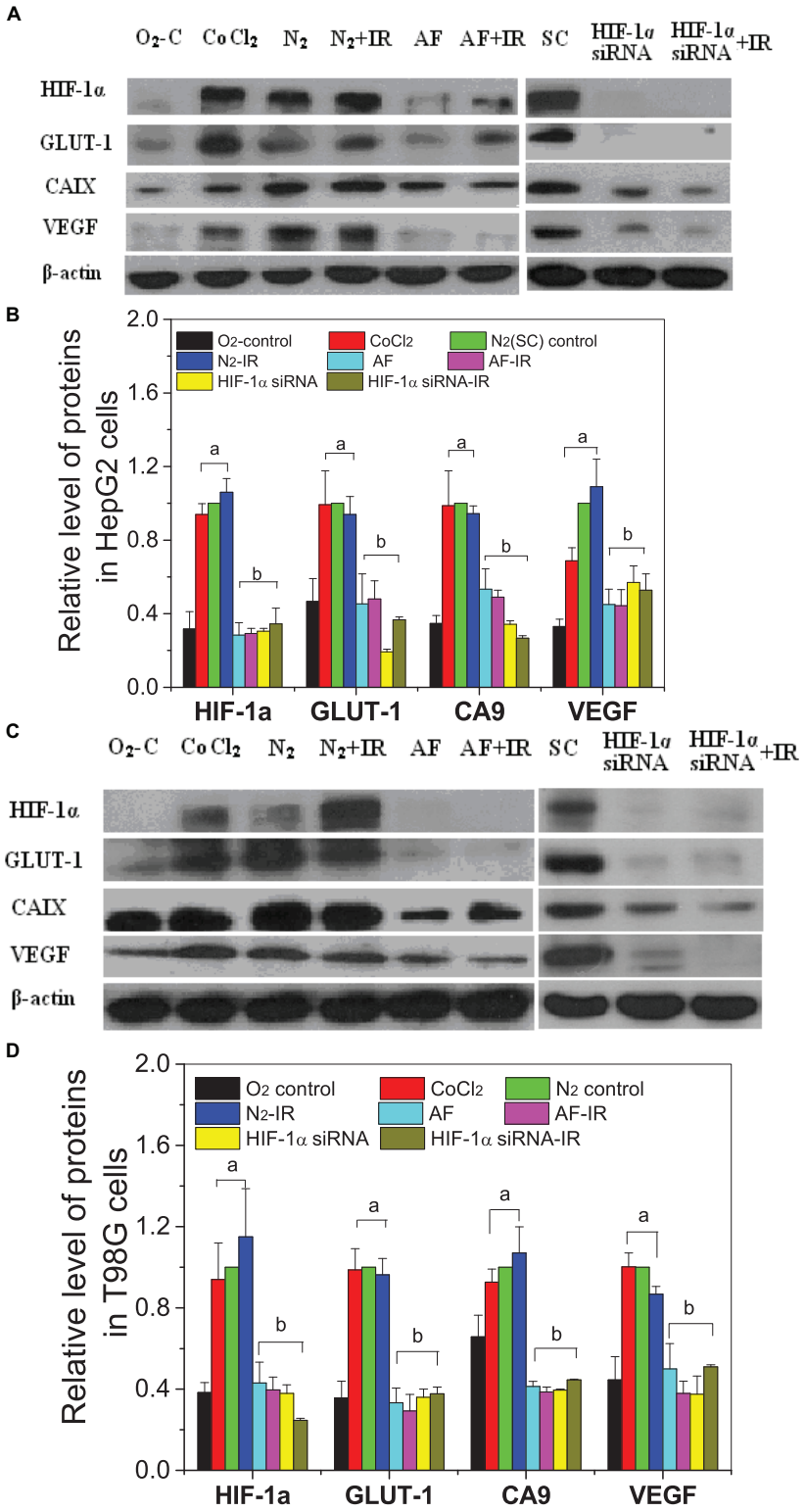

FIGURE 7 | Expressions of HIF-1α and downstream proteins in hypoxic-irradiated cells pretreated with HIF-1α inhibitor treatment. The HepG2 cells **(A,C)** and T98G cells **(B,D)** were pretreated with or without 100 μM $CoCl_2$, 5 μM 7-aminoflavone for 4 h, and HIF-1α siRNA for 24 h before irradiation under normoxic or hypoxic conditions, then nuclear or whole proteins were collected and analyzed at 4 h post 5 Gy X-irradiation. The HIF-1α signal and its downstream proteins were compared with the corresponding β-actin and then normalized to that protein under hypoxia. a, $p < 0.05$ compared with the normoxic control; b, $p < 0.05$ compared with the hypoxic control without irradiation.

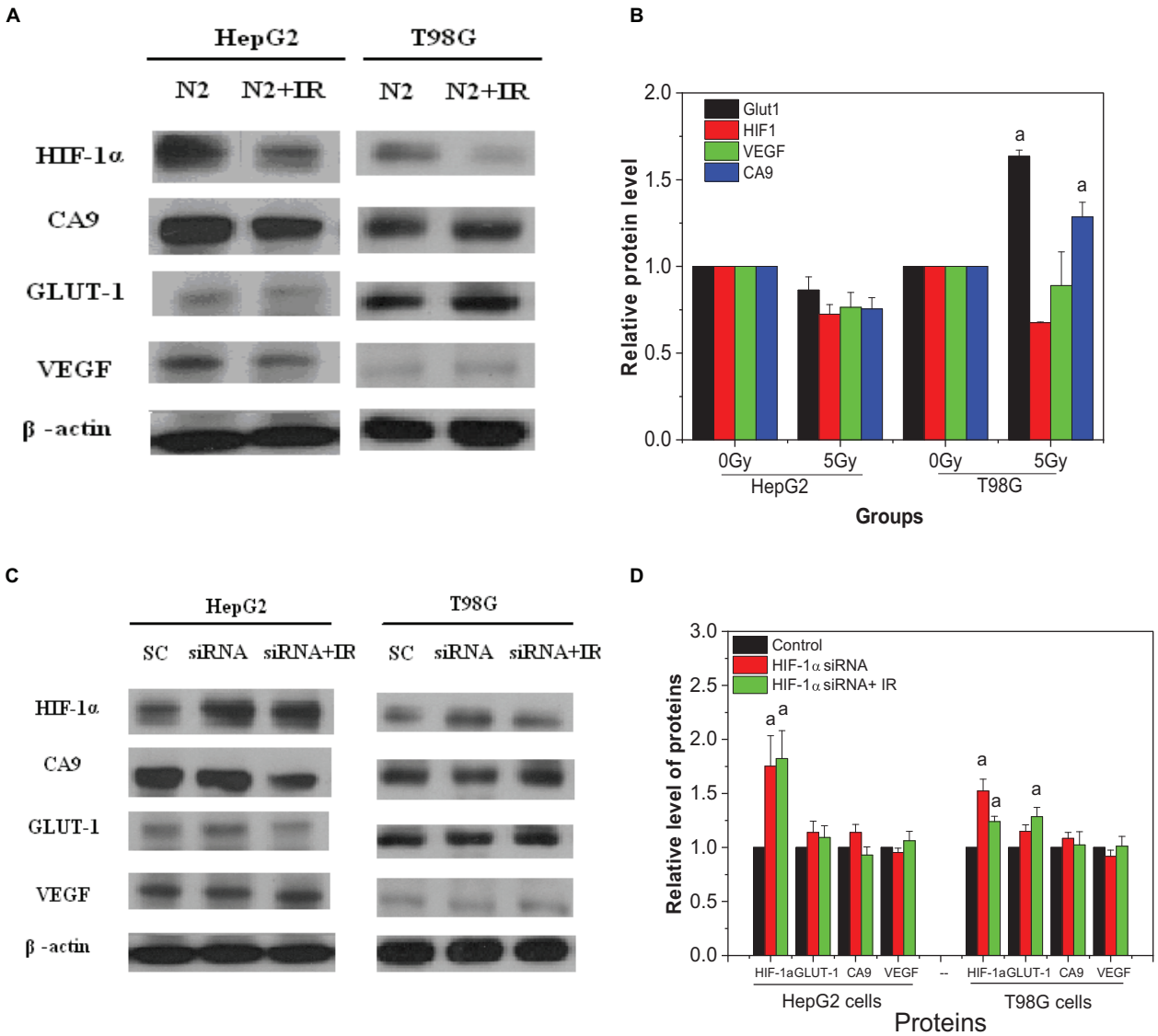

FIGURE 8 | Expression of HIF-1α and related downstream proteins on the bystander cells induced by the conditioned medium under hypoxic conditions. **(A,B)** Hypoxic bystander cells were treated with the conditioned medium from hypoxic-irradiated HepG2 and T98G cells. **(C,D)** Hypoxic bystander cells were exposed to the conditioned medium from irradiated cells with or without inhibitor pretreatment. Each HIF-1α signal and its downstream protein were compared with the corresponding β-actin signal and then normalized to that protein under hypoxia conditions. a, $p < 0.05$ compared with the hypoxic control without irradiation.

radiotherapy. Since the radiosensitivity of hypoxic tumor cells is lower than that of normoxic cells, the cell killing effect of bystander response could play a key role in radiation-induced lethal effect in tumor cells. In our study, two methods, i.e., conditioned medium transfer and cell co-culture, were used for RIBE investigation and it was found that they could lead to the measurement of similar levels of bystander damage (shown in **Figures 2A,B**). During cell co-culture, signaling factors released from irradiated cells can diffuse freely interacting with non-irradiated bystander cells leading to the induction of bystander damage. During a few hours of cell co-culture, bystander damage can accumulate, while some damaged cells may disappear by necrosis. For the medium transfer experiment, the signaling factors released from irradiated cells are concentrated in the conditioned medium and affect the bystander cells at a defined time. Since conditioned-medium and cell-co-culture treatment leads to similar bystander responses, this suggests that the bystander signaling factors are relatively stable in the medium. Recent studies have also investigated the potential impact of modulated beams on the response of hypoxic cells to mimic the steep gradients observed with advanced radiotherapies. By using shielding strategies, bystander signaling between irradiated and non-irradiated areas of a cell culture can be compared (Butterworth et al., 2011). Similarly to what is observed here, although an oxygen dependency of directly irradiated cells was observed, under hypoxia no significant

difference in the out-of-field (bystander) response was observed (Thompson et al., 2017).

It has been known that the generation of ROS and NO is an early event of RIBE on both normal cells and tumor cells under normoxic conditions (Shao et al., 2008c; He et al., 2012; Zhang et al., 2012), which is consistent with present results in **Figure 3** where DMSO and AG partly suppressed the RIBE in HepG2 and T98G cells. Importantly, it is reported here that ROS and NO also contribute to the RIBE in these tumor cells under hypoxic conditions. Others also reported that ROS could be induced in the irradiated hypoxic cells. Lee et al. (2008) found that intracellular ROS was significantly increased in proton-irradiated HCT116 cells under hypoxia conditions and this contributed to radiation-induced apoptosis that could be abolished by treatment with the antioxidant N-acetyl cysteine (NAC). NO can act as an effective hypoxic cell radiosensitizer, by mimicking the effects of oxygen via fixation of radiation-induced DNA damage; however, the required levels cannot be observed *in vivo* because of vasoactive complications (De Ridder et al., 2008a,b). However, ROS and NO free radicals have very short half-lives and cannot be maintained stably in the conditioned medium, and thus they may partly play roles as bystander signaling factors by regulating other downstream cytokines (Meng et al., 2018). For instance, radiation-induced cytochrome C (Cyt-C) has a significant role in regulating bystander effect through an iNOS-triggered NO signal (He et al., 2012), and transforming growth factor β1 (TGF-β1) can be activated by NO stress in a dose- or time-dependent fashion and it can further induce bystander responses including secondary free radicals and chromosome damage (Shao et al., 2008b,c). Our data support the concept that there must be other biological mechanisms mediating a hypoxic radiation-inducible bystander effect, in addition to the free radical effect induced directly by irradiation.

Among various intrinsic and extrinsic factors, HIF-1α is the key mediator of hypoxic signal transduction, controlling the expression of more than 100 genes and exerting a diverse and complex impact on tumor radiotherapy. In response to hypoxia, HIF-1α induces VEGF and PDGF, which leads to angiogenesis and also promotes cell survival by increasing glucose transport, converting cellular metabolism to the glycolytic system (Clara et al., 2014; Bajbouj et al., 2017). HIF-1 can also induce cell-cycle arrest (Clara et al., 2014) and inhibit apoptosis signals (Sun et al., 2015), which could result in decreased radiosensitivity. Our study has shown that HIF-1α can be activated and induced not only by hypoxia but also by irradiation (**Figure 6**) in both HepG2 cells and T98G cells, and its expression increased following time under hypoxic and post-irradiation time. Downstream protein (VEGF, GLUT-1, and CA9) expression also increased following increased HIF-1α expression. Cells were pretreated with HIF-1α siRNA or a chemical inhibitor of HIF-1α (7-aminoflavone, AF) before irradiation, showing a significantly decreased expression of HIF-1α and its downstream proteins (shown in **Figure 7**). Radiosensitivity, measured using a cell survival assay (shown in **Figure 1**), under hypoxic conditions, was increased by suppression of HIF-1α expression. These results confirm that HIF-1α can play an important role in hypoxia-induced radioresistance. HIF-1α becomes activated in response to radiation exposure in hypoxic solid tumors and functions by protecting tumor blood vessels from the cytotoxic effects of radiation via inducing the expressions of VEGF, GLUT-1, or CA9, assuring the delivery of oxygen and nutrients to cells, and eventually accelerating tumor (Horsman et al., 2012; Towner et al., 2013). So, a blockade of activity of HIF-1 enhances the therapeutic effect of radiation.

In addition, based on our results that bystander effects play an important role in radiation-induced lethal effects of tumor cells under hypoxic conditions, greater than that under normoxic conditions, we determined the effect of HIF-1α on RIBE. When hypoxic-irradiated tumor cells were pretreated with an HIF-1α inhibitor, the DNA damage in the non-irradiated bystander cells was attenuated, while cell survival of bystander cells was increased. Interestingly, this was only observed when either irradiated only or irradiated and bystander cells were inhibited. If Hif-1α is inhibited only in hypoxic bystander cells, cell survival does not change and a decreased level of micronucleus yield is observed in comparison to inhibition of irradiated or irradiated plus bystander cells. In contrast to irradiated cells, the expression of HIF-1α in hypoxic bystander cells was decreased following the treatment with the conditioned medium from hypoxic-irradiated cells (shown in **Figures 8A,B**), and no changes in downstream proteins were observed. In the HepG2 cell line, the expression of CA9 and VEGF reduced coinciding with the decrease of HIF-1α, but no change was observed in GLUT-1. However, in T98G cells, there was no change in VEGF, whereas GLUT1 and CA9 were both increased significantly. When irradiated cells were pretreated with an inhibitor of HIF-1α, the expression of bystander HIF-1α was increased, but there was no change in the other three proteins (shown in **Figures 8C,D**). It is thus evident that the mechanism underlying a bystander effect is dependent on cell-type specificity. Overall, combining our results, it could be postulated that the contribution of HIF-1α in irradiated (directly targeted) cells is greater than that of non-irradiated bystander cells to produce a hypoxic-dependent RIBE. Also, HIF-1α plays a direct stimulating role in the hypoxia-induced radioresistance of targeted cells via regulating downstream genes but plays an adverse effect regarding a bystander effect. This result is supported by previous reports that the gene expression profiles of irradiated cells and bystander cells are significantly different and that more than 50% of the genes upregulated in irradiated cells could be downregulated in bystander cells. For example, the NF-κB, $p21^{Waf1}$ (Iwakawa et al., 2008), and CSE/CBS (enzymes which endogenously synthesize H_2S) genes were activated in irradiated cells, but not in bystander cells (Zhang et al., 2011, 2012). Downregulation of HIF-1α in bystander cells could reduce the protective effect of HIF-1α, making bystander cells more susceptible to bystander stress signaling, but not via downstream genes such as VEGF, CA9, and GLUT-1 which were quantified in our experiments.

In summary, hypoxia occurs in the microenvironment of solid tumors as a result of the complex interaction of numerous factors, including blood vessels, interstitial tissues, and tumor cells. A radiation-inducible bystander effect plays a more significant role in the overall damage response in tumor cells exposed under hypoxic conditions. As well as free radicals, such as NO

and ROS, induced by irradiation, HIF-1α and its downstream-regulated proteins were involved. Under hypoxic conditions, irradiated hepatoma carcinoma HepG2 or glioblastoma T98G cells can promote the expression of HIF-1α, which would result in radioresistance, but the conditioned medium from these cells can inhibit HIF-1α expression and induce cell damage in bystander cells. These findings suggest that inhibition of HIF-1α may enhance radiosensitivity and reduce bystander cell damage, and these could help deliver potential benefits to strategies for therapeutic treatment of hypoxic tumors.

DATA AVAILABILITY STATEMENT

The raw data supporting the conclusions of this article will be made available by the authors, without undue reservation.

AUTHOR CONTRIBUTIONS

CS, KP, and JZ contributed to the overall conception and design of the study. GP and KB performed the acquisition and analysis of the data. YZ and FM performed further processing of the images. JZ constructed the first draft of the manuscript. CS and KP revised the manuscript prior to submission. All authors contributed to the article and approved the submitted version.

FUNDING

We acknowledge the support of Cancer Research UK (C1513/A7047), Brainwaves NI, National Key R&D Program of China (No. 2017YFC0108604), and National Natural Science Foundation of China (Nos. 81672985 and 31770910).

REFERENCES

Ahn, G. O., Seita, J., Hong, B. J., Kim, Y. E., Bok, S., Lee, C. J., et al. (2014). Transcriptional activation of hypoxia-inducible factor-1 (HIF-1) in myeloid cells promotes angiogenesis through VEGF and S100A8. *Proc. Natl. Acad. Sci. U.S.A.* 111, 2698–2703. doi: 10.1073/pnas.1320243111

Bajbouj, K., Shafarin, J., Abdalla, M. Y., Ahmad, I. M., and Hamad, M. (2017). Estrogen-induced disruption of intracellular iron metabolism leads to oxidative stress, membrane damage, and cell cycle arrest in MCF-7 cells. *Tumour Biol. J. Int. Soc. Oncodev. Biol. Med.* 39, 1–12.

Behar, A. (2008). [Radiobiology base change: long term effects of ionizing radiation]. *Bull. Mem. Acad. R. Med. Belg.* 163, 133–142;discussion143.

Bewicke-Copley, F., Mulcahy, L. A., Jacobs, L. A., Samuel, P., Akbar, N., Pink, R. C., et al. (2017). Extracellular vesicles released following heat stress induce bystander effect in unstressed populations. *J. Extracell. Vesicles* 6, 1340746. doi: 10.1080/20013078.2017.1340746

Busk, M., Overgaard, J., and Horsman, M. R. (2020). Imaging of tumor hypoxia for radiotherapy: current status and future directions. *Semin. Nucl. Med.* 50, 562–583. doi: 10.1053/j.semnuclmed.2020.05.003

Butterworth, K. T., McGarry, C. K., Trainor, C., O'Sullivan, J. M., Hounsell, A. R., and Prise, K. M. (2011). Out-of-field cell survival following exposure to intensity-modulated radiation fields. *Int. J. Radiat. Oncol. Biol. Phys.* 79, 1516–1522. doi: 10.1016/j.ijrobp.2010.11.034

Chiche, J., Ilc, K., Laferriere, J., Trottier, E., Dayan, F., Mazure, N. M., et al. (2009). Hypoxia-inducible carbonic anhydrase IX and XII promote tumor cell growth by counteracting acidosis through the regulation of the intracellular pH. *Cancer Res.* 69, 358–368. doi: 10.1158/0008-5472.can-08-2470

Clara, C. A., Marie, S. K., de Almeida, J. R., Wakamatsu, A., Oba-Shinjo, S. M., Uno, M., et al. (2014). Angiogenesis and expression of PDGF-C, VEGF, CD105 and HIF-1alpha in human glioblastoma. *Neuropathol. J. Jpn. Soc. Neuropathol.* 34, 343–352.

De Ridder, M., Van Esch, G., Engels, B., Verovski, V., and Storme, G. (2008a). Hypoxic tumor cell radiosensitization: role of the iNOS/NO pathway. *Bull. Cancer* 95, 282–291.

De Ridder, M., Verellen, D., Verovski, V., and Storme, G. (2008b). Hypoxic tumor cell radiosensitization through nitric oxide. *Nitric Oxide* 19, 164–169. doi: 10.1016/j.niox.2008.04.015

Dong, C., He, M., Tu, W., Konishi, T., Liu, W., Xie, Y., et al. (2015). The differential role of human macrophage in triggering secondary bystander effects after either gamma-ray or carbon beam irradiation. *Cancer Lett.* 363, 92–100. doi: 10.1016/j.canlet.2015.04.013

Dungwa, J. V., Hunt, L. P., and Ramani, P. (2011). Overexpression of carbonic anhydrase and HIF-1alpha in Wilms tumours. *BMC Cancer* 11:390. doi: 10.1186/1471-2407-11-390

Fenech, M., and Morley, A. A. (1986). Cytokinesis-block micronucleus method in human lymphocytes: effect of *in vivo* ageing and low dose X-irradiation. *Mutat. Res.* 161, 193–198. doi: 10.1016/0027-5107(86)90010-2

Formenti, S. C., and Demaria, S. (2009). Systemic effects of local radiotherapy. *Lancet. Oncol.* 10, 718–726. doi: 10.1016/s1470-2045(09)70082-8

Frank, D. K., Szymkowiak, B., and Hughes, C. A. (2006). Connexin expression and gap junctional intercellular communication in human squamous cell carcinoma of the head and neck. *Otolaryngol. Head Neck Surg. J. Am. Acad. Otolaryngol. Head Neck Surg.* 135, 736–743. doi: 10.1016/j.otohns.2006.06.1242

Gaziev, A. I., Guliaeva, N. A., Bel'skaia, I. I., Muksinova, K. N., Zakharova, M. L., Fomenko, L. A., et al. (2008). [The use of temporal temperature gradient gel electrophoresis to reveal mutations in peripheral blood mitochondrial DNA]. *Radiat. Biol. Radioecol.* 48, 133–138.

Griffin, R. J., Ahmed, M. M., Amendola, B., Belyakov, O., Bentzen, S. M., Butterworth, K. T., et al. (2020a). Understanding high-dose, ultra-high dose-rate and, spatially fractionated radiotherapy. *Int. J. Radiat. Oncol. Biol. Phys.* 107, 766–778.

Griffin, R. J., Prise, K. M., McMahon, S. J., Zhang, X., Penagaricano, J., and Butterworth, K. T. (2020b). History and current perspectives on the biological effects of high-dose spatial fractionation and high dose-rate approaches: GRID, Microbeam & FLASH radiotherapy. *Br. J. Radiol.* 93, 20200217. doi: 10.1259/bjr.20200217

Gupta, N., Lamborn, K., and Deen, D. F. (1996). A statistical approach for analyzing clonogenic survival data. *Radiat. Res.* 145, 636–640. doi: 10.2307/3579284

He, M., Ye, S., Ren, R., Dong, C., Xie, Y., Yuan, D., et al. (2012). Cytochrome-c mediated a bystander response dependent on inducible nitric oxide synthase in irradiated hepatoma cells. *Br. J. Cancer* 106, 889–895. doi: 10.1038/bjc.2012.9

Heeran, A. B., Berrigan, H. P., and O'Sullivan, J. (2019). The radiation-induced bystander effect (RIBE) and its connections with the hallmarks of cancer. *Radiat. Res.* 192, 668–679. doi: 10.1667/rr15489.1

Horsman, M. R., Mortensen, L. S., Petersen, J. B., Busk, M., and Overgaard, J. (2012). Imaging hypoxia to improve radiotherapy outcome. *Nat. Rev. Clin. Oncol.* 9, 674–687. doi: 10.1038/nrclinonc.2012.171

Iwakawa, M., Hamada, N., Imadome, K., Funayama, T., Sakashita, T., Kobayashi, Y., et al. (2008). Expression profiles are different in carbon ion-irradiated normal human fibroblasts and their bystander cells. *Mutat. Res.* 642, 57–67. doi: 10.1016/j.mrfmmm.2008.04.007

Kamochi, N., Nakashima, M., Aoki, S., Uchihashi, K., Sugihara, H., Toda, S., et al. (2008). Irradiated fibroblast-induced bystander effects on invasive growth of squamous cell carcinoma under cancer-stromal cell interaction. *Cancer Sci.* 99, 2417–2427. doi: 10.1111/j.1349-7006.2008.00978.x

Lee, K. B., Kim, K. R., Huh, T. L., and Lee, Y. M. (2008). Proton induces apoptosis of hypoxic tumor cells by the p53-dependent and p38/JNK MAPK signaling pathways. *Int. J. Oncol.* 33, 1247–1256.

Li, Q., Zhang, J., Wang, W., Liu, J., Zhu, H., Chen, W., et al. (2010). Connexin40 modulates pulmonary permeability through gap junction channel in acute lung injury after thoracic gunshot wounds. *J. Trauma* 68, 802–809. doi: 10.1097/ta.0b013e3181bb80ea

Logsdon, D. P., Grimard, M., Luo, M., Shahda, S., Jiang, Y., Tong, Y., et al. (2016). Regulation of HIF1alpha under Hypoxia by APE1/Ref-1 Impacts CA9 expression: dual targeting in patient-derived 3D pancreatic cancer models. *Mol. Cancer Ther.* 15, 2722–2732. doi: 10.1158/1535-7163.mct-16-0253

Lorimore, S. A., Chrystal, J. A., Robinson, J. I., Coates, P. J., and Wright, E. G. (2008). Chromosomal instability in unirradiated hemaopoietic cells induced by macrophages exposed *in vivo* to ionizing radiation. *Cancer Res.* 68, 8122–8126. doi: 10.1158/0008-5472.can-08-0698

Mayer, A., Schneider, F., Vaupel, P., Sommer, C., and Schmidberger, H. (2012). Differential expression of HIF-1 in glioblastoma multiforme and anaplastic astrocytoma. *Int. J. Oncol.* 41, 1260–1270. doi: 10.3892/ijo.2012.1555

Meng, L., Cheng, Y., Tong, X., Gan, S., Ding, Y., Zhang, Y., et al. (2018). Tumor oxygenation and hypoxia inducible factor-1 functional inhibition via a reactive oxygen species responsive nanoplatform for enhancing radiation therapy and Abscopal effects. *ACS Nano* 12, 8308–8322. doi: 10.1021/acsnano.8b03590

Moeller, B. J., Richardson, R. A., and Dewhirst, M. W. (2007). Hypoxia and radiotherapy: opportunities for improved outcomes in cancer treatment. *Cancer Metastasis Rev.* 26, 241–248. doi: 10.1007/s10555-007-9056-0

Nikitaki, Z., Mavragani, I. V., Laskaratou, D. A., Gika, V., Moskvin, V. P., Theofilatos, K., et al. (2016). Systemic mechanisms and effects of ionizing radiation: a new 'old' paradigm of how the bystanders and distant can become the players. *Semin. Cancer Biol.* 37-38, 77–95. doi: 10.1016/j.semcancer.2016.02.002

Noman, M. Z., Hasmim, M., Lequeux, A., Xiao, M., Duhem, C., Chouaib, S., et al. (2019). Improving cancer immunotherapy by targeting the hypoxic tumor microenvironment: new opportunities and challenges. *Cells* 8, 1083. doi: 10.3390/cells8091083

Palayoor, S. T., John-Aryankalayil, M., Makinde, A. Y., Falduto, M. T., Magnuson, S. R., and Coleman, C. N. (2014). Differential expression of stress and immune response pathway transcripts and miRNAs in normal human endothelial cells subjected to fractionated or single-dose radiation. *Mol. Cancer Res. MCR* 12, 1002–1015. doi: 10.1158/1541-7786.mcr-13-0623

Peitzsch, C., Tyutyunnykova, A., Pantel, K., and Dubrovska, A. (2017). Cancer stem cells: the root of tumor recurrence and metastases. *Semin. Cancer Biol.* 44, 10–24. doi: 10.1016/j.semcancer.2017.02.011

Prise, K. M., and O'Sullivan, J. M. (2009). Radiation-induced bystander signalling in cancer therapy. *Nat. Rev. Cancer* 9, 351–360. doi: 10.1038/nrc2603

Semenza, G. L. (2009). Regulation of cancer cell metabolism by hypoxia-inducible factor 1. *Semin. Cancer Biol.* 19, 12–16. doi: 10.1016/j.semcancer.2008.11.009

Shao, C., Folkard, M., Held, K. D., and Prise, K. M. (2008a). Estrogen enhanced cell-cell signalling in breast cancer cells exposed to targeted irradiation. *BMC Cancer* 8:184. doi: 10.1186/1471-2407-8-184

Shao, C., Folkard, M., Michael, B. D., and Prise, K. M. (2005). Bystander signaling between glioma cells and fibroblasts targeted with counted particles. *Int. J. Cancer* 116, 45–51. doi: 10.1002/ijc.21003

Shao, C., Folkard, M., and Prise, K. M. (2008b). Role of TGF-beta1 and nitric oxide in the bystander response of irradiated glioma cells. *Oncogene* 27, 434–440. doi: 10.1038/sj.onc.1210653

Shao, C., Furusawa, Y., Aoki, M., and Ando, K. (2003). Role of gap junctional intercellular communication in radiation-induced bystander effects in human fibroblasts. *Radiat. Res.* 160, 318–323. doi: 10.1667/rr3044

Shao, C., Lyng, F. M., Folkard, M., and Prise, K. M. (2006). Calcium fluxes modulate the radiation-induced bystander responses in targeted glioma and fibroblast cells. *Radiat. Res.* 166, 479–487. doi: 10.1667/rr3600.1

Shao, C., Prise, K. M., and Folkard, M. (2008c). Signaling factors for irradiated glioma cells induced bystander responses in fibroblasts. *Mutat. Res.* 638, 139–145. doi: 10.1016/j.mrfmmm.2007.09.007

Shikazono, N., Noguchi, M., Fujii, K., Urushibara, A., and Yokoya, A. (2009). The yield, processing, and biological consequences of clustered DNA damage induced by ionizing radiation. *J. Radiat. Res.* 50, 27–36. doi: 10.1269/jrr.08086

Span, P. N., and Bussink, J. (2015). Biology of hypoxia. *Semin. Nucl. Med.* 45, 101–109.

Sun, Y., Xing, X., Liu, Q., Wang, Z., Xin, Y., Zhang, P., et al. (2015). Hypoxia-induced autophagy reduces radiosensitivity by the HIF-1alpha/miR-210/Bcl-2 pathway in colon cancer cells. *Int. J. Oncol.* 46, 750–756. doi: 10.3892/ijo.2014.2745

Thompson, H. F., Butterworth, K. T., McMahon, S. J., Ghita, M., Hounsell, A. R., and Prise, K. M. (2017). The impact of hypoxia on out-of-field cell survival after exposure to modulated radiation fields. *Radiat. Res.* 188, 636–644.

Towner, R. A., Gillespie, D. L., Schwager, A., Saunders, D. G., Smith, N., Njoku, C. E., et al. (2013). Regression of glioma tumor growth in F98 and U87 rat glioma models by the Nitrone OKN-007. *Neuro Oncol.* 15, 330–340. doi: 10.1093/neuonc/nos337

Xie, Y., Tu, W., Zhang, J., He, M., Ye, S., Dong, C., et al. (2015). SirT1 knockdown potentiates radiation-induced bystander effect through promoting c-Myc activity and thus facilitating ROS accumulation. *Mutat. Res.* 772, 23–29. doi: 10.1016/j.mrfmmm.2014.12.010

Xie, Y., Ye, S., Zhang, J., He, M., Dong, C., Tu, W., et al. (2016). Protective effect of mild endoplasmic reticulum stress on radiation-induced bystander effects in hepatocyte cells. *Sci. Rep.* 6, 38832.

Yasui, H., Yamamoto, K., Suzuki, M., Sakai, Y., Bo, T., Nagane, M., et al. (2017). Lipophilic triphenylphosphonium derivatives enhance radiation-induced cell killing via inhibition of mitochondrial energy metabolism in tumor cells. *Cancer Lett.* 390, 160–167. doi: 10.1016/j.canlet.2017.01.006

Zhang, J., Xie, Y., Xu, Y., Pan, Y., and Shao, C. (2011). Hydrogen sulfide contributes to hypoxia-induced radioresistance on hepatoma cells. *J. Radiat. Res.* 52, 622–628. doi: 10.1269/jrr.11004

Zhang, J., Xie, Y., Xu, Y., and Shao, C. (2012). Suppression of endogenous hydrogen sulfide contributes to the radiation-induced bystander effects on hypoxic HepG2 cells. *Radiat. Res.* 178, 395–402. doi: 10.1667/rr2967.1

Zhu, L., Han, W., Chen, S., Zhao, Y., Jiang, E., Bao, L., et al. (2008). Radiation-induced bystander effects enhanced by elevated sodium chloride through sensitizing cells to bystander factors. *Mutat. Res.* 644, 43–47. doi: 10.1016/j.mrfmmm.2008.06.011

Conflict of Interest: The authors declare that the research was conducted in the absence of any commercial or financial relationships that could be construed as a potential conflict of interest.

frontiers in Cell and Developmental Biology

ORIGINAL RESEARCH
published: 09 April 2021
doi: 10.3389/fcell.2021.595108

miR-151 Affects Low-Temperature Tolerance of *Penaeus vannamei* by Modulating Autophagy Under Low-Temperature Stress

*QingJian Liang†, WenNa Dong†, MuFei Ou, ZhongHua Li, Can Liu, FeiFei Wang, Yuan Liu and WeiNa Wang**

Guangzhou Key Laboratory of Subtropical Biodiversity and Biomonitoring, Guangdong Provincial Key Laboratory for Healthy and Safe Aquaculture, Key Laboratory of Ecology and Environmental Science in Guangdong Higher Education, College of Life Sciences, South China Normal University, Guangzhou, China

MicroRNAs (miRNAs) play key roles in many physiologic and pathologic processes, including autophagy. Autophagy is cellular in an emergency response mechanism of environment stress, but their complex molecular regulatory mechanism under low-temperature stress is largely unknown in shrimp, especially miRNA-mediated regulation of autophagy in low-temperature tolerance. In this article, a shrimp *PvTOR* and miRNA pva-miR-151 cooperation in response to low-temperature stress has been reported. Pva-miR-151 showed expression patterns opposite to target *PvTOR* under low-temperature stress. The pva-miR-151 targets the 3′-UTR region of *PvTOR*, regulate the formation of autophagosome, which contribute to the degradation and recycling of damaged organelles. In addition, the low-temperature tolerance was correlated positively with autophagy in shrimp. Silenced pva-miR-151 increased sensitivity to low-temperature stress, whereas overexpression pva-miR-151 decreased the expression of PvTOR and p-TOR and increased tolerance to low-temperature stress by improving the formation of autophagosome and total hemocyte count. In addition, the TOR activator 3BDO can partially rescue autophagy induced by overexpression of pva-miR-151; these results indicate that miR-151 was necessary for the low-temperature tolerance in shrimp. Taken together, we provide a novel strategy and mechanism for shrimp breeding to improve shrimp low-temperature tolerance.

Keywords: autophagy, low temperature, *P. vannamei*, miR-151, target of rapamycin

OPEN ACCESS

Edited by:
Shengmin Xu,
Anhui University, China

Reviewed by:
Deniz Gulfem Ozturk,
Koç University, Turkey
Ye Zhao,
Anhui Medical University, China

****Correspondence:***
WeiNa Wang
wangwn@scnu.edu.cn

† These authors have contributed equally to this work

Specialty section:
This article was submitted to Cell Death and Survival, a section of the journal Frontiers in Cell and Developmental Biology

Received: *15 August 2020*
Accepted: *11 March 2021*
Published: *09 April 2021*

Citation:
Liang Q, Dong W, Ou M, Li Z, Liu C, Wang F, Liu Y and Wang W (2021) miR-151 Affects Low-Temperature Tolerance of Penaeus vannamei by Modulating Autophagy Under Low-Temperature Stress. Front. Cell Dev. Biol. 9:595108. doi: 10.3389/fcell.2021.595108

INTRODUCTION

Crustaceans have developed a complete protection system during the long-term evolution that responds to external factors by adjusting their vital functions to current needs (Lago-Lestón et al., 2007). There are external factors such as water temperature, salinity, dissolved oxygen, pH, nutrition, and stress (Wang et al., 2009; Qiu et al., 2011; Liang et al., 2019b). Low temperature is one of the main stress factors for aquaculture. *Penaeus vannamei* is one of the most important cultured shrimp in the world and has been adversely affected by low temperatures. Frequent periods of low temperatures have led to large-scale economic losses for several decades (Zhou et al., 2011;

Li et al., 2013). Recent studies have shown that low-temperature stress directly affects the survival, growth, and metabolism and also induces the generation of reactive oxygen species (ROS), hemocyte apoptosis, and autophagy, reduces the immune functions, and causes DNA damage in shrimp (Cheng et al., 2005; Qiu et al., 2011; Li et al., 2013). Thus, studies on cold-adaptation mechanisms to enhance its cold tolerance will be great value to the aquaculture industry of *P. vannamei*.

Many stresses could trigger autophagy, and autophagy becomes a strategy to adapt and copes with stress (Marino et al., 2014). It is an essential process for eukaryotes, which via the lysosome degrade cytoplasm and organelles to recycle misfolded proteins or damaged organelles to resynthesize macromolecules and/or ATP generation (Wang and Klionsky, 2003; Tettamanti et al., 2008). Therefore, autophagy is a self-survival mechanism under external stress, hypoxia, and endoplasmic reticulum stress. Previous studies have shown that hypothermia can cause an increase in the number of liver lysosomes and autophagosomes, endoplasmic reticulum disorder, and swelling of mitochondria (Salas et al., 1977). Fish oil alleviated liver injury induced by intestinal ischemia/reperfusion via AMPK/SIRT-1 autophagy pathway (Jing et al., 2018). In addition, autophagy plays a vital role in the innate immunity of *P. vannamei* (Wu et al., 2019). The mechanistic target of rapamycin (mTOR), an atypical serine/threonine protein kinase that belongs to the phosphatidylinositol-3-kinase (PI3K)–related kinase (PIKK) family, is a key molecule in the process of autophagy induction (Hu et al., 2015). There is increasing evidence that mTOR signaling pathway is inactivated in response to diverse environmental (Laplante and Sabatini, 2012; Sun et al., 2015). Subsequently, the inactivated TOR causes the activation of ULK1 to initiate phagophore formation, and the beclin1–Vps34 complex extends the nascent autophagosome to form a mature double-membrane autophagosome. Finally, autophagosomes fuse with lysosomes to degrade cytoplasmic content, thereby recovering energy for cells (Mukhopadhyay et al., 2020). In addition, researchers found that mTOR in the balance between growth and autophagy is crucial when organisms respond to environmental stress (Liu et al., 2018b). However, the underlying regulatory mechanism of TOR/autophagy pathway in low-temperature stress that induced hepatopancreas injury remains incompletely understood.

MicroRNAs (miRNAs) are a family of small non-coding RNA about 20–24 nt and inhibit the expression of their target mRNA at posttranscriptional level by directly binding to 3′-UTRs (Carthew and Sontheimer, 2009). MiRNA has been reported to participate in the various biological and metabolic processes in cells, such as development, metabolism, apoptosis, autophagy, and signal transduction, which are associated with abiotic and/or biotic stress responses (Plasterk, 2006; Zeng et al., 2015). Recent studies suggest that 63 miRNAs of shrimp responding to WSSV infection have been identified (Huang and Zhang, 2012). Twenty-four miRNAs of shrimp were closely related to phagocytosis, apoptosis, and the pro-phenoloxidase system (Yang et al., 2012). Studies have found that increased susceptibility to arrhythmias in response to acute myocardial estrogen deprivation is dependent on the up-regulation of miR-151 in the rat (Zhang et al., 2013), and miR-151-3p is closely related to improved survival in resected cholangiocarcinoma (McNally et al., 2013), suggesting that miR-151 is a vital factor. In addition, STAT is a typical transduction factor involved in the regulation of autophagy. MiR-151 could target 3′-untranslated region (3′-UTR) of STAT3 gene, which suggests a possible connection between miR-151 and autophagy regulation (Liu et al., 2018a). However, little is known about the molecular mechanism of miR-151 and autophagy.

In our study, RNA-seq was used to screen the miRNAs involved in autophagy to respond to low-temperature stress. The present study showed that in shrimp miRNAs, which were conserved in animals, the level of miR-151 increased significantly in low-temperature stress. Application of abnormal expression, transmission electron microscope (TEM), cumulative mortality, etc., connect shrimp autophagy with the low-temperature challenge. Finally, using a luciferase reporter assay identified miR-151 directly targeted mTOR to regulate autophagy. This study provided a novel insight that miRNA could activate autophagy to alleviate hepatopancreas injury induced by acute low-temperature stress in *P. vannamei*.

MATERIALS AND METHODS

Shrimp Culture and Low-Temperature Stress

Healthy *P. vannamei* were cultured in 200 L (approximately 3‰ salinity) aquariums at 23°C–25°C, pH 7.4, continuous aeration, which with length range 6.1 ± 0.6 cm and weight 5.2 ± 0.9 g, were obtained from a shrimp farm in Panyu, Guangdong Province, China. All animal procedures were licensed under the Institutional Animal Care and Use Committee of the Institute of Zoology, Chinese Academy of Sciences.

From healthy shrimp that had been acclimated to 25°C ± 0.5°C for 2 weeks, 30 shrimp were randomly assigned in different groups and were directly transferred to 12°C ± 0.5°C for acute low-temperature stress, 25°C ± 0.5°C as the control group. At different times after low-temperature stress (0, 1.5, 3, 6, 12, and 24 h), there were randomly collected three shrimp tissue samples for each group. Different tissue samples were immediately frozen in liquid nitrogen and stored at -80°C.

Quantitative Real-Time Polymerase Chain Reaction (RT-qPCR)

Total RNA was extracted using Trizol (Invitrogen) according to the manufacturer's recommendations and previous description (Liang et al., 2019c). The concentration and quality of the RNA were determined by the 260/280-nm spectrophotometer (NanoDrop Technologies, Montchanin, DE) and 1.5% agarose gel electrophoresis. First-strand cDNA was synthesized from total RNA (1 μg in each reaction) using a PrimeScript RT reagent kit with gDNA Eraser (Takara, Dalian, China) according to the manufacturer's protocol. Quantitative polymerase chain reaction (qPCR) used an ABI 7500 thermal cycler (Applied Biosystems, Foster City, CA) using SYBR Premix Ex Taq (Takara) in a 20-μL reaction volume with three biological and three technical replicates. Shrimp small nuclear RNA (U6), eukaryotic elongation factor 1α, and β-actin were used as endogenous

controls. All gene-specific primers used in this study were designed using Primer Premier 5.0 (**Supplementary Table 1**).

miRNA Library Analysis

The RNA was enriched in a size range of 18–30 nt by polyacrylamide gel electrophoresis (PAGE). Then, the 3′ adapters were added, and 5′ adapter RNAs were sequenced using Illumina HiSeq^{TM} 2500 by Gene *De novo* Biotechnology Co. (Guangzhou, China). The data from the miRNA-seq are available on NCBI (NO. PRJNA560613). Clear data normalization was performed with the weighted regression method. False discovery rate (FDR) $\leq$ 0.001 and $|\log_2 FC| \geq 2.5$ miRNA were chosen for further analyses. The heat map of differentially expressed miRNAs expression profile was drawn with ggplots heatmap 0.2. The RNAhybrid v2.1.2[1], TargetScan 7.0[2], and miRanda 3.3[3] were used to predict targets of miRNAs with default parameters. Enrichment analysis of the predicted target genes was conducted with Gene Ontology (GO)[4] and Kyoto Encyclopedia of Genes and Genomes (KEGG) pathway[5].

Gene Cloning and Sequence Analyses

The primary transcript of pva-miR-151 (pri–pva-miR-151) and 3′-UTR were isolated from the shrimp cDNA library by PCR using PrimeSTAR® Max DNA polymerase (Takara). The PCR product was verified by Sanger sequencing. The mfold Web server[6] was used to detect hairpin structures with pre-miRNA sequence. By using the ClustalW2 program, multiple sequence alignment can be performed. On the basis of the sequence alignment and using the neighbor-joining algorithm as implemented in the MEGA 5.1 software package, a phylogenetic tree was constructed, with 1,000 bootstrap replications.

Silencing or Overexpression of miR-151 in Shrimp

To silence miR-151, the antago-151 (5′- CCUCAAAGAGCUU CAGUCCAGU-3′) and antago normal control (NC) (5′- CAGUACUUUGUGU AGUACAA-3′) were synthesized (GenePharm, Shanghai, China) with a 5′ and 3′ phosphorothioate backbone, a 3′ end cholesterol modified, and a 2′-O-methyl modification at all nucleotides. The antago-151 (2 nM/g) and a control antago NC were injected intramuscularly into healthy shrimp. After low-temperature stress, the tissue of three randomly selected shrimp was collected at different time points.

For overexpression of miR-151, ago-151 (5′- ACUGGACU GAAGCUCUUUGAGG-3′) and ago NC (5′- UUCUCCGA ACGUGUCACGUTT-3′) were synthesized *in vitro*. The formation of double-stranded RNAs was modified with a 5′ and 3′ phosphorothioate backbone, a 3′ end cholesterol modified, and a 2′-O-methyl modification at the anticoding strand nucleotide. The ago-151 (2 nM/g) and a control ago NC were injected intramuscularly into healthy shrimp. After low-temperature stress, the tissue of three randomly selected shrimp was collected at different time points. All the assays were biologically repeated three times.

Total Hemocyte Count

Hemolymph samples were analyzed by using a hemocytometer. A drop of diluted hemolymph sample with anticoagulant (4.2 g · L^{-1} sodium chloride, 8 g · L^{-1} sodium citrate, 20.5 g · L^{-1} glucose, pH 7.5) was placed in a hemocytometer and observed under a light microscope (Olympus CX31RBSF, Beijing, China) to measure total hemocyte count (THC). Each sample was quantified nine consecutive times. THC was calculated as cells per milliliter.

Primary Hemocyte Culture

Primary hemocyte culture was made following a published protocol with minor modification (George et al., 2011; Thansa et al., 2016). Hemolymph was withdrawn into a syringe half-filled with Alsever solution as anticoagulant and then centrifuged at 2,500 rpm for 5 min at 4◦C. The cell pellet was roughly washed with 10% sodium acetate twice before being washed once with culture medium [2 × Leibovitz's L-15, 100 units/mL penicillin, 100 mg/mL streptomycin, 10% each of fetal bovine serum (FBS), and shrimp meat extract]. In order to prepare shrimp muscle extract, 10 g muscle tissue was dissected from surface sterilized live shrimp and homogenized in 100 mL with phosphate-buffered saline (PBS), and centrifuged at 4,500 × *g* for 5 min to remove cell debris. The supernatant was again centrifuged at 4,500 × *g* for 10 min to remove the coagulated proteins, sterilized by sequentially passing through filters (0.45 followed by 0.22 μm), and kept at 4°C until being mixed with the cell culture medium. Then, a culture medium was used to resuspend the pellet, and cells were seeded at the density of 5 × 10^6 cells/well in a 24-well plate. Trypan blue staining was used to determine the cell viability of primary hemolymph. If the positive result of trypan blue staining of primary hemolymph was less than 5%, cells isolated from that shrimp would be further used in the experiments.

Dual-Luciferase Reporter Assay

The 3′-UTR fragments were cloned into psiCHECK^{TM}-2 vector (Promega, United States) as a Renilla luciferase reporter vector, which contains the predicted pva-miR-151 target sites of *PvTOR*, using the *Xho*I and *Not*I site with primers in **Supplementary Table 1**. To further identify the binding site of pva-miR-151, a mutated site was also constructed into psiCHECK^{TM}-2 vector by ClonExpress® Ultra One Step Cloning Kit (Vazyme, Nanjing, China). The overexpression of pva-miR-151 or pva-pre-miR-151 used pcDNA^{TM} 6.2-GW/miR vector (Invitrogen, Carlsbad, CA, United States) in hemocyte. Using FuGENE® HD Transfection Reagent (Invitrogen) according to the manufacturer's instructions, cotransfection was done with luciferase reporter vector and pcDNA-miR-151, or pcDNA-pre-miR-151, respectively. After transfection at 48 h, activities of the luciferases were measured using the Clarity^{TM} Western ECL substrate (Bio-Rad, United States) with EnSpire^{TM} multiscan

[1]https://omictools.com/rnahybrid-tool
[2]http://www.targetscan.org/
[3]http://www.microrna.org/
[4]http://www.geneontology.org/
[5]http://www.genome.jp/kegg/
[6]http://unafold.rna.albany.edu/?q=mfold

spectrum (PerkinElmer, Germany). Data were represented as the ratio of Renilla to firefly luciferase activity with three independent replicates after normalization.

Flow Cytometer Detected Hemolymph Autophagy Flux

Hemocyte autophagy fluxes were quantified using the commercial Cyto ID® autophagy detection kit (ENZO Life Sciences, ENZ-KIT175-0200) following the manufacturer's protocol. Briefly, the primary hemocytes (1×10^6 cells) were incubated for 24 h with dimethyl sulfoxide (DMSO), 2 μM rapamycin (Rap), 50 μM 3BDO, 8 μM chloroquine (CLQ), and 0.4 μg empty vector or pcDNA-miR-151 according to specific experiments. The cells were washed with PBS, and then suspended cells were resuspended using 1 mL buffer containing 5% FBS and Cyto ID® Green Detection Reagent. Incubation was performed for 30 min under room temperature (25○C). Cells were washed with DPBS once, and cells were resuspended in PBS containing 2% FBS. Cyto ID® fluorescence was detected using BD FACSAria III flow cytometer (BD Biosciences); data of cell counts were plotted as fluorescein isothiocyanate (FL1) fluorescence intensity. The experiment was performed in triplicate.

Histological Analysis by Hematoxylin–Eosin Stain

For all experiments, at least three samples were stained per treatment sampled. Hepatopancreas was fixed with the 4% paraformaldehyde fixative for 24 h and subsequently replaced by ethanol for at least 24 h using the methods described (Ng et al., 2018). The hepatopancreas was then sectioned and stained with hematoxylin–eosin stain (H&E) following standard histological methods. Hepatopancreas structures were observed using light microscopy (DM6, Germany).

Western Blotting

Hepatopancreas was lysed in lysis RIPA buffer (Beyotime, China) for 30 min on ice. After incubation, lysates were centrifuged (14,000 × *g*, 15 min) at 4°C, and each supernatant was collected. Total protein was quantified using the traditional BCA method. Fifty micrograms of protein was separated by 15% sodium dodecyl sulfate–PAGE and electrotransferred onto polyvinylidene difluoride membrane (Bio-Rad). The membranes were incubated in 20 mM tris-buffered saline (TBS) containing 5% BSA for 1 h at room temperature. The membranes were washed with tris-buffered saline and tween 20 (TBST) for 5 min and incubated with the anti-LC3I/II (1:500, Abcam), beclin1 (1:1,000, CST), TOR (1:500, CST), p-TOR (1:500, CST), and actin (1:1,000, CST) at 4°C overnight in a shaking incubator and then washed with (3 × 5 min per wash), and the protein was detected using alkaline phosphatase (1:2,000) as the secondary antibody was incubated for 2 h at room temperature. The membrane was detected with 5-bromo-4-chloro-3-indolyl-phosphate/nitroblue tetrazolium substrate (Sangon Biotech, Shanghai, China). To quantify the signals, gray intensities of Western blots were calculated using ImageJ[7].

[7]https://imagej.nih.gov/ij/

Transmission Electron Microscopy

Transmission electron microscopy (TEM) was used to observe the cell ultrastructure. Changes regarding mitochondrial state and nuclear condensation indicated cellular damage, and the formation of autophagosome indicated autophagy. Tissues were first fixed with 2.5% glutaraldehyde and subsequently fixed with 1% osmium tetroxide. Cells were embedded in Epon after dehydration with different concentrations of alcohol. Ultrathin sections (0.5 μm) were generated for observation under a transmission electron microscope (JEOL, United States) at 100 kV.

Statistical Analyses

All data analyses were used SPSS (version 20.0 for Windows). The data were expressed in the form of mean ± SD. Different groups of data were analyzed by using *t* test. We set the threshold for statistical significance at $p < 0.05$.

RESULTS

miRNAs Involved in Low-Temperature Response of Shrimp Hepatopancreas

To evaluate the miRNAs associated with the low-temperature response, the expression profile analysis was performed on miRNA or mRNA extracted from the hepatopancreas of adult shrimp, which were subjected to low-temperature stress for 3 h. Hundreds of shrimp miRNAs were identified by the hepatopancreas expression profiles. MiRNAs with a threshold of the FDR ≤ 0.001 and an absolute value of $|\log_2 FC| \geq 2.5$ were chosen for further analyses. The results indicated a dynamic regulation of 36 miRNAs ($P < 0.05$) during the period in which there was low-temperature stress at 3 h (**Figure 1A** and **Supplementary Table 2**). To further understand the function of miRNA through the predicted target genes (**Supplementary Table 3**), GO and KEGG pathway enrichment analysis was performed. In terms of biological process class, it was found that the response to a stimulus may be associated with the antistress capability. In the field of molecular function, approximately half of the genes were involved in catalytic activity, and antioxidant activity was found (i.e., oxidoreductase, peroxidase) (**Figure 1B**). In terms of pathway classification, both endocytosis and an mTOR signaling pathway were significantly enriched (**Figure 1C** and **Supplementary Table 4**). Finally, the comprehensive analysis found that the most significant of miRNA in combination with the mTOR 3′-UTR was miR-151. Thus, miR-151 was selected, which may be involved in TOR signal pathway in response to stress for further analyses.

Characteristics of miR-151

The primary transcript of pri–pva-miR-151 was cloned from the hepatopancreas of *P. vannamei*. The pri–pva-miR-151 was composed of 311-nt, which contained a 63-nt precursor sequence (pre–pva-miR-151) and 22-nt mature sequence (pva-miR-151) (**Supplementary Table 5**). In addition, the secondary structure

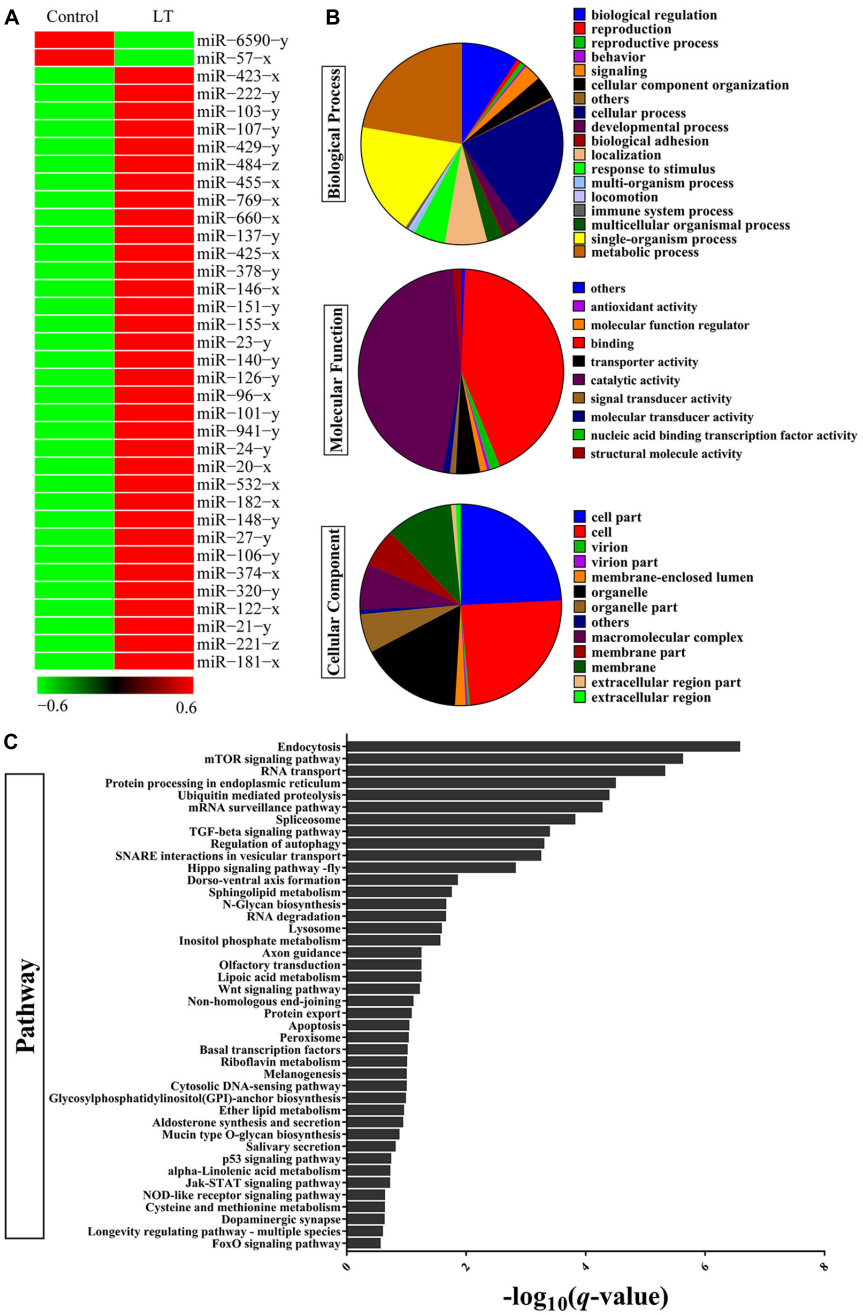

FIGURE 1 | Identification of differentially expressed miRNAs and target gene in shrimp response to low-temperature stress. **(A)** Heat map analysis of significant DE miRNAs after low-temperature stress. Low-temperature stress 3 h later, the miRNAs of shrimp hepatopancreas were subjected to miRNA library analysis. **(B)** GO and **(C)** KEGG pathway analysis of significant DE miRNAs target gene after low-temperature stress.

analysis performed by the mfold Web server predicted a well-developed hairpin structure in the pre–pva-miR-151 sequence (**Figure 2A** and **Supplementary Figure 1**). Mature miR-151 and miR-151 precursor were found to be conserved across multiple species (**Figure 2B**). However, the bases located at positions 4 and 14 of the mature miR-151 sequence are "G" and "U" in mammals. The pre-miR-151 sequences were used to construct a phylogenetic tree, which revealed that miR-151 was divided into two distinct branches invertebrate and vertebrata (**Figure 2C**).

Expression Analysis of *PvTOR* and pva-miR-151

To further analyze the expression patterns of *PvTOR* and pva-miR-151 in shrimp, the following experiments were carried out

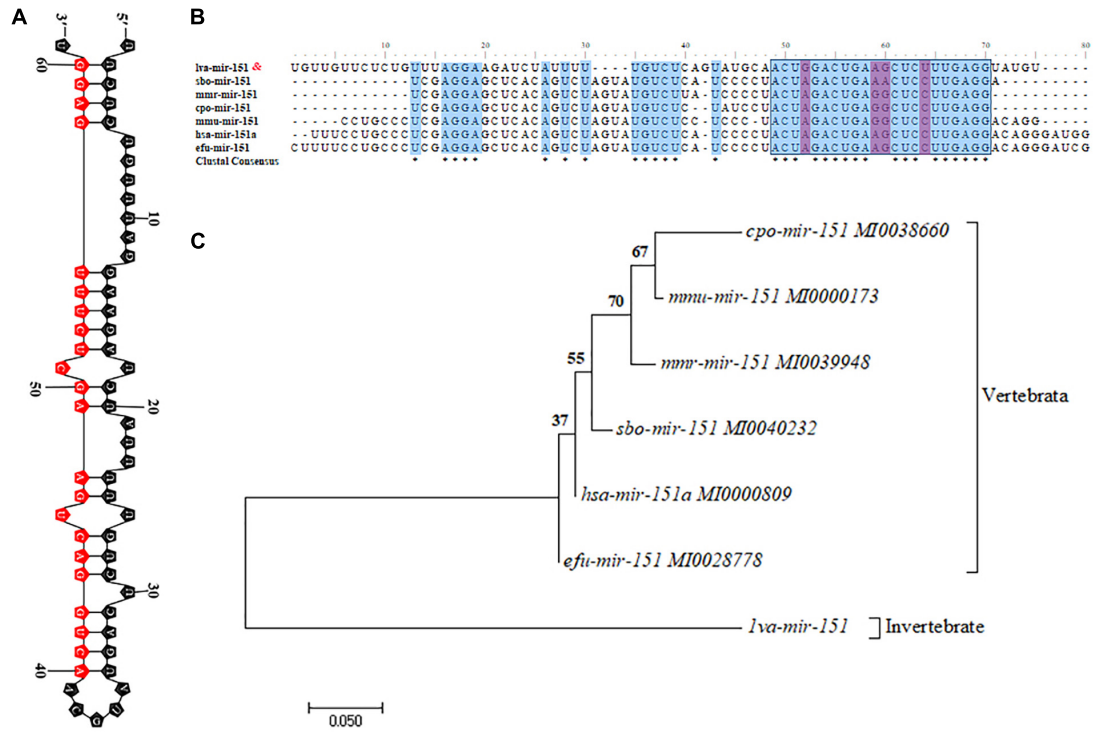

FIGURE 2 | Characteristic analysis of miR-151. **(A)** The hairpin structures of pre-miR-151 from *Epinephelus coioides* and mature miR-151 sequences are indicated in the red box. **(B)** Precursor miR-151 multiple sequence alignment. **(C)** The phylogenetic tree of precursor miR-151 with other species reconstructed by the neighbor-joining (NJ) method using the MEGA 7. The accession numbers used in this analysis are listed in the figure.

in this study. The results showed that the expression of pva-miR-151 was induced by various abiotic and biotic stresses, including ammonia nitrogen, low temperature, and *Vibrio alginolyticus* challenge (**Figure 3A**). To verify whether these miRNAs and TOR were indeed changed in low-temperature stress, qPCR was used to quantify the levels of these pva-miR-151 and *PvTOR* after low-temperature challenge. The results showed that the expression of pva-miR-151 was decreased at 1.5 h and then increased at 3 to 24 h. An opposite pattern was observed in the expression of *PvTOR* in response to low-temperature stress (**Figure 3B**). These results indicated that *PvTOR* might be regulated by pva-miR-151 *in vivo* in response to low-temperature stress. In addition, tissue-specific expression of pva-miR-151 showed that pva-miR-151 was expressed in almost all examined tissue types, such as hepatopancreatic, hemolymph, heart, muscle, gill, stomach, intestine, and eye (**Figure 3C**).

Low-Temperature Stress Induced Autophagy *in vivo*

LC3 is a key autophagy-related protein, and previous studies showed that LC3 level is closely related to the autophagic flux (Zhu et al., 2017). To evaluate whether autophagy occurred in shrimp, rapamycin (autophagy activator) was used to induce autophagy of shrimp hepatopancreas, followed by the detection of LC3II/β-actin and beclin1. After different concentrations of rapamycin were injected into shrimp, there is a significant increase in LC3II/β-actin ratio, and beclin1 expressions were found in the 100 or 500 nM rapamycin compared to the control group (**Figures 4A–C**). Nevertheless, high concentration of rapamycin was cytotoxic to shrimp. Therefore, 100 nM rapamycin was chosen for further study. The results showed that autophagy was induced at 24 h after injection of rapamycin compared with the control (**Figures 4D–F**). These results indicated that autophagy of shrimp hepatopancreas could be activated at an early stage of rapamycin challenge. To explore the effect of low temperature–induced autophagy, the shrimp were treated with low-temperature stress. Western blotting revealed that the autophagy-related proteins LC3 and beclin1 of shrimp hepatopancreas dramatically increased in response to low-temperature stress. At an early stage of low-temperature stress (1.5 h), the shrimp autophagy was induced (**Figures 4G–I**). The results indicated that low-temperature stress was an inducer of autophagy in shrimp *in vivo*, which was similar to that of rapamycin.

Furthermore, to further determine the occurrence of autophagy, we performed a degradation experiment. Primary cells were treated with mTOR inhibitor rapamycin and lysosomal protease inhibitor chloride. Primary cells were treated with 2 μM rapamycin and 8 μM CLQ for 24 h. CYTO-ID® Green Detection Reagent 2 was stained for 30 min and analyzed by flow cytometry. Compared with untreated cells, the fluorescence was increased, with treatment with RAP + CLQ (**Figures 4J,K**).

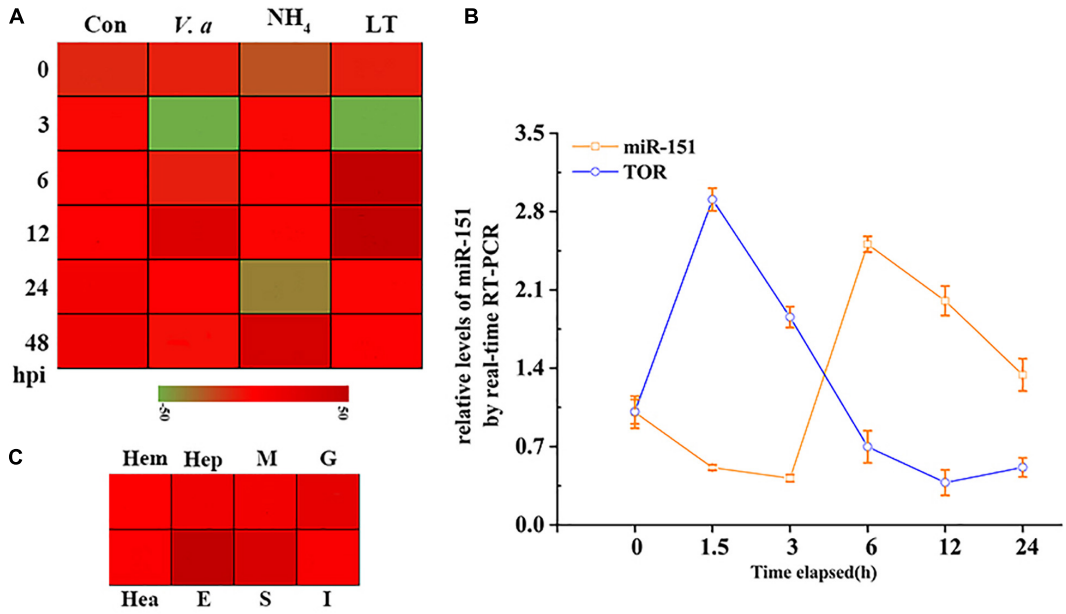

FIGURE 3 | Expression pattern analysis of *PvTOR* and pva-miR-151. **(A)** Transcriptional profiling of pva-miR-151. The values calculated by qRNA data were shown as a heat map. **(B)** Different tissues expression profiles of pva-miR-151 in shrimp. The colors of the bar shown to the right of the heat map varied from red to green, representing the relative expression levels from high to low. Hepatopancreatic (Hep), hemolymph (Hem), heart (Hea), muscle (M), gill (G), stomach (S), intestine (I), and eye (E). **(C)** pva-miR-151 and *PvTOR* expression patterns in shrimp under low-temperature stress. cDNAs were synthesized from total RNA extracted from various tissues of shrimp. The expression levels of pva-miR-151 were normalized using U6, and *PvTOR* was normalized using β-actin. Error bars represented standard deviations of the mean values from three independent experiments.

The results indicated that autophagy can be induced under stress conditions.

Alters of pva-miR-151 Impact Low-Temperature Tolerance of Shrimp

To investigate a possible role of pva-miR-151 in response to low-temperature stress in shrimp, ago-151 or antago-151 was used to overexpress or silence pva-miR-151 in *P. vannamei*, respectively. The efficiency was analyzed by qPCR. We chose the period 24–36 h for the experiment in which the overexpression efficiency was more than 100-fold or the silencing efficiency was less than 50% (**Supplementary Figure 2**). The results showed that low-temperature challenge significantly increased the mortality of shrimp ($P < 0.01$; **Figure 5A**). Importantly, overexpression of pva-miR-151 significantly reduced mortality ($P < 0.01$; **Figure 5B**), while silencing pva-miR-151 significantly enhanced the mortality of shrimp in low-temperature challenge ($P < 0.05$; **Figure 5C**).

Previous studies have shown that loss of circulating hemocytes or hemocyte DNA damage would endanger survival (Li et al., 2013; Liang et al., 2019a). Thus, this possibility was observed, and results showed that overexpression of pva-miR-151 significantly elevated THC, while silencing pva-miR-151 significantly reduced the THC in low-temperature challenge (**Figures 5D,E**). In addition, the hepatopancreas is a sensitive organ that can show ultrastructural alterations at the early stages of stress (Xu et al., 2018). Low temperature caused the vacuoles cells to increase and cell atrophy. Excitingly, silencing pva-miR-151 appeared to accelerate the lesions such that the vacuole cells occurred at 1.5 h, while vacuoles cells have occurred in 3 h in the NC group. Conversely, in overexpression of pva-miR-151, vacuole cells were the first to appear, at 6 h, after temperature challenge compared with the NC group (**Figure 5F** and **Supplementary Figure 3**). All these data indicated that pva-miR-151 protects against damage in response to low-temperature stress in shrimp.

Pva-miR-151 Affects Low-Temperature Tolerance of Shrimp by Inducing Autophagy

To further investigate the biological role of pva-miR-151 under low-temperature stress, ago or antago was used to overexpress or silence pva-miR-151 in shrimp. The results showed that overexpression of pva-miR-151 inhibited the protein levels of p-TOR (**Figures 6A,B**). Importantly, silenced pva-miR-151 reversed the inhibitory effect on TOR signaling pathway (**Figures 6E,F**). Based on the above results and those from previous studies, the hypothesis presented that low-temperature stress induced the occurrence of autophagy and increased the expression of pva-miR-151 to decrease the protein level of p-TOR. With the decrease of PvTOR activation, the accumulation of autophagy increases, thereby alleviating the damage of the hepatopancreas under low-temperature stress. To confirm our hypothesis, the LC3I/II and beclin1 protein levels were determined in aberration shrimp. The results disclosed that overexpression of pva-miR-151 induced expression of

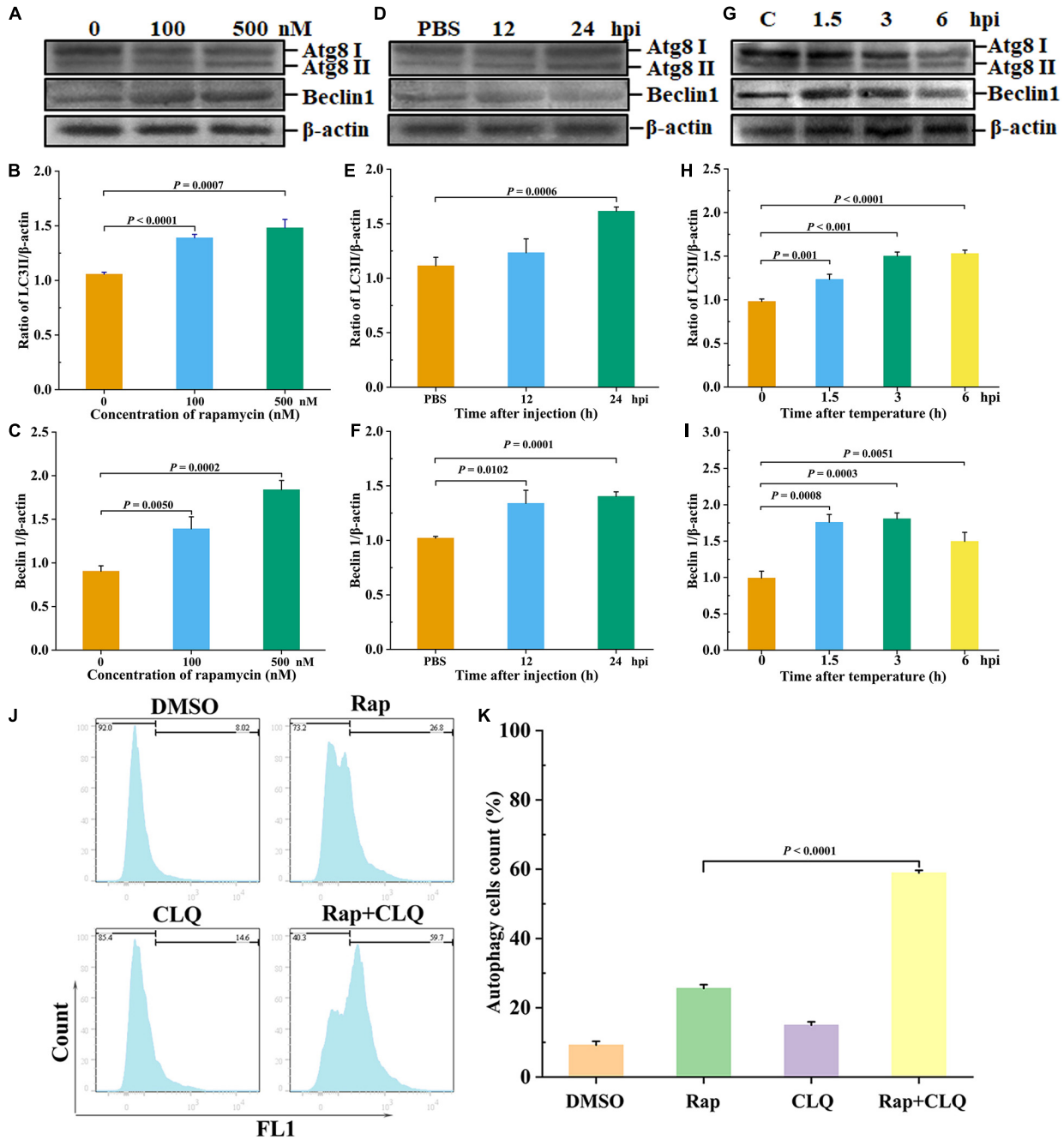

FIGURE 4 | Low temperature induced autophagy *in vivo*. Shrimp were injected with rapamycin at different concentrations. At 12 and 24 h after rapamycin injection, the shrimp hepatopancreas specimens was collected for Western blot analysis with an LC3 and beclin1 antibody. Dosage of rapamycin for autophagy induction Western blot analysis **(A)**, LC3 **(B)**, and beclin1 **(C)** statistical analysis. Time-course detections of autophagy Western blot analysis **(D)**, LC3 **(E)**, and beclin1 **(F)** statistical analysis. Low-temperature stress induction for autophagy Western blot analysis **(G)**, LC3 **(H)**, and beclin1 **(I)** statistical analysis. The ratios of LC3II/β-actin and beclin1/β-actin gray-scale value were calculated with three independent experiments. Shrimp primary hemolymph cells were treated with DMSO, 2 μM rapamycin (Rap), 8 μM chloroquine (CLQ), or Rap + CLQ for 24 h to induce autophagy and then used CYTO-ID® Green Detection Reagent 2 stain for 30 min and analyzed by flow cytometry **(J)** and statistical analysis **(K)**. Data were shown as fold changes and mean ± SD.

LC3II/β-actin and beclin1 protein level when shrimp were exposed to low-temperature stress (**Figures 6A,C,D**). On the contrary, silenced pva-miR-151 had an opposite result (**Figures 6E,G,H**).

To further determine the role of the miR-151 in low-temperature stress–induced autophagy, we performed a degradation experiment. Primary cells were treated with mTOR inhibitor rapamycin and lysosomal protease inhibitor chloride.

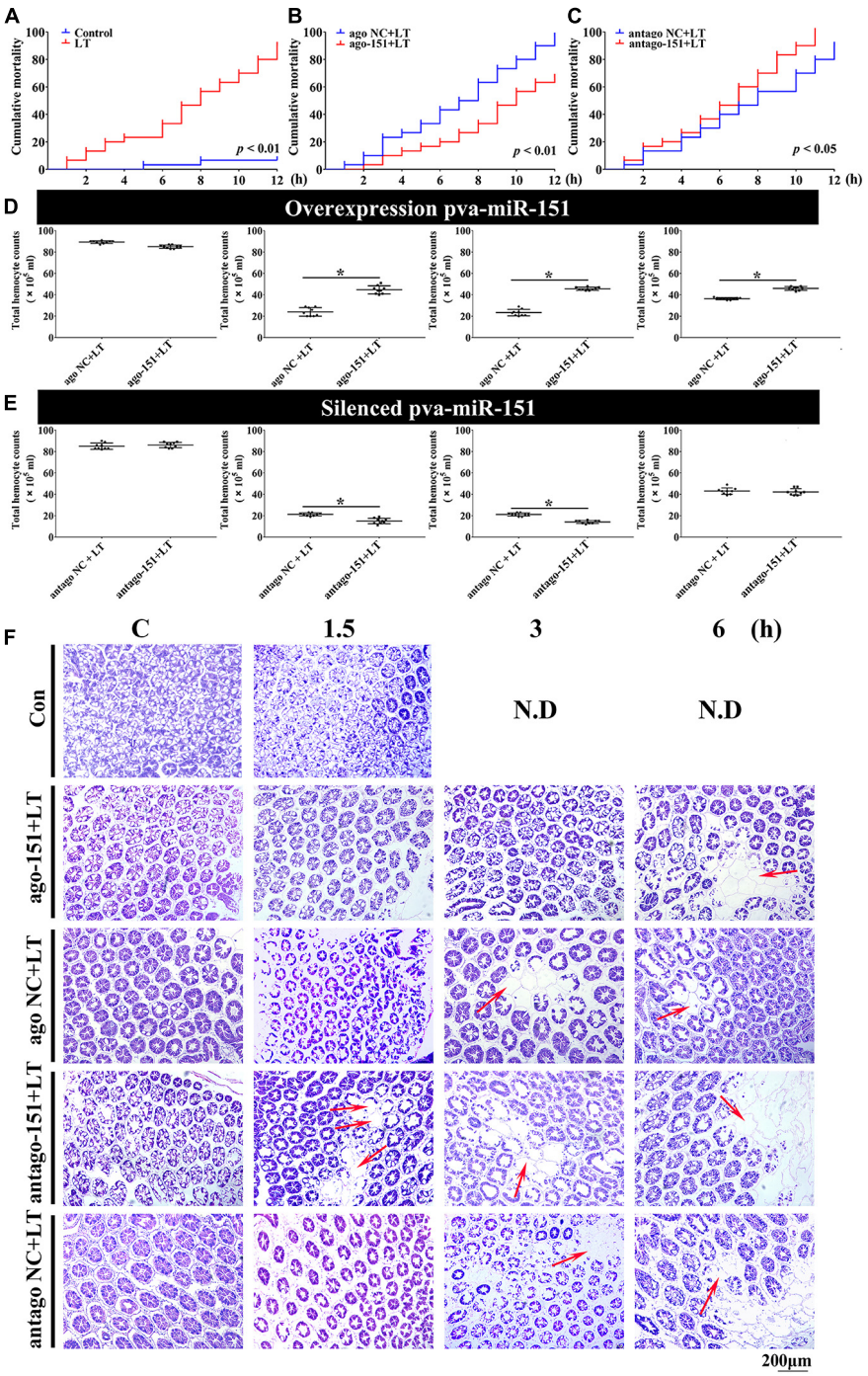

FIGURE 5 | Alterations of pva-miR-151 impact low-temperature tolerance of shrimp. **(A)** The shrimp were treated with low temperature at various times after challenge; the shrimp mortality was examined. In low temperature–challenged shrimp, mortality was reduced after pretreatment with ago-151 **(B)** and increased after pretreatment with antago-151 **(C)**. Differences in mortality curves between each group were analyzed by the log–rank test. THC was increased after pretreatment with ago-151 **(D)** and reduced after pretreatment with antago-151 **(E)**. Differences in THC between each group were analyzed by *t* test. *Significantly different ($p < 0.05$). **(F)** H&E-stained hepatopancreas collected from ago-151, ago NC, antago-151, and antago NC groups after low-temperature challenge at 0–6 hpi. Pretreatment with ago-151 alleviates the vacuole cells, and cell atrophy occurred. ND, no data. Scale bar, 200 μm.

Primary cells were treated with 50 μM 3BDO, 8 μM CLQ, ago NC and ago-151, for 24 h. CYTO-ID® Green Detection Reagent 2 was stained for 30 min and analyzed by flow cytometry. Overexpression miR-151 in primary cells and treating them with or without 3BDO were used to detect the autophagy flux. The autophagy flux was significantly increased by overexpression

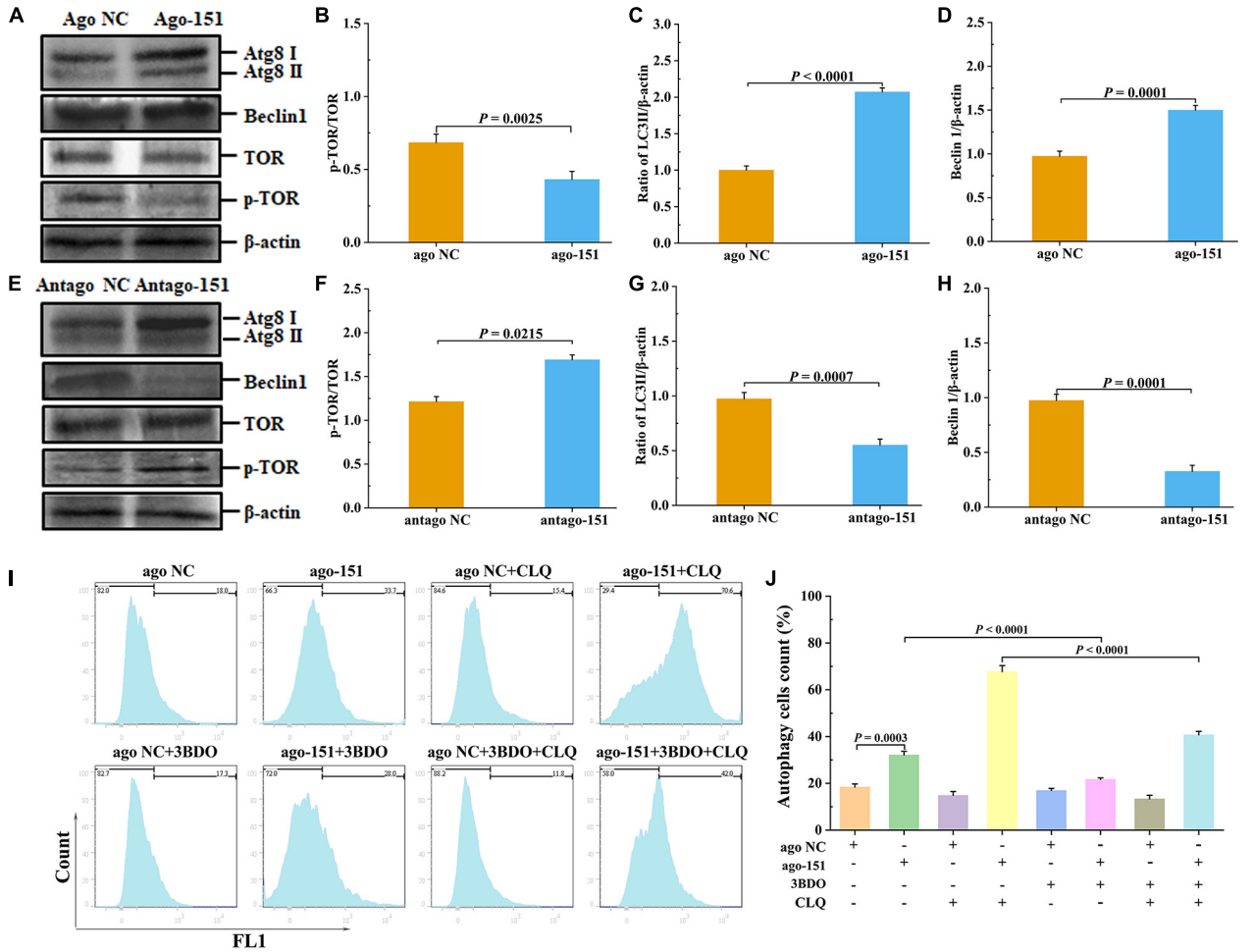

FIGURE 6 | Pva-miR-151 affects low-temperature tolerance of shrimp by inducing the occurrence of autophagy. Shrimp were injected with 2 nM/g ago-151 or antago-151. After 24 h, the shrimp hepatopancreas was collected for Western blot. The Western blot evaluation of shrimp autophagy after ago-151 treatment **(A)**, p-TOR **(B)**, LC3 **(C)**, and beclin1 **(D)** statistical analysis. The evaluation Western blot of shrimp autophagy after antago-151 treatment **(E)**, p-TOR **(F)**, LC3 **(G)**, and beclin1 **(H)** statistical analysis. β-Actin was used as the control. The ratios of pTOR/TOR, LC3II/β-actin, and beclin1/β-actin gray-scale value were calculated with three independent experiments. Shrimp primary hemolymph cells were treatments with DMSO, 20 pmol NC or miR-151, 8 μM chloroquine (CLQ), and 50 μM 3BDO for 24 h to induce autophagy and then used CYTO-ID® Green Detection Reagent 2 stain for 30 min and analyzed by flow cytometry **(I)** and statistical analysis **(J)**. Data were shown as fold changes and mean ± SD.

miR-151, but suppressed with 3BDO and miR-151 coprocessing treatment cells (**Figures 6I,J**). Excitingly, the autophagy flux was significantly increased by overexpression miR-151 and CLQ coprocessing, but significantly suppressed with 3BDO, miR-151, and CLQ coprocessing treatment cells (**Figures 6I,J**).

In addition, ultrastructural observation of the hepatopancreas by TEM showed that the overexpression pva-miR-151 induced autophagy formation when shrimp were exposed to low-temperature stress, reducing damaged organelle fragments. For example, mitochondria are round or elongated, the matrix electron density is higher, and the ridges are aligned after pretreatment with ago-151. On the contrary, silenced pva-miR-151 had an opposite result (**Figure 7**). Nuclear (N) shrinkage and mitochondria are sparsely distributed, with varying oval sizes, and the ridges are slightly expanded, disordered, and broken after pretreatment with antago-151.

All these data indicated that when shrimp were exposed to low-temperature stress, the up-regulated expression of pva-miR-151 inhibited PvTOR, leading to a decrease in p-TOR expression level and the elevation of autophagy formation, which further resulted in increased scavenging of the damaged organelle injury accumulation by low-temperature stress induced in shrimp hepatopancreas cells.

PvTOR Is an Immediate Target of pva-miR-151

To detect that *PvTOR* was the target gene of pva-miR-151, using the bioinformatics software TargetScan, RNAhybrid, and miRDB intersection was carried out to predict results. The predicted binding site between miR-151 and *PvTOR* 3′-UTR was shown at 7656–7678 (**Figure 8A**). The pre-miR-151 was cloned into a

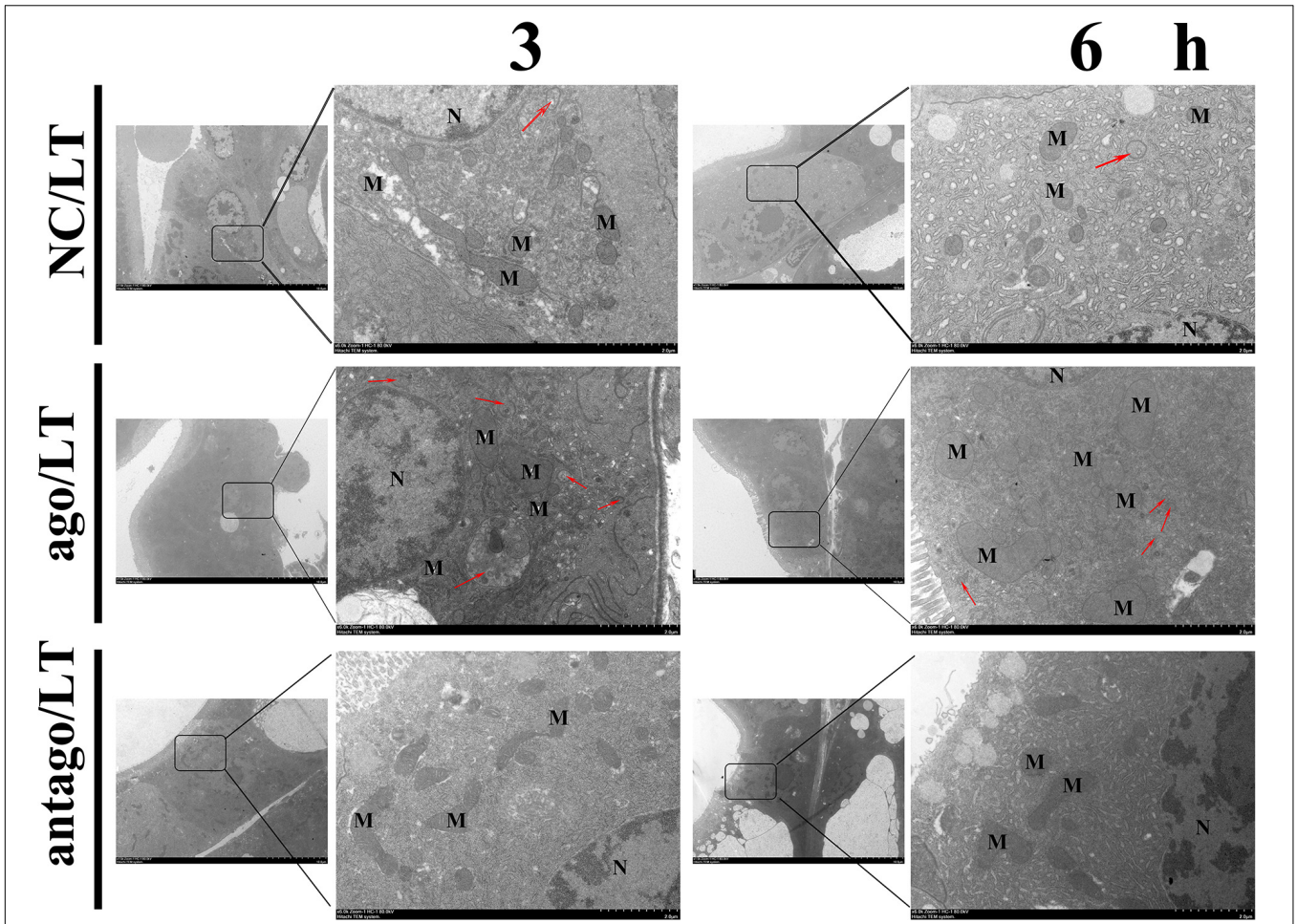

FIGURE 7 | TEM observation the hepatopancreas ultrastructure after pretreatment with ago-151 or antago-151. Mitochondria (M) are round or elongated, the matrix electron density is higher, the ridges are aligned, and there is obvious autophagy (red arrow) after pretreatment with ago-151. Nuclear (N) shrinkage and mitochondria (M) are sparsely distributed, with varying oval sizes, and the ridges are slightly expanded, disordered, and broken after pretreatment with antago-151.

pcDNA6.2 GW miR vector, and *PvTOR* 3′-UTR was cloned into a luciferase reporter plasmid (**Figure 8B**). The luciferase reporter assay results showed that overexpression of miR-151 significantly suppressed luciferase activity of reporter genes containing 3′-UTR-WT of *PvTOR* (**Figure 8C**), and the transfection of pre-miR-151 had similar results (**Figure 8D**). In addition, overexpression miR-151 significantly suppressed the mRNA expression of *PvTOR* (**Figure 8E**), and the transfection of pre-miR-151 had similar results (**Figure 8F**). These results suggested that miR-151 bound directly to the predicted binding site(s) in the *PvTOR* 3′-UTR and negatively regulated *PvTOR* expression.

DISCUSSION

In nature, aquatic organisms trigger adjustments to their physiology and behavior to adapt to the fluctuation environment (de Souza et al., 2016). Therefore, temperature is one of the most important environmental factors for aquatic animals. Crustaceans are cold-blooded thermophilic animals whose body temperature changes with the water temperature of living waters. As a sensitive organ, ultrastructural alterations can occur in the hepatopancreas at the early stages of stress (Xu et al., 2018). Recent studies have indicated that hypothermia was a critical factor to hepatic ultrastructural changes, notably autophagy (Salas et al., 1977). In addition, autophagy has been described in many studies that it constitutes a strategy to adapt to and cope with stress by removing misfolded proteins and damaged organelles (Marino et al., 2014; Wu et al., 2019). Recent studies have also shown that rapamycin induced autophagy involved in the immune regulation of *P. vannamei* (Wu et al., 2019). Chlorpyrifos also can induce autophagy that occurs by activating the AMPK/TOR pathway in common carp (Zhang et al., 2019). Accumulating evidence suggests that TOR plays a gating role in autophagy, and its activity is the key to the formation and maturation of autophagy (Wang and Klionsky, 2003). However, the role of miRNA-mediated TOR genes in the occurrence of autophagy has been studied only in invertebrates.

miRNAs, as critical regulators of transcription, RNA processing, RNA stability, and translation, were involved in

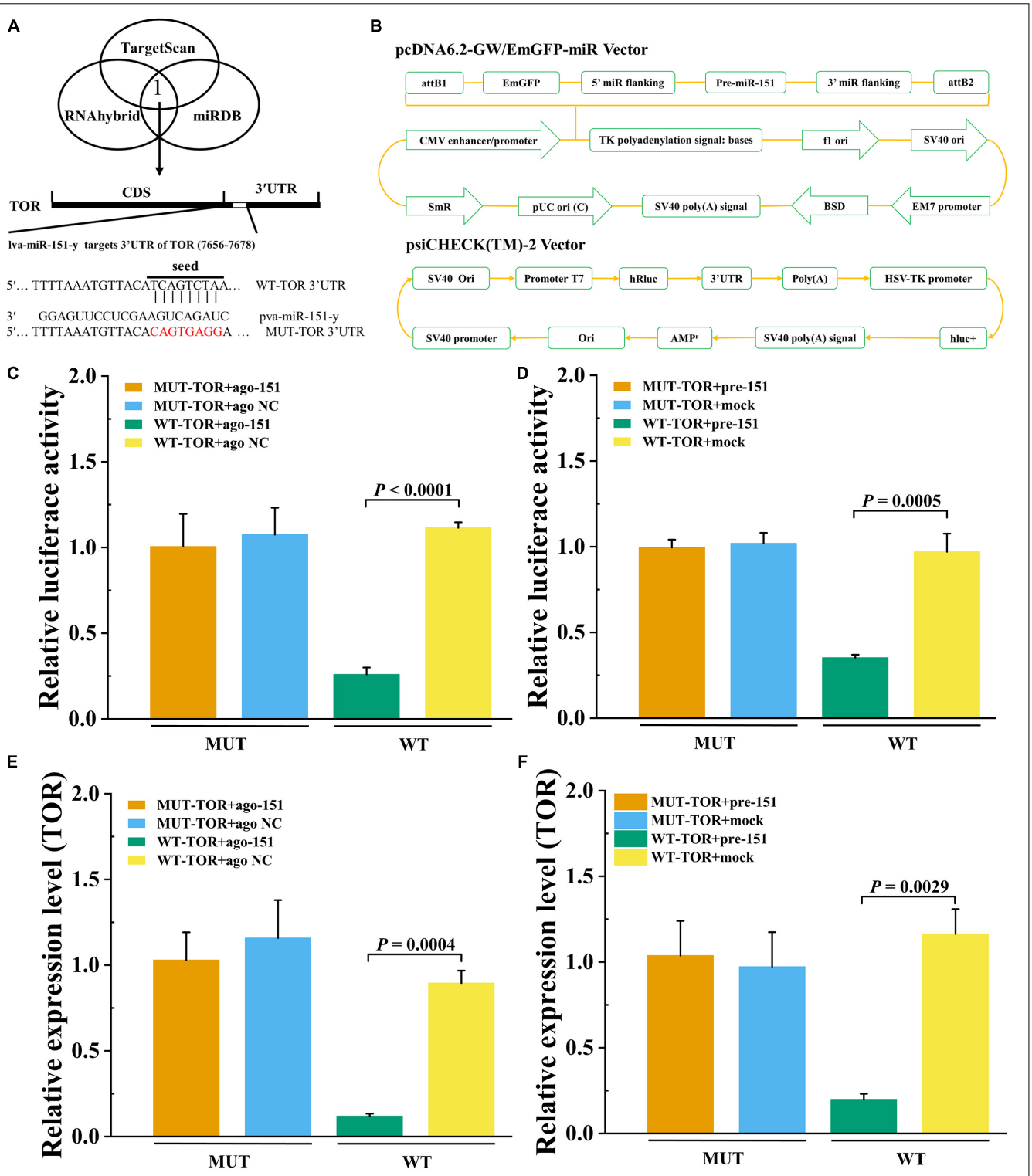

FIGURE 8 | Prediction and validation of pva-iR-151 target genes *PvTOR*. **(A)** Predicted target genes of pva-miR-151. The 3′-UTR of the PvTOR gene was predicted to be targeted by miR-13b used TargetScan, miRDB, and RNAhybrid. Schematic diagram miR-151 to binding 3′-UTR of PvTOR and wild or mutant type 3′-UTR of PvTOR. **(B)** Schematic diagram of pcDNA-pre-miR-151 and psiCHECK-3′-UTR$_{PvTOR}$ vector. The luciferase activity was determined using reporter gene assay. Data were shown as fold changes and mean ± SD. Primary cells were transfected with ago-151 **(C)** or pcDNA-pre-miR-151 **(D)** and psiCHECK-3′-UTR$_{PvTOR}$ cotransfection with Lipofectamine 2000. After incubation at 27∘C for 24 h, the luciferase activity was determined. The mTOR expression levels after primary cells were transfected with ago-151 **(E)** or pcDNA-pre-miR-151 **(F)**. Data were shown as fold changes and mean ± SD.

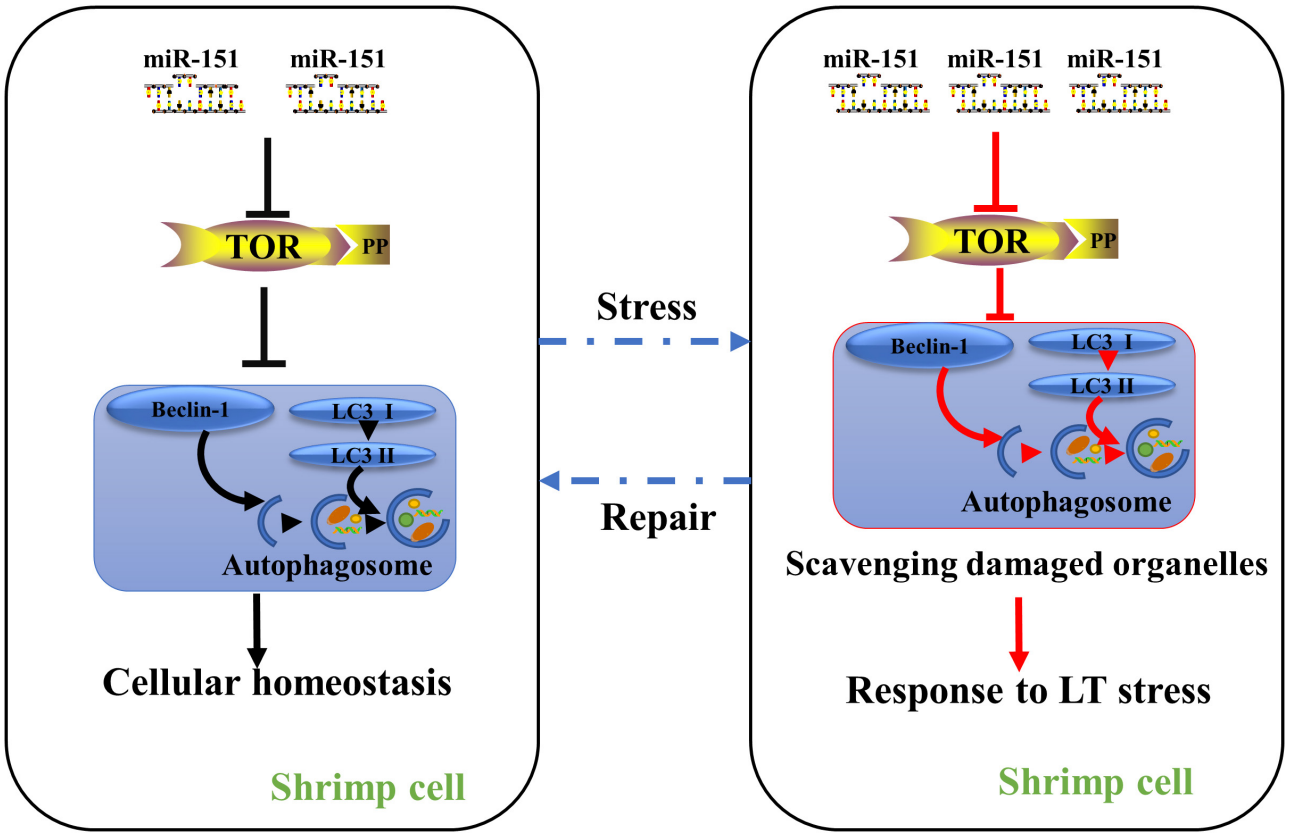

FIGURE 9 | A proposed model for the role of miR-151 in low-temperature tolerance. Under normal physiological conditions, miR-151 mediates the expression of PvTOR to maintain intracellular homeostasis. When the shrimp were exposed to low-temperature stress, inhibiting miR-151 reduces the accumulation of TOR and p-tor, thereby regulating the expression of autophagy-related proteins, resulting in increasing the accumulation of autophagosomes. The accumulated autophagosomes contribute to degrading these organelles such as damaged mitochondria. To alleviate hepatopancreas injury induced by acute low temperature in shrimp. Red lines indicate increased pathways, whereas blank lines indicate maintain intracellular homeostasis pathways.

the regulation of cell proliferation, differentiation, autophagy, and apoptosis regulation (Carthew and Sontheimer, 2009). Many miRNAs have recently been identified to play key roles in regulating autophagy. In the diabetic mesangial cell, Oleanolic acid activation of autophagy via miRNA-142-5p/PTEN signaling attenuates cell injury (Chen et al., 2019). miR-71 and miR-13b are necessary for viral infection and host autophagy of shrimp (He et al., 2017). Furthermore, miRNA regulates autophagy mainly through the regulation of the expression of key proteins in the process of autophagosome formation. ULK1 can be inhibited by mir-20a or mir-106b expression, thereby inhibiting leucine deficiency–induced autophagy (Wu et al., 2012). miR-30a inhibits autophagy by inhibiting the expression of Beclin1 and Atg5 proteins during nucleation and elongation of autophagosomes (Zhai et al., 2013). However, the regulation of autophagosome formation process proteins is more limited. Because the initiation of autophagy is regulated by numerous signaling pathways such as PI3K/AKT/mTOR, ERK1/2, elF-2, AMPK, and MAPK signaling pathway (Lim et al., 2019; Wang et al., 2019), therefore, PI3K/AKT/mTOR signaling pathway is an important upstream regulatory factor on the formation of autophagosomes. For instance, mTOR is a target gene such as miR-7, miR-199a-3p, and miR-100 and can block autophagy induced by the mTOR signaling pathway (Alqurashi et al., 2013). Fortunately, crustacean miRNAs, which are involved in the regulation of autophagy, have also been gradually discovered. Twenty-four miRNAs were also found to play a role in autophagy, phagocytosis, and apoptosis in *Marsupenaeus japonicus* (Tianzhi Huang, 2012). In this context, the posttranscriptional regulation mediated by miRNAs may shed light on the interaction between autophagy and damage.

This data indicate that 36 differentially expressed miRNAs were identified under low-temperature stress, and their target genes were significantly enriched in endocytosis and mTOR signaling pathway. Studies show that mTOR can drive protein synthesis (Aramburu et al., 2014). Shrimps need to consume energy under low-temperature stress. Thus, the expression of pva-miR-151 was decreased at 1.5 h after low-temperature stress, suggesting that down-regulation of pva-miR-151 could partially promote activities of mTOR to protect stressed cells by increasing the rate of biosynthesis and the cellular energy demand. However, constitutively active mTOR could increase ROS production and induced cell damage. Thus, the expression of pva-miR-151 was increased at 3 to 24 h

after low-temperature stress, suggesting that up-regulation pva-miR-151 could partially inhibit activities of mTOR activating an autophagic response that clears protein aggregates and damaged organelles and improves cell survival. Additionally, low-temperature stress can induce hepatopancreatic injury and autophagy accumulation. The results revealed that miRNAs are involved in the regulation of autophagy under low-temperature stress. Currently, the mechanism associated with autophagy and miRNA, which controlled shrimp response to low-temperature stress, is still unclear. In this study, we characterized the expression patterns and biological functions of pva-miR-151 in shrimp and provided a new regulatory mechanism by which pva-miR-151 mediated *PvTOR* regulation in shrimp response to low-temperature stress. Sequence analysis revealed that mature pva-miR-151 is completely conserved in mammals, and LUC reporter experiment confirmed that the pva-miR-151 precursor can be folded into a hairpin structure. In addition, pva-miR-151 directly targeted the 3′-UTR gene to regulate *PvTOR* expression by confirming experimentally. As reported, the significant reduction of miRNA-151 was associated with severe liver injury (Cheng et al., 2018). Up-regulation of miR-151-3p was closely related to the overall survival rate in resected cholangiocarcinoma (McNally et al., 2013). The data of this study indicate that the accumulation of autophagy induced by overexpression of pva-miR-151 can alleviate hepatopancreas injury caused by low-temperature stress and reduce the mortality of shrimp and *vice versa* (**Figure 9**). Autophagy is a necessary process in which cell recycling degrades cytoplasm and organelles by the lysosomal pathway in all eukaryotic cells (Yan et al., 2019). Autophagy has been shown to be a survival mechanism under different stress conditions (Wei et al., 2015; Jing et al., 2018). These findings showed that pva-miR-151 through target gene *PvTOR* regulating the autophagy accumulation involved in *P. vannamei* response.

Loss and damage of circulating hemocytes in shrimp can lead to decreasing the immune ability, augment the susceptibility against pathogens, and even threaten survival, demonstrating that hemocytes play an important role in physiology and immune defense (Smith et al., 1995; Li et al., 2013). It was documented that acute low-temperature stress could result in a reduction of the THC (Qiu et al., 2011). It is suggested that overexpression of pva-mir-151 can alleviate THC reduction caused by low-temperature stress. In crustaceans, there are three morphologically different hemolymph types: hyaline, semigranular, and granular cells (Johansson et al., 2000). Both hyaline and semigranular have phagocytosis. Thus, we speculate that pva-miR-151 might regulate hemolymph autophagy or phagocytosis-related protein expression to inhibit hemolymph apoptosis. There was no evidence in this article to explain this molecular mechanism; the results showed that pva-miR-151 is closely related to shrimp THC, which needs to be investigated in further research.

Taken together, the present study indicated that both pva-miR-151 and *PvTOR* were involved in shrimp response to low-temperature stress. Ectopic expression of pva-miR-151 resulted in low-temperature tolerance phenotype. A low-temperature hypersensitive phenotype was observed in silenced pva-miR-151 in *P. vannamei*. The present study provides a much-needed framework that pva-miR-151 responds to low-temperature tolerance of *P. vannamei* by increased autophagy accumulation and THC under low-temperature stress by its target gene *PvTOR* expression.

DATA AVAILABILITY STATEMENT

The original contributions presented in the study are included in the article/**Supplementary Material**, further inquiries can be directed to the corresponding author/s.

ETHICS STATEMENT

The animal study was reviewed and approved by animal protocols conform to the University Animal Care and Use Committee of the South China Normal University.

AUTHOR CONTRIBUTIONS

QL: software and writing-original draft preparation. QL, MO, and WD: validation and writing-review and editing. ZL, CL, and FW: prepare the experiment materials. YL and WW: project administration and funding acquisition. All authors have read and agreed to the published version of the manuscript.

FUNDING

This research was supported by the National Natural Science Foundation of China (Grant Nos. 31670423 and 31971417) and Guangdong Provincial Natural Science Foundation of China (Grant No. 2019A1515011442).

SUPPLEMENTARY MATERIAL

The Supplementary Material for this article can be found online at: https://www.frontiersin.org/articles/10.3389/fcell.2021.595108/full#supplementary-material

Supplementary Figure 1 | The energy dot plot of pva-miR-151 precursor. The hairpin structures of pva-miR-151 precursor were formed by the mfold Web server (http://unafold.rna.albany.edu/?q~=~mfold). The dots represent the superposition of all possible folding within p% of ΔGmfe, the minimum free energy, where *p* is the maximum percent deviation from ΔGmfe. Different colors are used to indicate varying levels of suboptimality. The explanations of relevant parameters were detailed in the mfold Web server.

Supplementary Figure 2 | The shrimp were injected with ago-151 or antago-151. After different hours that the efficiency was analyzed by qRT-PCR in hepatopancreas.

Supplementary Table 1 | Sequences of PCR primers used in this study.

Supplementary Table 2 | Differential miRNA after low-temperature stress 3 h.

Supplementary Table 3 | Differential miRNA target genes predicted.

Supplementary Table 4 | Differential miRNA target genes by KEGG analysis.

Supplementary Table 5 | Sequences of miR-151 (red) and its precursor (blue).

REFERENCES

Alqurashi, N., Hashimi, S. M., and Wei, M. Q. (2013). Chemical Inhibitors and microRNAs (miRNA) Targeting the Mammalian Target of Rapamycin (mTOR) Pathway: Potential for Novel Anticancer Therapeutics. *Int. J. Mole. Sci.* 14, 3874–3900. doi: 10.3390/ijms14023874

Aramburu, J., Ortells, M. C., Tejedor, S., Buxade, M., and Lopez-Rodriguez, C. (2014). Transcriptional regulation of the stress response by mTOR. *Sci. Signal.* 7:re2.

Carthew, R. W., and Sontheimer, E. J. (2009). Origins and Mechanisms of miRNAs and siRNAs. *Cell* 136, 642–655. doi: 10.1016/j.cell.2009.01.035

Chen, J., Cui, Y., Zhang, N., Yao, X., Wang, Z., and Yang, L. (2019). Oleanolic acid attenuated diabetic mesangial cell injury by activation of autophagy via miRNA-142-5p/PTEN signaling. *Cytotechnology* 71, 925–933. doi: 10.1007/s10616-019-00335-0

Cheng, J.-L., Zhao, H., Yang, S.-G., Chen, E.-M., Chen, W.-Q., and Li, L.-J. (2018). Plasma miRNA-122-5p and miRNA-151a-3p identified as potential biomarkers for liver injury among CHB patients with PNALT. *Hepatol. Int.* 12, 277–287. doi: 10.1007/s12072-018-9871-0

Cheng, W. T., Wang, L. U., and Chen, J. C. (2005). Effect of water temperature on the immune response of white shrimp *Litopenaeus vannamei* to *Vibrio alginolyticus*. *Aquaculture* 250, 592–601. doi: 10.1016/j.aquaculture.2005.04.060

de Souza, D. M., Borges, V. D., Furtado, P., Romano, L. A., Wasielesky, W., Monserrat, J. M., et al. (2016). Antioxidant enzyme activities and immunological system analysis of *Litopenaeus vannamei* reared in biofloc technology (BFT) at different water temperatures. *Aquaculture* 451, 436–443. doi: 10.1016/j.aquaculture.2015.10.006

George, S. K., Kaizer, K. N., Betz, Y. M., and Dhar, A. K. (2011). Multiplication of Taura syndrome virus in primary hemocyte culture of shrimp (*Penaeus vannamei*). *J. Virol. Methods* 172, 54–59. doi: 10.1016/j.jviromet.2010.12.020

He, Y., Sun, Y., and Zhang, X. (2017). Noncoding miRNAs bridge virus infection and host autophagy in shrimp in vivo. *FASEB J.* 31, 2854–2868. doi: 10.1096/fj.201601141rr

Hu, G., McQuiston, T., Bernard, A., Park, Y. D., Qiu, J., Vural, A., et al. (2015). TOR-dependent post-transcriptional regulation of autophagy. *Autophagy* 11, 2390–2392. doi: 10.1080/15548627.2015.1091142

Huang, T., and Zhang, X. (2012). Contribution of the argonaute-1 isoforms to invertebrate antiviral defense. *PLoS One* 7:e50581. doi: 10.1371/journal.pone.0050581

Jing, H. R., Luo, F. W., Liu, X. M., Tian, X. F., and Zhou, Y. (2018). Fish oil alleviates liver injury induced by intestinal ischemia/reperfusion via AMPK/SIRT-1/autophagy pathway. *World J. Gastroenterol.* 24, 833–843. doi: 10.3748/wjg.v24.i7.833

Johansson, M. W., Keyser, P., Sritunyalucksana, K., and Soderhall, K. (2000). Crustacean haemocytes and haematopoiesis. *Aquaculture* 191, 45–52. doi: 10.1016/s0044-8486(00)00418-x

Lago-Lestón, A., Ponce, E., and Muñoz, M. E. (2007). Cloning and expression of hyperglycemic (CHH) and molt-inhibiting (MIH) hormones mRNAs from the eyestalk of shrimps of *Litopenaeus vannamei* grown in different temperature and salinity conditions. *Aquaculture* 270, 343–357. doi: 10.1016/j.aquaculture.2007.04.014

Laplante, M., and Sabatini, D. M. (2012). mTOR signaling in growth control and disease. *Cell* 149, 274–293. doi: 10.1016/j.cell.2012.03.017

Li, B., Xian, J.-A., Guo, H., Wang, A.-L., Miao, Y.-T., Ye, J.-M., et al. (2013). Effect of temperature decrease on hemocyte apoptosis of the white shrimp *Litopenaeus vannamei*. *Aquacult. Int.* 22, 761–774. doi: 10.1007/s10499-013-9704-z

Liang, Q., Ou, M., Li, Z., Ren, Y., Wei, W., Qiao, X., et al. (2019a). Functional analysis target of rapamycin (TOR) on the *Penaeus vannamei* in response to acute low-temperature stress. *Fish Shellfish Immunol.* 96, 53–61. doi: 10.1016/j.fsi.2019.11.070

Liang, Q., Ou, M., Ren, Y., Yao, Z., Hu, R., Li, J., et al. (2019b). Molecular cloning, characterization and expression analysis of S- adenosyl- L-homocysteine hydrolase (SAHH) during the pathogenic infection of *Litopenaeus vannamei* by *Vibrio alginolyticus*. *Fish Shellfish Immunol.* 88, 284–292. doi: 10.1016/j.fsi.2019.02.058

Liang, Q., Wu, X., Yang, P., Kong, J., Wei, W., Qiao, X., et al. (2019c). The role of delta-1-pyrroline-5-carboxylate dehydrogenase (P5CDh) in the Pacific white shrimp (*Litopenaeus vannamei*) during biotic and abiotic stress. *Aquatic Toxicol.* 208, 1–11. doi: 10.1016/j.aquatox.2018.12.016

Lim, V., Zhu, H., Diao, S., Hu, L., and Hu, J. (2019). PKP3 interactions with MAPK-JNK-ERK1/2-mTOR pathway regulates autophagy and invasion in ovarian cancer. *Biochem. Biophys. Res. Commun.* 508, 646–653. doi: 10.1016/j.bbrc.2018.11.163

Liu, X., Su, X., Xu, S., Wang, H., Han, D., Li, J., et al. (2018a). MicroRNA in vivo precipitation identifies miR-151-3p as a computational unpredictable miRNA to target Stat3 and inhibits innate IL-6 production. *Cell Mol. Immunol.* 15, 99–110. doi: 10.1038/cmi.2017.82

Liu, X. W., Wang, M. Q., Sun, G. Q., Wang, B. J., Jiang, K. Y., Shao, J. C., et al. (2018b). Mechanistic target of rapamycin inhibition with rapamycin induces autophagy and correlative regulation in white shrimp (*Litopenaeus vannamei*). *Aquacult. Nutr.* 24, 1509–1520. doi: 10.1111/anu.12688

Marino, G., Niso-Santano, M., Baehrecke, E. H., and Kroemer, G. (2014). Self-consumption: the interplay of autophagy and apoptosis. *Nat. Rev. Mole. Cell Biol.* 15, 81–94. doi: 10.1038/nrm3735

McNally, M. E., Collins, A., Wojcik, S. E., Liu, J., Henry, J. C., Jiang, J., et al. (2013). Concomitant dysregulation of microRNAs miR-151-3p and miR-126 correlates with improved survival in resected cholangiocarcinoma. *HPB* 15, 260–264. doi: 10.1111/j.1477-2574.2012.00523.x

Mukhopadhyay, S., Praharaj, P. P., Naik, P. P., Talukdar, S., Emdad, L., Das, S. K., et al. (2020). Identification of Annexin A2 as a key mTOR target to induce roller coaster pattern of autophagy fluctuation in stress. *Biochim. Biophys. Acta Mol. Basis Dis.* 1866:165952. doi: 10.1016/j.bbadis.2020.165952

Ng, T. H., Lu, C. W., Lin, S. S., Chang, C. C., Tran, L. H., Chang, W. C., et al. (2018). The Rho signalling pathway mediates the pathogenicity of AHPND-causing V. parahaemolyticus in shrimp. *Cell Microbiol.* 20:e12849.

Plasterk, R. H. A. (2006). Micro RNAs in Animal Development. *Cell* 124, 877–881. doi: 10.1016/j.cell.2006.02.030

Qiu, J., Wang, W. N., Wang, L. J., Liu, Y. F., and Wang, A. L. (2011). Oxidative stress, DNA damage and osmolality in the Pacific white shrimp, *Litopenaeus vannamei* exposed to acute low-temperature stress. *Compar. Biochem. Phys. Toxicol. Phar. CBP* 154, 36–41. doi: 10.1016/j.cbpc.2011.02.007

Salas, M., Tuchweber, B., and Kourounakis, P. (1977). Temperature-dependence of stress-induced hepatic autophagy. *Experientia* 33, 612–614. doi: 10.1007/bf01946531

Smith, V. J., Swindlehurst, R. J., Johnston, P. A., and Vethaak, A. D. (1995). Disturbance of Host-Defense Capability in the Common Shrimp, Crangon-Crangon, by Exposure to Harbor Dredge Spoils. *Aquat. Toxicol.* 32, 43–58. doi: 10.1016/0166-445x(94)00078-5

Sun, S. J., Wang, B. J., Jiang, K. Y., Sun, J., Liu, M., and Wang, L. (2015). Target of rapamycin (TOR) in *Fenneropenaeus chinensis*: cDNA cloning, characterization, tissue expression and response to amino acids. *Aquac. Nutr.* 21, 1–9. doi: 10.1111/anu.12133

Tettamanti, G., Salo, E., Gonzalez-Estevez, C., Felix, D. A., Grimaldi, A., and de Eguileor, M. (2008). Autophagy in invertebrates: insights into development, regeneration and body remodeling. *Curr. Pharm. Des.* 14, 116–125. doi: 10.2174/138161208783378716

Thansa, K., Yocawibun, P., and Suksodsai, H. (2016). The cellular death pattern of primary haemocytes isolated from the black tiger shrimp (*Penaeus monodon*). *Fish Shellfish Immunol.* 57, 243–251. doi: 10.1016/j.fsi.2016.08.045

Tianzhi Huang, D. X. A. X. Z. (2012). Characterization of host microRNAs that respond to DNA virus infection in a crustacean. *Genomics* 13, 2–10.

Wang, C. W., and Klionsky, D. J. (2003). The molecular mechanism of autophagy. *Mol. Med.* 9, 65–76. doi: 10.1007/bf03402040

Wang, J., Hu, J., Chen, X., Huang, C., Lin, J., Shao, Z., et al. (2019). BRD4 inhibition regulates MAPK, NF-kappaB signals, and autophagy to suppress MMP-13 expression in diabetic intervertebral disc degeneration. *FASEB J.* 33, 11555–11566. doi: 10.1096/fj.201900703r

Wang, W. N., Zhou, J., Wang, P., Tian, T. T., Zheng, Y., Liu, Y., et al. (2009). Oxidative stress, DNA damage and antioxidant enzyme gene expression in the Pacific white shrimp, *Litopenaeus vannamei* when exposed to acute pH stress. *Compar. Biochem. Physiol. Toxicol. Pharmacol. CBP* 150, 428–435. doi: 10.1016/j.cbpc.2009.06.010

Wei, J., Ma, Z., Li, Y., Zhao, B., Wang, D., Jin, Y., et al. (2015). miR-143 inhibits cell proliferation by targeting autophagy-related 2B in non-small cell lung cancer H1299 cells. *Mol. Med. Rep.* 11, 571–576. doi: 10.3892/mmr.2014.2675

Wu, H., Wang, F., Hu, S., Yin, C., Li, X., Zhao, S., et al. (2012). MiR-20a and miR-106b negatively regulate autophagy induced by leucine deprivation via suppression of ULK1 expression in C2C12 myoblasts. *Cell. Signal.* 24, 2179–2186. doi: 10.1016/j.cellsig.2012.07.001

Wu, W. L., Lin, X. S., Wang, C. F., Ke, J. Y., Wang, L., and Liu, H. P. (2019). Transcriptome of white shrimp *Litopenaeus vannamei* induced with rapamycin reveals the role of autophagy in shrimp immunity. *Fish Shellfish Immunol.* 86, 1009–1018. doi: 10.1016/j.fsi.2018.12.039

Xu, Z., Regenstein, J. M., Xie, D., Lu, W., Ren, X., Yuan, J., et al. (2018). The oxidative stress and antioxidant responses of *Litopenaeus vannamei* to low temperature and air exposure. *Fish Shellfish Immunol.* 72, 564–571. doi: 10.1016/j.fsi.2017.11.016

Yan, S., Khambu, B., Hong, H., Liu, G., Huda, N., and Yin, X. M. (2019). Autophagy, Metabolism, and Alcohol-Related Liver Disease: Novel Modulators and Functions. *Int. J. Mole. Sci.* 2019:20.

Yang, G., Yang, L., Zhao, Z., Wang, J., and Zhang, X. (2012). Signature miRNAs involved in the innate immunity of invertebrates. *PLoS One* 7:e39015. doi: 10.1371/journal.pone.0039015

Zeng, D. G., Chen, X. L., Xie, D. X., Zhao, Y. Z., Yang, Q., Wang, H., et al. (2015). Identification of highly expressed host microRNAs that respond to white spot syndrome virus infection in the Pacific white shrimp *Litopenaeus vannamei* (Penaeidae). *Genet. Mole. Res.* 14, 4818–4828. doi: 10.4238/2015.may.11.14

Zhai, H., Fesler, A., and Ju, J. (2013). MicroRNA: a third dimension in autophagy. *Cell Cycle* 12, 246–250. doi: 10.4161/cc.23273

Zhang, Q., Zheng, S., Wang, S., Wang, W., Xing, H., and Xu, S. (2019). Chlorpyrifos induced oxidative stress to promote apoptosis and autophagy through the regulation of miR-19a-AMPK axis in common carp. *Fish Shellfish Immunol.* 93, 1093–1099. doi: 10.1016/j.fsi.2019.07.022

Zhang, Y., Wang, R., Du, W., Wang, S., Yang, L., Pan, Z., et al. (2013). Downregulation of miR-151-5p contributes to increased susceptibility to arrhythmogenesis during myocardial infarction with estrogen deprivation. *PLoS One* 8:e72985. doi: 10.1371/journal.pone.0072985

Zhou, M., Wang, A.-L., and Xian, J.-A. (2011). Variation of free amino acid and carbohydrate concentrations in white shrimp, *Litopenaeus vannamei*: Effects of continuous cold stress. *Aquaculture* 317, 182–186. doi: 10.1016/j.aquaculture.2011.04.033

Zhu, J., Yu, W., Liu, B., Wang, Y., Shao, J., Wang, J., et al. (2017). Escin induces caspase-dependent apoptosis and autophagy through the ROS/p38 MAPK signalling pathway in human osteosarcoma cells *in vitro* and *in vivo*. *Cell Death Dis.* 8:e3113. doi: 10.1038/cddis.2017.488

Conflict of Interest: The authors declare that the research was conducted in the absence of any commercial or financial relationships that could be construed as a potential conflict of interest.

frontiers in Cell and Developmental Biology

REVIEW
published: 12 April 2021
doi: 10.3389/fcell.2021.668735

Autophagic Organelles in DNA Damage Response

*Jeongha Kim[1], Sungmin Lee[1], Hyunwoo Kim[1], Haksoo Lee[1], Ki Moon Seong[2], HyeSook Youn[3] and BuHyun Youn[1,4]**

[1] Department of Integrated Biological Science, Pusan National University, Busan, South Korea, [2] Laboratory of Low Dose Risk Assessment, National Radiation Emergency Medical Center, Korea Institute of Radiological and Medical Sciences, Seoul, South Korea, [3] Department of Integrative Bioscience and Biotechnology, Sejong University, Seoul, South Korea, [4] Department of Biological Sciences, Pusan National University, Busan, South Korea

Autophagy is an important subcellular event engaged in the maintenance of cellular homeostasis *via* the degradation of cargo proteins and malfunctioning organelles. In response to cellular stresses, like nutrient deprivation, infection, and DNA damaging agents, autophagy is activated to reduce the damage and restore cellular homeostasis. One of the responses to cellular stresses is the DNA damage response (DDR), the intracellular pathway that senses and repairs damaged DNA. Proper regulation of these pathways is crucial for preventing diseases. The involvement of autophagy in the repair and elimination of DNA aberrations is essential for cell survival and recovery to normal conditions, highlighting the importance of autophagy in the resolution of cell fate. In this review, we summarized the latest information about autophagic recycling of mitochondria, endoplasmic reticulum (ER), and ribosomes (called mitophagy, ER-phagy, and ribophagy, respectively) in response to DNA damage. In addition, we have described the key events necessary for a comprehensive understanding of autophagy signaling networks. Finally, we have highlighted the importance of the autophagy activated by DDR and appropriate regulation of autophagic organelles, suggesting insights for future studies. Especially, DDR from DNA damaging agents including ionizing radiation (IR) or anti-cancer drugs, induces damage to subcellular organelles and autophagy is the key mechanism for removing impaired organelles.

Keywords: DNA damage response, mitophagy, ER-phagy, ribophagy, therapeutic approach

OPEN ACCESS

Edited by:
Guoping Zhao,
Hefei Institutes of Physical Science (CAS), China

Reviewed by:
Yushan Zhu,
Nankai University, China
Yanrong Zheng,
Zhejiang University, China
Jin Rui Liang,
ETH Zürich, Switzerland

****Correspondence:***
BuHyun Youn
bhyoun72@pusan.ac.kr

Specialty section:
This article was submitted to Cell Death and Survival, a section of the journal Frontiers in Cell and Developmental Biology

Received: *17 February 2021*
Accepted: *23 March 2021*
Published: *12 April 2021*

Citation:
Kim J, Lee S, Kim H, Lee H, Seong KM, Youn H and Youn B (2021) Autophagic Organelles in DNA Damage Response. Front. Cell Dev. Biol. 9:668735. doi: 10.3389/fcell.2021.668735

INTRODUCTION

Human cells receive several DNA lesions on $\sim 10^{13}$ cells per day in response to various genotoxic insults (Lindahl and Barnes, 2000). DNA damage, due to its potential for mutagenicity, has been shown to be involved in aging, disease, and cancer development. However, there are also positive aspects of DNA damage: both chemotherapy and radiation therapy are typically known to trigger apoptosis in cancer cells by inducing DNA damage. When DNA damage occurs, cells detect it *via* various mechanisms and monitoring systems, resulting in systematic responses to repair the damage, called DNA damage responses (DDRs). DNA damage is divided into double-strand break (DSB) and single-strand break (SSB). When DSB and SSB occur, DDR occurs to maintain the intracellular environment in a normal manner, and signal transduction begins through protein kinase in both DSB and SSB. Ataxia-telangiectasia mutated (ATM) is involved

in DSB, and ATM/Rad3-related (ATR) is involved in SSB. The ATM pathway begins when the MRE11/RAD50/NBS1 (MRN) complex binds to the DSB site and recruits ATM. Recruited ATM phosphorylates substrates such as checkpoint kinase 2 (CHK2) or mediator of DNA damage checkpoint protein 1 (MDC1). In the case of MDC1, it is known that a really interesting new gene (RING) finger protein 8 (RNF8), an E3 ubiquitin ligase, recognizes MDC1 and causes ATM to phosphorylate (Yan et al., 2014; Mirza-Aghazadeh-Attari et al., 2018; Tšuiko et al., 2019). Several studies described that DDR occurs through various mechanisms in subcellular organelles within a cell (Boesch et al., 2011). It has been reported that DDR can progress in four directions: activation of cell cycle checkpoint and transcriptional program, DNA repair, and apoptosis (Sancar et al., 2004). For example, radiotherapy and chemotherapy trigger DNA damage to promote cellular apoptosis or senescence as the consequence of the DDR. Recently, DNA damage emerged as a causal factor of aging. DNA damage has a role in aging and age-related diseases and it is further demonstrated by congenital progeroid syndromes.

The autophagy we usually know is macro-autophagy which is not selective. However, an increasing number of recent studies have drawn that autophagy can be greatly selective (Nakatogawa et al., 2009). In contrast to macro-autophagy, in which cytosolic components are engulfed randomly, selective autophagy targets specific cellular components and packages them into membrane vesicles (Mizushima et al., 2011; Rogov et al., 2014). In selective autophagy, these particular substrates are targeted to the autophagosome *via* specific receptors, and the targeted cargo can include protein aggregates, damaged mitochondria, or pathogens, such as bacteria. Besides, numerous studies have reported the selective autophagic degradation of several organelles, including mitochondria, peroxisomes, lysosomes, endoplasmic reticulum (ER), and the nucleus (Gatica et al., 2018). Since damaged such organelles need to be removed, autophagy machinery is activated. Many factors cause damage to organelles, and in the case of damage by DNA damaging agents, studies are continuing to show that autophagy is activated to control cell fate to maintain homeostasis in cells (Stagni et al., 2020). ATM, the major sensor of DSB, is involved in generating signal transduction by recognizing the damaged area when DNA damage occurs, and autophagy is activated by this ATM pathway (Eliopoulos et al., 2016). Ionizing radiation, one of DNA damaging agents, can induce DSB and is known to act as a trigger of autophagy through AKT signaling (Seiwert et al., 2017). In addition to the suggested DSB-related proteins, it is known that proteins required for SSB, such as Poly ADP-ribose polymerase 1 (PARP1), repair also regulate autophagy (Muñoz-Gámez et al., 2009). Autophagosomes engulf cytoplasmic material and organelles, including mitochondria, peroxisomes, lipid droplets, ribosomes, and parts of the nucleus, as part of the processes also known as mitophagy, pexophagy, lipophagy, ribophagy, and nucleophagy, respectively (Eliopoulos et al., 2016). During the autophagy processes, proteins with the LC3 interacting regions (LIR) in mammals are essential in dragging the organelles to autophagosomes (Anding and Baehrecke, 2017). The specificity of selective autophagy is divided according to the type of receptor and interaction with ubiquitin-like proteins through ubiquitin-like modifiers (UBLs) (Shaid et al., 2013). UBLs are directly involved in the autophagosome nucleation machinery, and this regulatory mechanism is a general selective autophagy mechanism; however, various types of selective autophagy activate specific pathways. For example, the PTEN-induced kinase 1 (PINK1)/Parkin pathway is specific to mitophagy, and pexophagy is associated with peroxisomal targeting signal 1 receptor (PTS1R), while the protein phosphatase 1D (PPM1D) pathway is to related lipophagy (Chu, 2019).

The role of autophagy in managing cellular DNA aberrations has been demonstrated by numerous studies. Currently, autophagic degradation of subcellular organelles, including mitochondria, ER, and ribosome, is involved in the determination of cell fates after DNA damage. In this review, we summarize the molecular mechanisms of subcellular autophagic degradation of organelles induced by DDRs and their contribution to managing DNA damage. In addition, we present the pathological mechanisms of the autophagy-related DDR and its potential as a therapeutic target.

DDR AND AUTOPHAGIC ORGANELLES

Mitophagy

Mitochondria are organelles with a double membrane that play a central role in the energy metabolism of cells *via* oxidative phosphorylation. Mitochondria also contain genetic information called mitochondrial DNA (mtDNA) (Henze and Martin, 2003). There are several differences between mtDNA and the nuclear genome. Unlike the linear nuclear genome, the circular mitochondrial genome is not enveloped and it is not packaged into chromatin. Thirteen mitochondrial genes play a pivotal role in the survival of cells that produce the subunits of enzymes necessary for oxidative phosphorylation; however, the mitochondrial genome is very small and cannot produce all functionally necessary proteins. As a result, mitochondria are highly dependent on imported nuclear gene products (Taanman, 1999). The mitochondrial genome is exposed to the harmful agents that adversely affect the nuclear genome. Therefore, the DDR in mitochondria can also play a critical role in determining cell fate (Babbar et al., 2020). For this reason, the regulation of mitochondrial homeostasis through mitochondrial biogenesis, bioenergetics, dynamics, mitophagy, and DNA status is important from a cellular perspective (Yu et al., 2017).

Mitophagy is known as the process of removing mitochondria through the autophagy that regulates the homeostasis of mitochondria by eliminating dysfunctional mitochondria. Cell damage that changes energy requirements and developmental changes can all induce mitophagy (Hirota et al., 2015). When gemcitabine, a drug that destroys mtDNA, is used, mitochondrial dysfunction occurs and mitophagy pathway is activated (Inamura et al., 2019). As new mitophagy-related pathways have been demonstrated, the importance of mitophagy is emerging. Mitophagy is regulated by the p53-Spata18 axis (Dan et al., 2020), the PINK1/Parkin pathway, and BCL2 Interacting Protein 3 Like (BNIP3L)/NIX and FUN14 Domain

Containing 1 (FUNDC1) related pathway. Among them, the PINK1/Parkin is a key protein for mitophagy signals. Based on the paper, reactive oxygen species (ROS), one of the DNA damaging agents, occurred in the Dox-treated group, activating the PINK1/Parkin pathway and lowering the expression of mitochondrial proteins (Yin et al., 2018). Mitophagy is initiated when an autophagy receptor called PINK1 recognizes damaged mitochondria. In healthy mitochondria, PINK1 is imported into the inner mitochondrial membrane (IMM) through translocase of the outer membrane channel (TOM) and translocase of the inner membrane channel (TIM) by the membrane potential of mitochondria. This leads to the mitochondrial targeting signal being cleaved first by the matrix processing peptidase and then by the protease presenilin-associated rhomboid-like, resulting in the degradation of PINK1 by the proteasome. In damaged mitochondria, the membrane potential of the mitochondria is not maintained. Therefore, PINK1 is not imported into the IMM and accumulates in the membrane of the mitochondria (Nguyen et al., 2016). Accumulated PINK1 recruits an E3 ubiquitin ligase called Parkin that plays a critical role in ubiquitination. When PINK1 and Parkin bind, Parkin ubiquitinates OMM proteins such as mitochondrial profusion protein mitofusin 1 (MFN1), MFN2, voltage dependent anion channels (VDAC), and ras homolog family member T1 (RHOT1/MIRO1) (Shanbhag et al., 2012; Yao et al., 2020), and recruits mitophagy receptor optineurin (OPTN) and nuclear dot protein 52 kDa (NDP52) which is also known as calcium binding and coiled-coil domain 2 (Calcoco2) (Liu et al., 2019). These ubiquitinated proteins act as signals and recruit autophagic machinery to remove damaged mitochondria (McWilliams and Muqit, 2017). Fanconi anemia (FA) pathway genes, known as tumor suppressors, are involved in the repair of damaged nuclear DNA. Also, the association between Parkin and FA pathway genes was revealed, so these proteins may be an important factor in the induction of mitophagy (Sumpter et al., 2016). As such, Parkin and PINK1 are important proteins for mitophagy initiation, and recent paper results that prevent inflammation by removing damaged mitochondria by Parkin-mediated mitophagy suggest that mitophagy is crucial not only in DDR but also in the pathogenesis of other diseases (Sliter et al., 2018). Another mitophagy signal, the BNIP3L/NIX and FUNDC1 pathway, is initiated by FUNDC1 interacting with LC3. FUNDC1 is an outer mitochondrial membrane (OMM) protein, and its interaction with LC3 is regulated by multi-site phosphorylation. This pathway is activated in hypoxic conditions that cause DNA damage and is known to be important as a regulator of the mitochondrial network in the process of cell differentiation (Lampert et al., 2019; Fu et al., 2020).

Ataxia-telangiectasia mutated, a serine-threonine protein kinase, is a well-known mediator of DDR which plays a crucial role in maintaining cellular processes, such as hypoxia, oxidative stress, DNA repair, apoptosis, and senescence (Derheimer and Kastan, 2010; Guleria and Chandna, 2016). The intracellular ATM is primarily localized in the nucleus, while smaller amounts can be found in the cytosol and organelles, such as mitochondria and peroxisomes (Alexander et al., 2010). Based on the knowledge that ATM is kinase and affects the phosphorylation of PINK1 (**Figure 1**) which is indispensable for the biological function of Parkin activation (Gu et al., 2018). According to the latest research, ATM has been shown to regulate autophagy *via* tuberous sclerosis complex two or *via* the phosphorylation of hypoxia-inducible factor 1α. Furthermore, the role of ATM in mitophagy was confirmed in ATM-proficient cells and ATM-deficient cells with the spermidine-induced mitophagy model. Specifically, spermidine, which has a protective function against oxidative damage caused by hydrogen peroxide, induces mitophagy by causing mitochondrial depolarization (Eisenberg et al., 2009; Qi et al., 2016; Madeo et al., 2018). Depolarization of mitochondria means defective mitochondria, which causes accumulation of Pink1 and translocation of Parkin to damaged mitochondria leads to decreased mitochondrial mass in ATM-proficient cells (Qi et al., 2016). Whereas the loss of ATM results in mitochondrial abnormalities and the impairment of mitophagy, eliciting the accumulation of dysfunctional organelles (Valentin-Vega et al., 2012). Another research showed that by modulating DNA repair defects, it is possible to alleviate pathologies resulting from genome instability. PARP1 mediated immoderate poly ADP-ribosylation and it could alleviate the NAD^+ levels which result in defective mitophagy (Fang et al., 2014, 2016). Recently, this mechanism has been demonstrated in neuroblastoma cells. ATM depletion results in a similar mitochondrial phenotype and mitophagy alteration. These phenomena could be partially rescued by NAD^+ cofactor replenishment (Fang et al., 2016).

Ring finger protein 8 is a major factor in DNA DSB signaling pathway (Ma et al., 2011; Fang et al., 2016; Nakada, 2016). The RING finger-containing E3 ligase family is E3 ubiquitin ligases, and the specificity and ubiquitination type of substrate are determined by E3 ubiquitin ligase. In response to DNA damage, RNF8 mediates histone H2A and H2B mono-ubiquitination and facilitates the propagation of the DNA damage, the processes indispensable for DNA damage repair and activation of cell cycle checkpoint, and necessary to maintain genomic stability (Wu et al., 2009; Bohgaki et al., 2010). The primary function of RNF8 is to convert the DSB signal caused by exogenous or endogenous factors such as ionizing radiation (IR) or ROS, respectively (Yan and Jetten, 2008). A few recent reports confirmed the presence of RNF8 in the mitochondria; it was previously identified as a nuclear E3 ligase involved in non-homologous end-joining DNA damage repair. Ubiquitin receptors play the role of binding and transferring ubiquitinated cargo to the phagophore, initiate mitophagy (Husnjak and Dikic, 2012). In addition, it has been reported that 53BP1 (**Figure 1**), a DDR protein, is involved in damaged mitochondria clearance through mitophagy (Youn et al., 2017). Furthermore, it has already been reported that RNF8 is required for 53BP1 recruitment (Shao et al., 2009). These findings provide clear evidence that RNF8 can induce a DDR through mitophagy.

As a tumor suppressor, p53 has many different functions. A functional DDR prevents cells from uncontrolled proliferation; however, mutations could affect genes that control the DDR of the cell. DDR controls the biological signal a cell can enter and proceed through the cell cycle (Bartek and Lukas, 2007). p53 plays a crucial role in regulating cellular proliferation in response to DNA damage. Usually, p53 is a short-lived protein, and the

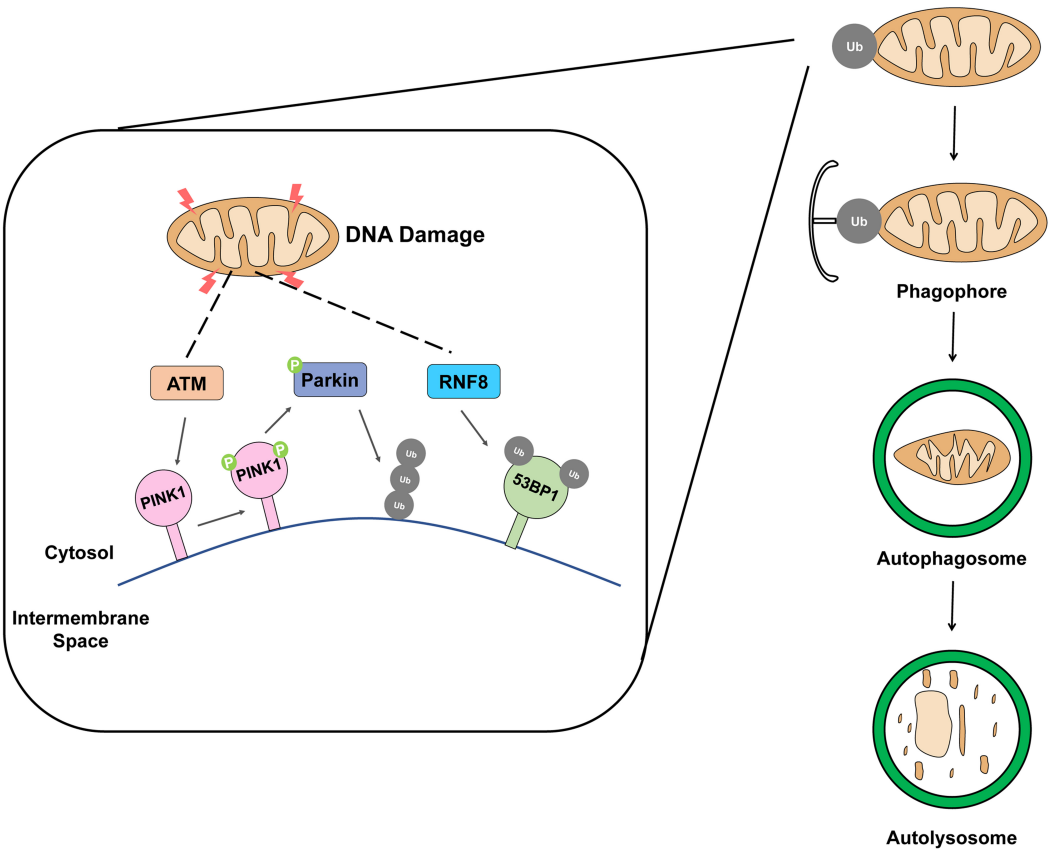

FIGURE 1 | Schematic representation of removing damaged mitochondria by mitophagy. The accumulation of damaged mitochondria is removed by mitophagy when mitochondria are exposed to DNA damage factors such as ionizing radiation, ROS, and drug.

activity of p53 is very strictly regulated through various processes including transcriptional and translational regulation and post-translational modifications (Honda et al., 1997). Moreover, p53 is rapidly ubiquitylated by mouse double minute 2 homolog (MDM2) and is subsequently targeted for degradation by the ubiquitin-dependent proteasomal system (Momand et al., 1992). However, when DNA damage occurs, p53 is stabilized by the DDR signaling system. In that particular case, p53 acts as a transcription factor and regulates the expression of target genes of p53 through a response factor in the promoter of that gene (Beckerman and Prives, 2010). The activity of p53 is also regulated by a number of post-translational modifications. As is widely known, p53 is involved in many signaling pathways and is known to have a bidirectional role in regulating autophagy. p53 plays a role in inducing the autophagy mechanism by activating AMPK, and also plays a role in inhibiting the autophagy mechanism by inhibiting the PI3K/Akt signaling pathway through the increase of PTEN expression (Zhang et al., 2015). Unlike ATM and RNF8, p53 binds to the RING0 region of Parkin, which interferes with the mitophagy process involved in Parkin, and affects mitochondria quality control, biosynthesis, kinetic regulation, and cellular redox homeostasis (Jung et al., 2017; Korolchuk et al., 2017). These results confirmed that mitophagy was increased by the downregulation of p53 in both *in vivo* and *in vitro* experiments using bone marrow mesenchymal stem cells (Zhang et al., 2020).

ER-phagy

After translation, newly synthesized proteins enter the ER lumen and are structured according to their characteristics. If the protein modification process in the ER has trouble such as protein misfolding, a process called unfolded protein response (UPR) occurs that activates the intracellular signaling pathway for cells to maintain homeostasis. ER performs several functions, including folding of protein molecules and transporting proteins synthesized from vesicles to the Golgi apparatus. Unfolded protein, disturbance of redox or calcium regulation, and glucose deficiency trigger UPR and activate ER stress response (Kober et al., 2012). Recent clinical and preclinical studies suggest that ER stress is related to various metabolic diseases such as insulin resistance, diabetes, obesity, non-alcoholic fatty liver disease, and atherosclerosis. Therefore, proper regulation of ER stress can be a way to prevent the causes of various diseases. The ER stress pathway generated by UPR is closely linked to biological pathways such as cell survival, proliferation, autophagy, and apoptosis (Jäger et al., 2012; Ciechomska et al., 2013). While damaged mitochondria undergo targeted removal *via* mitophagy, as a result of ER stress, the portions of the ER are sequestered

in autophagosomes in the process called ER-phagy, the type of selective autophagy to survive in severe ER stress condition. In general, ROS, one of the most representative factors known to cause DNA damage, induces ER stress. Several studies have reported that biological processes caused by ER stress are closely related to DNA damage (Groenendyk et al., 2010; Dicks et al., 2015). DNA damage induces the extension of tubular ER to facilitate ER-mitochondria signaling, thereby promoting apoptosis, a common mechanism of DDR (Zheng et al., 2018). Also, ER stress modulates the p53-related signaling pathway, leading to G2 arrest, thereby promoting apoptosis (Mlynarczyk and Fåhraeus, 2014). Studies are underway to reveal the link between DNA damage and ER stress, and it is known that p53 and C/EBP-homologous protein (CHOP) mainly regulate the life cycle of cells in ER stress conditions. p53 and CHOP are transcription factors and monitor genome integrity and stability. CHOP is upregulated by UPR, which is related to ER stress and generates ER stress response such as autophagy (Bernales et al., 2006; Hu et al., 2018).

Selective autophagy, ER-phagy, involves the formation of autophagosomes made from the ER membrane. ER is involved in the formation of autophagosome, and damaged ER is engulfed by itself by ER-phagy. Since ER-phagy also plays a role in removing the superfluous part from ER, ER-phagy activated against UPR can be said to be very important to establish homeostatic control (Bernales et al., 2007). ER-phagy could be similar to the regulation of peroxisome number, the balance between peroxisome biogenesis and pexophagy, and to the control of mitochondrial homeostasis (Dunn et al., 2005; Kundu and Thompson, 2005). TFEB and TFE3, nutrient responsive transcription factors, increase the expression of ER-phagy receptor reticulophagy regulator 1 (RETREG1)/FAM134B to induce ER-phagy (Cinque et al., 2020). C53, a cytosolic protein, is involved in the formation of autophagosome under ER stress condition (Stephani et al., 2020). A lot of effort is being put into identifying the ER-phagy mechanism. ER stress caused by the accumulation of unfolded proteins is the activation of UPR via three transmembrane proteins: inositol-requiring enzyme 1 (IRE1), protein kinase RNA-like ER kinase (PERK), and activating transcription factor 6 (ATF6) (Hetz, 2012). IRE1 and PERK are autophosphorylated, and ATF6 is exported to the Golgi apparatus and undergoes additional proteolytic cleavages. The downstream signaling pathways of these three proteins regulate the translation and transcription of proteins involved in relieving ER stress, and act as important factors in each step of the ER-phagy process, which removes damaged ER (Song et al., 2018).

Inositol-requiring enzyme 1 is a sensor that activates UPR in the ER transmembrane and is a necessary factor to maintain ER and cellular function in animals and plants. IRE1 monitors ER homeostasis and determines whether the ER environment is appropriate or not by the luminal domain of the ER stress sensor present in IRE1. Thereafter, IRE1 triggers UPR through kinase and RNase cytoplasmic domains (Hetz and Glimcher, 2009; Hetz et al., 2011). In the UPR process, when a signal goes from the luminal to the cytosolic side of the ER, the signaling cascade proceeds and ER swelling occurs. The connection between ER-phagy and IRE1 is not well understood, however, there are experiments to elucidate the mechanism between the two. Epr1, a soluble ER-phagy receptor, was severely diminished in Δ*ire1* indicating that Epr1 upregulation requires Ire1 (Zhao et al., 2020). In another study, an experiment using 3-methyladenine or *Atg5* knockdown, which can inhibit autophagy, resulted in the finding that inhibition of autophagy can inhibit the IRE1 pathway of UPR (Liao et al., 2019). It can be said that the presented study results well explain the mechanism between IRE1 and ER-phagy. In mammalian cells, vesicle-associated membrane protein-associated proteins (VAPs) are involved in autophagosome formation by recruitment of the ULK1 complex and promote the connection between the ER and the autophagosome membrane (Bissa and Deretic, 2018). IRE1 forms a complex with tumor necrosis factor receptor-associated factor-2 (TRAF2) and apoptosis signal-regulating kinase-1 (ASK1), resulting in the downstream activation of stress kinase Jun-N-terminal kinase (JNK) that promotes autophagy (Ron and Hubbard, 2008; Gardner and Walter, 2011). Bcl-2 phosphorylated by JNK becomes an activated form and the Beclin-1/Bcl-2 complex is not formed. Free Beclin-1, which cannot form a complex with Bcl-2, forms a complex with vacuolar protein sorting 34 (VPS34) and is involved in the nucleation stage of autophagy (Pattingre et al., 2005). In addition, X-box binding protein-1 (XBP-1) is also activated by IRE1, promoting the transcription of Beclin-1, which is involved in autophagy induction (**Figure 2**; Hetz et al., 2009).

Protein kinase RNA-like ER kinase is one of the major transducers of ER stress and participates in the regulation of basic cellular functions. Autophagy and apoptosis signals induced by ER stress can be transmitted through the PERK signaling pathway, which has a switch mechanism to regulate cell death or cell survival (Liu et al., 2015). PERK activates activating transcription factor 4 (ATF4), a major transducer, by inhibiting the general protein translation process through phosphorylation of eIF2α (Rutkowski and Hegde, 2010; Hetz, 2012). ATF4 transcriptionally regulates Atg12, and ATF4-mediated CHOP activation transcriptionally induces Atg5, which includes the elongation process during autophagy (B'Chir et al., 2013; Kang et al., 2017). ATF4 upregulates light chain 3 (LC3), which plays a key role in the elongation and maturation of autophagosomes. LC3 interacts with the receptor of ER to selectively recognize defective ER and recruitment to proceed with ER-phagy (**Figure 2**). In addition, PERK, like IRE1, activates Beclin-1 to regulate the induction and nucleation stages of ER-phagy (Deegan et al., 2013).

Activating transcription factor 6 is a transcription factor and is transported to the Golgi apparatus when ER stress occurs, and then the N-terminal cytosolic domain is cleaved and moved to the nucleus. ATF6 moved to the nucleus binds to the ATF-cAMP response element and promotes transcription of ER stress response factors such as *XBP-1* and *CHOP* (Adachi et al., 2008; Guo et al., 2014). The activation of ER stress occurs *via* the eukaryotic translation initiation factor 2 alpha kinase 3 (EIF2AK3) and ATF6 UPR pathways, but not the ER to nucleus signaling 1 (ERN1)-XBP1 pathway, along with the upregulation of downstream signaling pathway both ATF4 and DNA damage inducible transcript 3 (DDIT3) (Wang et al., 2018). The ATF6

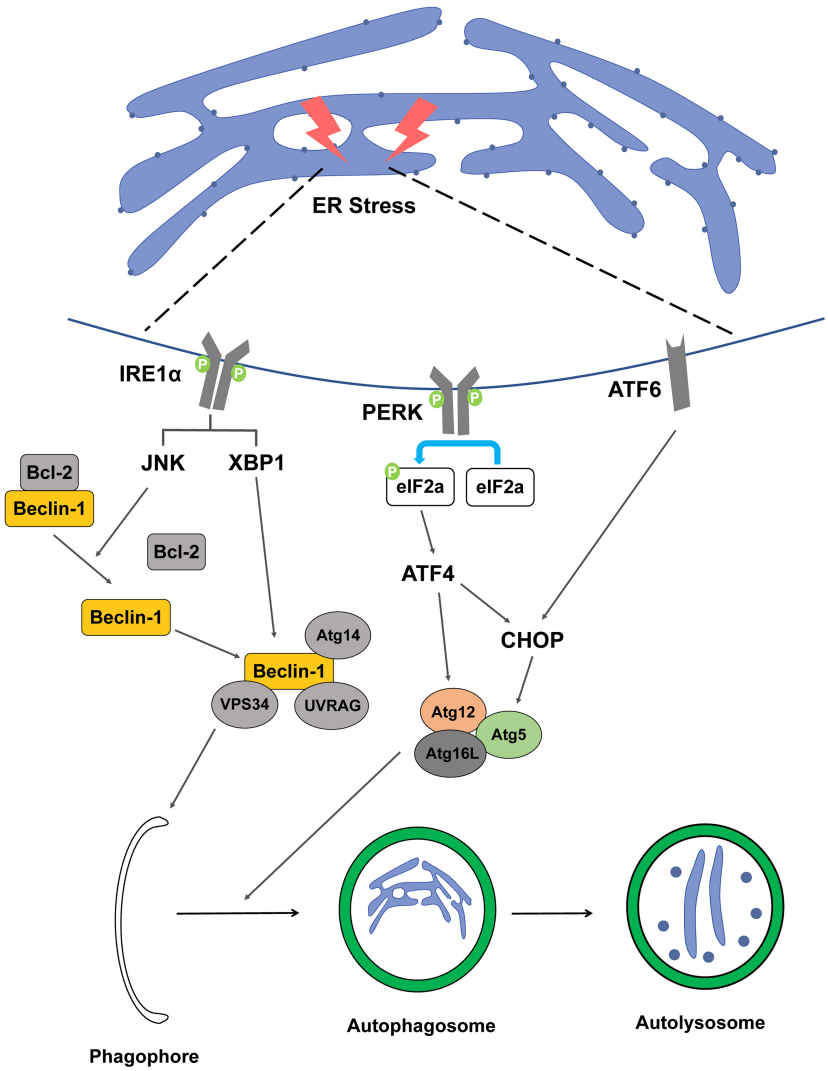

FIGURE 2 | Schematic representation between ER stress factor and ER-phagy. The figure represents a signaling pathway of ER-phagy while damaged ER is engulfed by autophagosome. When ER stress is induced by DNA damage, the IRE1a, PERK, and ATF6 signaling pathways are activated, resulting in the formation of autophagosomes.

signaling pathway is required for the activation of ER-phagy (**Figure 2**). ER-phagy proceeds in the same system as general macro-autophagy and ATF6 is involved in this process under ER stress (Song et al., 2018). In addition, ATF6 induces the expression of death-associated protein kinase 1 (DAPK1), a kinase that phosphorylates Beclin-1 to form a phagophore, and interacts with C/EBP-β to not only participate in ER expansion but also contribute to the ER-phagy process (Gade et al., 2012).

Ribophagy

Crosstalk between DDR and ribosome biogenesis has recently been reported. When the activated ATM n recruits NBS1 (Nijmegen Breakage Syndrome protein 1) to the nucleolus, this complex inhibits rDNA transcription (Larsen et al., 2014). This regulatory mechanism has a crucial role in the conservation of the stability of the rDNA genome which has a highly repetitive and actively transcribed feature. The ATM/NBS1/Treacle response is the particularly important response in the rDNA replication process. This response leads to forming DNA:RNA hybrids or R-loops and breakage of DNA double-strand (Pelletier et al., 2018). Thus, the ATM/NBS1/Treacle response is maintained at an appropriate level with the impaired ribosome synthesis checkpoint-p21 response to protect against DNA damage, which suggests that ribosome biogenesis in replicative stress is important (Pelletier et al., 2020). In addition, it has been found that ROS, one of the representatives DDR agents, not only attacks ribosome components but also affects ribosomes indirectly by altering the activities of ribosome-modifying enzymes. Ribosome modification by ubiquitin is one such example (Shcherbik and Pestov, 2019).

The molecular mechanisms of ribophagy have not been fully elucidated yet. Most studies have been performed using

yeast models, and only a few studies have been conducted in mammalian models. Specific regulation of ribophagy is mediated by the deubiquitination of listerin E3 ubiquitin protein ligase 1 (Ltn1) by the ubiquitin carboxyl-terminal hydrolase 3 (Ubp3)/brefeldin A sensitivity 5 (Bre5) complex. A previous study showed that DNA damaging reagents induced the activity of the Ubp3/Bre5 complex, supporting the significance of ribophagy as a DDR (Bilsland et al., 2007). In addition, Ltn1 has been reported to recover the production of misfolded proteins derived from damaged mRNA (Yan et al., 2019), while nuclear fragile X mental retardation-interacting protein 1 (NUFIP1) was shown to serve as the major receptor of ribophagy machinery through specific binding to LC3B *via* the LIR motif within the NUFIP1. NUFIP1 targets the 60S ribosomal subunit; however, the actual ligand for this mechanism is not known and still needs further investigation (Wyant et al., 2018). To find out the mechanism of ribophagy, an experiment was conducted using Purkinje cells (PC), and macro-segregation of nuclear components and heterochromatinization were observed in these cells. This indicates a serious dysfunction of nuclear and extranuclear transcription, and it was found that free polyribosomes are replaced by monoribosomes (Baltanás et al., 2011). These monoribosomes were closely wrapped and appeared isolated into cytoplasmic compartments bound by sequestered rough endoplasmic reticulum (RER) cisterns and known as autophagosomes (Kraft et al., 2008). Accumulation of DNA damage in PCs of PC degeneration (pcd) mice results in nucleosome destruction, polyribosomal and monoribosomal autophagic degradation. This observation suggests that autophagy-related pathways are involved in the selective degradation of ribosomes and can be said to be a study to investigate the mechanism of ribophagy (Baltanás et al., 2011).

In the case of ribophagy, the role in yeast was first identified. Ubp3 in Yeast forms a complex with Bre5, a pivotal positive regulator (Li et al., 2005). The Ubp3/Bre5 complex is responsible for a wide variety of intracellular functions such as transcription elongation (Kvint et al., 2008), DNA repair by non-homologous end joining (Bilsland et al., 2007), and protein kinase C-mediated signaling (Wang et al., 2008). Another Ubp3/Bre5 complex plays a role in the autophagy process. It regulates the cytoplasm-to-vacuole targeting pathway through its action on Atg19, as well as the degradation of mature ribosomes that occur in starvation situations (Kraft et al., 2008). Another factor known to regulate ribophagy, Ltn1, is a protein known to perform ribosome-associated quality control (Bengtson and Joazeiro, 2010). In the absence of Ltn1 alone, it cannot directly affect the ribophagy pathway, but in the absence of Ubp3, it regulates the ribophagy pathway involving Ubp3/Bre5 complex instead (Ossareh-Nazari et al., 2010).

Ribophagy has recently been identified in mammalian cells. NUFIP1, an autophagy receptor for ribosomes, is required for ribophagy. NUFIP1 has an LIR motif and can bind to LC3 and forms a heterodimer with zinc finger HIT domain-containing protein 3 (ZNHIT3) to participate in the ribophagy process (**Figure 3**; Quinternet et al., 2016). It is known that NUFIP1-ZNHIT3 has a high probability of interacting with the 60S ribosomal subunit, and further studies are needed for detailed this pathway (Klinge et al., 2011). In the cytoplasm, NUFIP1 interacts with LC3 and transfers ribosomal cargo directly to the autophagosome. The degradation of ribosome induced in a starvation environment is accomplished through ribophagy, and this process depends on the capacity of NUFIP1 to bind to LC3 (Wyant et al., 2018). However, a ribosomal factor which interacted with NUFIP1 has not yet been identified, so further research is needed.

CLINICAL ROLES OF THE AUTOPHAGIC ORGANELLES IN DDRS

Molecular Pathology of DDR-Related Autophagic Organelles

Defects in DNA repair pathways induce the modification of DNA, and if this modification continues, mutations may accumulate and defects in polymerization and transcription of DNA or RNA may occur. These defects in the DNA repair mechanism induce apoptosis and aging, which could soon become a starting point for various diseases (Tiwari and Wilson, 2019). Many studies have shown that various diseases are caused by defects in the DNA repair system. Diseases caused by these defects are mostly related to aging and cancer. Furthermore, recent studies have shown that defects in the DNA repair system are known as a new cause of diseases associated with polyglutamine disease, such as Huntington's disease, spinocerebellar ataxias, and other neurodegenerative disorders (Qi et al., 2007). Here, we summarize the latest research that connects diseases and autophagy in each subcellular organelle (mitochondria, ER, and ribosome), with the defects in the DNA repair system.

Mitochondrial dysfunction is associated with numerous biological phenomena including cancer. PINK1 is one of the representative factors related to mitochondrial function. Aging is known to be a major factor in causing cardiovascular disease (Liang and Gustafsson, 2020) and is also known as a major reason for age-related diseases such as Alzheimer's disease (AD), Parkinson's disease (PD), and Huntington's disease (HD), and amyotrophic lateral sclerosis. Such aging proceeds according to biological conditions such as oxidative damage, telomere length, and mitochondrial dysfunction, and it is known that mitophagy is involved in regulating these abnormal environments (Tran and Reddy, 2020). When mitochondria are damaged, it is widely known to affect aging and neurodegeneration. As the name of Parkin, this protein is widely known as the protein associated with PD. Neurodegeneration in PD is related to mitochondrial dysfunction, and recently, studies have shown that PINK1/Parkin-dependent mitophagy responding to mitochondrial damage is associated with PD (Malpartida et al., 2021). Besides, there has been a study on the pathogenesis of PD through the association between α-synuclein aggregation and neuroinflammation (Liu et al., 2019). Mitochondrial dysfunction was also observed in a nucleotide excision DNA repair disorder with severe neurodegeneration (Fang et al., 2014). Synthetically, mitophagy could be a promising strategy in the treatment of neurodegenerative disorders. PINK1 has been reported as a gene

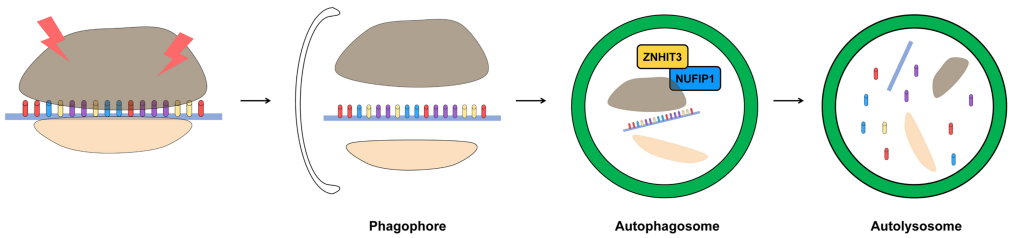

FIGURE 3 | Schematic representation of removing damaged ribosome by ribophagy. The accumulation of damaged ribosome is removed by ribophagy. For the most part, the ribosome is related to RNA but ribosome biogenesis is affected by DNA. DNA damage interrupts ribosome biogenesis and decreases the stability of rDNA. ZNHIT3 and NUFIP1 have been suggested as a major factors of ribophagy induction in mammalian cells.

whose expression is increased by overexpression of PTEN, a representative tumor suppressor in cancer cells. PINK1 has also been shown to be downregulated in the absence of PTEN (Unoki and Nakamura, 2001). Research over the past decade has shown that PINK1 is implicated in various cellular functions such as cell survival, stress resistance, and mitochondrial homeostasis in cancer cells (O'Flanagan and O'Neill, 2014). PTEN is one of the most frequently mutated genes in several cancers, including glioblastoma, endometrial, breast and prostate cancers (Steck et al., 1997). Since it was found that PINK1 is regulated by PTEN, studies on the relationship between PINK1 and PI3-kinase/Akt signaling system have been intensively conducted. PTEN-induced increase in PINK1 and decrease in PI3K/AKT have been found in PD and several cancers, suggesting that PINK1 plays an important pathological function (MacKeigan et al., 2005). PINK1 has an important pathophysiological function, so it could be a promising drug target in diseases such as neurodegeneration, aging, and cancer.

Ataxia-telangiectasia mutated gene mutations cause the development of Ataxia-Telangiectasia (AT). AT is a rare genetic disorder that affects body systems, including the nervous and immune systems. All AT patients have mutations in the *ATM* gene. Dysfunction in DNA damage repair, apoptosis, and cell cycle is due to mutations in the *ATM* gene. BNIP3, acting as an inducer of mitophagy, showed low expression levels in AT cells, suggesting that the mitophagy pathway malfunctions when the *ATM* gene is mutated (Sunderland et al., 2020). It is known that AT patients also have an increased risk of cancer due to the loss of ATM function (Friedenson, 2007). Usually, a heterozygous mutation of ATM is found in cancer. According to the Somatic Mutation Catalog of Cancer (COSMIC), the frequency of *ATM* gene mutation is 0.7% in 713 ovarian cancers, 0.9% in central nervous system cancers, 1.9% in 1,120 breast cancers, 2.1% in 847 kidney cancers, 18% in 74 colon cancer, 7.2% in 1,040 lung cancers, and 11.1% in 1,790 hematopoietic and lymphoid tissue cancers. In pancreatic cancer, one of the representative malignant carcinomas, it has been reported that 6.4% of 5,234 patients had an ATM mutation in germ cells or somatic cells (Cremona and Behrens, 2014).

RNF8 is an enzyme that plays an important role in DNA repair and an appropriate level must be maintained. It has been reported that RNF8 causes genomic instability, tumorigenesis, and malignant tumors when RNF8 exceeds appropriate levels and accumulates excessively (Singh et al., 2019). Additionally, RNF8 is an associated partner of estrogen receptor α (ERα) and activates ERα-mediated responses in breast cancer cells *in vitro*. As with the results *in vitro*, it was confirmed that RNF8 was positively correlated with ERα in breast cancer patient tissues (Wang et al., 2017). Conversely, even when the expression of RNF8 is reduced, pathological issues arise. It has been reported that the expression of RNF8 decreases when infection or disease progresses, causing genomic instability in adult T-cell leukemia (Zhi et al., 2020). Recent studies also reported that decreased expression of RNF8 increases genomic instability and vulnerability to tumorigenesis in prostate cancer (Li et al., 2010). These results indicate that RNF8, a key factor of DNA repair, has potential as a novel tumor suppressor.

p53 actually has many functions, and disease can occur if the level of this protein is not properly regulated. Recent studies have shown that mitophagy upregulates hepatic cancer stem cells (CSCs) by inhibiting p53, well known as a tumor suppressor. Transcription factors are important for maintaining the stemness and self-renewal capacity of CSCs. For example, when phosphorylated p53 binds to the NANOG promoter, it is important to reduce the hepatic CSC population by preventing transcription factors OCT4 and SOX2 from upregulating the expression of NANOG. Mitophagy regulates the ability of p53 to maintain hepatic CSCs, providing an explanation why autophagy is necessary for promoting hepatocarcinogenesis. p53 downregulates NANOG and is eliminated together with mitochondria by mitophagy (Liu et al., 2017).

Cellular stress can disturb the protein-folding functions of ER, driving many types of cancer cells to activate the UPR as the means of sustaining malignant growth while retaining viability (Wang and Kaufman, 2014). In estrogen receptor α positive ($ER\alpha^{+}$) breast cancer, the UPR in general, and XBP1 in particular, contribute to acquired resistance against anti-endocrine therapy (Clarke and Cook, 2015). A recent study revealed that triple-negative breast cancer (TNBC) cells highly depend on IRE1 to adapt their ER to *in vivo* stress and to accommodate the tumor microenvironment to promote malignant growth. Other studies have also linked the IRE1α–XBP1s pathway to the MYC, transcription factor and a potent driver of proliferation in TNBC, prostate cancer, and B-cell lymphoma. In addition, IRE1 mutations in glioblastoma multiforme were recently reported, with one mutated form of IRE1 characterized by elevated

regulated IRE1-dependent decay activity and reduced ability to form tumors *in vivo* (Sheng et al., 2019).

Recent studies investigating the role of PERK have suggested both pro- and anti-tumorigenic functions. PERK signaling pathway is used when both tumor initiation and expansion to maintain redox balance for facilitating tumorigenesis (Bobrovnikova-Marjon et al., 2010). The activation of PERK-eIF2α axis causes reduction of proliferation and increase of apoptosis and this pathway during the loss of intestinal epithelial stemness and enforced differentiation (Heijmans et al., 2013). Subsequent studies demonstrated that PERK signaling mediates arrest in the G1 phase. Activation of PERK and phosphorylation of eIF2α suppress protein translation, including cyclin D1 (Hamanaka et al., 2005). Because of its short half-life, expression of cyclin D1 is greatly decreased during ER stress. Decreased cyclin D1 expression results in the impaired activity of cyclin D1-CDK4 complex, thereby ensuring cell cycle arrest at the G1 phase (Brewer et al., 1999).

There is a significant correlation between the expression of ATF6 and inhibitor of DNA binding 1 (ID1) in high-grade serous ovarian cancer tissues. Furthermore, patients with high expression of ATF6 or ID1 have a resistance to platinum treatment and the overall survival rate was low (Meng et al., 2020). In addition, ATF6 was found to be highly expressed in areas undergoing pre-cancerous atypical change in both non-ulcerative colitis (UC) and UC-associated CRC, and this can be used to determine the grade level of UC patients (Hanaoka et al., 2018). In addition, in the mouse model with high ATF6 expression, after 4 days of the activation of ATF6, the bacteria were close to the colon epithelium, the cell proliferation rate was faster, and 100% tumors developed within 26 weeks. It suggests that these alterations are early events activation of ATF6 downstream. These findings suggest that activated ATF6 induces an innate immune response to promote colorectal tumorigenesis (Lavoie and Garrett, 2018).

TABLE 1 | Pharmacological targeting of DDR factors.

Target	Compound	Stage	References
ATM	KU55933	Preclinical	Hickson et al., 2004
	KU60019	Preclinical	Golding et al., 2009
	CP466722	Preclinical	Rainey et al., 2008
	Caffeine	Preclinical	Blasina et al., 1999
	Wortmannin	Preclinical	Sarkaria et al., 1998
	TPA	Preclinical	Truman et al., 2005
	Vitamin B3	Phase 2	NCT03962114
RNF8	Corilagin	Preclinical	Qiu et al., 2019
p53	STIMA-1	Preclinical	Zache et al., 2008
	APR-246	Preclinical	Bykov et al., 2002; Bykov et al., 2005b
	CP-31398	Preclinical	Foster et al., 1999
	MIRA-1	Preclinical	Bykov et al., 2005a
	RITA	Preclinical	Issaeva et al., 2004; Jones et al., 2012
IRE1	B-109	Preclinical	Tang et al., 2014
	STF-083010	Preclinical	Chen et al., 2018
	KIRA6–8	Preclinical	Ghosh et al., 2014; Morita et al., 2017
	Toyocamycin	Preclinical	Ri et al., 2012
	Doxorubicin	Preclinical	Jiang et al., 2016
PERK	GSK2606414	Preclinical	Mercado et al., 2018
	GSK2656157	Preclinical	Atkins et al., 2013
ATF6	Ceapin-A7	Preclinical	Gallagher and Walter, 2016
	PBA	Early Phase 1	NCT04041232

Pharmacological Approach to DDR-Related Autophagic Organelles

Based on the pathological mechanisms induced by defects in the DNA repair system related to autophagy for each organelle described above, we summarize here the research treatment strategies for each disease, as well as the potential for each factor as a drug target (**Table 1**).

In the latest research, several studies showed increased cellular sensitivity toward genotoxic agents by modulating the ATM signaling *via* the specific ATM kinase inhibition. This drug induced tumor senescence in breast, lung, and colon carcinoma cell lines and verified the ATM/ATR signaling pathway to be constitutively active in cancer cells. Furthermore, the addition of the ATM kinase-specific inhibitor KU55933 (Hickson et al., 2004) or another ATM/ATR dual inhibitor CGK733 (Alao and Sunnerhagen, 2009), caused the increase of apoptosis in these cancer cells. Interestingly, although this treatment was cytotoxic to these cells, it did not lead to apoptosis in the normal senescent human fibroblasts. ATM expression inhibition, through ATM gene silencing using shRNA or siRNA, is another strategy (Guha et al., 2000). Furthermore, using the KU55933 treatment, blocking the function of ATM in these cancer cells caused the increase of radiosensitivity because the cells cannot repair the damage caused by homologous recombination repair (Neijenhuis et al., 2010). 12-O-tetradecanoylphorbol 12-acetate (TPA), the protein kinase C activator, functions to decrease the cellular level of the ATM. TPA and ATM are related to each other in the radiosensitization of an otherwise radioresistant human prostate cancer cell line and in the induction of apoptosis. Treatment of cells with TPA decreases ATM activity and increases the level of apoptosis that induces the regulatory enzyme ceramide synthase, resulting in induction of apoptosis after IR treatment (Truman et al., 2005). Another advantage of targeting ATM such as KU-60019 is revealed in HD. ATM inhibitors have not been used before to treat brain disease conditions *in vivo*. But this research presents the reasons for future pharmacokinetic studies (Lu et al., 2014).

Ring finger protein 8 is known as a promising target for chemotherapy because it is aberrantly expressed in many breast cancer patients, promotes tumor metastasis, and plays a key role in the DDR pathway. Targeting of RNF8 not only suppresses or eliminates the metastatic capacity of cancer cells but also increases the sensitivity of cancer cells to anticancer drugs upon depletion of RNF8, which can greatly improve the efficacy of anticancer drugs (Kuang et al., 2016). For example, corilagin targeting RNF8 effectively inhibits cell proliferation of esophageal squamous cell carcinoma (ESCC) and induces apoptosis. This

compound caused significant DNA damage in ESCC cells and significantly attenuated the RNF8 expression through the ubiquitin-proteasome pathway, blocking the DNA damage repair pathway and causing cell apoptosis (Qiu et al., 2019).

SH-group targeting and induction of massive apoptosis (STIMA-1), a low molecular weight compound with some structural similarity to CP-31398, known as a p53 inhibitor, stimulates the binding of mutant p53 to DNA *in vitro*, induces the expression of the p53 target protein, and can cause cell death in tumor cells expressing the mutant p53 (Zache et al., 2008). A small molecule called p53 reactivation and induction of massive apoptosis-1 (PRIMA-1) was developed to restore the original function of the tumor causing mutant p53. The effect of PRIMA-1 and its derivative, PRIMA-1^{MET} (APR-246 was verified *in vitro*, and it was identified as a compound that specifically inhibits the growth of p53 mutant tumor cells (Bykov et al., 2002). Similarly to PRIMA-1 and mutant p53 reactivation and induction of rapid apoptosis (MIRA-3), which also rescued the function of mutant p53 *via* thiol modification in the DNA binding domain, PRIMA-1 upregulated p53 activity by recovering sequence-specific DNA binding and facilitated the mitochondrial dependent intrinsic apoptosis program through the activation of caspase-2 (Shen et al., 2008). Upon binding to p53, RITA (also known as NSC 652287) also reactivates it and promotes cell death by interfering with its interaction with MDM2. The IC_{50} value of RITA depends on which cancer cell it is, but growth inhibition is clearly more effective (Issaeva et al., 2004).

Endoplasmic reticulum stress can be induced by DDR, and autophagy can be activated by factors involved in ER stress, IRE1, PERK, and ATF6. Activated autophagy can be involved in a number of disease factors, and controlling ER stress factors can be a method of treatment. Drugs that target IRE1, an ER stress factor, to give clinical effects have been suggested *in vitro* and *in vivo*. Representatively, Studies have shown that RNA attenuator, KIRA, can inhibit IRE1. KIRA 6, one of the KIRAs, was found to inhibit IRE1 and promote cell survival (Ghosh et al., 2014). Another KIRA, KIRA 7, has been reported to decrease UPR signaling and protect lung fibrosis by inhibiting IRE1. Finally, it was found that KIRA8 is a compound having a structure different from KIRA7 but can inhibit pulmonary fibrosis by inhibiting IRE1 (Thamsen et al., 2019). These suggestions imply that proposed drugs can inhibit autophagy and some diseases, which is increased by IRE1.

The control of other ER stress factors, PERK and ATF6, has also proven the effectiveness of treatment in several papers. GSK2656157, an ATP-competitive inhibitor that lowers the enzyme activity of PERK, is used as an inhibitor of PERK and has been found to affect tumor growth. By administering this drug orally, it can target PERK and effectively control tumors under microenvironment stresses such as hypoxia or nutrient starvation (Atkins et al., 2013). GSK2606414, a drug targeting PERK in the same way as GSK2656157, shows that oral administration can effectively prevent PD, a disease that causes clinical symptoms by killing dopaminergic neurons in the midbrain of the brain, under ER stress. However, in the case of GSK2606414, it has been reported that pancreatic toxicity occurs, so continuous experiment is needed (Mercado et al., 2018). Studies have shown that drugs targeting ATF6, another ER stress factor, are effective in the treatment of diseases. As an example, Ceapin, a type of pyrazole amides, inhibits ATF6 signaling, which leads to the alleviation of ER stress (Gallagher and Walter, 2016).

CONCLUSION

Until now, the connection between DDR and autophagic organelles has been evaluated; however, there is a limited number of studies investigating DDR factors related to selective autophagy (mitophagy, ER-phagy, and ribophagy). In this review, we summarize not only the role of autophagy in DDR, but also the pathophysiology of a wide range of diseases, as well as potential pharmacological regulators affecting both DDR factors and selective autophagy. Since autophagy emerges as a promising drug target, our understanding of its exact mechanisms in DDR is crucial when targeting pathologies, such as cancer, liver diseases, and brain disorders. Therefore, the inactivation of DDR factors by small molecule inhibitors should provide a new strategy for the treatment of diverse diseases. Thus, further research of the molecular mechanisms related to the regulation of DDR and autophagy is one of the ways to increase treatment efficiency. We hope that this review presented a far deeper understanding of DDR and autophagic degradation of organelles and could guide researchers pursuing clinical investigations in this scientific field.

AUTHOR CONTRIBUTIONS

JK and BY: conceptualization and writing original draft preparation. JK, SL, HK, HL, KMS, HY, and BY: writing review and editing. BY: supervision and project administration. All authors contributed to the article and approved the submitted version.

FUNDING

This work was supported by the National Research Foundation of Korea (NRF) grant funded by the Korea Government (MSIT) (NRF-2020R1A2C2005793, BY), National Research Foundation of Korea (NRF) funded by the Ministry of Science and ICT (2020M2D9A2094156, BY), a grant of the Basic Science Research Program through NRF grant (2016R1D1A1B03931405, HY), Republic of Korea and BK21 FOUR Program by Pusan National University Research Grant, 2020 (JK), and a grant of the Korea Institute of Radiological and Medical Sciences (KIRAMS), funded by Nuclear Safety and Security Commission (NSSC) of the Republic of Korea (No. 50091-2020, KMS and BY).

ACKNOWLEDGMENTS

We would like to thank Editage (www.editage.co.kr) for English language editing.

REFERENCES

Adachi, Y., Yamamoto, K., Okada, T., Yoshida, H., Harada, A., and Mori, K. (2008). ATF6 is a transcription factor specializing in the regulation of quality control proteins in the endoplasmic reticulum. *Cell Struct. Funct.* 33, 75–89. doi: 10.1247/csf.07044

Alao, J. P., and Sunnerhagen, P. (2009). The ATM and ATR inhibitors CGK733 and caffeine suppress cyclin D1 levels and inhibit cell proliferation. *Radiat. Oncol.* 4:51. doi: 10.1186/1748-717x-4-51

Alexander, A., Cai, S. L., Kim, J., Nanez, A., Sahin, M., MacLean, K. H., et al. (2010). ATM signals to TSC2 in the cytoplasm to regulate mTORC1 in response to ROS. *Proc. Natl. Acad. Sci. U.S.A.* 107, 4153–4158. doi: 10.1073/pnas.0913860107

Anding, A. L., and Baehrecke, E. H. (2017). Cleaning house: selective autophagy of organelles. *Dev. Cell* 41, 10–22. doi: 10.1016/j.devcel.2017.02.016

Atkins, C., Liu, Q., Minthorn, E., Zhang, S. Y., Figueroa, D. J., Moss, K., et al. (2013). Characterization of a novel PERK kinase inhibitor with antitumor and antiangiogenic activity. *Cancer Res.* 73, 1993–2002. doi: 10.1158/0008-5472.Can-12-3109

Babbar, M., Basu, S., Yang, B., Croteau, D. L., and Bohr, V. A. (2020). Mitophagy and DNA damage signaling in human aging. *Mech. Ageing Dev.* 186:111207. doi: 10.1016/j.mad.2020.111207

Baltanás, F. C., Casafont, I., Weruaga, E., Alonso, J. R., Berciano, M. T., and Lafarga, M. (2011). Nucleolar disruption and cajal body disassembly are nuclear hallmarks of DNA damage-induced neurodegeneration in purkinje cells. *Brain Pathol.* 21, 374–388. doi: 10.1111/j.1750-3639.2010.00461.x

Bartek, J., and Lukas, J. (2007). DNA damage checkpoints: from initiation to recovery or adaptation. *Curr. Opin. Cell Biol.* 19, 238–245. doi: 10.1016/j.ceb.2007.02.009

B'Chir, W., Maurin, A. C., Carraro, V., Averous, J., Jousse, C., Muranishi, Y., et al. (2013). The eIF2α/ATF4 pathway is essential for stress-induced autophagy gene expression. *Nucleic Acids Res.* 41, 7683–7699. doi: 10.1093/nar/gkt563

Beckerman, R., and Prives, C. (2010). Transcriptional regulation by p53. *Cold Spring Harb. Perspect. Biol.* 2:a000935. doi: 10.1101/cshperspect.a000935

Bengtson, M. H., and Joazeiro, C. A. (2010). Role of a ribosome-associated E3 ubiquitin ligase in protein quality control. *Nature* 467, 470–473. doi: 10.1038/nature09371

Bernales, S., McDonald, K. L., and Walter, P. (2006). Autophagy counterbalances endoplasmic reticulum expansion during the unfolded protein response. *PLoS Biol.* 4:e423. doi: 10.1371/journal.pbio.0040423

Bernales, S., Schuck, S., and Walter, P. (2007). ER-phagy: selective autophagy of the endoplasmic reticulum. *Autophagy* 3, 285–287. doi: 10.4161/auto.3930

Bilsland, E., Hult, M., Bell, S. D., Sunnerhagen, P., and Downs, J. A. (2007). The Bre5/Ubp3 ubiquitin protease complex from budding yeast contributes to the cellular response to DNA damage. *DNA Repair.* 6, 1471–1484. doi: 10.1016/j.dnarep.2007.04.010

Bissa, B., and Deretic, V. (2018). Autophagosome formation: cutting the gordian knot at the ER. *Curr. Biol.* 28, R347–R349. doi: 10.1016/j.cub.2018.03.015

Blasina, A., Price, B. D., Turenne, G. A., and McGowan, C. H. (1999). Caffeine inhibits the checkpoint kinase ATM. *Curr. Biol.* 9, 1135–1138. doi: 10.1016/s0960-9822(99)80486-2

Bobrovnikova-Marjon, E., Grigoriadou, C., Pytel, D., Zhang, F., Ye, J., Koumenis, C., et al. (2010). PERK promotes cancer cell proliferation and tumor growth by limiting oxidative DNA damage. *Oncogene* 29, 3881–3895. doi: 10.1038/onc.2010.153

Boesch, P., Weber-Lotfi, F., Ibrahim, N., Tarasenko, V., Cosset, A., Paulus, F., et al. (2011). DNA repair in organelles: pathways, organization, regulation, relevance in disease and aging. *Biochim. Biophys. Acta* 1813, 186–200. doi: 10.1016/j.bbamcr.2010.10.002

Bohgaki, T., Bohgaki, M., and Hakem, R. (2010). DNA double-strand break signaling and human disorders. *Genome Integr.* 1:15. doi: 10.1186/2041-9414-1-15

Brewer, J. W., Hendershot, L. M., Sherr, C. J., and Diehl, J. A. (1999). Mammalian unfolded protein response inhibits cyclin D1 translation and cell-cycle progression. *Proc. Natl. Acad. Sci. U.S.A.* 96, 8505–8510. doi: 10.1073/pnas.96.15.8505

Bykov, V. J., Issaeva, N., Shilov, A., Hultcrantz, M., Pugacheva, E., Chumakov, P., et al. (2002). Restoration of the tumor suppressor function to mutant p53 by a low-molecular-weight compound. *Nat. Med.* 8, 282–288. doi: 10.1038/nm0302-282

Bykov, V. J., Issaeva, N., Zache, N., Shilov, A., Hultcrantz, M., Bergman, J., et al. (2005a). Reactivation of mutant p53 and induction of apoptosis in human tumor cells by maleimide analogs. *J. Biol. Chem.* 280, 30384–30391. doi: 10.1074/jbc.M501664200

Bykov, V. J., Zache, N., Stridh, H., Westman, J., Bergman, J., Selivanova, G., et al. (2005b). PRIMA-1(MET) synergizes with cisplatin to induce tumor cell apoptosis. *Oncogene* 24, 3484–3491. doi: 10.1038/sj.onc.1208419

Chen, Q. Q., Zhang, C., Qin, M. Q., Li, J., Wang, H., Xu, D. X., et al. (2018). Inositol-requiring enzyme 1 Alpha endoribonuclease specific inhibitor STF-083010 alleviates carbon tetrachloride induced liver injury and liver fibrosis in mice. *Front. Pharmacol.* 9:1344. doi: 10.3389/fphar.2018.01344

Chu, C. T. (2019). Mechanisms of selective autophagy and mitophagy: implications for neurodegenerative diseases. *Neurobiol. Dis.* 122, 23–34. doi: 10.1016/j.nbd.2018.07.015

Ciechomska, I. A., Gabrusiewicz, K., Szczepankiewicz, A. A., and Kaminska, B. (2013). Endoplasmic reticulum stress triggers autophagy in malignant glioma cells undergoing cyclosporine a-induced cell death. *Oncogene* 32, 1518–1529. doi: 10.1038/onc.2012.174

Cinque, L., De Leonibus, C., Iavazzo, M., Krahmer, N., Intartaglia, D., Salierno, F. G., et al. (2020). MiT/TFE factors control ER-phagy via transcriptional regulation of FAM134B. *EMBO J.* 39:e105696. doi: 10.15252/embj.2020105696

Clarke, R., and Cook, K. L. (2015). Unfolding the role of stress response signaling in endocrine resistant breast cancers. *Front. Oncol.* 5:140. doi: 10.3389/fonc.2015.00140

Cremona, C. A., and Behrens, A. (2014). ATM signalling and cancer. *Oncogene* 33, 3351–3360. doi: 10.1038/onc.2013.275

Dan, X., Babbar, M., Moore, A., Wechter, N., Tian, J., Mohanty, J. G., et al. (2020). DNA damage invokes mitophagy through a pathway involving Spata18. *Nucleic Acids Res.* 48, 6611–6623. doi: 10.1093/nar/gkaa393

Deegan, S., Saveljeva, S., Gorman, A. M., and Samali, A. (2013). Stress-induced self-cannibalism: on the regulation of autophagy by endoplasmic reticulum stress. *Cell Mol. Life. Sci.* 70, 2425–2441. doi: 10.1007/s00018-012-1173-4

Derheimer, F. A., and Kastan, M. B. (2010). Multiple roles of ATM in monitoring and maintaining DNA integrity. *FEBS Lett.* 584, 3675–3681. doi: 10.1016/j.febslet.2010.05.031

Dicks, N., Gutierrez, K., Michalak, M., Bordignon, V., and Agellon, L. B. (2015). Endoplasmic reticulum stress, genome damage, and cancer. *Front. Oncol.* 5:11. doi: 10.3389/fonc.2015.00011

Dunn, W. A. Jr., Cregg, J. M., Kiel, J. A., van der Klei, I. J., Oku, M., Sakai, Y., et al. (2005). Pexophagy: the selective autophagy of peroxisomes. *Autophagy* 1, 75–83. doi: 10.4161/auto.1.2.1737

Eisenberg, T., Knauer, H., Schauer, A., Büttner, S., Ruckenstuhl, C., Carmona-Gutierrez, D., et al. (2009). Induction of autophagy by spermidine promotes longevity. *Nat. Cell Biol.* 11, 1305–1314. doi: 10.1038/ncb1975

Eliopoulos, A. G., Havaki, S., and Gorgoulis, V. G. (2016). DNA damage response and autophagy: a meaningful partnership. *Front. Genet.* 7:204. doi: 10.3389/fgene.2016.00204

Fang, E. F., Kassahun, H., Croteau, D. L., Scheibye-Knudsen, M., Marosi, K., Lu, H., et al. (2016). NAD(+) Replenishment Improves Lifespan and Healthspan in Ataxia Telangiectasia Models via Mitophagy and DNA Repair. *Cell Metab.* 24, 566–581. doi: 10.1016/j.cmet.2016.09.004

Fang, E. F., Scheibye-Knudsen, M., Brace, L. E., Kassahun, H., SenGupta, T., Nilsen, H., et al. (2014). Defective mitophagy in XPA via PARP-1 hyperactivation and NAD(+)/SIRT1 reduction. *Cell* 157, 882–896. doi: 10.1016/j.cell.2014.03.026

Foster, B. A., Coffey, H. A., Morin, M. J., and Rastinejad, F. (1999). Pharmacological rescue of mutant p53 conformation and function. *Science* 286, 2507–2510. doi: 10.1126/science.286.5449.2507

Friedenson, B. (2007). The BRCA1/2 pathway prevents hematologic cancers in addition to breast and ovarian cancers. *BMC Cancer* 7:152. doi: 10.1186/1471-2407-7-152

Fu, Z. J., Wang, Z. Y., Xu, L., Chen, X. H., Li, X. X., Liao, W. T., et al. (2020). HIF-1α-BNIP3-mediated mitophagy in tubular cells protects against renal ischemia/reperfusion injury. *Redox Biol.* 36:101671. doi: 10.1016/j.redox.2020.101671

Gade, P., Ramachandran, G., Maachani, U. B., Rizzo, M. A., Okada, T., Prywes, R., et al. (2012). An IFN-γ-stimulated ATF6-C/EBP-β-signaling pathway critical

for the expression of death associated protein kinase 1 and induction of autophagy. *Proc. Natl. Acad. Sci. U.S.A.* 109, 10316–10321. doi: 10.1073/pnas.1119273109

Gallagher, C. M., and Walter, P. (2016). Ceapins inhibit ATF6α signaling by selectively preventing transport of ATF6α to the Golgi apparatus during ER stress. *Elife* 5:e11880. doi: 10.7554/eLife.11880

Gardner, B. M., and Walter, P. (2011). Unfolded proteins are Ire1-activating ligands that directly induce the unfolded protein response. *Science* 333, 1891–1894. doi: 10.1126/science.1209126

Gatica, D., Lahiri, V., and Klionsky, D. J. (2018). Cargo recognition and degradation by selective autophagy. *Nat. Cell Biol.* 20, 233–242. doi: 10.1038/s41556-018-0037-z

Ghosh, R., Wang, L., Wang, E. S., Perera, B. G., Igbaria, A., Morita, S., et al. (2014). Allosteric inhibition of the IRE1α RNase preserves cell viability and function during endoplasmic reticulum stress. *Cell* 158, 534–548. doi: 10.1016/j.cell.2014.07.002

Golding, S. E., Rosenberg, E., Valerie, N., Hussaini, I., Frigerio, M., Cockcroft, X. F., et al. (2009). Improved ATM kinase inhibitor KU-60019 radiosensitizes glioma cells, compromises insulin, AKT and ERK prosurvival signaling, and inhibits migration and invasion. *Mol. Cancer Ther.* 8, 2894–2902. doi: 10.1158/1535-7163.Mct-09-0519

Groenendyk, J., Sreenivasaiah, P. K., Kim, D. H., Agellon, L. B., and Michalak, M. (2010). Biology of endoplasmic reticulum stress in the heart. *Circ. Res.* 107, 1185–1197. doi: 10.1161/circresaha.110.227033

Gu, X., Qi, Y., Feng, Z., Ma, L., Gao, K., and Zhang, Y. (2018). Lead (Pb) induced ATM-dependent mitophagy via PINK1/Parkin pathway. *Toxicol. Lett.* 291, 92–100. doi: 10.1016/j.toxlet.2018.04.012

Guha, C., Guha, U., Tribius, S., Alfieri, A., Casper, D., Chakravarty, P., et al. (2000). Antisense ATM gene therapy: a strategy to increase the radiosensitivity of human tumors. *Gene Ther.* 7, 852–858. doi: 10.1038/sj.gt.3301174

Guleria, A., and Chandna, S. (2016). ATM kinase: much more than a DNA damage responsive protein. *DNA Repair.* 39, 1–20. doi: 10.1016/j.dnarep.2015.12.009

Guo, F. J., Xiong, Z., Lu, X., Ye, M., Han, X., and Jiang, R. (2014). ATF6 upregulates XBP1S and inhibits ER stress-mediated apoptosis in osteoarthritis cartilage. *Cell. Signal.* 26, 332–342. doi: 10.1016/j.cellsig.2013.11.018

Hamanaka, R. B., Bennett, B. S., Cullinan, S. B., and Diehl, J. A. (2005). PERK and GCN2 contribute to eIF2alpha phosphorylation and cell cycle arrest after activation of the unfolded protein response pathway. *Mol. Biol. Cell* 16, 5493–5501. doi: 10.1091/mbc.e05-03-0268

Hanaoka, M., Ishikawa, T., Ishiguro, M., Tokura, M., Yamauchi, S., Kikuchi, A., et al. (2018). Expression of ATF6 as a marker of pre-cancerous atypical change in ulcerative colitis-associated colorectal cancer: a potential role in the management of dysplasia. *J. Gastroenterol.* 53, 631–641. doi: 10.1007/s00535-017-1387-1

Heijmans, J., van Lidth de Jeude, J. F., Koo, B. K., Rosekrans, S. L., Wielenga, M. C., van de Wetering, M., et al. (2013). ER stress causes rapid loss of intestinal epithelial stemness through activation of the unfolded protein response. *Cell Rep.* 3, 1128–1139. doi: 10.1016/j.celrep.2013.02.031

Henze, K., and Martin, W. (2003). Evolutionary biology: essence of mitochondria. *Nature* 426, 127–128. doi: 10.1038/426127a

Hetz, C. (2012). The unfolded protein response: controlling cell fate decisions under ER stress and beyond. *Nat. Rev. Mol. Cell Biol.* 13, 89–102. doi: 10.1038/nrm3270

Hetz, C., and Glimcher, L. H. (2009). Fine-tuning of the unfolded protein response: assembling the IRE1alpha interactome. *Mol. Cell.* 35, 551–561. doi: 10.1016/j.molcel.2009.08.021

Hetz, C., Martinon, F., Rodriguez, D., and Glimcher, L. H. (2011). The unfolded protein response: integrating stress signals through the stress sensor IRE1α. *Physiol. Rev.* 91, 1219–1243. doi: 10.1152/physrev.00001.2011

Hetz, C., Thielen, P., Matus, S., Nassif, M., Court, F., Kiffin, R., et al. (2009). XBP-1 deficiency in the nervous system protects against amyotrophic lateral sclerosis by increasing autophagy. *Genes Dev.* 23, 2294–2306. doi: 10.1101/gad.1830709

Hickson, I., Zhao, Y., Richardson, C. J., Green, S. J., Martin, N. M., Orr, A. I., et al. (2004). Identification and characterization of a novel and specific inhibitor of the ataxia-telangiectasia mutated kinase ATM. *Cancer Res.* 64, 9152–9159. doi: 10.1158/0008-5472.Can-04-2727

Hirota, Y., Yamashita, S., Kurihara, Y., Jin, X., Aihara, M., Saigusa, T., et al. (2015). Mitophagy is primarily due to alternative autophagy and requires the MAPK1 and MAPK14 signaling pathways. *Autophagy* 11, 332–343. doi: 10.1080/15548627.2015.1023047

Honda, R., Tanaka, H., and Yasuda, H. (1997). Oncoprotein MDM2 is a ubiquitin ligase E3 for tumor suppressor p53. *FEBS Lett.* 420, 25–27. doi: 10.1016/s0014-5793(97)01480-4

Hu, H., Tian, M., Ding, C., and Yu, S. (2018). The C/EBP homologous protein (CHOP) transcription factor functions in endoplasmic reticulum stress-induced apoptosis and microbial infection. *Front. Immunol.* 9:3083. doi: 10.3389/fimmu.2018.03083

Husnjak, K., and Dikic, I. (2012). Ubiquitin-binding proteins: decoders of ubiquitin-mediated cellular functions. *Annu. Rev. Biochem.* 81, 291–322. doi: 10.1146/annurev-biochem-051810-094654

Inamura, A., Muraoka-Hirayama, S., and Sakurai, K. (2019). Loss of mitochondrial DNA by gemcitabine triggers mitophagy and cell death. *Biol. Pharm. Bull.* 42, 1977–1987. doi: 10.1248/bpb.b19-00312

Issaeva, N., Bozko, P., Enge, M., Protopopova, M., Verhoef, L. G., Masucci, M., et al. (2004). Small molecule RITA binds to p53, blocks p53-HDM-2 interaction and activates p53 function in tumors. *Nat. Med.* 10, 1321–1328. doi: 10.1038/nm1146

Jäger, R., Bertrand, M. J., Gorman, A. M., Vandenabeele, P., and Samali, A. (2012). The unfolded protein response at the crossroads of cellular life and death during endoplasmic reticulum stress. *Biol. Cell* 104, 259–270. doi: 10.1111/boc.201100055

Jiang, D., Lynch, C., Medeiros, B. C., Liedtke, M., Bam, R., Tam, A. B., et al. (2016). Identification of doxorubicin as an inhibitor of the IRE1α-XBP1 axis of the unfolded protein response. *Sci. Rep.* 6:33353. doi: 10.1038/srep33353

Jones, R. J., Bjorklund, C. C., Baladandayuthapani, V., Kuhn, D. J., and Orlowski, R. Z. (2012). Drug resistance to inhibitors of the human double minute-2 E3 ligase is mediated by point mutations of p53, but can be overcome with the p53 targeting agent RITA. *Mol. Cancer Ther.* 11, 2243–2253. doi: 10.1158/1535-7163.Mct-12-0135

Jung, Y. Y., Son, D. J., Lee, H. L., Kim, D. H., Song, M. J., Ham, Y. W., et al. (2017). Loss of Parkin reduces inflammatory arthritis by inhibiting p53 degradation. *Redox Biol.* 12, 666–673. doi: 10.1016/j.redox.2017.04.007

Kang, X., Yang, W., Feng, D., Jin, X., Ma, Z., Qian, Z., et al. (2017). Cartilage-specific autophagy deficiency promotes ER stress and impairs chondrogenesis in PERK-ATF4-CHOP-dependent manner. *J. Bone. Miner. Res.* 32, 2128–2141. doi: 10.1002/jbmr.3134

Klinge, S., Voigts-Hoffmann, F., Leibundgut, M., Arpagaus, S., and Ban, N. (2011). Crystal structure of the eukaryotic 60S ribosomal subunit in complex with initiation factor 6. *Science* 334, 941–948. doi: 10.1126/science.1211204

Kober, L., Zehe, C., and Bode, J. (2012). Development of a novel ER stress based selection system for the isolation of highly productive clones. *Biotechnol. Bioeng.* 109, 2599–2611. doi: 10.1002/bit.24527

Korolchuk, V. I., Miwa, S., Carroll, B., and von Zglinicki, T. (2017). Mitochondria in cell senescence: is mitophagy the weakest link? *EBioMedicine* 21, 7–13. doi: 10.1016/j.ebiom.2017.03.020

Kraft, C., Deplazes, A., Sohrmann, M., and Peter, M. (2008). Mature ribosomes are selectively degraded upon starvation by an autophagy pathway requiring the Ubp3p/Bre5p ubiquitin protease. *Nat. Cell Biol.* 10, 602–610. doi: 10.1038/ncb1723

Kuang, J., Li, L., Guo, L., Su, Y., Wang, Y., Xu, Y., et al. (2016). RNF8 promotes epithelial-mesenchymal transition of breast cancer cells. *J. Exp. Clin. Cancer Res.* 35:88. doi: 10.1186/s13046-016-0363-6

Kundu, M., and Thompson, C. B. (2005). Macroautophagy versus mitochondrial autophagy: a question of fate? *Cell Death Differ.* 12(Suppl. 2), 1484–1489. doi: 10.1038/sj.cdd.4401780

Kvint, K., Uhler, J. P., Taschner, M. J., Sigurdsson, S., Erdjument-Bromage, H., Tempst, P., et al. (2008). Reversal of RNA polymerase II ubiquitylation by the ubiquitin protease Ubp3. *Mol. Cell.* 30, 498–506. doi: 10.1016/j.molcel.2008.04.018

Lampert, M. A., Orogo, A. M., Najor, R. H., Hammerling, B. C., Leon, L. J., Wang, B. J., et al. (2019). BNIP3L/NIX and FUNDC1-mediated mitophagy is required for mitochondrial network remodeling during cardiac progenitor cell differentiation. *Autophagy* 15, 1182–1198. doi: 10.1080/15548627.2019.1580095

Larsen, D. H., Hari, F., Clapperton, J. A., Gwerder, M., Gutsche, K., Altmeyer, M., et al. (2014). The NBS1-Treacle complex controls ribosomal RNA transcription in response to DNA damage. *Nat. Cell Biol.* 16, 792–803. doi: 10.1038/ncb3007

Lavoie, S., and Garrett, W. S. (2018). The unfolding story of ATF6, microbial dysbiosis, and colorectal cancer. *Gastroenterology* 155, 1309–1311. doi: 10.1053/j.gastro.2018.10.011

Li, K., Zhao, K., Ossareh-Nazari, B., Da, G., Dargemont, C., and Marmorstein, R. (2005). Structural basis for interaction between the Ubp3 deubiquitinating enzyme and its Bre5 cofactor. *J. Biol. Chem.* 280, 29176–29185. doi: 10.1074/jbc.M502975200

Li, L., Halaby, M. J., Hakem, A., Cardoso, R., El Ghamrasni, S., Harding, S., et al. (2010). Rnf8 deficiency impairs class switch recombination, spermatogenesis, and genomic integrity and predisposes for cancer. *J. Exp. Med.* 207, 983–997. doi: 10.1084/jem.20092437

Liang, W. J., and Gustafsson, ÅB. (2020). The aging heart: mitophagy at the center of rejuvenation. *Front. Cardiovasc. Med.* 7:18. doi: 10.3389/fcvm.2020.00018

Liao, Y., Duan, B., Zhang, Y., Zhang, X., and Xia, B. (2019). Excessive ER-phagy mediated by the autophagy receptor FAM134B results in ER stress, the unfolded protein response, and cell death in HeLa cells. *J. Biol. Chem.* 294, 20009–20023. doi: 10.1074/jbc.RA119.008709

Lindahl, T., and Barnes, D. E. (2000). Repair of endogenous DNA damage. *Cold. Spring Harb. Symp. Quant. Biol.* 65, 127–133. doi: 10.1101/sqb.2000.65.127

Liu, J., Liu, W., Li, R., and Yang, H. (2019). Mitophagy in Parkinson's disease: from pathogenesis to treatment. *Cells* 8:712. doi: 10.3390/cells8070712

Liu, K., Lee, J., Kim, J. Y., Wang, L., Tian, Y., Chan, S. T., et al. (2017). Mitophagy controls the activities of tumor suppressor p53 to regulate hepatic cancer stem cells. *Mol. Cell.* 68, 281.e285–292.e285. doi: 10.1016/j.molcel.2017.09.022

Liu, Z., Lv, Y., Zhao, N., Guan, G., and Wang, J. (2015). Protein kinase R-like ER kinase and its role in endoplasmic reticulum stress-decided cell fate. *Cell Death Dis.* 6:e1822. doi: 10.1038/cddis.2015.183

Lu, X. H., Mattis, V. B., Wang, N., Al-Ramahi, I., van den Berg, N., Fratantoni, S. A., et al. (2014). Targeting ATM ameliorates mutant Huntingtin toxicity in cell and animal models of Huntington's disease. *Sci. Transl. Med.* 6:268ra178. doi: 10.1126/scitranslmed.3010523

Ma, T., Keller, J. A., and Yu, X. (2011). RNF8-dependent histone ubiquitination during DNA damage response and spermatogenesis. *Acta Biochim. Biophys. Sin.* 43, 339–345. doi: 10.1093/abbs/gmr016

MacKeigan, J. P., Murphy, L. O., and Blenis, J. (2005). Sensitized RNAi screen of human kinases and phosphatases identifies new regulators of apoptosis and chemoresistance. *Nat. Cell Biol.* 7, 591–600. doi: 10.1038/ncb1258

Madeo, F., Eisenberg, T., Pietrocola, F., and Kroemer, G. (2018). Spermidine in health and disease. *Science* 359:eaan2788. doi: 10.1126/science.aan2788

Malpartida, A. B., Williamson, M., Narendra, D. P., Wade-Martins, R., and Ryan, B. J. (2021). Mitochondrial dysfunction and mitophagy in Parkinson's disease: from mechanism to therapy. *Trends Biochem. Sci.* 46, 329–343. doi: 10.1016/j.tibs.2020.11.007

McWilliams, T. G., and Muqit, M. M. (2017). PINK1 and Parkin: emerging themes in mitochondrial homeostasis. *Curr. Opin. Cell Biol.* 45, 83–91. doi: 10.1016/j.ceb.2017.03.013

Meng, J., Liu, K., Shao, Y., Feng, X., Ji, Z., Chang, B., et al. (2020). ID1 confers cancer cell chemoresistance through STAT3/ATF6-mediated induction of autophagy. *Cell Death Dis.* 11, 137. doi: 10.1038/s41419-020-2327-1

Mercado, G., Castillo, V., Soto, P., López, N., Axten, J. M., Sardi, S. P., et al. (2018). Targeting PERK signaling with the small molecule GSK2606414 prevents neurodegeneration in a model of Parkinson's disease. *Neurobiol. Dis.* 112, 136–148. doi: 10.1016/j.nbd.2018.01.004

Mirza-Aghazadeh-Attari, M., Darband, S. G., Kaviani, M., Mihanfar, A., Aghazadeh Attari, J., Yousefi, B., et al. (2018). DNA damage response and repair in colorectal cancer: defects, regulation and therapeutic implications. *DNA Repair.* 69, 34–52. doi: 10.1016/j.dnarep.2018.07.005

Mizushima, N., Yoshimori, T., and Ohsumi, Y. (2011). The role of Atg proteins in autophagosome formation. *Annu. Rev. Cell Dev. Biol.* 27, 107–132. doi: 10.1146/annurev-cellbio-092910-154005

Mlynarczyk, C., and Fåhraeus, R. (2014). Endoplasmic reticulum stress sensitizes cells to DNA damage-induced apoptosis through p53-dependent suppression of p21(CDKN1A). *Nat. Commun.* 5:5067. doi: 10.1038/ncomms6067

Momand, J., Zambetti, G. P., Olson, D. C., George, D., and Levine, A. J. (1992). The mdm-2 oncogene product forms a complex with the p53 protein and inhibits p53-mediated transactivation. *Cell* 69, 1237–1245. doi: 10.1016/0092-8674(92)90644-r

Morita, S., Villalta, S. A., Feldman, H. C., Register, A. C., Rosenthal, W., Hoffmann-Petersen, I. T., et al. (2017). Targeting ABL-IRE1α signaling spares ER-stressed pancreatic β cells to reverse autoimmune diabetes. *Cell Metab.* 25, 883.e888–897.e888. doi: 10.1016/j.cmet.2017.03.018

Muñoz-Gámez, J. A., Rodríguez-Vargas, J. M., Quiles-Pérez, R., Aguilar-Quesada, R., Martín-Oliva, D., de Murcia, G., et al. (2009). PARP-1 is involved in autophagy induced by DNA damage. *Autophagy* 5, 61–74. doi: 10.4161/auto.5.1.7272

Nakada, S. (2016). Opposing roles of RNF8/RNF168 and deubiquitinating enzymes in ubiquitination-dependent DNA double-strand break response signaling and DNA-repair pathway choice. *J. Radiat. Res.* 57(Suppl. 1), i33–i40. doi: 10.1093/jrr/rrw027

Nakatogawa, H., Suzuki, K., Kamada, Y., and Ohsumi, Y. (2009). Dynamics and diversity in autophagy mechanisms: lessons from yeast. *Nat. Rev. Mol. Cell Biol.* 10, 458–467. doi: 10.1038/nrm2708

Neijenhuis, S., Verwijs-Janssen, M., van den Broek, L. J., Begg, A. C., and Vens, C. (2010). Targeted radiosensitization of cells expressing truncated DNA polymerase {beta}. *Cancer Res.* 70, 8706–8714. doi: 10.1158/0008-5472.Can-09-3901

Nguyen, T. N., Padman, B. S., and Lazarou, M. (2016). Deciphering the Molecular Signals of PINK1/Parkin Mitophagy. *Trends Cell Biol.* 26, 733–744. doi: 10.1016/j.tcb.2016.05.008

O'Flanagan, C. H., and O'Neill, C. (2014). PINK1 signalling in cancer biology. *Biochim. Biophys. Acta* 1846, 590–598. doi: 10.1016/j.bbcan.2014.10.006

Ossareh-Nazari, B., Bonizec, M., Cohen, M., Dokudovskaya, S., Delalande, F., Schaeffer, C., et al. (2010). Cdc48 and Ufd3, new partners of the ubiquitin protease Ubp3, are required for ribophagy. *EMBO Rep.* 11, 548–554. doi: 10.1038/embor.2010.74

Pattingre, S., Tassa, A., Qu, X., Garuti, R., Liang, X. H., Mizushima, N., et al. (2005). Bcl-2 antiapoptotic proteins inhibit Beclin 1-dependent autophagy. *Cell* 122, 927–939. doi: 10.1016/j.cell.2005.07.002

Pelletier, J., Riaño-Canalias, F., Almacellas, E., Mauvezin, C., Samino, S., Feu, S., et al. (2020). Nucleotide depletion reveals the impaired ribosome biogenesis checkpoint as a barrier against DNA damage. *EMBO J.* 39:e103838. doi: 10.15252/embj.2019103838

Pelletier, J., Thomas, G., and Volarevіæ, S. (2018). Ribosome biogenesis in cancer: new players and therapeutic avenues. *Nat. Rev. Cancer* 18, 51–63. doi: 10.1038/nrc.2017.104

Qi, M. L., Tagawa, K., Enokido, Y., Yoshimura, N., Wada, Y., Watase, K., et al. (2007). Proteome analysis of soluble nuclear proteins reveals that HMGB1/2 suppress genotoxic stress in polyglutamine diseases. *Nat. Cell Biol.* 9, 402–414. doi: 10.1038/ncb1553

Qi, Y., Qiu, Q., Gu, X., Tian, Y., and Zhang, Y. (2016). ATM mediates spermidine-induced mitophagy via PINK1 and Parkin regulation in human fibroblasts. *Sci. Rep.* 6:24700. doi: 10.1038/srep24700

Qiu, F., Liu, L., Lin, Y., Yang, Z., and Qiu, F. (2019). Corilagin inhibits esophageal squamous cell carcinoma by inducing DNA damage and down-regulation of RNF8. *Anticancer Agents Med. Chem.* 19, 1021–1028. doi: 10.2174/1871520619666190307120811

Quinternet, M., Chagot, M. E., Rothé, B., Tiotiu, D., Charpentier, B., and Manival, X. (2016). Structural features of the box C/D snoRNP Pre-assembly process are conserved through species. *Structure* 24, 1693–1706. doi: 10.1016/j.str.2016.07.016

Rainey, M. D., Charlton, M. E., Stanton, R. V., and Kastan, M. B. (2008). Transient inhibition of ATM kinase is sufficient to enhance cellular sensitivity to ionizing radiation. *Cancer Res.* 68, 7466–7474. doi: 10.1158/0008-5472.Can-08-0763

Ri, M., Tashiro, E., Oikawa, D., Shinjo, S., Tokuda, M., Yokouchi, Y., et al. (2012). Identification of Toyocamycin, an agent cytotoxic for multiple myeloma cells, as a potent inhibitor of ER stress-induced XBP1 mRNA splicing. *Blood Cancer J.* 2:e79. doi: 10.1038/bcj.2012.26

Rogov, V., Dötsch, V., Johansen, T., and Kirkin, V. (2014). Interactions between autophagy receptors and ubiquitin-like proteins form the molecular basis for selective autophagy. *Mol. Cell.* 53, 167–178. doi: 10.1016/j.molcel.2013.12.014

Ron, D., and Hubbard, S. R. (2008). How IRE1 reacts to ER stress. *Cell* 132, 24–26. doi: 10.1016/j.cell.2007.12.017

Rutkowski, D. T., and Hegde, R. S. (2010). Regulation of basal cellular physiology by the homeostatic unfolded protein response. *J. Cell Biol.* 189, 783–794. doi: 10.1083/jcb.201003138

Sancar, A., Lindsey-Boltz, L. A., Unsal-Kaçmaz, K., and Linn, S. (2004). Molecular mechanisms of mammalian DNA repair and the DNA damage checkpoints. *Annu. Rev. Biochem.* 73, 39–85. doi: 10.1146/annurev.biochem.73.011303.073723

Sarkaria, J. N., Tibbetts, R. S., Busby, E. C., Kennedy, A. P., Hill, D. E., and Abraham, R. T. (1998). Inhibition of phosphoinositide 3-kinase related kinases by the radiosensitizing agent wortmannin. *Cancer Res.* 58, 4375–4382.

Seiwert, N., Neitzel, C., Stroh, S., Frisan, T., Audebert, M., Toulany, M., et al. (2017). AKT2 suppresses pro-survival autophagy triggered by DNA double-strand breaks in colorectal cancer cells. *Cell Death Dis.* 8:e3019. doi: 10.1038/cddis.2017.418

Shaid, S., Brandts, C. H., Serve, H., and Dikic, I. (2013). Ubiquitination and selective autophagy. *Cell Death. Differ.* 20, 21–30. doi: 10.1038/cdd.2012.72

Shanbhag, R., Shi, G., Rujiviphat, J., and McQuibban, G. A. (2012). The emerging role of proteolysis in mitochondrial quality control and the etiology of Parkinson's disease. *Parkinsons Dis.* 2012:382175. doi: 10.1155/2012/382175

Shao, G., Lilli, D. R., Patterson-Fortin, J., Coleman, K. A., Morrissey, D. E., and Greenberg, R. A. (2009). The Rap80-BRCC36 de-ubiquitinating enzyme complex antagonizes RNF8-Ubc13-dependent ubiquitination events at DNA double strand breaks. *Proc. Natl. Acad. Sci. U.S.A.* 106, 3166–3171. doi: 10.1073/pnas.0807485106

Shcherbik, N., and Pestov, D. G. (2019). The impact of oxidative stress on ribosomes: from injury to regulation. *Cells* 8:1379. doi: 10.3390/cells8111379

Shen, J., Vakifahmetoglu, H., Stridh, H., Zhivotovsky, B., and Wiman, K. G. (2008). PRIMA-1MET induces mitochondrial apoptosis through activation of caspase-2. *Oncogene* 27, 6571–6580. doi: 10.1038/onc.2008.249

Sheng, X., Nenseth, H. Z., Qu, S., Kuzu, O. F., Frahnow, T., Simon, L., et al. (2019). IRE1α-XBP1s pathway promotes prostate cancer by activating c-MYC signaling. *Nat. Commun.* 10:323. doi: 10.1038/s41467-018-08152-3

Singh, A. N., Oehler, J., Torrecilla, I., Kilgas, S., Li, S., Vaz, B., et al. (2019). The p97-Ataxin 3 complex regulates homeostasis of the DNA damage response E3 ubiquitin ligase RNF8. *EMBO J.* 38:e102361. doi: 10.15252/embj.2019102361

Sliter, D. A., Martinez, J., Hao, L., Chen, X., Sun, N., Fischer, T. D., et al. (2018). Parkin and PINK1 mitigate STING-induced inflammation. *Nature* 561, 258–262. doi: 10.1038/s41586-018-0448-9

Song, S., Tan, J., Miao, Y., and Zhang, Q. (2018). Crosstalk of ER stress-mediated autophagy and ER-phagy: Involvement of UPR and the core autophagy machinery. *J. Cell. Physiol.* 233, 3867–3874. doi: 10.1002/jcp.26137

Stagni, V., Ferri, A., Cirotti, C., and Barilà, D. (2020). ATM kinase-dependent regulation of autophagy: a key player in senescence? *Front. Cell Dev. Biol.* 8:599048. doi: 10.3389/fcell.2020.599048

Steck, P. A., Pershouse, M. A., Jasser, S. A., Yung, W. K., Lin, H., Ligon, A. H., et al. (1997). Identification of a candidate tumour suppressor gene, MMAC1, at chromosome 10q23.3 that is mutated in multiple advanced cancers. *Nat. Genet.* 15, 356–362. doi: 10.1038/ng0497-356

Stephani, M., Picchianti, L., Gajic, A., Beveridge, R., Skarwan, E., Sanchez de Medina Hernandez, V., et al. (2020). A cross-kingdom conserved ER-phagy receptor maintains endoplasmic reticulum homeostasis during stress. *Elife* 9:e58396. doi: 10.7554/eLife.58396

Sumpter, R. Jr., Sirasanagandla, S., Fernández Á, F., Wei, Y., Dong, X., Franco, L., et al. (2016). Fanconi anemia proteins function in mitophagy and immunity. *Cell* 165, 867–881. doi: 10.1016/j.cell.2016.04.006

Sunderland, P., Augustyniak, J., Lenart, J., Bużańska, L., Carlessi, L., Delia, D., et al. (2020). ATM-deficient neural precursors develop senescence phenotype with disturbances in autophagy. *Mech. Ageing Dev.* 190:111296. doi: 10.1016/j.mad.2020.111296

Taanman, J. W. (1999). The mitochondrial genome: structure, transcription, translation and replication. *Biochim. Biophys. Acta* 1410, 103–123. doi: 10.1016/s0005-2728(98)00161-3

Tang, C. H., Ranatunga, S., Kriss, C. L., Cubitt, C. L., Tao, J., Pinilla-Ibarz, J. A., et al. (2014). Inhibition of ER stress-associated IRE-1/XBP-1 pathway reduces leukemic cell survival. *J. Clin. Invest.* 124, 2585–2598. doi: 10.1172/jci73448

Thamsen, M., Ghosh, R., Auyeung, V. C., Brumwell, A., Chapman, H. A., Backes, B. J., et al. (2019). Small molecule inhibition of IRE1α kinase/RNase has anti-fibrotic effects in the lung. *PLoS One* 14:e0209824. doi: 10.1371/journal.pone.0209824

Tiwari, V., and Wilson, D. M. III (2019). DNA damage and associated DNA repair defects in disease and premature aging. *Am. J. Hum. Genet.* 105, 237–257. doi: 10.1016/j.ajhg.2019.06.005

Tran, M., and Reddy, P. H. (2020). Defective autophagy and mitophagy in aging and Alzheimer's disease. *Front. Neurosci.* 14:612757. doi: 10.3389/fnins.2020.612757

Truman, J. P., Gueven, N., Lavin, M., Leibel, S., Kolesnick, R., Fuks, Z., et al. (2005). Down-regulation of ATM protein sensitizes human prostate cancer cells to radiation-induced apoptosis. *J. Biol. Chem.* 280, 23262–23272. doi: 10.1074/jbc.M503701200

Tšuiko, O., Jatsenko, T., Parameswaran Grace, L. K., Kurg, A., Vermeesch, J. R., Lanner, F., et al. (2019). A speculative outlook on embryonic aneuploidy: can molecular pathways be involved? *Dev. Biol.* 447, 3–13. doi: 10.1016/j.ydbio.2018.01.014

Unoki, M., and Nakamura, Y. (2001). Growth-suppressive effects of BPOZ and EGR2, two genes involved in the PTEN signaling pathway. *Oncogene* 20, 4457–4465. doi: 10.1038/sj.onc.1204608

Valentin-Vega, Y. A., Maclean, K. H., Tait-Mulder, J., Milasta, S., Steeves, M., Dorsey, F. C., et al. (2012). Mitochondrial dysfunction in ataxia-telangiectasia. *Blood* 119, 1490–1500. doi: 10.1182/blood-2011-08-373639

Wang, J., Li, Y., Duan, J., Yang, M., Yu, Y., Feng, L., et al. (2018). Silica nanoparticles induce autophagosome accumulation via activation of the EIF2AK3 and ATF6 UPR pathways in hepatocytes. *Autophagy* 14, 1185–1200. doi: 10.1080/15548627.2018.1458174

Wang, M., and Kaufman, R. J. (2014). The impact of the endoplasmic reticulum protein-folding environment on cancer development. *Nat. Rev. Cancer* 14, 581–597. doi: 10.1038/nrc3800

Wang, S., Luo, H., Wang, C., Sun, H., Sun, G., Sun, N., et al. (2017). RNF8 identified as a co-activator of estrogen receptor α promotes cell growth in breast cancer. *Biochim. Biophys. Acta Mol. Basis Dis.* 1863, 1615–1628. doi: 10.1016/j.bbadis.2017.02.011

Wang, Y., Zhu, M., Ayalew, M., and Ruff, J. A. (2008). Down-regulation of Pkc1-mediated signaling by the deubiquitinating enzyme Ubp3. *J. Biol. Chem.* 283, 1954–1961. doi: 10.1074/jbc.M705682200

Wu, J., Huen, M. S., Lu, L. Y., Ye, L., Dou, Y., Ljungman, M., et al. (2009). Histone ubiquitination associates with BRCA1-dependent DNA damage response. *Mol. Cell. Biol.* 29, 849–860. doi: 10.1128/mcb.01302-08

Wyant, G. A., Abu-Remaileh, M., Frenkel, E. M., Laqtom, N. N., Dharamdasani, V., Lewis, C. A., et al. (2018). NUFIP1 is a ribosome receptor for starvation-induced ribophagy. *Science* 360, 751–758. doi: 10.1126/science.aar2663

Yan, J., and Jetten, A. M. (2008). RAP80 and RNF8, key players in the recruitment of repair proteins to DNA damage sites. *Cancer Lett.* 271, 179–190. doi: 10.1016/j.canlet.2008.04.046

Yan, L. L., Simms, C. L., McLoughlin, F., Vierstra, R. D., and Zaher, H. S. (2019). Oxidation and alkylation stresses activate ribosome-quality control. *Nat. Commun.* 10:5611. doi: 10.1038/s41467-019-13579-3

Yan, S., Sorrell, M., and Berman, Z. (2014). Functional interplay between ATM/ATR-mediated DNA damage response and DNA repair pathways in oxidative stress. *Cell Mol. Life. Sci.* 71, 3951–3967. doi: 10.1007/s00018-014-1666-4

Yao, R. Q., Ren, C., Xia, Z. F., and Yao, Y. M. (2020). Organelle-specific autophagy in inflammatory diseases: a potential therapeutic target underlying the quality control of multiple organelles. *Autophagy* doi: 10.1080/15548627.2020.1725377 Online ahead of print

Yin, J., Guo, J., Zhang, Q., Cui, L., Zhang, L., Zhang, T., et al. (2018). Doxorubicin-induced mitophagy and mitochondrial damage is associated with dysregulation of the PINK1/parkin pathway. *Toxicol. In Vitro* 51, 1–10. doi: 10.1016/j.tiv.2018.05.001

Youn, C. K., Kim, H. B., Wu, T. T., Park, S., Cho, S. I., and Lee, J. H. (2017). 53BP1 contributes to regulation of autophagic clearance of mitochondria. *Sci. Rep.* 7:45290. doi: 10.1038/srep45290

Yu, W., Gao, B., Li, N., Wang, J., Qiu, C., Zhang, G., et al. (2017). Sirt3 deficiency exacerbates diabetic cardiac dysfunction: role of Foxo3A-parkin-mediated mitophagy. *Biochim. Biophys. Acta Mol. Basis Dis.* 1863, 1973–1983. doi: 10.1016/j.bbadis.2016.10.021

Zache, N., Lambert, J. M., Rökaeus, N., Shen, J., Hainaut, P., Bergman, J., et al. (2008). Mutant p53 targeting by the low molecular weight compound STIMA-1. *Mol. Oncol.* 2, 70–80. doi: 10.1016/j.molonc.2008.02.004

Zhang, D., Tang, B., Xie, X., Xiao, Y. F., Yang, S. M., and Zhang, J. W. (2015). The interplay between DNA repair and autophagy in cancer therapy. *Cancer Biol. Ther.* 16, 1005–1013. doi: 10.1080/15384047.2015.1046022

Zhang, F., Peng, W., Zhang, J., Dong, W., Wu, J., Wang, T., et al. (2020). P53 and Parkin co-regulate mitophagy in bone marrow mesenchymal stem cells to promote the repair of early steroid-induced osteonecrosis of the femoral head. *Cell Death Dis.* 11:42. doi: 10.1038/s41419-020-2238-1

Zhao, D., Zou, C. X., Liu, X. M., Jiang, Z. D., Yu, Z. Q., Suo, F., et al. (2020). A UPR-induced soluble ER-phagy receptor acts with VAPs to confer ER stress resistance. *Mol. Cell.* 79, 963.e963–977.e963. doi: 10.1016/j.molcel.2020.07.019

Zheng, P., Chen, Q., Tian, X., Qian, N., Chai, P., Liu, B., et al. (2018). DNA damage triggers tubular endoplasmic reticulum extension to promote apoptosis by facilitating ER-mitochondria signaling. *Cell Res.* 28, 833–854. doi: 10.1038/s41422-018-0065-z

Zhi, H., Guo, X., Ho, Y. K., Pasupala, N., Engstrom, H. A. A., Semmes, O. J., et al. (2020). RNF8 dysregulation and down-regulation during HTLV-1 infection promote genomic instability in adult T-cell leukemia. *PLoS Pathog.* 16:e1008618. doi: 10.1371/journal.ppat.1008618

Conflict of Interest: The authors declare that the research was conducted in the absence of any commercial or financial relationships that could be construed as a potential conflict of interest.

frontiers in Cell and Developmental Biology

ORIGINAL RESEARCH
published: 29 April 2021
doi: 10.3389/fcell.2021.672693

Association of Cancer Stem Cell Radio-Resistance Under Ultra-High Dose Rate FLASH Irradiation With Lysosome-Mediated Autophagy

Gen Yang[1], Chunyang Lu[1], Zhusong Mei[1], Xiaoyi Sun[1], Jintao Han[1], Jing Qian[2], Yulan Liang[1], Zhuo Pan[1], Defeng Kong[1], Shirui Xu[1], Zhipeng Liu[1], Ying Gao[1], Guijun Qi[1], Yinren Shou[1], Shiyou Chen[1], Zhengxuan Cao[1], Ye Zhao[2], Chen Lin[1], Yanying Zhao[1], Yixing Geng[1], Wenjun Ma[1]* and Xueqing Yan[1,3]**

[1] State Key Laboratory of Nuclear Physics and Technology, School of Physics, CAPT, Peking University, Beijing, China, [2] Teaching and Research Section of Nuclear Medicine, School of Basic Medical Sciences, Anhui Medical University, Hefei, China, [3] Collaborative Innovation Center of Extreme Optics, Shanxi University, Taiyuan, China

OPEN ACCESS

Edited by:
Daoxiang Zhang,
Washington University in St. Louis,
United States

Reviewed by:
Jinpeng Geng,
Hebei University of Technology, China
Cong Liu,
Second Military Medical University,
China

***Correspondence:**
Gen Yang
gen.yang@pku.edu.cn
Wenjun Ma
wenjun.ma@pku.edu.cn
Xueqing Yan
x.yan@pku.edu.cn

Specialty section:
This article was submitted to Cell Death and Survival, a section of the journal Frontiers in Cell and Developmental Biology

Received: 26 February 2021
Accepted: 06 April 2021
Published: 29 April 2021

Citation:
Yang G, Lu C, Mei Z, Sun X, Han J, Qian J, Liang Y, Pan Z, Kong D, Xu S, Liu Z, Gao Y, Qi G, Shou Y, Chen S, Cao Z, Zhao Y, Lin C, Zhao Y, Geng Y, Ma W and Yan X (2021) Association of Cancer Stem Cell Radio-Resistance Under Ultra-High Dose Rate FLASH Irradiation With Lysosome-Mediated Autophagy. Front. Cell Dev. Biol. 9:672693. doi: 10.3389/fcell.2021.672693

Cancer stem cell (CSC) is thought to be the major cause of radio-resistance and relapse post radiotherapy (RT). Recently ultra-high dose rate "FLASH-RT" evokes great interest for its decreasing normal tissue damages while maintaining tumor responses compared with conventional dose rate RT. However, the killing effect and mechanism of FLASH irradiation (FLASH-IR) on CSC and normal cancer cell are still unclear. Presently the radiation induced death profile of CSC and normal cancer cell were studied. Cells were irradiated with FLASH-IR ($\sim 10^9$ Gy/s) at the dose of 6–9 Gy via laser-accelerated nanosecond particles. Then the ratio of apoptosis, pyroptosis and necrosis were determined. The results showed that FLASH-IR can induce apoptosis, pyroptosis and necrosis in both CSC and normal cancer cell with different ratios. And CSC was more resistant to radiation than normal cancer cell under FLASH-IR. Further experiments tracing lysosome and autophagy showed that CSCs had higher levels of lysosome and autophagy. Taken together, our results suggested that the radio-resistance of CSC may associate with the increase of lysosome-mediated autophagy, and the decrease of apoptosis, necrosis and pyroptosis. To our limited knowledge, this is the first report shedding light on the killing effects and death pathways of CSC and normal cancer cell under FLASH-IR. By clarifying the death pathways of CSC and normal cancer cell under FLASH-IR, it may help us improve the understanding of the radio-resistance of CSC and thus help to optimize the future clinical FLASH treatment plan.

Keywords: ultra-high dose rate irradiation, FLASH, DNA damage, lysosome, cancer stem cell, autophagy, apoptosis, necrosis

Abbreviations: CSC, cancer stem cell; RT, radiotherapy; IL, interleukin; ROS, reactive oxygen species; FLASH-IR, FLASH irradiation; CLAPA, compact laser plasma accelerator system; FBS, fetal bovine serum; EGF, epidermal growth factor; bFGF, basic fibroblast growth factor; FWHM, full width at half maximum; TPS, Thomson parabola spectrometer; RCF, radiochromic film; PI, propidium iodide; MDC, dansylcadaverine; MOMP, mitochondrial outer membrane permeabilization; FADD, FAS Associated death domain; RIP3, receptor interacting protein 3.

INTRODUCTION

Cancer is one of the leading causes of death, more than half of cancer patients receive radiotherapy (RT) during treatment (Arnold et al., 2020). In RT, the common types of radiation are photon (such as X-rays and γ-rays) radiation and particle (such as electrons, protons, heavy ions and neutrons) radiation. RT exerts cell killing effect by inducing DNA damage, either directly or indirectly via generating free radicals by interacting with water molecules (YuN, 1992). Irradiation induces cell death mainly by damaging DNA. Among them, apoptosis and necrosis are very important death pathways (Mitteer et al., 2015; Bozhenko et al., 2019; Wang et al., 2019). Besides, studies have shown that irradiation can also cause cell pyroptosis (Liao et al., 2017; Li et al., 2019). Pyroptosis, as a highly pro-inflammatory programmed cell death, the feature is that it depends on the activation of caspase-1 and releases the inflammatory cytokines IL-1β and IL-18 (Westbom et al., 2015; Wang et al., 2017). In addition, irradiation can also induce cell autophagy. In the early years, autophagy was considered a mechanism by which cells produce nutrients and energy. However, in recent years, many studies have shown when cells were continuously exposed to stress conditions, autophagy acted as a cell stress protection mechanism (Turcotte and Giaccia, 2010), can remove macromolecules or mitochondria that were damaged by ionizing radiation and cytotoxic substances in the cell, and further promote cell survival (Han et al., 2018).

The radio-resistance of cancer stem cells (CSCs) is an important cause of RT failure, cancer recurrence and metastasis (Bao et al., 2006; Chiou et al., 2008; Arnold et al., 2020). Compared with normal cancer cells, the main reasons for CSCs radio-resistance are suggested as follows: (1) CSCs have stronger reactive oxygen species (ROS) removal ability, the ROS baseline in CSCs is lower, and the damage caused by irradiation is less (Diehn et al., 2009; Chang et al., 2014). (2) CSCs have enhanced DNA repair capability (Bao et al., 2006). (3) CSCs are usually in a stationary phase (Moore and Lyle, 2011; Batlle and Clevers, 2017). (4) CSCs have enhanced self-renewal ability (Woodward et al., 2007; Batlle and Clevers, 2017). (5) CSCs have an increased autophagy level (Lomonaco et al., 2009). Among them, in recent years, some studies have shown that lysosomes and autophagy may be related to the radio-resistance of CSC (Tang et al., 2018; Zhang et al., 2018). Through limited activation of autophagy, CSCs can achieve higher cell survival. Blocking autophagy is considered to be a feasible strategy to enhance radio-sensitivity, and autophagy inhibitors are considered as promising radiosensitizers (Zhang et al., 2018).

The ultra-high dose rate FLASH-RT has attracted widely attention in recent years (Bourhis et al., 2019). It greatly protects normal tissues from damage, while effectively killing tumor tissues. This significantly improves the therapeutic index during RT and may achieve better control of the tumor (Durante et al., 2018; Griffin et al., 2020). Compared with conventional dose rate irradiation (∼1 Gy/min), FLASH-RT has a higher dose rate (>40 Gy/s), and the irradiation process is usually completed in a very short time (<0.1 s) (Durante et al., 2018). In the last few decades, important progress on laser plasma acceleration provided a new method to study radiobiology effects (Ledingham et al., 2014). The laser-driven ion beams have ultra-short pulse duration in a range of nanoseconds and ultra-high dose rate in the order of 10^9 Gy/s (Bin et al., 2012; Doria et al., 2012; Pommarel et al., 2017; Hantonl et al., 2019), showing the potential for *in vitro* (Yogo et al., 2011; Zeil et al., 2013; Raschke et al., 2016; Bayart et al., 2019) and *in vivo* (Rosch et al., 2020) FLASH-RT besides cyclotrons, synchrotrons or synchrocyclotron (Patriarca et al., 2018). Presently, there are few articles on FLASH-RT, mainly because the realization of ultra-high dose rate is quite difficult (Griffin et al., 2020). The existing FLASH-RT articles mainly focus on the protective effect of FLASH on normal tissues (Field and Bewley, 1974; Favaudon et al., 2014; Montay-Gruel et al., 2017; Vozenin et al., 2019). For example, a number of animal FLASH-RT experiments showed that compared with conventional irradiation, FLASH-RT can significantly reduce damage to normal tissues, including reducing pulmonary fibrosis (Favaudon et al., 2014), reducing radiation-induced neurotoxicity (Montay-Gruel et al., 2017) and reducing radiation-induced skin reactions (Field and Bewley, 1974; Vozenin et al., 2019), etc. Besides, there were also several animal experiments proved that FLASH-RT has a tumor-killing effect similar to conventional irradiation (Favaudon et al., 2014; Rama et al., 2019). But there are few researches on the basic killing effect and specific killing mechanisms of FLASH on cancer cells, especially for the important problem of radiation biology, the CSC radio-resistance.

In this article, we used the CLAPA ultra-fast laser acceleration system to irradiate cells with ultra-high dose rate (∼10^9 Gy/s), and the dose was controlled at 6–9 Gy. The ratio of apoptosis, pyroptosis and necrosis was determined at 6, 12, and 24 h after irradiation. At the same time, we also labeled the lysosomes and detected autophagy in cells.

MATERIALS AND METHODS

Cell Culture

MCF-7 cells were cultured in DMEM high glucose medium (Hyclone) supplemented with 10% fetal bovine serum (FBS) (Bai Ling Biotechnology) and 1% penicillin-streptomycin (P/S) (Hyclone). MCF-7 CSCs were cultured in DME/F12 1:1 medium (Hyclone) supplemented with N2 (Gibco), B27 (Gibco), epidermal growth factor (EGF) (20 ng/mL, PeproTech), and basic fibroblast growth factor (bFGF) (10 ng/m, PeproTech). And the petri dishes used for CSCs were pre-coated with 1% Geltrex (Gibco) as described previously (Fu et al., 2017). All cells were cultured at 37°C under 5% CO_2 in a humidified incubator (Sanyo).

Flow Cytometry Analysis

MCF-7 CSCs were obtained by sorting as reported previously (Fu et al., 2017). In brief, the cells were concentrated to a few million/100 μL, and were stained by adding 10 μL anti-CD44-PE antibody (BD Pharmingen) and 10 μL anti-CD24-FITC antibody (BD Pharmingen). After the staining was completed, the cells were washed twice by PBS and analyzed/sorted on flow cytometer (BD Aria III).

Spheroids Formation Assay

MCF-7 cells and CSCs were digested, centrifuged and resuspended in serum-free medium (CSC culture medium, as mentioned above), the density was adjusted to 2,500 cells/mL, then the cell suspension was added to a low-adsorption 24-well plate (1 mL per well). Cells were cultured at 37°C under 5% CO_2. After 3 days, spheroids were imaged and with diameter larger than 50 μm were counted. Image acquisition and analysis were performed through automatic real-time live cell imaging detection system (Spark®Cyto, Tecan).

In vivo Tumor Formation Experiment in Mice

MCF-7 cells and CSCs were digested, washed three times using PBS, and diluted to a certain density, then mixed the cell suspension and Geltrex (Gibco) at 1:1. Same number (10,000) of MCF-7 cells and CSCs were injected on the left and right fat pads of each BALB/C nude mice, respectively. The growth of the tumor was recorded and the images were token 36 days after injection. All animal experiments and protocols were approved by the Peking University Institutional Animal Care and Use Committee (Approval ID: Physics-YangG-2).

Implementation of FLASH-IR

The FLASH radiation experiment was performed using CLAPA system in Peking University (Geng et al., 2018). The CLAPA was driven by a 200TW Ti: sapphire laser with central wavelength at 800 nm and full width at half maximum (FWHM) duration of 30 fs compressed. A single plasma mirror system was used to increase the temporal contrast of the laser to 10^8@5 ps. S-polarized laser was focused onto the 100 nm plastic target using an f/2.5 off-axis parabolic (OAP) with a focal length of 200 mm. The laser energy on target was ∼1 J and the diameter (FWHM) of focal spot was 4.2 μm, containing 36% of the total energy, resulting in the peak intensity of 5.6×10^{19} W/cm^2. The ion energy spectra were measured by a Thomson parabola spectrometer (TPS) positioned at 780 mm along the direction normal to the back surface of the target.

A 3.5 μm Mylar film was pasted at the bottom of the cell-culture hoop using glue in advance, and then was pre-treated with DMEM high glucose medium and/or 1% Geltrex for 24 h, respectively. The height and inner diameter of the stainless-steel cell-culture hoop were 13 and 10 mm, respectively. Cells were seeded 8 h before irradiation. MCF-7 cells and CSCs were digested and diluted to 150,000/mL, and 800 μL cell suspension was added to each cell-culture hoop. Before starting the irradiation, the medium in cell-culture hoop was aspirated, and the cell-culture hoop was screwed on the hoop holder and mounted vertically. The hoop holder was sealed with another 3.5 μm Mylar film to avoid contamination and dryout of the cell during irradiation. Then the cells irradiation system was plugged in, the ion beams entered the cell irradiation system through a vacuum window located 63 mm behind the target and irradiated the cells. The vacuum window consisted of two parts, a 10 μm Aluminum film to prevent cells from being exposed to scattered light and a 25 μm Kapton window for vacuum sealing. Aluminum films of different thicknesses and copper wire mesh were used in front of the sealing Mylar film to adjust the dose. After the irradiation was completed, the medium was added and the cells were inoculated in the incubator.

Detection of Apoptotic and Necrosis

Dead Cell Apoptosis Kit with Annexin V Alexa Fluor™ 488 & Propidium Iodide (PI) (Invitrogen) were used to detect apoptotic and necrosis. For a 96-well plate, 100 μL cell suspension, 1 μL of PI working solution (red), 5 μL of Annexin V (green) and appropriate volume of Hoechst (blue, Molecular Probes) were added into each well. The images were token after staining according to the manufactural protocol. The nucleus was marked as blue, living cells were blue+, apoptotic cells were blue+green+, and dead cells were marked as blue+green+red+. Image acquisition were performed via automatic real-time live cell imaging detection system (Spark®Cyto, Tecan).

Detection of Pyroptosis

Pyroptosis were detected using Caspase-glo 1 inflammasome assay (Promega), for a 96-well plate, 100 μL of cell suspension and 100 μL Z-WEHD substrate were added, then the chemiluminescence was detected after 1 h. The detection was performed via automatic real-time live cell imaging detection system (Spark®Cyto, Tecan).

Autophagy Detection

After the irradiation is completed, the cells were digested from the Mylar film and seeded into a 96-well plate. Autophagy was detected after 24 h using dansylcadaverine (MDC) autophagy detection kit (Leagene Biotechnology). In addition, lysosomes were labeled with lysoTracker (Invitrogen), nucleus were labeled with Hoechst 33342. Image acquisition was performed via automatic real-time live cell imaging detection system (Spark®Cyto, Tecan).

Data Analysis

All results were expressed as means ± SD, Student's *t*-test or one-way ANOVA were used for analyzing significance between the controls and the experimental groups, where $P < 0.05$ was marked as *, $P < 0.01$ was marked as **, and $P < 0.001$ was marked as ***.

RESULTS

Functional Verification of MCF-7 CSCs

MCF-7 CSCs were obtained by flow sorting as our research group reported previously (Fu et al., 2017). We used flow cytometry analysis, spheroids formation assay and *in vivo* tumor formation experiment to verify the sorted CSCs. For flow cytometry analysis, the cells were divided into five groups, the control (not stained), the single CD44 stained group, the single CD24 stained group and the CD44CD24 double stained group (MCF-7 cells and CSCs). By analyzing the expression of CD44 and CD24 on the cell surface, the results showed that MCF-7 CSCs maintains

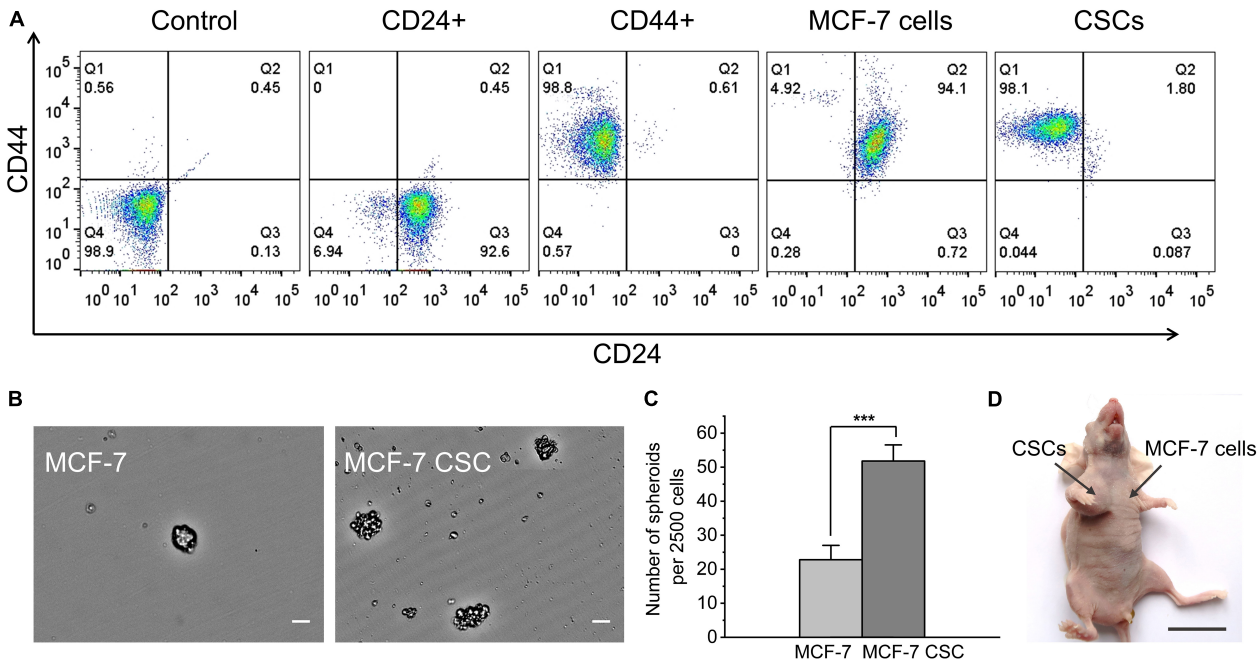

FIGURE 1 | Functional verification of MCF-7 CSCs. **(A)** Flow cytometry results for five groups of cells. From left to right are the control (not stained), the single CD44 stained group, the single CD24 stained group and the CD44CD24 double stained group (MCF-7 cells and CSCs). **(B)** Representative images of spheroids formed by MCF-7 cells and MCF-7 CSCs. Scale bars: 50 μm. **(C)** Quantification of the number of spheroids derived from MCF-7 cells and MCF-7 CSCs at day 3. **(D)** Representative image depicting *in vivo* tumor formation at the injection site of 10,000 CSCs, with no tumor formation seen at the injection site of 10,000 MCF-7 cells. Scale bar: 2 cm. ***$P < 0.001$.

the characteristics of CSC, and the percentage of CD44+CD24− cells is 98.1% (**Figure 1A**). In addition, MCF-7 CSCs also showed stronger self-renewal ability, its spheroids formation efficiency was ∼2.3 folds that of MCF-7 cells (**Figures 1B,C**). To investigate whether sorted CSCs display long-term tumorigenic potential, we also performed *in vivo* tumor formation experiment by injecting 10,000 MCF-7 cells and CSCs into BALB/C nude mice, and observed and counted the growth of the tumor. The results showed that CSCs have stronger tumorigenesis ability *in vivo*. 10,000 CSCs are capable of generating visible tumors after 36 days (**Table 1**). In contrast, no visible tumors were observed with MCF-7 cells under the same conditions (**Figure 1D**). Statistics on the size of tumors were shown in **Supplementary Table 1**.

Dose Monitoring and Conversion of FLASH-IR

During the cell irradiation, customized radiochromic films (RCFs) EBT3 were directly placed behind the Mylar film for dose verification. Since the RCF dose was known, we can get the deposit dose in cells. Considering the fluctuation of the energy spectrum between different shots, the result will have an error of ± 15%. In this experiment, the cells were irradiated with a single shot (∼6–9 Gy). The ion beam was generated within 1 ps. Considering the difference between the flight time of particles with different energy, the duration of radiation was ∼1.4 ns, so the dose rate was $\sim 10^9$ Gy/s. The specific RCF dose and deposit dose in cells for each shot were shown in **Table 2**. More detailed information about the dose was shown in **Supplementary Figure 1**.

TABLE 1 | *In vivo* tumor formation ability of MCF-7 cells and CSCs.

Cell type	Tumor formation efficiency
MCF-7 cells	0/3
CSCs	2/3

TABLE 2 | Dose summary for each shot of the laser accelerator.

	Dose in RCF film	Deposit dose (Median) in cells	Deposit dose (Range) in cells	Shot used
1	3.05	6.83	5.89–7.88	MCF-7 CSC 6 h
2	3.43	7.68	6.62–8.87	MCF-7 CSC 12 h
3	3.16	7.08	6.10–8.17	MCF-7 CSC 24 h
4	3.93	8.80	7.59–10.16	MCF-7 6 h
5	3.52	7.88	6.80–9.10	MCF-7 12 h
6	3.37	7.54	6.51–8.71	MCF-7 24 h
7	2.82	6.14	5.36–7.07	MCF-7 CSC autophagy
8	3.97	8.89	7.67–10.26	MCF-7 autophagy

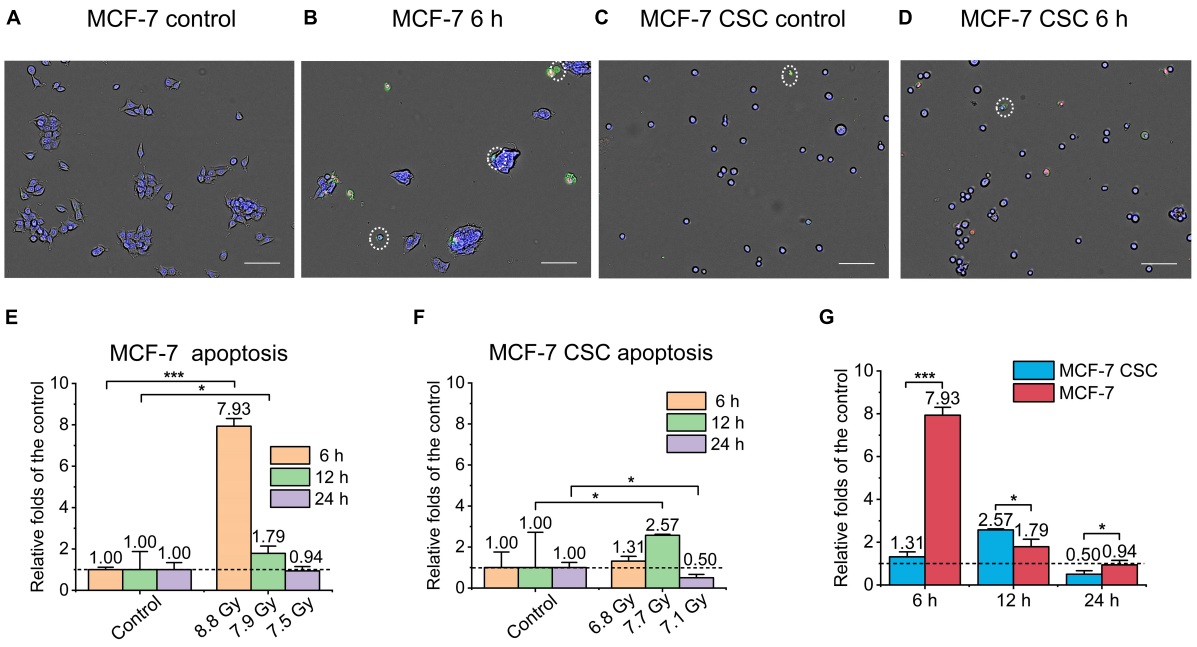

FIGURE 2 | Apoptosis of irradiated MCF-7 cells and MCF-7 CSCs. **(A–D)** Representative images of control groups and irradiated MCF-7 cells and MCF-7 CSCs at 6 h which were stained with annexin V and PI. Apoptotic cells were marked with white circles. Scale bars: 100 μm. **(E,F)** Compared with the relative controls, the relative increasement of the apoptosis proportion for irradiated groups at 6, 12, and 24 h. **(G)** The increasement of the apoptosis proportion between irradiated MCF-7 cells and MCF-7 CSCs. $^{*}P < 0.05$; $^{***}P < 0.001$.

CSCs Are More Resistant Than Normal Cancer Cell to FLASH Irradiation

To evaluate the killing effect of ultra-high dose rate FLASH irradiation (FLASH-IR) on MCF-7 and CSC, we assessed the apoptosis, necrosis and pyroptosis, at 6 h, 12 h and 24 h after irradiation. Annexin V Alexa Fluor^{TM}x 488 & Propidium Iodide (PI) was used to detect apoptosis and necrosis. Apoptotic cells were marked as blue+green+, and dead cells were marked as blue+green+red+. **Figures 2A–D** were the representative images showing the differences between MCF-7 and CSC after irradiation, compared with the control, the apoptosis level of irradiated MCF-7 at 6 h was significantly increased, which was ∼7.9 folds that of the control. In addition, there was also an increasement at 12 h, which was ∼1.8 folds of the control (**Figure 2E**). For CSC, apoptosis had a significant but much lower increasement at 12 h, which was ∼2.6 folds of relative control, while there was no significant change at any other time points (**Figure 2F**). Putting the apoptosis data of irradiated MCF-7 and CSC together, it can also be seen that the apoptosis level of irradiated MCF-7 was significantly higher than that of irradiated CSC, among them, MCF-7 had the highest response at 6 h after irradiation, while CSC had the highest response at 12 h after irradiation (**Figure 2G**).

Similarly, as shown in **Figure 3**, we also detected and analyzed the necrosis of the irradiated cells. **Figures 3A–D** were the representative images. It can be seen that, similar to the result of apoptosis, the necrosis of MCF-7 at 6 h after irradiation was ∼11 folds than that of the control (**Figure 3E**). On the other hand, the necrosis of CSC at 6 h after irradiation reached ∼9.3 folds than that of the control. In addition, CSC's necrosis at 12 and 24 h after irradiation also reached ∼2.3 folds that of the control (**Figure 3F**). Comparing the necrosis of irradiated CSC and MCF-7, the results showed that although the necrosis of CSC in the early stage was lower than MCF-7, in the late stage, it was significant higher (**Figure 3G**).

Pyroptosis is a highly pro-inflammatory programmed cell death. We made a rough assessment of pyroptosis by detecting the activity of caspase-1 in the cell. Mainly using Caspase-glo 1 inflammasome assay kit. The main principle of the kit is as follows, a single addition of this reagent results in cell lysis, substrate cleavage by caspase-1 and generation of light by a proprietary, thermostable, recombinant luciferase. The luminescent signal is proportional to caspase activity (O'Brien et al., 2017). As shown in **Figures 4A–C**, the overall normalized pyroptosis level of irradiated MCF-7 was also higher than that of irradiated CSC, the former reached ∼3.4 folds and ∼1.5 folds of the control at 6 and 12 h, respectively, while the latter only reached ∼1.4 folds of the relative control at 6 h, no significant change at any other time points.

CSCs Increase Autophagy

To further study the mechanism of CSCs' radio-resistance under FLASH-IR, we used MDC staining kit to detect the autophagy level of the two cell types. We labeled lysosomes and detected autophagy at 24 h after irradiation. The results showed that the autophagy of irradiated CSCs increased significantly compared with the control, which was ∼1.7 folds than that of the control, while the autophagy of irradiated normal cancer cell (MCF-7)

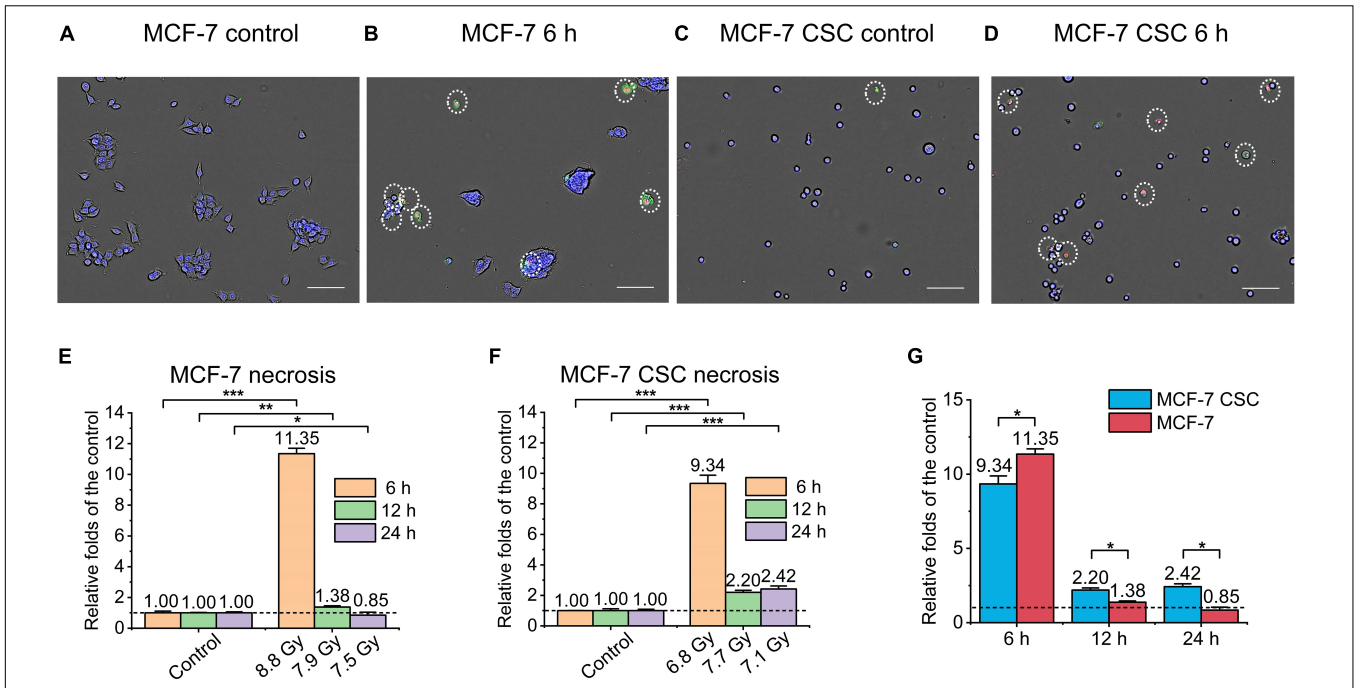

FIGURE 3 | Necrosis of irradiated MCF-7 cells and MCF-7 CSCs. **(A–D)** Representative images of control groups, irradiated MCF-7 cells and MCF-7 CSCs at 6 h which were stained with annexin V and PI. Necrosis cells were marked with white circles. Scale bars: 100 μm. **(E,F)** Compared with the relative controls, the increasement of the necrosis proportion for irradiated groups at 6, 12, and 24 h. **(G)** The increasement of the necrosis proportion between irradiated MCF-7 cells and MCF-7 CSCs. *$P < 0.05$; **$P < 0.01$; ***$P < 0.001$.

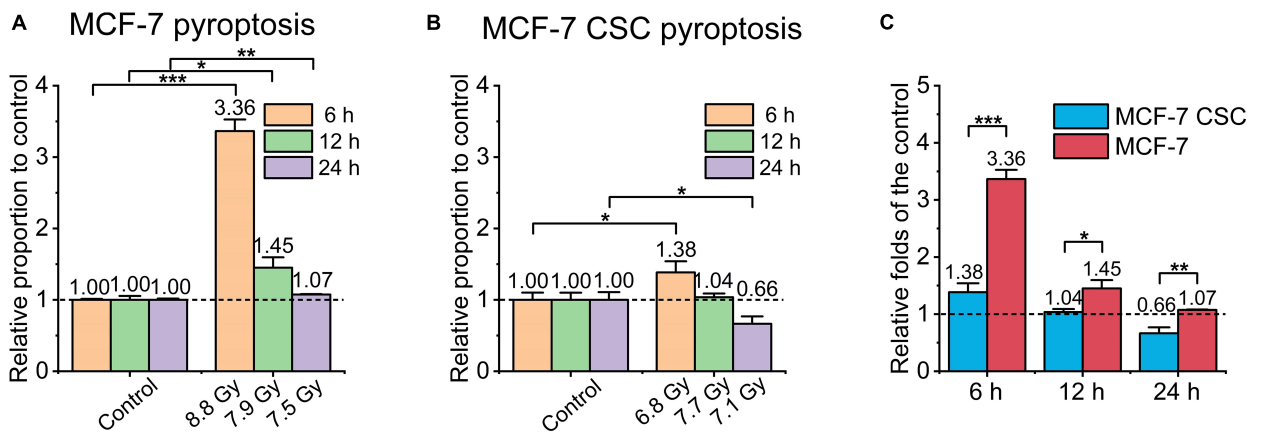

FIGURE 4 | Pyroptosis of irradiated MCF-7 cells and MCF-7 CSCs. **(A,B)** Compared with the relative controls, the increasement of pyroptosis proportion for irradiated groups at 6, 12, and 24 h, respectively. **(C)** The increasement of the pyroptosis proportion between irradiated MCF-7 cells and MCF-7 CSCs. *$P < 0.05$; **$P < 0.01$; ***$P < 0.001$.

almost showed no change compared to the relative control (**Figures 5A,B**). **Figures 5C,D** were the representative images.

Overall, our results showed that even under ultra-high dose rate FLASH-IR, MCF-7 CSC was more radio-resistant than normal cancer cells (MCF-7), the proportion of apoptosis was significantly lower. By detecting cell's autophagy after irradiation, we found that the autophagy in CSC was much higher, which may make it more resistant to radiation and appear less apoptosis. In addition, our experiments also found that the overall level of irradiated pyroptosis and necrosis of CSC was slightly lower than that of normal cells, and the response to irradiation also seemed slower.

DISCUSSION

In this article, we studied the killing effect of ultra-high dose rate FLASH-IR on MCF-7 and its CSCs. The results showed that the apoptosis of irradiated CSCs was significantly lower than that of MCF-7, and the pyroptosis and necrosis of irradiated CSCs were

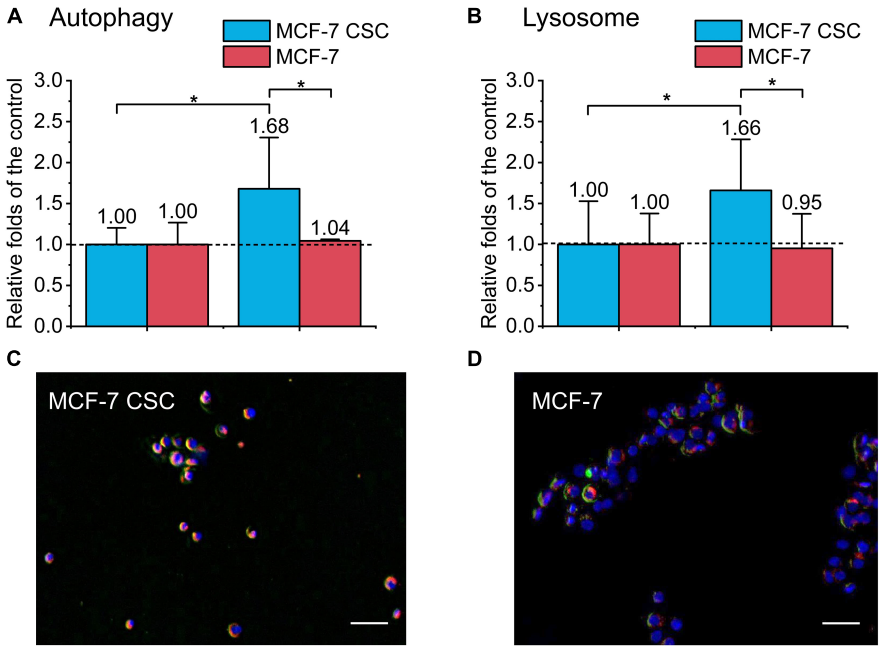

FIGURE 5 | Detection of autophagy and lysosome of irradiated MCF-7 cells and MCF-7 CSCs. **(A)** Compared with the control, the increasement of autophagy proportion for irradiated group. **(B)** Compared with the control, the increasement of lysosome for irradiated group. **(C,D)** Representative images of irradiated MCF-7 cells and MCF-7 CSCs stained with MDC autophagy detection kit and lysoTracker Red DND-99. The blue was the nucleus, the red was the lysosome, and the green labeled autophagy. Scale bars: 50 μm. *$P < 0.05$.

also slightly lower than that of MCF-7. In addition, the response of CSC to irradiation was slower. These results suggested the radio-resistance of CSCs under FLASH-IR. By detecting cell's autophagy as well as lysosomes after irradiation, we found that the lysosomes and autophagy in CSC are much higher, suggesting CSC may enhance the radio-resistance by increasing lysosome-mediated autophagy and decreasing apoptosis after FLASH-IR.

High levels of anti-apoptotic molecules make cancer cells resistant to RT and chemotherapy (Schmitt, 2003). Drugs targeting the apoptotic pathway have anticancer effects in many malignant tumors, and many of these new therapies have entered clinical trials (Hassan et al., 2014; Delbridge et al., 2016). Among them, CSCs seemed to be more resistant to apoptosis than normal cancer cells. Bao et al. (2006) reported that the apoptosis in CSCs was ∼4–5 folds lower than that in non-stem cancer cells (NSCCs), in addition, there were also results showing that the apoptosis of CSCs was ∼8 folds lower than that of NSCCs when irradiated by conventional dose rate γ-rays, and was ∼3–4 folds lower than that of NSCCs when irradiated by conventional dose rate proton (Fu et al., 2012). Present experimental results showed that the apoptosis of FLASH irradiated CSCs was ∼6 folds lower than that of irradiated MCF-7 cells, suggesting even under ultra-high dose rate irradiation, the radio-resistance of CSC still existed. The possible reasons for CSCs' apoptosis resistance are as follows, the critical step in the apoptotic cascade is mitochondrial outer membrane permeabilization (MOMP), and CSCs expressed higher levels of anti-apoptotic proteins related to MOMP, including Bcl-2 and Bcl-XL (Beroukhim et al., 2010). Our results indicated that CSCs produce less pyroptosis than normal cancer cells, which may be related to CSCs' stronger ROS removal ability (Chang et al., 2014). Ion irradiation induced the production of ROS, and at the same time, the excessive ROS destroyed the body's antioxidant system, thereby generating more ROS, forming a cascade of amplified inflammatory responses (Qiu et al., 2017). ROS mediates cell death by affecting mitochondria (Zorov et al., 2014), among them, ROS-mediated apoptosis has been well studied. Due to less research, the relationship between ROS and pyroptosis has not been fully reported. Recently, there have been research reported that pyroptosis was closely related to the ROS level (Dong et al., 2020), which was also consistent with our results. However, whether ROS is the cause of pyroptosis remains unclear and is worthy of in-depth study.

There were several results indicated that lysosomes were related to radio-resistance, and targeted lysosome therapy can increase radiation sensitivity (Zhang et al., 2017; Wang et al., 2018). Lysosome-mediated radio-resistance was mainly related to autophagy. In the late stage of autophagy, lysosomes combine with autophagosomes to form autophagy-lysosomes and act as scavengers. Existing researches showed that autophagy plays a dual role in cancer development. In anti-tumor therapy, inducing autophagy can achieve tumor suppression. However, for resistant tumors, autophagy appears to be a protective mechanism that reduces the damage caused by radiation/drug (Han et al., 2018). CSC is usually associated with an increase in the level of autophagy. Autophagy allows CSC to maintain pluripotency and develop resistance, etc. (Nazio et al., 2019). Presently, our results showed that compared with the control, the autophagy of irradiated CSCs increased significantly, ∼1.7 folds of the control,

while the autophagy of irradiated MCF-7 kept unchanged (**Figure 5A**). Studies have identified a pathway for autophagy regulation by synchronizing ATR checkpoints and double-strand break pathways (Robert et al., 2011). Therefore, CSC may use autophagy to inhibit DNA damage, thereby improving survival (Rahman et al., 2020).

For different death pathways, despite some differences, there are also some cross-talking among them. Apoptosis and necrosis are the two main pathways of cell death, and their molecular mechanisms have been extensively studied. Although originally thought to constitute a mutually exclusive cellular state, recent discoveries have revealed the need for a balanced and interactive cellular environment between these two death pathways. This was also supported by experimental data, the analysis of FAS Associated death domain (FADD)/receptor interacting protein 3 (RIP3 and FLIP/RIP3 double knockout showed that there is a complex cross-regulation of apoptosis and necrosis (Dillon et al., 2012). Besides, more and more evidences showed that autophagy and apoptosis can cooperate or antagonize with each other, thereby differentially affecting the fate of cells (Nikoletopoulou et al., 2013). In general, different death pathways interact with each other to produce the final effect. For the more precise mechanisms and the corresponding upstream and downstream influencing factors, further research is needed.

As an emerging thing, laser accelerators can complete irradiation in a very short time (∼ ns) and achieve ultra-high dose rates. But at the same time, it has stability issues, and the dose and particle types between different shots cannot be completely consistent (Lundh et al., 2012; Manti et al., 2017). We also marked in the figures. In general, more experiments are needed in the future, to further clarify the killing effect and mechanism of FLASH-RT on cancer cells and the protective mechanism of FLASH-RT on normal cells.

DATA AVAILABILITY STATEMENT

The original contributions presented in the study are included in the article/**Supplementary Material**, further inquiries can be directed to the corresponding author/s.

ETHICS STATEMENT

The animal study was reviewed and approved by the Peking University Institutional Animal Care and Use Committee (Approval ID: Physics-YangG-2).

AUTHOR CONTRIBUTIONS

GY, CL, WM, and XY conceived the research plan. GY and CL designed the biology experiments. GY, CL, JH, JQ, and XS performed the biology experiments. CL and JH analyzed the results and produced the figures. ZM, WM, and GY designed and constructed the irradiation setup. ZM, YL, ZP, DK, SX, ZL, YGao, GQ, YS, SC, ZC, YZ, and YGeng supervised by WM performed the laser acceleration and cell irradiation experiments. ZM and YL measured the proton radiation and provided the dose data. CL wrote the initial draft of the manuscript. GY wrote the final draft of the manuscript. All authors commented on the manuscript.

FUNDING

This study was supported by the National Natural Science Foundation of China (11875079, 61631001, and 119210067), the National Grand Instrument Project (2019YFF01014402), NSFC innovation group project (No. 11921006), and the State Key Laboratory of Nuclear Physics and Technology, PKU under Grant Nos. NPT2020KFY19 and NPT2020KFJ04.

ACKNOWLEDGMENTS

We are very grateful to Prof. Yugang Wang for helpful discussions.

SUPPLEMENTARY MATERIAL

The Supplementary Material for this article can be found online at: https://www.frontiersin.org/articles/10.3389/fcell.2021.672693/full#supplementary-material

REFERENCES

Arnold, C. R., Mangesius, J., Skvortsova, I. I., and Ganswindt, U. (2020). The Role of Cancer Stem Cells in Radiation Resistance. *Front. Oncol.* 10:164. doi: 10.3389/fonc.2020.00164

Bao, S., Wu, Q., McLendon, R. E., Hao, Y., Shi, Q., Hjelmeland, A. B., et al. (2006). Glioma stem cells promote radioresistance by preferential activation of the DNA damage response. *Nature* 444, 756–760. doi: 10.1038/nature05236

Batlle, E., and Clevers, H. (2017). Cancer stem cells revisited. *Nat. Med.* 23, 1124–1134. doi: 10.1038/nm.4409

Bayart, E., Flacco, A., Delmas, O., Pommarel, L., Leyy, D., Cayallone, M., et al. (2019). Fast dose fractionation using ultra-short laser accelerated proton pulses can increase cancer cell mortality, which relies on functional PARP1 protein. *Sci. Rep.* 9:10132. doi: 10.1038/s41598-019-46512-1

Beroukhim, R., Mermel, C. H., Porter, D., Wei, G., Raychaudhuri, S., Donovan, J., et al. (2010). The landscape of somatic copy-number alteration across human cancers. *Nature* 463, 899–905. doi: 10.1038/nature08822

Bin, J. H., Allinger, K., Assmann, W., Dollinger, G., Drexler, G. A., Friedl, A. A., et al. (2012). A laser-driven nanosecond proton source for radiobiological studies. *Appl. Phys. Lett.* 101:243701. doi: 10.1063/1.4769372

Bourhis, J., Sozzi, W. J., Jorge, P. G., Gaide, O., Bailat, C., Duclos, F., et al. (2019). Treatment of a first patient with FLASH-radiotherapy. *Radiother. Oncol.* 139, 18–22. doi: 10.1016/j.radonc.2019.06.019

Bozhenko, V. K., Ivanov, A. V., Kulinich, T. M., Smirnov, V. P., Shishkin, A. M., and Solodky, V. A. (2019). Comparison of Biological Effects of gamma-Radiation of Low and Ultra-High Dose Rate on Lymphocytes and Cultured Human Malignant Lymphoma Cells. *Bull. Exp. Biol. Med.* 166, 785–787. doi: 10.1007/s10517-019-04440-0

Chang, C. W., Chen, Y. S., Chou, S. H., Han, C. L., Chen, Y. J., Yang, C. C., et al. (2014). Distinct subpopulations of head and neck cancer cells with different levels of intracellular reactive oxygen species exhibit diverse stemness,

proliferation, and chemosensitivity. *Cancer Res.* 74, 6291–6305. doi: 10.1158/0008-5472.CAN-14-0626

Chiou, S. H., Kao, C. L., Chen, Y. W., Chien, C. S., Hung, S. C., Lo, J. F., et al. (2008). Identification of CD133-positive radioresistant cells in atypical teratoid/rhabdoid tumor. *PLoS One* 3:e2090. doi: 10.1371/journal.pone.0002090

Delbridge, A. R., Grabow, S., Strasser, A., and Vaux, D. L. (2016). Thirty years of BCL-2: translating cell death discoveries into novel cancer therapies. *Nat. Rev. Cancer* 16, 99–109. doi: 10.1038/nrc.2015.17

Diehn, M., Cho, R. W., Lobo, N. A., Kalisky, T., Dorie, M. J., Kulp, A. N., et al. (2009). Association of reactive oxygen species levels and radioresistance in cancer stem cells. *Nature* 458, 780–783. doi: 10.1038/nature07733

Dillon, C. P., Oberst, A., Weinlich, R., Janke, L. J., Kang, T. B., Ben-Moshe, T., et al. (2012). Survival Function of the FADD-CASPASE-8-cFLIP(L) Complex. *Cell Rep.* 1, 401–407. doi: 10.1016/j.celrep.2012.03.010

Dong, S., Lyu, X., Yuan, S., Wang, S., Li, W., Chen, Z., et al. (2020). Oxidative stress: a critical hint in ionizing radiation induced pyroptosis. *Radiat. Med. Prot.* 1, 179–185. doi: 10.1016/j.radmp.2020.10.001

Doria, D., Kakolee, K. F., Kar, S., Litt, S. K., Fiorini, F., Ahmed, H., et al. (2012). Biological effectiveness on live cells of laser driven protons at dose rates exceeding 10(9) Gy/s. *Aip Adv.* 2:011209. doi: 10.1063/1.3699063

Durante, M., Brauer-Krisch, E., and Hill, M. (2018). Faster and safer? FLASH ultra-high dose rate in radiotherapy. *Br. J. Radiol.* 91:20170628. doi: 10.1259/bjr.20170628

Favaudon, V., Caplier, L., Monceau, V., Pouzoulet, F., Sayarath, M., Fouillade, C., et al. (2014). Ultrahigh dose-rate FLASH irradiation increases the differential response between normal and tumor tissue in mice. *Sci. Transl. Med.* 6:245ra93. doi: 10.1126/scitranslmed.3008973

Field, S. B., and Bewley, D. K. (1974). Effects of dose-rate on the radiation response of rat skin. *Int. J. Radiat. Biol. Relat. Stud. Phys. Chem. Med.* 26, 259–267. doi: 10.1080/09553007414551221

Fu, Q., Huang, T., Wang, X., Lu, C., Liu, F., Yang, G., et al. (2017). Association of elevated reactive oxygen species and hyperthermia induced radiosensitivity in cancer stem-like cells. *Oncotarget* 8, 101560–101571. doi: 10.18632/oncotarget.21678

Fu, Q. B., Quan, Y., Wang, W. K., Mei, T., Wu, J. W., Li, J., et al. (2012). Response of cancer stem-like cells and non-stem cancer cells to proton and gamma-ray irradiation. *Nucl.Instrum. Methods Phys. Res. B* 286, 346–350. doi: 10.1016/j.nimb.2012.01.032

Geng, Y. X., Qing-Liao, Shou, Y. R., Zhu, J. G., Xu, X. H., Wu, M. J., et al. (2018). Generating Proton Beams Exceeding 10 MeV Using High Contrast 60TW Laser. *Chin. Phys Lett.* 35:092901. doi: 10.1088/0256-307x/35/9/092901

Griffin, R. J., Ahmed, M. M., Amendola, B., Belyakov, O., Bentzen, S. M., Butterworth, K. T., et al. (2020). Understanding High-Dose, Ultra-High Dose Rate, and Spatially Fractionated Radiation Therapy. *Int. J. Radiat. Oncol. Biol. Phys.* 107, 766–778. doi: 10.1016/j.ijrobp.2020.03.028

Han, Y., Fan, S., Qin, T., Yang, J., Sun, Y., Lu, Y., et al. (2018). Role of autophagy in breast cancer and breast cancer stem cells (Review). *Int. J. Oncol.* 52, 1057–1070. doi: 10.3892/ijo.2018.4270

Hantonl, F., Chaudhary, P., Doria, D., Gwynne, D., Maiorino, C., Scullion, C., et al. (2019). DNA DSB Repair Dynamics following Irradiation with Laser-Driven Protons at Ultra-High Dose Rates. *Sci. Rep.* 9:4471. doi: 10.1038/s41598-019-40339-6

Hassan, M., Watari, H., AbuAlmaaty, A., Ohba, Y., and Sakuragi, N. (2014). Apoptosis and molecular targeting therapy in cancer. *Biomed. Res. Int.* 2014:150845. doi: 10.1155/2014/150845

Ledingham, K. W. D., Bolton, P. R., Shikazono, N., and Ma, C. M. C. (2014). Towards Laser Driven Hadron Cancer Radiotherapy: a Review of Progress. *Appl. Sci. Basel* 4, 402–443. doi: 10.3390/app4030402

Li, C., Tian, M., Gou, Q., Jia, Y. R., and Su, X. (2019). Connexin43 Modulates X-Ray-Induced Pyroptosis in Human Umbilical Vein Endothelial Cells. *Biomed. Environ. Sci.* 32, 177–188. doi: 10.3967/bes2019.025

Liao, H., Wang, H., Rong, X., Li, E., Xu, R. H., and Peng, Y. (2017). Mesenchymal Stem Cells Attenuate Radiation-Induced Brain Injury by Inhibiting Microglia Pyroptosis. *Biomed. Res. Int.* 2017:1948985. doi: 10.1155/2017/1948985

Lomonaco, S. L., Finniss, S., Xiang, C., Decarvalho, A., Umansky, F., Kalkanis, S. N., et al. (2009). The induction of autophagy by gamma-radiation contributes to the radioresistance of glioma stem cells. *Int. J. Cancer* 125, 717–722. doi: 10.1002/ijc.24402

Lundh, O., Rechatin, C., Faure, J., Ben-Ismail, A., Lim, J., De Wagter, C., et al. (2012). Comparison of measured with calculated dose distribution from a 120-MeV electron beam from a laser-plasma accelerator. *Med. Phys.* 39, 3501–3508. doi: 10.1118/1.4719962

Manti, L., Perozziello, F. M., Borghesi, M., Candiano, G., Chaudhary, P., Cirrone, G. A. P., et al. (2017). The radiobiology of laser-driven particle beams: focus on sub-lethal responses of normal human cells. *J. Instrum.* 12:C03084. doi: 10.1088/1748-0221/12/03/C03084

Mitteer, R. A., Wang, Y. L., Shah, J., Gordon, S., Fager, M., Butter, P. P., et al. (2015). Proton beam radiation induces DNA damage and cell apoptosis in glioma stem cells through reactive oxygen species. *Sci. Rep.* 5:13961. doi: 10.1038/srep13961

Montay-Gruel, P., Petersson, K., Jaccard, M., Boivin, G., Germond, J. F., Petit, B., et al. (2017). Irradiation in a flash: unique sparing of memory in mice after whole brain irradiation with dose rates above 100Gy/s. *Radiother. Oncol.* 124, 365–369. doi: 10.1016/j.radonc.2017.05.003

Moore, N., and Lyle, S. (2011). Quiescent, slow-cycling stem cell populations in cancer: a review of the evidence and discussion of significance. *J. Oncol.* 2011:396076. doi: 10.1155/2011/396076

Nazio, F., Bordi, M., Cianfanelli, V., Locatelli, F., and Cecconi, F. (2019). Autophagy and cancer stem cells: molecular mechanisms and therapeutic applications. *Cell Death Differ.* 26, 690–702. doi: 10.1038/s41418-019-0292-y

Nikoletopoulou, V., Markaki, M., Palikaras, K., and Tavernarakis, N. (2013). Crosstalk between apoptosis, necrosis and autophagy. *Biochim. Biophys Acta* 1833, 3448–3459. doi: 10.1016/j.bbamcr.2013.06.001

O'Brien, M., Moehring, D., Munoz-Planillo, R., Nunez, G., Callaway, J., Ting, J., et al. (2017). A bioluminescent caspase-1 activity assay rapidly monitors inflammasome activation in cells. *J. Immunol. Methods* 447, 1–13. doi: 10.1016/j.jim.2017.03.004

Patriarca, A., Fouillade, C., Auger, M., Martin, F., Pouzoulet, F., Nauraye, C., et al. (2018). Experimental Set-up for FLASH Proton Irradiation of Small Animals Using a Clinical System. *Int. J. Radiat. Oncol. Biol Phys.* 102, 619–626. doi: 10.1016/j.ijrobp.2018.06.403

Pommarel, L., Vauzour, B., Megnin-Chanet, F., Bayart, E., Delmas, O., Goudjil, F., et al. (2017). Spectral and spatial shaping of a laser-produced ion beam for radiation-biology experiments. *Phys Rev. Accel. Beams* 20:032801. doi: 10.1103/PhysRevAccelBeams.20.032801

Qiu, S. Q., Liu, J., and Xing, F. Y. (2017). 'Hints' in the killer protein gasdermin D: unveiling the secrets of gasdermins driving cell death. *Cell Death Differ* 24, 588–596. doi: 10.1038/cdd.2017.24

Rahman, M. A., Saha, S. K., Rahman, M. S., Uddin, M. J., Uddin, M. S., Pang, M. G., et al. (2020). Molecular Insights Into Therapeutic Potential of Autophagy Modulation by Natural Products for Cancer Stem Cells. *Front. Cell Dev. Biol.* 8:283. doi: 10.3389/fcell.2020.00283

Rama, N., Saha, T., Shukla, S., Goda, C., Milewski, D., Mascia, A. E., et al. (2019). Improved Tumor Control Through T-cell Infiltration Modulated by Ultra-High Dose Rate Proton FLASH Using a Clinical Pencil Beam Scanning Proton System. *Int. J. Radiat. Oncol. Biol Phys.* 105, S164–S165.

Raschke, S., Spickermann, S., Toncian, T., Swantusch, M., Boeker, J., Giesen, U., et al. (2016). Ultra-short laser-accelerated proton pulses have similar DNA-damaging effectiveness but produce less immediate nitroxidative stress than conventional proton beams. *Sci. Rep.* 6:32441. doi: 10.1038/srep32441

Robert, T., Vanoli, F., Chiolo, I., Shubassi, G., Bernstein, K. A., Rothstein, R., et al. (2011). HDACs link the DNA damage response, processing of double-strand breaks and autophagy. *Nature* 471, 74–79. doi: 10.1038/nature09803

Rosch, T. F., Szabo, Z., Haffa, D., Bin, J. H., Brunner, S., Englbrecht, F. S., et al. (2020). A feasibility study of zebrafish embryo irradiation with laser-accelerated protons. *Rev. Sci. Instrum* 91:063303. doi: 10.1063/5.0008512

Schmitt, C. A. (2003). Senescence, apoptosis and therapy–cutting the lifelines of cancer. *Nat. Rev. Cancer* 3, 286–295. doi: 10.1038/nrc1044

Tang, L., Wei, F., Wu, Y., He, Y., Shi, L., Xiong, F., et al. (2018). Role of metabolism in cancer cell radioresistance and radiosensitization methods. *J. Exp. Clin. Cancer Res.* 37:87. doi: 10.1186/s13046-018-0758-7

Turcotte, S., and Giaccia, A. J. (2010). Targeting cancer cells through autophagy for anticancer therapy. *Curr. Opin Cell Biol* 22, 246–251. doi: 10.1016/j.ceb.2009.12.007

Vozenin, M. C., Hendry, J. H., and Limoli, C. L. (2019). Biological Benefits of Ultra-high Dose Rate FLASH Radiotherapy: sleeping Beauty Awoken. *Clin. Oncol. (R Coll Radiol)* 31, 407–415. doi: 10.1016/j.clon.2019.04.001

Wang, F., Tang, J. Y., Li, P. C., Si, S. H., Yu, H., Yang, X., et al. (2018). Chloroquine Enhances the Radiosensitivity of Bladder Cancer Cells by Inhibiting Autophagy and Activating Apoptosis. *Cell. Physiol. Biochem.* 45, 54–66. doi: 10.1159/000486222

Wang, L., Han, S., Zhu, J., Wang, X., Li, Y., Wang, Z., et al. (2019). Proton versus photon radiation-induced cell death in head and neck cancer cells. *Head Neck* 41, 46–55. doi: 10.1002/hed.25357

Wang, Y., Gao, W., Shi, X., Ding, J., Liu, W., He, H., et al. (2017). Chemotherapy drugs induce pyroptosis through caspase-3 cleavage of a gasdermin. *Nature* 547, 99–103. doi: 10.1038/nature22393

Westbom, C., Thompson, J. K., Leggett, A., MacPherson, M., Beuschel, S., Pass, H., et al. (2015). Inflammasome Modulation by Chemotherapeutics in Malignant Mesothelioma. *PLoS One* 10:e0145404. doi: 10.1371/journal.pone.0145404

Woodward, W. A., Chen, M. S., Behbod, F., Alfaro, M. P., Buchholz, T. A., and Rosen, J. M. (2007). WNT/beta-catenin mediates radiation resistance of mouse mammary progenitor cells. *Proc. Natl. Acad. Sci. U. S. A.* 104, 618–623. doi: 10.1073/pnas.0606599104

Yogo, A., Maeda, T., Hori, T., Sakaki, H., Ogura, K., Nishiuchi, M., et al. (2011). Measurement of relative biological effectiveness of protons in human cancer cells using a laser-driven quasimonoenergetic proton beamline. *Appl. Phys. Lett.* 98:053701. doi: 10.1063/1.3551623

YuN, K. (1992). Contributions of the direct and indirect effects of ionizing radiation to reproductive cell death. *Radiat. Res.* 129, 228–234. doi: 10.2307/3578162

Zeil, K., Baumann, M., Beyreuther, E., Burris-Mog, T., Cowan, T. E., Enghardt, W., et al. (2013). Dose-controlled irradiation of cancer cells with laser-accelerated proton pulses. *Appl. Phys. B.* 110, 437–444. doi: 10.1007/s00340-012-5275-3

Zhang, X., Wang, J., Li, X., and Wang, D. (2018). Lysosomes contribute to radioresistance in cancer. *Cancer Lett* 439, 39–46. doi: 10.1016/j.canlet.2018.08.029

Zhang, X., Xu, R., Zhang, C., Xu, Y. Y., Han, M. Z., Huang, B., et al. (2017). Trifluoperazine, a novel autophagy inhibitor, increases radiosensitivity in glioblastoma by impairing homologous recombination. *J. Exp. Clin. Cancer Res.* 36:118. doi: 10.1186/s13046-017-0588-z

Zorov, D. B., Juhaszova, M., and Sollott, S. J. (2014). Mitochondrial Reactive Oxygen Species (Ros) and Ros-Induced Ros Release. *Physiol. Rev.* 94, 909–950. doi: 10.1152/physrev.00026.2013

Conflict of Interest: The authors declare that the research was conducted in the absence of any commercial or financial relationships that could be construed as a potential conflict of interest.

frontiers in Cell and Developmental Biology

ORIGINAL RESEARCH
published: 30 April 2021
doi: 10.3389/fcell.2021.672929

Ultra-High Dose Rate FLASH Irradiation Induced Radio-Resistance of Normal Fibroblast Cells Can Be Enhanced by Hypoxia and Mitochondrial Dysfunction Resulting From Loss of Cytochrome C

Jintao Han[1†], Zhusong Mei[1†], Chunyang Lu[1†], Jing Qian[2†], Yulan Liang[1], Xiaoyi Sun[1], Zhuo Pan[1], Defeng Kong[1], Shirui Xu[1], Zhipeng Liu[1], Ying Gao[1], Guijun Qi[1], Yinren Shou[1], Shiyou Chen[1], Zhengxuan Cao[1], Ye Zhao[2], Chen Lin[1], Yanying Zhao[1], Yixing Geng[1], Jiaer Chen[1], Xueqing Yan[1,3], Wenjun Ma[1]* and Gen Yang[1]**

[1] State Key Laboratory of Nuclear Physics and Technology, School of Physics and CAPT, Peking University, Beijing, China, [2] Teaching and Research Section of Nuclear Medicine, School of Basic Medical Sciences, Anhui Medical University, Hefei, China, [3] Collaborative Innovation Center of Extreme Optics, Shanxi University, Taiyuan, China

Ultra-high dose rate FLASH irradiation (FLASH-IR) has got extensive attention since it may provide better protection on normal tissues while maintain tumor killing effect compared with conventional dose rate irradiation. The FLASH-IR induced protection effect on normal tissues is exhibited as radio-resistance of the irradiated normal cells, and is suggested to be related to oxygen depletion. However, the detailed cell death profile and pathways are still unclear. Presently normal mouse embryonic fibroblast cells were FLASH irradiated ($\sim 10^9$ Gy/s) at the dose of ~10–40 Gy in hypoxic and normoxic condition, with ultra-fast laser-generated particles. The early apoptosis, late apoptosis and necrosis of cells were detected and analyzed at 6, 12, and 24 h post FLASH-IR. The results showed that FLASH-IR induced significant early apoptosis, late apoptosis and necrosis in normal fibroblast cells, and the apoptosis level increased with time, in either hypoxic or normoxic conditions. In addition, the proportion of early apoptosis, late apoptosis and necrosis were significantly lower in hypoxia than that of normoxia, indicating that radio-resistance of normal fibroblast cells under FLASH-IR can be enhanced by hypoxia. To further investigate the apoptosis related profile and potential pathways, mitochondria dysfunction cells resulting from loss of cytochrome c (cyt $c^{-/-}$) were also irradiated. The results showed that compared with irradiated normal cells (cyt $c^{+/+}$), the late apoptosis and necrosis but not early apoptosis proportions of irradiated cyt $c^{-/-}$ cells were significant decreased in both hypoxia and normoxia, indicating mitochondrial dysfunction increased radio-resistance of FLASH irradiated cells. Taken together, to our limited knowledge, this is the first report shedding light on the death

OPEN ACCESS

Edited by:
Shengmin Xu,
Anhui University, China

Reviewed by:
Hailong Pei,
Soochow University, China
Chunlin Shao,
Fudan University, China

***Correspondence:**
Gen Yang
gen.yang@pku.edu.cn
Xueqing Yan
x.yan@pku.edu.cn
Wenjun Ma
wenjun.ma@pku.edu.cn

[†] These authors have contributed equally to this work

Specialty section:
This article was submitted to Cell Death and Survival, a section of the journal Frontiers in Cell and Developmental Biology

Received: 26 February 2021
Accepted: 08 April 2021
Published: 30 April 2021

Citation:
Han J, Mei Z, Lu C, Qian J, Liang Y, Sun X, Pan Z, Kong D, Xu S, Liu Z, Gao Y, Qi G, Shou Y, Chen S, Cao Z, Zhao Y, Lin C, Zhao Y, Geng Y, Chen J, Yan X, Ma W and Yang G (2021) Ultra-High Dose Rate FLASH Irradiation Induced Radio-Resistance of Normal Fibroblast Cells Can Be Enhanced by Hypoxia and Mitochondrial Dysfunction Resulting From Loss of Cytochrome C. Front. Cell Dev. Biol. 9:672929. doi: 10.3389/fcell.2021.672929

profile and pathway of normal and cyt $c^{-/-}$ cells under FLASH-IR in hypoxic and normoxic circumstances, which might help us improve the understanding of the FLASH-IR induced protection effect in normal cells, and thus might potentially help to optimize the future clinical FLASH treatment.

Keywords: ultra-high dose rate irradiation, FLASH, radio-resistance, cell death, hypoxia, normoxia, mitochondria, cytochrome c

INTRODUCTION

Radiotherapy (RT) makes up an essential part of cancer treatment and more than half of cancer patients receive radiotherapy during treatment (Vozenin et al., 2019a). In conventional radiotherapy, the radiation includes photons, electrons, protons and heavy ions (Valentini et al., 2020). Although major advances in precise treatment delivery and multimodal imaging allowed radiotherapy to apply to more patients, radiation resistance still remains an unsolved clinical problem, thus more powerful and better tolerated radiotherapy was needed (Vozenin et al., 2019a). A novel modality of irradiation, named FLASH radiotherapy (FLASH-RT), has got extensive attention in recent years, since it provides better protection on normal tissues while maintains tumor killing effects (Durante et al., 2018). At the biological level, the increased radio-resistance and reduced normal tissue toxicity has been named as the FLASH protection effect (Montay-Gruel et al., 2018). Compared with conventional irradiation (∼1 Gy/min), FLASH-RT provides ultra-high dose rate (>40 Gy/s) and is always delivered in an ultra-short time (<0.1 s) (Durante et al., 2018). Normal tissue sparing by FLASH of many organs has been demonstrated in previous experiments (Bourhis et al., 2019; Griffin et al., 2020). Favaudon et al. (2014) found that the pulmonary fibrosis of mouse didn't appear at 36 weeks after FLASH irradiation while it appeared at 8 weeks after the same dose with conventional dose rate. Montay-Gruel et al. found that spatial memory of mice was preserved after whole brain irradiation with >100 Gy/s dose rate while it was totally impaired with 0.1 Gy/s dose rate at same dose (Petersson et al., 2017). Loo et al. (2017) found that when receiving abdomen irradiation between 10 and 22 Gy, the median lethal dose (LD50) of mouse is 14.7 Gy for 0.05 Gy/s dose rate and 18.3 Gy for 210 Gy/s dose rate. The FLASH IR experiments could be performed on conventional accelerators and on compact laser-driven accelerators as well (Ledingham et al., 2014). The laser-driven proton beams with duration scale of nanosecond at the irradiation site can improve dose rates to about 10^9 Gy/s (Bin et al., 2012; Doria et al., 2012; Hanton et al., 2019). Several FLASH IR studies have been reported *in vitro* (Zeil et al., 2013; Raschke et al., 2016; Bayart et al., 2019) and *in vivo* (Rosch et al., 2020) with laser-driven protons, aiming to clarify the radiobiological effects of the high dose rate proton bunches.

Currently the exact mechanism of FLASH effect on normal tissues is not clear, and is suggested to be closely related to the oxygen consumption in tissues (Wilson et al., 2012). The hypothesis is as follows, FLASH with high total dose depletes oxygen within ultra-short time, and it is too quickly for diffusion and reoxygenation, so the normal tissue responds as hypoxic tissue (Durante et al., 2018). Therefore, ultra-high dose rate will increase the radio-resistance of the normal tissue while have small impact on the already hypoxic tumor tissue (Durante et al., 2018).

Irradiation induces cell death mainly by damaging DNA either directly or indirectly (Korystov, 1992). Among the cell death after irradiation, apoptosis is a highly regulated form with characteristic morphological and molecular features (Eriksson and Stigbrand, 2010; Sia et al., 2020). The mitochondrial apoptotic pathway is activated when the DNA damage repair machinery disrupts the balance between pro- and anti-apoptotic factors, resulting in the release of cytochrome c (cyt c) from mitochondria (Sia et al., 2020). The externalization of phosphatidylserine on the plasma membrane is a marker of early stage apoptosis (Yun and Lee, 2016) and can be detected by annexin-V (Xu and Leung, 2010; Liu et al., 2013), while late apoptosis and secondary necrosis have the feature of DNA and nuclear fragmentation and permeability of the plasma membrane to propidium iodide (Bacso et al., 2000; Troiano et al., 2007; Foldbjerg et al., 2011).

Cyt c is a pivotal protein residing in mitochondria, and acts as a component of mitochondria respiration and apoptosis initiator (Yang et al., 2009). It transports electrons from Complex III to Complex IV in respiratory chain and is crucial for ATP synthesis through oxidative phosphorylation (Yang et al., 2009; Wilson and Vinogradov, 2014). In response to stimuli such as radiation induced DNA damages, cytochrome c is released from intermembrane space of mitochondria, binds Apaf-1 with high affinity in cytosol and triggers oligomerization of Apaf-1/cyt c complexes that activate procaspase-9. And then activated caspase-9 cleaves and activates caspase-3, caspase-6 and caspase-7, which function as downstream effectors of the cell death (Li et al., 2000; Wang and Youle, 2009).

Due to its significant clinic potential of the fledging ultra-high dose rate FLASH-IR area, there are many fundamental questions need to be carefully re-visited as conventional low dose rate irradiation, especially the basic killing effect of FLASH on normal cells in hypoxic and normoxic condition. In this article, cyt c-normal (cyt $c^{+/+}$) and -null (cyt $c^{-/-}$) mouse embryonic fibroblast cells were irradiated and traced after FLASH-IR (>10^9 Gy/s) at a dose of ∼10 to 40 Gy in hypoxic

Abbreviations: Cyt c, cytochrome c; FBS, fetal bovine serum; PI, propidium iodide; RT, radiotherapy; FLASH-IR, FLASH irradiation; CLAPA, compact laser plasma accelerator system; FWHM, full width at half maximum; TPS, Thomson parabola spectrometer; RCF, radiochromic film.

and normoxic condition, using CLAPA ultra-fast laser-generated particles, and the dose was determined by the experimental ion spectra and dose spatial distribution combined with Monte Carlo simulations.

MATERIALS AND METHODS

Cell Culture

Cyt c-normal and -null mouse embryonic fibroblast cells are kind gifts from Dr. Xiaodong Wang (Li et al., 2000; Yang et al., 2009). The cells were cultured in Dulbecco's modified Eagle's medium (DMEM, HyClone) supplemented with 20% fetal bovine serum (FBS, Bai Ling Biotechnology), 100 U/ml penicillin and streptomycin (P/S) (HyClone), 50 mg/L uridine (Macklin), 2 mM glutamine (Boyobio), 1 × non-essential amino acids (Coolaber), 55 mM 2′-mercaptoethanol (Macklin), 2.5 M HEPES (Boyobio) and 5×10^5 unit/L mouse leukemia inhibitory factor (Yize). The cyt c-null cell culture medium was added with 110 mg/L pyruvate (Psaitong) for the compensation of the defect in mitochondrial respiration. And the petri dishes for both cell lines were pre-coated with 1% geltrex (Gibco) as described previously (Fu et al., 2017) and cells were cultured at 37°C in a humidified incubator (5% CO_2).

Detection of Viability

The Calcein-AM/PI staining kit (BestBio) was used to assay the viability of cyt $c^{+/+}$ and cyt $c^{-/-}$ cells. Cells were harvested at the confluence of 70–80%, transfered to 96-well plate and stained with Calcin-AM and PI. Live cells and dead cells showed green fluorescence and red fluorescence respectively.

Experimental Setup

The FLASH radiation experiment was performed using Compact Laser Plasma Accelerator (CLAPA) system at Peking University. The CLAPA laser is a Ti: sapphire laser with central wavelength of 800 nm and full-width-at-half-maximum duration of 30 fs. A single plasma mirror system was used to increase the temporal contrast to 10^8@5 ps. S-polarized laser was focused onto the 100 nm plastic target using an f/2.5 off-axis parabolic (OAP) with a focal length of 200 mm. The laser energy on target was ∼1 J and the diameter (FWHM) of focal spot was 4.2 μm, containing 36% of the total energy, resulting in the peak intensity of 5.6×10^{19} W/cm^2. The target got broken by the laser at each shot, generating ultra-short ion bunch. The ion energy spectra were measured by a Thomson parabola spectrometer (TPS) positioned at 780 mm along the direction normal to the back surface of the target. The cells irradiation system was plugged in after the ion energy spectra were measured (**Figure 1A**). The ion

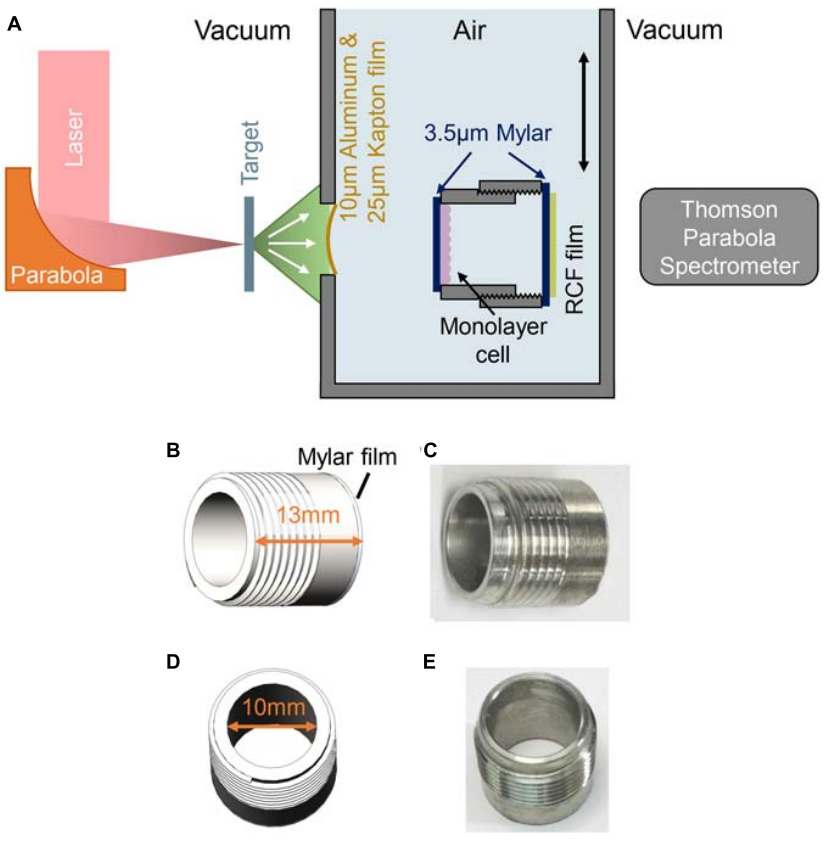

FIGURE 1 | Experimental setup for FLASH irradiation. **(A)** Schematic drawing of experimental setup. **(B,C)** Side view of the cell-culture cylinder, cells were cultured on the 3.5 μm Mylar film adhered to inner side of the cylinder. **(D,E)** Top view of the cell-culture cylinder.

beams entered cells radiation system through a vacuum window and irradiated the cells.

Dose Monitoring

The ions were accelerated in well-known Target Normal Sheath Acceleration (TNSA) regime (Passoni et al., 2010), which leads to exponentially decreasing energy spectra up to a cut-off energy around 5–6 MeV depending on the on-target laser intensity. The parabolic traces of ions were obtained by the Thomson Parabola Spectrometer, recorded by a micro-channel plate with a phosphor screen and imaged onto a 16-bit EMCCD camera. After the proton energy was known and the cells irradiation system moved in, customized radiochromic film (RCF) EBT3 (the clear polyester layer facing the target was removed) was placed behind the cell sample for dose measured. To obtain the dose deposited in the cell from the measured dose in EBT3 films, the Monte-Carlo code FLUKA (Bohlen et al., 2014) was put into use.

Irradiation Protocol

Cells were cultured on the 3.5 μm Mylar film pasted by glue at the bottom of cell cylinder for irradiation. The cell cylinder was pre-treated with 1% geltrex for 24 h and seeded cells 20 h before irradiation. Cyt c-normal and -null mouse embryonic fibroblast cells were digested and adjusted to appropriate density, and ∼120,000 cells were added to each cell cylinder. The hypoxic condition was mimicked by adding $CoCl_2$ (Sigma) at the final concentration of 100 μM to the medium for 6–12 h as reported previously (Wu and Yotnda, 2011).

The medium in the cell cylinder was aspirated right before irradiation, and after irradiation the cell cylinder was supplemented with medium immediately and put into the incubator. At 6, 12, and 24 h after the irradiation, the cells on the mylar film were digested, mixed and transferred to 96-well plate for detection of apoptosis.

Conventional Irradiation

Cyt $c^{+/+}$ and cyt $c^{-/-}$ cells were seeded on 24-well plate for adherence before irradiation, with ∼120,000 cells each well. Then cells were irradiated by Co-60 γ radation at 3 Gy/min for 10 min (30 Gy total doses). At 6, 12, and 24 h after the irradiation, cells were transferred to 96-well plate for detection of apoptosis by Dead Cell Apoptosis Kit with Alexa Fluor 488 annexin V and PI (Invitrogen).

Detection of Apoptosis

To detect apoptosis of cells after FLASH radiation, we used Dead Cell Apoptosis Kit with Alexa Fluor 488 annexin V and PI (Invitrogen). Cells digested from the mylar film were added to 96-well plate with 100 μL for each well. Then 1 μL 100 μg/mL PI, 5 μL Alexa Fluor 488 annexin V and 0.2 μL Hoechst 33342 (Thermo Fisher) working solution were added to the well. Cells were stained 15 min in the incubator and then imaged by Spark® Cyto automatic real-time live cell imaging detection system (TECAN). The cell nuclei are stained by Hoechst, cells with Hoechst+, annexin V+ and PI− were recognized as early

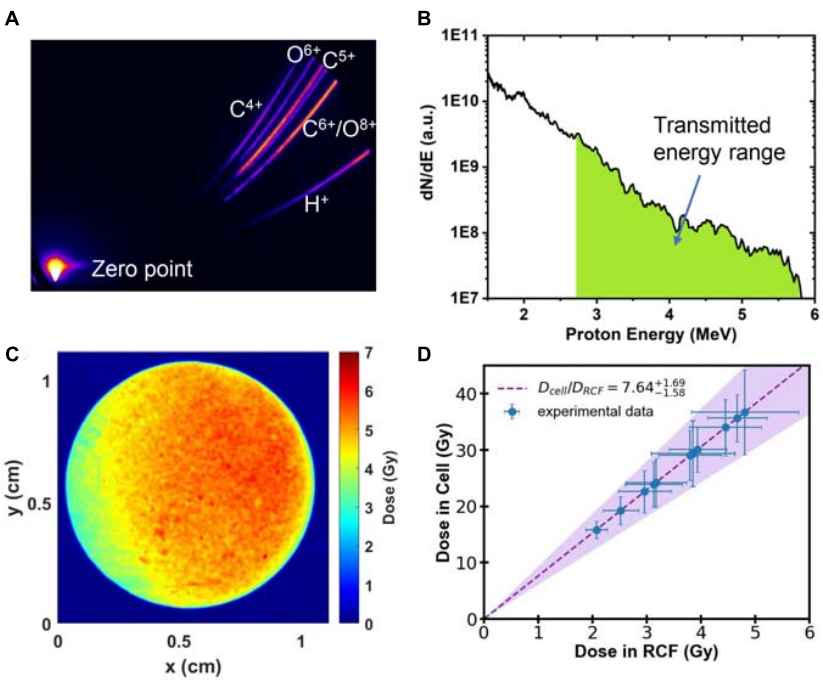

FIGURE 2 | (A) Raw image obtained by the Thomson Parabola Spectrometer. **(B)** Typical energy spectra of laser-accelerated protons. Protons with energy in the green area can pass through the monolayer cell. **(C)** Spatial distribution of dose detected by RCF film from a single shot. **(D)** The dose deposited in the monolayer cell as a function of the measured dose with RCF film.

TABLE 1 | Summary of laser accelerator dose for each FLASH experiment.

	Dose in RCF film	SD. Of Dose in RCF film	Calculated average dose in cells	SD of dose in cells	Shot used
1	3.9	0.5	30.1	4.1	cyt $c^{+/+}$ hypoxia 6 h
2	4.8	1.0	36.8	7.6	cyt $c^{+/+}$ hypoxia 12 h
3	4.7	0.6	35.7	4.2	cyt $c^{+/+}$ hypoxia 24 h
4	3.2	0.6	24.2	4.3	cyt $c^{+/+}$ normoxia 6 h
5	3.0	0.5	22.6	3.7	cyt $c^{+/+}$ normoxia 12 h
6	3.9	0.8	29.4	5.9	cyt $c^{+/+}$ normoxia 24 h
7	3.1	0.5	23.9	4.1	cyt $c^{-/-}$ hypoxia 6 h
8	2.1	0.2	15.8	1.5	cyt $c^{-/-}$ hypoxia 12 h
9	2.5	0.3	19.3	2.5	cyt $c^{-/-}$ hypoxia 24 h
10	3.8	0.6	29.0	4.4	cyt $c^{-/-}$ normoxia 6 h
11	3.9	0.8	29.4	5.8	cyt $c^{-/-}$ normoxia 12 h
12	4.5	0.7	34.0	5.0	cyt $c^{-/-}$ normoxia 24 h
13	3.5	0.5	32.1	4.7	cyt $c^{+/+}$ hypoxia 6 h
14	4.5	0.8	41.1	7.0	cyt $c^{+/+}$ hypoxia 12 h
15	4.4	0.6	40.9	5.9	cyt $c^{+/+}$ hypoxia 24 h
16	3.6	0.4	33.5	4.1	cyt $c^{+/+}$ normoxia 6 h
17	5.2	1.0	47.5	9.2	cyt $c^{+/+}$ normoxia 12 h
18	6.1	1.6	56.0	14.4	cyt $c^{+/+}$ normoxia 24 h
19	3.1	0.5	28.1	4.2	cyt $c^{-/-}$ hypoxia 6 h
20	4.7	0.7	42.8	6.4	cyt $c^{-/-}$ hypoxia 12 h
21	4.8	0.8	43.8	6.9	cyt $c^{-/-}$ hypoxia 24 h
22	2.4	0.5	5.2	1.2	cyt $c^{+/+}$ hypoxia 12 h
23	1.3	0.2	2.8	0.4	cyt $c^{+/+}$ hypoxia 24 h
24	0.9	0.1	1.8	0.2	cyt $c^{+/+}$ normoxia 12 h
25	1.0	0.1	2.0	0.2	cyc $c^{+/+}$ normoxia 24 h
26	2.2	0.3	4.9	0.4	cyc $c^{+/+}$ hypoxia 12 h
27	3.9	0.8	8.6	1.7	cyc $c^{+/+}$ hypoxia 24 h
28	2.7	0.6	5.9	1.2	cyc $c^{-/-}$ hypoxia 12 h
29	4.2	1.1	9.2	2.5	cyc $c^{-/-}$ hypoxia 24 h

apoptotic cells, while Hoechst+/annexin V+/PI+ represent late apoptotic and necrotic cells.

Detection of Caspase-3/7

Caspase-3/7 were detected using Caspase-Glo® 3/7 Assay (Promega) at 24 h after conventional irradiation. In a 96-well plate, 100 μL of cell suspension and 100 μL Caspase-Glo® 3/7 Reagent were added, and the chemiluminescence was detected after 1 h. The detection was performed by Spark® Cyto automatic real-time live cell imaging detection system (TECAN).

Data Analysis

Results were expressed as means ± SD, and one-way ANOVA was used to analyze the significant differences between control and experimental group. $P < 0.05$ was marked as *, $P < 0.01$ was marked as **, $P < 0.001$ was marked as ***. At least 3,000 cells were counted in each group.

RESULTS

FLASH Irradiation Setup

The schematic of the experimental setup was shown in **Figure 1A**, the ion beams entered cells irradiation system through a vacuum window located 63 mm behind the target and irradiated the cells. The vacuum window is composed of a 10 μm Aluminum film for light-shielding, and a 25 μm Kapton film for vacuum sealing. Monolayer cells cultured on a 3.5 μm Mylar film were mounted on a stainless-steel cell-culture cylinder, facing to the inner space of the cylinder as shown in **Figures 1C,E**. The inner diameter and the height of the cylinder were 10 and 13 mm, respectively (**Figures 1B,D**), and the cylinder was mounted on a holder, locating the cell-cultured Mylar film vertically to receive the irradiation. The distance from the vacuum window to the cell plane is 7 mm. Another 3.5 μm Mylar film was taped on the other side of the holder to seal the cylinder, avoiding the contamination and dryout of the cell during irradiation. Each cell sample was irradiated by a single shot.

Dose Calculation

The parabolic traces of ions were obtained by the Thomson Parabola Spectrometer, recorded by a micro-channel plate with a phosphor screen and imaged onto a 16-bit EMCCD camera. A typical raw image of the parabolic traces measured by the Thomson Parabola Spectrometer is shown in **Figure 2A**. The corresponding energy spectra of protons with cut-off energy of 5.8 MeV are shown in **Figure 2B**. Protons in the energy range marked in green can pass through the monolayer cell and detected by the EBT3 film. Generated oxygen/carbon ions and protons lower than 2.7 MeV were completely stopped by the vacuum window and the air.

Customized EBT3 film for dose verification was placed 25 mm away from the cells, directly behind the sealing Mylar film. The irradiated EBT3 films were scanned with an Epson Perfection V700 scanner in transmission mode. The dose response of EBT3 was calibrated following the literature reported

previously (Reinhardt et al., 2012). The spatial distribution of dose detected by EBT3 film in a single laser shot is shown in **Figure 2C**, which has RMS (root mean square) variation of 16%.

We employed the Monte-Carlo code FLUKA (Bohlen et al., 2014), input all the setup parameters and the measured energy spectra of protons, to determine the dose deposited in the cell from the measured dose in EBT3 films. The calculated dose delivered to the cell is shown in **Figure 2D**. The filled area shows the calculation result considering the shot-to-shot fluctuations and the error bar of the data represents the RMS variation of the dose distributions. The summary of the dose in both layers for each shot is shown in **Table 1**.

In TNSA regime, the laser acceleration is completed within 1 ps (Bayart et al., 2019). Considering the broadening of the beam duration due to the difference of the flying speed of protons, the duration of the proton pulse delivered to the cell plane was ∼10 ns, corresponding to the dose rate in the order of 10^9 Gy/s.

Detection of Cell Viability

As shown in **Supplementary Figure 5**, the survival proportion of cyt $c^{+/+}$ and cyt $c^{-/-}$ cells were 93.4 and 92.5%, respectively. Cyt $c^{+/+}$ cells showed a little bit higher viability, but the difference between the two type of cells was not significant.

Mouse Embryonic Fibroblast Cells Are More Resistant to FLASH Irradiation in Hypoxic Condition

For the evaluation of mouse embryonic fibroblast cell performance under ultra-high dose rate FLASH irradiation, we assessed the apoptosis proportion of cyt c-normal cells at 6, 12, and 24 h after the irradiation by Dead Cell Apoptosis Kit with Alexa Fluor 488 annexin V and PI. Cells with Hoechst+/annexin V+/ PI- or Hoechst+/annexin V+/PI+ were recognized as early apoptotic cells, late apoptotic and necrotic cells respectively, representive images were shown in (**Figures 3A–C**). As shown in **Supplementary Figure 1**, compared with the unirradiated control, the relative early apoptosis level of irradiated normal fibroblast cells was increased with time in both hypoxic and normoxic conditions, and the proportion of early apoptosis at 6 h was relatively low (**Supplementary Figures 1A,B**). For the comparison of the irradiated cells in hypoxia and normoxia, the early apoptosis level in hypoxia was significantly lower than that of normoxia, with 0.73, 0.76, and 0.63-fold of the normoxic group at 6, 12, and 24 h, respectively (**Figures 3D–F**). And the overall proportion of early apoptosis of irradiated cells in the hypoxic condition was obviously lower than that of the normoxic condition (**Supplementary Figures 1A,B**).

We also detected and analyzed the late apoptosis and necrosis level of irradiated normal fibroblast cells after FLASH-IR, as

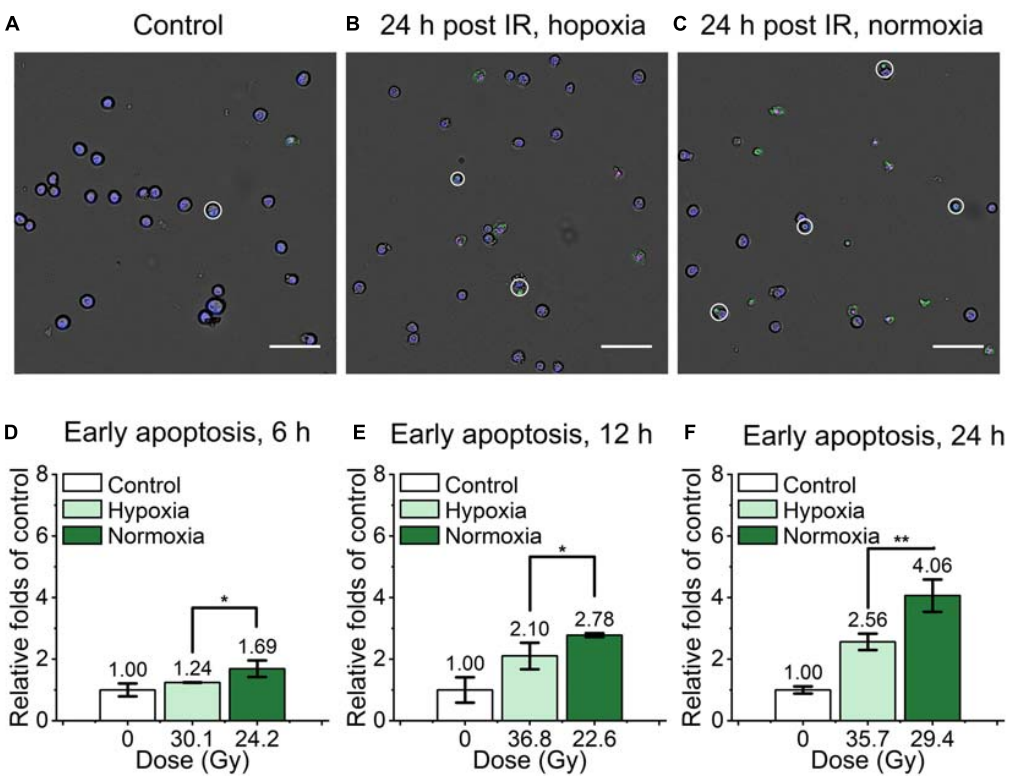

FIGURE 3 | Early apoptosis of irradiated normal fibroblast cells after FLASH irradiation. **(A–C)** Representative images of control **(A)**, irradiated cells in hypoxic **(B)** and normoxic condition **(C)** at 24 h after radiation. Early apoptotic cells were marked with white circles. Scale bars: 100 μm. **(D–F)** The relative increasement of early apoptosis in irradiated cells between hypoxia and normoxia at 6 h **(D)**, 12 h **(E)** and 24 h **(F)** after radiation.

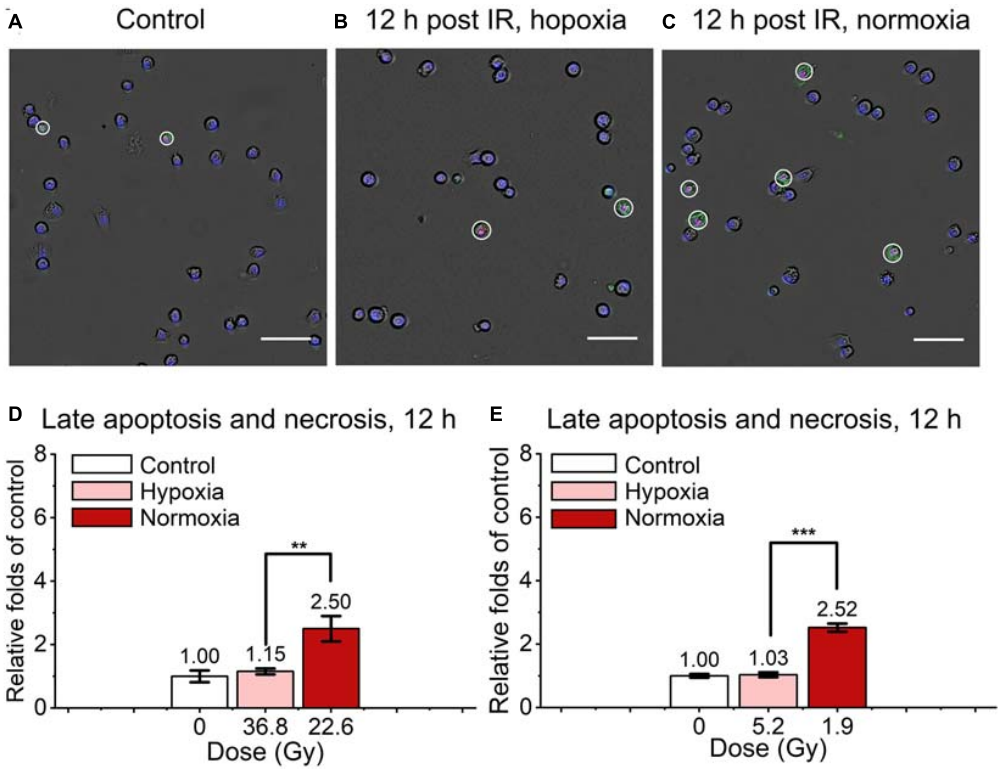

FIGURE 4 | Late apoptosis and necrosis of irradiated normal fibroblast cells after FLASH irradiation. **(A–C)** Representative images of control **(A)**, irradiated cells in hypoxic **(B)** and normoxic condition **(C)** at 12 h after radiation. Late apoptotic and necrotic cells were marked with white circles. Scale bars: 100 μm. **(D,E)** The relative increasement of late apoptosis and necrosis in irradiated cells between hypoxia and normoxia at 12 h after high **(D)** or low **(E)** doses of radiation.

shown in **Figure 4**. Similar with the results of early apoptosis, the relative late apoptosis and necrosis level of irradiated cells were increased with time in both hypoxic and normoxic conditions (**Supplementary Figures 1C,D**). And compared with the irradiated group in normoxic condition, the irradiated cells in hypoxic condition showed significant lower level of late apoptosis and necrosis at 12 h, both after high doses and low doses irradiaion (**Figures 4D,E**). However, at 24 h, irradiated cells reached high level of late apoptosis and necrosis but without significant difference between them in both hypoxic and normoxic conditions (**Supplementary Figures 2A,B**).

Cyt c-Null Mouse Embryonic Fibroblast Cells Show Lower Apoptosis Proportion After FLASH Irradiation

As shown in the **Figure 5**, the relative early apoptosis level of irradiated normal (cyt $c^{+/+}$) and cyt c-null (cyt $c^{-/-}$) cells at different time and condition was compared. There was slightly decrease of early apoptosis proportion of cyt $c^{-/-}$ cells at 6 h hypoxia (**Figure 5E** and **Supplementary Figure 3A**), 12 h in hypoxia (**Figure 5F** and **Supplementary Figure 3B**), and 24 h in normoxia (**Figure 5J** and **Supplementary Figure 3F**) compared with relative cyt $c^{+/+}$ cells in certain conditions. The rest of the groups show similar relative early apoptosis level between irradiated cyt $c^{+/+}$ and cyt $c^{-/-}$ cells (**Figures 5G–I** and **Supplementary Figures 3AC–E**), showing no obvious difference of FLASH irradiation induced early apoptosis between cyt $c^{+/+}$ and cyt $c^{-/-}$ cells.

The comparison of relative late apoptosis and necrosis level of irradiated cyt $c^{+/+}$ and cyt $c^{-/-}$ cells at different time were shown in **Figure 6**. The difference of late apoptosis and necrosis proportion between irradiated cyt $c^{+/+}$ and cyt $c^{-/-}$ cells is significant at 12 h in hypoxia (**Figure 6E**), 12 h in normoxia (**Figure 6G**), 24 h in hypoxia (**Figure 6F**) and 24 h in normoxia (**Figure 6H**), and the relative late apoptosis and necrosis level of irradiated cyt $c^{-/-}$ cells were 0.83, 0.60, 0.74 and 0.67 folds of irradiated cyt $c^{+/+}$ cells in certain conditions, respectively, indicating mitochondrial dysfunction enhanced radio-resistance of normal fibroblast cells with less late apoptosis and necrosis after FLASH irradiation. And similar results of cyt $c^{-/-}$ cells were also shown when receiving lower doses of FLASH irradiation (**Supplementary Figures 4A,B**).

Apoptosis and Caspase-3/7 Detection After Conventional Irradiation

As shown in **Supplementary Figure 6**, the irradiated normal fibroblast cells in hypoxia showed lower early apoptosis level as well as late apoptosis and necrosis level compared with normoxia after conventional irradiation. The difference between hypoxia and normoxia is significant

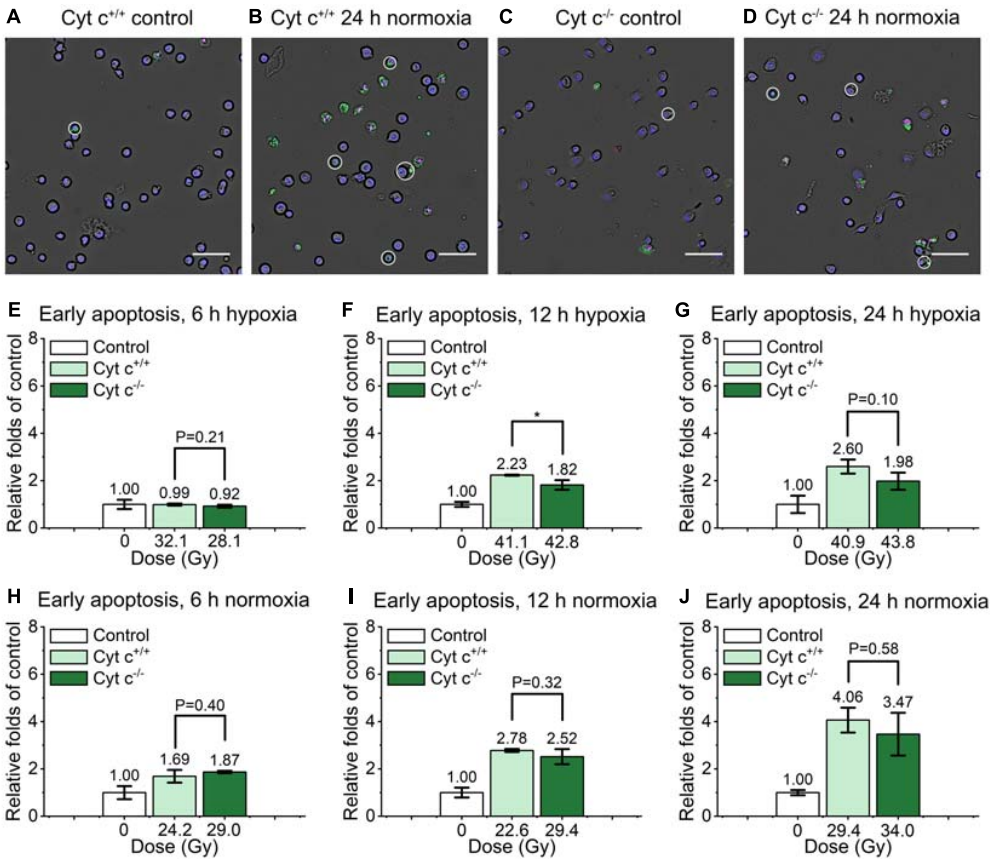

FIGURE 5 | Comparison of early apoptosis between irradiated cyt $c^{+/+}$ and cyt $c^{-/-}$ cells after FLASH irradiation. **(A–D)** Representative images of cyt $c^{+/+}$ control **(A)**, cyt $c^{+/+}$ irradiated **(B)**, cyt $c^{-/-}$ control **(C)** and cyt $c^{-/-}$ irradiated cells **(D)** at 24 h in normoxic condition. Early apoptotic cells were marked with white circles. Scale bars: 100 μm. **(E–J)** The relative increasement of early apoptosis for irradiated cyt $c^{+/+}$ and cyt $c^{-/-}$ cells at 6 h in hypoxia **(E)**, 6 h in normoxia **(H)**, 12 h in hypoxia **(F)**, 12 h in normoxia **(I)**, 24 h in hypoxia **(G)** and 24 h in normoxia **(J)**.

at 6 h (**Supplementary Figure 6A**), 12 h (**Supplementary Figures 6B,D**) and 24 h (**Supplementary Figures 6C,E**), indicating the radio-resistance enhancement of cyt $c^{+/+}$ cells at hypoxic condition.

The caspase-3/7 chemiluminescence also revealed significant lower level at hypoxia compared with normoxia at 24 h after irradiation for cyt $c^{+/+}$ cells (**Supplementary Figure 8A**) and cyt $c^{-/-}$ cells (**Supplementary Figure 8B**). Besides, compared with conventional irradiation, FLASH irradiation showed high overall level of relative increment of early apoptosis, late apoptosis and necrosis, especially at 24 h both hypoxic and normoxic condition.

The comparison of relative apoptosis level of irradiated cyt $c^{+/+}$ and cyt $c^{-/-}$ cells at different time or condition were shown in **Supplementary Figure 7**. There was certain decrease of early apoptosis proportion of cyt $c^{-/-}$ cells at all time points, in which the difference was significant at 6 h normoxia (**Supplementary Figure 7D**), 12 h hypoxia (**Supplementary Figure 7B**), 24 h hypoxia (**Supplementary Figure 7C**) and 24 h normoxia (**Supplementary Figure 7F**) compared with relative cyt $c^{+/+}$ cells.

Similarly, the difference of late apoptosis and necrosis proportion between irradiated cyt $c^{+/+}$ and cyt $c^{-/-}$ cells is significant at 12 h in hypoxia (**Supplementary Figure 7G**), 12 h in normoxia (**Supplementary Figure 7H**), 24 h in hypoxia (**Supplementary Figure 7I**) and 24 h in normoxia (**Supplementary Figure 7J**), indicating the crucial role of mitochondrial function in apoptosis of normal fibroblast cells induced by radiation.

As shown in **Supplementary Figures 8C,D**, caspase-3/7 level of both cyt $c^{+/+}$ and cyt $c^{-/-}$ cells were low at hypoxia, caspase-3/7 level of cyt $c^{-/-}$ cells decreased slightly compared with cyt $c^{+/+}$ cells but the difference was not significant. At normoxia, the caspase-3/7 level of cyt $c^{-/-}$ cells was significantly lower compared with cyt $c^{+/+}$ cells.

DISCUSSION

In this article, we revealed early apoptosis, late apoptosis and necrosis induced by FLASH irradiation in both cyt $c^{+/+}$ and cyt $c^{-/-}$ mouse embryonic fibroblast cells. The apoptosis proportion of cyt $c^{+/+}$ cell was significantly lower in hypoxia than that of in normoxia, indicating the increased resistance of normal fibroblast cell after FLASH

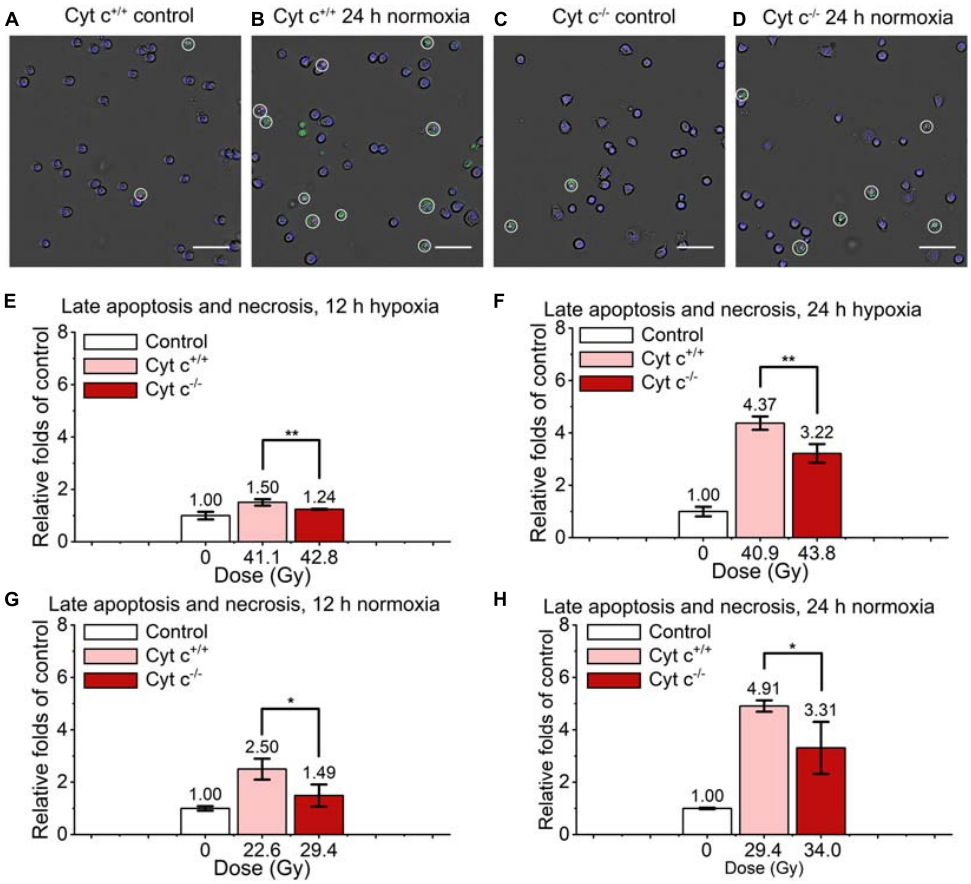

FIGURE 6 | Comparison of late apoptosis and necrosis between irradiated cyt $c^{+/+}$ and cyt $c^{-/-}$ cells after FLASH irradiation. **(A–D)** Representative images of cyt $c^{+/+}$ control **(A)**, cyt $c^{+/+}$ irradiated **(B)**, cyt $c^{-/-}$ control **(C)** and cyt $c^{-/-}$ irradiated cells **(D)** at 24 h in normoxic condition. Late apoptotic and necrosis cells were marked with white circles. Scale bars: 100 μm. **(E–H)** The relative increasement of late apoptotic and necrosis for irradiated cyt $c^{+/+}$ and cyt $c^{-/-}$ cells at 12 h in hypoxia **(E)**, 12 h in normoxia **(G)**, 24 h in hypoxia **(F)**, and 24 h in normoxia **(H)**.

irradiation in hypoxia. The late apoptosis and necrosis proportion of irradiated cyt $c^{-/-}$ was significantly lower in both hypoxia and normoxia compared with irradiated normal cyt $c^{+/+}$ cells, indicating mitochondrial dysfunction enhanced radio-resistance of mouse embryonic fibroblast cells after FLASH irradiation.

Due to the shot-to-shot fluctuations during laser acceleration, doses of laser-driven ion beams were different in every shot of irradiation and it is hard to keep it constant. Besides, the assay used to detect apoptosis and necrosis was an endpoint method so the doses were not same in experiments. We tried to use similar doses in the comparison group or choose the low doses for high apoptosis level. Although the doses were not completely consistent, the lower doses showed a higher value, indicating that the conclusion was reliable.

The normal tissue protection and tumor growth delay in animal models under FLASH irradiation suggested a potential role for FLASH in treating humans (Vozenin et al., 2019b). Our results showed that the apoptosis level of normal fibroblast cell was significantly lower in hypoxia compared with that in normoxia. Given the known role of oxygen in modulating radio-sensitivity, it is rationalized that FLASH irradiation could cause a rapid consumption of local oxygen that is much faster than tissue reoxygenation kinetics (Vozenin et al., 2019b). The types of cell death after radiation depend on a number of factors including cell type, radiation dose and quality, oxygen tension and so on (Sia et al., 2020). Oxygen tension modulates cell death after irradiation, with reduction in chromosomal aberrations of cells irradiated in hypoxic conditions (Sia et al., 2020). And it is presumed to related to kinetic competition between the oxygen 'fixation' of DNA damage and chemical repair processes (Sia et al., 2020).

Mitochondria plays crucial part in cell fate after irradiation. The mitochondria apoptotic pathway is the principal pathway of cell death after conventional low dose rate irradiation (Sinha et al., 2013; Li et al., 2019), in which cyt c serves as key component of apoptosis initiator (Jiang and Wang, 2004). The release of cyt c from mitochondria in response to multiple apoptotic stimuli can induce a series of biochemical responses leading to caspase activation and subsequent cell death (Jiang and Wang, 2004). There have been reports that mitochondrial permeabilization is generally more closely linked to events

of late apoptosis and necrosis (Kinnally et al., 2011). And cells lacking cyt c show reduced caspase-3 activation and are resistant to the proapoptotic effects of UV irradiation, serum withdrawal, or staurosporine (Li et al., 2000). In our results, late apoptosis and necrosis proportion of irradiated cyt $c^{-/-}$ cells showed significant decrease in both hypoxia and normoxia compared with irradiated normal cyt $c^{+/+}$ cells, indicating that the deficiency of cyt c in mouse embryonic fibroblast cells also reduced the proportion of mitochondrial-mediated apoptosis under FLASH-IR. In addition, functional changes in mitochondria in response to radiation exposure could influence epigenetic parameters and genome stability (Baulch, 2019). And cyt c independent ceramide apoptotic pathway is also related to mitochondria. Research showed that by regulating mitochondrial function, DDR pathway and MAPK pathway, ceramide could potentially mediated gamma radiation-induced apoptosis (Yang et al., 2021). Presently we cannot exclude the impact of the apoptosis in cyt c independent apoptotic pathway after FLASH irradiation. More validating experiments need to be further performed.

The ultra-high dose rates and ultra-short irradiation time implemented by laser accelerators is promising, but the instability in different shots is also a concern (Lundh et al., 2012; Manti et al., 2017), which is sure to impede the interpretation and repetition of FLASH experimental results. The more stable, easily controlled and widely applicable FLASH irradiation as well as more biological experiments for scientific and clinical use are further expected.

DATA AVAILABILITY STATEMENT

The original contributions presented in the study are included in the article/**Supplementary Material**, further inquiries can be directed to the corresponding author/s.

AUTHOR CONTRIBUTIONS

GY, WM, and XY conceived the research plan. JH, CLu, and JQ designed and performed the biology experiments, analyzed results, and produced figures. ZM, WM, and GY designed and constructed the irradiation setup. ZM, YL, ZP, DK, SX, ZL, YGa, GQ, YS, SC, ZC, YZ, and YGe supervised by WM performed the laser acceleration and cell irradiation experiments. ZM and YL measured the proton radiation and provided the dose data. JH wrote the initial draft of the manuscript. GY wrote the final draft of the manuscript. All authors commented on the manuscript.

FUNDING

This study was supported by the National Natural Science Foundation of China (11875079, 61631001 and 119210067) and the National Grand Instrument Project (2019YFF01014402), NSFC innovation group project (No. 11921006), and the State Key Laboratory of Nuclear Physics and Technology, PKU under Grant No. NPT2020KFY19.

ACKNOWLEDGMENTS

We are very grateful to Professor Yugang Wang for helpful discussions.

SUPPLEMENTARY MATERIAL

The Supplementary Material for this article can be found online at: https://www.frontiersin.org/articles/10.3389/fcell.2021.672929/full#supplementary-material

REFERENCES

Bacso, Z., Everson, R. B., and Eliason, J. F. (2000). The DNA of annexin V-binding apoptotic cells is highly fragmented. *Cancer Res.* 60, 4623–4628.

Baulch, J. E. (2019). Radiation-induced genomic instability, epigenetic mechanisms and the mitochondria: a dysfunctional menage a trois? *Intern. J. Radiat. Biol.* 95, 516–525. doi: 10.1080/09553002.2018.1549757

Bayart, E., Flacco, A., Delmas, O., Pommarel, L., Levy, D., Cavallone, M., et al. (2019). Fast dose fractionation using ultra-short laser accelerated proton pulses can increase cancer cell mortality, which relies on functional PARP1 protein. *Sci. Rep.* 9:10132. doi: 10.1038/s41598-019-46512-1

Bin, J. H., Allinger, K., Assmann, W., Dollinger, G., Drexler, G. A., Friedl, A. A., et al. (2012). A laser-driven nanosecond proton source for radiobiological studies. *Appl. Phys. Lett.* 101:243701. doi: 10.1063/1.4769372

Bohlen, T. T., Cerutti, F., Chin, M. P. W., Fosso, A., Ferrari, A., Ortega, P. G., et al. (2014). The FLUKA code: developments and challenges for high energy and medical applications. *Nuclear Data Sheets* 120, 211–214. doi: 10.1016/j.nds.2014.07.049

Bourhis, J., Sozzi, W. J., Jorge, P. G., Gaide, O., Bailat, C., Duclos, F., et al. (2019). Treatment of a first patient with FLASH-radiotherapy. *Radiother. Oncol.* 139, 18–22. doi: 10.1016/j.radonc.2019.06.019

Doria, D., Kakolee, K. F., Kar, S., Litt, S. K., Fiorini, F., Ahmed, H., et al. (2012). Biological effectiveness on live cells of laser driven protons at dose rates exceeding 109Gy/s. *AIP Adv.* 2:011209. doi: 10.1063/1.3699063

Durante, M., Brauer-Krisch, E., and Hill, M. (2018). Faster and safer? FLASH ultra-high dose rate in radiotherapy. *Br. J. Radiol.* 91:20170628. doi: 10.1259/bjr.20170628

Eriksson, D., and Stigbrand, T. (2010). Radiation-induced cell death mechanisms. *Tumour Biol.* 31, 363–372. doi: 10.1007/s13277-010-0042-8

Favaudon, V., Caplier, L., Monceau, V., Pouzoulet, F., Sayarath, M., Fouillade, C., et al. (2014). Ultrahigh dose-rate FLASH irradiation increases the differential response between normal and tumor tissue in mice. *Sci. Transl. Med.* 6:245ra293. doi: 10.1126/scitranslmed.3008973

Foldbjerg, R., Dang, D. A., and Autrup, H. (2011). Cytotoxicity and genotoxicity of silver nanoparticles in the human lung cancer cell line, A549. *Archiv. Toxicol.* 85, 743–750. doi: 10.1007/s00204-010-0545-5

Fu, Q., Huang, T., Wang, X., Lu, C., Liu, F., Yang, G., et al. (2017). Association of elevated reactive oxygen species and hyperthermia induced radiosensitivity in cancer stem-like cells. *Oncotarget* 8, 101560–101571. doi: 10.18632/oncotarget.21678

Griffin, R. J., Ahmed, M. M., Amendola, B., Belyakov, O., Bentzen, S. M., Butterworth, K. T., et al. (2020). Understanding high-dose, ultra-high dose rate, and spatially fractionated radiation therapy. *Int. J. Radiat. Oncol. Biol. Phys.* 107, 766–778. doi: 10.1016/j.ijrobp.2020.03.028

Hanton, F., Chaudhary, P., Doria, D., Gwynne, D., Maiorino, C., Scullion, C., et al. (2019). DNA DSB repair dynamics following irradiation with laser-driven protons at ultra-high dose rates. *Sci. Rep.* 9:4471. doi: 10.1038/s41598-019-40339-6

Jiang, X., and Wang, X. (2004). Cytochrome C-mediated apoptosis. *Annu. Rev. Biochem.* 73, 87–106. doi: 10.1146/annurev.biochem.73.011303.073706

Kinnally, K. W., Peixoto, P. M., Ryu, S. Y., and Dejean, L. M. (2011). Is mPTP the gatekeeper for necrosis, apoptosis, or both? *Biochim. Biophys. Acta* 1813, 616–622. doi: 10.1016/j.bbamcr.2010.09.013

Korystov, Y. N. (1992). Contributions of the direct and indirect effects of ionizing-radiation to reproductive cell-death. *Radiat. Res.* 129, 228–234. doi: 10.2307/3578162

Ledingham, K., Bolton, P., Shikazono, N., and Ma, C. M. (2014). Towards laser driven hadron cancer radiotherapy: a review of progress. *Appl. Sci.* 4, 402–443. doi: 10.3390/app4030402

Li, K., Li, Y., Shelton, J. M., Richardson, J. A., Spencer, E., Chen, Z. J., et al. (2000). Cytochrome c deficiency causes embryonic lethality and attenuates stress-induced apoptosis. *Cell* 101, 389–399. doi: 10.1016/s0092-8674(00)80849-1

Li, X., Fang, F., Gao, Y., Tang, G., Xu, W., Wang, Y., et al. (2019). ROS induced by KillerRed targeting mitochondria (mtKR) enhances apoptosis caused by radiation via Cyt c/Caspase-3 pathway. *Oxid. Med. Cell Longev.* 2019:4528616. doi: 10.1155/2019/4528616

Liu, T. Y., Tan, Z. J., Jiang, L., Gu, J. F., Wu, X. S., Cao, Y., et al. (2013). Curcumin induces apoptosis in gallbladder carcinoma cell line GBC-SD cells. *Cancer Cell Intern.* 13:64. doi: 10.1186/1475-2867-13-64

Loo, B. W., Schuler, E., Lartey, F. M., Rafat, M., King, G. J., Trovati, S., et al. (2017). (P003) delivery of ultra-rapid flash radiation therapy and demonstration of normal tissue sparing after abdominal irradiation of mice. *Intern. J. Radiat. Oncol. Biol. Phys.* 98:101. doi: 10.1016/j.ijrobp.2017.02.101

Lundh, O., Rechatin, C., Faure, J., Ben-Ismail, A., Lim, J., De Wagter, C., et al. (2012). Comparison of measured with calculated dose distribution from a 120-MeV electron beam from a laser-plasma accelerator. *Med. Phys.* 39, 3501–3508. doi: 10.1118/1.4719962

Manti, L., Perozziello, F. M., Borghesi, M., Candiano, G., Chaudhary, P., Cirrone, G. A. P., et al. (2017). The radiobiology of laser-driven particle beams: focus on sub-lethal responses of normal human cells. *J. Instrument.* 12:C03084. doi: 10.1088/1748-0221/12/03/c03084

Montay-Gruel, P., Bouchet, A., Jaccard, M., Patin, D., Serduc, R., Aim, W., et al. (2018). X-rays can trigger the FLASH effect: ultra-high dose-rate synchrotron light source prevents normal brain injury after whole brain irradiation in mice. *Radiother. Oncol.* 129, 582–588. doi: 10.1016/j.radonc.2018.08.016

Passoni, M., Bertagna, L., and Zani, A. (2010). Target normal sheath acceleration: theory, comparison with experiments and future perspectives. *New J. Phys.* 12:045012. doi: 10.1088/1367-2630/12/4/045012

Petersson, K., Montay-Gruel, P., Jaccard, M., Boivin, G., Germond, J., Petit, B., et al. (2017). OC-0039: unique sparing of spatial memory in mice after whole brain irradiation with dose rates above 100Gy/s. *Radiotherapy Oncol.* 123, S15–S16. doi: 10.1016/s0167-8140(17)30483-8

Raschke, S., Spickermann, S., Toncian, T., Swantusch, M., Boeker, J., Giesen, U., et al. (2016). Ultra-short laser-accelerated proton pulses have similar DNA-damaging effectiveness but produce less immediate nitroxidative stress than conventional proton beams. *Sci. Rep.* 6:32441. doi: 10.1038/srep32441

Reinhardt, S., Hillbrand, M., Wilkens, J. J., and Assmann, W. (2012). Comparison of Gafchromic EBT2 and EBT3 films for clinical photon and proton beams. *Med. Phys.* 39, 5257–5262. doi: 10.1118/1.4737890

Rosch, T. F., Szabo, Z., Haffa, D., Bin, J. H., Brunner, S., Englbrecht, F. S., et al. (2020). A feasibility study of zebrafish embryo irradiation with laser-accelerated protons. *Rev. Sci. Instrum.* 91:63303. doi: 10.1063/5.0008512

Sia, J., Szmyd, R., Hau, E., and Gee, H. E. (2020). Molecular mechanisms of radiation-induced cancer cell death: a primer. *Front. Cell Dev. Biol.* 8:41. doi: 10.3389/fcell.2020.00041

Sinha, K., Das, J., Pal, P. B., and Sil, P. C. (2013). Oxidative stress: the mitochondria-dependent and mitochondria-independent pathways of apoptosis. *Arch. Toxicol.* 87, 1157–1180. doi: 10.1007/s00204-013-1034-4

Troiano, L., Ferraresi, R., Lugli, E., Nemes, E., Roat, E., Nasi, M., et al. (2007). Multiparametric analysis of cells with different mitochondrial membrane potential during apoptosis by polychromatic flow cytometry. *Nat. Protoc.* 2, 2719–2727. doi: 10.1038/nprot.2007.405

Valentini, V., Boldrini, L., Mariani, S., and Massaccesi, M. (2020). Role of radiation oncology in modern multidisciplinary cancer treatment. *Mol. Oncol.* 14, 1431–1441. doi: 10.1002/1878-0261.12712

Vozenin, M. C., De Fornel, P., Petersson, K., Favaudon, V., Jaccard, M., Germond, J. F., et al. (2019a). The advantage of FLASH radiotherapy confirmed in mini-pig and cat-cancer patients. *Clin. Cancer Res.* 25, 35–42. doi: 10.1158/1078-0432.CCR-17-3375

Vozenin, M. C., Hendry, J. H., and Limoli, C. L. (2019b). Biological benefits of ultra-high dose rate FLASH radiotherapy: sleeping beauty awoken. *Clin. Oncol.* 31, 407–415. doi: 10.1016/j.clon.2019.04.001

Wang, C., and Youle, R. J. (2009). The role of mitochondria in apoptosis*. *Annu. Rev. Genet.* 43, 95–118. doi: 10.1146/annurev-genet-102108-134850

Wilson, D. F., and Vinogradov, S. A. (2014). Mitochondrial cytochrome c oxidase: mechanism of action and role in regulating oxidative phosphorylation. *J. Appl. Physiol.* 117, 1431–1439. doi: 10.1152/japplphysiol.00737.2014

Wilson, P., Jones, B., Yokoi, T., Hill, M., and Vojnovic, B. (2012). Revisiting the ultra-high dose rate effect: implications for charged particle radiotherapy using protons and light ions. *Br. J. Radiol.* 85:e0933-39. doi: 10.1259/bjr/17827549

Wu, D., and Yotnda, P. (2011). Induction and testing of hypoxia in cell culture. *J. Vis. Exp.* 2011:2899. doi: 10.3791/2899

Xu, C. S., and Leung, A. W. N. (2010). Light-activated hypericin induces cellular destruction of nasopharyngeal carcinoma cells. *Laser Phys. Lett.* 7, 68–72. doi: 10.1002/lapl.200910095

Yang, G., Wu, L., Chen, S., Zhu, L., Huang, P., Tong, L., et al. (2009). Mitochondrial dysfunction resulting from loss of cytochrome c impairs radiation-induced bystander effect. *Br. J. Cancer* 100, 1912–1916. doi: 10.1038/sj.bjc.6605087

Yang, Y., Xu, G., Xu, Y., Cheng, X., Xu, S., Chen, S., et al. (2021). Ceramide mediates radiation-induced germ cell apoptosis via regulating mitochondria function and MAPK factors in *Caenorhabditis elegans*. *Ecotoxicol. Environ. Saf.* 208:111579. doi: 10.1016/j.ecoenv.2020.111579

Yun, J., and Lee, D. G. (2016). A novel fungal killing mechanism of propionic acid. *FEMS Yeast Res.* 16:fow089. doi: 10.1093/femsyr/fow089

Zeil, K., Baumann, M., Beyreuther, E., Burris-Mog, T., Cowan, T. E., Enghardt, W., et al. (2013). Dose-controlled irradiation of cancer cells with laser-accelerated proton pulses. *Appl. Phys. B Lasers Opt.* 110, 437–444. doi: 10.1007/s00340-012-5275-3

Conflict of Interest: The authors declare that the research was conducted in the absence of any commercial or financial relationships that could be construed as a potential conflict of interest.

frontiers in Cell and Developmental Biology

MINI REVIEW
published: 12 May 2021
doi: 10.3389/fcell.2021.669379

The Mitochondrial Response to DNA Damage

Ziye Rong[1], Peipei Tu[2], Peiqi Xu[1], Yan Sun[1], Fangfang Yu[1], Na Tu[1], Lixia Guo[3] and Yanan Yang[1]**

[1] Department of Immunology, School of Basic Medical Science, Anhui Medical University, Hefei, China, [2] Department of Microbiology and Bioengineering, School of Life Sciences, Anhui Medical University, Hefei, China, [3] Division of Pulmonary and Critical Care Medicine, Mayo Clinic, Rochester, MN, United States

Mitochondria are double membrane organelles in eukaryotic cells that provide energy by generating adenosine triphosphate (ATP) through oxidative phosphorylation. They are crucial to many aspects of cellular metabolism. Mitochondria contain their own DNA that encodes for essential proteins involved in the execution of normal mitochondrial functions. Compared with nuclear DNA, the mitochondrial DNA (mtDNA) is more prone to be affected by DNA damaging agents, and accumulated DNA damages may cause mitochondrial dysfunction and drive the pathogenesis of a variety of human diseases, including neurodegenerative disorders and cancer. Therefore, understanding better how mtDNA damages are repaired will facilitate developing therapeutic strategies. In this review, we focus on our current understanding of the mtDNA repair system. We also discuss other mitochondrial events promoted by excessive DNA damages and inefficient DNA repair, such as mitochondrial fusion, fission, and mitophagy, which serve as quality control events for clearing damaged mtDNA.

Keywords: mitochondrial DNA, DNA repair, mitochondrial fusion, mitochondrial fission, mitophagy

OPEN ACCESS

Edited by:
Daoxiang Zhang,
Washington University in St. Louis, United States

Reviewed by:
Konstantinos Palikaras,
National and Kapodistrian University of Athens, Greece
Yushan Zhu,
Nankai University, China

****Correspondence:***
Ziye Rong
2021500003@ahmu.edu.cn
Yanan Yang
yang.yanan@ahmu.edu.cn

Specialty section:
This article was submitted to Cell Death and Survival, a section of the journal Frontiers in Cell and Developmental Biology

Received: *18 February 2021*
Accepted: *20 April 2021*
Published: *12 May 2021*

Citation:
Rong Z, Tu P, Xu P, Sun Y, Yu F, Tu N, Guo L and Yang Y (2021) The Mitochondrial Response to DNA Damage. Front. Cell Dev. Biol. 9:669379. doi: 10.3389/fcell.2021.669379

INTRODUCTION

The mitochondria provide most of the cell energy in the form of adenosine triphosphate (ATP) through oxidative phosphorylation (OXPHOS), which is executed by the electron transport chain (ETC) within the mitochondria. In addition, mitochondria provide other key metabolic intermediates to many other basic cellular processes, such as lipid biogenesis and the synthesis of amino acids (Zong et al., 2016).

In the 1960s, nucleic acids and DNA were discovered in the mitochondria (Saki and Prakash, 2017). The mitochondrial DNA (mtDNA) is circular, and its length is varied in different species, from 75∼85 kb in *Saccharomyces cerevisiae* to around 16.5 kb in mammalian cells (Anderson et al., 1981; Foury et al., 1998). Although most of the mitochondrial proteins are transcribed in the nucleus, synthesized in the cytosol, and then transported into the mitochondria (Gray, 2012), the mtDNA is not non-sense. For example, in human cells, it encodes for 22 tRNAs and two ribosomal RNAs, as well as 13 polypeptides that comprise core subunits of the ETC Complex I, III, IV, and V, which are essential for the OXPHOS activity.

In mammalian cells, mtDNA is tightly linked with proteins to form complexes called nucleoids, which localize to the mitochondrial inner membrane (Chen and Butow, 2005; Holt et al., 2007). Some replication- and transcription-related proteins, such as mitochondrial transcription factor A (TFAM), DNA polymerase gamma (POLG), mitochondrial single-strand binding protein (mtSSB), and mtDNA helicase Twinkle, have been reported to interact with mtDNA (Garrido et al., 2003; Wang and Bogenhagen, 2006; Farge and Falkenberg, 2019).

Similar to nuclear DNA, the mtDNA is constantly assaulted by both exogenous and endogenous stresses, such as ultraviolet (UV) radiation and reactive oxygen species (ROS) (Alexeyev et al., 2013). However, evidence suggests that the mtDNA is more susceptible to certain stress-induced damages (e.g., oxidized DNA damages) than nuclear DNA due to its proximity to the sites of oxidative phosphorylation and lack of the protection by histones (Yakes and Van Houten, 1997; Druzhyna et al., 2008).

Excessive mtDNA damages, if not repaired efficiently, may increase ROS production, which in turn leads to mitochondrial dysfunction and provokes the pathogenesis of many human diseases, including Kearns-Sayre Syndrome, Alzheimer's, Parkinson's disease (PD), cancer, and diabetes (Wallace, 2005; Nakabeppu et al., 2007; Tsang et al., 2018; Llanos-Gonzalez et al., 2020). Therefore, accurate maintenance of the mtDNA is essential for a healthy life. In this review, we discuss how mitochondria respond to DNA damages, with an emphasis on how such damages are repaired. We also discuss a series of mitochondrial quality control events, including fission, fusion, and mitophagy, which are important for clearing damaged mtDNA that cannot be efficiently repaired.

AN OVERVIEW OF THE mtDNA DAMAGE REPAIR

Compared with nuclear DNA repair mechanisms, which have been extensively studied, the mtDNA repair mechanisms are much less understood. Unlike nuclear DNA, mtDNA is multi-copied (Yasukawa and Kang, 2018). Due to such nature, it was previously thought that DNA repair mechanisms might not be present or necessary in the mitochondria. For many years, this had led to a hypothesis that damaged mtDNA was simply degraded without being repaired, while the remained undamaged mtDNA served as the template for mtDNA synthesis (Druzhyna et al., 2008). This hypothesis was primarily based on the experiments showing that pyrimidine dimers induced by UV were not repaired in mammalian mitochondria (Clayton et al., 1974). Given that the nucleotide base repair (NER) is a highly efficient nuclear repair pathway for correcting a variety of DNA damages caused by UV radiation and many other environmental insults (Lee and Kang, 2019), these data suggest that the NER is absent for mtDNA damage repair.

However, more and more studies have shown that several other DNA repair pathways, including base excision repair (BER), direct reversal (DR), mismatch repair (MMR), and possibly double-strand break repair (DSBR), exist in the mammalian mitochondria (Kazak et al., 2012; Saki and Prakash, 2017; **Figure 1**). Key components of these pathways are encoded by nuclear genes and transported to the mitochondria after being synthesized in the cytosol.

BASE EXCISION REPAIR IN THE MITOCHONDRIA

Base excision repair is highly conserved from bacteria to human and has been considered as the primary repair pathway in the mitochondria, responsible for the removal of non-bulky DNA lesions caused predominantly by oxidation, alkylation, deamination, and methylation (Kazak et al., 2012; Krokan and Bjoras, 2013). Its basic process includes damaged DNA base recognition and removal, leaving an apurinic/apyrimidinc (AP) site (or called an abasic site), and subsequently the cleavage of the resulted AP site, end processing, gap filling, and ligation to complete the BER (Fortini et al., 2003).

At the initiation step of the BER, DNA glycosylases play important roles in damaged DNA recognition and removal (Jacobs and Schar, 2012). Seven of eleven known DNA glycosylases have mitochondrial targeting signal and have been identified in mammalian mitochondria (Sharma et al., 2019). They are categorized into two groups, namely the mono-functional glycosylases and bi-functional DNA glycosylases (Mullins et al., 2019). Mono-functional glycosylases include alkyladenine DNA glycosylase (AAG) (van Loon and Samson, 2013), MutY glycosylase homolog (MUTYH) (Ohtsubo et al., 2000), and uracil N-glycosyalse (UNG) (Slupphaug et al., 1993). Bi-functional DNA glycosylases include 8-oxoguanine DNA glycosylase-1 (OGG1) (Nishioka et al., 1999), Nei-like 1 (NEIL1) and Nei-like 2 (NEIL2) (Han et al., 2019), and Nth-Like 1 (NTHL1) (Imai et al., 1998).

Mono-functional glycosylases lack lyase activity and cleave the *N*-glycosidic bonds to generate AP sites, which are further processed by apurinic/apyrimidinic endonuclease 1 (APE1). Bi-functional DNA glycosylases with intrinsic lyase activity are capable of cleaving the abasic sites, and the DNA strand on the 3′ end of the AP site (Kazak et al., 2012; Stein and Sia, 2017). During the end processing, APE1 processes the ends generated by OGG1 and NTHL1 glycosylases (Hegde et al., 2008). The polynucleotide kinase/phosphatase (PNKP) processes the ends generated by the NEIL glycosylases (Tahbaz et al., 2012).

During short-patch BER (SP-BER), 5′-deoxyribose phosphate moiety created by APEI is excised by polymerase γ (Pol γ) with its lyase activity (Longley et al., 1998). Next, Pol γ inserts a single nucleotide to fill the gap. In long patch BER (LP-BER), 2–6 nucleotides are incorporated at the nick by Pol γ through its strand displacement synthesis activity (Longley et al., 1998; Akbari et al., 2008). Then, the 5′ flap is possibly cleaved by flap endonuclease 1 (FEN1) (Liu et al., 2008). Previous reports have shown that other enzymes, including DNA replication helicase/nuclease 2 (DNA2) and 5′-exo/endonuclease (EXOG) are important for removing 5′ flaps during mitochondrial LP-BER (Duxin et al., 2009; Tann et al., 2011). In both SP-BER and LP-BER, DNA ligase III seals the

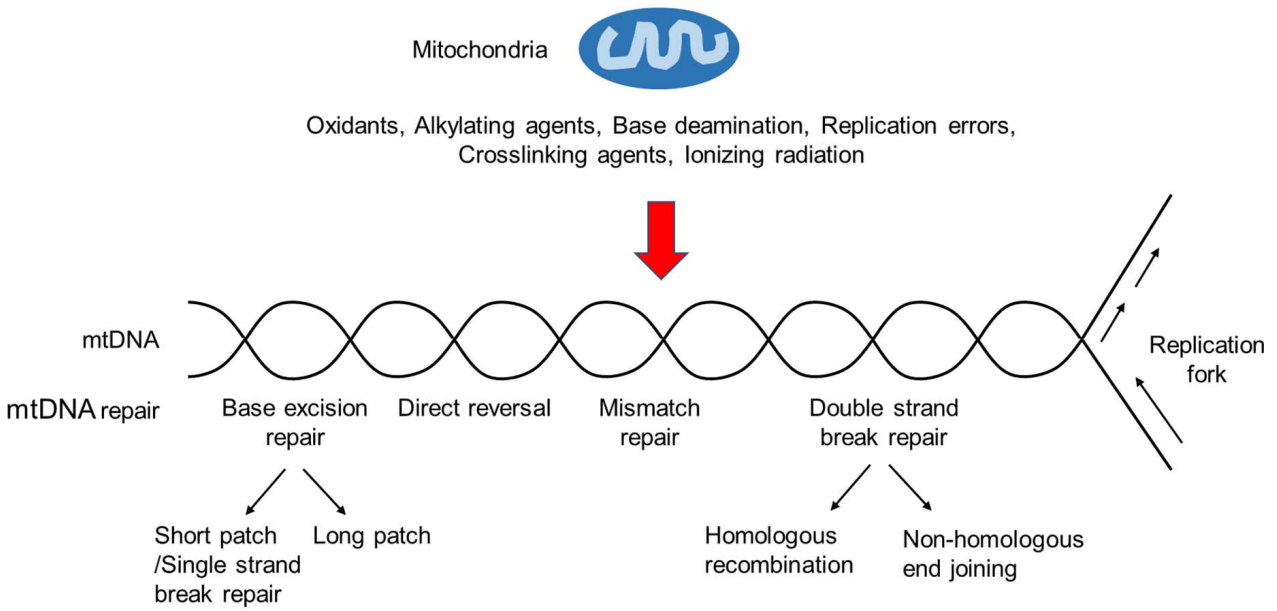

FIGURE 1 | An overview of the mtDNA damage repair. Ionizing radiation, base deamination, replication errors, and DNA damaging agents, such as oxidants, alkylating agents, and crosslinking agents, can cause mtDNA damages. BER is the primary mtDNA damage repair pathway, whereas NER is not observed in mitochondria. In addition, other repair pathways, such as DR, MMR and DSBR, may exist in the mitochondria.

nick to complete the final ligation step of the mitochondrial BER (Simsek et al., 2011).

The single strand break repair (SSBR) pathway is also likely to be present in the mitochondria (Hegde et al., 2012). SSBR can be considered as a form of BER, because many of the proteins involved in BER are important for SSBR. The two pathways have common gap filling and ligation steps. Previously, poly-ADP-ribose polymerase 1 (PARP1), which is required for recognizing single-strand breaks, has been reported to localize to the mitochondria (Rossi et al., 2009). However, the exact role for PARP1 in mammalian mtDNA SSBR is still unclear, and conflicting results have been reported (Szczesny et al., 2014).

During the end processing step, besides of APE1 and PNKP, tyrosyl DNA phosphodiesterase 1 (TDP1) and aprataxin (APTX) have been found to be involved in the mitochondrial SSBR pathway (Hegde et al., 2012; Meagher and Lightowlers, 2014). In the mitochondria, TDP1 typically hydrolyzes the phosphodiester bond between a tyrosyl moiety and a 3′-DNA end. It can also hydrolyze other 3′-end DNA alterations including 3′-phosphoglycolate and 3′-abasic sites. Therefore, TDP1 may function as a general 3′-end-processing DNA repair enzyme to remove a variety of adducts that are poor substrates for APE1 (Das et al., 2010). APTX belongs to the histidine triad (HIT) superfamily of nucleotide hydrolases and transferasese (Kijas et al., 2006). It removes 5′-adenylate (5′-AMP) group from DNA (Zheng et al., 2019). 5′-AMP group is an abortive DNA ligation product during DNA repair and replication, and it must be removed for the later DNA ligation. Previously, a slow rate of 5′-AMP removal was reported in the mitochondrial extracts compared with nuclear extracts (Akbari et al., 2015). Biochemical and cell biological analysis indicated it due to the lack of back up enzymes or repair mechanisms in mtDNA (Caglayan et al., 2017). All these results suggest that APTX is more critical in mtDNA repair than in the nuclear DNA repair.

Notably, mtDNA modifications are also involved in BER. For example, an enrichment of N^6-methyldeoxyadenosine (m^6A) in mammalian mtDNA has been recently reported (Hao et al., 2020). M^6A could repress DNA binding and bending by TFAM, which possesses a greater affinity for oxidized lesions and inhibits the activity of OGG1, UNG, and APE1 (Canugovi et al., 2010). Increased m^6A in the mtDNA affect the binding between TFAM and DNA so that the BER glycosylases are stimulated.

OTHER mtDNA DAMAGE REPAIR MECHANISMS

Direct Reversal

Direct reversal is responsible for the repair of DNA O-alkylated and N-alkylated damages caused by DNA alkylating agents (Fu et al., 2012). This repair process does not require excision, synthesis, and ligation. In mammalian cells, DR is performed by O^6-methylguanine DNA methyltransferase (MGMT) or ALKBH (AlkB homolog) proteins in the nucleus (Ragg et al., 2000; Ahmad et al., 2015). MGMT repairs the O^6-methylguanine lesions by removing methyl groups, whereas ALKBH repairs certain N-alkyl lesions *via* dealkylation. According to previous studies, mitochondrial localization of ALKBH has not been confirmed, and a protein with similar molecular weight to MGMT may localize to mammalian mitochondria (Myers et al., 1988). However, different groups have reported conflicting results, and

whether DR is present in the mammalian mitochondria remain to be further clarified (Cai et al., 2005).

Mismatch Repair

In 2003, MMR activity in rat liver mitochondrial extracts was reported (Mason et al., 2003). Notably, unlike nuclear MMR, there is no evidence that such activity relies on any well-known nuclear MMR proteins, such as MSH and MLH. Instead, it may depend on the Y-box binding protein YB-1 (de Souza-Pinto et al., 2009; Lyabin et al., 2014). This is supported by the facts that depleting YB-1 leads to both a decrease of MMR activity in the mitochondrial extracts and an increase of mtDNA mutations in YB-1-depleted cells. While these findings strongly suggest the presence of YB-1-dependent MMR in the mitochondria, more investigations are needed for better characterizing its detailed mechanism, especially the mitochondrial YB-1-associated cofactor(s) involved in this process.

Double-Strand Break Repair

Double-strand breaks (DSBs) are the most cytotoxic DNA lesions if not efficiently repaired (Stein and Sia, 2017). DSBs can be induced by ROS, replication stalling, or radiation. In the nucleus, DSBs are mainly repaired by two pathways, including homologous recombination (HR) and non-homologous end joining (NHEJ) pathways (Pannunzio et al., 2018; Wright et al., 2018). HR is considered as an "error-free" repair pathway due to its use of homologous partner as the template to repair DNA lesions. Several lines of evidence support the presence of HR in the mitochondria. For instance, the recombination intermediates containing four-way junctions can be detected in human mitochondria (Pohjoismaki et al., 2009), and Rad51, a RecA homolog, has been reported to execute HR in mammalian mitochondria (Sage et al., 2010). In addition, Rad51 related proteins, e.g., XRCC3, also exist in human mitochondria and may participate in HR (Mishra et al., 2018).

Compared with HR, NHEJ is more error-prone and results in large deletions. DNA end-joining activity has been observed in mitochondrial extracts prepared from mammalian cells, where both cohesive and blunt-ended DNA molecules can be repaired (Lakshmipathy and Campbell, 1999). Breast cancer type 1 susceptibility protein (BRCA1) and p53-binding protein 1 (53BP1) oppositely affect the extent of DNA end resection and are key determinants for the choice of HR or NHEJ (Panier and Boulton, 2014). During G2/S phase, BRCA1 promotes DNA end resection and thus induces HR. During G1 phase, 53BP1 protects the broken DNA end and inhibits long-range end resection, thereby promoting NHEJ. Both BRCA1 and 53BP1 have been identified in the mammalian mitochondria (Coene et al., 2005; Youn et al., 2017).

Taken together, previous findings suggest that both DSB and its related proteins are present in the mitochondria (Coffey and Campbell, 2000; Coene et al., 2005; Sage et al., 2010). However, whether DSB plays a major role in the mtDNA damage repair and whether the mitochondrial HR and NHEJ exert pathophysiological functions in disease contexts remain to be further elucidated.

THE MITOCHONDRIAL RESPONSE TO UNREPAIRED DNA DAMAGES

To maintain a healthy mitochondrial network, mammalian cells have developed several mechanisms to respond to unrepaired DNA damages, including *trans*-lesion synthesis, mitochondrial fusion and fission, and mitophagy. The interactions between some of them have also been reported (**Figure 2**).

Mitochondrial DNA Damage Tolerance Pathway: *Trans*-Lesion Synthesis

Trans-lesion synthesis (TLS) can bypass the DNA replication block caused by DNA damages (Waters et al., 2009; Sale, 2013). It is an error-prone process, in which the polymerases with low fidelity are involved (Ma X. et al., 2020). In TLS, nucleotides are incorporated to repair DNA lesions but convert them to DNA mutations. It requires DNA polymerase selection and switching (Friedberg et al., 2005). A group of specialized DNA polymerases termed TLS polymerases are utilized in this process, which are categorized into several families (Sale, 2013; Ma X. et al., 2020). Rev1, Polκ, Polη, and Polι belong to the best characterized Y-family polymerases, while polymerase zeta (Polζ) is a B-family polymerase (Yang and Gao, 2018). In mammalian mitochondria, there are evidence that REV3, the catalytic subunit of Polζ localizes to the mitochondria (Singh et al., 2015). REV3 associates with POLG and prevents the mtDNA damage. PrimPol is another TLS polymerase that has been detected in the mammalian mitochondria (Garcia-Gomez et al., 2013; Rudd et al., 2014). This enzyme has both DNA primase activity and DNA polymerase activity. It is capable of bypassing DNA lesions such as 8-oxoG (Guilliam et al., 2015).

Mitochondrial Fusion, Fission, and Mitophagy

If mtDNA damages cannot be repaired, they will accumulate and subsequently evoke mtDNA quality control events, including mitochondrial fusion, fission, and mitophagy (Youle and van der Bliek, 2012).

Mitochondrial fusion and fission are essential for cell metabolic activities as well as re-distribution of mtDNA (Tilokani et al., 2018). Both fusion and fission are mediated by GTPases (Hoppins et al., 2007). Specifically, Mitofusin 1 (Mfn1), Mitofusin 2 (Mfn2), and Optic Atrophy 1 (OPA1) are involved in the regulation of mitochondrial fusion (Delettre et al., 2000; Chen et al., 2003; Olichon et al., 2003; Detmer and Chan, 2007), and Drp1 is involved in mitochondrial fission (Fonseca et al., 2019).

Damaged and undamaged mtDNAs yield a heteroplasmic mixture of normal and mutant mitochondrial genomes within the same cell (Wonnapinij et al., 2008; Aryaman et al., 2018). Mitochondrial fusion allows the mitochondria with normal mtDNA to compensate for defects in the mitochondria with damaged mtDNA (Nakada et al., 2001; Ono et al., 2001; Yang et al., 2015). Through fusion, essential functional and structural components (e.g., proteins and lipids) in the two types of mitochondria can be diffused and shared, thereby rescuing the mitochondria with damaged mtDNA and mitigating the effects

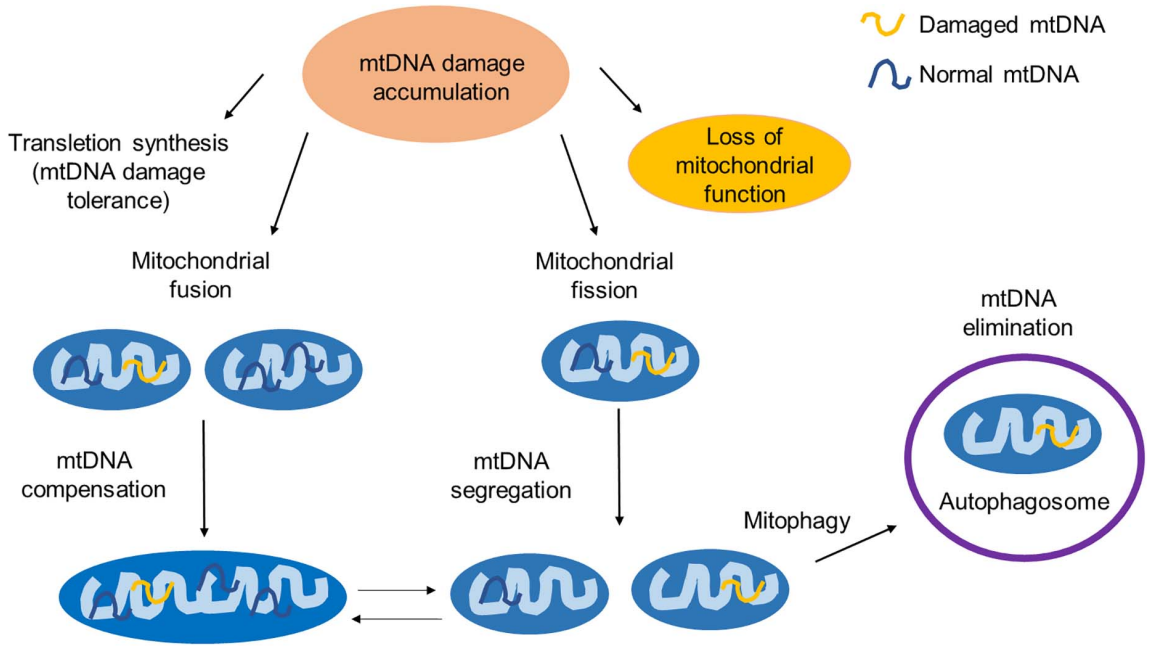

FIGURE 2 | The mitochondrial response to unrepaired DNA damages. Unrepaired mtDNA damages can be accumulated and lead to the mitochondrial dysfunction. To maintain its function, the mitochondria have developed several quality control events. TLS is an mtDNA damage tolerance pathway to bypass the mtDNA replication block. Mitochondrial fusion provides mtDNA complementation by mixing damaged and normal mtDNA. Mitochondrial fission segregates the part of a mitochondrion with damaged mtDNA and maintains the integrity of the healthy part of a mitochondrion. Mitochondria with excessive damaged mtDNA are selectively degraded through mitophagy. The interaction between the mitophagy and the mitochondrial fission/fusion has also been reported.

of environmental stresses on the mitochondria if the stress level is below a critical threshold (Stewart and Chinnery, 2015).

Mitochondrial fission allows mtDNAs to be divided into two mitochondria and provides a chance for a mitochondrion to re-fuse with another mitochondrion (Tilokani et al., 2018). It is suggested that fission divides a mitochondrion into two parts and distributes the damaged mtDNA and other harmful components asymmetrically to eliminate the part with most seriously damaged mtDNA but preserve the healthier part with normal mtDNA (Meyer et al., 2017).

Homoplasmy in mtDNA is rarely observed because of inherited or sporadic mutations that result in heteroplasmy (Wei et al., 2020). A broad range of heteroplasmy among different cell types and tissues are observed. The dynamics of heteroplasmy is one of the most challenging aspects of mtDNA disease. The mechanisms regulating heteroplasmy shifts are still needed to be elucidated. In T cell lineage, purifying selection occurs and heteroplasmy ratio is dramatically reduced (Walker et al., 2020). This process may enrich for certain mtDNA sequences and eliminate the pathogenic mutant mtDNA.

Irreparably damaged mtDNA may trigger mitophagy, a process through which depolarized or damaged mitochondria are selectively degraded by autophagy (Lemasters, 2005; Pickles et al., 2018). During autophagy, unwanted cellular materials are sequestered by double-membrane autophagosomes and delivered to lysosomes for degradation (Wollert, 2019). In normal cells, autophagy is utilized to clear and recycle almost all types of cellular materials, including proteins, lipids, damaged organelles, and etc. Mitophagy is an important mitochondrial quality control mechanism to maintain a healthy mitochondrial network (Ma K. et al., 2020). In mammalian cells, two pathways of mitophagy have been described. The first is an ubiquitin-mediated pathway, in which PINK1 (PTEN-induced putative protein kinase 1) has been shown to play an important role by recruiting the E3 ubiquitin ligase Parkin from the cytosol to the mitochondria with damaged DNA (Narendra et al., 2008; Matsuda et al., 2010; Pickrell and Youle, 2015). The other pathway is a receptor-mediated pathway, in which mitophagy receptors on the mitochondria with at least one LC3-interacting region have been identified. Some examples are BCL2 interacting protein 3 (BNIP3) (Chourasia and Macleod, 2015), FUN14 domain containing 1 (FUNDC1) (Chen M. et al., 2016), and mitochondria inner membrane protein Prohibitin 2 (PHB2) (Wei et al., 2017). These receptors mediate mitophagy by binding with LC3 to recruit the autophagosome (Yoo and Jung, 2018).

Previous reports also suggest that mitophagy may be linked to mitochondrial fission and fusion (Shirihai et al., 2015; Yoo and Jung, 2018). For example, overexpression of Opa1 or dominant-negative mutant of Drp1 can inhibit mitophagy (Twig et al., 2008). An interaction between the PINK1/Parkin pathway and the fission/fusion machinery has also been reported (Yu et al., 2011; Murata et al., 2020). It is proposed that fission is prerequisite for mitophagy by segregating the damaged part of a mitochondrion and targeting it for autophagic degradation. It is suspected that the damaged mtDNA and unwanted debris should distribute unevenly in the mitochondria to achieve such

asymmetric fission (Zorov et al., 2017). However, the underlying mechanism remains largely unknown.

As above-discussed, the UV-radiation induced mtDNA damages cannot be repaired by mtDNA repair mechanisms. However, the mitochondria with photo-damaged mtDNA undergoes mitophagy (Kim and Lemasters, 2011). It was confirmed that mitophagy can be induced by different types of mtDNA damage stimuli, and it at least partially depends on DNA damage response pathways (Furda et al., 2012). It should be noted that the modulation of mitophagy after DNA damage is independent of the type of mtDNA damage stimuli. Recently, it has been suggested that Spata18, a p53 inducible protein, is critical in mitophagy after mtDNA damage (Dan et al., 2020). Knocking down Spata18 suppresses mitophagy, promotes mtDNA damage, and attenuates mtDNA repair. To better understand the mitophagy process in response to mtDNA damage, it is important to identify related proteins and figure out how a mitochondrion, or its part, with damaged mtDNA can be selectively removed.

MITOPHAGY IN IMMUNITY AND HUMAN DISEASES

The interplay of mitophagy with mitochondrial dynamics is critical for maintaining mitochondrial homeostasis in normal and stressed conditions. Damaged mitochondria may either induce innate immunity or trigger cell death to drive aging-related diseases when mtDNA damages are beyond repairable (Ma K. et al., 2020).

Previous reports suggest that the mtDNA is implicated in the regulation of inflammation and innate immunity, and a major mediator for these processes is the "cGAS-STING" pathway (West et al., 2015; Chen Q. et al., 2016). For instance, internalized bacterial endotoxin lipopolysaccharide (LPS) can trjgger the mitochondrial membrane localization of active GSDMD, which in turn stimulates the release of mtDNA into the cytosol (Huang et al., 2020). The released mtDNA can be detected by the cyclic AMP-GMP synthase (cGAS), which generates cyclic GMP-AMP (cGAMP) to activate the pro-inflammatory stimulator of interferon genes (STING), eventually leading to increased production of type 1 interferons (IFNs).

In cancer cells, the mitochondrial outer membrane permeabilization (MOMP) has been shown to promote the cytosolic release of mtDNA, the activation of the cGAS-STING pathway, and the production of type I IFNs, which collectively facilitate an effective radiation therapy (Yamazaki et al., 2020); whereas Bcl2-dependent mitophagy can deplete MOMP, thereby limiting the release of mtDNA and associated immune responses.

Age-related accumulation of mtDNA mutations in human somatic and germ cells have also been reported (Arbeithuber et al., 2020). Replication errors are likely the main sources of *de novo* mtDNA mutations. Accumulation of certain types of mtDNA mutations may trigger cell death and lead to age-related diseases, such as PD, Cockayne syndrome (CS), and Werner syndrome (WS) (Palikaras et al., 2015; Fang et al., 2019; Lopes et al., 2020).

Parkinson's disease is a progressive neurodegenerative disorder with movement problems due to the loss of dopamine-producing neurons (Kalia and Lang, 2015). Interestingly, most of PD-related proteins have been shown to lead to dysfunctional mitochondria and/or accumulated damaged mitochondria (Martin-Jimenez et al., 2020). Some of them, including PINK1 and Parkin and LRRK2, play important roles in the execution of mitophagy (Vives-Bauza et al., 2010; Wallings et al., 2015). These facts not only establish a strong link between mitophagy and the pathogenesis of PD, but also suggest that manipulating mitophagy may have diagnostic/therapeutic values.

Werner syndrome is a human premature aging disease caused by mutations in the gene encoding for Werner protein (WRN), which is an important DNA helicase involved in DNA repair (Fang et al., 2019). WRN regulates the transcription of nicotinamide nucleotide adenylyltransferase 1 and NAD^+ biosynthesis. Accordingly, decreased NAD^+ levels and impaired mitophagy have been reported in WS patient samples.

In CS patient samples, there is a reduction in the activation of AMP-activated kinase (AMPK) and its downstream target, autophagy protein unc-51 like autophagy activating kinase 1 (ULK1), suggesting dysfunctional mitochondrial dynamics and impaired mitophagy (Okur et al., 2020). Reduced NAD^+ metabolism level was discovered in all three diseases. NAD^+ precursors can be used for treatment by promoting mitophagy *via* increasing the levels of key mitophagy-related proteins, such as PINK1, ULK1, and DCT-1 (Aman et al., 2020). Mitochondrial quality is improved and mitochondrial defects are reversed. These results further implicate that promoting mitophagy can be a promising approach to treat some age-related diseases.

CONCLUSION

We have known that cells are continuously exposed to both internal and external stresses, which may cause mtDNA damages. In response to such damages, the mitochondria have developed multiple ways to maintain its DNA integrity and function. Nevertheless, we still lack a comprehensive understanding of how distinct pathways/mechanisms act together to maintain a functional mitochondrial genome.

In this review, we have mainly focused on the mitochondrial response that repairs, attenuates, or eliminate mtDNA damages. Compared with nuclear DNA repair pathways, the pathways for repairing mtDNA damages are less understood. Many nuclear DNA repair proteins, especially those found in the nuclear BER pathway, are also found in the mitochondria (**Supplementary Table 1**). Previous data suggest that BER is the major mtDNA repair pathway, whereas NER has not been confirmed in the mitochondria. DR, MMR and DSBR may exist in the mitochondria. However, key components involved in these pathways have not been fully elucidated. To that end, further efforts are needed to identify the proteins/enzymes participating in distinct mtDNA damage repair processes.

Mitochondria have multiple quality control pathways to maintain its function in response to stresses. Herein, we have briefly discussed several such pathways, including TLS,

mitochondrial fission, fusion, and mitophagy. TLS can also be considered as a post-replication repair pathway. It utilizes damaged mtDNA as template to replicate with low-fidelity polymerases. Mitochondrial fusion and fission are dynamic to balance mtDNA damage compensation and elimination, and mitophagy is primarily responsible for the elimination of mitochondria with damaged mtDNA. Mis-regulation of such mtDNA damage responses has been linked to the immunity and pathogenesis of human diseases, including neurodegenerative disorders and cancer. In-depth understanding of these processes will provide insights for developing novel treatment strategies.

AUTHOR CONTRIBUTIONS

ZR and YY wrote the manuscript. All authors discussed and approved the contents.

FUNDING

This work was partly supported by the National Natural Science Foundation of China (NSFC) Project 82073257 (to YY) and University Natural Science Research Project of Anhui Province (China) (KJ2020A0159) (to PT).

SUPPLEMENTARY MATERIAL

The Supplementary Material for this article can be found online at: https://www.frontiersin.org/articles/10.3389/fcell.2021.669379/full#supplementary-material

Supplementary Table 1 | Enzymes/proteins in mtDNA repair. Important enzymes/proteins in mammalian mitochondria in different mtDNA damage repair mechanisms are present. Functions of each enzyme/protein are also listed.

REFERENCES

Ahmad, A., Nay, S. L., and O'Connor, T. R. (2015). Direct reversal repair in mammalian cells. *Adv. DNA Repair* 95–128. doi: 10.5772/60037

Akbari, M., Sykora, P., and Bohr, V. A. (2015). Slow mitochondrial repair of 5'-AMP renders mtDNA susceptible to damage in APTX deficient cells. *Sci. Rep.* 5:12876. doi: 10.1038/srep12876

Akbari, M., Visnes, T., Krokan, H. E., and Otterlei, M. (2008). Mitochondrial base excision repair of uracil and AP sites takes place by single-nucleotide insertion and long-patch DNA synthesis. *DNA Repair (Amst.)* 7, 605–616. doi: 10.1016/j.dnarep.2008.01.002

Alexeyev, M., Shokolenko, I., Wilson, G., and LeDoux, S. (2013). The maintenance of mitochondrial DNA integrity–critical analysis and update. *Cold Spring Harb. Perspect. Biol.* 5:a012641. doi: 10.1101/cshperspect.a012641

Aman, Y., Frank, J., Lautrup, S. H., Matysek, A., Niu, Z., Yang, G., et al. (2020). The NAD(+)-mitophagy axis in healthy longevity and in artificial intelligence-based clinical applications. *Mech. Ageing Dev.* 185:111194. doi: 10.1016/j.mad.2019.111194

Anderson, S., Bankier, A. T., Barrell, B. G., de Bruijn, M. H., Coulson, A. R., Drouin, J., et al. (1981). Sequence and organization of the human mitochondrial genome. *Nature* 290, 457–465. doi: 10.1038/290457a0

Arbeithuber, B., Hester, J., Cremona, M. A., Stoler, N., Zaidi, A., Higgins, B., et al. (2020). Age-related accumulation of de novo mitochondrial mutations in mammalian oocytes and somatic tissues. *PLoS Biol.* 18:e3000745. doi: 10.1371/journal.pbio.3000745

Aryaman, J., Johnston, I. G., and Jones, N. S. (2018). Mitochondrial heterogeneity. *Front. Genet.* 9:718. doi: 10.3389/fgene.2018.00718

Caglayan, M., Prasad, R., Krasich, R., Longley, M. J., Kadoda, K., Tsuda, M., et al. (2017). Complementation of aprataxin deficiency by base excision repair enzymes in mitochondrial extracts. *Nucleic Acids Res.* 45, 10079–10088. doi: 10.1093/nar/gkx654

Cai, S., Xu, Y., Cooper, R. J., Ferkowicz, M. J., Hartwell, J. R., Pollok, K. E., et al. (2005). Mitochondrial targeting of human O6-methylguanine DNA methyltransferase protects against cell killing by chemotherapeutic alkylating agents. *Cancer Res.* 65, 3319–3327. doi: 10.1158/0008-5472.CAN-04-3335

Canugovi, C., Maynard, S., Bayne, A. C., Sykora, P., Tian, J., de Souza-Pinto, N. C., et al. (2010). The mitochondrial transcription factor A functions in mitochondrial base excision repair. *DNA Repair (Amst.)* 9, 1080–1089. doi: 10.1016/j.dnarep.2010.07.009

Chen, H., Detmer, S. A., Ewald, A. J., Griffin, E. E., Fraser, S. E., and Chan, D. C. (2003). Mitofusins Mfn1 and Mfn2 coordinately regulate mitochondrial fusion and are essential for embryonic development. *J. Cell Biol.* 160, 189–200. doi: 10.1083/jcb.200211046

Chen, M., Chen, Z., Wang, Y., Tan, Z., Zhu, C., Li, Y., et al. (2016). Mitophagy receptor FUNDC1 regulates mitochondrial dynamics and mitophagy. *Autophagy* 12, 689–702. doi: 10.1080/15548627.2016.1151580

Chen, Q., Sun, L., and Chen, Z. J. (2016). Regulation and function of the cGAS-STING pathway of cytosolic DNA sensing. *Nat. Immunol.* 17, 1142–1149. doi: 10.1038/ni.3558

Chen, X. J., and Butow, R. A. (2005). The organization and inheritance of the mitochondrial genome. *Nat. Rev. Genet.* 6, 815–825. doi: 10.1038/nrg1708

Chourasia, A. H., and Macleod, K. F. (2015). Tumor suppressor functions of BNIP3 and mitophagy. *Autophagy* 11, 1937–1938. doi: 10.1080/15548627.2015.1085136

Clayton, D. A., Doda, J. N., and Friedberg, E. C. (1974). The absence of a pyrimidine dimer repair mechanism in mammalian mitochondria. *Proc. Natl. Acad. Sci. U. S. A.* 71, 2777–2781. doi: 10.1073/pnas.71.7.2777

Coene, E. D., Hollinshead, M. S., Waeytens, A. A., Schelfhout, V. R., Eechaute, W. P., Shaw, M. K., et al. (2005). Phosphorylated BRCA1 is predominantly located in the nucleus and mitochondria. *Mol. Biol. Cell* 16, 997–1010. doi: 10.1091/mbc.e04-10-0895

Coffey, G., and Campbell, C. (2000). An alternate form of Ku80 is required for DNA end-binding activity in mammalian mitochondria. *Nucleic Acids Res.* 28, 3793–3800. doi: 10.1093/nar/28.19.3793

Dan, X., Babbar, M., Moore, A., Wechter, N., Tian, J., Mohanty, J. G., et al. (2020). DNA damage invokes mitophagy through a pathway involving Spata18. *Nucleic Acids Res.* 48, 6611–6623. doi: 10.1093/nar/gkaa393

Das, B. B., Dexheimer, T. S., Maddali, K., and Pommier, Y. (2010). Role of tyrosyl-DNA phosphodiesterase (TDP1) in mitochondria. *Proc. Natl. Acad. Sci. U. S. A.* 107, 19790–19795. doi: 10.1073/pnas.1009814107

de Souza-Pinto, N. C., Mason, P. A., Hashiguchi, K., Weissman, L., Tian, J., Guay, D., et al. (2009). Novel DNA mismatch-repair activity involving YB-1 in human mitochondria. *DNA Repair (Amst.)* 8, 704–719. doi: 10.1016/j.dnarep.2009.01.021

Delettre, C., Lenaers, G., Griffoin, J. M., Gigarel, N., Lorenzo, C., Belenguer, P., et al. (2000). Nuclear gene OPA1, encoding a mitochondrial dynamin-related protein, is mutated in dominant optic atrophy. *Nat. Genet.* 26, 207–210. doi: 10.1038/79936

Detmer, S. A., and Chan, D. C. (2007). Complementation between mouse Mfn1 and Mfn2 protects mitochondrial fusion defects caused by CMT2A disease mutations. *J. Cell Biol.* 176, 405–414. doi: 10.1083/jcb.200611080

Druzhyna, N. M., Wilson, G. L., and LeDoux, S. P. (2008). Mitochondrial DNA repair in aging and disease. *Mech. Ageing Dev.* 129, 383–390. doi: 10.1016/j.mad.2008.03.002

Duxin, J. P., Dao, B., Martinsson, P., Rajala, N., Guittat, L., Campbell, J. L., et al. (2009). Human Dna2 is a nuclear and mitochondrial DNA maintenance protein. *Mol. Cell Biol.* 29, 4274–4282. doi: 10.1128/MCB.01834-08

Fang, E. F., Hou, Y., Lautrup, S., Jensen, M. B., Yang, B., SenGupta, T., et al. (2019). NAD(+) augmentation restores mitophagy and limits accelerated aging in Werner syndrome. *Nat. Commun.* 10:5284. doi: 10.1038/s41467-019-13172-8

Farge, G., and Falkenberg, M. (2019). Organization of DNA in mammalian mitochondria. *Int. J. Mol. Sci.* 20:2770. doi: 10.3390/ijms20112770

Fonseca, T. B., Sanchez-Guerrero, A., Milosevic, I., and Raimundo, N. (2019). Mitochondrial fission requires DRP1 but not dynamins. *Nature* 570, E34–E42. doi: 10.1038/s41586-019-1296-y

Fortini, P., Pascucci, B., Parlanti, E., D'Errico, M., Simonelli, V., and Dogliotti, E. (2003). The base excision repair: mechanisms and its relevance for cancer susceptibility. *Biochimie* 85, 1053–1071. doi: 10.1016/j.biochi.2003.11.003

Foury, F., Roganti, T., Lecrenier, N., and Purnelle, B. (1998). The complete sequence of the mitochondrial genome of Saccharomyces cerevisiae. *FEBS Lett.* 440, 325–331. doi: 10.1016/s0014-5793(98)01467-7

Friedberg, E. C., Lehmann, A. R., and Fuchs, R. P. (2005). Trading places: how do DNA polymerases switch during translesion DNA synthesis? *Mol. Cell* 18, 499–505. doi: 10.1016/j.molcel.2005.03.032

Fu, D., Calvo, J. A., and Samson, L. D. (2012). Balancing repair and tolerance of DNA damage caused by alkylating agents. *Nat. Rev. Cancer* 12, 104–120. doi: 10.1038/nrc3185

Furda, A. M., Marrangoni, A. M., Lokshin, A., and Van Houten, B. (2012). Oxidants and not alkylating agents induce rapid mtDNA loss and mitochondrial dysfunction. *DNA Repair (Amst.)* 11, 684–692. doi: 10.1016/j.dnarep.2012.06.002

Garcia-Gomez, S., Reyes, A., Martinez-Jimenez, M. I., Chocron, E. S., Mouron, S., Terrados, G., et al. (2013). PrimPol, an archaic primase/polymerase operating in human cells. *Mol. Cell* 52, 541–553. doi: 10.1016/j.molcel.2013.09.025

Garrido, N., Griparic, L., Jokitalo, E., Wartiovaara, J., van der Bliek, A. M., and Spelbrink, J. N. (2003). Composition and dynamics of human mitochondrial nucleoids. *Mol. Biol. Cell* 14, 1583–1596. doi: 10.1091/mbc.e02-07-0399

Gray, M. W. (2012). Mitochondrial evolution. *Cold Spring Harb. Perspect. Biol.* 4:a011403. doi: 10.1101/cshperspect.a011403

Guilliam, T. A., Jozwiakowski, S. K., Ehlinger, A., Barnes, R. P., Rudd, S. G., Bailey, L. J., et al. (2015). Human PrimPol is a highly error-prone polymerase regulated by single-stranded DNA binding proteins. *Nucleic Acids Res.* 43, 1056–1068. doi: 10.1093/nar/gku1321

Han, D., Schomacher, L., Schule, K. M., Mallick, M., Musheev, M. U., Karaulanov, E., et al. (2019). NEIL1 and NEIL2 DNA glycosylases protect neural crest development against mitochondrial oxidative stress. *Elife* 8:e49044. doi: 10.7554/eLife.49044

Hao, Z., Wu, T., Cui, X., Zhu, P., Tan, C., Dou, X., et al. (2020). N(6)-deoxyadenosine methylation in mammalian mitochondrial DNA. *Mol. Cell* 78, 382–395.e8. doi: 10.1016/j.molcel.2020.02.018

Hegde, M. L., Hazra, T. K., and Mitra, S. (2008). Early steps in the DNA base excision/single-strand interruption repair pathway in mammalian cells. *Cell Res.* 18, 27–47. doi: 10.1038/cr.2008.8

Hegde, M. L., Mantha, A. K., Hazra, T. K., Bhakat, K. K., Mitra, S., and Szczesny, B. (2012). Oxidative genome damage and its repair: implications in aging and neurodegenerative diseases. *Mech. Ageing Dev.* 133, 157–168. doi: 10.1016/j.mad.2012.01.005

Holt, I. J., He, J., Mao, C. C., Boyd-Kirkup, J. D., Martinsson, P., Sembongi, H., et al. (2007). Mammalian mitochondrial nucleoids: organizing an independently minded genome. *Mitochondrion* 7, 311–321. doi: 10.1016/j.mito.2007.06.004

Hoppins, S., Lackner, L., and Nunnari, J. (2007). The machines that divide and fuse mitochondria. *Annu. Rev. Biochem.* 76, 751–780. doi: 10.1146/annurev.biochem.76.071905.090048

Huang, L. S., Hong, Z., Wu, W., Xiong, S., Zhong, M., Gao, X., et al. (2020). mtDNA activates cGAS signaling and suppresses the YAP-mediated endothelial cell proliferation program to promote inflammatory injury. *Immunity* 52, 475–486.e5. doi: 10.1016/j.immuni.2020.02.002

Imai, K., Sarker, A. H., Akiyama, K., Ikeda, S., Yao, M., Tsutsui, K., et al. (1998). Genomic structure and sequence of a human homologue (NTHL1/NTH1) of *Escherichia coli* endonuclease III with those of the adjacent parts of TSC2 and SLC9A3R2 genes. *Gene* 222, 287–295. doi: 10.1016/s0378-1119(98)00485-5

Jacobs, A. L., and Schar, P. (2012). DNA glycosylases: in DNA repair and beyond. *Chromosoma* 121, 1–20. doi: 10.1007/s00412-011-0347-4

Kalia, L. V., and Lang, A. E. (2015). Parkinson's disease. *Lancet* 386, 896–912. doi: 10.1016/S0140-6736(14)61393-3

Kazak, L., Reyes, A., and Holt, I. J. (2012). Minimizing the damage: repair pathways keep mitochondrial DNA intact. *Nat. Rev. Mol. Cell Biol.* 13, 659–671. doi: 10.1038/nrm3439

Kijas, A. W., Harris, J. L., Harris, J. M., and Lavin, M. F. (2006). Aprataxin forms a discrete branch in the HIT (histidine triad) superfamily of proteins with both DNA/RNA binding and nucleotide hydrolase activities. *J. Biol. Chem.* 281, 13939–13948. doi: 10.1074/jbc.M507946200

Kim, I., and Lemasters, J. J. (2011). Mitophagy selectively degrades individual damaged mitochondria after photoirradiation. *Antioxid. Redox Signal.* 14, 1919–1928. doi: 10.1089/ars.2010.3768

Krokan, H. E., and Bjoras, M. (2013). Base excision repair. *Cold Spring Harb. Perspect. Biol.* 5:a012583. doi: 10.1101/cshperspect.a012583

Lakshmipathy, U., and Campbell, C. (1999). Double strand break rejoining by mammalian mitochondrial extracts. *Nucleic Acids Res.* 27, 1198–1204. doi: 10.1093/nar/27.4.1198

Lee, T. H., and Kang, T. H. (2019). DNA oxidation and excision repair pathways. *Int. J. Mol. Sci.* 20:6092. doi: 10.3390/ijms20236092

Lemasters, J. J. (2005). Selective mitochondrial autophagy, or mitophagy, as a targeted defense against oxidative stress, mitochondrial dysfunction, and aging. *Rejuvenation Res.* 8, 3–5. doi: 10.1089/rej.2005.8.3

Liu, P., Qian, L., Sung, J. S., de Souza-Pinto, N. C., Zheng, L., Bogenhagen, D. F., et al. (2008). Removal of oxidative DNA damage via FEN1-dependent long-patch base excision repair in human cell mitochondria. *Mol. Cell Biol.* 28, 4975–4987. doi: 10.1128/MCB.00457-08

Llanos-Gonzalez, E., Henares-Chavarino, A. A., Pedrero-Prieto, C. M., Garcia-Carpintero, S., Frontinan-Rubio, J., Sancho-Bielsa, F. J., et al. (2020). Interplay between mitochondrial oxidative disorders and proteostasis in Alzheimer's disease. *Front. Neurosci.* 13:ARTN1444. doi: 10.3389/fnins.2019.01444

Longley, M. J., Prasad, R., Srivastava, D. K., Wilson, S. H., and Copeland, W. C. (1998). Identification of 5'-deoxyribose phosphate lyase activity in human DNA polymerase gamma and its role in mitochondrial base excision repair in vitro. *Proc. Natl. Acad. Sci. U. S. A.* 95, 12244–12248. doi: 10.1073/pnas.95.21.12244

Lopes, A. F. C., Bozek, K., Herholz, M., Trifunovic, A., Rieckher, M., and Schumacher, B. (2020). A C. elegans model for neurodegeneration in Cockayne syndrome. *Nucleic Acids Res.* 48, 10973–10985. doi: 10.1093/nar/gkaa795

Lyabin, D. N., Eliseeva, I. A., and Ovchinnikov, L. P. (2014). YB-1 protein: functions and regulation. *Wiley Interdiscip. Rev. RNA* 5, 95–110. doi: 10.1002/wrna.1200

Ma, K., Chen, G., Li, W., Kepp, O., Zhu, Y., and Chen, Q. (2020). Mitophagy, mitochondrial homeostasis, and cell fate. *Front. Cell Dev. Biol.* 8:467. doi: 10.3389/fcell.2020.00467

Ma, X., Tang, T. S., and Guo, C. (2020). Regulation of translesion DNA synthesis in mammalian cells. *Environ. Mol. Mutagen.* 61, 680–692. doi: 10.1002/em.22359

Martin-Jimenez, R., Lurette, O., and Hebert-Chatelain, E. (2020). Damage in mitochondrial DNA associated with Parkinson's disease. *DNA Cell Biol.* 39, 1421–1430. doi: 10.1089/dna.2020.5398

Mason, P. A., Matheson, E. C., Hall, A. G., and Lightowlers, R. N. (2003). Mismatch repair activity in mammalian mitochondria. *Nucleic Acids Res.* 31, 1052–1058. doi: 10.1093/nar/gkg167

Matsuda, N., Sato, S., Shiba, K., Okatsu, K., Saisho, K., Gautier, C. A., et al. (2010). PINK1 stabilized by mitochondrial depolarization recruits Parkin to damaged mitochondria and activates latent Parkin for mitophagy. *J. Cell Biol.* 189, 211–221. doi: 10.1083/jcb.200910140

Meagher, M., and Lightowlers, R. N. (2014). The role of TDP1 and APTX in mitochondrial DNA repair. *Biochimie* 100, 121–124. doi: 10.1016/j.biochi.2013.10.011

Meyer, J. N., Leuthner, T. C., and Luz, A. L. (2017). Mitochondrial fusion, fission, and mitochondrial toxicity. *Toxicology* 391, 42–53. doi: 10.1016/j.tox.2017.07.019

Mishra, A., Saxena, S., Kaushal, A., and Nagaraju, G. (2018). RAD51C/XRCC3 facilitates mitochondrial DNA replication and maintains integrity of the mitochondrial genome. *Mol. Cell Biol.* 38:e00489–17. doi: 10.1128/MCB.00489-17

Mullins, E. A., Rodriguez, A. A., Bradley, N. P., and Eichman, B. F. (2019). Emerging roles of DNA glycosylases and the base excision repair pathway. *Trends Biochem. Sci.* 44, 765–781. doi: 10.1016/j.tibs.2019.04.006

Murata, D., Arai, K., Iijima, M., and Sesaki, H. (2020). Mitochondrial division, fusion and degradation. *J. Biochem.* 167, 233–241. doi: 10.1093/jb/mvz106

Myers, K. A., Saffhill, R., and O'Connor, P. J. (1988). Repair of alkylated purines in the hepatic DNA of mitochondria and nuclei in the rat. *Carcinogenesis* 9, 285–292. doi: 10.1093/carcin/9.2.285

Nakabeppu, Y., Tsuchimoto, D., Yamaguchi, H., and Sakumi, K. (2007). Oxidative damage in nucleic acids and Parkinson's disease. *J. Neurosci. Res.* 85, 919–934. doi: 10.1002/jnr.21191

Nakada, K., Inoue, K., Ono, T., Isobe, K., Ogura, A., Goto, Y. I., et al. (2001). Inter-mitochondrial complementation: mitochondria-specific system preventing mice from expression of disease phenotypes by mutant mtDNA. *Nat. Med.* 7, 934–940. doi: 10.1038/90976

Narendra, D., Tanaka, A., Suen, D. F., and Youle, R. J. (2008). Parkin is recruited selectively to impaired mitochondria and promotes their autophagy. *J. Cell Biol.* 183, 795–803. doi: 10.1083/jcb.200809125

Nishioka, K., Ohtsubo, T., Oda, H., Fujiwara, T., Kang, D., Sugimachi, K., et al. (1999). Expression and differential intracellular localization of two major forms of human 8-oxoguanine DNA glycosylase encoded by alternatively spliced OGG1 mRNAs. *Mol. Biol. Cell* 10, 1637–1652. doi: 10.1091/mbc.10.5.1637

Ohtsubo, T., Nishioka, K., Imaiso, Y., Iwai, S., Shimokawa, H., Oda, H., et al. (2000). Identification of human MutY homolog (hMYH) as a repair enzyme for 2-hydroxyadenine in DNA and detection of multiple forms of hMYH located in nuclei and mitochondria. *Nucleic Acids Res.* 28, 1355–1364. doi: 10.1093/nar/28.6.1355

Okur, M. N., Fang, E. F., Fivenson, E. M., Tiwari, V., Croteau, D. L., and Bohr, V. A. (2020). Cockayne syndrome proteins CSA and CSB maintain mitochondrial homeostasis through NAD(+) signaling. *Aging Cell* 19:e13268. doi: 10.1111/acel.13268

Olichon, A., Baricault, L., Gas, N., Guillou, E., Valette, A., Belenguer, P., et al. (2003). Loss of OPA1 perturbates the mitochondrial inner membrane structure and integrity, leading to cytochrome c release and apoptosis. *J. Biol. Chem.* 278, 7743–7746. doi: 10.1074/jbc.C200677200

Ono, T., Isobe, K., Nakada, K., and Hayashi, J. I. (2001). Human cells are protected from mitochondrial dysfunction by complementation of DNA products in fused mitochondria. *Nat. Genet.* 28, 272–275. doi: 10.1038/90116

Palikaras, K., Lionaki, E., and Tavernarakis, N. (2015). Coordination of mitophagy and mitochondrial biogenesis during ageing in C. elegans. *Nature* 521, 525–528. doi: 10.1038/nature14300

Panier, S., and Boulton, S. J. (2014). Double-strand break repair: 53BP1 comes into focus. *Nat. Rev. Mol. Cell Biol.* 15, 7–18. doi: 10.1038/nrm3719

Pannunzio, N. R., Watanabe, G., and Lieber, M. R. (2018). Nonhomologous DNA end-joining for repair of DNA double-strand breaks. *J. Biol. Chem.* 293, 10512–10523. doi: 10.1074/jbc.TM117.000374

Pickles, S., Vigie, P., and Youle, R. J. (2018). Mitophagy and quality control mechanisms in mitochondrial maintenance. *Curr. Biol.* 28, R170–R185. doi: 10.1016/j.cub.2018.01.004

Pickrell, A. M., and Youle, R. J. (2015). The roles of PINK1, parkin, and mitochondrial fidelity in Parkinson's disease. *Neuron* 85, 257–273. doi: 10.1016/j.neuron.2014.12.007

Pohjoismaki, J. L., Goffart, S., Tyynismaa, H., Willcox, S., Ide, T., Kang, D., et al. (2009). Human heart mitochondrial DNA is organized in complex catenated networks containing abundant four-way junctions and replication forks. *J. Biol. Chem.* 284, 21446–21457. doi: 10.1074/jbc.M109.016600

Ragg, S., Xu-Welliver, M., Bailey, J., D'Souza, M., Cooper, R., Chandra, S., et al. (2000). Direct reversal of DNA damage by mutant methyltransferase protein protects mice against dose-intensified chemotherapy and leads to in vivo selection of hematopoietic stem cells. *Cancer Res.* 60, 5187–5195.

Rossi, M. N., Carbone, M., Mostocotto, C., Mancone, C., Tripodi, M., Maione, R., et al. (2009). Mitochondrial localization of PARP-1 requires interaction with mitofilin and is involved in the maintenance of mitochondrial DNA integrity. *J. Biol. Chem.* 284, 31616–31624. doi: 10.1074/jbc.M109.025882

Rudd, S. G., Bianchi, J., and Doherty, A. J. (2014). PrimPol-A new polymerase on the block. *Mol. Cell Oncol.* 1:e960754. doi: 10.4161/23723548.2014.960754

Sage, J. M., Gildemeister, O. S., and Knight, K. L. (2010). Discovery of a novel function for human Rad51: maintenance of the mitochondrial genome. *J. Biol. Chem.* 285, 18984–18990. doi: 10.1074/jbc.M109.099846

Saki, M., and Prakash, A. (2017). DNA damage related crosstalk between the nucleus and mitochondria. *Free Radic. Biol. Med.* 107, 216–227. doi: 10.1016/j.freeradbiomed.2016.11.050

Sale, J. E. (2013). Translesion DNA synthesis and mutagenesis in eukaryotes. *Cold Spring Harb. Perspect. Biol.* 5:a012708. doi: 10.1101/cshperspect.a012708

Sharma, N., Pasala, M. S., and Prakash, A. (2019). Mitochondrial DNA: epigenetics and environment. *Environ. Mol. Mutagen.* 60, 668–682. doi: 10.1002/em.22319

Shirihai, O. S., Song, M., and Dorn, G. W. II (2015). How mitochondrial dynamism orchestrates mitophagy. *Circ. Res.* 116, 1835–1849. doi: 10.1161/CIRCRESAHA.116.306374

Simsek, D., Furda, A., Gao, Y., Artus, J., Brunet, E., Hadjantonakis, A. K., et al. (2011). Crucial role for DNA ligase III in mitochondria but not in Xrcc1-dependent repair. *Nature* 471, 245–248. doi: 10.1038/nature09794

Singh, B., Li, X., Owens, K. M., Vanniarajan, A., Liang, P., and Singh, K. K. (2015). Human REV3 DNA polymerase zeta localizes to mitochondria and protects the mitochondrial genome. *PLoS One* 10:e0140409. doi: 10.1371/journal.pone.0140409

Slupphaug, G., Markussen, F. H., Olsen, L. C., Aasland, R., Aarsaether, N., Bakke, O., et al. (1993). Nuclear and mitochondrial forms of human uracil-DNA glycosylase are encoded by the same gene. *Nucleic Acids Res.* 21, 2579–2584. doi: 10.1093/nar/21.11.2579

Stein, A., and Sia, E. A. (2017). Mitochondrial DNA repair and damage tolerance. *Front. Biosci. (Landmark Ed.)* 22:920–943. doi: 10.2741/4525

Stewart, J. B., and Chinnery, P. F. (2015). The dynamics of mitochondrial DNA heteroplasmy: implications for human health and disease. *Nat. Rev. Genet.* 16, 530–542. doi: 10.1038/nrg3966

Szczesny, B., Brunyanszki, A., Olah, G., Mitra, S., and Szabo, C. (2014). Opposing roles of mitochondrial and nuclear PARP1 in the regulation of mitochondrial and nuclear DNA integrity: implications for the regulation of mitochondrial function. *Nucleic Acids Res.* 42, 13161–13173. doi: 10.1093/nar/gku1089

Tahbaz, N., Subedi, S., and Weinfeld, M. (2012). Role of polynucleotide kinase/phosphatase in mitochondrial DNA repair. *Nucleic Acids Res.* 40, 3484–3495. doi: 10.1093/nar/gkr1245

Tann, A. W., Boldogh, I., Meiss, G., Qian, W., Van Houten, B., Mitra, S., et al. (2011). Apoptosis induced by persistent single-strand breaks in mitochondrial genome: critical role of EXOG (5'-EXO/endonuclease) in their repair. *J. Biol. Chem.* 286, 31975–31983. doi: 10.1074/jbc.M110.215715

Tilokani, L., Nagashima, S., Paupe, V., and Prudent, J. (2018). Mitochondrial dynamics: overview of molecular mechanisms. *Essays Biochem.* 62, 341–360. doi: 10.1042/EBC20170104

Tsang, S. H., Aycinena, A. R. P., and Sharma, T. (2018). Mitochondrial disorder: kearns-sayre syndrome. *Adv. Exp. Med. Biol.* 1085, 161–162. doi: 10.1007/978-3-319-95046-4_30

Twig, G., Elorza, A., Molina, A. J., Mohamed, H., Wikstrom, J. D., Walzer, G., et al. (2008). Fission and selective fusion govern mitochondrial segregation and elimination by autophagy. *EMBO J.* 27, 433–446. doi: 10.1038/sj.emboj.7601963

van Loon, B., and Samson, L. D. (2013). Alkyladenine DNA glycosylase (AAG) localizes to mitochondria and interacts with mitochondrial single-stranded binding protein (mtSSB). *DNA Repair (Amst.)* 12, 177–187. doi: 10.1016/j.dnarep.2012.11.009

Vives-Bauza, C., Zhou, C., Huang, Y., Cui, M., de Vries, R. L., Kim, J., et al. (2010). PINK1-dependent recruitment of Parkin to mitochondria in mitophagy. *Proc. Natl. Acad. Sci. U. S. A.* 107, 378–383. doi: 10.1073/pnas.0911187107

Walker, M. A., Lareau, C. A., Ludwig, L. S., Karaa, A., Sankaran, V. G., Regev, A., et al. (2020). Purifying selection against pathogenic mitochondrial DNA in human T cells. *N. Engl. J. Med.* 383, 1556–1563. doi: 10.1056/NEJMoa2001265

Wallace, D. C. (2005). A mitochondrial paradigm of metabolic and degenerative diseases, aging, and cancer: a dawn for evolutionary medicine. *Annu. Rev. Genet.* 39, 359–407. doi: 10.1146/annurev.genet.39.110304.095751

Wallings, R., Manzoni, C., and Bandopadhyay, R. (2015). Cellular processes associated with LRRK2 function and dysfunction. *FEBS J.* 282, 2806–2826. doi: 10.1111/febs.13305

Wang, Y., and Bogenhagen, D. F. (2006). Human mitochondrial DNA nucleoids are linked to protein folding machinery and metabolic enzymes at the mitochondrial inner membrane. *J. Biol. Chem.* 281, 25791–25802. doi: 10.1074/jbc.M604501200

Waters, L. S., Minesinger, B. K., Wiltrout, M. E., D'Souza, S., Woodruff, R. V., and Walker, G. C. (2009). Eukaryotic translesion polymerases and their roles and regulation in DNA damage tolerance. *Microbiol. Mol. Biol. Rev.* 73, 134–154. doi: 10.1128/MMBR.00034-08

Wei, W., Pagnamenta, A. T., Gleadall, N., Sanchis-Juan, A., Stephens, J., Broxholme, J., et al. (2020). Nuclear-mitochondrial DNA segments resemble paternally inherited mitochondrial DNA in humans. *Nat. Commun.* 11:1740. doi: 10.1038/s41467-020-15336-3

Wei, Y., Chiang, W. C., Sumpter, R. Jr., Mishra, P., and Levine, B. (2017). Prohibitin 2 is an inner mitochondrial membrane mitophagy receptor. *Cell* 168(1–2), 224–238.e10. doi: 10.1016/j.cell.2016.11.042

West, A. P., Khoury-Hanold, W., Staron, M., Tal, M. C., Pineda, C. M., Lang, S. M., et al. (2015). Mitochondrial DNA stress primes the antiviral innate immune response. *Nature* 520, 553–557. doi: 10.1038/nature14156

Wollert, T. (2019). Autophagy. *Curr. Biol.* 29, R671–R677. doi: 10.1016/j.cub.2019.06.014

Wonnapinij, P., Chinnery, P. F., and Samuels, D. C. (2008). The distribution of mitochondrial DNA heteroplasmy due to random genetic drift. *Am. J. Hum. Genet.* 83, 582–593. doi: 10.1016/j.ajhg.2008.10.007

Wright, W. D., Shah, S. S., and Heyer, W. D. (2018). Homologous recombination and the repair of DNA double-strand breaks. *J Biol Chem* 293, 10524–10535. doi: 10.1074/jbc.TM118.000372

Yakes, F. M., and Van Houten, B. (1997). Mitochondrial DNA damage is more extensive and persists longer than nuclear DNA damage in human cells following oxidative stress. *Proc. Natl. Acad. Sci. U. S. A.* 94, 514–519. doi: 10.1073/pnas.94.2.514

Yamazaki, T., Kirchmair, A., Sato, A., Buque, A., Rybstein, M., Petroni, G., et al. (2020). Mitochondrial DNA drives abscopal responses to radiation that are inhibited by autophagy. *Nat. Immunol.* 21, 1160–1171. doi: 10.1038/s41590-020-0751-0

Yang, L., Long, Q., Liu, J., Tang, H., Li, Y., Bao, F., et al. (2015). Mitochondrial fusion provides an 'initial metabolic complementation' controlled by mtDNA. *Cell Mol. Life Sci.* 72, 2585–2598. doi: 10.1007/s00018-015-1863-9

Yang, W., and Gao, Y. (2018). Translesion and repair DNA polymerases: diverse structure and mechanism. *Annu. Rev. Biochem.* 87, 239–261. doi: 10.1146/annurev-biochem-062917-012405

Yasukawa, T., and Kang, D. (2018). An overview of mammalian mitochondrial DNA replication mechanisms. *J. Biochem.* 164, 183–193. doi: 10.1093/jb/mvy058

Yoo, S. M., and Jung, Y. K. (2018). A molecular approach to mitophagy and mitochondrial dynamics. *Mol. Cells* 41, 18–26. doi: 10.14348/molcells.2018.2277

Youle, R. J., and van der Bliek, A. M. (2012). Mitochondrial fission, fusion, and stress. *Science* 337, 1062–1065. doi: 10.1126/science.1219855

Youn, C. K., Kim, H. B., Wu, T. T., Park, S., Cho, S. I., and Lee, J. H. (2017). 53BP1 contributes to regulation of autophagic clearance of mitochondria. *Sci. Rep.* 7:45290. doi: 10.1038/srep45290

Yu, W., Sun, Y., Guo, S., and Lu, B. (2011). The PINK1/Parkin pathway regulates mitochondrial dynamics and function in mammalian hippocampal and dopaminergic neurons. *Hum. Mol. Genet.* 20, 3227–3240. doi: 10.1093/hmg/ddr235

Zheng, J., Croteau, D. L., Bohr, V. A., and Akbari, M. (2019). Diminished OPA1 expression and impaired mitochondrial morphology and homeostasis in Aprataxin-deficient cells. *Nucleic Acids Res.* 47, 4086–4110. doi: 10.1093/nar/gkz083

Zong, W. X., Rabinowitz, J. D., and White, E. (2016). Mitochondria and cancer. *Mol. Cell* 61, 667–676. doi: 10.1016/j.molcel.2016.02.011

Zorov, D. B., Popkov, V. A., Zorova, L. D., Vorobjev, I. A., Pevzner, I. B., Silachev, D. N., et al. (2017). Mitochondrial aging: is there a mitochondrial clock? *J. Gerontol. A Biol. Sci. Med. Sci.* 72, 1171–1179. doi: 10.1093/gerona/glw184

Conflict of Interest: The authors declare that the research was conducted in the absence of any commercial or financial relationships that could be construed as a potential conflict of interest.

frontiers in Cell and Developmental Biology

ORIGINAL RESEARCH
published: 21 June 2021
doi: 10.3389/fcell.2021.692269

Ser^{71} Phosphorylation Inhibits Actin-Binding of Profilin-1 and Its Apoptosis-Sensitizing Activity

Faliang Wang[1,2†], Cuige Zhu[1†], Shirong Cai[3,4], Aaron Boudreau[5], Sun-Joong Kim[1], Mina Bissell[5] and Jieya Shao[1]*

[1] Division of Oncology, Department of Medicine, Washington University School of Medicine, St. Louis, MO, United States, [2] Department of Surgical Oncology, The Children's Hospital, Zhejiang University School of Medicine, National Clinical Research Center for Child Health, Hangzhou, China, [3] Department of Cell Biology and Physiology, Washington University School of Medicine, St. Louis, MO, United States, [4] Department of Cancer Biology, The University of Texas MD Anderson Cancer Center, Houston, TX, United States, [5] Life Sciences Division, Lawrence Berkeley National Laboratory, Berkeley, CA, United States

OPEN ACCESS

Edited by:
Guoping Zhao,
Hefei Institutes of Physical Science, Chinese Academy of Sciences (CAS), China

Reviewed by:
Wang Minghui,
Sun Yat-sen University, China
Bart Tummers,
St. Jude Children's Research Hospital, United States

***Correspondence:**
Jieya Shao
shao.j@wustl.edu

[†] These authors have contributed equally to this work

Specialty section:
This article was submitted to Cell Death and Survival, a section of the journal Frontiers in Cell and Developmental Biology

Received: 08 April 2021
Accepted: 28 May 2021
Published: 21 June 2021

Citation:
Wang F, Zhu C, Cai S, Boudreau A, Kim S-J, Bissell M and Shao J (2021) Ser^{71} Phosphorylation Inhibits Actin-Binding of Profilin-1 and Its Apoptosis-Sensitizing Activity. Front. Cell Dev. Biol. 9:692269. doi: 10.3389/fcell.2021.692269

The essential actin-binding factor profilin-1 (Pfn1) is a non-classical tumor suppressor with the abilities toboth inhibit cellular proliferation and augment chemotherapy-induced apoptosis. Besides actin, Pfn1 interacts with proteins harboring the poly-L-proline (PLP) motifs. Our recent work demonstrated that both nuclear localization and PLP-binding are required for tumor growth inhibition by Pfn1, and this is at least partially due to Pfn1 association with the PLP-containing ENL protein in the Super Elongation Complex (SEC) and the transcriptional inhibition of pro-cancer genes. In this paper, by identifying a phosphorylation event of Pfn1 at Ser^{71} capable of inhibiting its actin-binding and nuclear export, we provide *in vitro* and *in vivo* evidence that chemotherapy-induced apoptotic sensitization by Pfn1 requires its cytoplasmic localization and actin-binding. With regard to tumor growth inhibition byPfn1, our data indicate a requirement for dynamic actin association and dissociation rendered by reversible Ser^{71}phosphorylation and dephosphorylation. Furthermore, genetic and pharmacological experiments showed that Ser^{71} of Pfn1 can be phosphorylated by protein kinase A (PKA). Taken together, our data provide novel mechanistic insights into the multifaceted anticancer activities of Pfn1 and how they are spatially-defined in the cell and differentially regulated by ligand-binding.

Keywords: profilin-1, phosphorylation, actin, poly-L-proline, apoptosis, breast cancer, chemotherapy, protein kinase A

INTRODUCTION

As the first actin-binding protein identified more than four decades ago (Carlsson et al., 1977), profilin-1 (Pfn1) has been extensively studied in the context of actin regulation. By binding monomeric G-actin, Pfn1 exchanges ADP for ATP and facilitates the addition of ATP-bound G-actin to the barbed ends of filamentous actin (Haarer and Brown, 1990; Witke, 2004; Jockusch et al., 2007; Birbach, 2008). In addition, Pfn1 interacts with a wide range of poly-L-proline (PLP)-containing proteins many of which are actin-regulatory factors and cooperate with Pfn1 to control actin polymerization (Haarer and Brown, 1990; Witke, 2004; Jockusch et al., 2007; Birbach, 2008).

Pfn1 is essential for the development and survival of multiple eukaryotic organisms including mice, Drosophila and yeast (Balasubramanian et al., 1994; Verheyen and Cooley, 1994; Witke et al., 2001; Bottcher et al., 2009). Paradoxically, Pfn1 also shows anti-tumor and anti-metastatic activities for various types of cancer (breast, pancreatic, and liver) (Janke et al., 2000; Roy and Jacobson, 2004; Wittenmayer et al., 2004; Ding et al., 2006; Wu et al., 2006; Zou et al., 2007, 2009, 2010; Bae et al., 2009, 2010; Das et al., 2009; Yao et al., 2014; Diamond et al., 2015). Our prior study suggested that some of these anticancer activities may stem from nuclear Pfn1 (Diamond et al., 2015). Our more recent work supported this theory and demonstrated that nuclear Pfn1 functions as a transcriptional repressor by binding and inhibiting the Super Elongation Complex (SEC), a positive regulator of transcriptional elongation of many pro-cancer genes (Zhu et al., 2021). Furthermore, we provided evidence that Pfn1 undergoes spatial deregulation in a broad range of cancer due to overexpression of its nuclear exporter exportin-6. This explains, to some extent, how anticancer activity of nuclear Pfn1 can be inhibited while its essential cytoplasmic functions are sustained. However, given that Pfn1 influences distinct cancer phenotypes including proliferation, metastasis, and survival upon chemotherapy treatments (Zou et al., 2010; Yao et al., 2013; Zaidi et al., 2016), it remains unclear whether these activities stem from the same or different subcellular locations and whether there are additional regulatory mechanisms besides exportin-6-dependent nuclear export.

We have found in prior and recent studies that PLP-binding is important for the tumor-inhibitory function of Pfn1 (Diamond et al., 2015), at least partially due to the direct interaction of nuclear Pfn1 with ENL, a PLP-containing protein, in the SEC complex (Zhu et al., 2021). We and others found that PLP-binding of Pfn1 can be abolished by Ser^{137} phosphorylation in its C-terminus (Shao et al., 2008b; Diamond et al., 2015). In addition to PLP-binding, actin-binding was also suggested to be important for tumor inhibition by Pfn1. This was based on the loss-of-function effect of Y59A, an actin-binding mutation of Pfn1 (Schluter et al., 1998; Wittenmayer et al., 2004). However, despite being the first actin-binding protein identified several decades ago, it remains unknown whether phosphorylation events exist in Pfn1 which can inhibit its actin-binding and modulate its anticancer activities.

In this paper, we identified a protein kinase A (PKA)-dependent phosphorylation site in Pfn1 at Ser^{71}. Residing in the actin-binding site of Pfn1, Ser^{71} phosphorylation abolishes the Pfn1/actin interaction and causes nuclear retention of Pfn1. Functional characterization using breast cancer cell lines revealed that Ser^{71} phosphorylation regulates both cell proliferation and chemotherapy-induced apoptosis but in different fashions. Dissection of the functional influences of subcellular localization further indicated that while tumor inhibition by Pfn1 is driven largely by its nuclear activities, apoptosis-sensitizing effect depends on its cytoplasmic localization. Thus, by identifying and characterizing a previously unknown inhibitory phosphorylation event for actin-binding of Pfn1, we provided further mechanistic insights into its multifaceted tumor-inhibitory activities which are regulated both by ligand-binding and subcellular localization.

MATERIALS AND METHODS

DNA Constructs

Untagged, Myc-tagged, and HA-tagged Pfn1 in pcDNA3, His-tagged Pfn1 in pRK172, untagged Pfn1 in pLenti-CMV/TO-Neo-DEST, and YFP-Pfn1 with and without NES or NLS tag in pFLRu-FH vector have been described previously (Shao et al., 2008b; Diamond et al., 2015; Zhu et al., 2021). Point mutations (S71A and S71D) within Pfn1 were introduced by site-directed mutagenesis using QuikChange. GFP-tagged PKA catalytic subunit in EGFP-C1 was purchased from Addgene (plasmid # 61091).

Antibodies

Primary antibodies used for Western blots are as follows: mouse anti-HA-tag (Convance, MMS-101P through BioLegend, United States), mouse anti-Myc-tag (Santa Cruz, United States, sc-40), mouse anti-β-actin (Santa Cruz, United States, sc-47778; Cell Signaling, United States, #3700), mouse anti-α-tubulin (Cell Signaling, United States, #3873), mouse GAPDH (Santa Cruz, United States, sc-47724), rabbit anti-Pfn1 (Cell Signaling, United States, #3246), rabbit anti-VASP (Bethyl laboratories, United States, A304-769A), rabbit anti-cleaved caspase-7 (Cell Signaling, United States, #8438), rabbit anti-cleaved PARP (Cell signaling, United States, #9541), rabbit anti-GFP (Cell Signaling, United States, #2956). To raise the polyclonal pSer^{71}-Pfn1 antibody (F5675), a synthetic phospho-Pfn1 peptide harboring pSer^{71} [Ac-CLGGQKC(pS)VIRDSL-amide] was conjugated to keyhole limpet hemocyanin and used to immunize rabbits. Antiserum was subjected to double affinity purification using both the antigenic phospho-peptide and the same peptide without the phosphate on Ser^{71} (New England Peptide, Inc., United States).

Cell Culture

All cell lines were purchased from ATCC with the exception of MDA-MB-231 cells stably expressing a tri-modal reporter fusion used to inject NOD/SCID mice as previously described (Diamond et al., 2015). All cell lines were authenticated and tested for mycoplasma within 3 months prior to the experiments. MDA-MB-231, MCF-7, and BT-549 were grown in RPM1 1,640 containing 5 or 10% fetal bovine serum (FBS) with gentamicin and supplements (50 μg/mL gentamycin, 1mM sodium pyruvate, 10 mM HEPES and glucose to 4.5 g/L). HEK293T cells were grown in high glucose DMEM supplemented with 5 or 10% fetal bovine serum and 50 μg/mL gentamicin. Transient transfection was performed using Fugene HD or Lipofectamine 2000. Lentiviruses were generated using HEK293T cells as previously described (Diamond et al., 2015).

Pull-Down Assays

To study Pfn1 interaction with actin and VASP, HEK293T cells grown in 6-well dishes were transfected with Myc-tagged or HA-tagged Pfn1 constructs (WT and mutants), lysed by RIPA buffer, and subjected to immunoprecipitation using antibodies against Myc or HA tags as described previously (Shao et al., 2008b;

Diamond et al., 2015). To affinity purify endogenous Pfn1, parental MDA-MB-231 cells were lysed and bound to PLP-conjugated agarose beads as described previously (Shao et al., 2008b; Diamond et al., 2015).

In Vitro Drug Treatment

For drug treatment in 2D cultures, MDA-MB-231 or BT-549 stable cells were seeded at 1,000 cells per well in 96-well plates or 500 cells per well in 24-well plates, and treated on the next day with vehicle or paclitaxel in quadruplicate wells. Viable cells were quantified 5–7 days later by the Alamar Blue assay (Diamond et al., 2015; Zhu et al., 2021). Briefly, they were incubated with 100ul (for 96-well) or 500ul (for 24-well) growth media containing 44 μM resazurin for 2–4 h at 37°C, and the fluorescence intensity of resorufin (converted product) in the media was measured at 540λ Ex/590λ Em on a fluorescence plate reader (Tecan Infinite M200). Relative drug effects were calculated as the percentage of live cells in drug vs. vehicle wells.

Mouse Xenografts

The animal experiment was carried out in strict accordance with the guidelines recommended for care and use of laboratory animals by the National Institutes of Health. The Animal Studies Committee at Washington University (St. Louis, MO, United States) approved all animal protocols. Five-week old female NOD/SCID and NU/NU mice were purchased from Charles River and kept under standard institutional care. Experimental details for orthotopically inoculating MDA-MB-231 stable cells were previously described (Diamond et al., 2015; Zhu et al., 2021). For paclitaxel dosing, when tumors in the NU/NU mice reached an average of ∼70 mm^3, they were randomly divided and treated with 0.9% sodium chloride or paclitaxel (10 mg/kg) by weekly intraperitoneal injection for two consecutive weeks. Clinical grade paclitaxel (6 mg/ml) was purchased from Siteman Cancer Center pharmacy at Washington University School of Medicine. Primary tumors were measured by Caliper on a weekly (for NOD/SCID) and semiweekly (NU/NU) basis until tumor resection and euthanasia of the mice.

Statistical Analysis

Unpaired two-tailed student *t*-test was used to determine the statistical significance of the differences in cell growth rates, tumor sizes and weights between control and experimental groups. All statistical analyses were performed using GraphPad Prism 7.0. *P*-values < 0.05 were considered significant.

RESULTS

Ser^{71} Phosphorylation Abolishes Actin-Binding of Pfn1

Hypothesizing that actin-binding of Pfn1 can be inhibited by phosphorylation, we selected five candidate serine/threonine residues at the actin-binding region of Pfn1 guided by the actin/Pfn1 co-crystal structure (**Figure 1A**; Ferron et al., 2007). Each residue was mutated to alanine (S/A) or aspartate (S/D) to prevent or mimic phosphorylation. The resulting Myc-tagged Pfn1 mutants were transfected into HEK293T cells and immunoprecipitated using an anti-Myc antibody followed by Western blot to determine their actin-binding. All mutants were successfully expressed except T89D which was likely due to a destabilizing effect on Pfn1 structure and its consequent degradation. Out of the five candidate residues, Ser^{71} appears to be a bona fide phosphorylation site as preventing (S71A) and mimicking (S71D) phosphorylation had opposite effects on actin-binding of Pfn1. While Pfn1(S71A) binds more actin than Pfn1(WT), Pfn1(S71D) completely fails to bind actin (**Figure 1B**). Introducing the S71A and S71D mutations into an HA-tagged Pfn1 showed the same effects on actin-binding as for Myc-Pfn1, but neither mutation had detectable effect on Pfn1 interaction with vasodilator-stimulated phosphoprotein (VASP), a well-known PLP-containing ligand of Pfn1 (Reinhard et al., 1995; Kang et al., 1997; Ferron et al., 2007; **Figure 1C**).

A search at PhosphoSitePlus revealed that Ser^{71} phosphorylation of Pfn1 has been detected in several unbiased mass spectrometry datasets (Klammer et al., 2012; Mertins et al., 2013, 2016). To confirm this, we developed a polyclonal antibody

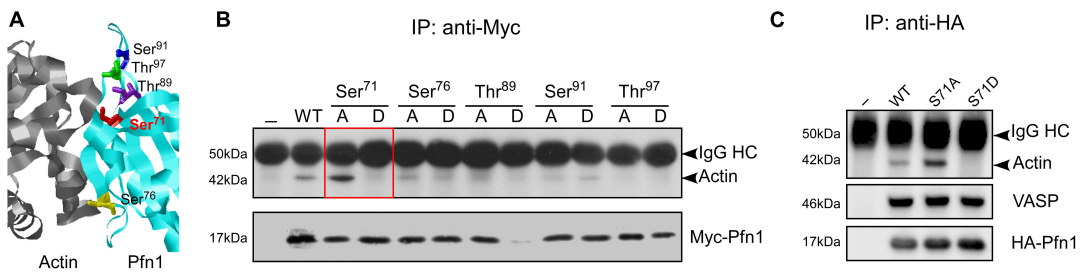

FIGURE 1 | Mimicking Ser^{71} phosphorylation by the S71D mutation abolishes actin-binding of Pfn1. **(A)** X-ray diffraction structure of human Pfn1 (right, cyan) bound with actin (left, purple) (Protein Data Bank ID 2PAV) (Ferron et al., 2007). Ser^{71} and four other serine and threonine residues in the actin-binding region of Pfn1 are displayed in the sticks mode. **(B)** HEK293T cells were transfected with Myc-tagged wild type or mutant Pfn1 containing alanine (A) or aspartate (D) substitutions on the five candidate serine or threonine residues. Lysates were subjected to immunoprecipitation using a Myc-tag antibody, and Western blot was used to detect Myc-Pfn1 and co-precipitated actin. **(C)** HEK293T cells were transfected with wild type or mutant forms of HA-tagged Pfn1 containing S71A or S71D, which were subsequently immunoprecipitated by an anti-HA tag antibody. Lysates were subjected to immunoprecipitation, and samples were blotted for actin, VASP, and HA-tag (to visualize HA-Pfn1).

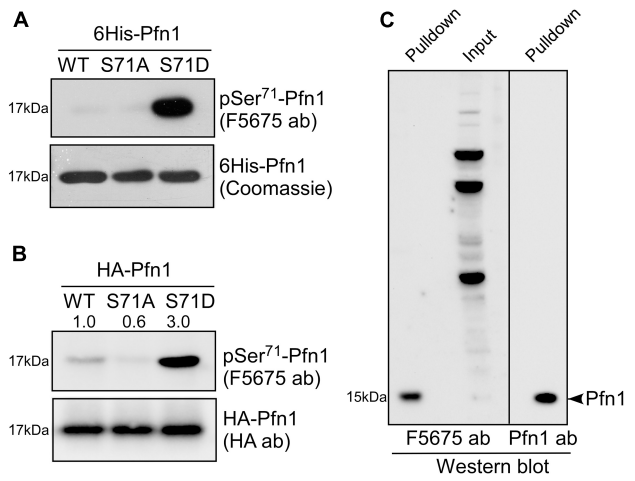

FIGURE 2 | Pfn1 is phosphorylated at Ser^{71} in cultured cells. **(A)** Equal amounts of recombinant 6His-Pfn1 (WT, S71A, or S71) purified from bacteria was stained by Coomassie blue or analyzed by Western blot using the pSer^{71}-Pfn1 antibody F5675. **(B)** HA-tagged Pfn1 (WT, S71A, or S71D) was transfected into HEK293 cells and immunoprecipitated using an anti-HA antibody. Samples were analyzed by Western blot using the pSer^{71}-Pfn1 antibody (F5675) or the anti-HA antibody. Densitometry was used to quantify the intensity of bands detected by F5675 and expressed as relative values to HA-Pfn1(WT). **(C)** Endogenous Pfn1 was purified from MDA-MB-231 cell lysates using poly-L-proline (PLP)-conjugated agarose beads, and subjected to Western blot analysis using the pSer^{71}-Pfn1 antibody (F5675) or a pan anti-Pfn1 antibody. Input was also blotted with the pSer^{71}-Pfn1 antibody (F5675) for comparison.

named F5675 using an antigenic Pfn1 peptide harboring pSer^{71}. Using recombinant 6His-Pfn1 purified from bacteria (where serines/threonines are largely unphosphorylated), we observed by Western blot little detection of Pfn1(WT) and the phospho-resistant Pfn1(S71A) but robust detection of the phosphomimetic Pfn1(S71D) by F5675 (**Figure 2A**). Though chemically different from phospho-serines, phosphomimetic amino acids such as aspartate (D) or glutamate (E) have been reported by us and others to react with phospho-antibodies raised against different proteins (Shao et al., 2008b; Shu et al., 2008). This thus supports the phospho-specificity of the pSer^{71}-Pfn1 antibody. Consistent with this, HA-Pfn1 immunoprecipitated from HEK293T cells was positively detected by the pSer^{71}-Pfn1 antibody, and the signal was significantly reduced by the S71A mutation while enhanced by S71D (**Figure 2B**). However, we could not readily detect endogenous Pfn1 within whole cell lysates using the pSer^{71}-Pfn1 antibody because it recognizes many other proteins due to its non-specific, polyclonal nature (**Figure 2C**, input, second lane). To overcome this, we used PLP-conjugated agarose beads to purify and enrich endogenous Pfn1 from the triple-negative breast cancer MDA-MB-231 cell line. This resulted in clear detection of endogenous Pfn1 by the pSer^{71}-Pfn1 antibody (**Figure 2C**, first lane), as confirmed by the side-by-side blotting with a pan Pfn1 antibody (third lane). Thus, our data suggest that Pfn1 is phosphorylated on Ser^{71} in mammalian cells.

Ser^{71} Is Phosphorylated by Protein Kinase A

By comparing Pfn1 and Pfn2 (a functionally related isoform) (Haarer and Brown, 1990; Witke, 2004; Jockusch et al., 2007; Birbach, 2008) sequences from various species, we find that Ser^{71} is evolutionarily conserved in vertebrates (a chemically similar threonine is present in zebrafish Pfn1) (**Figure 3A**). Ser^{71} is invariably preceded at −2 position by a basic residue (most commonly Arg), suggesting that it could be phosphorylated by the AGC kinase family (Pearce et al., 2010). A closer examination of the sequence surrounding Ser^{71} and comparing it with the phosphorylation consensus sites of common AGC kinases at Human Protein Kinase Knowledgebase revealed that cAMP-dependent protein kinase [also known as protein kinase A (PKA)] is a possibility. The preferred amino acids at +1 and +2 positions for PKA substrates are hydrophobic (F, I, L, and V) while those for +5 and +6 positions are leucine. The Ser^{71}-containing motif in Pfn1 meets all these requirements in particular a perfect match at +5/+6 positions. To test whether PKA is indeed the kinase for Ser^{71}, we co-transfected HEK293T cells with GFP or GFP-tagged alpha catalytic subunit of PKA with HA-Pfn1, and examined the level of Ser^{71} phosphorylation by Western blot after anti-HA immunoprecipitation. While equal amount of HA-Pfn1 was pulled down, co-transfection with GPKA significantly increased its pSer^{71} level detected by the F5675 antibody (**Figure 3B**). We next treated HEK293T cells co-transfected with HA-Pfn1 and GPKA with DMSO or PKA-specific inhibitor H89, and performed the same anti-HA immunoprecipitation and Western blot analyses. H89 significantly decreased pSer^{71}-Pfn1 level without affecting the total level of HA-Pfn1 (**Figure 3C**). To confirm that Ser^{71}, as opposed to other PKA phosphorylation sites in Pfn1, is detected by the F5675 antibody, we performed the same co-transfection experiment using either wild type or S71A mutant form of HA-Pfn1 with GFP or GPKA. We observed no GPKA-induced increase in the detection of HA-Pfn1(S71A) by the pSer^{71}-Pfn1 antibody in contrast to HA-Pfn1(WT) (**Figure 3D**). As a separate control, mutating Ser^{137} to alanine (S137A) did not affect the ability of GPKA to increase the detection of HA-Pfn1 by the F5675 antibody (**Figure 3E**). Taken together, our data suggest that Ser^{71} is the site of PKA-dependent phosphorylation of Pfn1.

Antitumor Activity of Pfn1 Requires Reversible Ser^{71} Phosphorylation and Dephosphorylation

Pfn1 overexpression inhibits the growth of various cancer cell lines *in vitro* and *in vivo* (Janke et al., 2000; Wittenmayer et al., 2004; Wu et al., 2006; Zou et al., 2007, 2010; Das et al., 2009; Yao et al., 2014). We have previously demonstrated that the antitumor effect of Pfn1 requires its PLP-binding ability which is inhibited by Ser^{137} phosphorylation (Diamond et al., 2015). To determine the effect of Ser^{71} phosphorylation, we virally expressed untagged wild type Pfn1 and its S71A or S71D mutants in the MDA-MB-231 breast cancer cells at levels 2–3-folds over endogenous Pfn1 (**Figure 4A**). GUS, a reporter gene encoding bacterial β-glucuronidase, was expressed as the negative

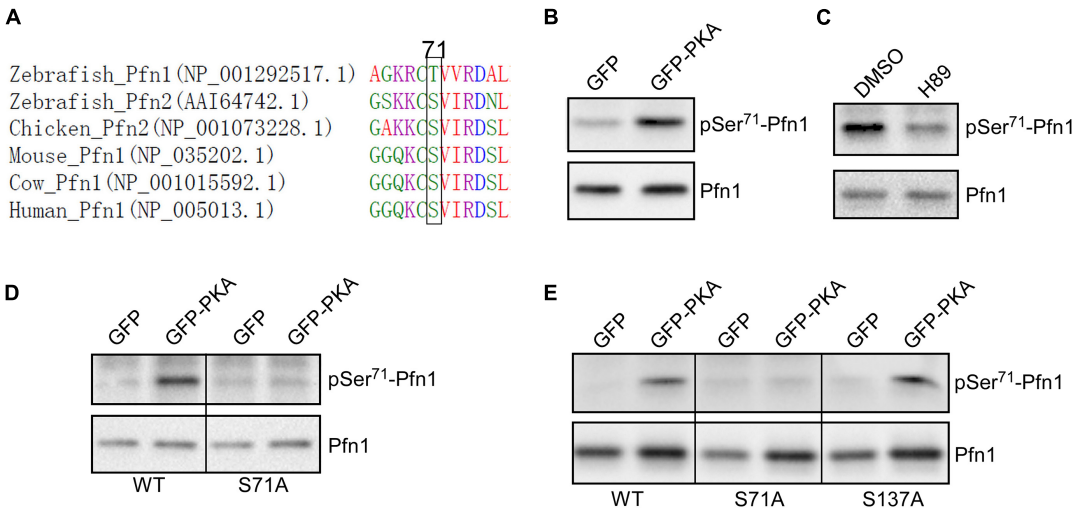

FIGURE 3 | Pfn1 is phosphorylated at Ser^{71} by protein kinase A (PKA). **(A)** sequence alignment of Pfn1 and Pfn2 proteins from multiple vertebrate organisms shows that a phosphorylatable serine or threonine residue is highly conserved at position 71. **(B)** HEK293T cells were co-transfected with HA-tagged Pfn1 with GFP or GFP-PKA, followed by anti-HA immunoprecipitation. Pulldown samples were blotted using the pSer^{71}-Pfn1 or pan Pfn1 antibodies. **(C)** HEK293T cells were transfected with HA-Pfn1 followed by the treatment with DMSO or 10 μM H89 for 24 h. HA-Pfn1 was subsequently immunoprecipitated and blotted as in **(B)**. **(D)** HEK293T cells were co-transfected with HA-Pfn1(WT) or HA-Pfn1(S71A) with GFP or GFP-PKA, followed by immunoprecipitation and Western blot analysis as in **(B, C)**. **(E)** HEK293T cells were co-transfected with wild type or mutant HA-Pfn1 (S71A or S137A) with GFP or GFP-PKA, followed by immunoprecipitation and Western blot analysis as in **(B–D)**.

control as previously described (Diamond et al., 2015). We first compared the cell proliferation rates *in vitro* by Alamar blue assay. While Pfn1(WT) showed anti-proliferative effect as observed previously, both Pfn1(S71A) and Pfn1(S71D) mutants were inactive (**Figure 4B**). We next determined the *in vivo* effects by injecting the same stable cells orthotopically in the mammary fat pads of female NOD/SCID mice as previously described (Diamond et al., 2015). Caliper measurements showed that both S71A and S71D mutations abolish the antitumor effect of Pfn1 and caused an additional increase in tumor growth compared to the GUS control (**Figure 4C**). End-point tumor weights confirmed these effects (**Figure 4D**). Thus, unlike the toggling effect of Ser^{137} phosphorylation, tumor inhibition by Pfn1 appears to require reversible Ser^{71} phosphorylation and dephosphorylation.

Ser^{71} Phosphorylation Inhibits the Apoptosis-Sensitizing Activity of Pfn1 in Response to Paclitaxel

In addition to suppressing proliferation, Pfn1 also sensitizes cancer cells to apoptosis induced by cytotoxic agents (Zou et al., 2010; Yao et al., 2013; Zaidi et al., 2016). When transfecting MDA-MB-231 cells using lipofectamine (which is cytotoxic), we consistently observed higher number of surviving cells expressing Pfn1(S71D) than those expressing Pfn1(WT) and Pfn1(S71A) (**Supplementary Figure 1A**). A similar effect was also observed in the transfected MCF-7 cells (**Supplementary Figure 1B**). Hypothesizing that Ser^{71} phosphorylation may be a pro-survival event by inhibiting the pro-apoptotic activity of Pfn1, we treated the stable MDA-MB-231 cells with paclitaxel, a commonly used chemotherapy agent which was reported to cause apoptosis in breast cancer cells more effectively upon Pfn1 overexpression (Zaidi et al., 2016). Indeed, we detected significantly decreased viability of Pfn1(WT)-expressing cells compared to the control cells. While Pfn1(S71A) showed a similar drug-sensitizing effect as Pfn1(WT), Pfn1(S71D) was completely inactive (**Figure 5A**). Western blot for cleaved caspase-7 confirmed the pro-apoptotic effect of Pfn1(WT) and Pfn1(S71A) but not Pfn1(S71D) upon paclitaxel treatment (**Figure 5B**). Similar results were also observed in MDA-MB-231 stable cells treated with doxorubicin and staurosporine (**Supplementary Figure 1C,D**), two other cytotoxic agents whose apoptosis-inducing abilities can be augmented by Pfn1 overexpression (Yao et al., 2013; Zaidi et al., 2016).

To confirm the toggling effect of Ser^{71} phosphorylation of Pfn1 on chemotherapy-induced apoptosis *in vivo*, we inoculated the MDA-MB-231 stable cells expressing Pfn1(S71A) vs. Pfn1(S71D) in the mammary fat pads of female nude mice. Tumors formed by both cell lines grew at similar rates as observed in the NOD/SCID mice. When the average tumor volumes in both groups reached ∼70 mm^3, mice were randomly divided into two subgroups (n = 5 per group) which were treated with vehicle or paclitaxel (10 mg/kg, weekly intraperitoneal injection) for 2 weeks. Semiweekly Caliper measurement showed an obvious tumor-regressing effect of paclitaxel in the Pfn1(S71A) group, with the tumor volume difference between the vehicle and paclitaxel groups being statistically significant at the last two time points (**Figure 5C**). In contrast, tumors in the Pfn1(S71D) group responded much less to paclitaxel and no statistically significant difference in tumor volumes between vehicle and drug groups was detected.

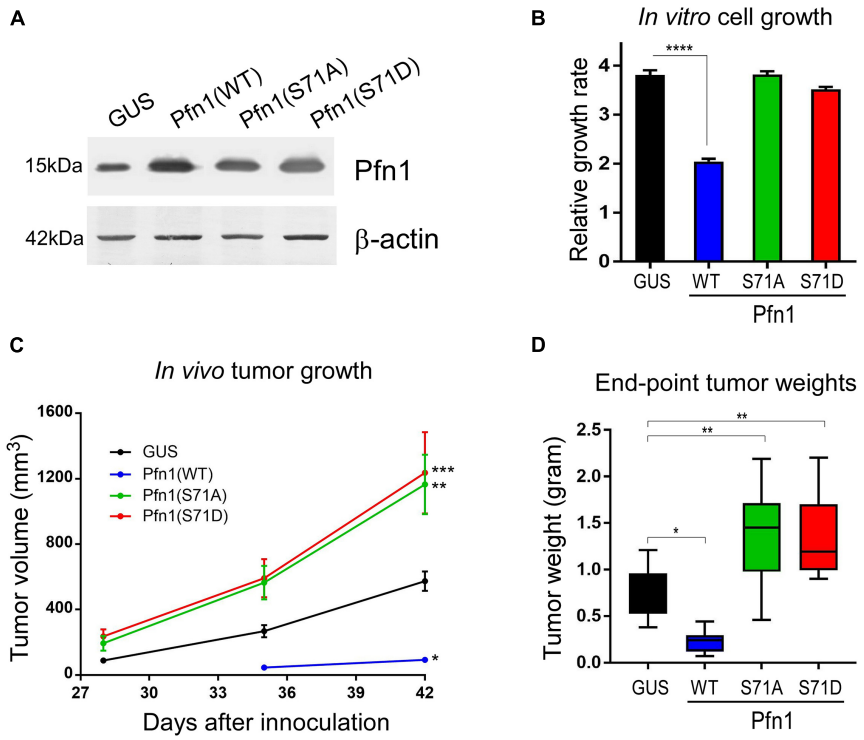

FIGURE 4 | Preventing and mimicking Ser^{71} phosphorylation similarly abolish the antitumor activity of Pfn1. **(A)** Western blot analysis of exogenous wild type and mutant Pfn1 expression in stable MDA-MB-231 cells using a pan Pfn1 antibody, controlled by actin. **(B)** Stable MDA-MB-231 cells from A were seeded in 96-well plates and grown for 7 days. Relative growth rates were calculated by normalizing Alamar blue values of each subline at Day 7 to those at Day 1. Data are mean ± SEM of four technical replicates in one experiment. *P*-values were based on two-tailed unpaired *t*-test. Same results were confirmed by more than three independent experiments. **(C)** Stable MDA-MB-231 cells were injected bilaterally into the 4th mammary fat pads of 5-week-old female NOD/SCID mice (10^6 cells per side, five mice per group). Caliper measurement of tumor volumes started at 4 weeks after injection. Data are the mean ± SEM of 10 tumors within each group. *P*-values were based on two-tailed unpaired *t*-test (versus GUS control) at day 42. **(D)** End-point tumor weights. Data are the mean ± SEM. *P*-values were based on two-tailed unpaired *t*-test (versus GUS control). $^*p < 0.05$; $^{**}p < 0.01$; $^{***}p < 0.001$, $^{****}p < 0.0001$. GUS and Pfn1(WT) tumor values were published in our prior study (Diamond et al., 2015) as they were the same controls for Pfn1(S137A vs. S137D) (published) and Pfn1(S71A vs. S71D) (shown here, unpublished) in the same mouse xenograft experiment.

Western blot using tumor lysates showed significantly higher levels of cleaved caspase-7 in the paclitaxel-treated Pfn1(S71A) tumors than the Pfn1(S71D) tumors (**Figure 5D**). Interestingly, baseline cleaved caspase-7 levels in untreated tumors, though much lower than in paclitaxel-treated tumors, were also higher in the Pfn1(S71A) vs. Pfn1(S71D) tumors. Collectively, these data suggest that Ser^{71} phosphorylation, by blocking actin-binding of Pfn1, abolishes the apoptosis-sensitizing activity of Pfn1 particularly in response to chemotherapy agents such as paclitaxel.

Apoptotic Sensitization by Pfn1 Rrequires Actin-Binding and Cytoplasmic Localization

The ability of Pfn1 to bind actin is crucial for its nuclear export by exportin-6 (Stuven et al., 2003). Since Ser^{71} phosphorylation disrupts actin-binding of Pfn1, we examined its effect on Pfn1 subcellular localization. Upon transfection into HEK293T cells, YFP-tagged Pfn1(WT) and Pfn1(S71A) were predominantly localized in the cytoplasm. However, YFP-Pfn1(S71D) was diffusely present within cytoplasm and nucleus (**Figure 2A**). We observed the same phenotype using lentivirus-infected MDA-MB-231 cells (**Figure 6A**). The opposite effects of S71A vs. S71D mutations on cell survival upon paclitaxel treatment were observed in the context of YFP-Pfn1 similar to untagged Pfn1 (**Supplementary Figure 2B**). Intrigued by the effects of Ser^{71} phosphorylation on both Pfn1 subcellular localization and chemo-sensitizing activity, we tested whether these two phenotypes are causally linked. To do that, we forced YFP-Pfn1 expression either in the cytoplasm or nucleus by tagging it with a nuclear export sequence (NES, recognized by exportin-1) or nuclear localization sequence (NLS) as previously described (Diamond et al., 2015; Zhu et al., 2021). We virally introduced YFP, YFP-NES-Pfn1, or YFP-NLS-Pfn1 into MDA-MB-231 cells and determined their relative responses to paclitaxel treatment. Compared to YFP control cells, YFP-NES-Pfn1 cells showed higher sensitivity to paclitaxel treatment while YFP-NLS-Pfn1 cells showed less (**Figure 6B**). These opposite effects on cellular survival by YFP-NES-Pfn1 and YFP-NLS-Pfn1 were also observed in BT-549 cells, another triple-negative breast cancer cell line (**Figure 6B**).

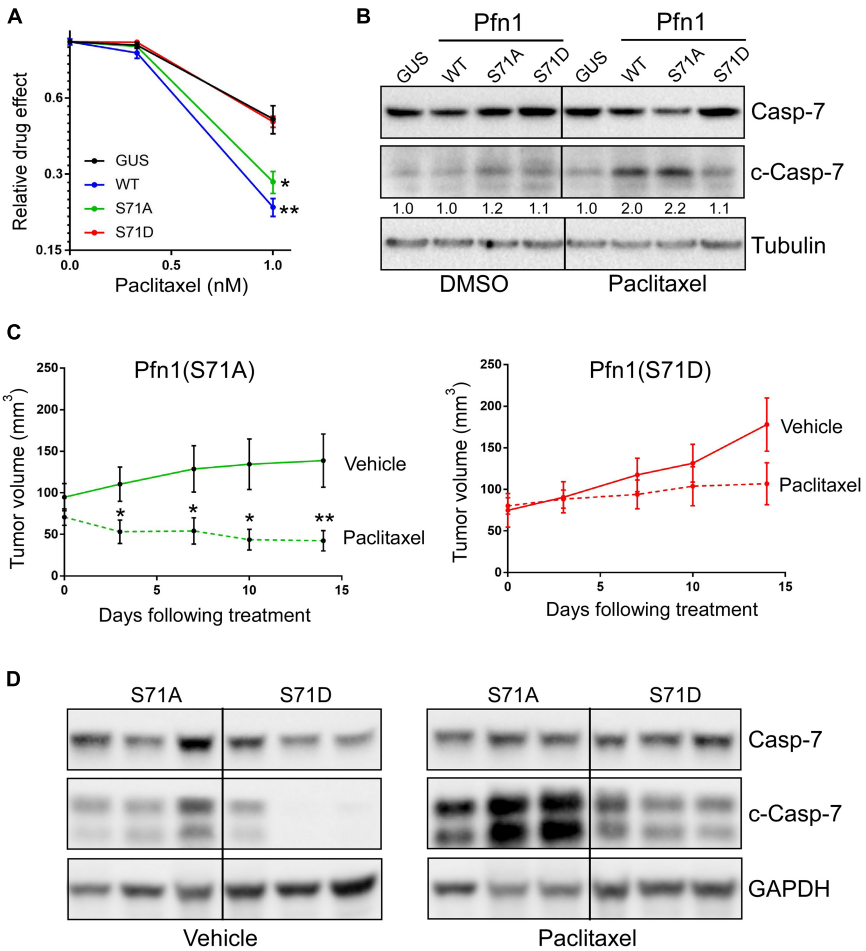

FIGURE 5 | Ser^{71} phosphorylation abolishes the pro-apoptotic activity of Pfn1 in response to paclitaxel. **(A)** Stable MDA-MB-231 cells were seeded in 96-well plates and treated with DMSO or paclitaxel for 7 days. Relative drug effects were calculated by normalizing Alamar blue values of drug-treated cells by DMSO-treated cells. Data are mean ± SEM of four technical replicates in one experiment. Similar results were observed in three independent experiments. *P*-values were based on two-tailed unpaired *t*-test (versus GUS control). **(B)** Stable MDA-MB-231 cells were treated with DMSO or 5 nM paclitaxel for 48 h, followed by Western blot analysis for full-length or cleaved caspase-7 or tubulin. Cleaved caspase-7 levels were quantified by densitometry and normalized by the levels in GUS control cells in DMSO or paclitaxel groups. **(C)** MDA-MB-231 stable cells expressing Pfn1(S71A) or Pfn1(S71D) were injected bilaterally into the 4th mammary fat pads of female nude mice (10 mice per group). Tumor-bearing mice were evenly divided and treated with vehicle (0.9% sodium chloride) or paclitaxel (10 mg/kg) by intraperitoneal injection for 2 weeks. Tumor volumes were measured semiweekly by Caliper. Data are mean ± SEM. *P*-values were based on two-tailed unpaired *t*-test between vehicle and paclitaxel treatment groups at individual time points. *$p < 0.05$; **$p < 0.01$. **(D)** Randomly selected tumors harvested from vehicle or paclitaxel-treated mice in **(C)** were blotted for full-length or cleaved caspase-7 and GAPDH. Each tumor was from a different mouse.

Next, we examined whether the drug-sensitizing effect of NES-Pfn1 is still under the regulation of Ser^{71} phosphorylation by introducing the S71A vs. S71D mutations (**Supplementary Figure 2C**). Indeed, MDA-MB-231 and BT-549 cells expressing NES-Pfn1(S71D) showed significantly higher resistance to paclitaxel treatment than those expressing NES-Pfn1(S71A) in colony formation assays (**Figure 6C**). Western blot against cleaved caspase-7 and cleaved PARP confirmed that paclitaxel-induced apoptosis in NES-Pfn1(S71D)-expressing cells was indeed significantly lower than in NES-Pfn1(S71A)-expressing cells (**Figure 6D**).

The pro-apoptotic activity of Pfn1 has been causally linked to its ability to increase p53 and IκBα (negative regulator of NFκB) levels in breast cancer cell lines (Yao et al., 2013; Zaidi and Manna, 2016; Zaidi et al., 2016). We found that MDA-MB-231 stable cells expressing untagged Pfn1(S71D) contain significantly lower levels of IκBα than those expressing Pfn1(S71A) (**Figure 6E**). The difference in IκBα levels between MDA-MB-231 cells expressing NES-Pfn1(S71A) and NES-Pfn1(S71D) can also be seen but to a lesser extent (**Figure 6E**). Interestingly, p53 levels did not differ significantly between Pfn1(S71A) and Pfn1(S71D) cells regardless of whether Pfn1 is untagged or NES-tagged (**Figure 6E**). Collectively, our data suggest that cytoplasmic Pfn1 promotes apoptosis in response to cytotoxic treatments and such an activity is abolished by Ser^{71} phosphorylation via abolishing actin-binding of Pfn1 as well as causing its nuclear retention, both of which contribute to IκBα destabilization and increased NFκB signaling.

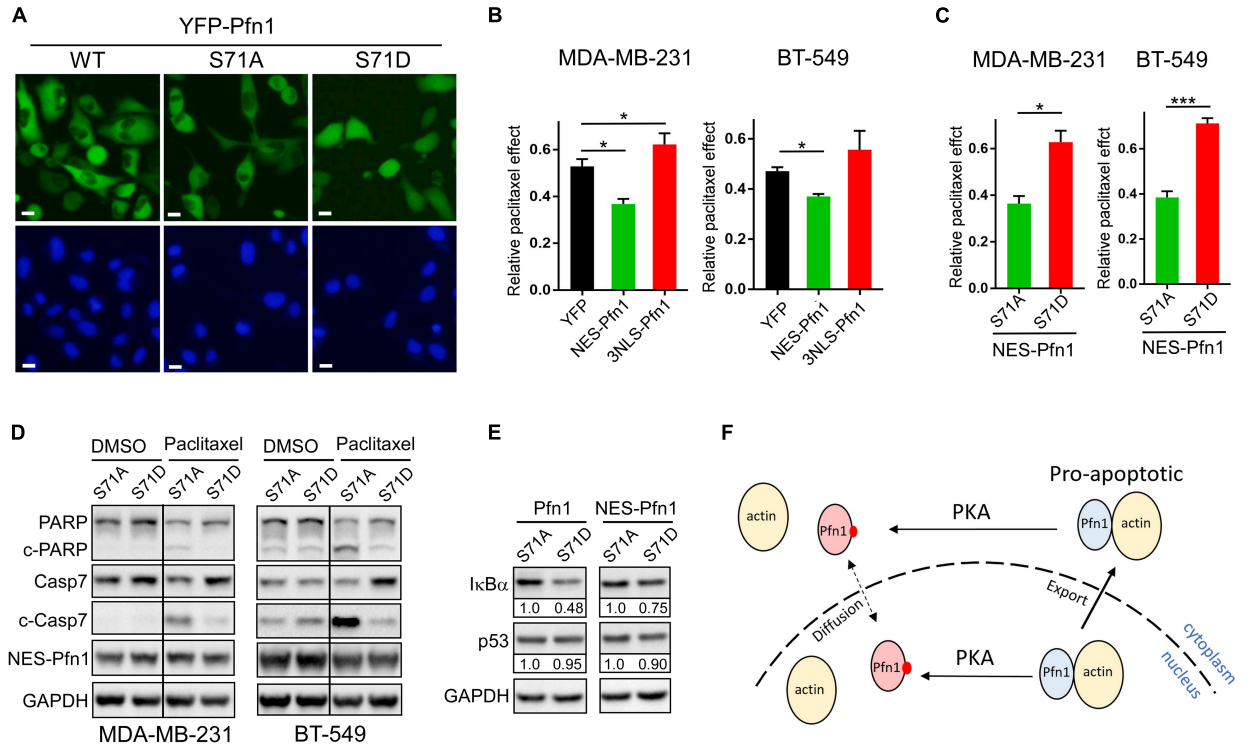

FIGURE 6 | Apoptotic sensitization by Pfn1 requires actin-binding and cytoplasmic localization. **(A)** Direct fluorescence imaging of MDA-MB-231 stably infected with wild type or mutant YFP-Pfn1. Scale bars represent 20 μm. **(B)** Stable MDA-MB-231 and BT-549 cells expressing YFP, NES-Pfn1, or NLS-Pfn1 were subjected to colony formation assays in 24-well plates with vehicle (DMSO) or 0.5 nM paclitaxel for 7 days. Relative drug effects were calculated as the ratios between cell numbers (based on Alamar blue values) in the paclitaxel-treated vs. vehicle conditions. **(C)** Stable MDA-MB-231 and BT-549 cells expressing NES-Pfn1(S71A) or NES-Pfn1(S71D) were treated with vehicle or paclitaxel in colony formation assays and analyzed as in **(B)**. Data are mean ± SEM of three technical replicates in one biological experiment. Similar results were observed in three independent experiments. *P*-values were based on two-tailed unpaired *t*-test. $^{*}p < 0.05$; $^{***}p < 0.001$. **(D)** MDA-MB-231 and BT-549 stable cells expressing NES-Pfn1(S71A) or NES-Pfn1(S71D) were treated with DMSO or 5 nM paclitaxel for 48 h, and analyzed for full-length or cleaved PARP and caspase-7, YFP-NES-Pfn1 (with GFP ab) and GAPDH by Western blot. **(E)** MDA-MB-231 stable cells expressing untagged or NES-tagged Pfn1(S71A) vs. Pfn1(S71D) were treated with 10 nM paclitaxel for 48 h, and analyzed for IκBα, p53, and GAPDH by Western blot. **(F)** Hypothetical model for the pro-apoptotic activity of cytoplasmic Pfn1 which requires actin-binding and is abolished by PKA-dependent Ser^{71} phosphorylation. Ser^{71} may also be phosphorylated by PKA in the nucleus. Actin-free pSer^{71}-Pfn1, due to its small size, can freely diffuse in and out of nucleus. However, nuclear pSer^{71}-Pfn1 cannot be actively transported into the cytoplasm by exportin-6 due to its loss of actin-binding.

DISCUSSION

Pfn1 was the first actin-binding protein identified more than four decades ago (Carlsson et al., 1977), yet it remains uncertain to this day whether its actin-binding ability undergoes negative regulation by post-translational modifications. In this paper, through candidate mutagenesis and validation using public proteomic data and a custom-made phospho-specific antibody, we provided evidence that the evolutionarily conserved Ser^{71} is a *bona fide* phosphorylation site in Pfn1 selectively inhibiting its actin-binding with little effect on its PLP-binding. This is consistent with the fact that Ser^{71} is located within the actin-binding site of Pfn1 and distal to its PLP-binding pocket (Ferron et al., 2007). Sequence analysis combined with genetic and pharmacological testing suggested that PKA may be one of the kinases phosphorylating Ser^{71}. Interestingly, it was recently suggested that PKA can also phosphorylate Ser^{137} of Pfn1 (Gau et al., 2019), a shared target site for PKC and ROCK which specifically inhibits Pfn1 interaction with PLPs (Singh et al., 1996; Sathish et al., 2004; Shao et al., 2008a). Nonetheless, based on co-immunoprecipitation data using HA-Pfn1-transfected HEK293T cells, the stoichiometry of PKA-mediated Ser^{71} phosphorylation of total cellular pool of Pfn1 appeared low, as overexpression of the alpha catalytic subunit of PKA did not cause detectable reduction in the levels of associated actin (data not shown), despite increasing Ser^{71} phosphorylation levels. This could be due to several possible reasons. First, PKA-mediated Ser^{71} phosphorylation may occur to a small fraction of total cellular Pfn1 either transiently or at specific subcellular locations. Given the high cellular abundance of Pfn1 (>50 μM in most tissues) (Witke, 2004), the net effect on steady-state actin-binding would not be detectable by co-IP using whole cell lysates. Second, PKA activity is regulated by complex mechanisms including inhibitory binding of the regulatory subunits as well as tethering to specific subcellular locations via the diverse A-kinase-anchoring proteins (AKAP) (Francis and Corbin, 1994; Harada et al., 1999). Therefore, it is possible that overexpressing the catalytic subunit of PKA alone is insufficient to achieve

optimal Pfn1 phosphorylation. In either case, more molecular details regarding the newly identified PKA/pSer^{71}-Pfn1 axis and the possible involvement of other kinases remain to be determined in the future.

Despite being an essential actin-binding protein, Pfn1 simultaneously functions as a non-classical tumor suppressor across different malignancies including breast (Roy and Jacobson, 2004; Wittenmayer et al., 2004; Zou et al., 2007, 2009, 2010; Bae et al., 2009, 2010; Das et al., 2009; Diamond et al., 2015), pancreatic (Yao et al., 2014), and liver (Wu et al., 2006) cancers. Its ability to inhibit cell cycle progression and tumor cell growth has been demonstrated by many *in vitro* and *in vivo* studies. Our recent work suggested that tumor growth inhibition by Pfn1 is mediated at least in part by its nuclear function in repressing SEC-dependent transcription of pro-cancer genes including c-MYC (Diamond et al., 2015; Zhu et al., 2021). Such an activity can be toggled off and on by Ser^{137} phosphorylation and dephosphorylation (mimicked by S137D and S137A) which, respectively, blocks and enables Pfn1 binding to PLPs that are present in the SEC component ENL (Diamond et al., 2015; Zhu et al., 2021). In this paper, by analyzing the effects of pSer^{71}-resistant and mimetic mutants (S71A and S71D) in MDA-MB-231 cells, we made the unexpected observation that both cannot inhibit tumor growth. This indicates that, rather than functioning as an on/off switch, reversible phosphorylation and dephosphorylation at Ser^{71}, causing dynamic actin dissociation and rebinding, are required for Pfn1 to inhibit tumor growth. Given that actin-binding promotes nuclear export of Pfn1 (Stuven et al., 2003), this raises an interesting possibility that Ser^{71} phosphorylation may occur in a transient and tightly controlled manner to nuclear Pfn1 to allow its escape from nuclear export, which is subsequently followed by Ser^{71} dephosphorylation to render actin-rebinding by Pfn1 for its functional engagement in transcriptional repression. Though speculative at the moment, this theory is consistent with our current knowledge regarding Pfn1 functions and can be tested in the future.

In addition to suppressing tumor growth, Pfn1 also sensitizes cancer cells to drug-induced apoptosis. This has been best demonstrated in breast cancer cells treated with cytotoxic agents many of which are common cancer chemotherapies including paclitaxel (Zou et al., 2010; Yao et al., 2013; Zaidi et al., 2016). Although detailed molecular mechanisms underlying apoptosis-sensitization by Pfn1 remain unknown, such an activity has been linked to p53 and NFκB signaling. It was found that Pfn1 and p53 co-exist in the same complex in breast cancer cells, and Pfn1 overexpression increases total p53 protein levels as well as its redistribution to cytoplasm and mitochondria (Yao et al., 2013; Zaidi et al., 2016) where p53 can drive intrinsic apoptotic pathway in a transcription-independent fashion (Marchenko et al., 2000; Chipuk et al., 2004). In support of the functional link between Pfn1 and p53, apoptosis-sensitizing effect of Pfn1 was greatly reduced in p53-null and knockdown cells (Yao et al., 2013; Zaidi et al., 2016). In addition to enhancing p53 activity, Pfn1 was also found to decrease NFκB signaling by preventing cytotoxin-induced IκBα phosphorylation and degradation and consequently preventing p65 nuclear translocation and transcription of pro-survival genes (Zaidi and Manna, 2016; Zaidi et al., 2016). Although these studies implicate the involvement of cytoplasmic Pfn1 in apoptotic sensitization, direct evidence was unavailable. In this study, by tagging Pfn1 with NES or NLS, we showed that apoptotic sensitization by Pfn1 indeed requires its cytoplasmic localization. Interestingly, such an activity of Pfn1 can be switched off and on by pSer^{71}-Pfn1 mimicking and preventing mutants both *in vitro* and *in vivo*, indicating an essential role of actin-binding. Our data suggested that pSer^{71}-Pfn1 could be a novel predictive biomarker for cancer chemotherapy response. They are also consistent with the well-known pro-survival effects of PKA, which have been mechanistically linked to activating phosphorylation of the cAMP-response element binding protein (CREB) in the nucleus (Wilson et al., 1996; De Cesare and Sassone-Corsi, 2000; Mayr and Montminy, 2001; Naqvi et al., 2014) and deactivating phosphorylation of the pro-apoptotic protein Bad in the cytoplasm (Harada et al., 1999; Lizcano et al., 2000). Thus, Pfn1 may be a previously unknown downstream effector of PKA function in apoptotic inhibition through Ser^{71} phosphorylation. Given that Ser^{71} phosphorylation prevents nuclear Pfn1 export, we speculate that it may inhibit the apoptosis-sensitizing effect of Pfn1 via a two-pronged mechanism by abolishing its actin-binding and reducing its cytoplasmic levels (**Figure 6F**). Taken together, our data in this paper demonstrated that Ser^{71} is a *bona fide* phosphorylation site of Pfn1 capable of inhibiting its actin-binding ability, preventing its nuclear export, and influencing its tumor-inhibitory functions.

DATA AVAILABILITY STATEMENT

The raw data supporting the conclusions of this article will be made available by the authors, without undue reservation.

ETHICS STATEMENT

The animal study was reviewed and approved by The Animal Studies Committee at Washington University in St. Louis.

AUTHOR CONTRIBUTIONS

JS conceived of the project and wrote the manuscript with input from all authors. JS, FW, CZ, and S-JK performed the experiments. JS, FW, CZ, SC, and S-JK performed the experiments and analyzed the data. AB and MB provided technical expertise and intellectual input.

FUNDING

The Siteman Cancer Center is supported in part by an NCI Cancer Center Support Grant #P30 CA091842. This work was supported by the NIH/NCI R01CA181671 (JS), the Susan G. Komen Foundation Career Catalyst Research Grant (JS), American Cancer Society Institutional Research Grant (JS),

United States Department of Defense Innovator Expansion Award (W81XWH0810736) (MB), Breast Cancer Research Foundation (BCRF) (MB), and the NIH/NCI R01CA064786 (MB). FW was supported by the National Natural Science Foundation of China (81801939).

ACKNOWLEDGMENTS

We thank Byron Hann for the MDA-MB-231 cell line stably expressing the tri-modal reporter fusion, Eric Campeau for the pLenti-CMV/TO-Neo-DEST (685–3) destination vector, and Marc Diamond for scientific advice. We also thank the Alvin J. Siteman Cancer Center at Washington University School of Medicine and Barnes-Jewish Hospital in St. Louis, MO, for the use of the Siteman Flow Cytometry, which provided the cell cycle analysis service.

SUPPLEMENTARY MATERIAL

The Supplementary Material for this article can be found online at: https://www.frontiersin.org/articles/10.3389/fcell.2021.692269/full#supplementary-material

REFERENCES

Bae, Y. H., Ding, Z., Das, T., Wells, A., Gertler, F., and Roy, P. (2010). Profilin1 regulates PI(3,4)P2 and lamellipodin accumulation at the leading edge thus influencing motility of MDA-MB-231 cells. *Proc. Natl. Acad. Sci. U.S.A.* 107, 21547–21552. doi: 10.1073/pnas.1002309107

Bae, Y. H., Ding, Z., Zou, L., Wells, A., Gertler, F., and Roy, P. (2009). Loss of profilin-1 expression enhances breast cancer cell motility by Ena/VASP proteins. *J. Cell Physiol.* 219, 354–364. doi: 10.1002/jcp.21677

Balasubramanian, M. K., Hirani, B. R., Burke, J. D., and Gould, K. L. (1994). The Schizosaccharomyces pombe cdc3+ gene encodes a profilin essential for cytokinesis. *J. Cell Biol.* 125, 1289–1301. doi: 10.1083/jcb.125.6.1289

Birbach, A. (2008). Profilin, a multi-modal regulator of neuronal plasticity. *Bioessays* 30, 994–1002. doi: 10.1002/bies.20822

Bottcher, R. T., Wiesner, S., Braun, A., Wimmer, R., Berna, A., Elad, N., et al. (2009). Profilin 1 is required for abscission during late cytokinesis of chondrocytes. *Embo J.* 28, 1157–1169. doi: 10.1038/emboj.2009.58

Carlsson, L., Nystrom, L. E., Sundkvist, I., Markey, F., and Lindberg, U. (1977). Actin polymerizability is influenced by profilin, a low molecular weight protein in non-muscle cells. *J. Mol. Biol.* 115, 465–483. doi: 10.1016/0022-2836(77)90166-8

Chipuk, J. E., Kuwana, T., Bouchier-Hayes, L., Droin, N. M., Newmeyer, D. D., Schuler, M., et al. (2004). Direct activation of Bax by p53 mediates mitochondrial membrane permeabilization and apoptosis. *Science* 303, 1010–1014. doi: 10.1126/science.1092734

Das, T., Bae, Y. H., Wells, A., and Roy, P. (2009). Profilin-1 overexpression upregulates PTEN and suppresses AKT activation in breast cancer cells. *J. Cell Physiol.* 218, 436–443. doi: 10.1002/jcp.21618

De Cesare, D., and Sassone-Corsi, P. (2000). Transcriptional regulation by cyclic AMP-responsive factors. *Prog. Nucleic Acid. Res. Mol. Biol.* 64, 343–369. doi: 10.1016/s0079-6603(00)64009-6

Diamond, M. I., Cai, S., Boudreau, A., Carey, C. J. Jr., Lyle, N., Pappu, R. V., et al. (2015). Subcellular localization and Ser-137 phosphorylation regulate tumor-suppressive activity of profilin-1. *J. Biol. Chem.* 290, 9075–9086. doi: 10.1074/jbc.m114.619874

Ding, Z., Lambrechts, A., Parepally, M., and Roy, P. (2006). Silencing profilin-1 inhibits endothelial cell proliferation, migration and cord morphogenesis. *J. Cell Sci.* 119, 4127–4137. doi: 10.1242/jcs.03178

Ferron, F., Rebowski, G., Lee, S. H., and Dominguez, R. (2007). Structural basis for the recruitment of profilin-actin complexes during filament elongation by Ena/VASP. *EMBO J.* 26, 4597–4606. doi: 10.1038/sj.emboj.7601874

Francis, S. H., and Corbin, J. D. (1994). Structure and function of cyclic nucleotide-dependent protein kinases. *Annu. Rev. Physiol.* 56, 237–272. doi: 10.1146/annurev.ph.56.030194.001321

Gau, D., Veon, W., Shroff, S. G., and Roy, P. (2019). The VASP-profilin1 (Pfn1) interaction is critical for efficient cell migration and is regulated by cell-substrate adhesion in a PKA-dependent manner. *J. Biol. Chem.* 294, 6972–6985. doi: 10.1074/jbc.ra118.005255

Haarer, B. K., and Brown, S. S. (1990). Structure and function of profilin. *Cell Motil. Cytoskeleton* 17, 71–74.

Harada, H., Becknell, B., Wilm, M., Mann, M., Huang, L. J., Taylor, S. S., et al. (1999). Phosphorylation and inactivation of BAD by mitochondria-anchored protein kinase A. *Mol. Cell* 3, 413–422. doi: 10.1016/s1097-2765(00)80469-4

Janke, J., Schluter, K., Jandrig, B., Theile, M., Kolble, K., Arnold, W., et al. (2000). Suppression of tumorigenicity in breast cancer cells by the microfilament protein profilin 1. *J. Exp. Med.* 191, 1675–1686. doi: 10.1084/jem.191.10.1675

Jockusch, B. M., Murk, K., and Rothkegel, M. (2007). The profile of profilins. *Rev. Physiol. Biochem. Pharmacol.* 159, 131–149. doi: 10.1007/112_2007_704

Kang, F., Laine, R. O., Bubb, M. R., Southwick, F. S., and Purich, D. L. (1997). Profilin interacts with the Gly-Pro-Pro-Pro-Pro-Pro sequences of vasodilator-stimulated phosphoprotein (VASP): implications for actin-based Listeria motility. *Biochemistry* 36, 8384–8392. doi: 10.1021/bi970065n

Klammer, M., Kaminski, M., Zedler, A., Oppermann, F., Blencke, S., Marx, S., et al. (2012). Phosphosignature predicts dasatinib response in non-small cell lung cancer. *Mol. Cell Proteomics* 11, 651–668. doi: 10.1074/mcp.m111.016410

Lizcano, J. M., Morrice, N., and Cohen, P. (2000). Regulation of BAD by cAMP-dependent protein kinase is mediated via phosphorylation of a novel site. Ser155. *Biochem. J.* 349, 547–557. doi: 10.1042/0264-6021:3490547

Marchenko, N. D., Zaika, A., and Moll, U. M. (2000). Death signal-induced localization of p53 protein to mitochondria. A potential role in apoptotic signaling. *J. Biol. Chem.* 275, 16202–16212. doi: 10.1074/jbc.275.21.16202

Mayr, B., and Montminy, M. (2001). Transcriptional regulation by the phosphorylation-dependent factor CREB. *Nat. Rev. Mol. Cell Biol.* 2, 599–609. doi: 10.1038/35085068

Mertins, P., Mani, D. R., Ruggles, K. V., Gillette, M. A., Clauser, K. R., Wang, P., et al. (2016). Proteogenomics connects somatic mutations to signalling in breast cancer. *Nature* 534, 55–62. doi: 10.1038/nature18003

Mertins, P., Qiao, J. W., Patel, J., Udeshi, N. D., Clauser, K. R., Mani, D. R., et al. (2013). Integrated proteomic analysis of post-translational modifications by serial enrichment. *Nat. Methods* 10, 634–637. doi: 10.1038/nmeth.2518

Naqvi, S., Martin, K. J., and Arthur, J. S. (2014). CREB phosphorylation at Ser133 regulates transcription via distinct mechanisms downstream of cAMP and MAPK signalling. *Biochem. J.* 458, 469–479. doi: 10.1042/bj20131115

Pearce, L. R., Komander, D., and Alessi, D. R. (2010). The nuts and bolts of AGC protein kinases. *Nat. Rev. Mol. Cell Biol.* 11, 9–22. doi: 10.1038/nrm2822

Reinhard, M., Giehl, K., Abel, K., Haffner, C., Jarchau, T., Hoppe, V., et al. (1995). The proline-rich focal adhesion and microfilament protein VASP is a ligand for profilins. *Embo J.* 14, 1583–1589. doi: 10.1002/j.1460-2075.1995.tb07146.x

Roy, P., and Jacobson, K. (2004). Overexpression of profilin reduces the migration of invasive breast cancer cells. *Cell Motil. Cytoskeleton* 57, 84–95. doi: 10.1002/cm.10160

Sathish, K., Padma, B., Munugalavadla, V., Bhargavi, V., Radhika, K. V., Wasia, R., et al. (2004). Phosphorylation of profilin regulates its interaction with actin and poly (L-proline). *Cell Signal* 16, 589–596. doi: 10.1016/j.cellsig.2003.10.001

Schluter, K., Schleicher, M., and Jockusch, B. M. (1998). Effects of single amino acid substitutions in the actin-binding site on the biological activity of bovine profilin I. *J. Cell Sci.* 111(Pt 22), 3261–3273. doi: 10.1242/jcs.111.22.3261

Shao, J., Welch, W. J., and Diamond, M. I. (2008a). ROCK and PRK-2 mediate the inhibitory effect of Y-27632 on polyglutamine aggregation. *FEBS Lett.* 582, 1637–1642. doi: 10.1016/j.febslet.2008.04.009

Shao, J., Welch, W. J., Diprospero, N. A., and Diamond, M. I. (2008b). Phosphorylation of profilin by ROCK1 regulates polyglutamine aggregation. *Mol. Cell Biol.* 28, 5196–5208. doi: 10.1128/mcb.00079-08

Shu, Y., Liu, X., Yang, Y., Takahashi, M., and Gillis, K. D. (2008). Phosphorylation of SNAP-25 at Ser187 mediates enhancement of exocytosis by a phorbol ester in INS-1 cells. *J. Neurosci.* 28, 21–30. doi: 10.1523/jneurosci.2352-07.2008

Singh, S. S., Chauhan, A., Murakami, N., Styles, J., Elzinga, M., and Chauhan, V. P. (1996). . Phosphoinositide-dependent in vitro phosphorylation of profilin by protein kinase C. Phospholipid specificity and localization of the phosphorylation site. *Recept. Signal. Transduct.* 6, 77–86.

Stuven, T., Hartmann, E., and Gorlich, D. (2003). Exportin 6: a novel nuclear export receptor that is specific for profilin.actin complexes. *Embo J.* 22, 5928–5940. doi: 10.1093/emboj/cdg565

Verheyen, E. M., and Cooley, L. (1994). Profilin mutations disrupt multiple actin-dependent processes during *Drosophila* development. *Development* 120, 717–728. doi: 10.1242/dev.120.4.717

Wilson, B. E., Mochon, E., and Boxer, L. M. (1996). Induction of bcl-2 expression by phosphorylated CREB proteins during B-cell activation and rescue from apoptosis. *Mol. Cell Biol.* 16, 5546–5556. doi: 10.1128/mcb.16.10.5546

Witke, W. (2004). The role of profilin complexes in cell motility and other cellular processes. *Trends Cell Biol.* 14, 461–469. doi: 10.1016/j.tcb.2004.07.003

Witke, W., Sutherland, J. D., Sharpe, A., Arai, M., and Kwiatkowski, D. J. (2001). Profilin I is essential for cell survival and cell division in early mouse development. *Proc. Natl. Acad. Sci. U.S.A.* 98, 3832–3836. doi: 10.1073/pnas.051515498

Wittenmayer, N., Jandrig, B., Rothkegel, M., Schluter, K., Arnold, W., Haensch, W., et al. (2004). Tumor suppressor activity of profilin requires a functional actin binding site. *Mol. Biol. Cell* 15, 1600–1608. doi: 10.1091/mbc.e03-12-0873

Wu, N., Zhang, W., Yang, Y., Liang, Y. L., Wang, L. Y., Jin, J. W., et al. (2006). Profilin 1 obtained by proteomic analysis in all-trans retinoic acid-treated hepatocarcinoma cell lines is involved in inhibition of cell proliferation and migration. *Proteomics* 6, 6095–6106. doi: 10.1002/pmic.200500321

Yao, W., Cai, X., Liu, C., Qin, Y., Cheng, H., Ji, S., et al. (2013). Profilin 1 potentiates apoptosis induced by staurosporine in cancer cells. *Curr. Mol. Med.* 13, 417–428. doi: 10.2174/156652413805076812

Yao, W., Ji, S., Qin, Y., Yang, J., Xu, J., Zhang, B., et al. (2014). Profilin-1 suppresses tumorigenicity in pancreatic cancer through regulation of the SIRT3-HIF1alpha axis. *Mol. Cancer* 13:187. doi: 10.1186/1476-4598-13-187

Zaidi, A. H., and Manna, S. K. (2016). Profilin-PTEN interaction suppresses NF-kappaB activation via inhibition of IKK phosphorylation. *Biochem. J.* 473, 859–872. doi: 10.1042/bj20150624

Zaidi, A. H., Raviprakash, N., Mokhamatam, R. B., Gupta, P., and Manna, S. K. (2016). Profilin potentiates chemotherapeutic agents mediated cell death via suppression of NF-kappaB and upregulation of p53. *Apoptosis* 21, 502–513. doi: 10.1007/s10495-016-1222-9

Zhu, C., Kim, S. J., Mooradian, A., Wang, F., Li, Z., Holohan, S., et al. (2021). Cancer-associated exportin-6 upregulation inhibits the transcriptionally repressive and anticancer effects of nuclear profilin-1. *Cell Rep.* 34:108749. doi: 10.1016/j.celrep.2021.108749

Zou, L., Ding, Z., and Roy, P. (2010). Profilin-1 overexpression inhibits proliferation of MDA-MB-231 breast cancer cells partly through p27kip1 upregulation. *J. Cell Physiol.* 223, 623–629.

Zou, L., Hazan, R., and Roy, P. (2009). Profilin-1 overexpression restores adherens junctions in MDA-MB-231 breast cancer cells in R-cadherin-dependent manner. *Cell Motil. Cytoskeleton.* 66, 1048–1056. doi: 10.1002/cm.20407

Zou, L., Jaramillo, M., Whaley, D., Wells, A., Panchapakesa, V., Das, T., et al. (2007). Profilin-1 is a negative regulator of mammary carcinoma aggressiveness. *Br. J. Cancer* 97, 1361–1371. doi: 10.1038/sj.bjc.6604038

Conflict of Interest: The authors declare that the research was conducted in the absence of any commercial or financial relationships that could be construed as a potential conflict of interest.

frontiers in Cell and Developmental Biology

ORIGINAL RESEARCH
published: 22 June 2021
doi: 10.3389/fcell.2020.597993

A Negative Feedback Loop in Ultraviolet A-Induced Senescence in Human Dermal Fibroblasts Formed by SPCA1 and MAPK

Hongfu Xie[1†], Xiao Xiao[2†], Yuxin Yi[1†], Mingxing Deng[1,3], Peihui Li[1,3], Dan Jian[1,3], Zhili Deng[1*] and Ji Li[1,3,4,5,6,7*]*

[1] Department of Dermatology, Xiangya Hospital, Central South University, Changsha, China, [2] Department of Dermatology, Hunan Provincial People's Hospital, Changsha, China, [3] Center for Molecular Medicine, Xiangya Hospital, Central South University, Changsha, China, [4] Key Laboratory of Organ Injury, Aging and Regenerative Medicine of Hunan Province, Changsha, China, [5] National Clinical Research Center for Geriatric Disorders, Changsha, China, [6] Science and Technology Aid Program, Xinjiang Uygur Autonomous Region, Urumqi, China, [7] Hunan Key Laboratory of Aging Biology, Xiangya Hospital, Central South University, Changsha, China

OPEN ACCESS

Edited by:
Randy Y. C. Poon,
Hong Kong University of Science and Technology, Hong Kong

Reviewed by:
Mallikarjuna Korivi,
Zhejiang Normal University, China
Qun Wang,
Duke University, United States
Uraiwan Panich,
Mahidol University, Thailand

***Correspondence:**
Ji Li
liji_xy@csu.edu.cn
Dan Jian
569085332@qq.com
Zhili Deng
dengzhili@csu.edu.cn

[†] These authors have contributed equally to this work

Specialty section:
This article was submitted to Cell Death and Survival, a section of the journal Frontiers in Cell and Developmental Biology

Received: 23 August 2020
Accepted: 30 December 2020
Published: 22 June 2021

Citation:
Xie H, Xiao X, Yi Y, Deng M, Li P, Jian D, Deng Z and Li J (2021) A Negative Feedback Loop in Ultraviolet A-Induced Senescence in Human Dermal Fibroblasts Formed by SPCA1 and MAPK. Front. Cell Dev. Biol. 8:597993. doi: 10.3389/fcell.2020.597993

Secretory pathway calcium ATPase 1 (SPCA1) is a calcium pump localized specifically to the Golgi. Its effects on UVA-induced senescence have never been examined. In our study, expression of SPCA1 was increased in UVA-irradiated human dermal fibroblasts (HDFs) by activating mitogen-activated protein kinase (MAPK) and its downstream transcription factor, c-jun. Dual-luciferase reporter and chromatin immunoprecipitation assays revealed that c-jun regulated SPCA1 by binding to its promoter. Furthermore, downregulating SPCA1 with siRNA transfection aggravated UVA-induced senescence due to an elevation of intracellular calcium concentrations and a subsequent increase in reactive oxygen species (ROS) and MAPK activity. In contrast, overexpression of SPCA1 reduced calcium overload, consequently lowering the ROS level and suppressing MAPK activation. This alleviated the cellular senescence caused by UVA irradiation. These results indicated that SPCA1 might exert a protective effect on UVA-induced senescence in HDFs via forming a negative feedback loop. Specifically, activation of MAPK/c-jun triggered by UVA transcriptionally upregulated SPCA1. In turn, the increased SPCA1 lowered the intracellular Ca^{2+} level, probably through pumping Ca^{2+} into the Golgi, leading to a reduction of ROS, eventually decreasing MAPK activity and diminishing UVA-induced senescence.

Keywords: SPCA1, UVA, intracellular calcium concentration, ROS, MAPK pathway, negative feedback

INTRODUCTION

Ultraviolet (UV) irradiation is the primary environmental cause of premature skin aging and cell senescence (Bosch et al., 2015). UV radiation can be divided into three parts: UVA (320–400 nm), UVB (280–320 nm), and UVC (200–280 nm). Among three types of UV irradiation, UVA is well-known to be responsible for most of the chronic skin damage associated with cell senescence, due to its abundance and deep penetration into the dermis (Krutmann, 2001). UVA radiation primarily initiates photo-damage through the generation of reactive oxygen species (ROS) (Rinnerthaler et al., 2015). ROS reduce the cellular antioxidant status resulting in oxidative stress, which is one of the most crucial pathogenic factors for cellular senescence.

ROS can directly attack cellular molecules causing telomere shortening, mitochondrial damage, membrane degradation, and oxidation of structural and enzymatic proteins (Yaar and Gilchrest, 2007). More importantly, numerous signal transduction pathways such as mitogen-activated protein kinase (MAPK), nuclear factor-kappa beta/p65, janus kinase, signal transduction and activation of transcription, and nuclear factor erythroid 2-related factor 2 are activated by ROS. Among these, MAPK and its downstream transcription factor, activator protein-1 (AP-1), play crucial roles in cell senescence (Fisher et al., 2002). MAPK pathway is well known to be responsible for the activation of p53 and p16, which are the main causes for cell senescence (Bulavin et al., 1999; Singh et al., 2003). UVA also can upregulate matrix metalloproteinase 1 (MMP1) via the MAPK/AP-1-signaling cascade (Chaiprasongsuk et al., 2017). Moreover, Zheng et al. (2013) reported that 10-hydroxy-2-decenoic acid reduced UVA-induced activation of the c-Jun N-terminal kinase (JNK) and inhibited the expression of MMP-1 and MMP-3, thereby preventing skin photoaging.

SPCA1 is a Golgi-localized transmembrane protein, encoded by the ATPase, Ca^{2+} transporting, type2C, member 1 (ATP2C1) gene, that pumps Ca^{2+} as well as Mn^{2+} into the Golgi apparatus in an ATP-dependent manner (Missiaen et al., 2007; Shull et al., 2011; Praitis et al., 2013). Current studies of SPCA1 are mainly focused on its association with Hailey-Hailey disease (Micaroni et al., 2016; Nellen et al., 2017), secretory cargo sorting (von Blume et al., 2011, 2012), neuron differentiation (Sepulveda et al., 2008, 2009), secretory pathway mammary calcium transport (Reinhardt and Lippolis, 2009), breast cancer (Grice et al., 2010), and focal cerebral ischemia-reperfusion injury (Lehotsky et al., 2009). However, the role of SPCA1 in aging and senescence has never been explored.

One characteristic of SPCA1 attracted our attention. Specifically, SPCA1 expression correlates with oxidative stress and ROS. Pavlikova et al. (2009) demonstrated that ischemic preconditioning could partially suppress lipid and protein oxidation and reverse the depression of SPCA1 induced by ischemia/reperfusion injury in rat hippocampal membranes. Additionally, in neuro-2a cells, SPCA1 knockdown increases the H_2O_2-induced production of nitric oxide, 3-nitrotyrosine, and lactate dehydrogenase in a concentration-dependent manner (Fan et al., 2016b). Moreover, SPCA1 plays an important role in cytosolic and intra-Golgi Ca^{2+} homeostasis by transporting Ca^{2+} into the Golgi lumen (Missiaen et al., 2004; Micaroni et al., 2010).

Expression and activity changes of SPCA1 are associated with changes in the intracellular-free Ca^{2+} concentration ($[Ca^{2+}]i$). However, growing evidence indicates a mutual interplay between $[Ca^{2+}]i$ and ROS. Abnormally high levels of $[Ca^{2+}]i$ induce overproduction of free radicals that can result in oxidative stress. In turn, inordinate accumulation of ROS can exacerbate calcium overload, which further alters ROS production (Gorlach et al., 2015). Because oxidative stress and ROS are the most crucial factors of cell senescence, we speculate that SPCA1 might also play an protected role in skin cell senescence by effecting $[Ca^{2+}]i$ and ROS levels.

Therefore, we investigated the role of SPCA1 on UVA-induced cellular senescence and its regulatory mechanism in HDFs.

MATERIALS AND METHODS

Isolation of Dermal Fibroblasts and Cell Culture

Skin samples were collected from healthy male children at 6–12 years of age who were circumcised in the Department of Urology, Xiangya Hospital, Central South University. Primary HDFs were obtained by explantation from samples. The cells were grown in complete Dulbecco's modified Eagle's medium (Gibco, Grand Island, NY, USA) containing 10% fetal bovine serum (Gibco) and antibiotics (penicillin, 100 U/ml; streptomycin, 100 μg/ml) at 37°C in a humidified incubator with 5% CO_2. Medium was refreshed every 2–3 days, and fibroblasts were split 1:2–1:3 when they reached 80–90% confluence. For all experiments, cells were used at passages 4–6. Before harvesting primary HDFs, written informed consent was obtained from legal guardians of donors in accordance with a protocol approved by the Clinical Research Ethics Committee at the Xiang Ya Hospital of Central South University in Changsha, China.

UVA Irradiation

Irradiation was carried out using a UVA phototherapy instrument (SS-03A, Sigma, Shanghai, China). After two washes with phosphate-buffered saline (PBS), cells were incubated in PBS under UVA irradiation. Cells were irradiated with a UVA dose of 10 J/cm^2/day for 3 days. The time interval of these three UVA irradiations is 24 h. After each UVA exposure, cells were fed fresh complete culture medium with or without 10 μM SP600125 (#S1876; Beyotime) or 10 μM SB203580 (#S1863; Beyotime) for 24 h before being collected for further analysis.

Western Blots

Proteins were extracted from cultured cells by homogenization on ice in radio immunoprecipitation assay lysis buffer (Beyotime, Haimen, China) containing Protease Inhibitor Cocktail (Sigma-Aldrich, St. Louis, MO, USA). Supernatants were obtained after centrifugation at 12,000 × g at 4°C for 10 min. Protein concentrations were determined using a Pierce BCA Protein Assay Kit (ThermoFisher Scientific, Waltham, MA, USA). The remainder of the lysates was mixed with 5× sodium dodecyl sulfate (SDS) loading buffer (Dingguo, Beijing, China) at a ratio of 1:4. Protein samples were heated at 100°C for 5 min and separated by SDS-polyacrylamide gel electrophoresis. The separated proteins were then transferred to a polyvinylidene difluoride membrane and blocked in 1× PBST containing 5% (*w*/*v*) skim milk. The membrane blots were incubated overnight at 4°C with primary antibodies.

The primary antibody for ATP2C1 was purchased from Proteintech (Rosemont, IL, USA), and the primary antibody for P16INK4A was purchased from Boster (Wuhan, China). Primary antibodies for phospho-p38, p38, phospho-JNK, JNK, phospho-ERK1/2, and ERK1/2 were purchased from Cell Signaling Technology (Danvers, MA, USA). All antibodies were diluted in 1× PBST containing 5% BSA and 0.02% sodium azide and were

then incubated overnight at 4°C. This was followed by incubation with horseradish peroxidase-conjugated secondary antibodies (Sigma-Aldrich) for 1 h at room temperature. Each membrane was washed in 1× PBST and developed using a ChemiDo MP System (Bio-Rad, Hercules, CA, USA). The chemiluminescence signal was detected using Image Lab software (Bio-Rad). Protein levels were first normalized to β-actin (Bioworld Technology, St. Louis Park, MN, USA) and then to experimental controls.

Quantitative Real-Time Polymerase Chain Reaction

Cells were lysed in Trizol (Invitrogen, Carlsbad, CA, USA), and the homogenate was separated into aqueous and organic phases by adding bromochloropropane. Next, total RNA was precipitated from the aqueous phase with isopropanol, and finally washed with ethanol and solubilized in diethyl pyrocarbonate. cDNA was synthesized by reverse transcription from 3 μg of total RNA using the RevertAid First-Strand cDNA Synthesis Kit (Fermentas, Burlington, ON, Canada). The cDNA was diluted 10:1 and amplified using specific primers for ATP2C1 or GAPDH (purchased from Sangon Biotech, Shanghai, China). The following primer pairs were used: 5′-GTA AAA TAC TGC AAC CTT TGG-3′ and 5′-GGT GTG AAA GAA GCT GTT ACA AC-3′ for ATP2C1; 5′-CATTGACCTCAACTACATGGTTTAC-3′ and 5′-GTGATGGGATTTCCATTGATGAC-3′ for GAPDH. Signal detection was performed in triplicate using CFX Manager Software (Bio-Rad). The reaction was performed with initial denaturation at 95°C for 10 min, followed by 40 PCR cycles of 95°C for 15 s and 60°C for 60 s. Data were collected and analyzed using the $2^{\Delta\Delta Ct}$ method. Values of genes were first normalized against GAPDH, and then compared with the experimental controls.

Small Interfering RNA Transfection

HDFs were transfected with SPCA1 siRNA using Lipofectamine 2000 Transfection Reagent (Thermo Fisher Scientific). The transfection mix (100 pmol RNA and 5 μl Lipofectamine 2000), each diluted in 500 μl Opti-MEM per 60-mm dish was added followed by a 20-min incubation at room temperature. The medium was changed after 6 h. Subsequent operations were done after 48-h incubation. siRNA against SPCA1 targeting the sequence 5′-AAGGTTGCACGTTTTCAAAAA-3′ in the SPCA1 cDNA was purchased from GenePharma (Shanghai, China). The level of knockdown of SPCA1 expression was determined by Western blot.

Senescence-Associated β-Galactosidase (SA-β-gal) Staining

The Senescence-Associated β-Galactosidase Staining Kit (Cell Signaling Technology) was used according to the manufacturer's instructions. Stained cells were observed under an inverted microscope for the development of blue color. The population of SA-β-gal-positive cells was determined by counting 10 microscopic fields per dish randomly, and then computing an average. The proportions of cells positive for SA-β-gal activity are given as percentages of the total number of cells counted in every dish.

3-(4,5-Dimethylthiazol-2-yl)-2,5-Diphenyltetrazolium Bromide Assay

SPCA1-siRNA, SPCA1-cDNA, and control (NS-siRNA, SPCA1-vector)-transfected HDF cells were planted on 96-well plates at an density of 4,000 cells per well in triplicate and exposed to UVA or not. After additional incubation for 0, 24, 48, or 72 h, 20 ml of 3-(4,5-dimethylthiazol-2-yl)-2,5-diphenyltetrazolium bromide (MTT) stock solution (5 mg/ml MTT reagent diluted in PBS; Sigma-Aldrich, USA) was added to each well. The plates were further incubated for 4 h at 37°C and 5% CO_2 in the dark. The supernatant was carefully removed without disturbing the sediment, and 150 μl dimethyl sulfoxide (Sigma-Aldrich, USA) was added to the wells to dissolve the purple formazan crystals. The absorbance at 490 nm was obtained from a microplate reader (BioRad).

$[Ca^{2+}]i$ Measurements

HDFs were loaded with 4 μM Fluo-4/AM (Dojindo Laboratories, Kumamoto, Japan) for 60 min at 37°C in the dark and washed thrice with PBS. Then, they were digested by trypsin, centrifuged at 2,000 rpm for 5 min, washed two times with PBS, and incubated for another 30 min. Fluorescence was measured using a flow cytometer.

ROS Measurements

The intracellular ROS level was measured using a Reactive Oxygen Test Kit (Beyotime). After three times UVA exposure, HDFs were fed fresh complete culture medium for 24 h before ROS measurements. HDFs were loaded with dichlorofluorescin diacetate for 20 min at 37°C in the dark and washed thrice with PBS. Fluorescence was measured using a Multiskan Spectrum microplate reader (Thermo Fisher Scientific).

Plasmids

The SPCA1 promoter reporter [SPCA1-luc (luciferase)] was prepared by inserting an approximately 1.0 kb upstream sequence (based on the putative translation starting codon) into the pGL3-basic vector. This fragment was generated by PCR with 5′-CGGGGTACCAAGTGGTTCTGCAGTAT-3′ and 5′-CCCAAGCTTATATTAGCTAGCTGGTGACTT-3′ as the primers (Sangon Biotech).The SPCA1 overexpression plasmid was prepared by inserting a coding sequence into pcDNA3.1 (+). This fragment was generated by PCR with the following primers: 5′-CCCAAGCTTATGAAGGTTGCACGTT-3′ and 5′-CGGGGTACCTCATACTTCAAGAAAAGATG-3′ (Sangon Biotech). The pGL3-basic and PLR-TK vectors were purchased from Promega. pcDNA3.1 (+) was purchased from Thermo Fisher Scientific. p6600 MSCV-IP N-HA only JUN, pLX304-FOS-V5 were purchased from addgene (Cambridge, MA, USA). All constructs were subjected to sequence analysis.

Dual-Luciferase Reporter Gene Assay

HEK293T cells were cultured in DMEM (Gibco) containing 10% fetal bovine serum (Gibco) to approximately 60% confluence in a 96-well plate, then co-transfected with different DNA mixes for 24–36 h. Firefly and Renilla luciferase activities were measured using the Dual-Luciferase Reporter Assay System (Promega). Renilla luciferase activity was normalized to firefly luciferase activity. Two thousand base pairs (bp) before transcription initiation sites within the DNMT1 promoter were cloned and inserted into a pGL4 control vector (Promega). Additionally, mutant reporter genes were created using the QuikChange Lightning Multi Site-Directed Mutagenesis kit (Stratagene, La Jolla, CA, USA). The primer used to clone the DNMT1 promoter was following: 5′-GCCGGTACCAAGTGGTTCTGCAGTATACAG-3′ and 5′-GCCCTCGAGTATTAGCTAGCTGGTGACTT-3′ (Sangon Biotech).

Chromatin Immunoprecipitation Assay

The chromatin immunoprecipitation (ChIP) assay was performed according to the manufacturer's manual using an EZ ChIP kit purchased from Millipore (Temecula, CA, USA). The immunoprecipitated complexes were incubated at 4°C overnight with the indicated antibodies. Bound DNA fragments were analyzed by RT-PCR using the HotStart Taq enzyme (Takara, Dalian, China). Primers were specific for the predicted binding sites (**Supplementary Table 2**). GAPDH was used as the negative control.

Nucleofector for Fibroblasts

Cultured primary HDFs (1×10^6) were transfected with the 4D-Nucleofector System (Lonza, Walkersville, MD, USA) according to manufacturer's instructions using the program U-023 preset with 2 μg plasmid DNA or 2 μg pmax GFP vector.

Statistical Analyses

Data are shown as means ± SD of at least three independent experiments. Statistical significance was assessed using Student's *t*-test or two-way ANOVA with SPSS 17.0 (IBM, Chicago, IL, USA).We considered $P < 0.05$ to be statistically significant.

RESULTS

UVA Irradiation Increases the Expression of SPCA1 by Activating the MAPK Pathway

Primary HDFs were irradiated with 10 J/cm^2 UVA/day for 3 days. Both the mRNA and protein levels of SPCA1 were remarkably increased in HDFs after UVA irradiation (**Figures 1A,B**). Then, we investigated the possible signaling pathway regulating SPCA1 expression. UVA irradiation enhanced phosphorylation of P38 and JNK, while inhibitors of MAPK (SB203580 and SP600125) suppressed this phosphorylation, as well as the SPCA1 expression induced by UVA irradiation (**Figures 1C,D**). These results indicate that UVA irradiation increases the expression of SPCA1 by activating the MAPK pathway.

MAPK Transcriptionally Regulates SPCA1 via Activating c-Jun

AP-1 is a classical transcription factor activated by MAPK. Phosphorylation of c-jun was increased after UVA irradiation, which could be blocked by MAPK inhibitors (**Figures 2A,B**). We predicted three high score binding sites of c-jun on the SPCA1 promoter through JASPAR bioinformatics software. Basic information about these three binding sites is presented in the Supporting Information (**Supplementary Table 1**). We cloned the promoter of SPCA1 (−2,000 to 0 bp) and generated a SPCA1 promoter luciferase reporter and cotransfected to HEK293T cell with p6600 MSCV-IP N-HA only JUN or pLX304-FOS-V5 (c-jun and c-fos expression plasmid). The dual-luciferase reporter assay revealed that c-jun markedly enhanced activity of SPCA1 promoter luciferase reporter, but c-fos (another component of AP-1) had no effect on SPCA1 promoter activity (**Figure 2C**). Furthermore, ChIP assay was applied to determine whether c-jun was bound to these sequences directly. The primers for amplifying these predicted binding sites in ChIP assays is shown in **Supplementary Table 2**. The results showed that the sequences at the predicted binding sites 2 and 3 were amplified to a greater extent following immunoprecipitation with an anti-c-jun antibody than with the non-specific IgG control (**Figure 2D**). These data suggest that AP-1 might bind directly to the predicted binding sites 2 and/or 3 of the SPCA1 promoter and regulates its transcription level. This indicated that c-jun might bind to the predicted sequence.

SPCA1 siRNA Exacerbates UVA-Induced Senescence and Phosphorylation of MAPK

To identify the role of SPCA1 in UVA-induced senescence in HDFs, SPCA1 siRNA was transfected to decrease its expression. SA-β-gal activity, and the expression of p16 (hallmark of cellular senescence), were measured to evaluate cellular senescence. Downregulation of SPCA1 exacerbated the increase of SA-β-gal-positive cells and the expression of p16 induced by UVA irradiation (**Figures 3A,C,D**); 24, 48, and 72 h after UVA radiation, SPCA1 and NS siRNA-transfected HDFs both decreased in cell viability, but the cell viability dropped severely in SPCA1 siRNA-transfected groups (**Figure 3B**). Downregulation of SPCA1 also promoted the phosphorylation of MAPK caused by UVA (**Figure 3E**). Thus, we demonstrated that downregulating SPCA1 exacerbates UVA-induced senescence and MAPK activation.

SPCA1 cDNA Attenuates UVA-Induced Senescence and Phosphorylation of MAPK

SPCA1 cDNA was nucleofected into HDFs to further investigate the role of SPCA1 in UVA-induced senescence. Upregulation of SPCA1 partially reversed the increased number of SA-β-gal-positive cells (**Figures 4C,D**), and p16 expression (**Figure 4A**), as well as phosphorylation of MAPK caused by UVA irradiation (**Figure 4E**). Simultaneously, the UVA-induced reduction of cell viability was partially reversed by SPCA1 cDNA (**Figure 4B**). These results indicate that overexpression of SPCA1 attenuates

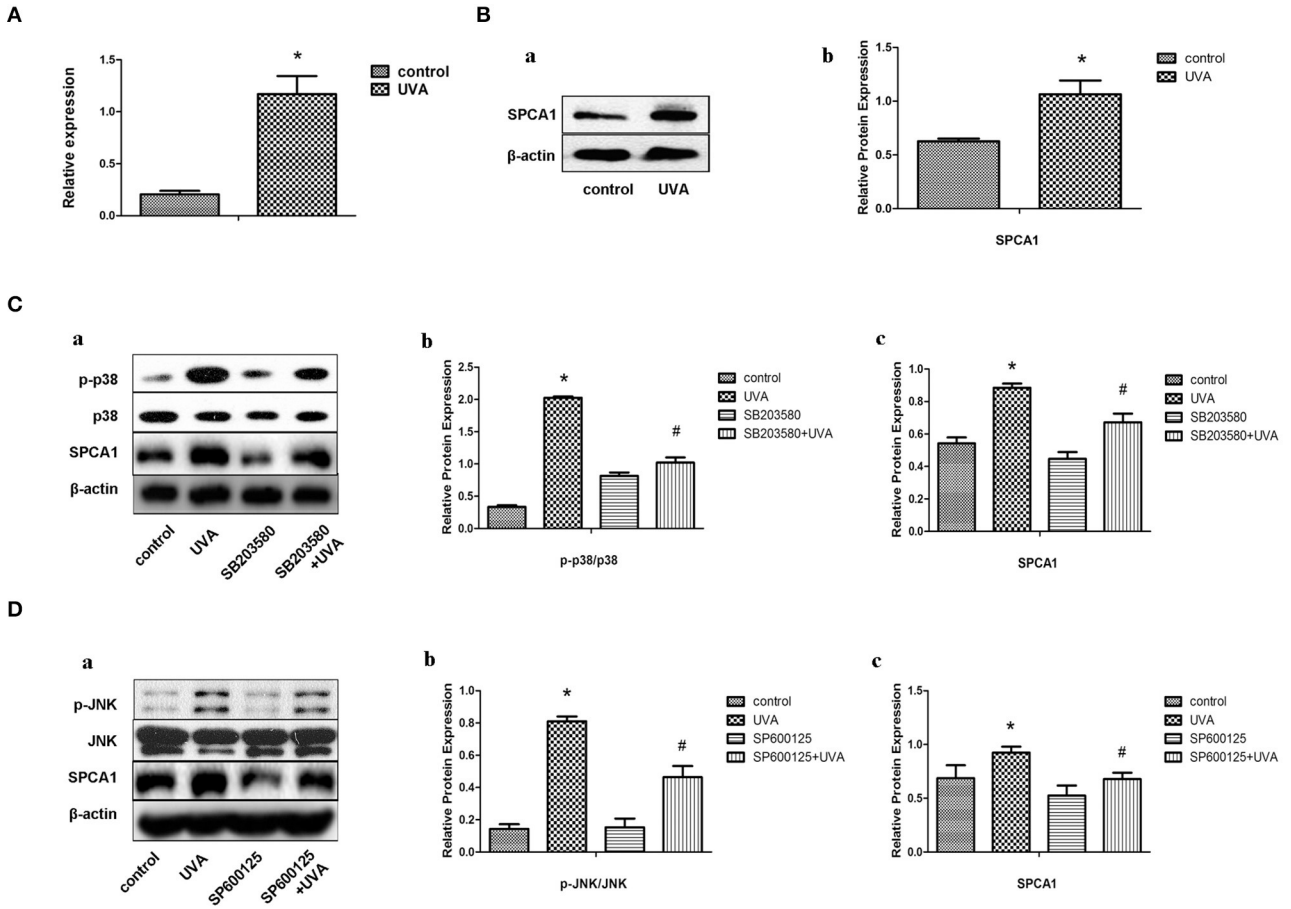

FIGURE 1 | UVA irradiation increases the expression of SPCA1 by activating the MAPK pathway. **(A)** SPCA1 mRNA expression in control and UVA-irradiated HDFs, as determined by real-time PCR. Each sample was analyzed in triplicate. Data are shown as the mean of three independent experiments. *$P < 0.05$ vs. control. **(B)** (a) SPCA1 protein expression in control and UVA-irradiated HDFs, as determined by Western blot analysis. Images are representative of three independent experiments. (b) Bar graphs show quantitative analysis of scanning densitometric values of SPCA1 as ratios to β-actin, which was used as a loading control. Data are representative of three independent experiments. *$P < 0.05$ vs. control. **(C,D)** Effects of SB203580 and SP600125 (inhibiter of p38 and JNK) on UVA-induced SPCA1 protein expression and phosphorylation of p38 and JNK as determined by Western blot analysis. Control and UVA-irradiated HDFs were treated with or without 10 μM SB203580 and SP600125, respectively. Images are representative of three independent experiments. (b,c) Bar graphs show quantitative analysis of scanning densitometric values of SPCA1 as ratios to β-actin and phospho-JNK, p38 proteins as ratios to their total JNK, and p38, respectively. Data are representative of three independent experiments. *$P < 0.05$ vs. control; #$P < 0.05$ vs. UVA.

UVA-induced senescence and phosphorylation of MAPK in HDFs.

SPCA1 Affects UVA-Induced ROS and MAPK Activation via Regulating [Ca^{2+}]i

To investigate the possible mechanism of the effects of SPCA1 on UVA-induced senescence, we evaluated the levels of [Ca^{2+}]i and ROS. Downregulating SPCA1 further elevated the increase of calcium, ROS, and MAPK activity induced by UVA. Moreover, compared with HDFs transfected with NC siRNA, UVA-irradiated HDFs transfected with SPCA1 siRNA have no difference in ROS level and phosphorylation of MAPK at the presence of BAPTA (**Figures 5A–C**). On the contrary, the elevations of intracellular calcium, ROS, and MAPK activity initiated by UVA were partially reversed by SPCA1 cDNA transfection (**Figures 5D,E**). Thus, our results demonstrate that SPCA1 influence UVA-induced ROS and MAPK activation by regulating [Ca^{2+}]i.

DISCUSSION

In this study, we found that UVA irradiation promoted the expression of SPCA1 through activation of MAPK and its downstream transcription factor, c-jun, which directly binds to the SPCA1 promoter. Increased SPCA1 suppressed UVA-induced MAPK activity by lowering the [Ca^{2+}]i and ROS levels, thereby alleviating cellular senescence caused by UVA. Thus, a novel negative feedback loop to maintain homeostasis in HDFs under UVA irradiation was discovered. This is the initial research concerning a role for SPCA1 and its regulatory mechanism in

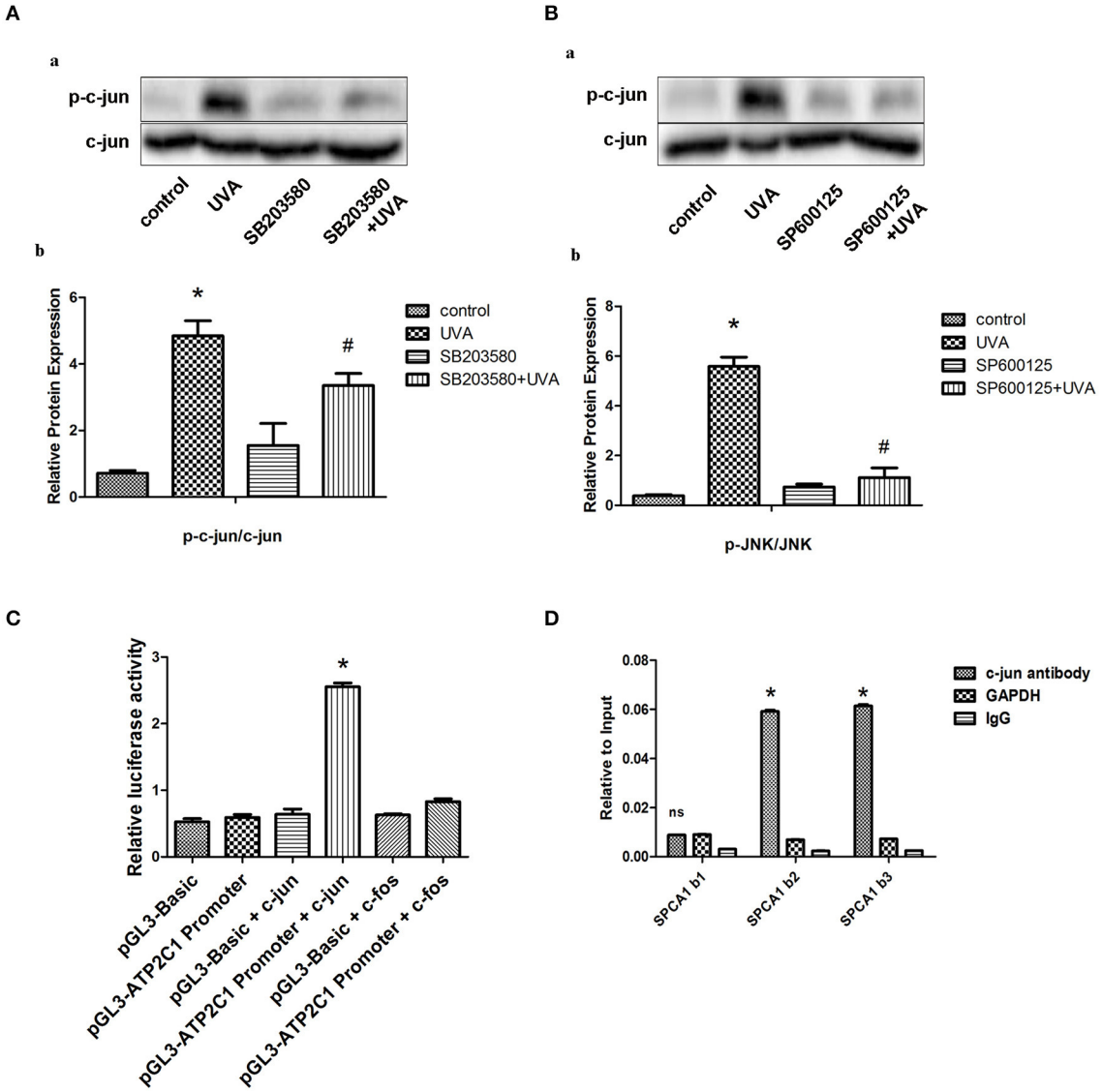

FIGURE 2 | MAPK transcriptionally regulates SPCA1 via activating c-jun. **(A,B)** Western blot images and quantitative analysis show effects of SB203580 and SP600125 on UVA-induced phosphorylation of c-jun. Images are representative of three independent experiments. $^{*}P < 0.05$ vs. control; $^{\#}P < 0.05$ vs. SB203580 + UVA or SP600125 + UVA. The treatment of SB203580 and SP600125 is described above. **(C)** Luciferase reporter assay data, showing the activity of SPCA1 promoter. Cells were transfected with the following plasmids: c-jun, c-jun-cDNA-expressing vector; c-fos, c-fos-cDNA-expressing vector; ATP2C1, reporter plasmid containing SPCA1 promoter. Experiments were performed in triplicate. $^{*}P < 0.05$ vs. pGL3-ATP2C1 promoter. **(D)** Chromatin immunoprecipitation data from HDFs incubated with either anti-SPCA1 antibody or non-specific control IgG, showing the amplification of each of the four predicted c-jun-binding sites within the SPCA1 promoter (termed SPCA1 b1, b2, and b3). Experiments were performed in triplicate.$^{*}P < 0.05$ vs. IgG; $^{ns}P < 0.05$ vs. IgG.

cellular senescence, suggesting that SPCA1 is involved in self-defense in UVA-induced senescence.

Oxidative stress and ROS are decisive factors of UVA-induced senescence and MAPK activation. Several reports in different areas congruously found that SPCA1 was associated with oxidative stress and ROS due to its capability of regulating $[Ca^{2+}]i$; some refer to this as "Golgi stress" (Okunade et al., 2007; Shull et al., 2011). Keratinocytes derived from Hailey–Hailey disease patients, which lack one functional copy of the ATP2C1 gene, underwent oxidative stress, while ATP2C1 inactivation increased oxidative stress in cultured human keratinocytes (Cialfi et al., 2010, 2016). In addition, there is a correlation between SPCA1 and oxidative stress in ischemia/reperfusion and ischemic preconditioning of brain cells (Pavlikova et al., 2009). Similarly, our findings suggested that SPCA1 played a very important role in UVA-induced senescence by altering oxidative stress. Silencing SPCA1 exacerbated the increased $[Ca^{2+}]i$ induced by UVA irradiation, leading to higher ROS levels and MAPK activity and eventually aggravating cellar senescence in HDFs. In contrast, overexpression of SPCA1 yielded the opposite

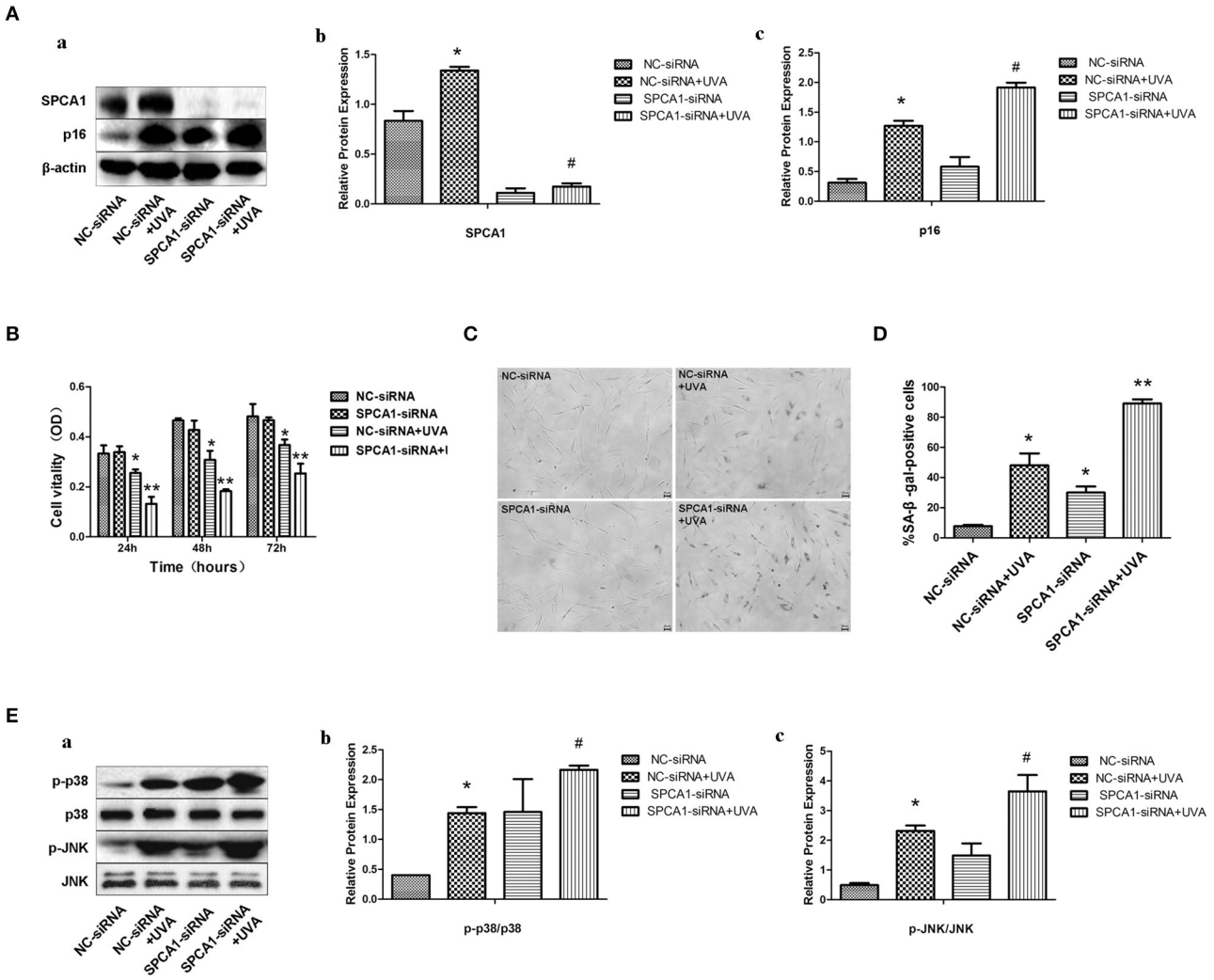

FIGURE 3 | SPCA1 siRNA exacerbates UVA-induced senescence and phosphorylation of MAPK. **(A)** Western blot images and quantitative analysis show SPCA1 and p16 protein expression in control and UVA-irradiated HDFs, with or without SPCA1 siRNA transfection. $^{*}P < 0.05$ vs. NC-siRNA; $^{\#}P < 0.05$ vs. NC-siRNA + UVA. Data are representative of three independent experiments. **(B)** Cell vitality determined by MTT analysis under indicated conditions. $^{*}P < 0.05$ vs. NC-siRNA; $^{**}P < 0.05$ vs. NC-siRNA + UVA. **(C,D)** Senescence-associated β-galactosidase (SA-β-gal) activity of cells under the indicated conditions. Representative images are shown (scale bar = 200 μm). The percentages of SA-β-gal-positive cells under each condition are presented as the mean ± standard deviation of three independent experiments. $^{*}P < 0.05$ vs. NC-siRNA; $^{**}P < 0.05$ vs. NC-siRNA + UVA. **(E)** Western blot images and quantitative analysis show phosphorylation of p38 and JNK in control and UVA-irradiated HDFs, with or without SPCA1 siRNA transfection. $^{*}P < 0.05$ vs. NC-siRNA; $^{\#}P < 0.05$ vs. NC-siRNA + UVA. Data are representative of three independent experiments.

result and exhibited a protective effect on senescence. The effects of SPCA1 siRNA on ROS and MAPK activity could be abolished by a calcium chelator, BAPTA. This indicates that $[Ca^{2+}]i$ acted as a mediator between SPCA1 and oxidative stress. Nevertheless, the specific underlying mechanism involved in regulating ROS by $[Ca^{2+}]i$ in this situation requires further study. It has been shown that intracellular calcium could cause mitochondria Ca^{2+} overload (Li et al., 2013), induce a three-dimensional conformation change of the respiratory chain complexes (Brookes et al., 2004), increase metabolic rate (Brookes et al., 2004), activate cytoplasmic NADPH oxidases (NOXes) (Crosas-Molist and Fabregat, 2015; Gorlach et al., 2015), and all eventually increase ROS production. Some of the processes mentioned above may be involved in our case.

Because SPCA1 has a protective role in UVA-induced cellular senescence, we examined its upstream regulatory mechanism. Loss of one functional copy of the ATP2C1 gene causes low expression of SPCA1 and Hailey–Hailey disease, a human autosomal dominant skin disorder characterized by suprabasal acantholysis of keratinocytes (Hu et al., 2000; Sudbrak et al., 2000). Short wave increased expression of SPCA1 in middle cerebral artery occlusion (Fan et al., 2016a), ischemia/reperfusion depressed SPCA1 expression, and ischemic preconditioning could partially reverse this kind of depression in hippocampal

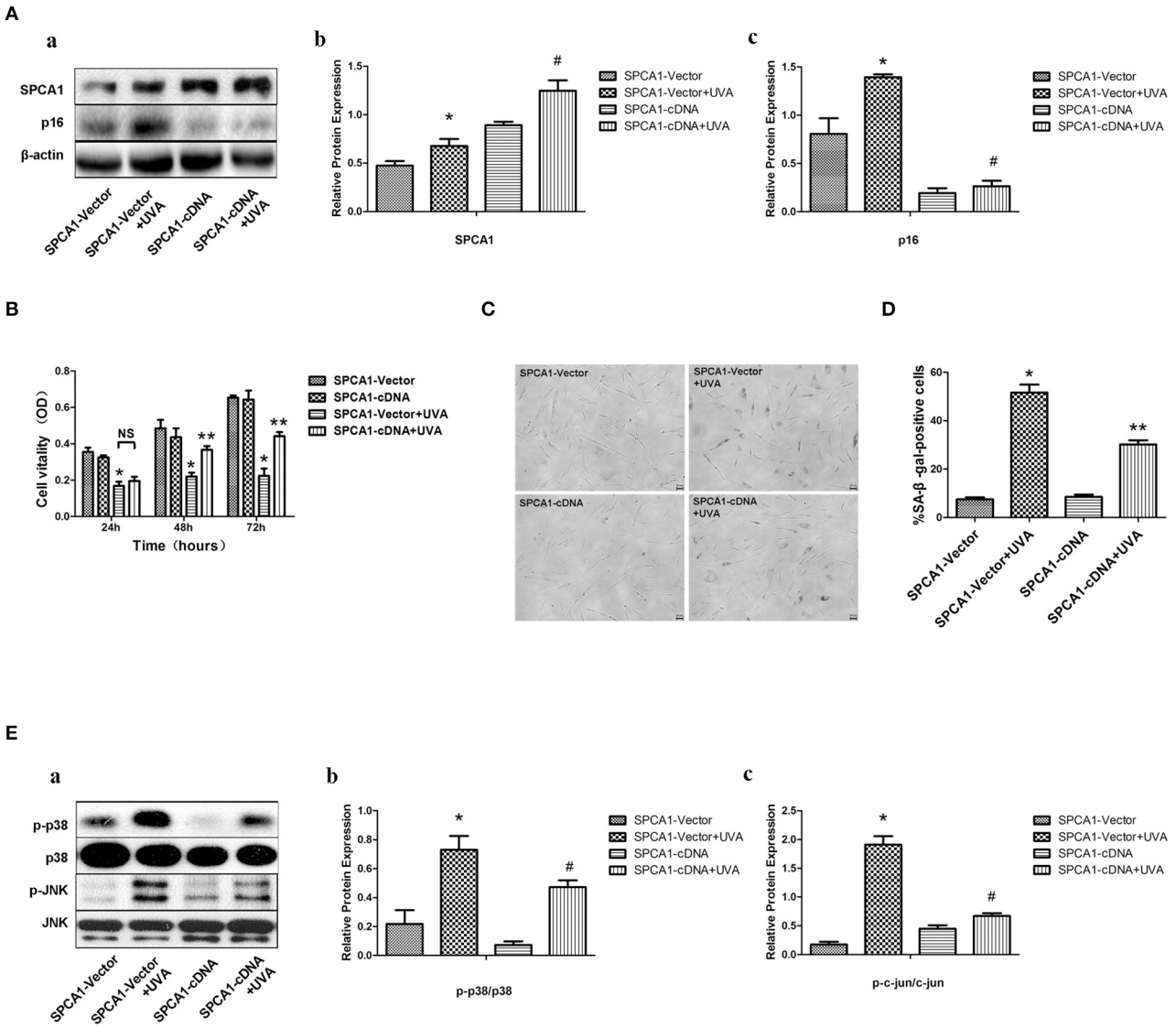

FIGURE 4 | SPCA1 cDNA attenuates UVA-induced senescence and phosphorylation of MAPK. **(A)** Western blot images and quantitative analysis show SPCA1 and p16 protein expression in control and UVA-irradiated HDFs, with or withoutSPCA1 cDNA transfection, $^{*}P < 0.05$ vs. SPCA1-vector; $^{\#}P < 0.05$ vs. SPCA1-vector+UVA. Data are representative of three independent experiments. **(B)** Cell vitality determined by MTT analysis under indicated conditions. $^{*}P < 0.05$, SPCA1-vector + UVA vs. SPCA1-vector; $^{**}P < 0.05$, SPCA1-cDNA+UVA vs. SPCA1-vector+UVA. **(C,D)** Senescence-associated β-galactosidase (SA-β-gal) activity of cells under the indicated conditions. Representative images are shown (scale bar = 200 μm). The percentages of SA-β-gal-positive cells under each condition are presented as the mean ± standard deviation of three independent experiments. $^{*}P < 0.05$ vs. SPCA1-vector; $^{**}P < 0.05$ vs. SPCA1-vector+UVA. **(E)** Western blot images and quantitative analysis show phosphorylation of p38 and JNK in control and UVA-irradiated HDFs, with or without SPCA1 cDNA transfection. $^{*}P < 0.05$ vs. SPCA1-vector; $^{\#}P < 0.05$ vs. SPCA1-vector + UVA. Data are representative of three independent experiments.

cells (Lehotsky et al., 2009). Serotonin deficiency decreased the expression of SPCA1 mRNA in mammary epithelial cells (Laporta et al., 2014). However, these reports only provided the expression changes of SPCA1 in certain conditions, without exploring the underlying mechanism. Aside from these findings, little is known about the regulatory mechanism of SPCA1, especially in skin.

In our study, we not only discovered a new condition that modified SPCA1 expression:UVA irradiation but also revealed a new regulatory mechanism of SPCA1. Specifically, UVA-activated MAPK and its downstream transcription factor c-jun, which, in turn, directly bound to the SPCA1 promoter and up-regulated its expression.

MAPK activation plays a crucial role in UVA-induced senescence. For example, MAPK increases MMP1, MMP3, and MMP9 through activating AP-1, leading to collagen degradation (Wang et al., 2005; Kim et al., 2013). Alternately, MAPK can directly phosphorylate p16 and p53 and initiate senescence of

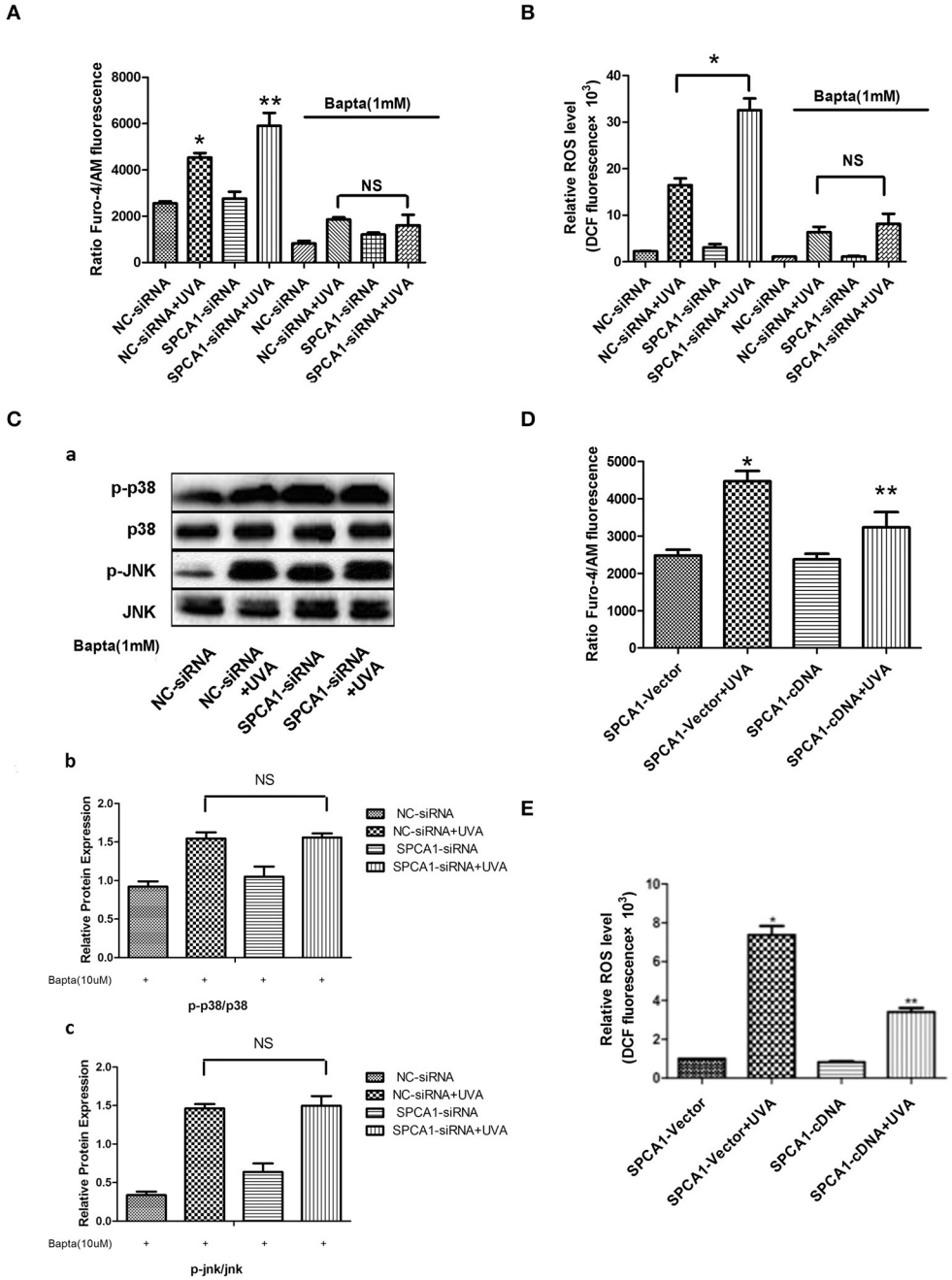

FIGURE 5 | SPCA1 affects UVA-induced ROS and MAPK activation via regulating $[Ca^{2+}]i$. **(A)** $[Ca^{2+}]i$ levels determined by Fluo-4/AM fluorescence under indicated conditions. Bapta (1 mM) abolish the effect of SPCA1 siRNA on $[Ca^{2+}]i$ levels in UVA-irradiated HDF. $^{*}P < 0.05$ vs. NC-siRNA; $^{**}P < 0.05$ vs. NC-siRNA + UVA; $^{ns}P < 0.05$. **(B)** ROS levels determined by dichlorofluorescin diacetate fluorescence under indicated conditions. Bapta (1 mM) abolish the effect of SPCA1 siRNA on ROS levels in UVA-irradiated HDF. $^{*}P < 0.05$ vs. NC-siRNA; $^{**}P < 0.05$ vs. NC-siRNA + UVA; $^{ns}P < 0.05$. **(C)** Western blot images and quantitative analysis show Bapta (1 mM) abolish the effect of SPCA1 siRNA on phosphorylation of p38 and JNK in UVA-irradiated HDF. $^{ns}P < 0.05$. Data are representative of three independent experiments. **(D,E)** $[Ca^{2+}]i$ and ROS level in control and UVA-irradiated HDFs, with or without SPCA1 cDNA transfection. $^{*}P < 0.05$ vs. SPCA1-vector; $^{**}P < 0.05$ vs. SPCA1-vector + UVA.

skin cells, especially dermal fibroblasts (Bulavin et al., 1999; Singh et al., 2003). In our previous studies, we demonstrated that the MAPK pathway was involved in UVA-induced senescence and apoptosis (Xie et al., 2013; Wang et al., 2015). In agreement with this finding, our present research also showed the activation of MAPK and c-jun, under UVA irradiation. Furthermore, we identified SPCA1 as a new target gene regulated by MAPK, in UVA-induced senescence in HDFs by using MAPK inhibitors.

MAPK activates c-jun by phosphorylation, and the latter binds to specific sequences called the tetradeconylphorbol-13-acetate response elements (TREs) in the promoters of AP-1-inducible genes, contributing to transcriptional activation or repression of target genes (Angel and Karin, 1991; Whitmarsh and Davis, 1996). We also found that UVA phosphorylated c-jun via activation of MAPK by using selective inhibitors. Using bioinformatic software (JASPAR), we predicted three TREs on the promoter of SPCA1. Dual-luciferase reporter and ChIP assays located the precise functional domain on the SPCA1 promoter that bound c-jun. To our knowledge, this regulatory mechanism of SPCA1 has not been reported previously and might provide a new direction for research concerning the regulation of SPCA1 in different circumstances.

Negative feedback is a core mechanism to maintain homeostasis and cope with stress in the human body. Examples of this are numerous, from the baroreflex in blood pressure to the regulation of hormone secretion. Overall, our research suggests that SPCA1 might exert a protective effect on UVA-induced senescence in HDFs through negative feedback of MAPK. Activation of MAPK/c-jun triggered by UVA could transcriptionally upregulate SPCA1. In turn, increased SPCA1 brings down the $[Ca^{2+}]i$, probably through pumping Ca^{2+} into the Golgi apparatus. This reduces ROS levels, eventually decreasing MAPK activity and easing UVA-induced senescence. Therefore, this negative feedback loop could partially break the signaling cascade of MAPK, alleviate damage caused by UVA, maintain cellular homeostasis, and prevent cells from senescence.

DATA AVAILABILITY STATEMENT

The original contributions presented in the study are included in the article/**Supplementary Material**, further inquiries can be directed to the corresponding author/s.

ETHICS STATEMENT

Before harvesting primary HDFs, written informed consent was obtained from legal guardians of donors in accordance with a protocol approved by the Clinical Research Ethics Committee at the Xiang Ya Hospital of Central South University in Changsha, China.

AUTHOR CONTRIBUTIONS

DJ and ZD performed the experiments, analyzed the data, and wrote the manuscript. MD and PL performed the experiments. YY and HX analyzed the data. JL and XX discussed the analyses, interpretation, and presentation and edited the manuscript. All authors contributed to the article and approved the submitted version.

FUNDING

This research was supported by the National Natural Science Foundation of China (Grant Nos. 81171520, 81371756, 81271775, 81472904, 91749114, and 2019E0289).

ACKNOWLEDGMENTS

We thank the Department of Dermatology in Xiangya Hospital of Central South University for collecting skin samples, and we especially thank the individuals who participated in this study.

SUPPLEMENTARY MATERIAL

The Supplementary Material for this article can be found online at: https://www.frontiersin.org/articles/10.3389/fcell.2020.597993/full#supplementary-material

REFERENCES

Angel, P., and Karin, M. (1991). The role of Jun, Fos and the AP-1 complex in cell-proliferation and transformation. *Bioch. Biophys. Acta* 1072, 129–157. doi: 10.1016/0304-419X(91)90011-9

Bosch, R., Philips, N., Suarez-Perez, J. A., Juarranz, A., Devmurari, A., Chalensouk-Khaosaat, J., et al. (2015). Mechanisms of photoaging and cutaneous photocarcinogenesis, and photoprotective strategies with phytochemicals. *Antioxidants* 4, 248–268. doi: 10.3390/antiox4020248

Brookes, P. S., Yoon, Y., Robotham, J. L., Anders, M. W., and Sheu, S. S. (2004). Calcium, A. T. P., and ROS: a mitochondrial love-hate triangle. *Am. J. Physiol. Cell Physiol.* 287, C817–C833. doi: 10.1152/ajpcell.00139.2004

Bulavin, D. V., Saito, S., Hollander, M. C., Sakaguchi, K., Anderson, C. W., Appella, E., et al. (1999). Phosphorylation of human p53 by p38 kinase coordinates N-terminal phosphorylation and apoptosis in response to UV radiation. *EMBO J.* 18, 6845–6854. doi: 10.1093/emboj/18.23.6845

Chaiprasongsuk, A., Lohakul, J., Soontrapa, K., Sampattavanich, S., Akarasereenont, P., and Panich, U. (2017). Activation of Nrf2 reduces UVA-Mediated MMP-1 upregulation via MAPK/AP-1 signaling cascades: the photoprotective effects of sulforaphane and hispidulin. *J. Pharmacol. Exp. Ther.* 360, 388–398. doi: 10.1124/jpet.116.238048

Cialfi, S., Le Pera, L., De Blasio, C., Mariano, G., Palermo, R., Zonfrilli, A., et al. (2016). The loss of ATP2C1 impairs the DNA damage response and induces altered skin homeostasis: consequences for epidermal biology in Hailey-Hailey disease. *Sci. Rep.* 6:31567. doi: 10.1038/srep31567

Cialfi, S., Oliviero, C., Ceccarelli, S., Marchese, C., Barbieri, L., Biolcati, G., et al. (2010). Complex multipathways alterations and oxidative stress are associated with Hailey-Hailey disease. *Br. J. Dermatol.* 162, 518–526. doi: 10.1111/j.1365-2133.2009.09500.x

Crosas-Molist, E., and Fabregat, I. (2015). Role of NADPH oxidases in the redox biology of liver fibrosis. *Redox Biol.* 6, 106–111. doi: 10.1016/j.redox.2015.07.005

Fan, Y., Zhang, C., Li, T., Peng, W., Yin, J., Li, X., et al. (2016a). A new approach of short wave protection against middle cerebral artery occlusion/reperfusion injury via attenuation of golgi apparatus stress by inhibition of downregulation of secretory pathway Ca(2+)-ATPase isoform 1 in rats. *J. Stroke Cerebrovasc. Dis.* 25, 1813–1822. doi: 10.1016/j.jstrokecerebrovasdis.2016.03.033

Fan, Y., Zhang, C., Peng, W., Li, T., Yin, J., Kong, Y., et al. (2016b). Secretory pathway Ca(2+)-ATPase isoform 1 knockdown promotes Golgi apparatus stress injury in a mouse model of focal cerebral ischemia-reperfusion: *in vivo* and *in vitro* study. *Brain Res.* 1642, 189–196. doi: 10.1016/j.brainres.2016.03.049

Fisher, G. J., Kang, S., Varani, J., Bata-Csorgo, Z., Wan, Y., Datta, S., et al. (2002). Mechanisms of photoaging and chronological skin aging. *Arch. Dermatol.* 138, 1462–1470. doi: 10.1001/archderm.138.11.1462

Gorlach, A., Bertram, K., Hudecova, S., and Krizanova, O. (2015). Calcium and ROS: a mutual interplay. *Redox Biol.* 6, 260–271. doi: 10.1016/j.redox.2015.08.010

Grice, D. M., Vetter, I., Faddy, H. M., Kenny, P. A., Roberts-Thomson, S. J., and Monteith, G. R. (2010). Golgi calcium pump secretory pathway calcium ATPase 1 (SPCA1) is a key regulator of insulin-like growth factor receptor (IGF1R) processing in the basal-like breast cancer cell line MDA-MB-231. *J. Biol. Chem.* 285, 37458–37466. doi: 10.1074/jbc.M110.163329

Hu, Z., Bonifas, J. M., Beech, J., Bench, G., Shigihara, T., Ogawa, H., et al. (2000). Mutations in ATP2C1, encoding a calcium pump, cause Hailey-Hailey disease. *Nat. Genet.* 24, 61–65. doi: 10.1038/71701

Kim, J. M., Noh, E. M., Kwon, K. B., Hwang, B. M., Hwang, J. K., You, Y. O., et al. (2013). Dihydroavenanthramide D prevents UV-irradiated generation of reactive oxygen species and expression of matrix metalloproteinase-1 and−3 in human dermal fibroblasts. *Exp. Dermatolo.* 22, 759–761. doi: 10.1111/exd.12243

Krutmann, J. (2001). The role of UVA rays in skin aging. *Eur. J. Dermatol.* 11, 170–171.

Laporta, J., Keil, K. P., Vezina, C. M., and Hernandez, L. L. (2014). Peripheral serotonin regulates maternal calcium trafficking in mammary epithelial cells during lactation in mice. *PLoS ONE.* 9:e110190. doi: 10.1371/journal.pone.0110190

Lehotsky, J., Racay, P., Pavlikova, M., Tatarkova, Z., Urban, P., Chomova, M., et al. (2009). Cross-talk of intracellular calcium stores in the response to neuronal ischemia and ischemic tolerance. *Gen. Physiol. Biophys.* 28:F104–F114.

Li, X., Fang, P., Mai, J., Choi, E. T., Wang, H., and Yang, X. F. (2013). Targeting mitochondrial reactive oxygen species as novel therapy for inflammatory diseases and cancers. *J. Hematol. Oncol.* 25, 6–19. doi: 10.1186/1756-8722-6-19

Micaroni, M., Giacchetti, G., Plebani, R., Xiao, G. G., and Federici, L. (2016). ATP2C1 gene mutations in Hailey-Hailey disease and possible roles of SPCA1 isoforms in membrane trafficking. *Cell Death Dis.* 7:e2259. doi: 10.1038/cddis.2016.147

Micaroni, M., Perinetti, G., Berrie, C. P., and Mironov, A. A. (2010). The SPCA1 Ca^{2+} pump and intracellular membrane trafficking. *Traffic* 11, 1315–1333. doi: 10.1111/j.1600-0854.2010.01096.x

Missiaen, L., Dode, L., Vanoevelen, J., Raeymaekers, L., and Wuytack, F. (2007). Calcium in the Golgi apparatus. *Cell Calcium* 41, 405–416. doi: 10.1016/j.ceca.2006.11.001

Missiaen, L., Raeymaekers, L., Dode, L., Vanoevelen, J., Van Baelen, K., Parys, J. B., et al. (2004). SPCA1 pumps and Hailey-Hailey disease. *Biochem. Biophys. Res. Commun.* 322, 1204–1213. doi: 10.1016/j.bbrc.2004.07.128

Nellen, R. G., Steijlen, P. M., van Steensel, M. A., Vreeburg, M., European Professional, C., Frank, J., et al. (2017). Mendelian disorders of cornification caused by defects in intracellular calcium pumps: mutation update and database for variants in ATP2A2 and ATP2C1 associated with darier disease and hailey-hailey disease. *Hum. Mutation* 38, 343–356. doi: 10.1002/humu.23164

Okunade, G. W., Miller, M. L., Azhar, M., Andringa, A., Sanford, L. P., Doetschman, T., et al. (2007). Loss of the Atp2c1 secretory pathway Ca(2+)-ATPase (SPCA1) in mice causes Golgi stress, apoptosis, and midgestational death in homozygous embryos and squamous cell tumors in adult heterozygotes. *J. Biol. Chem.* 282, 26517–26527. doi: 10.1074/jbc.M703029200

Pavlikova, M., Tatarkova, Z., Sivonova, M., Kaplan, P., Krizanova, O., and Lehotsky, J. (2009). Alterations induced by ischemic preconditioning on secretory pathways Ca^{2+}-ATPase (SPCA) gene expression and oxidative damage after global cerebral ischemia/reperfusion in rats. *Cell. Mol. Neurobiol.* 29, 909–916. doi: 10.1007/s10571-009-9374-6

Praitis, V., Simske, J., Kniss, S., Mandt, R., Imlay, L., Feddersen, C., et al. (2013). The secretory pathway calcium ATPase PMR-1/SPCA1 has essential roles in cell migration during *Caenorhabditis elegans* embryonic development. *PLoS Genet.* 9:e1003506. doi: 10.1371/journal.pgen.1003506

Reinhardt, T. A., and Lippolis, J. D. (2009). Mammary gland involution is associated with rapid down regulation of major mammary Ca^{2+}-ATPases. *Biochem. Biophys. Res. Commun.* 378, 99–102. doi: 10.1016/j.bbrc.2008.11.004

Rinnerthaler, M., Bischof, J., Streubel, M. K., Trost, A., and Richter, K. (2015). Oxidative stress in aging human skin. *Biomolecules* 5, 545–589. doi: 10.3390/biom5020545

Sepulveda, M. R., Marcos, D., Berrocal, M., Raeymaekers, L., Mata, A. M., and Wuytack, F. (2008). Activity and localization of the secretory pathway Ca^{2+}-ATPase isoform 1 (SPCA1) in different areas of the mouse brain during postnatal development. *Mol. Cell. Neurosci.* 38, 461–473. doi: 10.1016/j.mcn.2008.02.012

Sepulveda, M. R., Vanoevelen, J., Raeymaekers, L., Mata, A. M., and Wuytack, F. (2009). Silencing the SPCA1 (secretory pathway Ca^{2+}-ATPase isoform 1) impairs Ca^{2+} homeostasis in the Golgi and disturbs neural polarity. *J. Neurosci.* 29, 12174–12182. doi: 10.1523/JNEUROSCI.2014-09.2009

Shull, G. E., Miller, M. L., and Prasad, V. (2011). Secretory pathway stress responses as possible mechanisms of disease involving Golgi Ca^{2+} pump dysfunction. *BioFactors* 37, 150–158. doi: 10.1002/biof.141

Singh, S., Powell, D. W., Rane, M. J., Millard, T. H., Trent, J. O., Pierce, W. M., et al. (2003). Identification of the p16-Arc subunit of the Arp 2/3 complex as a substrate of MAPK-activated protein kinase 2 by proteomic analysis. *J. Biol. Chem.* 278, 36410–36417. doi: 10.1074/jbc.M306428200

Sudbrak, R., Brown, J., Dobson-Stone, C., Carter, S., Ramser, J., White, J., et al. (2000). Hailey-Hailey disease is caused by mutations in ATP2C1 encoding a novel Ca(2+) pump. *Hum. Mol. Genet.* 9, 1131–1140. doi: 10.1093/hmg/9.7.1131

von Blume, J., Alleaume, A. M., Cantero-Recasens, G., Curwin, A., Carreras-Sureda, A., Zimmermann, T., et al. (2011). ADF/cofilin regulates secretory cargo sorting at the TGN via the Ca^{2+} ATPase SPCA1. *Dev. Cell* 20, 652–662. doi: 10.1016/j.devcel.2011.03.014

von Blume, J., Alleaume, A. M., Kienzle, C., Carreras-Sureda, A., Valverde, M., and Malhotra, V. (2012). Cab45 is required for Ca(2+)-dependent secretory cargo sorting at the trans-Golgi network. *J. Cell Biol.* 199, 1057–1066. doi: 10.1083/jcb.201207180

Wang, B., Xie, H. F., Li, W. Z., Huang, Y. X., Shi, W., Jian, D., et al. (2015). Asymmetrical dimethylarginine promotes the senescence of human skin fibroblasts via the activation of a reactive oxygen species-p38 MAPK-microRNA-138 pathway. *J. Dermatol. Sci.* 78, 161–164. doi: 10.1016/j.jdermsci.2015.02.019

Wang, X., Bi, Z., Chu, W., and Wan, Y. (2005). IL-1 receptor antagonist attenuates MAP kinase/AP-1 activation and MMP1 expression in UVA-irradiated human fibroblasts induced by culture medium from UVB-irradiated human skin keratinocytes. *Int. J. Mol. Med.* 16, 1117–1124. doi: 10.3892/ijmm.16.6.1117

Whitmarsh, A. J., and Davis, R. J. (1996). Transcription factor AP-1 regulation by mitogen-activated protein kinase signal transduction pathways. *J. Mol. Med.* 74, 589–607. doi: 10.1007/s001090050063

Xie, H., Liu, F., Liu, L., Dan, J., Luo, Y., Yi, Y., et al. (2013). Protective role of AQP3 in UVA-induced NHSFs apoptosis via Bcl2 up-regulation. *Arch. Dermatol. Res.* 305, 397–406. doi: 10.1007/s00403-013-1324-y

Yaar, M., and Gilchrest, B. A. (2007). Photoageing: mechanism, prevention and therapy. *Br. J. Dermatol.* 157, 874–887. doi: 10.1111/j.1365-2133.2007.08108.x

Zheng, J., Lai, W., Zhu, G., Wan, M., Chen, J., Tai, Y., et al. (2013). 10-Hydroxy-2-decenoic acid prevents ultraviolet A-induced damage and matrix metalloproteinases expression in human dermal fibroblasts. *J. Eur. Acad. Dermatol. Venereol.* 27, 1269–1277. doi: 10.1111/j.1468-3083.2012.04707.x

Conflict of Interest: The authors declare that the research was conducted in the absence of any commercial or financial relationships that could be construed as a potential conflict of interest.

frontiers in Cell and Developmental Biology

ORIGINAL RESEARCH
published: 05 July 2021
doi: 10.3389/fcell.2021.672571

Connexin26 Modulates the Radiosensitivity of Cutaneous Squamous Cell Carcinoma by Regulating the Activation of the MAPK/NF-κB Signaling Pathway

Minqiong Sun[1†], Yuan Li[1†], Jing Qian[1], Siwei Ding[1], Mingyu Sun[1,2], Bowen Tan[1] and Ye Zhao[1]*

[1] Teaching and Research Section of Nuclear Medicine, School of Basic Medical Sciences, Anhui Medical University, Hefei, China, [2] Center of Medical Physics and Technology, Hefei Institutes of Physical Science, Chinese Academy of Sciences, Hefei, China

OPEN ACCESS

Edited by:
Daoxiang Zhang, Washington University in St. Louis, United States

Reviewed by:
Cuige Zhu, Washington University School of Medicine in St. Louis, United States
Zhonghua Wei, Shanghai Jiao Tong University, China

***Correspondence:**
Ye Zhao
zhaoye@ahmu.edu.cn
orcid.org/0000-0003-1384-6024

† These authors have contributed equally to this work and share first authorship

Specialty section:
This article was submitted to Cell Death and Survival, a section of the journal Frontiers in Cell and Developmental Biology

Received: *26 February 2021*
Accepted: *27 May 2021*
Published: *05 July 2021*

Citation:
Sun M, Li Y, Qian J, Ding S, Sun M, Tan B and Zhao Y (2021) Connexin26 Modulates the Radiosensitivity of Cutaneous Squamous Cell Carcinoma by Regulating the Activation of the MAPK/NF-κB Signaling Pathway. Front. Cell Dev. Biol. 9:672571. doi: 10.3389/fcell.2021.672571

Previous studies have confirmed that the gap junction protein Connexin26 (Cx26) is specifically expressed in human skin tissue. Cx26 can transmit radiation-induced damage signals. However, no study has yet reported whether Cx26 expression affects the radiosensitivity of human skin squamous cancer cells or the mechanism by which this occurs. In this study, we found that human skin squamous cell carcinoma cells (A431 cells) expressed significantly more Cx26 and were more sensitive to radiation compared to normal human keratinocytes (HaCaT cells). Knockdown of Cx26 in A431 cells ($A431^{Cx26-/-}$) decreased radiosensitivity relative to control cells and altered the expression of key proteins in the MAPK and NF-κB signaling pathways. These results demonstrate that Cx26 expression might play an important role in mediating radiation damage in A431 cells and could serve as a potential target for clinical radiotherapy for cutaneous squamous cell carcinoma.

Keywords: Connexin 26, cutaneous squamous cell carcinoma, radiosensitivity, MAPK/NF-κB signaling pathway, radiotherapy

INTRODUCTION

Squamous cell carcinoma of the skin, also known as cutaneous squamous cell carcinoma (cSCC), is a common malignant tumor of the skin. It originates from malignant lesions of the epidermis or accessory keratinocytes of the skin. cSCC accounts for four-fifths of basal cell carcinomas. Epidemiological data indicate that the ratio of chronic squamous cell carcinoma to basal cell carcinoma has been increasing in recent years. Because hematologic and lymphoid metastases occur early on in disease progression, approximately 5% of high-risk cSCC patients exhibit distant metastases at the time of diagnosis (Di et al., 2001). Although surgery is the first treatment choice for cSCC, radiotherapy is still useful in certain patients with unresectable tumors (Waldman and Schmults, 2019). Furthermore, adjuvant radiotherapy is widely used after surgery to improve therapeutic outcomes. Therefore, it is crucial to understand the mechanisms underlying the radiosensitivity of cSCC in order to improve the effects of radiotherapy for this disease.

Gap junction-mediated intercellular communication (GJIC) plays an important role in the coordination of normal keratinocyte differentiation. Connexins are expressed in the epidermis,

with Connexin26 (Cx26) specifically expressed in the basal layer of the epidermis (Sáez et al., 2005). Previous experimental results reported that overexpression of Cx26 in HeLa human cervical cancer cells ($HeLa^{Cx26+/+}$) significantly enhanced the ability of these cells to induce and transmit radiation damage relative to normal HeLa cells. Further, $HeLa^{Cx26+/+}$ cells displayed more rapid and intense radiation-induced bystander effects (RIBEs). Cx26 can interact with MLTK upstream of the MAPK signaling pathway, thereby affecting expression of the downstream molecules p38 and COX-2 (Zhao et al., 2014). In human normal skin keratinocytes (HaCaT cells), Cx26 expression levels affect both radiosensitivity and the activity of the MAPK and NF-κB signaling pathways.

Radiotherapy is a common treatment for cutaneous squamous cell carcinoma (cSCC); it has been used clinically for many years, and its efficacy is widely recognized. However, few studies have investigated the radiosensitivity of skin squamous cell carcinoma. In the present study, we used skin keratinocytes (HaCaT) and A431 cells to investigate the relationship between Cx26 and the radiosensitivity of skin squamous cell carcinoma cells as well as the mechanisms underlying the radiosensitivity of cSCC.

RESULTS

Cx26 Expression in Cutaneous Squamous Cell Carcinoma

First, western blotting was used to verify Cx26 expression levels in A431 and HaCaT cells. The results showed that A431 cells expressed more Cx26 than HaCaT cells under the same conditions (**Figure 1**, $p < 0.01$). This result provided a theoretical basis for our subsequent experiments. Previous studies have shown that Cx26 can mediate radiation damage, therefore we chose to further explore the differences in A431 and HaCaT radiation sensitivity.

Effects of Cx26 Expression on the Radiosensitivity of A431 Cells and HaCaT Cells

HaCaT and A431 cells were irradiated with X-rays at doses of 0, 1, 2, 3, and 5 Gy. 6 h and 24 h after irradiation, micronuclei formation and clone formation assays were performed. Our results revealed that the number of micronucleated HaCaT cells and A431 cells increased with increasing irradiation doses (**Figures 2A,B**). However, the number of micronuclei in A431 cells at 2 Gy, 3 Gy, and 5 Gy was significantly higher than that in HaCaT cells at the same doses (**Figures 2C,D**, $^{*}p < 0.05$, $^{**}p < 0.01$). The results also showed that the number of micronucleated cells was significantly lower at 24 h than at 6 h in both HaCaT cells and A431 cells. This was particularly true at the 3 Gy and 5 Gy doses ($^{**}p < 0.01$). In the clone formation experiments, the number of cloned cells was counted and used to calculate the fraction of surviving cells. The dose-survival curve was fitted using the multitarget model. In HaCaT cells and A431 cells, the clonal proliferation rate gradually decreased with increasing irradiation doses at both 6 and 24 h (**Figure 2E**). However, the dose-survival curve for A431 cells was lower than the curve for HaCaT cells at both 6 and 24 h (**Figure 2F**). These results showed that A431 cells were much more radiosensitive than HaCaT cells.

Validation of Cx26 Expression in A431 Cells Following Knockdown

To investigate the role of Cx26 in the radiosensitivity of A431 cells, the $A431^{Cx26-/-}$ cell line was constructed by transfecting parental A431 cells with the Cx26 CRISPR/Cas9 plasmid. An $A431^{vector}$ cell line was also constructed using an empty plasmid as a control. After transfection, protein expression was examined by western blotting. The results showed that the expression of Cx26 was significantly lower in $A431^{Cx26-/-}$ cells as compared with the control and wild-type cells (**Figure 3**, $^{**}p < 0.01$).

The effect of Cx26 Expression on the Radiosensitivity of A431 Cells

To measure the effects of Cx26 on the radiosensitivity of A431 cells, we performed micronuclei formation, CCK-8 proliferation and colony formation assays in A431, $A431^{vector}$ and $A431^{Cx26-/-}$ cells 6 and 24 h after irradiation. The results showed that micronuclei formation was lower in $A431^{Cx26-/-}$ cells at 2 Gy, 3 Gy, and 5 Gy compared with similarly treated A431 and $A431^{vector}$ cells (**Figures 4A,B**). In the clone formation experiment, the D_0 values of the $A431^{vector}$ and A431 cells were relatively close, while the D_0 value of the $A431^{Cx26-/-}$ cells was significantly higher than either of these (**Figures 4C–E**). The CCK-8 cell proliferation experiment results showed that the viability of $A431^{Cx26-/-}$ cells was significantly higher than that of the other two groups after 6 and 24 h irradiation. Further, radiation-induced damage was lower in $A431^{Cx26-/-}$ cells compared with $A431^{vector}$ and A431 cells even at increasing radiation doses (**Figures 4F,G**). These results suggested that $A431^{Cx26-/-}$ cells were less radiosensitive than the other two types of cells.

Cx26 Expression Affects the Radiation-Induced Activation of the MAPK and NF-κB Signaling Pathways in A431 Cells

A431, $A431^{vector}$, and $A431^{Cx26-/-}$ cells were X-ray irradiated with 0, 2, 3, and 5 Gy, as previously described. Treatment of A431 cells with increasing doses of irradiation altered expression of ERK but not p38. However, phospho-ERK and phospho-p38 protein expression levels were significantly increased in A431 cells after irradiation. Expression of phospho-ERK was significantly increased in A431 cells irradiated with 2 Gy, and 5 Gy compared to sham-irradiated cells (**Figures 5A,B**). Similarly, phospho-p38 expression was significantly higher in A431 cells after 5 Gy irradiation compared to sham-irradiated cells (**Figures 5C,D**). Expression of NF-κB, which is downstream of the MAPK signaling pathway, was increased in A431 cells irradiated with increasing doses, particularly 3 Gy and 5 Gy (**Figures 5E,F**). ERK and p38 protein expression was not significantly correlated with increased irradiation

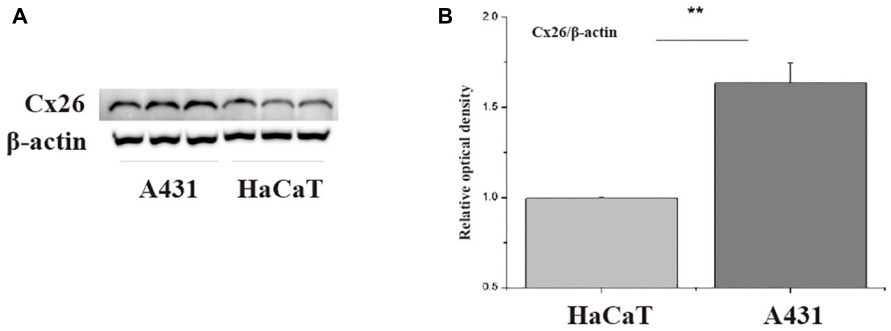

FIGURE 1 | Cx26 expression levels in A431 and HaCaT cells. **(A)** Cx26 expression levels in A431 and HaCaT cells. **(B)** Quantification of Cx26 expression in A431 and HaCaT cells. $^{**}p < 0.01$ between the two cell lines.

in A431$^{Cx26-/-}$ cells, however ERK expression levels were lower in A431$^{Cx26-/-}$ cells than in A431 cells and A431^{vector} cells. The p-ERK/ERK ratio was lower in 2 Gy-irradiated A431$^{Cx26-/-}$ cells compared to 2 Gy-irradiated A431^{vector} cells, however there was no significant difference at 3 Gy and 5 Gy (**Figures 5A,B**). In addition, the expression of ERK was lower in A431$^{Cx26-/-}$ cells compared with A431 and A431^{vector} cells. However, the expression of phospho-ERK was significantly lower in A431$^{Cx26-/-}$ cells than in A431 and A431^{vector} cells at 2 Gy and 5 Gy; this difference was statistically significant (**Supplementary Figure 2**). These results indicated that the expression of Cx26 influenced the expression and activation of ERK within the MAPK signaling pathway in A431 cells. The p-p38/p38 ratio was significantly lower in 5 Gy-irradiated A431$^{Cx26-/-}$ cells compared with similarly treated A431 cells and A431^{vector} cells (**Figures 5C,D**). Moreover, NF-κB protein expression in A431$^{Cx26-/-}$ cells did not vary according to radiation dose but was significantly lower than in 5 Gy-irradiated A431 cells (**Figures 5E,F**). In addition, we also verified the nuclear accumulation of NF-κB (p65) in A431 and A431$^{Cx26-/-}$ cells after irradiation. Using an immunofluorescence assay, we found that the nuclear accumulation of p65 was significantly higher in 5 Gy-irradiated A431 cells than in either sham-irradiated A431 cells or 5 Gy-irradiated A431$^{Cx26-/-}$ cells (**Supplementary Figure 1**). These results suggested that after irradiation, the expression of proteins involved in the MAPK and downstream NF-κB signaling pathways was affected by Cx26 expression levels.

DISCUSSION

The gap junction is the contact area between adjacent cells, which can allow for the exchange and interaction of some ions and other small molecules between adjacent cells. Therefore, gap junctions play an important role in intercellular communication and are widely found in various vertebrate tissues. Interstitial junctions are expressed throughout the body and are involved in many processes necessary for normal physiological functions. An increasing number of studies have shown that interstitial junction proteins, which are the main protein unit comprising interstitial junctions, are closely related to several human diseases. The half-channel of the gap junction protein can also function on the non-gap junction membrane, allowing for the exchange of solute with the extracellular space (Richard, 2000; Sáez et al., 2005).

Gap junction-mediated intercellular communication (GJIC) plays an important role in the differentiation and coordination of epidermal keratinocytes. In rodent skin, intercellular communication is highly regulated and is mediated by at least nine different junction proteins, including Cx30, Cx30.3, Cx31, Cx26, and Cx31.1 (Richard, 2000). Among these gap junction proteins, studies have shown that mutations in Cx26 occur more frequently in human populations (Lee and White, 2009). The results of a previous study of skin diseases also showed that Cx26-mediated intercellular communication plays an important role in regulating the radiation-induced bystander effect (RIBE) between neighboring cells after irradiation. In addition, some studies have concluded that the main roles of Cx26 in GJIC are to transmit radiation damage signals, stimulate radiation-induced bystander effects, and cause irradiated cells to produce more obvious radiation damage effects, thus aggravating the DNA radiation damage response. Each of these functions could potentially be co-opted to achieve our therapeutic goals in a clinical setting (Matesic et al., 1994; Richard, 2000; Apps et al., 2009; Lee and White, 2009).

In this study, we mainly investigated the effects of Cx26 expression levels on the radiosensitivity of cutaneous squamous cell carcinoma cells. We found that Cx26 expression was significantly higher in human skin squamous cell carcinoma cells (A431 cells) than in normal skin keratinocytes (HaCaT cells). Further, the radiosensitivity of A431 cells was significantly higher than that in HaCaT cells. These results suggested that skin squamous cell carcinoma may be more radiosensitive than the epidermis of normal human skin. We further explored whether the difference in radiosensitivity between these two types of cells was related to Cx26 expression levels. A431$^{Cx26-/-}$ cells were constructed using a CRISPR/Cas9 plasmid, and control A431^{vector} cells were constructed using an empty vector. Our results showed that A431$^{Cx26-/-}$ cells were significantly less radiosensitive than A431 cells and A431^{vector} cells.

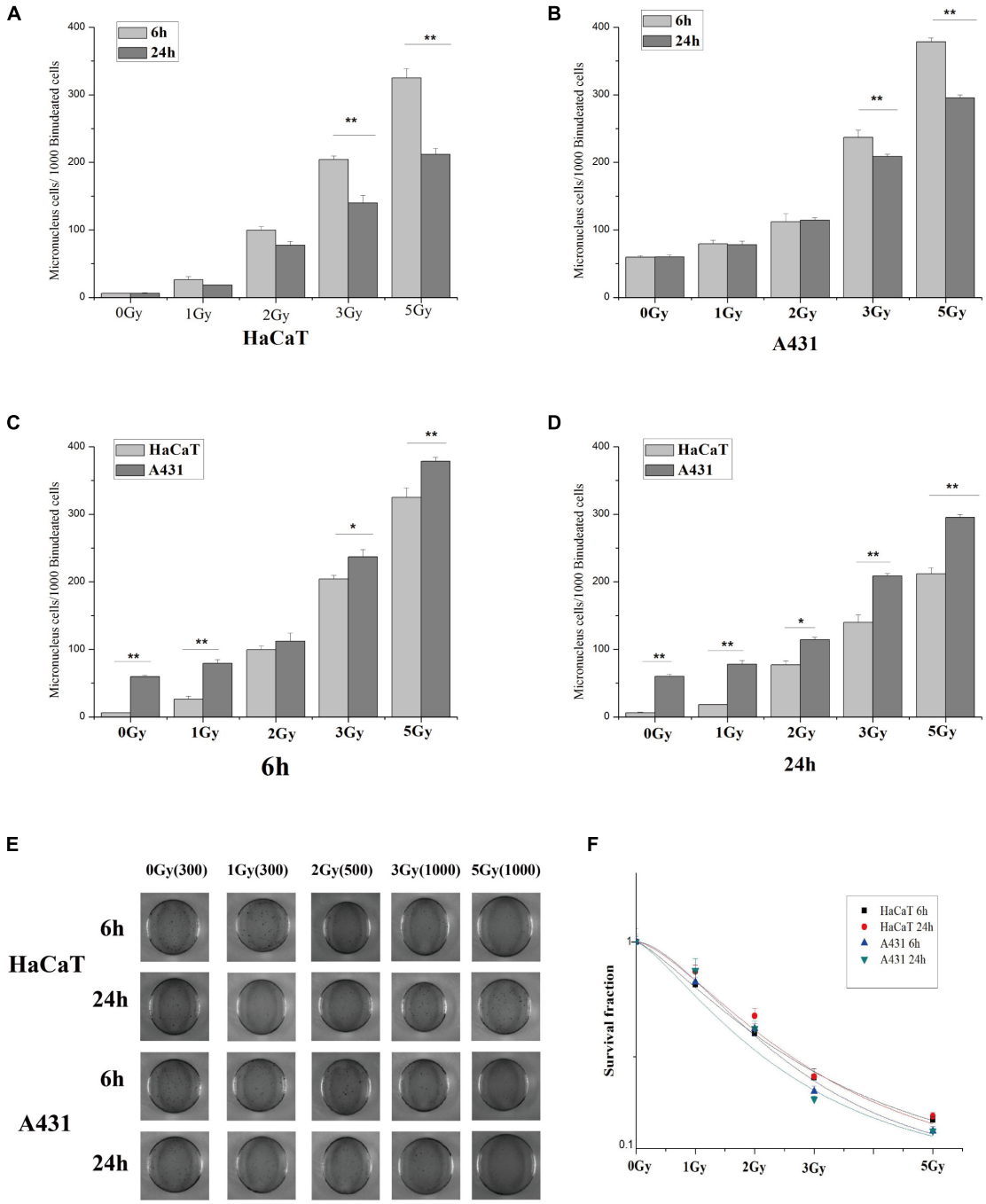

FIGURE 2 | Statistical analysis and schematic diagrams of micronuclei and clone formation assays in irradiated A431 and HaCaT cells. **(A)** Comparison of micronuclei formation in HaCaT cells 6 and 24 h after irradiation. **(B)** Comparison of micronuclei formation in A431 cells 6 and 24 h after irradiation. **(C)** Comparison of micronuclei formation in HaCaT and A431 cells 6 h after irradiation. **(D)** Comparison of micronuclei formation in HaCaT and A431 cells 24 h after irradiation. **(E)** Schematic diagram showing micronuclei formation in HaCaT and A431 cells 6 and 24 h after irradiation. **(F)** Dose-survival curves for HaCaT and A431 cells 6 and 24 h after irradiation. D_0 (HaCaT 6 h) = 2.84403, N = 1.32932; D_0 (HaCaT 24 h) = 2.49758, N = 1.6035; D_0 (A431 6 h) = 2.10442, N = 1.82945; D_0 (A431 24 h) = 2.29352, N = 1.38693. $^*p < 0.05$, $^{**}p < 0.01$ between the two cell lines.

We also detected activation of the MAPK and NF-κB signaling pathways in $A431^{Cx26-/-}$, $A431^{vector}$ and A431 cells after irradiation. The downstream modulators of the MAPK signaling pathway, including ERK1/2, $p38^{MAPK}$ and c-Jun amino-terminal kinase (JNK), have been thoroughly described (Kim, 2009). ERK1/2 is mainly activated by growth factors or mitogens, leading to cell differentiation, growth and survival, while JNK and p38 are mainly activated by oxidative stress

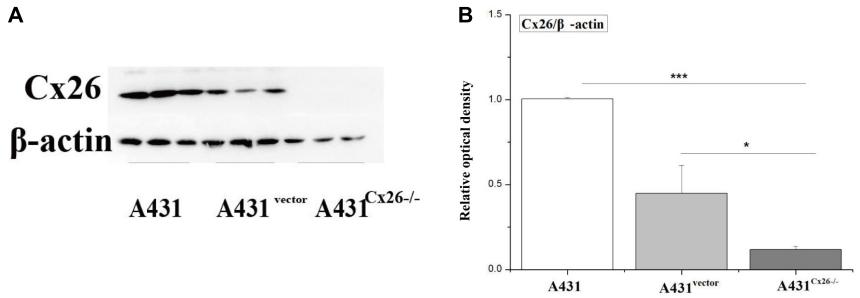

FIGURE 3 | Expression of Cx26 in A431, A431^{vector}, and A431$^{Cx26-/-}$ cells. **(A)** Cx26 expression levels in A431, A431^{vector}, and A431$^{Cx26-/-}$ cells. **(B)** Quantification of Cx26 expression in A431, A431^{vector}, and A431$^{Cx26-/-}$ cells. ***$p < 0.001$, *$p < 0.05$ between each cell line.

and cytokines, leading to inflammation and apoptosis (Fan and Chambers, 2001). However, certain stimuli can cause the simultaneous activation of all three proteins. Previous studies have shown that the MAPK signaling pathway plays a role in GJIC (Rummel et al., 1999; Wada and Penninger, 2004; Kim, 2009). Differential expression of various pathway proteins can affect gene expression and cell survival and death (Upham et al., 1997; Richard, 2000; Ruch et al., 2001; Rabionet et al., 2002; Kim et al., 2009). Within the MAPK signaling pathway, the key proteins we observed, including ERK and p38, play an important role in the processes of cell proliferation, differentiation and apoptosis (Matesic et al., 1994; Hwang et al., 2005; Kim, 2009). Previous studies have shown that ERK1/2, p38^{MAPK} and JNK are significantly enhanced in the common skin disease psoriasis. Indeed, H_2O_2 can enter keratinocytes through aquaporin 3, activating the NF-κB signaling pathway and thus participating in the development of psoriasis. This signaling pathway further drives the formation of Th1, Th17, and keratinocytes and promotes the accumulation of inflammatory cytokines and vascular endothelial growth factor, ultimately leading to skin damage (Xu et al., 2019). Currently, there has been no specific research in this field devoted to cutaneous squamous cell carcinoma. In this study, we used GJIC-mediated radiation injury to investigate the effects of Cx26 expression on radiation sensitivity and apoptosis-related signaling pathways in A431 cells. We found that the expression of ERK was reduced in A431$^{Cx26-/-}$ cells, but the expression of p38 and NF-κB (p65) was not significantly altered. Therefore, we speculated that ERK expression would be affected by Cx26 knockout in A431 cells. Our results showed that phospho-ERK, phospho-p38 and p65 expression levels were significantly lower in A431$^{Cx26-/-}$ cells than in A431 or A431^{vector} cells after irradiation. The nuclear accumulation of p65 protein was also significantly higher in irradiated A431 cells than in irradiated A431$^{Cx26-/-}$ cells. Therefore, expression of the Cx26 protein may play an important role in the regulation of the MAPK signaling pathway and the downstream NF-κB signaling pathway in A431 cells, thus affecting cell proliferation and apoptosis.

Based on the results of this study, we believe that Cx26 can transmit radiation damage signals in A431 cells and that A431 cells are highly sensitive to radiation. However, additional studies should be performed to address the relevance of this finding for the treatment of cutaneous squamous cell carcinoma. Specifically, future research should investigate how to apply radiotherapy to cancer patients to improve the anti-tumor effects and to reduce the recurrence and mortality rates of patients.

MATERIALS AND METHODS

Cell Culture

The human immortalized keratinocyte cell line HaCaT and human skin squamous cell line A431 were gifted by the Cell Bank of Shanghai, Chinese Academy of Sciences. The A431$^{Cx26-/-}$ cell line was generated *via* transfection of A431 cells with a Cx26 knockout CRISPR/Cas9 plasmid. The A431^{vector} cell line was constructed by transfecting A431 cells with an empty plasmid. HaCaT and A431 cells were cultured in high glucose DMEM (Gibco, Grand Island, NY, United States) containing 10% FBS. A431$^{Cx26-/-}$ and A431^{vector} cells were cultured in high glucose DMEM containing 10% FBS and 1 μg/ml puromycin. All cells were incubated at 37°C in a humidified atmosphere containing 95% air and 5% carbon dioxide.

Western Blot

Cells in each treatment group were scraped off the culture dishes and lysed in lysis buffer containing 10% glycerol, 10 mM Tris–HCl (pH 6.8), 1% sodium dodecyl sulfate (SDS), 5 mM dithiothreitol (DTT), and 1 × complete protease inhibitor cocktail (Sigma-Aldrich). The concentration of proteins in the supernatant were quantified and then 20 μg of each protein sample was separated on 12% SDS-polyacrylamide gels. The separated proteins were transferred to a polyvinylidene difluoride membrane and blocked for 1 h at room temperature in 5% skim milk in Tris-buffered saline (TBS) containing 0.1% Tween-20. Then, the membrane was incubated overnight at 4°C with primary antibody. The primary monoclonal antibodies used were: anti-Connexin26, anti-ERK1/2, anti-phospho-ERK1/2, anti-p38, anti-phospho-p38, and anti-NF-κB (Cell Signaling Technology, Beverly, MA, United States). After exposure, the relative optical density of the bands was analyzed in ImageJ. The data were normalized and statistically analyzed using SPSS and plotted using Origin 8.0.

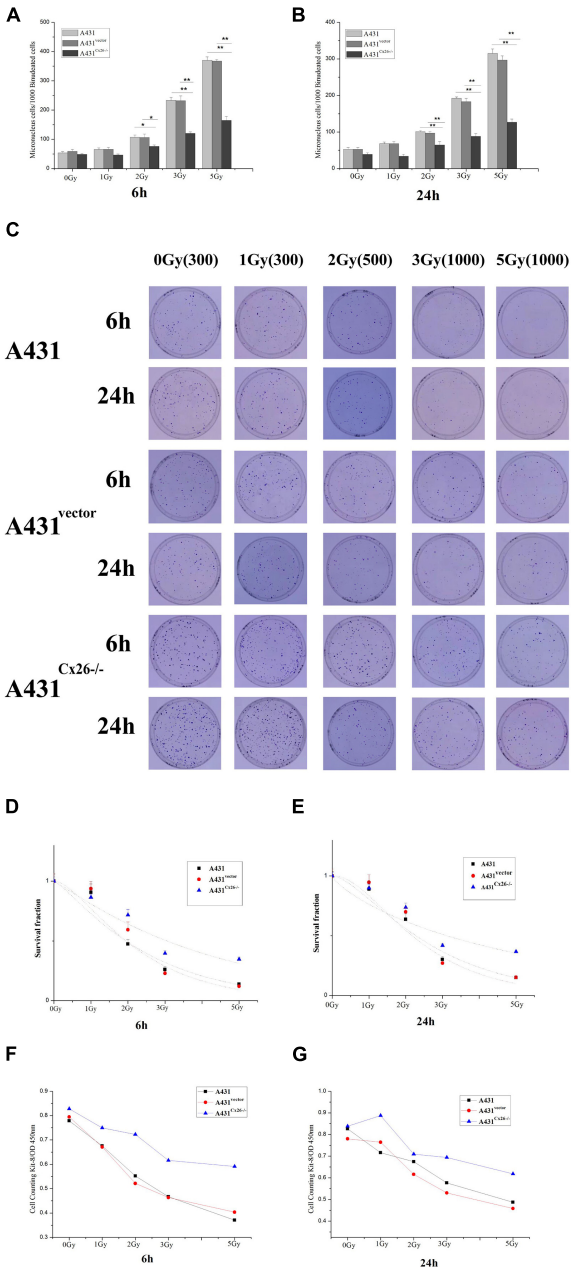

FIGURE 4 | Micronuclei and colony formation assays in irradiated A431, A431^{vector}, and A431$^{Cx26-/-}$ cells. **(A)** Statistical analysis of micronuclei formation in A431, A431^{vector}, and A431$^{Cx26-/-}$ cells 6 h after irradiation. **(B)** Statistical analysis of micronuclei formation in A431, A431^{vector}, and A431$^{Cx26-/-}$ cells 24 h after irradiation. **(C)** Quantification of clone formation in A431, A431^{vector}, and A431$^{Cx26-/-}$ cells 6 and 24 h after irradiation. **(D)** Dose-survival curves for A431, A431^{vector}, and A431$^{Cx26-/-}$ cells 6 h after irradiation; D_0 (A431 6 h) = 2.2214, N = 1.2845; D_0 (A431^{vector} 6 h) = 1.6945, N = 1.8206; D_0 (A431$^{Cx26-/-}$ 6 h) = 4.0250, N = 1.0966. **(E)** Dose-survival curves for A431, A431^{vector}, and A431$^{Cx26-/-}$ cells 24 h after irradiation, D_0 (A431 24 h) = 2.0667, N = 1.7154; D_0 (A431^{vector} 24 h) = 1.5955, N = 2.3482; D_0 (A431$^{Cx26-/-}$ 24 h) = 5.9810, N = 0.7704. **(F)** OD values for A431, A431^{vector}, and A431$^{Cx26-/-}$ cells 6 h after irradiation, as detected by CCK-8 assay. **(G)** OD values for A431, A431^{vector}, and A431$^{Cx26-/-}$ cells 24 h after irradiation, as detected by CCK-8 assay. *p<0.05, **p<0.01 between each cell line.

Plasmid Transfection

Cells were transfected with a mixture of Connexin26 Double Nickase Plasmid (h) (sc-402132-NIC, Santa Cruz Biotechnology, Inc., United States), transfection reagent and transfection medium (Santa Cruz Biotechnology, Inc., United States) in a certain proportion. The plasmid targets the following gene sequences for knockout: (A) tcgcattatgatcctcgttg and (B) gagccagatctttccaatgc. Then, the most effective concentration of puromycin was determined through a preliminary experiment. After 1–2 weeks of screening, monoclones were cultured for 10–14 days. The monoclones were removed and placed into 24-well plates and successfully transfected cells were selected with puromycin. Finally, the cells were amplified to form stable cell lines.

Micronuclei Formation Assay

Micronuclei, a form of chromosomal damage that arises mainly from DNA double-strand breaks, were evaluated using the cytokinesis block technique. After irradiation, the cells were hydrolyzed with trypsin at intervals of 6 and 24 h. A total of 50,000 cells were seeded in a 35 mm dish and cultured in high glucose DMEM containing 10% FBS. After cell attachment, the medium was changed, and cytochalasin B (Sigma) was added at a final concentration of 2.5 μg/ml. After 48 h, the cells were fixed with anhydrous ethanol and stained with acridine orange for cell counting. At least 1,000 binucleated cells were examined in each dish.

Proliferation Assay

The prepared cells were irradiated with 0, 1, 2, 3, or 5 Gy and then incubated for 6 or 24 h. Cells were seeded in 60 mm dishes according to the radiation dose received. The dishes were kept in an incubator for 10–12 days to allow for colony formation. Then, cells were fixed with anhydrous ethanol for 30 min and stained with 0.1% crystal violet solution for 2–3 h. The data were collected and analyzed in Excel to obtain the cell survival score. Then, the dose-survival curve was fitted and the D_0 value obtained using Origin8.0.

CCK-8 Cell Proliferation Assay

Approximately 2,000 cells were plated into each well of a 96-well plate. After stabilization, X-ray irradiation was performed at doses of 0, 1, 2, 3, and 5 Gy. After irradiation, cells were incubated for 6 or 24 h. Then, cells were incubated with 20 μl CCK-8 solution for 1.5 h. The absorbance value was measured at 450 nm using a microplate reader.

Immunofluorescence Assay

The cells were X-ray irradiated and incubated at 37°C for 6 h. Then, the cells were washed with PBS and fixed with 4% paraformaldehyde solution. Cells were then incubated with 0.3% Triton in PBS for 30 min and blocked with 1% goat serum. Then, the cells were incubated overnight in the primary antibody. The next day, the primary antibody solution was washed off. The cells were washed 3 × 5 min with PBST and then incubated with the secondary antibody for 2 h. Then, the cells were

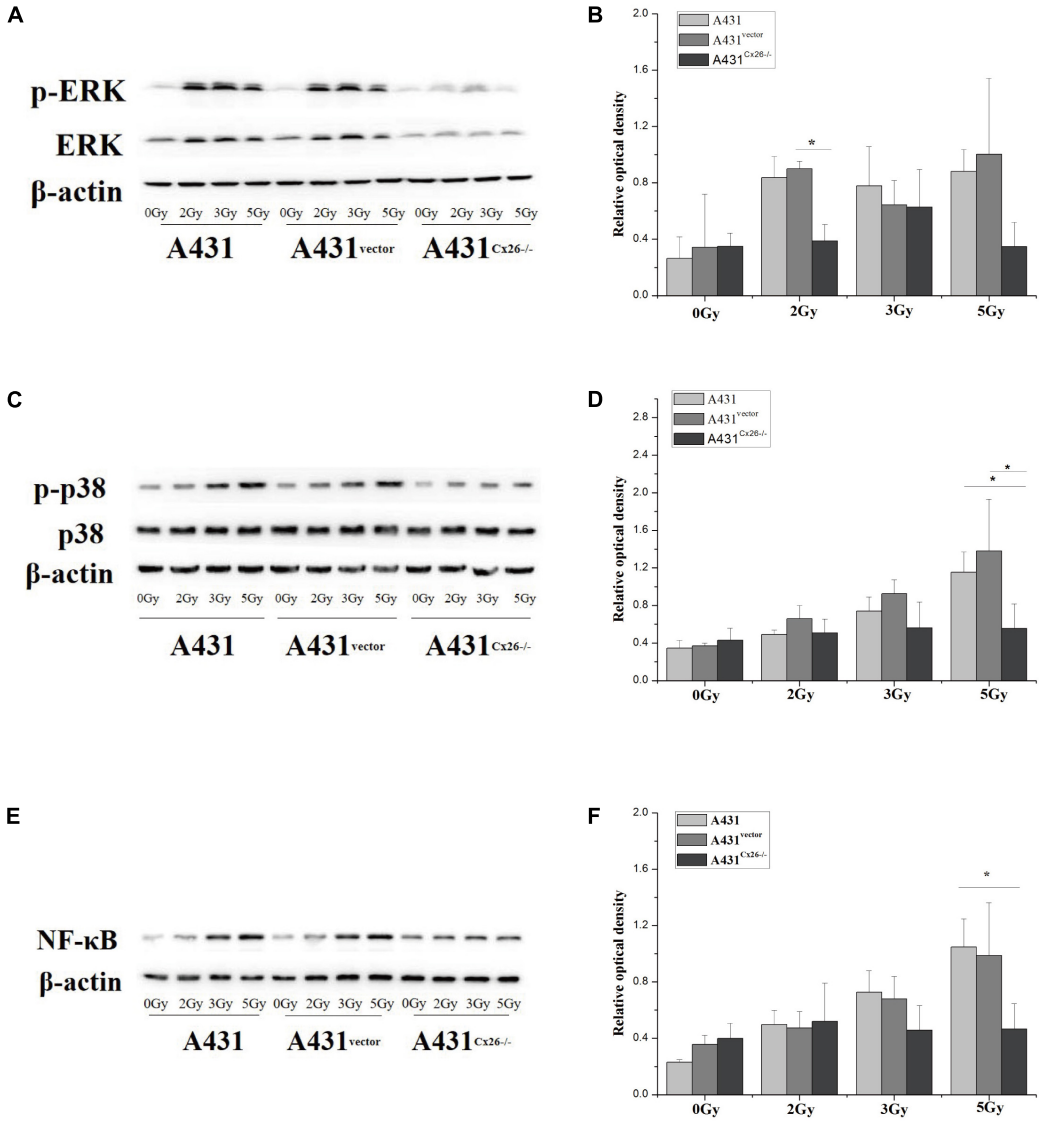

FIGURE 5 | Activation of the MAPK and NF-κB signaling pathways in A431, A431^{vector}, and A431$^{Cx26-/-}$ cells after irradiation. **(A)** p-ERK/ERK expression in irradiated A431, A431^{vector}, and A431$^{Cx26-/-}$ cells. **(B)** Quantification of p-ERK/ERK expression in irradiated A431, A431^{vector}, and A431$^{Cx26-/-}$ cells. **(C)** Expression of p-p38/p38 in irradiated A431, A431^{vector}, and A431$^{Cx26-/-}$ cells. **(D)** Quantification of p-p38/p38 expression in irradiated A431, A431^{vector}, and A431$^{Cx26-/-}$ cells. **(E)** NF-κB expression in irradiated A431, A431^{vector}, and A431$^{Cx26-/-}$ cells. **(F)** Quantification of NF-κB expression in irradiated A431, A431^{vector}, and A431$^{Cx26-/-}$ cells. *$p < 0.05$ between each cell line.

stained with the nuclear dye Hoechst 33342 (Sigma). Finally, fluorescence microscopy was performed, and images were taken at random in each dish.

Statistical Analyses

Data were statistically analyzed using SPSS software. The independent sample *t*-test was used for comparisons between two groups. Comparisons between multiple groups were performed using one-way analysis of variance $p < 0.05$. A value of $p < 0.05$ was considered to be statistically significant. All experiments in this study were performed in both technical and biological triplicate.

DATA AVAILABILITY STATEMENT

The original contributions presented in the study are included in the article/**Supplementary Material**, further inquiries can be directed to the corresponding author/s.

AUTHOR CONTRIBUTIONS

YZ conceived this study and designed. MQS and YL conducted the main experiments. JQ, SD, MYS, and BT also conducted some experiments. MQS and YL analyzed the experimental data. MQS

and YZ prepared the manuscript. All authors contributed to the article and approved the submitted version.

FUNDING

This study was supported by the National Natural Science Foundation of China (Grant No. 81673099, 31600680, 31670860, and 31800702) and the State Key Laboratory of Nuclear Physics and Technology, Peking University (Grant No. NPT2020KFY19).

SUPPLEMENTARY MATERIAL

The Supplementary Material for this article can be found online at: https://www.frontiersin.org/articles/10.3389/fcell.2021.672571/full#supplementary-material

REFERENCES

Apps, S. A., Rankin, W. A., and Kurmis, A. P. (2009). Connexin 26 mutations in autosomal recessive deafness disorders: a review. *Int. J. Audiol.* 46, 75–81. doi: 10.1080/14992020600582190

Di, W., Common, J. E. A., and Elsell, D. P. (2001). Connexin 26 expression and mutation analysis in epidermal disease. *Cell Commun. Adhes.* 8, 415–418. doi: 10.3109/15419060109080763

Fan, M., and Chambers, T. C. (2001). Role of mitogen-activated protein kinases in the response of tumor cells to chemotherapy. *Drug Resist. Updat.* 4, 253–267. doi: 10.1054/drup.2001.0214

Hwang, J. W., Park, J. S., Jo, E. H., Kim, S. J., Yoon, B. S., and Kim, S. H. (2005). Chinese cabbage extracts and sulforaphane can protect H2O2-induced inhibition of gap junctional intercellular communication through the inactivation of ERK1/2 and p38 MAP kinases. *J. Agric. Food Chem.* 21, 8205–8510. doi: 10.1021/jf051747h

Kim, J. S., Ha, T. Y., Ahn, J., Kim, H. K., and Kim, S. (2009). Pterostilbene from Vitis coignetiae protect H2O2-induced inhibition of gap junctional intercellular communication in rat liver cell line. *Food Chem. Toxicol.* 2009, 404–409. doi: 10.1016/j.fct.2008.11.038

Kim, J.-S. (2009). MAPK and mTOR pathways are involved in cadmium-induced neuronal apoptosis. *Food Chem. Toxicol.* 2, 404–409.

Lee, J. R., and White, T. W. (2009). Connexin-26 mutations in deafness and skin disease. *Expert Rev. Mol. Med.* 11:e35.

Matesic, D. F., Rupp, H. L., Bonney, W. J., and Di, W. L. (1994). Changes in gap-junction permeability, phosphorylation, and number mediated by phorbol ester and non-phorbol-ester tumor promoters in rat liver epithelial cells. *Mol. Carcinog.* 4, 226–236. doi: 10.1002/mc.2940100407

Rabionet, R., López-Bigas, N., Arbonès, M. L., and Estivill, X. (2002). Connexin mutations in hearing loss. *TRENDS Mol. Med.* 5, 205–211.

Richard, G. (2000). Connexins: a connection with the skin. *Exp. Dermatol.* 9, 77–96. doi: 10.1034/j.1600-0625.2000.009002077.x

Ruch, R. J., Trosko, J. E., and Madhukar, B. V. (2001). Inhibition of connexin43 gap junctional intercellular communication by TPA requires ERK activation. *J. Cell Biochem.* 1, 163–169. doi: 10.1002/jcb.1227

Rummel, A. M., Trosko, J. E., Wilson, M. R., and Upham, B. L. (1999). Polycyclic aromatic hydrocarbons with bay-like regions inhibited gap junctional intercellular communication and stimulated MAPK activity. *Toxicol. Sci.* 2, 232–240. doi: 10.1093/toxsci/49.2.232

Sáez, J. C., Retamal, M. A., Basilio, D., Bukauskas, F. F., and Bennett, M. V. (2005). Connexin-based gap junction hemichannels: gating mechanisms. *Biochim. Biophys. Acta Biomembr.* 1711, 215–224. doi: 10.1201/9781315369396-10

Upham, B. L., Kang, K. S., Cho, H. Y., and Trosko, J. E. (1997). Hydrogen peroxide inhibits gap junctional intercellular communication in glutathione sufficient but not glutathione deficient cells. *Carcinogenesis* 18, 37–42. doi: 10.1093/carcin/18.1.37

Wada, T., and Penninger, J. M. (2004). Mitogen-activated protein kinases in apoptosis regulation. *Oncogene* 16, 2838–2849. doi: 10.1038/sj.onc.1207556

Waldman, A., and Schmults, C. (2019). Cutaneous squamous cell carcinoma. *Hematol. Oncol. Clin. North Am.* 33, 1–12.

Xu, F., Xu, J., Xiong, X., and Deng, Y. (2019). Salidroside inhibits MAPK, NF-κB, and STAT3 pathways in psoriasis-associated oxidative stress via SIRT1 activation. *Redox Rep.* 24, 70–74. doi: 10.1080/13510002.2019.1658377

Zhao, Y., de Toledo, S. M., Hu, G., Hei, T. K., and Azzam, E. I. (2014). Connexins and cyclooxygenase-2 crosstalk in the expression of radiation-induced bystander effects. *Br. J. Cancer* 111, 125–131. doi: 10.1038/bjc.2014.276

Conflict of Interest: The authors declare that the research was conducted in the absence of any commercial or financial relationships that could be construed as a potential conflict of interest.

frontiers in Cell and Developmental Biology

REVIEW
published: 10 August 2021
doi: 10.3389/fcell.2021.671698

An Insight Into the Mechanism of Plant Organelle Genome Maintenance and Implications of Organelle Genome in Crop Improvement: An Update

*Kalyan Mahapatra†, Samrat Banerjee†, Sayanti De‡, Mehali Mitra‡, Pinaki Roy and Sujit Roy**

Department of Botany, UGC Center for Advanced Studies, The University of Burdwan, Burdwan, India

OPEN ACCESS

Edited by:
Guoping Zhao,
Hefei Institutes of Physical Science (CAS), China

Reviewed by:
Malgorzata Anna Garstka,
Xi'an Jiaotong University, China
Anita Mukherjee,
University of Calcutta, India

***Correspondence:**
Sujit Roy
sujitroy2006@gmail.com

†*These authors share first authorship*

‡*These authors have contributed equally to this work*

Specialty section:
This article was submitted to Cell Death and Survival, a section of the journal Frontiers in Cell and Developmental Biology

Received: *24 February 2021*
Accepted: *21 July 2021*
Published: *10 August 2021*

Citation:
Mahapatra K, Banerjee S, De S, Mitra M, Roy P and Roy S (2021) An Insight Into the Mechanism of Plant Organelle Genome Maintenance and Implications of Organelle Genome in Crop Improvement: An Update. Front. Cell Dev. Biol. 9:671698. doi: 10.3389/fcell.2021.671698

Besides the nuclear genome, plants possess two small extra chromosomal genomes in mitochondria and chloroplast, respectively, which contribute a small fraction of the organelles' proteome. Both mitochondrial and chloroplast DNA have originated endosymbiotically and most of their prokaryotic genes were either lost or transferred to the nuclear genome through endosymbiotic gene transfer during the course of evolution. Due to their immobile nature, plant nuclear and organellar genomes face continuous threat from diverse exogenous agents as well as some reactive by-products or intermediates released from various endogenous metabolic pathways. These factors eventually affect the overall plant growth and development and finally productivity. The detailed mechanism of DNA damage response and repair following accumulation of various forms of DNA lesions, including single and double-strand breaks (SSBs and DSBs) have been well documented for the nuclear genome and now it has been extended to the organelles also. Recently, it has been shown that both mitochondria and chloroplast possess a counterpart of most of the nuclear DNA damage repair pathways and share remarkable similarities with different damage repair proteins present in the nucleus. Among various repair pathways, homologous recombination (HR) is crucial for the repair as well as the evolution of organellar genomes. Along with the repair pathways, various other factors, such as the MSH1 and WHIRLY family proteins, WHY1, WHY2, and WHY3 are also known to be involved in maintaining low mutation rates and structural integrity of mitochondrial and chloroplast genome. SOG1, the central regulator in DNA damage response in plants, has also been found to mediate endoreduplication and cell-cycle progression through chloroplast to nucleus retrograde signaling in response to chloroplast genome instability. Various proteins associated with the maintenance of genome stability are targeted to both nuclear and organellar compartments, establishing communication between organelles as well as organelles and nucleus. Therefore, understanding the mechanism of DNA damage repair and inter compartmental crosstalk mechanism in various sub-cellular organelles

following induction of DNA damage and identification of key components of such signaling cascades may eventually be translated into strategies for crop improvement under abiotic and genotoxic stress conditions. This review mainly highlights the current understanding as well as the importance of different aspects of organelle genome maintenance mechanisms in higher plants.

Keywords: crop improvement, DNA damage response, homologous recombination, MSH1, organelle genome, retrograde signaling, SOG1, WHIRLY family proteins

INTRODUCTION

In plants, mitochondria and chloroplast are double membrane bound semi autonomous organelles having self contained genetic materials (mt-DNA and cp-DNA, respectively) and equipped with the associated molecular machinery for regulation of gene expression (Gutman and Niyogi, 2009; Smith and Keeling, 2015; Gray, 2017; Peralta-Castro et al., 2020). Both chloroplast and mitochondrial DNA have originated endosymbiotically from cyanobacteria and α-proteobacteria, respectively (Sagan, 1967; Dyall et al., 2004; Chevigny et al., 2020). The organellar DNA has also been shown to encode at least part of the genetic information required to accomplish some of the fundamental processes, such as photosynthesis and respiration (Saki and Prakash, 2017; Sakamoto and Takami, 2018; Duan et al., 2020). Plant mitochondrial DNA exhibits remarkable variation in size and predominantly linear in structure, while the characteristic features of chloroplast genome remain fairly constant across various plant species and may exist in both linear and circular forms (Morley et al., 2019; Chevigny et al., 2020). Both of the organellar genomes are present in high copy numbers. However, the copy number usually varies within different tissue types during different stages of plant development (Oldenburg and Bendich, 2015; Krupinska et al., 2020).

Due to their proximity with the reactive oxygen species (ROS) generating electron transport system, both mitochondrial and chloroplast genome are threatened by diverse forms of oxidative damages (Boesch et al., 2009). Therefore, maintenance of the stability of the organellar genome along with the nuclear genome is an absolute requirement for plants for sustaining their normal growth and development. Thus, as like the nuclear genome, faithful replication and repair of organellar genomes are also crucial to avoid genome instability, which may eventually cause potentially detrimental effects on phenotypes (Ahmad and Nielsen, 2020). To maintain genome integrity under adverse conditions, plant mitochondria and chloroplast have evolved with an extensive regulatory mechanisms to counteract the deleterious effects of DNA damage (Maréchal and Brisson, 2010; Oldenburg and Bendich, 2015; Ahmad and Nielsen, 2020). Plant mitochondria and chloroplast have been found to possess well-developed base excision repair (BER) pathways, comparable to the nuclear genome to cope up with different forms of oxidative DNA damages (Boesch et al., 2009; Peralta-Castro et al., 2020). Besides oxidative lesions, double-strand breaks (DSBs), which are also generated in the organellar genome either spontaneously or in response to other stress signals, are predominantly repaired by various homology-dependent repair pathways, as unlike the nuclear genome, both the organelles lack the non-homologous end-joining NHEJ pathways (Maréchal and Brisson, 2010).

The endosymbiotic origin of mitochondria and chloroplast from cyanobacteria and α-proteobacteria, respectively has indicated the presence of prokaryotic mode of replication and repair machineries in both the organelles (Ahmad and Nielsen, 2020). However, these replication or recombination/repair proteins, which participate in genome stability maintenance mechanisms in mitochondria and chloroplast, are encoded by either of these organellar genomes (Morley et al., 2019; Brieba, 2019). Analyses of the replication and repair machinery in mitochondria and chloroplast have revealed that the protein components involved in replication and repair machinery are mainly encoded by the nuclear genome and then subsequently targeted to the respective organelle (Saki and Prakash, 2017; Ahmad and Nielsen, 2020; Duan et al., 2020). Except for about 13 mitochondrial genome encoded proteins, more than 1500 proteins in the overall mitochondrial proteome are encoded by various nuclear genes and are targeted to mitochondria for maintenance of mitochondrial genome stability (Chacinska et al., 2009; Van Houten et al., 2016; Saki and Prakash, 2017). On the other hand, more than 95% of chloroplast proteins, including those associated with the maintenance of cp-DNA have been shown to be encoded by the nuclear genome (Green, 2011), which contains all the required genetic information for chloroplast functioning and plant survival (Woodson and Chory, 2008).

Both mitochondria and chloroplast genomes have been shown to experience considerable magnitude of homologous recombination and gene conversion events between comparable DNA sequences (Maréchal and Brisson, 2010; Wu et al., 2020). Chloroplast genome contains large inverted repeats, which generally exhibit slower sequence evolution as compared to single-copy regions, suggesting improved precision of error correction in the presence of easily available homologous templates (Wolfe et al., 1987; Zhu et al., 2016). Various DNA repair mechanisms in the organelles have been found to play important roles in protecting their genome stability and showed close association regarding their evolution. However, despite the highly oxidative environment, the rate of sequence evolution in both chloroplast and mitochondrial genome has been much slower as compared to nuclear genome. The comparatively slower rate of evolution of plant mt-DNA and cp-DNA with reduced substitution rate might be due to the activity highly efficient homologous recombination pathway, which mainly corrects the lesions by gene conversion (Wolfe et al., 1987;

Gualberto and Newton, 2017; Chevigny et al., 2020). Recent studies have revealed that members of *mutS* mismatch repair family protein MSH1, unique in plants, is dually targeted to both chloroplast and mitochondria and play crucial role for maintaining the slow rate of mutation in the organellar genome (Virdi et al., 2016; Wu et al., 2020). Disrupting the function of this gene has been found to increase the frequency of mitochondrial and chloroplast sequence variants approximately 10-fold to 1,000-fold in the model plant *Arabidopsis thaliana* (Wu et al., 2020).

As both mitochondria and chloroplast are believed to have originated from the engulfment of bacterium by eukaryotic cell and most genes were either lost or transferred to the nucleus after the endosymbiosis through endosymbiotic gene transfer (Timmis et al., 2004), the proper coordination of nuclear and organellar genome is therefore essential for ensuring the stability of both the organelles as well as retaining the cellular integrity (Kobayashi et al., 2009; Duan et al., 2020). Studies on genome communication mechanisms, including anterograde (nucleus to organelle) and retrograde (organelle to the nucleus) signaling has been primarily focused regarding the coordination of gene expression between nuclear and organellar genomes (Woodson and Chory, 2008; Chan et al., 2016). Interestingly, the activation and suppression of DNA damage response or DDR in plant organelles depends on the transportation of different proteins from the nucleus to the organelles. Organellar double-strand breaks are shown to be processed by different organellar single-strand binding proteins (OSBs) or the WHIRLY family proteins (Cappadocia et al., 2010). These nuclear genome encoded proteins are either mitochondrial-targeted (OSB1, OSB4, WHY2), chloroplast targeted (OSB2, WHY1, WHY3), or targeted to both the organelles (OSB3) through the anterograde signaling pathway (Krause et al., 2005; Marechal et al., 2008, 2009). The loss of function of *WHIRLY* family genes leads to disruption of homologous recombination repair and reduction in recombination events within sequences exhibiting microhomology (Cappadocia et al., 2010). In addition, some recent studies have demonstrated that chloroplast genome instability also affects the status of the nuclear genome, as the SOG1 transcription factor (the plant homolog of mammalian tumor suppressor p53), which acts as the central regulator of plants' DNA damage responses, has been shown to promote endoreduplication and modulate cell-cycle progression from chloroplast to nucleus through retrograde signaling in response to chloroplast genome instability (Duan et al., 2020). Therefore, maintenance of mitochondrial and chloroplast genomes and the transcription of genes encoded by the organellar genomes are primarily under the control of the nucleus.

The homologous recombination (HR) based repair is considered as the most error free mechanism of DSB repair and represent one of the essential source of genetic diversity and new allelic combination in plants. Therefore, understanding the HR pathway and its interactions with other repair pathways is essential for manipulation of HR events as part of the crop improvement program. The presence of highly efficient homology-dependent DSB repair in the organellar genome has opened up new possibilities in the area of genome transformation in the context of the overall goal of crop improvement (Li et al., 2021). Along with highly efficient homologous recombination system for precise transgene insertion, other characteristics, including absence of epigenetic regulations (such as gene silencing and positional effects) with the potential for expressing foreign proteins at a considerably higher level (approximately 70%) and increased biosafety due to the exclusion of chloroplasts from pollen transmission, chloroplast genome manipulation thus offers attractive alternative over nuclear genome for transgene integration (Oey et al., 2009; Bock, 2015; Boehm and Bock, 2019; Li et al., 2021). Recent studies have demonstrated highly efficient chloroplast transformation in *Arabidopsis thaliana* (Ruf and Bock, 2011). Furthermore, striking similarities between chloroplast and mitochondrial genome have also indicated the possibility of mitochondrial transformation by designing suitable strategies. However, successful mitochondrial transformation in higher plants has not been reported so far. Based on this information, this review mainly summarizes the current understanding of different aspects of organelle genome maintenance mechanisms in higher plants along with the possible applications of genetic manipulations of organellar genomes in crop improvement.

PLANT ORGANELLAR GENOME ARCHITECTURE

Plant mitochondria and chloroplast genomes are typically represented by small circular molecules of DNA. These organellar genomes appear to share very similar structural organization with prokaryotic genomes and the mode of replication. Conversely, unlike prokaryotes, these organelles have been found to possess multiple copies of their genome (Clark et al., 2019). However, organelle genomes do not contain enough genes to survive by themselves and thus rely mainly on the nuclear genome encoded proteins.

Mitochondrial and chloroplast genomes vary greatly in size and architecture both within and between eukaryotic organisms. The structure of mitochondrial genome in most animal cells is very similar, generally consisting of a circular DNA molecule of 14-20 kb (Kolesnikov and Gerasimov, 2012). It usually codes for two ribosomal RNAs, 13 polypeptides, and up to 25 tRNAs (Gualberto et al., 2014). In comparison to animals, plants possess mitochondrial genomes that are large, more complex in structure (**Figure 1A**) and in general the genome size ranges between 200-2000 kb (Gualberto et al., 2014). The relatively large size of the genome is mainly due to the additional amount of DNA found in large introns, non-coding regions, and repeated sequences (organized either in direct or indirect orientation) dispersed throughout the genome (Morley et al., 2019). The main difference between animal and plant mitochondrial DNA lies in the fact that in plants, it mostly exists as a collection of linear DNAs combined with smaller circular and branched molecules. Previous studies have shown that plant mitochondrial genome undergoes extensive high-frequency homologous recombination events between large repeats, resulting in multiple configurations of the genome. Plant mitochondria generally lack nuclei, but

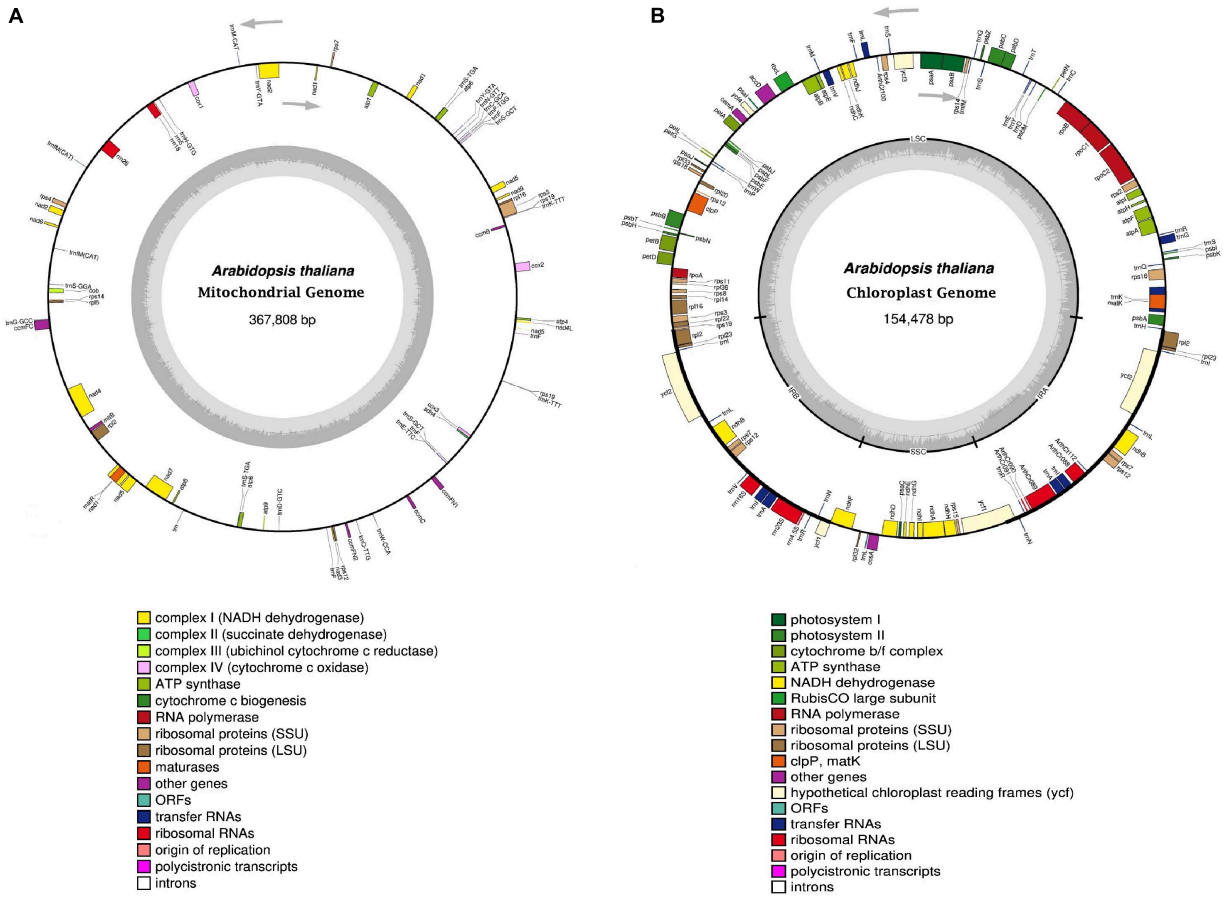

FIGURE 1 | Structural organization of organelle genomes in *Arabidopsis thaliana*. **(A)** and **(B)** Circular gene map of mitochondrial and chloroplast genome, respectively. The gray arrowheads indicate the direction of genes. Genes shown inside and outside the outer circle are transcribed clockwise and anticlockwise respectively. Genes belonging to different groups are color coded. The genome coordinate and GC content are shown in the inner circle. The darker gray region corresponds to GC content, whereas the lighter gray region corresponds to AT content. In the chloroplast genome, the thick lines indicate inverted repeats (IRA and IRB), which separate the genome into small (SSC) and large (LSC) single copy regions. Genome diagrams are adapted from the output of OGDRAW (Greiner et al., 2019).

the DNA is packed into nucleoprotein particles, called nucleoids (Kucej and Butow, 2007). These are membrane-anchored particles associated with DNA and influence transcriptional regulation of mt-DNA. Mitochondrial nucleoids encompass a set of core proteins involved in the maintenance of DNA and some peripheral components of signaling pathways (Gilkerson et al., 2013). Commonly, both plant and animal mitochondrial genomes include genes encoding nine subunits (nad1, nad2, nad3, nad4, nad4L, nad5, nad6, nad7, and nad9) of the respiratory-chain complex-I, NADH dehydrogenase; one subunit of complex III, cytochrome bc_1 (cob); three subunits of complex IV, cytochrome oxidase (cox1, cox2, cox3); and two subunits of complex V, ATP-synthase subunits (atp6, atp8), respectively. The mitochondrial genome also includes genes for ribosomal RNAs and tRNAs. Apart from these genes, plant mitochondrial genome also includes genes encoding proteins for cytochrome c biogenesis (*ccm*) and an mtt-B-like transporter (Cupp and Nielsen, 2014). The replication process of mt-DNA is much more complex in plants than in animals. Due to the large size and complexity of mitochondrial genomes, the exact mechanism for replication of mt-DNA remains unclear. However, accumulating evidences have indicated that plants use multiple strategies, like recombination-dependent replication (RDR), rolling circle mechanism similar to bacteriophage T4 DNA replication, and also the conventional bidirectional replication mechanism to replicate their mt-DNA (Gualberto et al., 2014; Morley et al., 2019).

Besides mitochondria, chloroplasts present in plant cells also contain their own genome and gene expression system. The chloroplast genome in higher plants possesses a highly conserved structural organization. In general, chloroplast genome exists in the circular form of DNA, comprising of a quadripartite structure (**Figure 1B**). The chloroplast genome consists of two large inverted repeats separated by a large single-copy region (LSC) and a small single-copy region (SSC), respectively (Wang and Lanfear, 2019). The chloroplast genome associated inverted repeats (IRs) are highly conserved and their length generally ranges between 20000–25000 bp (Morley et al., 2019).

Genes encoded by the chloroplast genome play crucial role in photosynthesis and carbon fixation and also serve as valuable resources for molecular identification in phylogenetic studies because of their compact size, less recombination, maternal inheritance, high copy number, and moderate substitution rates, respectively (Wang W. et al., 2014; Xie et al., 2018). Generally, the chloroplast genome in angiosperms encodes about 110-130 genes and the overall size of the genome ranges between 120-180 kb, respectively (Lin et al., 2018). Initially, the chloroplast genome was thought to form only a circular structure, but recent advances have revealed that multi-branched linear structures may also exist in many angiosperms (Mower and Vickrey, 2018). The chloroplast genome typically possesses four copies of rRNA genes, several tRNA genes, and some other protein-coding genes such as ribosomal proteins, thylakoid proteins, and the large Rubisco subunit (Palmer, 1985). However, most of the chloroplast proteins are nuclear-encoded. In majority of photosynthetic organisms, chloroplast DNA is packed into nucleoids. On an average, plant, the cell possesses nearly 1000-1700 copies of chloroplast nucleoids (Dobrogojski et al., 2020). The chloroplast genome has been shown to possess approximately 45 genes, which encode the proteins involved in photosynthesis. These genes mainly include subunits of cytochrome b6f complex (6 genes), photosystem I (5 genes), photosystem II (15 genes), ATPase of chloroplast (6 genes), NADH dehydrogenase (12 genes), and Rubisco large subunit (1 gene), respectively (Dobrogojski et al., 2020). *Arabidopsis* chloroplast genome also consists of 29 genes, including 4 genes for chloroplast RNA polymerase subunits and 25 genes for components of the ribosome (Sato et al., 1999). Chloroplasts have been shown to utilize a double displacement loop strategy to initiate their DNA replication (Kunnimalaiyaan and Nielsen, 1997). In addition, the rolling circle and recombinant-dependent replication (RDR) process have also been proposed for cp-DNA replication. Several studies have revealed that just like mitochondria, chloroplasts also possess two organellar DNA polymerases, Pol1A and Pol1B, resembling bacterial DNA Pol1 (Moriyama and Sato, 2014).

Organelle Genome Faces High Level of Oxidative Damage Due to Proximity With the ROS Generating Electron Transport Machinery

Plant mitochondria and chloroplast possess a complex network of enzyme systems for the transport of electrons associated with respiration and photosynthesis, respectively. Various ROS are generated continuously as metabolic by-products from both these organelles (Taylor and Millar, 2007; Kim, 2020). ROS are well-acknowledged for their benefits as well as deleterious effects. When present at optimum or moderate concentrations, ROS have been found to act as second messengers, thus regulating different cellular pathways. On the other hand, at high concentrations, ROS can cause substantial damage to various biomolecules, including nucleic acids and other cellular biomolecules (Sharma et al., 2012).

Since mitochondria represent one of the predominant cellular sources of ROS production, oxidative damages are by far the most studied mechanism affecting the mt-DNA stability (Meagher and Lightowlers, 2014). Different types of reactive oxygen species, including superoxide anion, hydrogen peroxide, hydroxyl radical, and singlet oxygen molecules are generated continuously as a result of electron leakage from the several sites of mitochondrial electron transport chain (ETC) (Andreyev et al., 2005; Sharma et al., 2012; Alexeyev et al., 2013). Among various ROS, O_2^- is generated from direct reduction of oxygen in the flavoprotein region of NADH dehydrogenase complex, also known as complex I of the respiratory electron transport chain (Arora et al., 2002). Besides complex I, complex III or ubiquinone-cytochrome complex of the ETC is also involved in producing O_2^- from oxygen (Murphy, 2009). Under normal growth condition, functioning of ETC and ATP synthesis are tightly regulated, while under various abiotic stress conditions, components of ETC are modulated, resulting in excessive reduction of various electron carriers, ending up with overproduction of ROS (Noctor et al., 2007; Blokhina and Fagerstedt, 2010). Besides mitochondria, as a light-harvesting organelle, chloroplast has also been found to inevitably produce considerable level of ROS primarily through the Photosystems (PSI and PSII). Like mitochondria, several sites of ROS production are present in chloroplast. Electron transport system connecting PSI and PSII appeared to be the main source of ROS production in the chloroplast. Under stress conditions, decreased supply of electron acceptor (NADP) leads to leakage of electrons from ferredoxin, thus resulting in the generation of O_2^- from oxygen (Elstner, 1991). Leakage of the electron can also occur from 2Fe-2S and 4Fe-4S clusters, present in electron transport systems associated with PSI. In addition, electrons may also be released from the acceptor side of ETC containing Q_A and Q_B in PSII. All these contribute to the production of O_2^- from oxygen (Cleland and Grace, 1999).

Both mitochondria and chloroplast possess various antioxidant compounds as the preliminary line of defense, which protect the organelles from ROS-mediated DNA damage. The ROS molecules, which have been found to escape the antioxidant mediated detoxification, may induce DNA damage through the generation of various modified bases, including thymine glycol, 8-hydroxyguanine, 5,6-dihydroxycytosine, 2,6-diamino-4-hydroxy-5-formamidopyrimidine, respectively and also some sugar break down products like 2-deoxypentose-4-ulose, erythrose and 2-deoxypentonic acid lactone, respectively. All these oxidative modifications of the bases may generate base-free sites, eventually leading to DNA strand breaks, including DSBs (Dizdaroglu et al., 2002; Evans et al., 2004; Boesch et al., 2011).

DNA DAMAGE REPAIR MECHANISMS IN PLANT MITOCHONDRIA AND CHLOROPLAST

Maintenance of organelle genome stability is crucial for their proper functioning as well as for overall plant growth and development. Initially, it was thought that plant organelles

do not possess any dedicated machinery for repairing DNA damages, and a high copy number of mitochondrial and chloroplast genome probably restrict the deleterious effects of DNA damage (Chevigny et al., 2020). In animal system, although damaged mt-DNA copies have been found to be completely degraded, similar mechanism has not yet been detected in plant organelles (Zhao, 2019; Chevigny et al., 2020). However, it is now well established that plant organelles possess their own DNA repair machinery, while not all repair the pathways have been demonstrated to date. Various components of organellar genome maintenance machinery were probably inherited from the bacterial ancestors. However, plant organelles are still highly dependent on nuclear genome encoded damage repair proteins for repairing single-strand and double-strand breaks. On the other hand, to counteract the continuous threat from various forms of oxidative damages in the organellar genome, which mainly originate because of their intrinsic association with the electron transport chain, both mitochondria and chloroplast genomes have been found to develop efficient BER pathway as like the nuclear genome. BER pathway is the first organellar repair pathway described in plants (Boesch et al., 2011). Besides oxidative damages, DSBs are also considered as another major threat to organelle genome stability. Both plant mitochondria and chloroplast have been found to employ homology-based recombination for repairing DSBs (Li and Heyer, 2008; Maréchal and Brisson, 2010).

Oxidative Damage in Plant Organellar Genome Is Repaired by BER Pathway

Besides performing key cellular processes, including photosynthesis and respiration, both chloroplast and mitochondria are the major sites of reactive oxygen species production. However, despite the continuous assault of oxidative damage, sequence drift in both plant mitochondrial and chloroplast genomes remains very low, indicating the presence of an efficient organellar DNA damage repair system. Recently, several studies have demonstrated that as like nuclear genome, the BER pathway also participates in the repair of oxidative DNA damages in the organellar genome (Boesch et al., 2009; Gredilla, 2010; Boesch et al., 2011; Prakash and Doublié, 2015; Peralta-Castro et al., 2020). BER in plants is a crucial genome defense pathway, comprising of sequential steps, including excision of the damaged DNA base, splitting of the sugar-phosphate backbone of DNA at the AP (apurinic/apyrimidinic) site, reorganizing the resulting DNA ends, filling of gaps through DNA replication and finally DNA strand ligation (Roldán-Arjona et al., 2019).

As in the nucleus, the BER pathway in mitochondria and chloroplast has also been found to be initiated with the action of a DNA glycosylase (**Figure 2**; Jacobs and Schar, 2012). Based on the substrate specificity, DNA glycosylases can be distinguished into monofunctional (only glycosylase activity) and bifunctional (glycosylase plus apurinic/apyrimidinic (AP) lyase activities) types. Monofunctional DNA glycosylases have only been found to remove the target base, thus generating an AP site. On the other hand, bifunctional glycosylases hold an additional AP lyase activity, which catalyzes an incision at 3′ of the AP site by β-elimination after base excision, thus generating 3′-α, β unsaturated aldehyde (3′-PUA), and 5′-hydroxyl (OH) termini (**Figure 2**; Gutman and Niyogi, 2009; Roldán-Arjona et al., 2019). Uracil-DNA glycosylases (UDG) are important monofunctional glycosylases capable of recognizing the uracil residue resulting from misincorporation of dUMP in DNA during replication or cytosine deamination and excising its N-glycosidic bond, thus generating an AP site (Roldán-Arjona et al., 2019). Previously, AtUNG (AT3G18630), a member of Family-1 UDGs has been characterized in *Arabidopsis thaliana* (Cordoba-Cañero et al., 2010). Although direct evidence of targeting AtUNG protein to the subcellular organelles, including mitochondria and chloroplast other than the nucleus have not been reported, *in vitro* import assays have revealed the transportation of UNG protein in mitochondria in *Arabidopsis thaliana*. In addition, *in vitro* targeting assays have also revealed that a transiently expressed AtUNG-GFP fusion protein in *Nicotiana benthamiana* leaves is readily colocalized with mitochondria in protoplasts generated from the agro-infiltrated tissues (Boesch et al., 2009). Moreover, some *in-organelle* experiments have further indicated the presence of UNG activity in the mitochondria in *Arabidopsis*, potato, and also in the gymnosperm *Araucaria angustifolia*, respectively (Boesch et al., 2009; Furlanetto et al., 2019).

Among various bi-functional DNA glycosylases, 8-oxoguanine glycosylase (OGG1) and the members of the formamidopyrimidine glycosylase/endonuclease VIII (FPG/NEI) family are mainly involved in repairing various oxidative damaged pyrimidines, including 8-oxoG. Previous studies have indicated that loss of FPG and OGG1 enzyme activities in *Arabidopsis thaliana* results in an increased magnitude of oxidative damage in both mitochondrial and chloroplast genome (Córdoba-Cañero et al., 2014; Chevigny et al., 2020). This strongly suggests that along with the nucleus, the BER pathway in mitochondria and chloroplast also rely on these glycosylases. Earlier investigations have revealed that oxidatively damaged pyrimidines are repaired in *E. coli* by Endonuclease III (EndoIII), also known as Nth. Two functional homologs of bacterial Nth (AtNTH1and AtNTH2) have been reported from *Arabidopsis thaliana* (**Figure 2**; Roldan-Arjona and Ariza, 2009; Gutman and Niyogi, 2009). Recent studies have revealed the presence of DNA glycosylase-lyase/endonuclease activity in the chloroplast protein fractions of *Arabidopsis thaliana*, thus providing meaningful evidences of involvement of DNA glycosylase-lyase/endonuclease in repairing of oxidative damaged pyrimidines through BER pathway in chloroplast (Gutman and Niyogi, 2009). *In silico* studies have identified the components of BER pathway (two endonuclease III homologs and an apurinic/apyrimidinic endonuclease) in chloroplast, which are possibly involved in this glycosylase-lyase/endonuclease activity (Gutman and Niyogi, 2009). Additional *in vitro* localization activity using transiently expressed GFP tagged proteins have further demonstrated targeting of these three proteins to the chloroplast and co-localized with the chloroplast DNA in nucleoids (Gutman and Niyogi, 2009).

Processing of blocked termini at the 5′-P and 3′-OH ends by the action of glycosylases is followed by progression of gap-filling step either by short patch (SP) or long patch (LP) BER

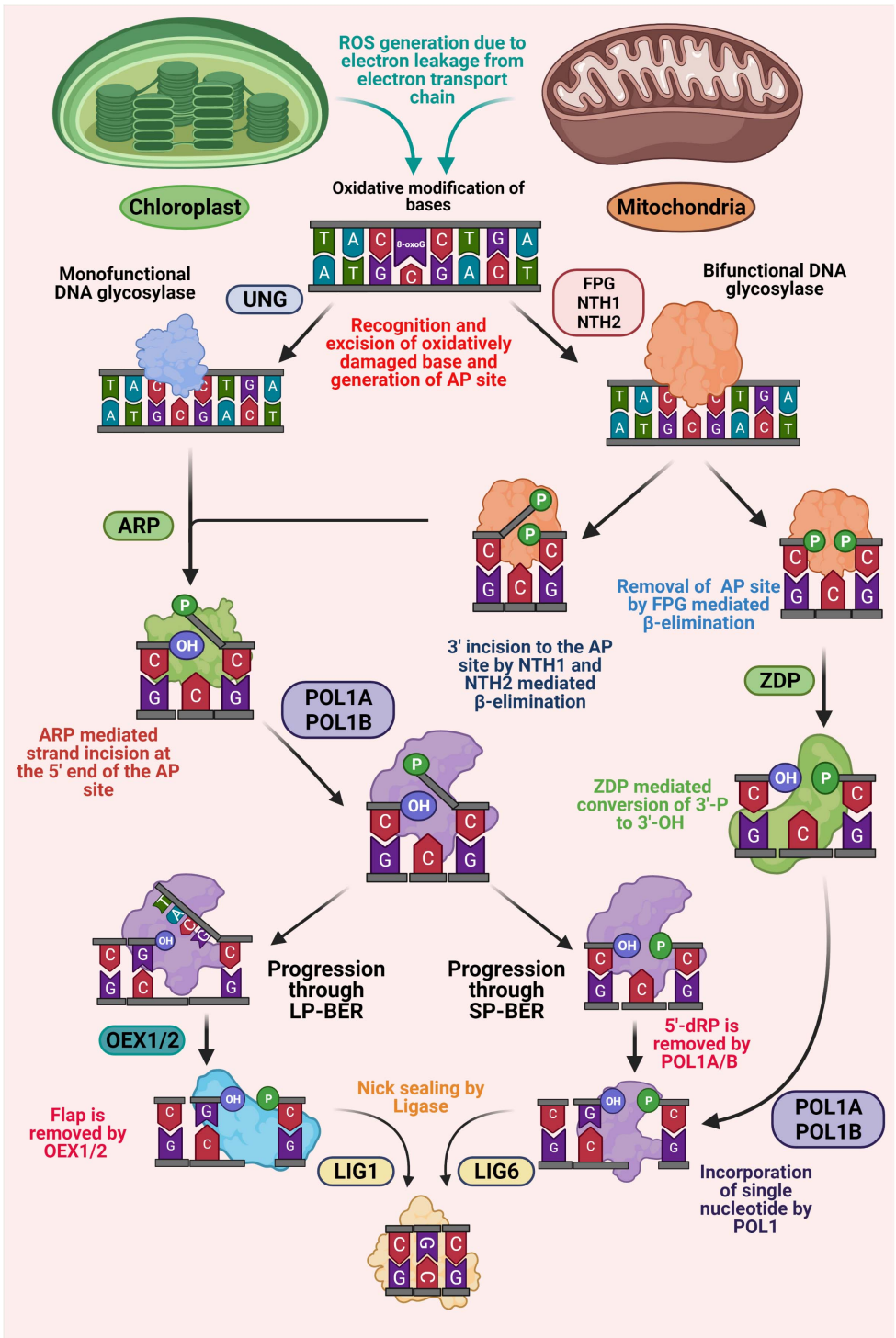

FIGURE 2 | Schematic representation of base excision repair (BER) in plant organelles. BER is initiated with recognition and removal of the oxidatively modified base by the action of DNA glycosylase, generating an AP site. Monofunctional glycosylase only possesses hydrolytic activity, while bifunctional glycosylases possess an additional lyase activity. An AP endonuclease (ARP) is associated with processing the AP sites produced by monofunctional glycosylases, thus generating 3′-OH and 5′-P ends. In addition, ARP also processes 3′-OH ends produced by bifunctional glycosylases generating 3′-OH and 5′-P ends. At this point, the BER pathway diverges into short-patch (SP) and long-patch (LP) sub pathways. The 50-flap generated by the action of POL1A and POL1B during LP-BER is cleaved by FEN1 endonuclease (OEX1 and OEX2). In SP-BER, the 5′-P moiety is processed by the lyase activity of POL1s and a single nucleotide is incorporated. DNA ligase is associated with the ligation process in both LP and SP-BER pathways. In addition, in an alternate pathway, a bifunctional glycosylase, FPG, remove oxidative DNA lesion, generating 3′-P and 5′-P ends. The 3′-P end is removed by ZDP phosphatase leaving a 3′-OH end, which is subsequently resolved through BER-SP.

pathway, respectively (**Figure 2**). Oxidative lesions processed by bifunctional glycosylases are generally repaired through the short-patch BER pathway (single nucleotide replacement). On the other hand, damages perceived by monofunctional glycosylases can be repaired alternatively either by long-patch (up to 10 nucleotide replacements) or short-patch BER (Van der Veen and Tang, 2015). Insertion of nucleotides through the SP or LP-BER pathway requires the activity of a DNA polymerase. Plant mitochondrial and chloroplast DNA polymerases have been shown to be phylogenetically linked to bacterial DNA polymerase I (Kimura et al., 2002; Shutt and Gray, 2006). In *Arabidopsis thaliana* and *Nicotiana tabacum*, two homologs of bacterial DNA polymerase I are found, which are indicated as POL1A and POL1B and shown to be targeted to both mitochondria and chloroplasts (Elo et al., 2003; Christensen et al., 2005; Mori et al., 2005; Ono et al., 2007). These plant organellar DNA polymerases have been found to possess the capability of replicating the complete organellar genome and exhibit excellent processivity without the requirement of any other accessory proteins (Takeuchi et al., 2007; Moriyama and Sato, 2014). In addition, both the polymerases have been shown to possess considerable fidelity as compared to the replicative DNA polymerases (Baruch-Torres and Brieba, 2017). Among the two plant organellar DNA polymerases, POL1A is only associated with DNA replication, whereas, POL1B is involved in DNA repair (Parent et al., 2011). Recent studies have revealed that both polymerases possess a 5′-P lyase activity, which is capable of removing 5′-P moieties formed during the short patch BER pathway (Trasvina-Arenas et al., 2018). Furthermore, it has also been found that POL1B is associated with efficient strand-displacement function on DNA containing a one-nucleotide gap, whereas POL1A shows moderate strand displacement activity, suggesting that both POL1A and POL1B can play a meaningful role in short-patch BER, while POL1B can also be involved in long-patch BER.

Homologous Recombination Represents the Primary Mechanism for Repairing DSBs in the Organellar Genome

As in other eukaryotes, DSBs are considered as one of most crucial and deleterious forms of DNA damages in plants. When remain unrepaired, DSBs can disrupt various fundamental cellular processes, including replication and transcription. In plants, most of the DSBs in the nuclear genome are repaired by non-homologous end joining (NHEJ) or homologous recombination (HR) (**Figure 3A**) mediated repair pathways (Britt, 1999; Puchta, 2005; Waterworth et al., 2011; Roy, 2014). DSBs are also generated in mitochondria and chloroplast genome due to exposure to various exogenous and endogenous stress factors, such as UV-B, ionizing radiation, and the ROS continuously generated within both these organelles. Although in animal mitochondria, both HR and NHEJ pathways are involved in repairing DSBs, plant organelles possess only HR pathways, completely lacking the NHEJ repair. In addition, DSBs in higher plant chloroplast and mitochondrial DNA are also repaired by the error-prone microhomology-mediated end joining (MMEJ) repair mechanism, which represents an alternate form of NHEJ repair (Kwon et al., 2010; Seol et al., 2017).

Homologous recombination is important for the repair of DSBs in the organellar genome and has generally been found to occur by the invasion of a homologous DNA strand followed by strand exchange (**Figure 3B**; Li and Heyer, 2008). Homologous recombination plays a crucial role in mitochondrial DSB repair and loss-of-function of any of the HR-associated protein results in significant rearrangements in the mitochondrial genome (Davila et al., 2011). Under genotoxic stress conditions, plant mt-DNA exhibits higher recombination frequency (Kuehn and Gualberto, 2012). Presence of large inverted repeats in the chloroplast genome provides increasing chances of availability of homologous sequences for homologous recombination, which involves repair of DNA lesions via gene conversion (Wolfe et al., 1987; Muse, 2000; Gualberto and Newton, 2017). Chloroplast employs all types of HR repair mechanisms, including double-strand break repair (DSBR), single-strand annealing (SSA), and synthesis-dependent strand annealing (SDSA) for DSB repair (Kohl and Bock, 2009). It has been suggested that because of their high homologous recombination frequencies, both mitochondrial and chloroplast genomes show a comparatively slower rate of evolution with a reduced substitution rate. In angiosperms, the rate of synonymous substitution in mitochondria, chloroplast, and nuclear genes appears as 1:3:10, exhibiting their high efficiency in genome repair (Drouin et al., 2008).

Two families of plant-specific single-strand binding proteins, including organellar single-strand binding proteins (OSBs) and plant-specific WHIRLY family proteins, are involved at the initial phase of homologous recombination in both mitochondria and chloroplast (Maréchal and Brisson, 2010). These proteins are encoded by the nuclear genome and have been targeted to either mitochondrion (OSB1, OSB4, and WHY2) or chloroplast (OSB2, WHY1, and WHY3) or both (OSB3) through anterograde signaling (Maréchal and Brisson, 2010; Garcia-Medel et al., 2019). All OSBs have been found to possess an N-terminal nuclear targeting peptide for their convenient targeting to the respective organelles. Although, not highly well conserved (30–50% similarity) in terms of amino acid residues, a domain having significant structural similarities with the oligonucleotide/oligosaccharide binding fold (OB-fold), a distinctive feature of many ssDNA-binding proteins, is has been found in the internal region of OSBs. Among various WHIRLY family proteins, chloroplast targeted WHY1 and WHY3 have been found to protect chloroplast genome from rearrangements (Marechal et al., 2009). On the other hand, WHY2 is targeted to mitochondria and is involved in strand resection following oligomerization (Maréchal and Brisson, 2010).

The bacterial recombinase RecA and its eukaryotic homologs of the Rad51 family are essential proteins that have been shown to play a central role in homologous recombination and thus are crucial for genome stability maintenance (Cox, 2007; Odahara et al., 2015). They are key factors involved in the accurate pairing of homologous DNA sequences, promotion of strand invasion, and branch migration during the recombination process. In bacterial recombination-based repair, the exonuclease

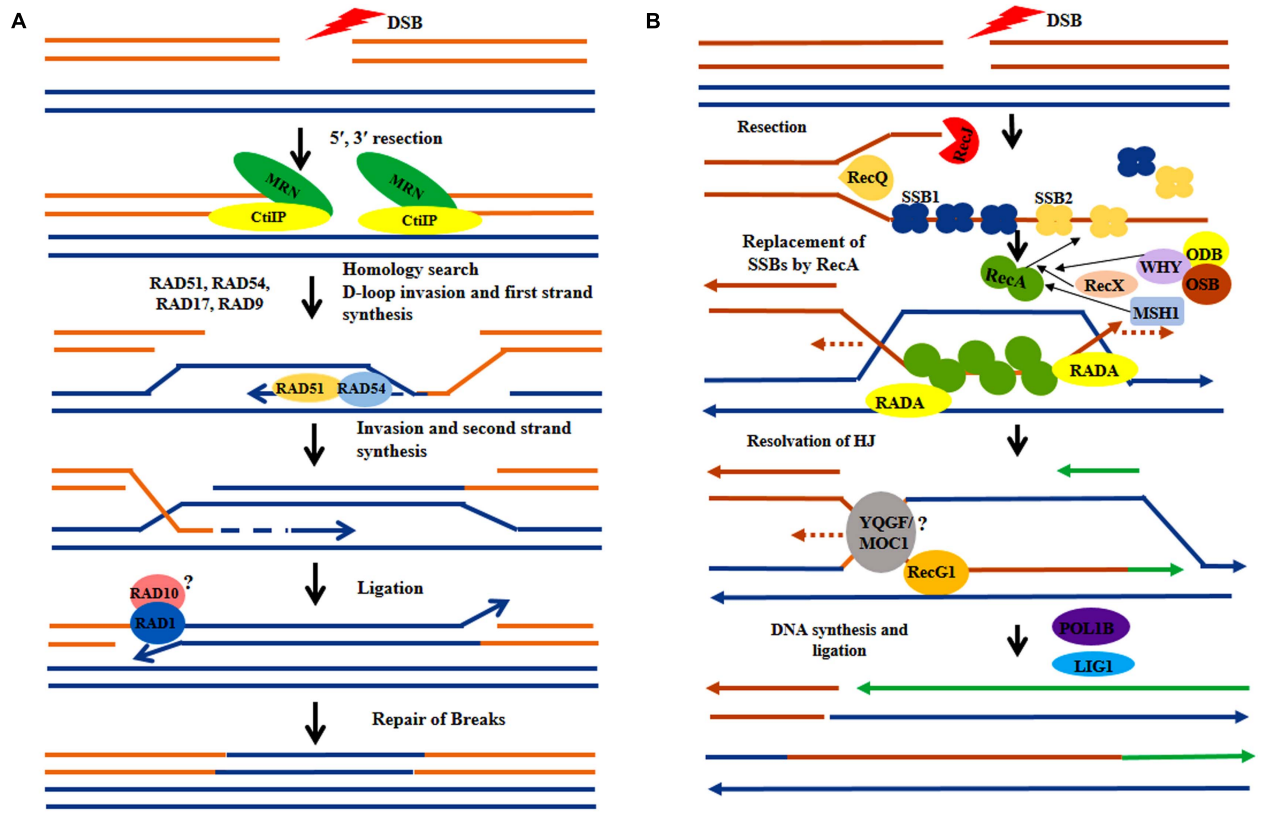

FIGURE 3 | Hypothetical model comparing recombination repair in nucleus and organelles. **(A)** Following the induction of double-strand breaks (DSBs) in nuclear DNA, the DNA lesions are processed by MRN complex (MRE11, RAD50, NBS1) protein. Then the RAD52 epistatic group of genes plays a crucial role in homology search (RAD54, RAD51) and subsequent strand invasion. The DNA breaks are sealed by the joined action of polymerase and ligase, **(B)** In the sub-cellular organelles the DSB sites are processed by RecJ and RecQ nuclease proteins followed by subsequent incorporation of nuclear-encoded by Single Strand Binding proteins (SSB1, SSB2). The nuclear-encoded WHIRLY (WHY) family gene along with RecX, ODB, and OSB facilitate incorporation of RecA protein which involves in strand invasion. The uncharacterized proteins, MOC1 and YQGF may be involved in HJ resolution. The ligations of breaks are done by the joined activity of polymerase and ligase.

activity of RecBCD helps in resection of the 5′ phosphate after induction of DSBs. Then RecA is involved in the formation of the presynaptic complex (Handa et al., 2009). Nucleation of RecA occurs in a RecFOR in protein-dependent manner and the dynamic nature of RecA initiates the homologous sequence finding process (Sandler and Clark, 1994). Plant nuclear genome characteristically encodes three bacterial−type RecA homologs, including RecA1, RecA2, and RecA3, which are localized in chloroplasts and/or mitochondria, in contrast to their nuclear counterpart Rad51. Among the three RecAs, RecA1 and RecA3 are specifically targeted to chloroplast and mitochondria, respectively. On the other hand, RecA2 is targeted to both, either chloroplast or mitochondria (Shedge et al., 2007; Odahara et al., 2009; Chevigny et al., 2020). Knockout of mitochondria-targeted RecA3 has resulted in large-scale rearrangements in the mitochondrial genome (Odahara et al., 2015). Besides higher plants, RecA1 has also been reported from *Physcomitrella patens* (moss) and disruption of PpRecA1 has been shown to cause considerable sequence rearrangements involving short repeats (Small, 1987; Odahara et al., 2009). The molecular function of RecA2 in homologous recombination in the organellar genome is further regulated by RecX protein in plants. The *recA3odb1* and *recA3msh1*double mutants are shown to exhibit developmental abnormalities (Chevigny et al., 2020). Therefore, it is suggested that organelle-targeted RecA homologs are involved in preventing recombination between short repeated sequences and thus promoting DNA damage repair.

The second branch point in the bacterial genome occurs in a RuvABC (helicase) mediated way. RuvABC has been shown to play a key role in branch migration during SDSA or SSA repair in bacterial cells. Although, no homolog of bacterial RuvABC is found in plant mitochondria, RadA and RecG proteins have been found to play a similar role in plant mitochondria (Whitby et al., 1994; Marie et al., 2017; Chevigny et al., 2019). RecG is involved in the migration of the holiday junctions to the very end of the DNA molecule and is also involved in D-loop formation. The activity of RecG further converts the D-loop to a holiday junction and subsequently, the endonucleases cleave the heteroduplex to recover the two sister chromosomes. The homolog of RecG protein is identified in both mitochondria and chloroplast (Wallet et al., 2015; Odahara et al., 2017). A knockout mutation of RecG results in an ectopic recombination event in

mitochondria with aberrant organellar structure (Odahara et al., 2017). RadA, also involved in branch migration, is a paralog of RecA and has already been characterized in *Arabidopsis thaliana* (Chevigny et al., 2020). Knockout of this gene in chloroplast and mitochondria results in the arrest of plant growth and development along with permanent impairment of mitochondrial genome stability (Chevigny et al., 2020). Although no functional organellar protein with resolvase activity has been reported, a nuclear-encoded protein is specifically recruited to chloroplast, which appears to play a similar function to bacterial RuvC resolvase (Wardrope et al., 2009; Kobayashi et al., 2017). In addition, monokaryotic chloroplast 1 or MOC1 has been found to resolve the holiday junction in the chloroplast genome, and absence of this protein may result in aberrant chloroplast segregation and complete loss of cp-DNA (Kobayashi et al., 2017). Together these pieces of evidences have indicated the similarity of bacterial and organellar homologous recombination processes, which also further supports the notion of the endosymbiotic origin of the organelles.

A MutS homolog, MSH1 was identified in both chloroplast and mitochondria. Beside their precise role in recognition of DNA damage associated with mismatches, plant MSH1 also contain a C-terminal endonuclease domain, GIY-YIG, which introduces DSBs and recruit homologous DNA damage repair machinery for accurate repair. Thus, the function of MSH1 is more than a mismatch repair protein in both chloroplast and mitochondria (Abdelnoor et al., 2003). In *Physcomitrella patens* (moss), duplicated genes of MSH1, MSH1A, and MSH1B are present. Among these two, MSH1B genetically interacts with RecA2 and RecG to maintain organellar genome stability (Odahara et al., 2017). Furthermore, the *msh1breca2* and *msh1brecg* double mutants have been shown to increase recombination between short dispersed repeats (SDRs) in chloroplasts and mitochondria synergistically (Odahara et al., 2017).

The organellar DNA not always requires long homologous repeats to repair DSBs. It has been reported that chloroplast DNA in *Arabidopsis thaliana* may also repair DSBs via microhomology-mediated end joining (MMEJ), distinct from homologous recombination (HR) (Kwon et al., 2010). MMEJ is a sub-type of alternative non-homologous end-joining (A-NHEJ) mechanism that requires very short regions (2-14 bp) of homology. In this process, DSBs have sealed microhomology (MH)-mediated base-pairing of DNA single strands, followed by the steps including nucleolytic trimming of DNA flaps, DNA gap filling, and DNA ligation (Seol et al., 2017). Although this process is error-prone, but possibly have further contributed to land plant genome evolution (Heacock et al., 2004; Kwon et al., 2010).

Coordination of Nuclear and Organellar Genome via Inter-Compartmental Crosstalk Is Crucial for the Maintenance of Organelle Genome Stability in Plants

Plants require the coordinated action of all three genomic compartments for their harmonious growth and development. The endosymbiotic origin of mitochondria and chloroplast and the subsequent transfer of a significant amount of genetic material to the nuclear compartment through horizontal gene transfer leaving few active genes to be encoded by the organellar genome (Pfannschmidt and Yang, 2012; Nakashima et al., 2014). Proteins associated with various cellular functions in plants are found to be encoded by the genome of different compartments. So, there must be a coordinated mechanism existing between various organelles within the plant cell that is involved in regulating the inter-organellar crosstalk during organellar biogenesis or stress responses (Busi et al., 2011; Ng et al., 2014). The inter-organellar crosstalk is of two types, including anterograde (nucleus to organelle) and retrograde (organelle to the nucleus) signaling (Busi et al., 2011; Bobik and Burch-Smith, 2015). Anterograde signaling initiates from the nucleus, appears to sense both the endogenous and exogenous environmental cues that may lead to modulate the expression of various mitochondrial and chloroplast genes. On the other hand, the retrograde mechanism is found to rely on the physiological state of organelles, which regulates the expression of nuclear genes (Ng et al., 2014; Chan et al., 2016; Börner, 2017). The balance of the protein pool in the nucleus and organelles can be modulated by two primary mechanisms. One of these mechanisms is dual targeting from the cytoplasm to either nucleus or organelles. Another one is targeting organelles and then subsequent relocation to the nucleus (Krause and Krupinska, 2009). Recently, various pathways have been identified that are probably involved in retrograde signaling including genome uncoupled (GUN) loci mediated chloroplast to nucleus signal transduction pathway, SAL1-PAP pathway, methylerythritol mediated pathway, and carotenoid mediated pathway, respectively (Strand et al., 2003; Cordoba et al., 2009; Estavillo et al., 2011; Giuliano, 2014).In yeast and animal, the inter-genomic signals between mitochondria and the nucleus not only regulate the mitochondrial biogenesis but also modulate gene expression throughout different developmental stages (Poyton and McEwen, 1996; Hess and Bo"rner, 1999). In mitochondria, the oxidized guanines (8-oxoG) are repaired by a specific bi-functional glycosylase, OGG1 (8-oxoguanine glycosylase) through base excision repair pathway (Córdoba-Cañero et al., 2014). It was found that in humans, the *OGG1* gene is differentially spliced at exon 7 and exon 8 and directed to both nucleus and mitochondria, respectively (Seeberg et al., 2000). In plants also, genomic compartments including, mitochondria and chloroplast are shown to be dependent on the nuclear genome and most of the proteins have been imported post-translationally during the growth and development (Zhang et al., 2011; Krupinska et al., 2020). The proteins targeted to mitochondria or chloroplast generally possess an N-terminal mitochondrial or chloroplast targeting signal, which enables them to be translocated through the outer and inner membranes (TOM, TIM; TOC, TIC) of chloroplast and mitochondria (Richly and Leister, 2004; Melonek et al., 2012; Saki and Prakash, 2017).

In plants, organelles act as the intracellular sensors of stress cues and convey the signal to the nucleus, followed by activation of an array of molecular signals. Efficient regulation of energy-producing reactions in organelles and inter compartmental crosstalk following various abiotic stresses is essential for

maintaining cellular homeostasis and also survival of plants (Jazwinski, 2013; Cagin and Enriquez, 2015). In animal cells, after induction of DNA damage, different signaling networks, including Ca^{2+}, NAD^{+}/NADH, AMPK, redox signaling, and mitochondrial unfolded protein response (UPR) mediated pathways have been found to be activated (Janssen-Heininger et al., 2008; Rizzuto et al., 2012; Stein and Imai, 2012; Tripathi et al., 2013; Jovaisaite et al., 2014). Introducing mutation in the nuclear gene *DAG* in *Antirrhinum majus* and *DCL1* in tomato has been shown to hamper chloroplast development, resulting in small chloroplasts with impaired internal membrane system (Keddie et al., 1996). The interdependence of chloroplast and mitochondria has already been proven from the loss-of-function mutants of non-chromosomal striped (NCS) in maize containing deletions in *COXII*, *NAD4,* and *NAD7* genes at coding regions (Li et al., 2018). Furthermore, albostrian barley with impaired photosynthetic activity and chloroplast development showed elevated expression of several mitochondrial genes encoding cytochrome c oxidase and ATPase subunits, including *COXII*, *COXIII*, *ATPA*, *ATP6* and *ATP9*, respectively (Hedtke et al., 1999). Defects in plant mitochondrial glycine decarboxylase have resulted in developmental deformities in chloroplast, including excessive excitation and reduction (Sabar et al., 2000; Heineke et al., 2001). Together these investigations have suggested the interdependence of organelles and the existence of a strong inter compartmental signaling network within plant cell.

Plethora of studies has revealed that retrograde signaling is activated in plants under different biotic and abiotic stress conditions (**Figure 4**; Huang et al., 2003). In *Arabidopsis thaliana*, loss-of-function of IM genes in nuclear genome encoding a terminal oxidase in chloroplast has resulted in overproduction of ROS and subsequent oxidation of genomic elements (Foudree et al., 2012). Another study has shown that *CHM* (chloroplast mutator) gene in *Arabidopsis* encodes a mitochondrion targeted protein, which is associated with maintaining mitochondrial genome stability and integrity (Abdelnoor et al., 2003). In yeast, NTG1, a bi-functional DNA glycosylase with lyase activity, possess both nuclear localization signal and mitochondrial matrix targeting sequence and is found to be located both in mitochondria and nucleus (Swartzlander et al., 2010). During excessive oxidative stress, NTG1 has been shown to modulate the stress response and activate base excision repair pathway in mitochondria. Oxidatively damaged pyrimidines are repaired in *E. coli* by Endonuclease III (EndoIII), also known as Nth. Two functional homologs of bacterial Nth (AtNTH1and AtNTH2, respectively) have been characterized from *Arabidopsis thaliana* (Roldan-Arjona and Ariza, 2009). Recent studies have revealed the presence of DNA glycosylase-lyase/endonuclease activity in the chloroplast protein fractions of *Arabidopsis thaliana* (Gutman and Niyogi, 2009). In yeast, fumarase, a mitochondrial genome encoded protein that converts fumarate to malate, is also involved in the activation of DNA damage repair in the nucleus by inhibiting histone H3 demethylation (Jiang et al., 2015). Proteins encoded by the *WHIRLY* (*WHY*) family of genes in the nuclear genome act as organellar single-strand binding proteins and can be targeted to either chloroplast or mitochondria or both (Zaegel et al., 2006). These proteins play a crucial role in the initial stages of recombination-mediated repair in organellar genomes. In *Arabidopsis thaliana*, two *WHIRLY* family genes; *AtWHY1* and *AtWHY3* are specifically targeted to chloroplast where they suppress chloroplast genome rearrangements (Mare'chal et al., 2009). On the other hand, *AtWHY2,* another member of this family is targeted to mitochondria. In *Arabidopsis thaliana*, among the six SWIB (SWI/SNF complex B) domain-containing proteins, four proteins are found to be targeted to chloroplast and associated with the chloroplast nucleoids. Among these chloroplast-targeted SWIB members, SWIB-6 and SWIB-4 have been shown to exhibit a second localization in mitochondria and nucleus, respectively (Melonek et al., 2012). The recombinant SWIB-4 has been shown to influence the compaction and condensation of nucleoids. In *Arabidopsis*, DNA ligase I (AtLIG1) is found to be located in both nucleus and mitochondria along with type I and type II isomerases (Sunderland et al., 2006; Moriyama and Sato, 2014). The AtLIG1 activity is modulated in different cell types and metabolic states. Besides the role in ligation, this mitochondrial targeting protein is also involved in excision repair (Sunderland et al., 2006). Initial studies have reported a complete absence of photoreactivation in plant organelles (Chen et al., 1996; Hada et al., 2000). However, in rice and *Arabidopsis*, a nuclear-encoded photolyase was detected in both mitochondria, and chloroplast, respectively (Kleine et al., 2003; Takahashi et al., 2011). A single Mismatch repair (MMR) protein, MSH1, is nuclear-encoded and targeted to both chloroplast and mitochondria to repair the mismatches and also facilitates the recruitment of HR repair proteins in organelles (Chevigny et al., 2020).

Besides the DNA repair proteins, several transcription factors have been shown to play crucial role in anterograde signaling, where they participate in regulating the expression of different stress-responsive mitochondrial and chloroplast genes (**Figure 4**). In plants, a NAC domain transcription factor SOG1 (SUPPRESSOR OF GAMMA RESPONSE 1), the functional homolog of mammalian p53, has been found to regulate various aspects of DNA damage response in the nucleus, including DNA damage repair, cell cycle checkpoint control, and endoreduplication for ensuring genome integrity and stability (Adachi et al., 2011; Yoshiyama et al., 2017; Mahapatra and Roy, 2020). SOG1, the central regulator of DNA damage responses in plants, is also found to mediate endoreplication and cell-cycle progression through retrograde signaling from chloroplast to nucleus in response to chloroplast genome instability. *Arabidopsis thaliana* triple mutant *recA1why1why3* with considerable chloroplast genome instability have shown elevated expression of *RAD51* and *KU70*, the DNA repair marker genes associated with nuclear DSB repair (Horvath et al., 2017). In the same triple mutant, upregulation of various genes associated with cell cycle inhibition including *SMR5* and *SMR7* has also been detected, indicating arrest of cell cycle and induction of endoreduplication in response to chloroplast genome instability. Possibly, this response is regulated by SOG1, as all these genes are the direct target of SOG1 (Ogita et al., 2018; Mahapatra and Roy, 2020; Duan et al., 2020). This probably showcases a novel example of a retrograde signaling pathway, where nuclear gene expression is modulated

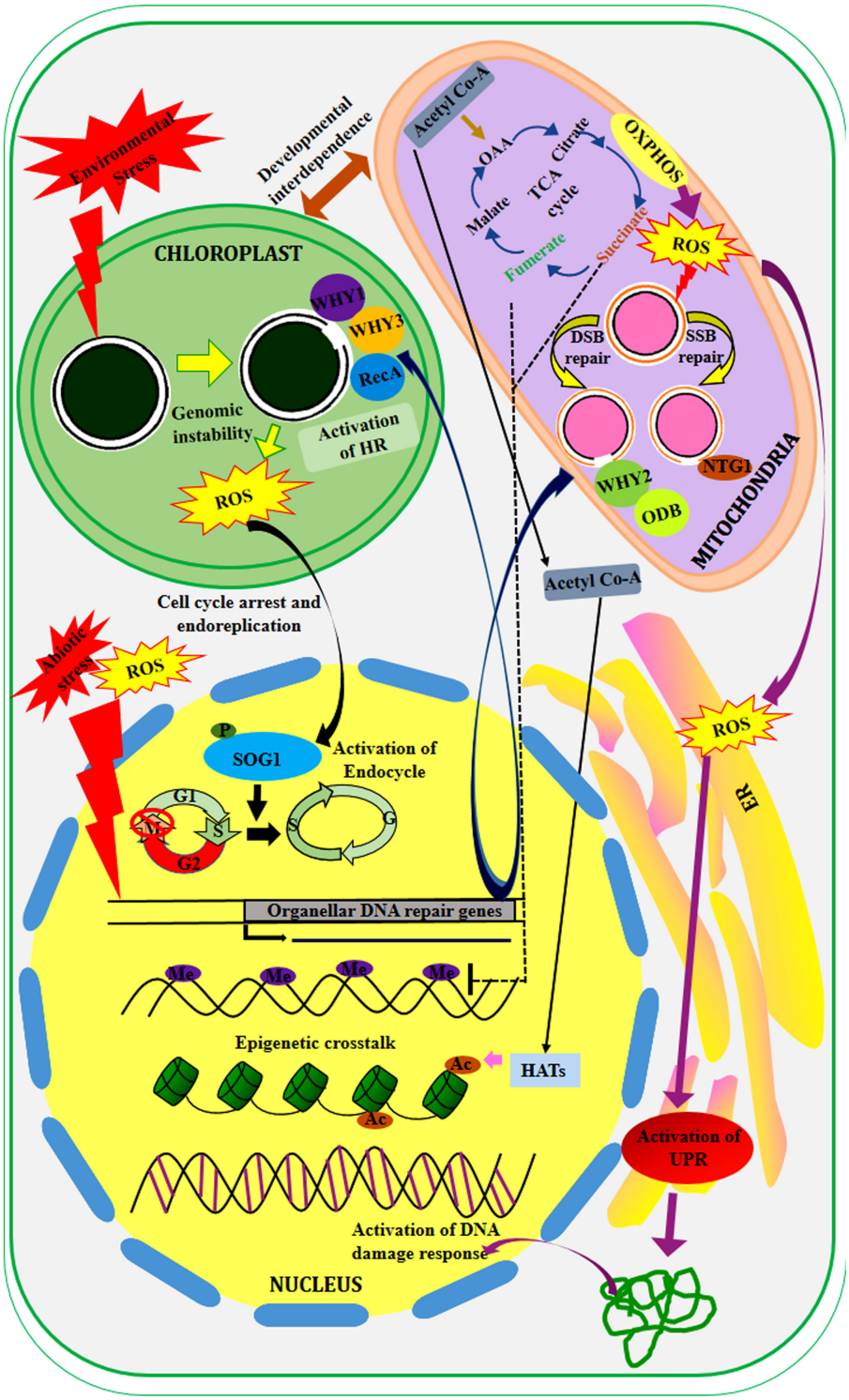

FIGURE 4 | Inter-compartmental crosstalk in the plant cell. The organelles are developmentally interdependent. The mutation of chloroplast genes affects the expression of several important genes (not shown here). In response to different environmental stress, the chloroplast genome become unstable which leads to the production of ROS in this compartment. This signal is received by the transcription factor, SOG1 that promotes endoreduplication and cell cycle arrest in the nucleus. While the nuclear-encoded proteins related to organellar DNA repair of both single and double-strand break repair are transported to the chloroplast (WHY3, WHY1, and RecA) and mitochondria (WHY2, ODB, NTG1) via anterograde signaling. The products of the TCA cycle (Succinate and fumarate) epigenetically modulate the gene expression via activation or repression. Moreover, the metabolic by-product (ROS) generated in mitochondria activates unfolded protein response (UPR) in ER which subsequently promotes DNA damage response in the nucleus.

by organellar genome instability and dysfunction (Chi et al., 2013; Hudik et al., 2014).

EPIGENETIC MODIFICATIONS ARE INVOLVED IN MAINTAINING THE STABILITY OF THE ORGANELLAR GENOME

Epigenetic changes affect an array of cellular processes in both prokaryotes and eukaryotes and these changes are not associated with permanent alterations in DNA sequence, while modify gene expression. Such changes are still heritable to the next generation (Kinoshita and Seki, 2014). Epigenetic modifications are generally caused by post-translational modifications (PTMs) that exist in the nuclear genome, including methylation, acetylation, phosphorylation, ubiquitination, PARylation, and sumoylation of protein. In addition, methylation of mainly cytosine residues in the promoter and intergenic regions also represents another important epigenetic modification in plants. These modifications are collectively involved in mediating various biotic and abiotic stress responses in plants (Bannister and Kouzarides, 2011; Kim, 2019). Besides these post-translational modifications, recent studies have revealed that different non-coding RNAs are also involved in epigenetic regulation (Agarwal and Miller, 2016). In plants, two subcellular organelles, mitochondria and chloroplast with self-contained genetic material have been found to coexist with the nucleus. However, very little information is available in the context of epigenetic modification and regulation of organellar genomes in plants.

Epigenetic Regulation by Post-translational Modifications

Among the various forms of post-translational modifications, cytosine DNA methylation has been identified as one of important heritable epigenetic marks found in many eukaryotes. Although DNA methylation is found to perform a conserved role in gene silencing, the levels and patterns of DNA methylation appear to differ significantly among different organisms. Methylation of DNA bases, as well as N and C-terminal tails of histone proteins modulate the nuclear gene expression. Cytosine residues are the major targets of methyltransferases (Methylation enzyme), which convert cytosine to 5-methyl cytosine (Richards, 2006). Methylation has also been found to play crucial role in organellar genome maintenance in plants (Gauly and Kössel, 1989). DNA methylation in the organellar genome has been a topic of research for past couple of decades. Although organellar DNA generally remains unmethylated, some of the cytosine residues in chloroplast DNA in the unicellular green alga *Chlamydomonas reinhardtii* have been found to be methylated (Dyer, 1982; Sager et al., 1984). During reproduction in *Chlamydomonas reinhardtii*, the chloroplast DNA gets degraded due to activation of zygote maturation process (Umen and Goodenough, 2001). However, methylation has been found to prevent the degradation of chloroplast DNA during mating (Sager et al., 1984; Umen and Goodenough, 2001). Subsequently, cytosine methylation in plastome was also reported in many higher plants, including *Acer*, tomato, and maize (Ngernprasirtsiri et al., 1988a,b; Gauly and Kössel, 1989). Leaf chloroplast in rice becomes more methylated with aging (Muniandy et al., 2019). In addition, the differential methylation pattern of CpG and CHG islands could be detected in leaf chloroplast and grain amyloplast of rice with identical DNA sequences (Muniandy et al., 2019). Besides chloroplast, a more recent study has indicated cytosine methylation in rice mitochondrial genome (Muniandy et al., 2020). In rice, leaf mitochondrial DNA showed higher proportions of methylation as compared to the grain mitochondrial DNA (Muniandy et al., 2020).

Cytosine methylation in plants can occur at different sites, like CG, CHG, and CHH, where H indicates nucleotide other than G (Law and Jacobsen, 2010). Earlier studies have indicated a tissue-specific organellar methylation pattern of cytosine residues, while in some cases methylation was completely absent (Yan et al., 2010). Furthermore, the same study has also revealed the presence of about 22 methylation sites in the coding region of the organellar DNA and about 146 positions dispersed in intergenic parts, indicating the variation in the position of methylation (Yan et al., 2010). Though nuclear methylases have been well characterized in plants, the information on methylation mechanism via specific methylases in organellar genome remains mostly inadequate. Previous studies have employed cyanobacterial methylase for the characterization of epigenetic regulation in plant chloroplast (Ahlert et al., 2009). In the nucleus, DNA methylation of cytosines has been found to occur specifically in CpG islands, which are dinucleotide repeat elements of typically 500-1500 bp length. In mitochondria, the story is somehow different as the CpG islands are absent in the mitochondrial genome due to their relatively smaller size (Muniandy et al., 2020).

Organellar genomes also affect the intricacy of the plant nuclear genome. Chloroplast and mitochondrion are the salient plant organelles with their own genetic material. During the course of evolution, most of the genetic information of organelles have been transferred to the nucleus and subsequently integrated with the nuclear genome, leading to the formation of NUPTs (Nuclear integrant of plastid DNA) and NUMTs (Nuclear integrant of mitochondrial DNA) (Yoshida et al., 2019; Zhang et al., 2020). In plants, NUPTs are shown to be involved in centromere formation and sex chromosome evolution (Li et al., 2019). The regulation and expression of integrated organellar DNA fragments in the nucleus are controlled via methylation. Considerable decrease in methylation level of NUPTs has been detected during evolution after being integrated into nuclear genomes (Paszkowski and Whitham, 2001; Bender, 2004). Thus, DNA methylation on nuclear organellar DNA fragments may also contribute toward the maintenance of genome stability and evolutionary dynamics of symbiotic organellar as well as their host's genomes. Although, there has been no direct evidence of plant organellar genome methylation, methylome data analysis using various epigenetic mutants have revealed the establishment and maintenance of methylation of NUPTs (Nuclear integrant of plastid DNA) in *Arabidopsis thaliana* by

several methyltransferases including DDM1, CMT3, CMT2, and SUVH4/KYP proteins, respectively (Yoshida et al., 2019; Zhang et al., 2020). In the absence of histone proteins, mitochondrial gene expression is regulated by the epigenetic changes of nucleoid-associated proteins. In animal system, multiple lysine acetylation and phosphorylation sites have been detected in the organellar genome (Zhao et al., 2010). Mitochondrial transcription factor A (TFAM) has been shown to be post-transcriptionally modified via glycosylation, acetylation as well as phosphorylation (Lu et al., 2013; King et al., 2018). However, corresponding information in plant mitochondria genome remains much limited and further investigation is required. In humans, poly ADP ribosylation is considered as one of the key post-translational modifications regulated by poly ADP ribose polymerases (PARP). Three canonical PARP proteins are encoded by *Arabidopsis* nuclear genome (Gu et al., 2019). Among the three PARP proteins, PARP1 has been found to be conserved throughout the plant and animal kingdom, while PARP2 proteins are broadly conserved across diverse plant groups. In contrast, PARP3 is mainly expressed in seed tissues in plants, but can also be detected in the seedlings and roots in adult plants (Feng et al., 2016; Rissel and Peiter, 2019). In *Arabidopsis,* AtPARP2 plays a predominant role in poly-ADP ribosylation than AtPARP1. AtPARP2 is localized in the nucleus, as evidenced from the expression of *AtPARP2-GFP* constructs in *Nicotiana benthamiana* and *Arabidopsis* (Song et al., 2015; Pham et al., 2015; Chen et al., 2018). Recent studies have demonstrated that nuclear import of AtPARP2 is mediated via importin-α (Chen et al., 2018). In addition to its nuclear localization, AtPARP2 has been suggested to be partially localized in chloroplasts (Pham et al., 2015). As with AtPARP2, the AtPARP1-GFP fusion protein was detected in nucleus in *Nicotiana benthamiana* and in *Arabidopsis* cell suspension culture (Song et al., 2015; Pham et al., 2015). Furthermore, PARP1-GFP localization was detected in chloroplasts and mitochondria when expressed in *Arabidopsis* protoplasts (Pham et al., 2015). In plants, PARP2 regulates response to various genotoxic agents such as bleomycin, mitomycin-c, or γ-radiation, respectively (Song et al., 2015). Nuclear encoded PARP2 also regulates plant immunity via interacting with fork head associated (FHA) domain protein, DAWDLE (DDL) (Feng et al., 2016). Recent studies have revealed that PARP1 is located both nucleus and mitochondria (Pankotai et al., 2009). PARP1 binds to the promoter of several mitochondrial-targeted nuclear protein-encoding genes, which are specifically involved in mitochondrial DNA damage repair. PARP1 also modulates the expression of many DNA damage repair genes, including *APE1*, *UNG1*, *MYH1*, and various transcription factors including TFB1M and TFB2M, respectively (Lapucci et al., 2011).

Epigenetic Regulation of Organellar Genome by Non-coding RNAs and MicroRNAs

Besides the precise role of cytosine methylation in the regulation of epigenetic responses in the organellar genome, several non-coding RNAs are also found to be involved in the regulation of expression of organellar proteins encoded by nuclear genes (Lung et al., 2006). Intra-organellar non-coding RNAs also alter the expression of both mitochondrial and chloroplast genes (Zhang et al., 2016; Matsui and Corey, 2017). These non-coding RNAs are either synthesized *de novo* via the transcription of mitochondrial or chloroplast genome or may be generated from the degradation of the organelle transcriptome, as it was evidenced from Pentatricopeptide Repeat Proteins (PPR) (Hotto et al., 2012). Various reports have claimed the location of intermediate size non-coding RNAs in the protein-coding genes, including *ATP*, *RPL*, *NAD,* and *COX3*, respectively in *Arabidopsis thaliana* (Wang Y. et al., 2014). In barley grains and leaves, exonic regions of mitochondrial DNA produce different circular RNAs and their expression varies in response to different micronutrients and they are also involved in an array of metabolic pathways (Darbani et al., 2016). Previous studies have revealed abiotic stress mediated up-regulation of various microRNAs (miRNAs) in chloroplasts and among which, mi-408 was found to be highly induced under cold stress (Liu et al., 2008). However, the information regarding involvement of various non-coding RNAs in regulating DNA damage response in plant organellar genome remains largely unknown. Therefore, further studies are required for the characterization of role of different non-coding RNAs in organellar genome maintenance.

Besides non-coding RNAs, various miRNAs are also found to be associated with several biological processes, including animal cell development and differentiation. It has been observed that miR125a is involved in the sex-determination and development of mammalian gonads (Reza et al., 2019). Many human diseases are associated with the aberrant expression of miRNAs (Paul et al., 2018). Moreover, muscle-specific miR-1 is capable of enhancing the expression of mt-DNA encoded proteins during muscle differentiation, which also requires argonaut 2 (AGO2) (Zhang et al., 2014).

TARGETING ORGANELLAR GENOME FOR CROP IMPROVEMENT

The detrimental effects of global climate change along with the augmented increase in human population have put a substantial impact on agriculture and thus, emphasis has now been given toward ensuring food security for a sustainable future (Foley et al., 2011; Tilman et al., 2011; Verma et al., 2020). Conventional plant breeding for generating plants with high productivity is often found to be a comparatively labor-intensive and time-consuming procedure as compared to plant genetic engineering approaches, which is believed to enhance crop productivity more efficiently (Christou, 2013).

Genetic diversity is one of the very essential components for crop improvement to generate novel combinations of genes to achieve desired phenotypes (Glaszmann et al., 2010). Although DNA damage has been considered for its mutagenic effect, the persistence of damaged bases in DNA also harms plant growth and development. Due to their immobile nature and obligatory dependence on sunlight for photosynthesis, as like the other plants, crop plants' genome also remains continuously

exposed to various genotoxic factors, including solar UV and ionizing radiation, soil salinity, heavy metal contamination and also the by-products of endogenous metabolic processes, such as ROS, which may frequently result in the accumulation of spontaneous mutations (Verma et al., 2020). Although these mutations have been found to enrich the genetic diversity in the already existing genetic pool, the process is too slow to keep pace with the ever-increasing demand. At present, various crop improvement tools are used, which can be broadly categorized into major three types, such as the chemical and physical mutagenesis, transgenics, and genome editing approaches (Manova and Gruszka, 2015; Verma et al., 2020). Intriguingly, DNA damage response or DDR has taken the central stage in almost all crop improvement techniques. Techniques of mutagenesis appeared to be one of the effective tools for developing various germplasm collections in both model and crop plants and have facilitated the discovery of desired loci and alleles (Manova and Gruszka, 2015). Significant advancement has been made for the past couple of years to decipher the underlying mechanisms of organellar genome stability maintenance in plants. Further identification and functional characterization of different genes involved in these processes therefore may provide important insight into the molecular mechanisms of DNA repair. Induction of mutations in the crucial genes involved in DNA damage response and repair in organellar genomes have been found to alter the efficacy of these important processes, resulting in more effective mutagenesis (Verma et al., 2020).

Nuclear genome transformation has been employed extensively to increase productivity of some economically important crop plants (Li et al., 2021). However, one of the major constraints of nuclear transformation is the uncertain expression of the gene of interest along with the random location of insert DNA integration, resulting in gene silencing (Meyers et al., 2010). In this context, the presence of highly efficient homology-dependent DSB repair in the organellar genome has opened up new possibilities in the area of genome transformation and overall crop improvement (Li et al., 2021). Along with the highly efficient homologous recombination process for precise transgene insertion, some other attractive characteristics, including high intensity of transgene expression, multiple transgenes stacking through operon transfer to the organellar genome, absence of epigenetic regulation mediated gene silencing, and expression of native bacterial proteins, respectively have provided a better option for settlement of transgene within the organellar genome (Bansal and Saha, 2012; Li et al., 2021). Chloroplast transformation has been successfully performed in the model plant *Arabidopsis thaliana* (Ruf et al., 2019). However, successful transformation of mitochondria in higher plant systems has not been reported so far. In crop plants, chloroplast transformation has been limited due to technical difficulties. However, it has been suggested that the development of species-specific transgene delivery vectors with homologous recombination sequences along with regulatory elements for methodical transgene integration would effectively facilitate chloroplast transformation (Bansal and Saha, 2012).

Targeting DNA Damage Response and Repair System in Subcellular Organelle for Crop Improvement

Plants have evolved with vast array of DNA damage response and repair systems for efficient detection and repair of the damages in the genome for maintaining genome stability and to cope up with various genotoxic threats. However, information regarding mechanisms of DNA damage repair in plant organellar genome and their implications is rather limited. Various genes involved in DDR are known to be responsive to different abiotic and biotic stress factors and targeting these genes by altering their expression or protein structure may help in generating improved stress tolerance in crop plants (Baillo et al., 2019). Many DNA glycosylases involved in repairing oxidative damages, including the repair of one of the highly mutagenic lesions, 8-oxo guanine (8-oxoG) via base excision repair (BER) pathway and have been shown to play an essential role in developing oxidative stress tolerance. In *Arabidopsis*, overexpression of *AtOGG1* (codes for AtOGG1 DNA glycosylase) improves seed longevity (Chen et al., 2012) while, overexpression of *AtMBD4* (codes for MBD4L DNA glycosylases) has been shown to enhance tolerance to oxidative stress in *Arabidopsis* (Nota et al., 2015). Studies carried out with the nuclear genome have provided important clues regarding the altered expression of DNA glycosylases associated with the BER pathway in mitochondria and chloroplast for developing enhanced tolerance to biotic and abiotic stress factors in plants. Therefore, it would be highly interesting to understand the functional aspects of DNA glycosylases associated with organellar base excision repair to get further insight into the potential scope of utilization of BER pathway components in crop improvement.

Although, the homology-dependent DNA repair has been primarily demonstrated in nuclear and prokaryote genome, accumulating evidences have revealed the presence of fairly well-developed homologous recombination pathway in both mitochondria and chloroplast in many plant species (extensively reviewed by Barr et al., 2005; Kmiec et al., 2006). Frequent and easily noticeable flip-flop recombination events between large inverted repeats could be detected in chloroplasts of many angiosperms, resulting in equimolar plastome isoforms with different orientations of the two single-copy regions (Palmer, 1983). Homologous recombination can be employed as a fundamental and potential driving force for the generation of new allelic combinations as well as enhancement of genetic diversity. Thus, understanding the in-depth mechanism of homologous recombination and its possible interlinking with other pathways of the organellar DNA damage response may provide an effective tool for modulating HR frequencies for achieving the goal of crop improvement. In addition, it may also provide one possible mechanism to ease the homologous recombination between divergent sequences.

Chloroplast Genome Editing for Genetic Analysis

The present nuclease based genome editing approach relies on the induction of DSBs at the targeted DNA sequences of targeted

genome alterations in the context of crop improvement (Puchta and Fauser, 2015; Schmidt et al., 2019). The resulting DSBs can be repaired by both the non-homologous end joining (NHEJ) and homologous recombination (HR) mediated repair pathways. However, the skewness of the former pathway normally results in imprecise repair as well as random mutations (Ray and Raghavan, 2020). On the other hand, the homology-directed repair has been considered as one of the most error-free pathway as it involves a precise sequence alteration based on a homologous DNA sequence as template (Chen et al., 2019). In plants, in both mitochondria and chloroplast, DSBs are mainly repaired via homologous recombination and microhomology-mediated end joining pathway, while the NHEJ repair pathway appears to be either completely absent in plant organellar genome or may be present in few cases (Kwon et al., 2010). In the chloroplast of the green algae *Chlamydomonas*, all three forms of HR pathways, including DSBR, SDSA, and SSA have been reported (Odom et al., 2008; Kwon et al., 2010). CRISPR-Cas9-mediated genome alteration approach was applied in *Chlamydomonas* by introducing two plasmids. One of the plasmid was used for carrying Cas9 and a guide RNA (gRNA) expression cassette, while the other plasmid carried the precise donor DNA fragment for incorporation between the two specific DSB sites created by the targeted action of CRISPR-Cas9 (Yoo et al., 2020). Interestingly, at one of the Cas9 incision sites in the *Chlamydomonas* chloroplast, no insertions or deletion could be detected, indicating the absence of error-prone NHEJ repair pathway in the *Chlamydomonas* chloroplast genome. However, the possibility of activation of the CRISPR-Cas9 system in the chloroplast of *Chlamydomonas* cannot be discarded. For now, one of the major constraints for employing the CRISPR-Cas9 genome editing system to manipulate organellar genomes in higher plants is the presence of double-membrane boundary of the organelles, which efficiently restricts the import of various biomolecules, including the nucleic acids (Gammage et al., 2018). One of the possible approaches for genome editing in chloroplast may involve direct expression of both Cas9 and gRNA in the chloroplast genome by using the privilege of chloroplast transformation technology. However, one of the major limitations in this approach is the high copy number of the chloroplast genome (Shaver et al., 2006). Possible risk of gene conversion between wild-type and disrupted genome may occur in such condition if the chloroplast genome with insertion and/or deletions, generated by CRISPR-Cas9, fails to achieve a homoplasmic state (Khakhlova and Bock, 2006). This may eliminate the insertion and/or deletions (indels) and the desire edited plastome will not be obtained.

Because of the presence of efficient homologous recombination in chloroplasts, genes in the chloroplast genome can be disrupted easily by inserting or replacing them with a selectable marker gene cassette. More subtle changes, such as induction of point mutations and small indels can be achieved by co-transformation of the selectable marker gene and a target gene with a specific mutation (Krech et al., 2013). Various chloroplast genes have been characterized by knockout mutations (Scharff and Bock, 2014). Variations in the selectable markers and their recycling techniques have made it possible to construct double and triple knockout mutants and the induction of mutations in multiple chloroplast genes, thereby allowing the discovery of various molecular interactions between the components of the photosynthetic complex (Fleischmann et al., 2011).

Improving Photosynthesis Through Chloroplast Engineering

Ribulose-1,5-bisphosphate carboxylase/oxygenase, also known as Rubisco is the most abundant class of protein in nature and appeared to be the major enzyme of the Calvin–Benson cycle, which is responsible for fixing atmospheric CO_2 into the C_3 organic acid 3−phosphoglycerate (3−PGA) for its further utilization to regenerate the substrate ribulose−1,5−bisphosphate (RuBP) or form the building blocks of carbohydrate synthesis (Sharwood, 2017). Rubisco is a large protein complex consisting of eight large catalytic subunits (rbcL) and eight small catalytic subunits (rbcS). The large subunits are encoded by the chloroplast genome itself, whereas, the small subunits are encoded by the nuclear genome, respectively. Rubisco has been shown to exhibit catalytic inefficiencies, including slow catalysis and imperfect discrimination between CO_2 and O_2, thus considered as the most obvious target for crop improvement to enhance the photosynthetic capacity of plants (**Figure 5**; Parry et al., 2013; Galmés et al., 2014; Pottier et al., 2018). The distinct locations of the genes responsible for encoding the Rubisco large (chloroplast) and small (nucleus) subunits have made the engineering of Rubisco complicated in higher plants. In this context, development of chloroplast transformation was the first breakthrough in engineering the Rubisco large subunit (Sharwood, 2017).

Among some of the initial trials of Rubisco large subunit engineering, the substitution of tobacco rbcL was achieved with the sunflower and cyanobacterial counterparts (Kanevski et al., 1999). Although, the resulting hybrid Rubisco was catalytically inactive or inefficient, this initial study provided proof-of-concept for this new technology. Another approach was to assemble the functional Rubisco enzyme within the chloroplast. To achieve this, Rubisco small subunit gene (rbcS) was relocated back into its pre-endosymbiotic location within the plastome (Whitney and Andrews, 2001; Zhang et al., 2002; Dhingra et al., 2004). One very recent study has demonstrated the effectiveness of various sequences on Rubisco protein production from synthetic rbcL-rbcS operons transformed into the chloroplast genome to replace rbcM. For this, a tobacco bRrDs line was generated, in which endogenous *rbcS* genes were silenced and the rbcL gene of tobacco was replaced using the *rbcM* gene of *Rhodospirillum rubrum* (Avila et al., 2020). The *rbcM* gene of *Rhodospirillum rubrum* has been found to encode the L2 form of Rubisco that does not assemble with the small subunit. Although the production of Rubisco was achieved only up to 50% of the wild type, this research has explored the possibilities of modulating different Rubisco subunit assemblies for increasing the production of Rubisco by chloroplast engineering. Apart from Rubisco engineering, another interesting strategy to enhance photosynthesis includes the introduction of a CO_2-concentrating mechanism from

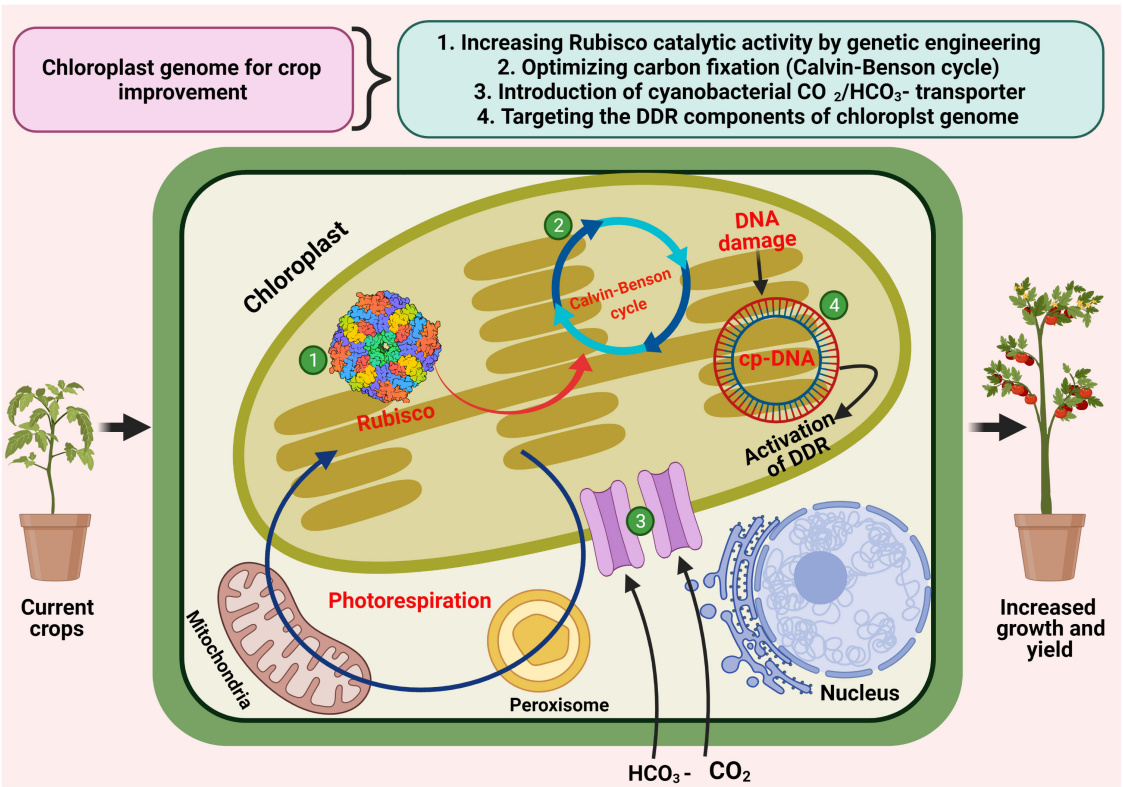

FIGURE 5 | Modulation of chloroplast genome for crop improvement. Various aspects of employment of chloroplast genome for improving photosynthesis and crop productivity including modifications of Rubisco subunits through plastome engineering, optimization of carbon fixation, the introduction of cyanobacterial HCO_3– and CO_2 transporters, and targeting various components of DNA damage response (DDR).

cyanobacteria into transplastomic plants to maximize their carbon fixation (Lin et al., 2014; Occhialini et al., 2016).

Molecular Breeding Through Modifications of Mitochondrial Genome

Although, the structure of angiosperm mitochondrial genome has been studied in detail, molecular analysis of mitochondrial genome for crop improvement has not been successful because of the lack of efficient transformation strategies. Genome editing in mitochondria has been made possible by employing transcription activator-like editing nucleases (TALEN)- mediated nuclear transformation, which resulted in new transformed rice and canola (**Figure 6**; Kazama et al., 2019). Generally, TALENs consist of two domains, including the DNA binding domain, which can be engineered to recognize any DNA sequences, and the nuclease domain, capable of nicking the DNA and causing deletions. For manipulating mitochondrial genes, the plant-adapted TALEN was modified with the inclusion of a mitochondrial localization signal sequence and the DNA binding domain was engineered in a way so that it can recognize the target genes of interest. The plasmid encoding the mito-TALEN was then transferred into plants by *Agrobacterium*-mediated transformation. In the above-mentioned study, two mito-TALENs were constructed, which targeted two mitochondrial genes, including *orf79* (rice) and *orf125* (rapeseed), respectively (Kazama et al., 2019). The resulting deletions have established role of these genes in male sterility, which appeared to prevent self-fertilization in certain hermaphroditic plants. Another recent study has demonstrated utilization of mito-TALENs to knock out the function of two mitochondrial genes, including *atp6-1*and *atp6-2*, respectively in the model plant *Arabidopsis thaliana* (Arimura et al., 2020). In addition to TALEN-mediated plant mitochondrial genome editing, recent studies have reported development of a CRISPR-free technique for human mitochondrial genome base editing (Mok et al., 2020). This newly developed genome editing technique utilizes a double-stranded DNA-specific interbacterial cytidine deaminase toxin to induce targeted mutation in the human mitochondrial genome with approximately 5-50% efficiency (Mok et al., 2020). Although, additional research is required to further decipher the efficiency of this approach.

Conclusion and Prospects

Since their discovery about half a century ago, significant progress has been made on the sequencing and characterization of mitochondrial and chloroplast genome. Maintenance of organellar genome stability in the context of permanent threat from oxidative damage is one of the major challenges for eukaryotic cells. Despite this, it has long been considered that bona fide DNA damage repair mechanism is absent in

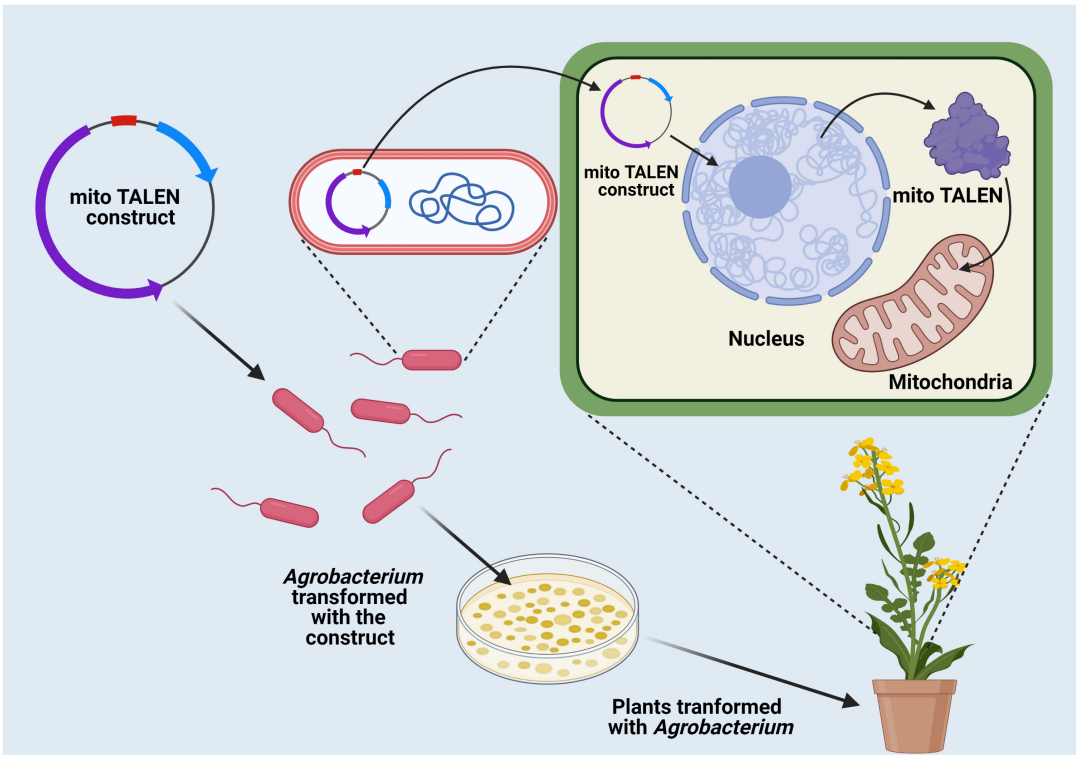

FIGURE 6 | Transformation of the mitochondrial genome. Genome editing in mitochondria through transcription activator-like editing nucleases (TALEN) mediated nuclear transformation and generated new types of crop plants with improved productivity.

both plant mitochondria and chloroplast genomes. However, recent advancements on the structure-function aspects of organellar genome have demonstrated the existence of highly efficient DNA damage repair machinery in both chloroplast and mitochondria and has become an emerging field of research within a little more than a decade for better understanding plant cell function under stress conditions. Previous studies have indicated the functioning of base excision repair and homologous recombination repair pathways for repairing oxidative damages and double-strand breaks, respectively in the organellar genomes. Besides its role in repairing DSBs, the HR pathway appears to be involved in organellar genome replication and maintenance of low mutation rates. However, corresponding knowledge on the mechanistic details of HR mediated functions remains still elusive and deserves further extensive research. In addition, there are still potential questions regarding the evolution and variation of plant organellar genomes and how the various DNA repair mechanisms in organellar genomes became closely associated during their evolution. These aspects needs further research to get more insight into the evolutionary aspects DNA damage response and repair mechanisms in the context of genome stability mechanisms in plants.

After the origin of mitochondria and chloroplast following the engulfment of ancestral α-proteobacteria and cyanobacteria, most genes were subsequently either lost or transferred to the nucleus through horizontal gene transfer after the endosymbiosis, and thus both organelles are dependent on nuclear-encoded proteins for their DNA damage response and genome stability maintenance. As organelles are critical integrators of both internal and external cues, various activities in the organelles are needed to be tightly coordinated with nuclear activities to enable plant development and stress signaling. Various crucial proteins for organelle genome maintenance, such as the WHIRLY family proteins are found to be under coordinated control of organelle and nuclear genomes. Dual localization of proteins associated with various important cellular responses in eukaryotic organisms has eventually been accepted as an important phenomenon linked with multi-functionalization and also proposed to have an evolutionary advantage.

To meet the demand for food for a rapidly growing world population in the face of an unsure global climate change and reduced arable land, improvement in crop production is emerging as an immediate priority. In this context, along with nuclear transformation, plants also offer the opportunity to transform the comparably smaller genomes of two semi-autonomous organelles, including chloroplast and mitochondria. The chloroplast genome has been modified genetically for improvement of crop yield, nutritional quality, and resistance to various abiotic and biotic stresses. However, mitochondrial transformation in higher plants was not been successful initially, but stepwise progress has been made for manipulation mitochondrial genes and their transcripts. In addition, emphasis

has also been given to target various DNA damage responses and repair components associated with organellar genome maintenance for crop improvement. However, further research is required in this exciting field of research to unveil plant cell response under changing environment.

AUTHOR CONTRIBUTIONS

SR, KM, and SB researched and developed the idea. SR, KM, SB, SD, MM, and PR wrote the review. KM, SB, and SD created the figures. SR and KM edited the manuscript. All authors have read and approved the manuscript.

FUNDING

The authors gratefully acknowledge Council of Scientific and Industrial Research, Govt. of India, [Ref. No. 38(1417)/16/EMR-II, dated:17/05/2016 to SR], SERB, DST, Govt. of India (Ref. No: ECR/2016/000539 to SR), and DST and BT, Govt. of WB (Ref. No: ST/P/S and T/1G-5/2018 to SR) for the financial support for performing related research in the lab. KM is the recipient of SRF fellowship from CSIR, Govt. of India [09/025(0220)/2017-EMRI]. SB is the recipient of the JRF fellowship from CSIR, Govt. of India [09/025(0261)/2018-EMR-I]. MM is the recipient of Inspire Fellowship from DST, Govt. of India (DST/INSPIRE Fellowship/2017/IF17001).

REFERENCES

Abdelnoor, R. V., Yule, R., Elo, A., Christensen, A. C., Meyer-Gauen, G., and Mackenzie, S. A. (2003). Substoichiometric shifting in the plant mitochondrial genome is influenced by a gene homologous to MutS. *Proc. Natl. Acad. Sci. U.S.A.* 100, 5968–5973. doi: 10.1073/pnas.1037651100

Adachi, S., Minamisawa, K., Okushima, Y., Inagaki, S., Yoshiyama, K., Kondou, Y., et al. (2011). Programmed induction of endoreduplication by DNA double-strand breaks in Arabidopsis. *Proc. Natl. Acad. Sci. U.S.A.* 108, 10004–10009. doi: 10.1073/pnas.1103584108

Agarwal, P., and Miller, K. M. (2016). The nucleosome: orchestrating DNA damage signaling and repair within chromatin. *Biochem. Cell Biol.* 94, 381–395. doi: 10.1139/bcb-2016-0017

Ahlert, D., Stegemann, S., Kahlau, S., Ruf, S., and Bock, R. (2009). Insensitivity of chloroplast gene expression to DNA methylation. *Mol. Genet. Genomics* 282, 17–24. doi: 10.1007/s00438-009-0440-z

Ahmad, N., and Nielsen, B. L. (2020). Plant Organelle DNA Maintenance. *Plants* 9:683. doi: 10.3390/plants9060683

Alexeyev, M., Shokolenko, I., Wilson, G., and LeDoux, S. (2013). The maintenance of mitochondrial DNA integrity - critical analysis and update. *Cold Spring Harb. Perspect. Biol.* 5:a012641. doi: 10.1101/cshperspect.a012641

Andreyev, A. Y., Kushnareva, Y. E., and Starkov, A. A. (2005). Mitochondrial metabolism of reactive oxygen species. *Biochemistry* 70, 200–214. doi: 10.1007/s10541-005-0102-7

Arimura, S. I., Ayabe, H., Sugaya, H., Okuno, M., Tamura, Y., Tsuruta, Y., et al. (2020). Targeted gene disruption of *ATP synthases 6-1* and *6-2* in the mitochondrial genome of *Arabidopsis thaliana* by mitoTALENs. *Plant J.* 104, 1459–1471. doi: 10.1111/tpj.15041

Arora, A., Sairam, R. K., and Srivastava, G. C. (2002). Oxidative stress and antioxidative system in plants. *Curr. Sci.* 82, 1227–1238.

Avila, E. M., Lim, Y. L., Birch, R., Dirk, L. M. A., Buck, S., Rhodes, T., et al. (2020). Modifying plant photosynthesis and growth via simultaneous chloroplast transformation of Rubisco large and small subunits. *Plant Cell* 20:288. doi: 10.1105/tpc.20.00288

Baillo, E. H., Kimotho, R. N., Zhang, Z., and Xu, P. (2019). Transcription Factors Associated with Abiotic and Biotic Stress Tolerance and Their Potential for Crops Improvement. *Genes* 10:771. doi: 10.3390/genes10100771

Bannister, A. J., and Kouzarides, T. (2011). Regulation of chromatin by histone modifications. *Cell Res.* 21, 381–395. doi: 10.1038/cr.2011.22

Bansal, K. C., and Saha, D. (2012). Chloroplast Genomics and Genetic Engineering for Crop Improvement. *Agric. Res.* 1, 53–66. doi: 10.1007/s40003-011-0010-6

Barr, C. M., Neiman, M., and Taylor, D. R. (2005). Inheritance and recombination of mitochondrial genomes in plants, fungi, and animals. *New Phytol.* 168, 39–50. doi: 10.1111/j.1469-8137.2005.01492.x

Baruch-Torres, N., and Brieba, L. G. (2017). Plant organellar DNA polymerases are replicative and translesion DNA synthesis polymerases. *Nucleic Acids Res.* 45, 10751–10763. doi: 10.1093/nar/gkx744

Bender, J. (2004). Chromatin-based silencing mechanisms. *Curr. Opin. Plant Biol.* 7, 521–526. doi: 10.1016/j.pbi.2004.07.003

Blokhina, O., and Fagerstedt, K. V. (2010). Reactive oxygen species and nitric oxide in plant mitochondria: origin and redundant regulatory systems. *Physiol. Plant.* 138, 447–462. doi: 10.1111/j.1399-3054.2009.01340.x

Bobik, K., and Burch-Smith, T. M. (2015). Chloroplast signaling within, between, and beyond cells. *Front. Plant Sci.* 6:781. doi: 10.3389/fpls.2015.00781

Bock, R. (2015). Engineering plastid genomes: methods, tools, and applications in basic research and biotechnology. *Annu. Rev. Plant Biol.* 66, 211–241. doi: 10.1146/annurev-arplant-050213-040212

Boehm, C. R., and Bock, R. (2019). Recent advances and current challenges in synthetic biology of the plastid genetic system and metabolism. *Plant Physiol.* 179, 794–802. doi: 10.1104/pp.18.00767

Boesch, P., Ibrahim, N., Paulus, F., Cosset, A., Tarasenko, V., and Dietrich, A. (2009). Plant mitochondria possess a short-patch base excision DNA repair pathway. *Nucleic Acids Res.* 37, 5690–5700. doi: 10.1093/nar/gkp606

Boesch, P., Weber-Lotfi, F., Ibrahim, N., Tarasenko, V., Cosset, A., Paulus, F., et al. (2011). A. DNA repair in organelles: Pathways, organization, regulation, relevance in disease and aging. *Biochim. Biophys. Acta* 1813, 186–200. doi: 10.1016/j.bbamcr.2010.10.002

Börner, T. (2017). The discovery of plastid-to-nucleus retrograde signaling—a personal perspective. *Protoplasma* 254, 1845–1855. doi: 10.1007/s00709-017-1104-1

Brieba, L. (2019). Structure-Function Analysis Reveals the Singularity of Plant Mitochondrial DNA Replication Components: A Mosaic and Redundant System. *Plants* 2019:533. doi: 10.3390/plants8120533

Britt, A. B. (1999). Molecular genetics of DNA repair in higher plants. *Trends Plant Sci.* 4, 20–25. doi: 10.1016/s1360-1385(98)01355-7

Busi, M. V., Gomez-Lobato, M. E., Rius, S. P., Casati, P., Zabaleta, E. J., et al. (2011). Effect of mitochondrial dysfunction on carbon metabolism and gene expression in flower tissues of Arabidopsis thaliana. *Mol. Plant* 4, 127–143. doi: 10.1093/mp/ ssq065

Cagin, U., and Enriquez, J. A. (2015). The complex crosstalk between mitochondria and the nucleus: What goes in between? *Int. J. Biochem. Cell Biol.* 63, 10–15. doi: 10.1016/j.biocel.2015.01.026

Cappadocia, L., Marechal, A., Parent, J. S., Lepage, E., Sygusch, J., and Brisson, N. (2010). Crystal structures of DNA–Whirly complexes and their role in *Arabidopsis* organelle genome repair. *Plant Cell.* 22, 1849–1867. doi: 10.1105/tpc.109.071399

Chacinska, A., Koehler, C. M., Milenkovic, D., Lithgow, T., and Pfanner, N. (2009). Importing mitochondrial proteins: machineries and mechanisms. *Cell* 138, 628–644. doi: 10.1016/j.cell.2009.08.005

Chan, K. X., Phua, S. Y., Crisp, P., McQuinn, R., and Pogson, B. J. (2016). Learning the languages of the chloroplast: retrograde signaling and beyond. *Annu. Rev. Plant Biol.* 67, 25–53. doi: 10.1146/annurevarplant-043015-111854

Chen, C., De Masi, R., Lintermann, R., and Wirthmueller, L. (2018). Nuclear import of *Arabidopsis* poly(ADP-ribose) polymerase 2 is mediated by importin-α and a nuclear localization sequence located between the predicted SAP domains. *Front. Plant Sci.* 9:1581. doi: 10.3389/fpls.2018.01581

Chen, H., Chu, P., Zhou, Y., Li, Y., Liu, J., Ding, Y., et al. (2012). Overexpression of AtOGG1, a DNA glycosylase/AP lyase, enhances seed longevity and abiotic

stress tolerance in Arabidopsis. *J. Exp. Bot.* 63, 4107–4121. doi: 10.1093/jxb/ers093

Chen, J. J., Jiang, C. Z., and Britt, A. B. (1996). Little or no repair of cyclobutyl pyrimidine dimers is observed in the organellar genomes of the young Arabidopsis seedling. *Plant Physiol.* 111, 19–25. doi: 10.1104/pp.111.1.19

Chen, K., Wang, Y., Zhang, R., Zhang, H., and Gao, C. (2019). CRISPR/Cas genome editing and precision plant breeding inagriculture. *Annu. Rev. Plant Biol.* 70, 667–697. doi: 10.1146/annurev-arplant-050718-100049

Chevigny, N., Nadiras, C., Raynaud, C., Monique, L., Bichara, M., Mathieu, E., et al. (2019). RADA is the main branch migration factor in plant mitochondrial recombination and its defect leads to mtDNA instability and cell cycle arrest. *bioRxiv* 856716. [preprint]. doi: 10.1101/85671

Chevigny, N., Schatz-Daas, D., Lotfi, F., and Gualberto, J. M. (2020). DNA Repair and the Stability of the Plant Mitochondrial Genome. *Int. J. Mol. Sci.* 21:328. doi: 10.3390/ijms21010328

Chi, W., Sun, X., and Zhang, L. (2013). Intracellular signaling from plastid to nucleus. *Annu. Rev. Plant Biol.* 64, 559–582. doi: 10.1146/annurev-arplant-050312-120147

Christensen, A. C., Lyznik, A., Mohammed, S., Elowsky, C. G., Elo, A., Yule, R., et al. (2005). Dual-domain, dual-targeting organellar protein presequences in *Arabidopsis* can use non-AUG start codons. *Plant Cell* 17, 2805–2816. doi: 10.1105/tpc.105.035287

Christou, P. (2013). Plant genetic engineering and agricultural biotechnology 1983-2013. *Trends Biotechnol.* 31, 125–127. doi: 10.1016/j.tibtech.2013.01.006

Clark, D. P., Pazdernik, N. J., and McGehee, M. R. (2019). *Molecular Biology (Third Edition)*. Netherland: Elsevier.

Cleland, R. E., and Grace, S. C. (1999). Voltametric detection of superoxide production by photosystem II,". *FEBS Lett.* 457, 348–352. doi: 10.1016/s0014-5793(99)01067-4

Cordoba, E., Salmi, M., and Leon, P. (2009). Unravelling the regulatory mechanisms that modulate the MEP pathway in higher plants. *J. Exp. Bot.* 60, 2933–2943. doi: 10.1093/jxb/erp190

Cordoba-Cañero, D., Dubois, E., Ariza, R. R., Doutriaux, M. P., and Roldan-Arjona, T. (2010). Arabidopsis uracil DNA glycosylase (UNG) is required for base excision repair of uracil and increases plant sensitivity to 5-fluorouracil. *J. Biol. Chem.* 285, 7475–7483. doi: 10.1074/jbc.M109.067173

Córdoba-Cañero, D., Roldán-Arjona, T., and Ariza, R. R. (2014). Arabidopsis ZDP DNA 3'-phosphatase and ARP endonuclease function in 8-oxoG repair initiated by FPG and OGG1 DNA glycosylases. *Plant J.* 79, 824–834. doi: 10.1111/tpj.12588

Cox, M. M. (2007). Regulation of bacterial RecA protein function. *Crit. Rev. Biochem. Mol. Biol.* 42, 41–63. doi: 10.1080/10409230701260258

Cupp, J. D., and Nielsen, B. L. (2014). Minireview: DNA replication in plant mitochondria. *Mitochondrion* 19, 231–237. doi: 10.1016/j.mito.2014.03.008

Darbani, B., Noeparvar, S., and Borg, S. (2016). Identification of circular RNAs from the parental genes involved in multiple aspects of cellular metabolism in barley. *Front. Plant. Sci.* 7:776. doi: 10.3389/fpls.2016.00776

Davila, J., Arrieta-Montiel, M., Wamboldt, Y., Cao, J., Hagmann, J., Shedge, V., et al. (2011). Mackenzie S. Double-strand break repair processes drive evolution of the mitochondrial genome in Arabidopsis. *BMC Biol.* 2011:64. doi: 10.1186/1741-7007-9-64

Dhingra, A., Portis, A. J., and Daniell, H. (2004). Enhanced translation of a chloroplast-expressed *RbcS* gene restores small subunit levels and photosynthesis in nuclear *RbcS* antisense plants. *Proc. Natl. Acad. Sci. U.S.A* 101, 6315–6320. doi: 10.1073/pnas.0400981101

Dizdaroglu, M., Jaruga, P., Birincioglu, M., and Rodriguez, H. (2002). Free radical-induced damage to DNA: mechanisms and measurement. *Free Radical Biol. Med.* 32, 1102–1115. doi: 10.1016/s0891-5849(02)00826-2

Dobrogojski, J., Adamiec, M., and Luciński, R. (2020). The chloroplast genome: a review. *Acta Physiol. Plant.* 2020:98.

Drouin, G., Daoud, H., and Xia, J. (2008). Relative rates of synonymous substitutions in the mitochondrial, chloroplast, and nuclear genomes of seed plants. *Mol. Phylogenet. E* 49, 827–831. doi: 10.1016/j.ympev.2008.09.009

Duan, S., Hu, L., Dong, B., Jin, H. L., and Wang, H. B. (2020). Signaling from Plastid Genome Stability Modulates Endoreplication and Cell Cycle during Plant Development. *Cell Rep.* 32:108019. doi: 10.1016/j.celrep.2020.108019

Dyall, S. D., Brown, M. T., and Johnson, P. J. (2004). Ancient invasions: From endosymbionts to organelles. *Science* 304, 253–257. doi: 10.1126/science.1094884

Dyer, T. (1982). Methylation of chloroplast DNA in *Chlamydomonas*. *Nature* 298, 422–423. doi: 10.1038/298422a0

Elo, A., Lyznik, A., Gonzalez, D. O., Kachman, S. D., and Mackenzie, S. A. (2003). Nuclear genes that encode mitochondrial proteins for DNA and RNA metabolism are clustered in the *Arabidopsis* genome. *Plant Cell* 15, 1619–31. doi: 10.1105/tpc.010009

Elstner, E. F. (1991). "Mechanisms of oxygen activation in different compartments of plant cells," in *Active Oxygen/Oxidative Stress and Plant Metabolism.* eds, E. J. Pell and K. L. Steffen, (Rockville MD: American Society of Plant Physiologists Press), 13–25.

Estavillo, G. M., Crisp, P. A., Pornsiriwong, W., Wirtz, M., Collinge, D., Carrie, C., et al. (2011). Evidence for a SAL1-PAP chloroplast retrograde pathway that functions in drought and high light signaling in Arabidopsis. *Plant Cell* 23, 3992–4012. doi: 10.1105/tpc.111.091033

Evans, M. D., Dizdaroglu, M., and Cooke, M. S. (2004). Oxidative DNA damage and disease: induction, repair, and significance. *Mutat. Res. Rev. Mutat. Res.* 567, 1–61. doi: 10.1016/j.mrrev.2003.11.001

Feng, B., Ma, S., Chen, S., Zhu, N., Zhang, S., Yu, B., et al. (2016). PARylation of the forkhead-associated domain protein DAWDLE regulates plant immunity. *EMBO Rep.* 17, 1799–1813. doi: 10.15252/embr.201642486

Fleischmann, T. T., Scharff, L. B., Alkatib, S., Hasdorf, S., Schottler, M. A., and Bock, R. (2011). Nonessential plastid-encoded ribosomal proteins in tobacco: a developmental role for plastid translation and implications for reductive genome evolution. *Plant Cell* 23, 3137–3155. doi: 10.1105/tpc.111.088906

Foley, J. A., Ramankutty, N., Brauman, K. A., Cassidy, E. S., Gerber, J. S., Johnston, M., et al. (2011). Solutions for a cultivated planet. *Nature* 478, 337–342.

Foudree, A., Putarjunan, A., Kambakam, S., Nolan, T., Fussell, J., Pogorelko, G., et al. (2012). The mechanism of variegation in immutans provides insight into chloroplast biogenesis. *Front. Plant Sci.* 3:260. doi: 10.3389/fpls.2012.00260

Furlanetto, A. L. D. M., Cadena, S. M. S. C., Martinez, G. R., Ferrando, B., Stevnsner, T., and Moller, I. M. (2019). Short-term high temperature treatment reduces viability and inhibits respiration and DNA repair enzymes in *Araucaria angustifolia* cells. *Physiol. Plant.* 166, 513–524. doi: 10.1111/ppl.12793

Galmés, J., Conesa, M. À, Díaz-Espejo, A., Mir, A., Perdomo, J. A., Niinemets, Ü, et al. (2014). Rubisco catalytic properties optimized for present and future climatic conditions. *Plant Sci.* 226, 61–70. doi: 10.1016/j.plantsci.01.008

Gammage, P. A., Moraes, C. T., and Minczuk, M. (2018). Mitochondrial genome engineering: the revolution may not be CRISPR-ized. *Trends Genet.* 34, 101–110. doi: 10.1016/j.tig.2017.11.001

Garcia-Medel, P. L., Baruch-Torres, N., Peralta-Castro, A., Trasvina-Arenas, C. H., Torres-Larios, A., and Brieba, L. G. (2019). Plant organellar DNA polymerases repair double-stranded breaks by microhomology-mediated end-joining. *Nucleic Acids Res.* 47, 3028–3044. doi: 10.1093/nar/gkz039

Gauly, A., and Kössel, H. (1989). Evidence for tissue-speciWc cytosine methylation of plastid DNA from Zea mays. *Curr. Genet.* 15, 371–376. doi: 10.1007/bf00419918

Gilkerson, R., Bravo, L., Garcia, I., Gaytan, N., Herrera, A., Maldonado, A., et al. (2013). The mitochondrial nucleoid: integrating mitochondrial DNAinto cellular homeostasis. *Cold Spring Harb. Perspect. Biol.* 5:a011080. doi: 10.1101/cshperspect.a011080

Giuliano, G. (2014). Plant carotenoids: genomics meets multi-gene engineering. *Curr. Opin. Plant Biol.* 19, 111–117. doi: 10.1016/j.pbi.2014.05.006

Glaszmann, J. C., Kilian, B., Upadhyaya, H. D., and Varshney, R. K. (2010). Accessing genetic diversity for crop improvement. *Curr. Opin. Plant Biol.* 13, 167–173. doi: 10.1016/j.pbi.2010.01.004

Gray, M. W. (2017). Lynn Margulis and the endosymbiont hypothesis: 50 years later. *Mol. Biol. Cell.* 28, 1285–1287. doi: 10.1091/mbc.e16-07-0509

Gredilla, R. (2010). DNA damage and base excision repair in mitochondria and their role in aging. *J. Aging Res.* 2011:257093.

Green, B. R. (2011). Chloroplast genomes of photosynthetic eukaryotes. *Plant J.* 66, 34–44. doi: 10.1111/j.1365-313x.2011.04541.x

Greiner, S., Lehwark, P., and Bock, R. (2019). OrganellarGenomeDRAW (OGDRAW) version 1.3.1: expanded toolkit for the graphical visualization of organellar genomes. *Nucleic Acids Res.* 47, W59–W64.

Gu, Z., Pan, W., Chen, W., Lian, Q., Wu, Q., Lv, Z., et al. (2019). New perspectives on the plant PARP family: *Arabidopsis* PARP3 is inactive, and PARP1 exhibits predominant poly (ADP-ribose) polymerase activity in response to DNA damage. *BMC Plant Biol.* 19:364. doi: 10.1186/s12870-019-1958-9

Gualberto, J. M., and Newton, K. J. (2017). Plant Mitochondrial Genomes: Dynamics and Mechanisms of Mutation. *Annu. Rev. Plant Biol.* 68, 225–252. doi: 10.1146/annurev-arplant-043015-112232

Gualberto, J. M., Mileshina, D., Wallet, C., Niazi, A. K., Weber-Lotfi, F., and Dietrich, A. (2014). The plant mitochondrial genome: dynamics and maintenance. *Biochimie* 100, 107–120. doi: 10.1016/j.biochi.2013.09.016

Gutman, B. L., and Niyogi, K. K. (2009). Evidence for base excision repair of oxidative DNA damage in chloroplasts of Arabidopsis thaliana. *J. Biol. Chem.* 284, 25.17006–17012. doi: 10.1074/jbc.M109.008342

Hada, M., Hino, K., Buchholz, G., Goss, J., Wellmann, E., and Shin, M. (2000). Assay of DNA Photolyase Activity in Spinach Leaves in Relation to Cell Compartmentation-Evidence for Lack of DNA Photolyase in Chloroplasts. *Biosci. Biotechnol. Biochem.* 64, 1288–1291. doi: 10.1271/bbb.64.1288

Handa, N., Amitani, I., Gumlaw, N., Sandler, S. J., and Kowalczykowski, S. C. (2009). Single Molecule Analysis of a Red Fluorescent RecA Protein Reveals a Defect in Nucleoprotein Filament Nucleation That Relates to its Reduced Biological Functions. *J. Biol. Chem.* 284, 18664–18673. doi: 10.1074/jbc.m109.004895

Heacock, M., Spangler, E., Riha, K., Puizina, J., and Shippen, D. E. (2004). Molecular analysis of telomere fusions in *Arabidopsis*: multiple pathways for chromosome end-joining. *EMBO J.* 23, 2304–2313. doi: 10.1038/sj.emboj.7600236

Hedtke, B., Wagner, I., Börner, T., and Hess, W. R. (1999). Inter-organellar crosstalk in higher plants: Impaired chloroplast development affects mitochondrial gene and transcript levels. *Plant J.* 19, 635–643. doi: 10.1046/j.1365-313x.1999.00554.x

Heineke, D., Bykova, N., Gardestrom, P., and Bauwe, H. (2001). Metabolic response of potato plants to an antisense reduction of the P-protein of glycine decarboxylase. *Planta* 212, 880–887. doi: 10.1007/s004250000460

Hess, W. R., and Bo"rner, T. (1999). Organellar RNA polymerases of higher plants. *Int. Rev. Cytol.* 190, 1–59. doi: 10.1016/s0074-7696(08)62145-2

Horvath, B. M., Kourova, H., Nagy, S., Nemeth, E., Magyar, Z., Papdi, C., et al. (2017). Arabidopsis RETINOBLASTOMA RELATED directly regulates DNA damage responses through functions beyond cell cycle control. *EMBO J.* 36, 1261–1278. doi: 10.15252/embj.201694561

Hotto, A., Germain, A., and Stern, D. (2012). Plastid non-coding RNAs: Emerging candidates for gene regulation. *Trends Plant Sci.* 17:20. doi: 10.1016/j.tplants.2012.08.002

Huang, C. Y., Ayliffe, M. A., and Timmis, J. N. (2003). Direct measurement of the transfer rate of chloroplast DNA into the nucleus. *Nature* 422, 72–76. doi: 10.1038/nature01435

Hudik, E., Yoshioka, Y., Domenichini, S., Bourge, M., Soubigout-Taconnat, L., Mazubert, C., et al. (2014). Chloroplast dysfunction causes multiple defects in cell cycle progression in the Arabidopsis crumpled leaf mutant. *Plant Physiol.* 166, 152–167. doi: 10.1104/pp.114.242628

Jacobs, A. L., and Schar, P. (2012). DNA glycosylases: in DNA repair and beyond. *Chromosoma* 121, 1–20. doi: 10.1007/s00412-011-0347-4

Janssen-Heininger, Y. M., Mossman, B. T., Heintz, N. H., Forman, H. J., Kalyanaraman, B., Finkel, T., et al. (2008). Redox-based regulation of signal transduction: principles, pitfalls, and promises. *Free Radic. Biol. Med.* 45, 1–17. doi: 10.1016/j.freeradbiomed.2008.03.011

Jazwinski, S. M. (2013). The retrograde response: when mitochondrial quality control is not enough. *Biochim. Biophys. Acta.* 1833, 400–409. doi: 10.1016/j.bbamcr.2012.02.010

Jiang, Y., Qian, X., Shen, J., Wang, Y., Li, X., Liu, R., et al. (2015). Local generation of fumarate promotes DNA repair through inhibition of histone H3 demethylation. *Nat. Cell Biol.* 17, 1158–1168. doi: 10.1038/ncb3209

Jovaisaite, V., Mouchiroud, L., and Auwerx, J. (2014). The mitochondrial unfolded proteinresponse, a conserved stress response pathway with implications in health anddisease. *J. Exp. Biol.* 217, 137–143. doi: 10.1242/jeb.090738

Kanevski, I., Maliga, P., Rhoades, D. F., and Gutteridge, S. (1999). Plastome engineering of ribulose−1,5−bisphosphate carboxylase/oxygenase in tobacco to form a sunflower large subunit and tobacco small subunit hybrid. *Plant Physiol.* 119, 133–141. doi: 10.1104/pp.119.1.133

Kazama, T., Okuno, M., Watari, Y., Yanase, S., Koizuka, C., Tsuruta, Y., et al. (2019). Curing cytoplasmic male sterility via TALEN-mediated mitochondrial genome editing. *Nat. Plants* 5, 722–730. doi: 10.1038/s41477-019-0459-z

Keddie, J. S., Carroll, B., Jones, J. D., and Gruissem, W. (1996). The DCL gene of tomato is required for chloroplast development and palisade cell morphogenesis in leaves. *EMBO J.* 15, 4208–4217. doi: 10.1002/j.1460-2075.1996.tb00795.x

Khakhlova, O., and Bock, R. (2006). Elimination of deleterious mutations in plastid genomes by gene conversion. *Plant J.* 46, 85–94. doi: 10.1111/j.1365-313x.2006.02673.x

Kim, C. (2020). ROS-Driven Oxidative Modification: Its Impact on Chloroplasts-Nucleus Communication. *Front. Plant Sci.* 10:1729. doi: 10.3389/fpls.2019.01729

Kim, J. H. (2019). Chromatin Remodeling and Epigenetic Regulation in Plant DNA Damage Repair. *Int. J. Mol. Sci.* 20:4093. doi: 10.3390/ijms20174093

Kimura, S., Uchiyama, Y., Kasai, N., Namekawa, S., Saotome, A., Ueda, T., et al. (2002). A novel DNA polymerase homologous to *E. coli* DNA polymerase I from a higher plant, rice (*Oryzasativa*L.). *Nucleic Acids Res.* 30, 1585–1592. doi: 10.1093/nar/30.7.1585

King, G. A., Hashemi-Shabestari, M., Taris, K. H., Pandey, A. K., Venkatesh, S., Thilagavathi, J., et al. (2018). Acetylation and phosphorylation of human TFAM regulate TFAM-DNA interactions via contrasting mechanisms. *Nucleic Acids Res.* 46, 3633–3642. doi: 10.1093/nar/gky204

Kinoshita, T., and Seki, M. (2014). Epigenetic memory for stress response and adaptation in plants. *Plant Cell Physiol.* 55, 1859–1863. doi: 10.1093/pcp/pcu125

Kleine, T., Lockhart, P., and Batschauer, A. (2003). An Arabidopsis protein closely related to Synechocystiscryptochrome is targeted to organelles. *Plant J.* 35, 93–103. doi: 10.1046/j.1365-313x.2003.01787.x

Kmiec, B., Woloszynska, M., and Janska, H. (2006). Heteroplasmy as a common state of mitochondrial genetic information in plants and animals. *Curr. Genet.* 50, 149–159. doi: 10.1007/s00294-006-0082-1

Kobayashi, Y., Kanesaki, Y., Tanaka, A., Kuroiwa, H., Kuroiwa, T., and Tanaka, K. (2009). Tetrapyrrole signal as a cell-cycle coordinator from organelle to nuclear DNA replication in plant cells. *Proc. Natl. Acad. Sci. U.S.A.* 106, 803–807. doi: 10.1073/pnas.0804270105

Kobayashi, Y., Misumi, O., Odahara, M., Ishibashi, K., Hirono, M., Hidaka, K., et al. (2017). Holliday junction resolvases mediate chloroplast nucleoid segregation. *Science* 356, 631–634. doi: 10.1126/science.aan0038

Kohl, S., and Bock, R. (2009). Transposition of a bacterial insertion sequence in chloroplasts. *Plant J.* 58, 423–436. doi: 10.1111/j.1365-313X.2009.03787.x

Kolesnikov, A. A., and Gerasimov, E. S. (2012). Diversity of mitochondrial genome organization. *Biochem. Moscow* 77, 1424–1435. doi: 10.1134/S0006297912130020

Krause, K., and Krupinska, K. (2009). Nuclear regulators with a second home in organelles. *Trends Plant Sci.* 14, 194–199. doi: 10.1016/j.tplants.2009.01.005

Krause, K., Kilbienski, I., Mulisch, M., Ro"diger, A., Scha"fer, A., and Krupinska, K. (2005). DNA-binding proteins of the Whirly family in Arabidopsis thaliana are targeted to the organelles. *FEBS Lett.* 579, 3707–3712. doi: 10.1016/j.febslet.2005.05.059

Krech, K., Fu, H. Y., Thiele, W., Ruf, S., Schottler, M. A., and Bock, R. (2013). Reverse genetics in complex multigene operons by co-transformation of the plastid genome and its application to the open reading frame previously designated *psbN*. *Plant J.* 75, 1062–1074. doi: 10.1111/tpj.12256

Krupinska, K., Blanco, N. E., Oetke, S., and Zottini, M. (2020). Genome communication in plants mediated by organelle–nucleus-located proteins. *Phil. Trans. R. Soc. B* 375:20190397. doi: 10.1098/rstb.2019.0397

Kucej, M., and Butow, R. A. (2007). Evolutionary tinkering with mitochondrial nucleoids. *Trends Cell Biol.* 17, 586–592. doi: 10.1016/j.tcb.2007.08.007

Kuehn, K., and Gualberto, J. (2012). Recombination in the Stability, Repair, and Evolution of the Mitochondrial Genome. *Adv. Bot. Res.* 63, 215–252. doi: 10.1016/B978-0-12-394279-1.00009-0

Kunnimalaiyaan, M., and Nielsen, B. L. (1997). Chloroplast DNA replication: Mechanism, enzymes, and replication origins. *J. Plant Biochem. Biot.* 6, 1–7. doi: 10.1007/bf03263000

Kwon, T., Huq, E., and Herrin, D. (2010). Microhomology-mediated and nonhomologous repair of a double-strand break in the chloroplast genome of

Arabidopsis. *Proc. Natl. Acad. Sci. U.S.A.* 107, 13954–13959. doi: 10.1073/pnas.1004326107

Lapucci, A., Pittelli, M., Rapizzi, E., Felici, R., Moroni, F., and Chiarugi, A. (2011). Poly(ADP-ribose) polymerase-1 is a nuclear epigenetic regulator of mitochondrial DNA repair and transcription. *Mol. Pharmacol.* 79, 932–940. doi: 10.1124/mol.110.070110

Law, J. A., and Jacobsen, S. E. (2010). Establishing, maintaining, and modifying DNA methylation patterns in plants and animals. *Nat. Rev. Genet.* 11, 204–220. doi: 10.1038/nrg2719

Li, H., Ji, G., Wang, Y., Qian, Q., Xu, J., Sodmergen, L. G., et al. (2018). WHITE PANICLE3, a Novel Nucleus-Encoded Mitochondrial Protein, Is Essential for Proper Development and Maintenance of Chloroplasts and Mitochondria in Rice. *Front. Plant Sci.* 9:762. doi: 10.3389/fpls.2018.00762

Li, S. F., Li, J. R., Wang, J., Dong, R., Jia, K. L., Zhu, H. W., et al. (2019). Cytogenetic and genomic organization analyses of chloroplast DNA invasions in the nuclear genome of Asparagus officinalis L. provides signatures of evolutionary complexity and informativity in sex chromosome evolution. *BMC Plant Biol.* 19:361. doi: 10.1186/s12870-019-1975-8

Li, S., Chang, L., and Zhang, J. (2021). Advancing organelle genome transformation and editing for crop improvement. *Plant Comm.* 2:100141. doi: 10.1016/j.xplc.2021.100141

Li, X., and Heyer, W. D. (2008). Homologous recombination in DNA repair and DNA damage tolerance. *Cell Res.* 18, 99–113. doi: 10.1038/cr.2008.1

Lin, M. T., Occhialini, A., Andralojc, P. J., Parry, M. A., and Hanson, M. R. (2014). A faster Rubisco with potential to increase photosynthesis in crops. *Nature* 513, 547–550. doi: 10.1038/nature13776

Lin, M., Qi, X., Chen, J., Sun, L., Zhong, Y., Fang, J., et al. (2018). The complete chloroplast genome sequence of *Actinidiaarguta*using the PacBio RSII platform. *PLoS One* 13:e0197393. doi: 10.1371/journal.pone.0197393

Liu, H. H., Tian, X., Li, Y. J., Wu, C. A., and Zheng, C. C. (2008). Microarray−based analysis of stress−regulated microRNAs in Arabidopsis thaliana. *RNA* 14, 836–843. doi: 10.1261/rna.895308

Lu, B., Lee, J., Nie, X., Li, M., Morozov, Y. I., Venkatesh, S., et al. (2013). Phosphorylation of human TFAM in mitochondria impairs DNA binding and promotes degradation by the AAA+ Lon protease. *Mol. Cell.* 49, 121–132. doi: 10.1016/j.molcel.2012.10.023

Lung, B., Zemann, A., Madej, M. J., Schuelke, M., Techritz, S., Ruf, S., et al. (2006). Identification of small non-coding RNAs from mitochondria and chloroplasts. *Nucleic Acids Res.* 34, 3842–3852. doi: 10.1093/nar/gkl448

Mahapatra, K., and Roy, S. (2020). An insight into the mechanism of DNA damage response in plants-role of suppressor of gamma response 1: an overview. *Mutat. Res. Fund. Mol. Mech. Mutagen.* 2020:111689. doi: 10.1016/j.mrfmmm.2020.111689

Manova, V., and Gruszka, D. (2015). DNA damage and repair in plants - from models to crops. *Front. Plant Sci.* 23:885. doi: 10.3389/fpls.2015.00885

Mare'chal, A., Parent, J. S., Sabar, M., Ve'ronneau-Lafortune, F., Abou-Rached, C., and Brisson, N. (2008). Overexpression of mtDNA-associated AtWhy2 compromises mitochondrial function. *BMC Plant Biol.* 8:42. doi: 10.1186/1471-2229-8-42

Mare'chal, A., Parent, J. S., Ve'ronneau-Lafortune, F., Joyeux, A., Lang, B. F., and Brisson, N. (2009). Whirly proteins maintain plastid genome stability in Arabidopsis. *Proc. Natl. Acad. Sci. U.S.A.* 106, 14693–14698. doi: 10.1073/pnas.0901710106

Maréchal, A., and Brisson, N. (2010). Recombination and the maintenance of plant organelle genome stability. *New Phytol.* 186, 299–317. doi: 10.1111/j.1469-8137.2010.03195 x

Marie, L., Rapisarda, C., Morales, V., Bergé, M., Perry, T., Soulet, A. L., et al. (2017). Bacterial RadA is a DnaB-type helicase interacting with RecA to promote bidirectional D-loop extension. *Nat. Commun.* 8:15638.

Matsui, M., and Corey, D. R. (2017). Non-coding RNAs as drug targets. *Nat. Rev. Drug Discov.* 16, 167–179. doi: 10.1038/nrd.2016.117

Meagher, M., and Lightowlers, R. N. (2014). The role of TDP1 andAPTX in mitochondrial DNA repair. *Biochimie* 100, 121–124. doi: 10.1016/j.biochi.2013.10.011

Melonek, J., Matros, A., Trösch, M., Mock, H. P., and Krupinska, K. (2012). The core of chloroplast nucleoids contains architectural SWIB domain proteins. *Plant Cell* 24, 3060–3073. doi: 10.1105/tpc.112.099721

Meyers, B., Zaltsman, A., Lacroix, B., Kozlovsky, S. V., and Krichevsky, A. (2010). Nuclear and plastid genetic engineering of plants: comparison of opportunities and challenges. *Biotechnol. Adv.* 28, 747–756. doi: 10.1016/j.biotechadv.2010.05.022

Mok, B. Y., de Moraes, M. H., and Zeng, J. (2020). A bacterial cytidine deaminase toxin enables CRISPR-free mitochondrial base editing. *Nature* 583, 631–637. doi: 10.1038/s41586-020-2477-4

Mori, Y., Kimura, S., Saotome, A., Kasai, N., Sakaguchi, N., Uchiyama, Y., et al. (2005). Plastid DNA polymerases from higher plants *Arabidopsis thaliana*. *Biochem. Biophys. Res. Commun.* 334, 43–50. doi: 10.1016/j.bbrc.2005.06.052

Moriyama, T., and Sato, N. (2014). Enzymes involved in organellar DNA replication in photosynthetic eukaryotes. *Front. Plant Sci.* 5:480. doi: 10.3389/fpls.2014.00480

Morley, S., Ahmad, N., and Nielsen, B. (2019). Plant Organelle Genome Replication. *Plants* 8:358. doi: 10.3390/plants8100358

Mower, J. P., and Vickrey, T. L. (2018). Chapter nine—structural diversityamong plastid genomes of land plants. *Adv. Bot. Res.* 85, 263–292. doi: 10.1016/bs.abr.2017.11.013

Muniandy, K., Tan, M. H., Shehnaz, S., Song, B. K., Ayub, Q., and Rahman, S. (2020). Cytosine methylation of rice mitochondrial DNA from grain and leaf tissues. *Planta* 251:57. doi: 10.1007/s00425-020-03349-7

Muniandy, K., Tan, M. H., Song, B. K., Ayub, Q., and Rahman, S. (2019). Comparative sequence and methylation analysis of chloroplast and amyloplast genomes from rice. *Plant Mol Biol.* 100, 33–46. doi: 10.1007/s11103-019-00841-x

Murphy, M. P. (2009). How mitochondria produce reactive oxygen species. *Biochem. J.* 417, 1–13. doi: 10.1042/bj20081386

Muse, S. V. (2000). Examining rates and patterns of nucleotide substitution in plants. *Plant Mol. Biol.* 42, 25–43. doi: 10.1007/978-94-011-4221-2_2

Nakashima, K., Yamaguchi-Shinozaki, K., and Shinozaki, K. (2014). The transcriptional regulatory network in the drought response and its crosstalk in abiotic stress responses including drought, cold, and heat. *Front. Plant Sci.* 5:170. doi: 10.3389/fpls.2014.00170

Ng, S., De Clercq, I., Van Aken, O., Law, S. R., Ivanova, A., Willems, P., et al. (2014). Anterograde and retrograde regulation of nuclear genes encoding mitochondrial proteins during growth, development, and stress. *Mol. Plant* 7, 1075–1093. doi: 10.1093/mp/ssu037

Ngernprasirtsiri, J., Kobayashi, H., and Akazawa, T. (1988a). DNA methylation as a mechanism of transcriptional regulation in nonphotosynthetic plastids in plant cells. *Proc. Natl. Acad. Sci. U.S.A.* 85, 4750–4754. doi: 10.1073/pnas.85.13.4750

Ngernprasirtsiri, J., Kobayashi, H., and Akazawa, T. (1988b). DNA methylation occurred around lowly expressed genes of plastid DNA during tomato fruit development. *Plant Physiol.* 88, 16–20. doi: 10.1104/pp.88.1.16

Noctor, G., De Paepe, R., and Foyer, C. H. (2007). Mitochondrial redox biology and homeostasis in plants,". *Trends Plant Sci.* 12, 125–134. doi: 10.1016/j.tplants.2007.01.005

Nota, F., Cambiagno, D. A., Ribone, P., and Alvarez, M. E. (2015). Expression and function of AtMBD4L, the single gene encoding the nuclear DNA glycosylase MBD4L in Arabidopsis. *Plant Sci.* 235, 122–129. doi: 10.1016/j.plantsci.2015.03.011

Occhialini, A., Lin, M. T., Andralojc, P. J., Hanson, M. R., and Parry, M. A. (2016). Transgenic tobacco plants with improved cyanobacterial Rubisco expression but no extra assembly factors grow at near wild-type rates if provided with elevated CO_2. *Plant J.* 85, 148–160. doi: 10.1111/tpj.13098

Odahara, M., Inouye, T., Nishimura, Y., and Sekine, Y. (2015). RECA plays a dual role in the maintenance of chloroplast genome stability in Physcomitrella patens. *Plant J.* 84, 516–526. doi: 10.1111/tpj.13017

Odahara, M., Kishita, Y., and Sekine, Y. (2017). MSH1 maintains organelle genome stability and genetically interacts with RECA and RECG in the moss Physcomitrella patens. *Plant J.* 91, 455–465. doi: 10.1111/tpj.13573

Odahara, M., Kuroiwa, H., Kuroiwa, T., and Sekine, Y. (2009). Suppression ofrepeat-mediated gross mitochondrial genome rearrangements by RecAin the moss Physcomitrella patens. *Plant Cell.* 21, 1182–1194. doi: 10.1105/tpc.108.064709

Odom, O. W., Baek, K. H., Dani, R. N., and Herrin, D. L. (2008). *Chlamydomonas* chloroplasts can use short dispersed repeats and multiple pathways to repair a double-strand break in the genome. *Plant J.* 53, 842–853. doi: 10.1111/j.1365-313x.2007.03376.x

Oey, M., Lohse, M., Kreikemeyer, B., and Bock, R. (2009). Exhaustion of the chloroplast protein synthesis capacity by massive expression of a highly stable protein antibiotic. *Plant J.* 57, 436–445. doi: 10.1111/j.1365-313x.2008.03702.x

Ogita, N., Okushima, Y., Tokizawa, M., Yamamoto, Y. Y., Tanaka, M., Seki, M., et al. (2018). Identifying the target genes of SUPPRESSOR OF GAMMA RESPONSE 1, a master transcription factor controlling DNA damage response in *Arabidopsis*. *Plant J.* 94, 439–453. doi: 10.1111/tpj.13866

Oldenburg, D. J., and Bendich, A. J. (2015). DNA maintenance in plastids and mitochondria of plants. *Front. Plant Sci.* 6:883. doi: 10.3389/fpls.2015.00883

Ono, Y., Sakai, A., Takechi, K., Takio, S., Takusagawa, M., and Takano, H. (2007). NtPolI-like1 and NtPolI-like2, bacterial DNA polymerase I homologs isolated from BY-2 cultured tobacco cells, encode DNA polymerases engaged in DNA replication in both plastids and mitochondria. *Plant Cell Physiol.* 48, 1679–1692. doi: 10.1093/pcp/pcm140

Palmer, J. (1983). Chloroplast DNA exists in two orientations. *Nature* 301, 92–93. doi: 10.1038/301092a0

Palmer, J. D. (1985). Comparative Organization of Chloroplast Genomes. *Annu. Rev. Genet.* 19, 325–354. doi: 10.1146/annurev.ge.19.120185.001545

Pankotai, E., Lacza, Z., Muranyi, M., and Szabo, C. (2009). Intra-Mitochondrial Poly(ADP Ribosyl)Ation: Potential Role for Alpha-Ketoglutarate Dehydrogenase. *Mitochondrion* 9, 159–164. doi: 10.1016/j.mito.2009.01.013

Parent, J. S., Lepage, E., and Brisson, N. (2011). Divergent roles for the two PolI-like organelle DNA polymerases of *Arabidopsis*. *Plant Physiol.* 156, 254–262. doi: 10.1104/pp.111.173849

Parry, M. A. J., Andralojc, P. J., Scales, J., Salvucci, M. E., Carmo-Silva, A. E., Alonso, H., et al. (2013). Rubisco activity and regulation as targets for crop improvement. *J. Exp. Bot.* 64, 717–730. doi: 10.1093/jxb/ers336

Paszkowski, J., and Whitham, S. A. (2001). Gene silencing and DNA methylation processes. *Curr. Opin. Plant Biol.* 4, 123–129. doi: 10.1016/s1369-5266(00)00147-3

Paul, P., Chakraborty, A., Sarkar, D., Langthasa, M., Rahman, M., Bari, M., et al. (2018). Interplay between miRNAs and human diseases. *J. Cell Physiol.* 233, 2007–2018. doi: 10.1002/jcp.25854

Peralta-Castro, A., García-Medel, P. L., Baruch-Torres, N., Trasviña-Arenas, C. H., Juarez-Quintero, V., Morales-Vazquez, C. M., et al. (2020). Plant Organellar DNA Polymerases Evolved Multifunctionality through the Acquisition of Novel Amino Acid Insertions. *Genes* 11:1370. doi: 10.3390/genes11111370

Pfannschmidt, T., and Yang, C. (2012). The hidden function of photosynthesis: a sensing system for environmental conditions that regulates plant acclimation responses. *Protoplasma* 249, 125–136. doi: 10.1007/s00709-012- 0398-2

Pham, P. A., Wahl, V., Tohge, T., de Souza, L. R., Zhang, Y., Do, P. T., et al. (2015). Analysis of knockout mutants reveals non-redundant functions of poly(ADP-ribose)polymerase isoforms in Arabidopsis. *Plant Mol. Biol.* 89, 319–338. doi: 10.1007/s11103-015-0363-5

Pottier, M., Gilis, D., and Boutry, M. (2018). The hidden face of Rubisco. *Trends Plant Sci.* 23, 382–392. doi: 10.1016/j.tplants.2018.02.006

Poyton, R. O., and McEwen, J. E. (1996). Crosstalk between nuclear and mitochondrial genomes. *Annu. Rev. Biochem.* 65, 563–607. doi: 10.1146/annurev.bi.65.070196.003023

Prakash, A., and Doublié, S. (2015). Base excision repair in the mitochondria. *J. Cell. Biochem.* 116, 1490–1499. doi: 10.1002/jcb.25103

Puchta, H. (2005). The repair of double-strand breaks in plants: mechanisms and consequences for genome evolution. *J. Exp. Bot.* 56, 1–14. doi: 10.1093/jxb/eri02

Puchta, H., and Fauser, F. (2015). Double-Strand Break Repair and Its Application to Genome Engineering in Plants. *Adv. N. Technol. Target. Modif. Plant Genomes* 8, 1–20. doi: 10.1007/978-1-4939-2556-8-1

Ray, U., and Raghavan, S. C. (2020). Modulation of DNA double-strand break repair as a strategy to improve precise genome editing. *Oncogene* 39, 6393–6405. doi: 10.1038/s41388-020-01445-2

Reza, A. M. M. T., Choi, Y. J., Han, S. G., Song, H., Park, C., Hong, K., et al. (2019). Roles of microRNAs in mammalian reproduction: from the commitment of germ cells to peri−implantation embryos. *Biol. Rev.* 94, 415–438. doi: 10.1111/brv.12459

Richards, E. J. (2006). Inherited epigenetic variation—revisiting soft inheritance. *Nat. Rev. Genet.* 7, 395–401. doi: 10.1038/nrg1834

Richly, E., and Leister, D. (2004). An improved prediction of chloroplast proteins reveals diversities and commonalities in the chloroplast proteomes of Arabidopsis and rice. *Gene* 329, 11–16. doi: 10.1016/j.gene.2004.01.008

Rissel, D., and Peiter, E. (2019). Poly(ADP-Ribose) Polymerases in Plants and Their Human Counterparts: Parallels and Peculiarities. *Int. J. Mole. Sci.* 20:1638. doi: 10.3390/ijms20071638

Rizzuto, R., De Stefani, D., Raffaello, A., and Mammucari, C. (2012). Mitochondria as sensorsand regulators of calcium signaling. *Nat. Rev. Mol. Cell Biol.* 13, 566–578.

Roldan-Arjona, T., and Ariza, R. R. (2009). Repair and tolerance of oxidative DNA damage in plants. *Mutat. Res.* 681, 169–179. doi: 10.1016/j.mrrev.2008.07.003

Roldán-Arjona, T., Ariza, R. R., and Córdoba-Cañero, D. (2019). DNA Base Excision Repair in Plants: An Unfolding Story with Familiar and Novel Characters. *Front. Plant Sci.* 10:1055. doi: 10.3389/fpls.2019.01055

Roy, S. (2014). Maintenance of genome stability in plants: repairing DNA double strand breaks and chromatin structure stability. *Front. Plant Sci.* 5:487. doi: 10.3389/fpls.2014.00487

Ruf, S., and Bock, R. (2011). *In vivo* analysis of RNA editing in plastids. *Methods Mol. Biol.* 718, 137–150. doi: 10.1007/978-1-61779-018-8_8

Ruf, S., Forner, J., Hasse, C., Kroop, X., Seeger, S., Schollbach, L., et al. (2019). High-efficiency generation of fertile transplastomic Arabidopsis plants. *Nat. Plants* 5, 282–289. doi: 10.1038/s41477-019-0359-2

Sabar, M., De Paepe, R., and de Kouchkovsky, Y. (2000). Complex I impairment, respiratory compensations, and photosynthetic decrease in nuclear and mitochondrial male sterile mutants of Nicotiana sylvestris. *Plant Physiol.* 124, 1239–1250. doi: 10.1104/pp.124.3.1239

Sagan, L. (1967). On the origin of mitosing cells. *J. Theor. Biol.* 14, 255–274.

Sager, R., Sano, H., and Grabowy, C. T. (1984). Control of maternal inheritance by DNA methylation in Chlamydomonas. *Curr. Top. Microbiol. Immunol.* 108, 157–173. doi: 10.1007/978-3-642-69370-0_11

Sakamoto, W., and Takami, T. (2018). Chloroplast DNA Dynamics: Copy Number, Quality Control and Degradation. *Plant Cell Physiol.* 59, 1120–1127. doi: 10.1093/PCP/pcy084

Saki, M., and Prakash, A. (2017). DNA damage related crosstalk between the nucleus and mitochondria. *Free Radic. Biol. Med.* 107, 216–227. doi: 10.1016/j.freeradbiomed.2016.11.050

Sandler, S. J., and Clark, A. J. (1994). RecOR suppression of recF mutant phenotypes in E. coli K-12. *J. Bacteriol.* 176, 3661–3672. doi: 10.1128/jb.176.12.3661-3672.1994

Sato, S., Nakamura, Y., Kaneko, T., Asamizu, E., and Tabata, S. (1999). Complete Structure of the Chloroplast Genome of *Arabidopsis thaliana*. *DNA Res.* 6, 283–290. doi: 10.1093/dnares/6.5.283

Scharff, L. B., and Bock, R. (2014). Synthetic biology in plastids. *Plant J.* 78, 783–798. doi: 10.1111/tpj.12356

Schmidt, C., Pacher, M., and Puchta, H. (2019). DNA Break Repair in Plants and Its Application for Genome Engineering. *Methods Mol. Biol.* 1864, 237–266. doi: 10.1007/978-1-4939-8778-8-17

Seeberg, E., Luna, L., Morland, L., Eide, L., Johnson, B., Larsen, E., et al. (2000). Base remover and strand scissors: different strategies employed in base excision and strand incision at modified base residues in DNA. *Cold Spring Harb. Symp. Quant. Biol.* 65, 135–142. doi: 10.1101/sqb.2000.65.135

Seol, J. H., Eun Yong, E., Shim, S., and Lee, E. (2017). Microhomology-Mediated End Joining: Good, Bad and Ugly. *Mutat. Res.* 809, 81–87. doi: 10.1016/j.mrfmmm.2017.07.002

Sharma, P., Jha, A. B., Dubey, R. S., and Pessarakli, M. (2012). Reactive Oxygen Species, Oxidative Damage, and Antioxidative Defence Mechanism in Plants under Stressful Conditions. *J. Bot.* 27, 1–26. doi: 10.1155/2012/217037

Sharwood, R. E. (2017). Engineering chloroplasts to improve Rubisco catalysis: prospects for translating improvements into food and fibre crops. *New Phytol.* 213, 494–510. doi: 10.1111/nph.14351

Shaver, J. M., Oldenburg, D. J., and Bendich, A. J. (2006). Changes in chloroplast DNA during development in tobacco, *Medicagotruncatula*, pea, and maize. *Planta* 224, 72–82. doi: 10.1007/s00425-005-0195-7

Shedge, V., Arrieta-Montiel, M., Christensen, A. C., and Mackenzie, S. A. (2007). Plant mitochondrial recombination surveillance requires unusual RecA and MutS homologs. *Plant Cell* 19, 1251–1264. doi: 10.1105/tpc.106.048355

Shutt, T. E., and Gray, M. W. (2006). Bacteriophage origins of mitochondrial replication and transcription proteins. *Trends Genet.* 22, 90–95. doi: 10.1016/j.tig.2005.11.007

Small, G. D. (1987). Repair systems for nuclear and chloroplast DNA in Chlamydomonas reinhardtii. *Mutat. Res.* 181, 31–35. doi: 10.1016/0027-5107(87)90284-3

Smith, D. R., and Keeling, P. J. (2015). Mitochondrial and plastid genome architecture: Reoccurring themes, but significant differences at the extremes. *Proc. Natl. Acad. Sci. U.S.A.* 112, 10177–10184. doi: 10.1073/pnas.1422049112

Song, J., Keppler, B. D., Wise, R. R., and Bent, A. F. (2015). PARP2 Is the Predominant Poly (ADP-Ribose) Polymerase in Arabidopsis DNA Damage and Immune Responses. *PLoS Genet.* 11:e1005200. doi: 10.1371/journal.pgen.1005200

Stein, L. R., and Imai, S. (2012). The dynamic regulation of NAD metabolism inmitochondria. *Trends Endocrinol. Metab.* 23, 420–428. doi: 10.1016/j.tem.2012.06.005

Strand, A., Asami, T., Alonso, J., Ecker, J. R., and Chory, J. (2003). Chloroplast to nucleus communication triggered by accumulation of Mg-protoporphyrin IX. *Nature* 421, 79–83. doi: 10.1038/nature01204

Sunderland, P., West, C., Waterworth, W., and Bray, C. (2006). An evolutionarily conserved translation initiation mechanism regulates nuclear or mitochondrial targeting of DNA ligase 1 in Arabidopsis thaliana. *Plant J.* 47, 356–367. doi: 10.1111/j.1365-313X.2006.02791.x

Swartzlander, D. B., Griffiths, L. M., Lee, J., Degtyareva, N. P., Doetsch, P. W., and Corbett, A. H. (2010). Regulation of base excision repair: Ntg1 nuclear and mitochondrial dynamic localization in response to genotoxic stress. *Nucleic Acids Res.* 38, 3963–3974. doi: 10.1093/nar/gkq108

Takahashi, M., Teranishi, M., Ishida, H., Kawasaki, J., Takeuchi, A., Yamaya, T., et al. (2011). Cyclobutane pyrimidine dimer (CPD) photolyase repairs ultraviolet-B-induced CPDs in rice chloroplast and mitochondrial DNA: CPD photolyase in rice chloroplasts and mitochondria. *Plant J.* 66, 433–442. doi: 10.1111/j.1365-313x.2011.04500.x

Takeuchi, R., Kimura, S., Saotome, A., and Sakaguchi, K. (2007). Biochemical properties of a plastidial DNA polymerase of rice. *Plant Mol. Biol.* 64, 601–611. doi: 10.1007/s11103-007-9179-2

Taylor, N. L., and Millar, A. H. (2007). Oxidative stress and plant mitochondria. *Methods Mol Biol.* 372, 389–403. doi: 10.1007/978-1-59745-365-3-28

Tilman, D., Balzer, C., Hill, J., and Befort, B. L. (2011). Global food demand and the sustainable intensification of agriculture. *Proc. Natl. Acad. Sci. U.S.A* 108, 20260–20264.

Timmis, J., Ayliffe, M., and Huang, C. (2004). Endosymbiotic gene transfer: organelle genomes forge eukaryotic chromosomes. *Nat. Rev. Genet.* 5, 123–135. doi: 10.1038/nrg1271

Trasvina-Arenas, C. H., Baruch-Torres, N., Cordoba-Andrade, F. J., Ayala-Garcia, V. M., Garcia-Medel, P. L., Diaz-Quezada, C., et al. (2018). Identification of a unique insertion in plant organellar DNA polymerases responsible for 50-dRP lyase and strand-displacement activities: Implications for Base Excision Repair. *DNA Repair.* 65, 1–10. doi: 10.1016/j.dnarep.2018.02.010

Tripathi, D. N., Chowdhury, R., Trudel, L. J., Tee, A. R., Slack, R. S., Walker, C. L., et al. (2013). Reactive nitrogen species regulate autophagy through ATM-AMPK-TSC2-mediated suppression of mTORC1. *Proc. Natl. Acad. Sci. U.S.A.* 110, 2950–7.

Umen, J. G., and Goodenough, U. W. (2001). Chloroplast DNA methylation and inheritance in Chlamydomonas. *Genes Dev.* 15, 2585–2597. doi: 10.1101/gad.906701

Van der Veen, S., and Tang, C. M. (2015). The BER necessities: The repair of DNA damage in human-adapted bacterial pathogens. *Nat. Rev. Microbiol.* 13, 83–94. doi: 10.1038/nrmicro3391

Van Houten, B., Hunter, S. E., and Meyer, J. N. (2016). Mitochondrial DNA damage-induced autophagy, cell death, and disease. *Front. Biosci.* 21, 42–54. doi: 10.2741/4375

Verma, P., Tandon, R., Yadav, G., and Gaur, V. (2020). Structural Aspects of DNA Repair and Recombination in Crop Improvement. *Front. Genet.* 11:574549. doi: 10.3389/fgene.2020.574549

Virdi, K. S., Wamboldt, Y., Kundariya, H., Laurie, J. D., Keren, I., Kumar, K. R. S., et al. (2016). MSH1 Is a Plant Organellar DNA Binding and Thylakoid Protein under Precise Spatial Regulation to Alter Development. *Mole. Plant.* 9, 245–260. doi: 10.1016/j.molp.2015.10.011

Wallet, C., Le Ret, M., Bergdoll, M., Bichara, M., Dietrich, A., and Gualberto, J. M. (2015). The RECG1 DNA Translocase is a Key Factor in Recombination Surveillance, Repair, and Segregation of the Mitochondrial DNA in Arabidopsis. *Plant Cell* 27, 2907–2925.

Wang, W., and Lanfear, R. (2019). Long-Reads Reveal That the Chloroplast Genome Exists in Two Distinct Versions in Most Plants. *Genome Biol. Evolut.* 11, 3372–3381. doi: 10.1093/gbe/evz256

Wang, W., Haberer, G., Gundlach, H., Gläßer, C., Nussbaumer, T., Luo, M. C., et al. (2014). The *Spirodelapolyrhiza*genome reveals insights into its neotenous reduction fast growth and aquatic lifestyle. *Nat. Commun.* 5:3311. doi: 10.1038/ncomms4311

Wang, Y., Wang, X., Deng, W., Fan, X., Liu, T. T., He, G., et al. (2014). Genomic Features and Regulatory Roles of Intermediate-Sized Non-Coding RNAs in Arabidopsis. *Mol. Plant* 7, 514–527. doi: 10.1093/mp/sst177

Wardrope, L., Okely, E., and Leach, D. (2009). Resolution of joint molecules by RuvABC and RecG following cleavage of the E. coli chromosome by EcoKI. *PLoS One* 4:e6542. doi: 10.1371/journal.pone.0006542

Waterworth, W. M., Drury, G. E., Bray, C. M., and West, C. E. (2011). Repairing breaks in the plant genome: the importance of keeping it together. *New Phytol.* 192, 805–822. doi: 10.1105/tpc.108.060525

Whitby, M. C., Vincent, S. D., and Lloyd, R. G. (1994). Branch migration of Holliday junctions: Identification of RecG protein as a junction specific DNA helicase. *EMBO J.* 13, 5220–5228. doi: 10.1002/j.1460-2075.1994.tb06853.x

Whitney, S. M., and Andrews, T. J. (2001). The gene for the Rubisco small subunit relocated to the plastid genome of tobacco directs the synthesis of small subunits that assemble into Rubisco. *Plant Cell* 13, 193–205. doi: 10.2307/3871163

Wolfe, K. H., Li, W. H., and Sharp, P. M. (1987). Rates of nucleotide substitution vary greatly among plant mitochondrial, chloroplast, and nuclear DNAs. *Proc. Natl. Acad. Sci. U.S.A.* 84, 9054–9905. doi: 10.1073/pnas.84.24.9054

Woodson, J. D., and Chory, J. (2008). Coordination of gene expression between organellar and nuclear genomes. *Nat. Rev. Genet.* 9, 383–395. doi: 10.1038/nrg2348

Wu, Z., Waneka, G., Broz, A. K., King, C. R., and Sloan, D. B. (2020). *MSH1* is required for the maintenance of the low mutation rates in plant mitochondrial and plastid genomes. *Proc. Natl. Acad. Sci. U.S.A.* 117, 16448–16455. doi: 10.1073/pnas.2001998117

Xie, D. F., Yu, Y., Deng, Y. Q., Li, J., Liu, H. Y., Zhou, S. D., et al. (2018). Comparative analysis of the chloroplast genomes of the Chinese endemic genus and their contribution to chloroplast phylogeny and adaptive evolution. *Int. J. Mol. Sci.* 19:1847. doi: 10.3390/ijms19071847

Yan, H., Kikuchi, S., Neumann, P., Zhang, W., Wu, Y., Chen, F., et al. (2010). Genome-wide mapping of cytosine methylation revealed dynamic DNA methylation patterns associated with genes and centromeres in rice. *Plant J.* 63, 353–365. doi: 10.1111/j.1365-313x.2010.04246.x

Yoo, B. C., Yadav, N. S., Orozco, E. M., and Sakai, H. (2020). Cas9/gRNA-mediated genome editing of yeast mitochondria and *Chlamydomonas* chloroplasts. *PeerJ.* 8:e8362.

Yoshida, T., Furihata, H. Y., and To, T. K. (2019). Genome defense against integrated organellar DNA fragments from plastids into plant nuclear genomes through DNA methylation. *Sci. Rep.* 9:2060. doi: 10.1038/s41598-019-38607-6

Yoshiyama, K. O., Kaminoyama, K., Sakamoto, T., and Kimura, S. (2017). Increased Phosphorylation of Ser-Gln Sites on SUPPRESSOR OF GAMMA RESPONSE1 Strengthens the DNA Damage Response in Arabidopsis thaliana. *Plant Cell* 29, 3255–3268. doi: 10.1105/tpc.17.00267

Zaegel, V., Guermann, B., Le Ret, M., Andres, C., Meyer, D., Erhardt, M., et al. (2006). The plant-specific ssDNA binding protein OSB1 is involved in the stoichiometric transmission of mitochondrial DNA in Arabidopsis. *Plant Cell* 18, 3548–3563. doi: 10.1105/tpc.106.042028

Zhang, G. J., Dong, R., Lan, L. N., Li, S. F., Gao, W. J., and Niu, H. X. (2020). Nuclear Integrants of Organellar DNA contribute to genome structure and evolution in plants. *Int. J. Mol. Sci.* 21:707. doi: 10.3390/ijms 2103, 0707.

Zhang, W., Xie, Y., and Xu, L. (2016). Identification of microRNAs and their target genes explores miRNA mediated regulatory network of cytoplasmic male sterility occurrence during anther development in Radish (Raphanussativus L.). *Front. Plant Sci.* 7:1054. doi: 10.3389/fpls.2016.01054

Zhang, X. H., Ewy, R. G., Widholm, J. M., and Portis, A. R. Jr. (2002). Complementation of the nuclear antisense *RbcS*-induced photosynthesis

deficiency by introducing an *rbcS* gene into the tobacco plastid genome. *Plant Cell Physiol.* 43, 1302–1313. doi: 10.1093/pcp/pcf158

Zhang, X., Zuo, X., Yang, B., Li, Z., Xue, Y., Zhou, Y., et al. (2014). MicroRNA directly enhances mitochondrial translation during muscle differentiation. *Cell* 158, 607–619. doi: 10.1016/j.cell.2014.05.047

Zhang, Z. W., Yuan, S., Feng, H., Xu, F., Cheng, J., Shang, J., et al. (2011). Transient accumulation of Mg-protoporphyrin IX regulates expression of PhANGs – New evidence for the signaling role of tetrapyrroles in mature Arabidopsis plants. *J. Plant Physiol.* 168, 714–721. doi: 10.1016/j.jplph.2010.10.016

Zhao, L. (2019). Mitochondrial DNA degradation: A quality control measure for mitochondrial genome maintenance and stress response. *Enzymes* 45, 311–341. doi: 10.1016/bs.enz.2019.08.004

Zhao, S., Xu, W., Jiang, W., Yu, W., Lin, Y., Zhang, T., et al. (2010). Regulation of cellular metabolism by protein lysine acetylation. *Science* 327, 1000–1004.

Zhu, A., Guo, W., Gupta, S., Fan, W., and Mower, J. P. (2016). Evolutionary dynamics of the plastid inverted repeat: The effects of expansion, contraction, and loss on substitution rates. *New Phytol.* 209, 1747–1756. doi: 10.1111/nph.13743

Conflict of Interest: The authors declare that the research was conducted in the absence of any commercial or financial relationships that could be construed as a potential conflict of interest.

Advantages of publishing in Frontiers

OPEN ACCESS
Articles are free to read for greatest visibility and readership

FAST PUBLICATION
Around 90 days from submission to decision

HIGH QUALITY PEER-REVIEW
Rigorous, collaborative, and constructive peer-review

TRANSPARENT PEER-REVIEW
Editors and reviewers acknowledged by name on published articles

Frontiers
Avenue du Tribunal-Fédéral 34
1005 Lausanne | Switzerland

Visit us: www.frontiersin.org
Contact us: frontiersin.org/about/contact

REPRODUCIBILITY OF RESEARCH
Support open data and methods to enhance research reproducibility

DIGITAL PUBLISHING
Articles designed for optimal readership across devices

FOLLOW US
@frontiersin

IMPACT METRICS
Advanced article metrics track visibility across digital media

EXTENSIVE PROMOTION
Marketing and promotion of impactful research

LOOP RESEARCH NETWORK
Our network increases your article's readership